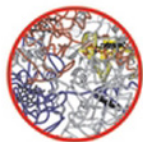


 WILEY



REDOX

BIOCHEMISTRY



Edited by RUMA BANERJEE

Associate Editors

DONALD BECKER • MARTIN DICKMAN
VADIM GLADYSHEV • STEPHEN RAGSDALE

REDOX BIOCHEMISTRY



THE WILEY BICENTENNIAL—KNOWLEDGE FOR GENERATIONS

Each generation has its unique needs and aspirations. When Charles Wiley first opened his small printing shop in lower Manhattan in 1807, it was a generation of boundless potential searching for an identity. And we were there, helping to define a new American literary tradition. Over half a century later, in the midst of the Second Industrial Revolution, it was a generation focused on building the future. Once again, we were there, supplying the critical scientific, technical, and engineering knowledge that helped frame the world. Throughout the 20th Century, and into the new millennium, nations began to reach out beyond their own borders and a new international community was born. Wiley was there, expanding its operations around the world to enable a global exchange of ideas, opinions, and know-how.

For 200 years, Wiley has been an integral part of each generation's journey, enabling the flow of information and understanding necessary to meet their needs and fulfill their aspirations. Today, bold new technologies are changing the way we live and learn. Wiley will be there, providing you the must-have knowledge you need to imagine new worlds, new possibilities, and new opportunities.

Generations come and go, but you can always count on Wiley to provide you the knowledge you need, when and where you need it!

A handwritten signature in black ink that reads "William J. Pesce".

WILLIAM J. PESCE
PRESIDENT AND CHIEF EXECUTIVE OFFICER

A handwritten signature in black ink that reads "Peter Booth Wiley".

PETER BOOTH WILEY
CHAIRMAN OF THE BOARD

REDOX BIOCHEMISTRY

Edited By

Ruma Banerjee

Department of Biological Chemistry
University of Michigan
Ann Arbor, Michigan

Associate Editors

Donald Becker

Redox Biology Center and Department of Biochemistry
University of Nebraska
Lincoln, Nebraska

Martin Dickman

Institute for Plant Genomics and Biotechnology
Texas A&M University
College Station, Texas

Vadim Gladyshev

Redox Biology Center and Department of Biochemistry
University of Nebraska
Lincoln, Nebraska

Stephen Ragsdale

Department of Biological Chemistry
University of Michigan
Ann Arbor, Michigan



**WILEY-
INTERSCIENCE**

A JOHN WILEY & SONS, INC., PUBLICATION

Copyright © 2008 by John Wiley & Sons, Inc. All rights reserved

Published by John Wiley & Sons, Inc., Hoboken, New Jersey
Published simultaneously in Canada

No part of this publication may be reproduced, stored in a retrieval system, or transmitted in any form or by any means, electronic, mechanical, photocopying, recording, scanning, or otherwise, except as permitted under Section 107 or 108 of the 1976 United States Copyright Act, without either the prior written permission of the Publisher, or authorization through payment of the appropriate per-copy fee to the Copyright Clearance Center, Inc., 222 Rosewood Drive, Danvers, MA 01923, (978) 750-8400, fax (978) 750-4470, or on the web at www.copyright.com. Requests to the Publisher for permission should be addressed to the Permissions Department, John Wiley & Sons, Inc., 111 River Street, Hoboken, NJ 07030, (201) 748-6011, fax (201) 748-6008, or online at <http://www.wiley.com/go/permission>.

Limit of Liability/Disclaimer of Warranty: While the publisher and author have used their best efforts in preparing this book, they make no representations or warranties with respect to the accuracy or completeness of the contents of this book and specifically disclaim any implied warranties of merchantability or fitness for a particular purpose. No warranty may be created or extended by sales representatives or written sales materials. The advice and strategies contained herein may not be suitable for your situation. You should consult with a professional where appropriate. Neither the publisher nor author shall be liable for any loss of profit or any other commercial damages, including but not limited to special, incidental, consequential, or other damages.

For general information on our other products and services or for technical support, please contact our Customer Care Department within the United States at (800) 762-2974, outside the United States at (317) 572-3993 or fax (317) 572-4002.

Wiley also publishes its books in a variety of electronic formats. Some content that appears in print may not be available in electronic formats. For more information about Wiley products, visit our web site at www.wiley.com.

Wiley Bicentennial Logo: Richard J. Pacifico.

Library of Congress Cataloging-in-Publication Data

Redox biochemistry / edited by Ruma Banerjee.

p. ; cm.

Includes bibliographical references and index.

ISBN 978-0-471-78624-5 (cloth)

1. Oxidation-reduction reaction—Physiological effect. I. Banerjee, Ruma.

[DNLM: 1. Oxidation-Reduction. QU 125 R3185 2008]

QP535.O1R433 2008

541'.393—dc22

2007036231

Printed in the United States of America

10 9 8 7 6 5 4 3 2 1

To our students, from whom we learn as we teach

CONTENTS

Contributors	xiii
List of Abbreviations	xvii
Preface	xix
1. Redox Metabolism and Life	1
<i>By Ruma Banerjee</i>	
1.1. Redox Biochemistry and the Evolution of Life	1
1.2. Global Redox Cycles	4
1.3. Major Bioenergetic Cycles	6
1.3.A. Photosynthesis	6
1.3.B. Aerobic Respiration	7
2. Antioxidant Molecules and Redox Cofactors	11
<i>Edited by Donald Becker</i>	
2.1. Glutathione	11
<i>By Joseph J. Barycki</i>	
2.1.A. Biological Functions	13
2.1.B. Biosynthesis	14
2.1.C. Degradation	16
2.1.D. Other Thiol-Based Redox Buffers	21
2.2. Ascorbate	22
<i>By Han Asard</i>	
2.2.A. Ascorbate Chemistry	22
2.2.B. Ascorbate Biosynthesis	23
2.2.C. Ascorbate Recycling	25
2.2.D. Ascorbate Transport	26
2.2.E. Importance of Ascorbate in Stress and Disease	26
2.3. Other Antioxidants	27
<i>By Julie M. Stone and Mark A. Wilson</i>	
2.3.A. Lipid-Soluble Antioxidants	28
	vii

2.3.B. Water-Soluble Antioxidants	31
2.3.C. Antioxidants and Human Health	32
2.4. Redox Coenzymes	35
<i>By Ruma Banerjee and Donald F. Becker</i>	
2.4.A. Flavin	35
2.4.B. NAD	39
2.4.C. Quinones	40
2.4.D. Pterins and Molybdopterins	42
2.4.E. Folic Acid	46
3. Antioxidant Enzymes	49
<i>Edited by Vadim Gladyshev</i>	
3.1. ROS-Dependent Enzymes	50
<i>By Irwin Fridovich and Leslie B. Poole</i>	
3.1.A. Catalase	50
3.1.B. Superoxide Dismutase	55
3.1.C. Peroxiredoxins	59
3.1.D. Alkyl Hydroperoxide Reductases	65
3.2. The Thioredoxin System	68
<i>By Arne Holmgren</i>	
3.2.A. Thioredoxin	68
3.2.B. Thioredoxin Reductase	71
3.3. The Glutathione System	74
<i>By Marjorie F. Lou</i>	
3.3.A. Glutathione Reductase	75
3.3.B. Glutaredoxin (Thioltransferase)	78
3.4. Repair Enzymes	84
<i>By Vadim N. Gladyshev, Sheila S. David, and By Leslie B. Poole</i>	
3.4.A. Methionine Sulfoxide Reductases	84
3.4.B. DNA Repair Enzymes	87
3.4.C. Sulfiredoxins	94
3.5. Detoxification Enzymes	97
<i>By Robert L. Osborne, John H. Dawson, and Shelly D. Copley</i>	
3.5.A. Cytochrome P450 Enzymes: Structure, Function, and Mechanism	97
3.5.B. GSH Transferases	104
3.6. Oxidative Folding	113
<i>By Hiroshi Kadokura, Jon Beckwith, and Hiram F. Gilbert</i>	

3.6.A. Disulfide Bond Formation in Bacteria	113
3.6.B. Disulfide Bond Formation in Eukaryotes	120
3.7. Other Antioxidant Enzymes	127
<i>By Vadim N. Gladyshev and Stephen W. Ragsdale</i>	
3.7.A. Selenoproteins	127
3.7.B. Heme Oxygenase	131
4. Redox Regulation of Physiological Processes	135
<i>Edited by Martin Dickman</i>	
4.1. Reactive Oxygen, Nitrogen, and Thiol-Based Signal Transduction	136
<i>By Ilsa I. Rovira and Toreen Finkel</i>	
4.1.A. Nitric Oxide Signaling	136
4.1.B. Carbon Monoxide Signaling	141
4.1.C. Superoxide and Hydrogen Peroxide	143
4.1.D. Other Novel Redox Molecules	147
4.2. Role of Nitric Oxide Synthases in Redox Signaling	148
<i>By Bettie Sue Masters</i>	
4.2.A. Characterization of the Nitric Oxide Synthases	149
4.2.B. Regulation of Nitric Oxide Synthases by Intrinsic Elements	150
4.2.C. Extrinsic Regulation of Nitric Oxide Synthases	152
4.2.D. Interactions of NO with Other Proteins and Enzymes	152
4.3. Redox Regulation of Genes	154
<i>By Martin B. Dickman</i>	
4.3.A. MAP Kinase/Cell Cycle	154
4.3.B. Redox Control of Gene Expression	155
4.3.C. Peptide Editing and Thiol-Mediated Redox Regulation	156
4.4. Redox Regulation of Apoptosis	158
<i>By Martin B. Dickman</i>	
4.4.A. Apoptotic Pathways	158
4.4.B. Reactive Oxygen Species and Apoptosis	159
4.5. Metal Homeostasis	162
<i>By Jaekwon Lee</i>	
4.5.A. Physiological Significance of Metal Metabolism	163
4.5.B. Metal Uptake from the Extracellular Environment	164
4.5.C. Intracellular Metal Distribution by Target-Specific Chaperones	165
4.5.D. Subcellular Membrane Metal Transporters	167

4.5.E. Heme and Iron–Sulfur Cluster Synthesis	168
4.5.F. Cellular Storage	168
4.5.G. Metal Export	168
4.5.H. Regulation of Metal Metabolism	169
4.5.I. Genetic Disorders in Metal Metabolism	171
4.5.J. Perturbation of Metal Homeostasis and Degenerative Disorders	172
4.6. Redox Enzymology <i>By Stephen W. Ragsdale</i>	173
4.7. Circadian Clock and Heme Biosynthesis <i>By Cheng Chi Lee</i>	177
4.7.A. Cyclic Expression of Heme Binding Proteins	177
4.7.B. Circadian Clock Mechanism	178
4.7.C. PAS Is a Heme Binding Domain	179
4.7.D. Expression of <i>Npas2</i> Is Controlled by mPER2	180
4.7.E. NPAS2 Regulates Expression of Aminolevulinate Synthase 1	180
5. Pathological Processes Related to Redox <i>Edited by Ruma Banerjee</i>	183
5.1. Protein Modification <i>By Earl R. Stadtman</i>	184
5.1.A. Protein Oxidation and Aging	184
5.1.B. Mechanisms of Protein Oxidation	184
5.1.C. Peptide Bond Cleavage	187
5.1.D. Oxidation of Amino Acid Residue Side Chains	188
5.1.E. Beta Scission of Amino Acid Side Chains	189
5.1.F. Generation of Protein Carbonyl Derivatives	189
5.1.G. Formation of Protein Cross-Linked Derivatives	193
5.1.H. Role of Protein Oxidation in Aging	193
5.2. Oxidative Stress in the Eye: Age-Related Cataract and Retinal Degeneration <i>By Marjorie F. Lou and John W. Crabb</i>	194
5.2.A. Oxidative Stress and Cataract	195
5.2.B. Oxidative Stress and Retinal Pathology	199
5.3. Redox Mechanisms in Cardiovascular Disease: Chronic Heart Failure <i>By George J. Rozanski</i>	204
5.3.A. Excitation–Contraction Coupling in Cardiac Myocytes	204
5.3.B. Role of Oxidative Stress in Chronic Heart Failure	206

5.3.C. Redox Modulation of Ca ²⁺ Handling Proteins	206
5.3.D. Hypertrophy and Cell Death	209
5.3.E. Extracellular Matrix Remodeling	209
5.4. Role of Reactive Oxygen Species in Carcinogenesis <i>By Suresh Veeramani and Ming-Fong Lin</i>	212
5.4.A. ROS Act as Growth Signaling Messengers	212
5.4.B. Phosphatases Are Prime Targets for ROS During Growth Stimulation	212
5.4.C. Uncontrolled Production of ROS is Carcinogenic	214
5.4.D. ROS Can Induce Carcinogenic DNA and Protein Adducts	215
5.4.E. ROS Can Affect DNA Methylation and Gene Expression	216
5.4.F. Mitochondrial DNA Mutations Are Induced by ROS	216
5.4.G. Clinical Trials on Antioxidant Supplementation Against Cancer	216
5.5. Oxidative Stress and the Host–Pathogen Interaction <i>By Greg A. Somerville</i>	218
5.5.A. Neutrophils and the Innate Immune Response	219
5.5.B. Bacterial Targets of Oxidative Damage	220
5.5.C. Regulating the Oxidative Stress Response	221
5.5.D. The Oxidative Stress Response	223
5.5.E. Evasion of the Innate Immune Response	223
6. Specialized Methods	227
<i>Edited by Stephen Ragsdale</i>	
6.1. Mass Spectrometry Applications for Redox Biology <i>By Ashraf Raza and John R. Engen</i>	228
6.1.A. Mass Spectrometer	228
6.1.B. Applications of Mass Spectrometry	231
6.1.C. Hydrogen Exchange Mass Spectrometry	236
6.2. Electron Paramagnetic Resonance (EPR) for the Redox Biochemist <i>By Stephen W. Ragsdale and Javier Seravalli</i>	237
6.2.A. Introduction to Magnetic Resonance Spectroscopy	237
6.2.B. Basic EPR Theory	239
6.2.C. Appearance of the EPR Spectrum	240
6.2.D. The EPR Experiment	240

6.2.E. The Conventional EPR Spectrometer: Detection of the Signal	241
6.2.F. Sensitivity and Saturation in EPR	244
6.2.G. Measuring the Concentration of Spins	244
6.2.H. Nuclear Hyperfine and Spin–Spin Interactions	246
6.3. Redox Potentiometry	247
<i>By Donald F. Becker</i>	
6.3.A. Midpoint Potential	247
6.3.B. Redox-Linked Processes	248
6.3.C. Potentiometric Technique	249
6.4. Bioinformatics Methods to Study Thiol-Based Oxidoreductases	251
<i>By Dmitri E. Fomenko and Vadim N. Gladyshev</i>	
6.4.A. Identification of Redox-Active Cysteines in Proteins	251
6.4.B. Cysteine-Based Redox Motifs	253
6.4.C. Conserved Cysteines in Metal-Binding Proteins	253
6.4.D. Secondary Structure Context of Redox-Active Cysteines	253
6.4.E. Structure Modeling	255
6.4.F. Comparative Sequence Analysis of Thiol-Based Oxidoreductases	255
6.5. Electrophysiology	256
<i>By Mark P. Thomas and Harold D. Schultz</i>	
6.5.A. Electrophysiology Part I: Ion Channel Physiology	256
6.5.B. Electrophysiology Part II	263
6.6. Methods to Detect Reactive Metabolites of Oxygen and Nitrogen	272
<i>By Matthew B. Grisham</i>	
6.6.A. Detection of the Superoxide Anion Radical	273
6.6.B. Detection of Hydrogen Peroxide	274
6.6.C. F2-Isoprostanes as Indicators of Lipid Peroxidation <i>In Vivo</i>	276
6.6.D. Measurement of the GSSG/GSH Redox Couple in Cells and Tissue	277
6.6.E. Methods to Detect NO and Its Oxidized Metabolites <i>In Vitro and In Vivo</i>	277
6.6.F. Detection of S-Nitrosothiols by Colorimetric and Fluorimetric Methods	281
6.6.G. Is the Presence of 3-Nitrotyrosine a Specific Footprint for Peroxynitrite?	283

CONTRIBUTORS

Han Asard, Department of Biology, University of Antwerp, Groenenborgerlaan 171, B-2020 Antwerp, Belgium

Ruma Banerjee, Department of Biological Chemistry, University of Michigan, 3220B MSRB III, 1150 West Medical Center Drive, Ann Arbor, MI 48109-0606

Joseph J. Barycki, Redox Biology Center and Department of Biochemistry, University of Nebraska, N222 Beadle Center, Lincoln, NE 68588-0664

Donald F. Becker, Redox Biology Center and Department of Biochemistry, University of Nebraska, N258 Beadle Center, Lincoln, NE 68588-0662

Jon Beckwith, Department of Microbiology and Molecular Genetics, Harvard Medical School, 200 Longwood Avenue, Boston, MA 02115

Shelley D. Copley, University of Colorado, MCDB, 347 UCB, Boulder, CO 80309-0347

John W. Crabb, Cole Eye Institute, Cleveland Clinic Foundation, Cleveland, OH 44195

Sheila S. David, Department of Chemistry, University of California–Davis, Chemistry Building, Davis, CA 95616

John H. Dawson, Department of Chemistry and Biochemistry, University of South Carolina, 631 Sumter Street, GSRC 410, Columbia, SC 29208

Martin B. Dickman, Institute for Plant Genomics and Biotechnology, Borlaug Center, Texas A&M University, 2123 TAMU, College Station, TX 77843-2123

John R. Engen, Department of Chemistry and Chemical Biology, Northeastern University—The Barnett Institute, 341 Mugar Life Sciences, 360 Huntington Avenue, Boston, MA 02115

Toren Finkel, Cardiology Branch, NHLBI NIH, Bldg 10/CRC 5-3330, 10 Center Drive, Bethesda, MD 20892

Dmitri E. Fomenko, Redox Biology Center and Department of Biochemistry, University of Nebraska, N152 Beadle Center, Lincoln, NE 68588-0664

Irwin Fridovich, Department of Biochemistry, Duke University Medical Center, 255 Nanaline H. Duke, Box 3711, DUMC, Durham, NC 27710

Hiram F. Gilbert, Department of Biochemistry and Molecular Biology, Baylor College of Medicine, One Baylor Plaza, Houston, TX 77030

Vadim N. Gladyshev, Redox Biology Center and Department of Biochemistry, University of Nebraska, N151 Beadle Center, Lincoln, NE 68588-0664

Matthew B. Grisham, Department of Molecular and Cellular Physiology, LSU Health Sciences Center, 1501 Kings Highway, Shreveport, LA 71130

Arne Holmgren, Department of Medical Biochemistry and Biophysics, Karolinska Institutet, S17177 Stockholm, Sweden

Hiroshi Kadokura, Department of Microbiology and Molecular Genetics, Harvard Medical School, 200 Longwood Avenue, Boston, MA 02115

Cheng Chi Lee, Department of Biochemistry and Molecular Biology, University of Texas–Houston Medical School, PO Box 20708, Houston, TX 77225

Jaekwon Lee, Redox Biology Center and Department of Biochemistry, University of Nebraska, N210 Beadle Center, Lincoln, NE 68588-0662

Ming-Fong Lin, Department of Biochemistry and Molecular Biology and Eppley Institute for Cancer Research, University of Nebraska Medical Center, 985870 Nebraska Medical Center, Omaha, NE 68198-5870

Marjorie F. Lou, Redox Biology Center and Department of Veterinary and Biomedical Sciences, University of Nebraska, 134 VBS, Lincoln, NE 68583-0905

Bettie Sue Masters, Department of Biochemistry—MSC 7760, The University of Texas Health Science Center at San Antonio, 7703 Floyd Curl Drive, San Antonio, TX 78229-3900

Robert L. Osborne, Department of Chemistry and Biochemistry, University of South Carolina, 631 Sumter Street, GSRC 410, Columbia, SC 29208

Leslie B. Poole, Department of Biochemistry and Center for Structural Biology, Wake Forest University School of Medicine, Medical Center Boulevard, Winston-Salem, NC 27157

Stephen W. Ragsdale, Department of Biological Chemistry, University of Michigan, 5220D MSRB III, 1150 West Medical Center Drive, Ann Arbor, MI 48109-0606

Ashraf Raza, Redox Biology Center and Department of Biochemistry, University of Nebraska, E154 Beadle Center, Lincoln, NE 68588-0662

Ilsa I. Rovira, Cardiology Branch, NHLBI NIH, Bldg 10/CRC 5-3330, 10 Center Drive, Bethesda, MD 20892

George J. Rozanski, Department of Cellular and Integrative Physiology, University of Nebraska Medical Center, 985850 Nebraska Medical Center, Omaha, NE 68198-5850

Harold D. Schultz, Department of Cellular and Integrative Physiology, University of Nebraska College of Medicine, 985850 Nebraska Medical Center, Omaha, NE 68198-5850

Javier Seravalli, Redox Biology Center and Department of Biochemistry, University of Nebraska, N113 Beadle Center, Lincoln, NE 68588-0664

Greg A. Somerville, Redox Biology Center and Department of Veterinary and Biomedical Sciences, University of Nebraska, 155 VBS, Lincoln, NE 68583-0905

Earl R. Stadtman, Laboratory of Biochemistry, National Heart, Lung, and Blood Institute, National Institutes of Health, Bldg 50—Louis B Stokes Labs, Rm 2140, 50 South Drive, Bethesda, MD 20892-0812

Julie M. Stone, Redox Biology Center and Department of Biochemistry, University of Nebraska, N230 Beadle Center, Lincoln, NE 68588-0664

Mark P. Thomas, School of Biological Sciences, University of Northern Colorado, College of Natural and Health Sciences, Greeley, CO 80639

Suresh Veeramani, Department of Biochemistry and Molecular Biology and Eppley Institute for Cancer Research, University of Nebraska Medical Center, 985870 Nebraska Medical Center, Omaha, NE 68198-5870

Mark A. Wilson, Redox Biology Center and Department of Biochemistry, University of Nebraska, N164 Beadle Center, Lincoln, NE 68588-0662

LIST OF ABBREVIATIONS

EPR	Electron paramagnetic resonance
GSH	Glutathionine
GSSG	Glutathione disulfide
H ₂ O ₂	Hydrogen peroxide
O ₂ [·]	Superoxide
OH [·]	Hydrogen radical
ROS	Reactive oxygen species
SOD	Superoxide dismutase

PREFACE

This book grew out of our efforts since 2001 to consolidate the area of redox biology at the University of Nebraska, in recognition of the centrality of redox reactions in the life sciences. Soon we were faced with the need to teach this subject to our students and quickly discovered the paucity of compiled information that would be more readily accessible than the primary literature to a recent inductee to the field. As one thing led to another, we decided to collectively write a textbook for our students and to invite experts in the redox biochemistry field to contribute to this project. I would be remiss if I did not acknowledge that the idea for this cooperative project was initially planted in my mind by Howie Gendelman (University of Nebraska Medical Center), who has since been repeatedly reminded that this project has felt like an albatross. Had it not been for the speedy and positive response that the book proposal received from our publisher, it is likely that the inspiration to undertake this project would have rapidly dissipated.

Redox biochemistry is an incredibly broad discipline and spans the gamut of physiological and pathological life processes. This book does not attempt to be comprehensive. It is, instead, an introduction, targeted for the beginner. It is organized into six chapters that cover: Redox Metabolism and Life, Antioxidant Molecules and Redox Cofactors, Antioxidant Enzymes, Redox Regulation of Physiological Processes, Pathological Processes Related to Redox and Specialized Methods. Each chapter is organized into multiple sections with most being written by different authors (with the exception of Chapter 1). This superfluity of writers presented obvious challenges for achieving stylistic uniformity and we decided to sacrifice some of that in favor of the substance that came from contributions by experts in the field. Due to the strict page limitations imposed by the publisher to keep costs within reach of student pockets, the associate editors and I have chosen a format in which each section is followed by selected references for further reading to guide the interested reader deeper into the relevant literature. However, this style of very limited referencing, although not uncommon for textbooks, is not ideal, and we apologize to our colleagues for not being able to cite the literature and their contributions completely. Most structural figures were generated with MolScript J. Kraulis (1991). MOLSCRIPT: a program to produce both detailed and schematic plots of protein structures, *Journal of Applied Crystallography* **24**:946–950. Some of them were generated with MolScript and Raster3D E. A. Merritt and D. J. Bacon (1997). Raster3D photorealistic molecular graphics, *Methods in Enzymology* **277**:505–524.

I thank my associate editors, Don Becker, Marty Dickman, Vadim Gladyshev, and Steve Ragsdale, for their assistance with planning, organizing, and editing this book. I

also thank each of the contributors for their patience in responding to my liberal editing pen. Lastly, this book would have literally not been possible without the diligence of Mamoru Yamanishi and Joyce Ore, both at the Redox Biology Center, who have done a superb job of formatting the text and editing its graphic content to compensate for the inability of the “redox experts” to follow formatting instructions! I hope that our student readers will find this book to be valuable for entering through the portals of the exciting area of redox biochemistry, which is rapidly gaining momentum.

RUMA BANERJEE
University of Michigan, Ann Arbor
January 2007

Redox Metabolism and Life

RUMA BANERJEE

Department of Biological Chemistry, University of Michigan, Ann Arbor, Michigan

- 1.1. Redox Biochemistry and the Evolution of Life
- 1.2. Global Redox Cycles
- 1.3. Major Bioenergetic Cycles
 - 1.3.A. Photosynthesis
 - 1.3.B. Aerobic Respiration

This chapter describes how, throughout the course of evolution, energy metabolism, which is based on redox reactions, has limited life and simultaneously exerted a strong selection pressure for innovation of more productive pathways. The redox biochemistry of organisms has in turn transformed the environment such that geochemical and biochemical cycles have become irrevocably intertwined. Today, the dominant bioenergetic pathways in the biosphere, oxygenic photosynthesis and respiration, are interlinked and thrive on a glut of reducing equivalents stored in water and oxidizing equivalents stored in oxygen.

1.1 REDOX BIOCHEMISTRY AND THE EVOLUTION OF LIFE

Life arose on our rocky planet more than 3.8 billion years ago (Fig. 1.1) using as its toolbox, the periodic table of elements, and as its energy currency, redox reactions. In as much as oxidation of fossil fuels powers motors, oxidation of inorganic and organic compounds (i.e., redox reactions) releases energy that is harnessed to power cellular functions. During the course of evolution, the carrying capacity of energy resources available to life forms on Earth, repeatedly limited expansion and spurred evolution of alternative energy portfolios by diversification of bioenergetic pathways. The early biosphere was rich in methane and hydrogen and had a surplus of reducing equivalents. Among the most primitive organisms were fermenting heterotrophs, dependent on abiotic sources of fermentable organic compounds and chemotrophs that eked out a

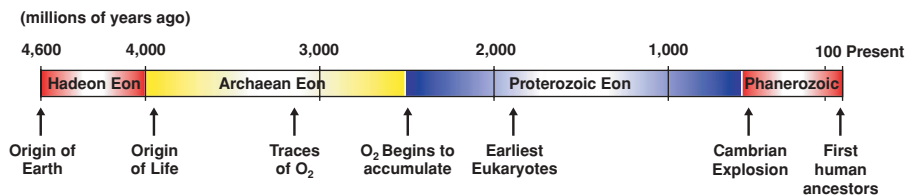


Figure 1.1. Time line for evolution of life on Earth.

meager subsistence on diets of hydrogen, hydrogen sulfide, and methane, using as electron acceptors, carbon dioxide and, less commonly, sulfate (Eqs. (1.1)–(1.4)).



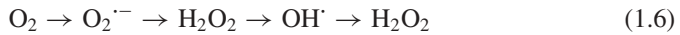
The use of N₂ as an alternative electron acceptor was restricted, despite its abundance, by the energetic price tag on reducing it to ammonia under physiological conditions. These early life forms were geographically confined to regions of volcanic and hydrothermal activity that spewed out abiotic compounds needed for their sustenance.

The innovation of anoxygenic bacterial photosynthesis coupled the redox chemistry of sulfur compounds (*viz.*, hydrogen sulfide, sulfur, or thiosulfate), hydrogen, or organic acids to solar energy to power metabolism. Purple and green sulfur bacteria and heliobacteria were probably among the first photosynthetic organisms. Their extant representatives use a variety of photoantenna designs to capture solar energy to drive electron transfer through a circuit that transduces light to chemical energy. The latter is then used for CO₂ fixation. The early anoxic environment lacked ozone and it has been speculated that pigments in the reaction centers used by photosynthetic bacteria may have evolved as shields against Ultraviolet (UV) radiation from the Sun. Even with the advent of anoxygenic photosynthetic capacity, only a pittance of energy could be extracted with the available electron acceptors and reducing agents. This constrained complexity of ancient organisms to uniseriate filamentous forms and exerted enormous selection pressure on the evolution of alternative and high yielding bioenergetic options.

Somewhere between 3.2 and 2.4 billion years ago, a cyanobacterial-like microbe emerged that was able to exploit solar energy to overcome the prohibitive cost of water oxidation and could thus tap into an abundant planetary electron donor pool. The chemical outcome of this water splitting reaction was the generation of one oxygen molecule from two molecules of water in a four-electron process (Eq. (1.5)).



The introduction of oxygen as a metabolic waste was, however, a double-edged sword. As a powerful oxidant, oxygen threatened the air-sensitive anaerobic metabolic networks that had evolved. Furthermore, the one-electron reduced intermediates between triplet oxygen and water include superoxide ($\text{O}_2^{\cdot-}$), hydrogen peroxide (H_2O_2), and hydroxyl radical (OH^{\cdot}), respectively (Eq. (1.6)).



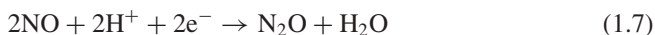
These are collectively known as reactive oxygen species (ROS) and can wreak havoc on DNA, proteins, and lipids, if uncontained. In addition, singlet oxygen ($^1\text{O}_2$) formed, for instance, by the reaction of triplet oxygen with triplet chlorophyll is highly reactive and destructive. Thus, in this changing metabolic landscape, organisms that had originally evolved under anaerobic conditions faced choices of adapting to contain the biotoxicity of oxygen, retreating to limited anaerobic niches or succumbing to extinction's knell.

Development of oxygenic photosynthesis heralded a permanent transformation to an oxygen-rich biosphere from one that was originally oxygen-poor. It is estimated that in the early Archaean period, the atmospheric partial pressure of oxygen was $\sim 10^{-12}$ -fold lower than its present value. As oxygen saturation of the oceans and the atmosphere rose, it forever changed evolution's trajectory. Geochemical evidence of red beds of sediments stained by oxidized iron deposits suggests that the transition to a stable oxygenic environment occurred between ~ 2.3 and 2.2 billion years ago. This "Great Oxidation Event" resulted in formation of a protective ozone layer and set the stage for the evolution of complex life forms that made a living on highly exergonic aerobic respiration.

With the exception of chlorine and fluorine in the periodic table, reduction of oxygen yields the largest free energy change per electron transferred. In contrast to the halogen gases, which are weakly bonded and whose high reactivity precludes their buildup in the planetary atmosphere, oxygen is stable, making it an excellent choice for a terminal electron acceptor in high yielding energy metabolism. It is believed that evolution of complex, mobile organisms in the 0.1–10 meter size range required the evolution of aerobic metabolism that extracted an order of magnitude more energy from glucose oxidation than anaerobic pathways. Oxygen also increased the repertoire of biochemical reactions leading to the appearance of at least one thousand new reactions not found in anaerobic metabolic networks. This precipitated an enormous increase in metabolic complexity and the appearance of novel secondary metabolites (viz., sterols, alkaloids, and certain antibiotics).

Aerobic respiration is an inherent trait of organisms in two of three domains of life—Bacteria and Archaea—while oxygenic photosynthesis occurs as a primary feature only in Bacteria. Eukaryotes that evolved ~ 1.5 billion years ago are believed to have acquired both bioenergetic capabilities secondarily via chance encounters with bacterial endosymbionts. Recent comparative genomic analyses reveal that homologs of cytochrome *c* oxidase, the protein that reduces molecular oxygen to water, are found both in Bacteria and in Archaea, indicating that aerobic respiration had a monophyletic origin that predated oxygenic photosynthesis. Traces of oxygen present

in the Archaean period could have been used for aerobic respiration in the last common universal ancestor of Bacteria and Archaea. In fact, even today, cytochrome oxidases in some organisms operate in niches containing very low oxygen pressure. Interestingly, nitric oxide reductase, which catalyzes a similar reaction (Eq. (1.7)), is speculated to have been a progenitor of cytochrome *c* oxidases, which is homologous.



The “Great Oxidation Event” thus led to an explosion of genomic and metabolic complexity culminating in the rise of metazoans in the Cambrian period (~600 million years ago). Based on the long “oxygenation time” on Earth—the time it took for atmospheric oxygen levels to reach present values (i.e., <1 billion years ago) needed to sustain large metazoan organisms—astrobiologists have argued that evolution of complex life forms on other habitable planets would be limited by the lifetime of the stars they orbit.

1.2 GLOBAL REDOX CYCLES

The evolution of life meant changes for the planetary environment and, today, nonequilibrium redox cycling of six principal elements—carbon, hydrogen, nitrogen, oxygen, phosphorus, and sulfur—shape and are, in turn, shaped by life on Earth. These biogeochemical cycles are interdependent and the major cycles are briefly discussed here (Fig. 1.2). Atmospheric carbon exists primarily in the form of carbon dioxide in the atmosphere (~0.04% but rising). Atmospheric carbon dioxide is captured by photosynthetic plants in a process that releases oxygen while the carbon is reduced to biomass that is utilized by animals and microbes (Fig. 1.2A) or becomes buried in organic sediments. In the oxidative half cycle, the energy captured in the biomass is extracted via respiration that consumes oxygen and returns carbon dioxide to the atmosphere. The vast majority of global carbon reserves is trapped in the lithosphere in sedimentary rock deposits and does not cycle while a smaller proportion is found in terrestrial and aquatic fossil fuel reserves that are being rapidly depleted. Deforestation and fossil fuel burning have had a major impact on atmospheric carbon levels in the postindustrial history of humankind, increasing levels of greenhouse gases that lead to global warming. In aquatic environments, fermentative microbes utilize anaerobic organic detritus that is converted to a variety of small molecules that bubble upward. Some of these products can be captured by acetogens to produce acetate or methanogens to produce methane. The latter can be converted to carbon dioxide by methanotrophs or can escape into the atmosphere, where it is a potent greenhouse gas, or it can be trapped in giant gas hydrates in the ocean that may in fact constitute the largest fuel reserves on the planet.

Nitrogen is the most abundant element in the atmosphere (78%); however, soluble and biologically available nitrogenous compounds are scarce commodities in natural environments. Nitrogen’s entry into the biogeochemical cycle results primarily from the activity of nitrogen-fixing bacteria that generate ammonia, which is utilized for the

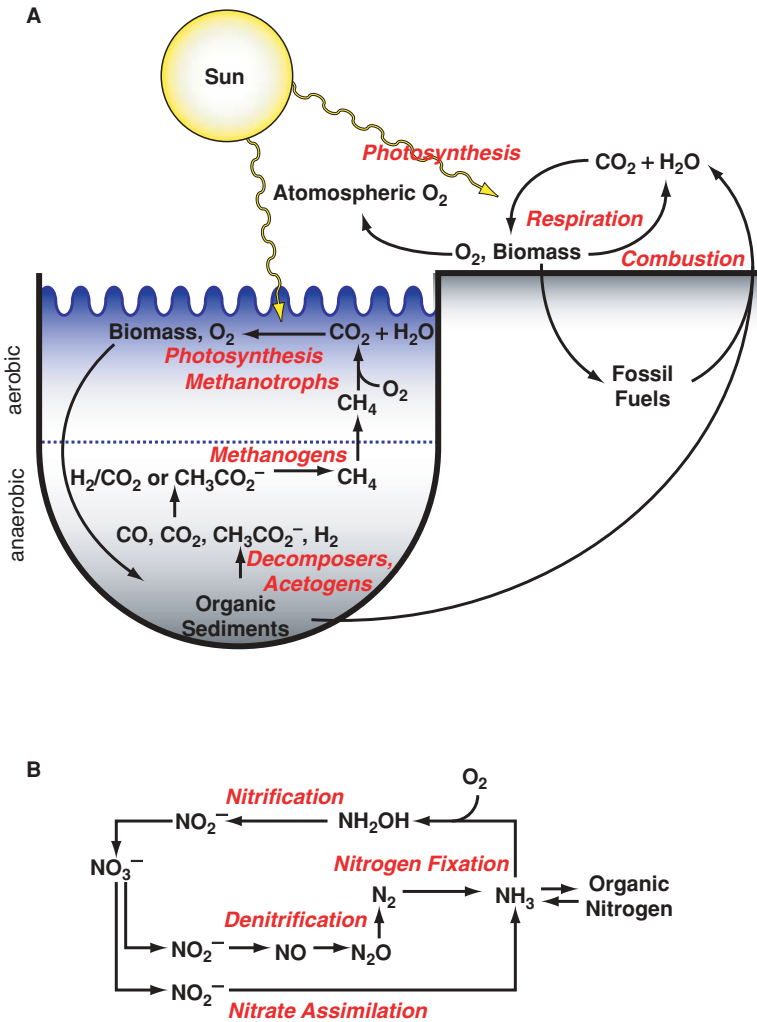


Figure 1.2. Simplified global biogeochemical cycles for carbon/hydrogen/oxygen (A) and nitrogen (B).

synthesis of organic nitrogen compounds (viz., amino acids) (Fig. 1.2B). Ammonia can also be used as an energy source by soil bacteria and be oxidized sequentially to nitrite and nitrate in a process known as nitrification. Plants and some microbes capable of nitrate assimilation can use nitrite and nitrate to generate ammonia. Anthropogenic alterations to the nitrogen biogeochemical cycle have resulted in an almost twofold increase in the transfer of inert nitrogen to biologically available forms. Chemical synthesis of fertilizers, cultivation of leguminous crops, and fossil fuel burning are contributing in major ways to large scale changes in the global nitrogen cycle.

1.3 MAJOR BIOENERGETIC CYCLES

Two of the most prevalent bioenergetic pathways in our biosphere are oxygenic photosynthesis and aerobic respiration, which together constitute the water–water cycle and have a major impact on global carbon/hydrogen and oxygen cycles. It is estimated that $\sim 75\%$ of the oxygen produced by photosynthesis is reduced to water, thus coupling two life-sustaining high energy pathways in the biosphere, which are briefly described here.

1.3.A Photosynthesis

Oxygenic photosynthesis enables life to tap into an abundant albeit poor electron donor, water ($E^{\circ'} = +0.82$ V), using the Sun's energy to drive an electron transfer cascade. The latter transduces light into chemical energy that is trapped as NADPH ($E^{\circ'} = -0.32$ V) and ATP. The stage for this remarkable set of reactions is a series of flattened membrane-encased sacs, the thylakoids, found in the chloroplast. In cyanobacteria, algae, and higher plants, two photosynthetic reaction centers (I and II) are arranged in tandem to yield a noncyclic architecture, which is referred to as the Z-scheme (Fig. 1.3). When solar energy reaches the special chlorophyll pair in the reaction center via exciton transfer from antenna molecules, it triggers a charge separation reaction. Transfer of an electron from chlorophyll in reaction center II to the acceptor, pheophytin, leaves behind an electron hole while initiating electron flow down a thermodynamically favorable gradient of acceptors including plastoquinones A and B and the cytochrome b_6f complex. Electron flow through the cytochrome b_6f complex is coupled to proton pumping and generates a proton gradient that is central for ATP synthesis. A soluble electron transfer protein, plastocyanin, serves as the intermediary carrier between photosystems II and I.

A similar chain of events unfold at photosystem I and a series of carriers transfer electrons from reaction center I (P700) to ferredoxin and then to ferredoxin:NADP⁺ oxidoreductase, resulting in NADPH synthesis (Fig. 1.3). Reduced plastocyanin donates its electron to fill the hole in reaction center I, which leaves a net electron deficit in reaction center II that is filled by the water-splitting reaction. Absorption of four photons of light is needed by the oxygen-evolving complex to abstract four electrons from water to generate oxygen (Eq. (1.5)).

The movement of electrons from water to NADPH via the Z-scheme results in the translocation of ~ 12 protons (4 by the oxygen-evolving complex and ~ 8 by the cytochrome b_6f complex). This represents the conservation of ~ 200 kJ of energy that is sufficient to drive the synthesis of several moles of ATP at a cost of ~ 50 kJ/mol. The transport of electrons through the photosynthetic circuit is imperfect and oxygen reduction to generate ROS is observed that increases with the intensity of illumination. Photosystem I and reduced plastoquinones are sites for reduction of oxygen to superoxide ($O_2^{\cdot-}$) and hydrogen peroxide (H_2O_2). In fact, under conditions of high light intensity, substantial short-circuiting in the photosynthetic electron transport chain and enhanced generation of H_2O_2 are observed. While this could be regarded simply as an unwanted consequence of electron transfer in an aerobic milieu, it is

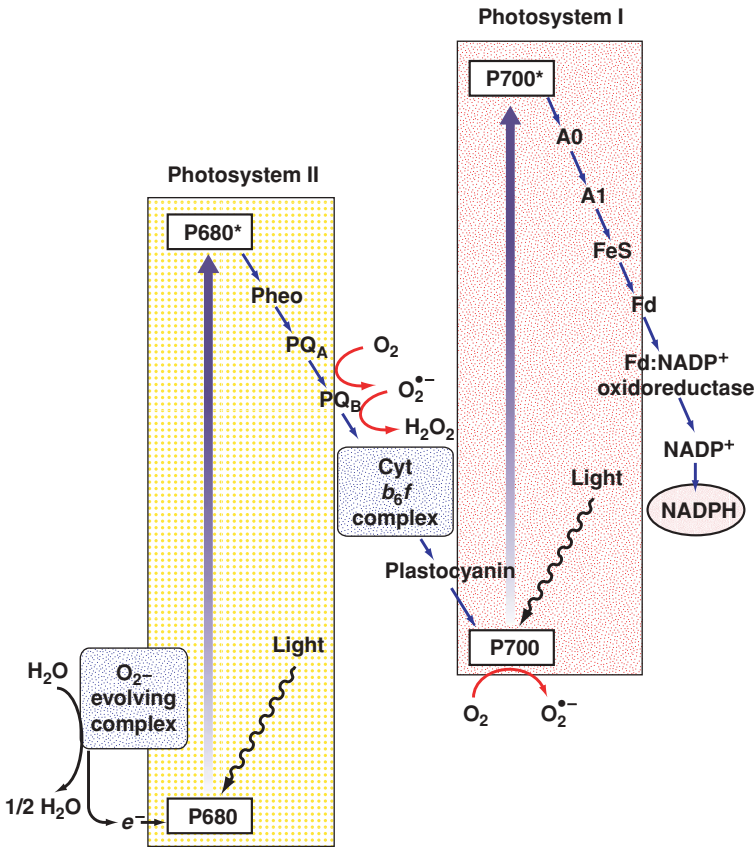


Figure 1.3. Architecture and operation of photosystems I and II in chloroplasts. Electrons flow through a noncyclic pathway, the Z-scheme, starting from water and ending in NADPH. At two points in this pathway, reaction centers P680 and P700, electrons' light energy is used to energize the electrons that are ultimately derived from water. As electrons then flow downhill, the energy is conserved in a proton gradient (which fuels ATP synthesis) and in NADPH. Pheo, PQA, PQB, A₀, and A₁ represent pheophytin, plastoquinone, second quinone, electron acceptor chlorophyll, and phyloquinone, respectively. The major sites of O₂^{•-} and H₂O₂ formation are shown.

increasingly viewed as having a potentially regulatory role. Thus, leakage of electrons from reduced plastoquinones to oxygen and O₂^{•-} could relieve the electron pressure in photosystem II and generate H₂O₂ as a signaling molecule that may be important for adaptive responses in the plant to varying light conditions.

1.3.B Aerobic Respiration

Reducing equivalents (NADH and FADH₂) harvested in catabolic pathways funnel their electrons into the respiratory chain, which represents the culmination of high

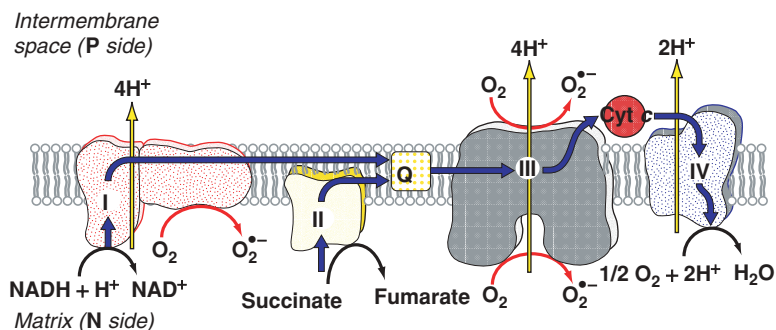


Figure 1.4. Organization of the mitochondrial respiratory chain and the sites for ROS generation. Electrons flow through four complexes in the respiratory chain and the major sites of “leakage” (i.e., O₂^{•-} formation) are complexes I and III that lead to ROS formation.

yielding energy metabolism in aerobes. In this bioenergetic pathway, electrons from reduced cofactors slide down a thermodynamic hill to oxygen, the terminal acceptor, and energy is conserved via vectorial proton pumping, which in turn drives ATP synthesis. The theater of this operation is the mitochondrion. The four major transit stations in this electron transfer pathway are complexes I–IV (Fig. 1.4). Complex I represents the point of entry of electrons from NADH, which are transferred via multiple redox cofactors to the first mobile electron carrier, oxidized coenzyme Q. The energy from this highly exergonic electron transfer reaction is captured via ejection of 4 protons from the mitochondrial matrix into the intermembrane space. Coenzyme Q also receives electrons from other sources, namely, complex II (succinate dehydrogenase), the electron transfer flavoprotein, and glycerol 3-phosphate dehydrogenase. Reduced coenzyme Q donates electrons to complex III for ultimate collection by cytochrome *c* present in the intermitochondrial space. The energy from this exergonic electron transfer reaction is also captured via a proton pumping mechanism. The final stop on the circuit is complex IV (cytochrome *c* oxidase), the site of reduction of molecular oxygen to water in 4 one-electron steps in a reversal of Eq. (1.5). The movement of each pair of electrons originating in complexes I and II leads to the translocation of ~10 and 6 protons, respectively, and corresponds to the conservation of ~200 kJ and ~120 kJ of energy, which is used to power ATP synthesis.

An inescapable consequence of electron currents flowing through the mitochondrial membrane in an aerobic milieu is occasional slippage, leading to formation of ROS. Estimates for the magnitude of precocious oxygen reduction in the respiratory chain vary from ~0.2% to ~2% of the total oxygen consumption. Originally viewed solely as an unproductive side reaction, ROS generation in the mitochondrion is increasingly seen as being important in various redox-dependent signaling pathways. The major sites of ROS generation are complexes I and III. While a number of cellular reactions contribute to ROS levels, it is estimated that mitochondria are a major source, accounting for ~90% of the total production.

SELECTED REFERENCES

1. Raymond, J., and Segrè, D. (2006). The effect of oxygen on biochemical networks and the evolution of complex life. *Science* 311:1764–1767.
2. Castresana, J., and Saraste, M. (1995). Evolution of energetic metabolism: the respiration-early hypothesis. *Trends Biochem. Sci.* 20:443–448.
3. Balaban, R.S., Nemoto, S., and Finkel, T. (2005). Mitochondria, oxidants and aging. *Cell* 120:483–495.
4. Samuilov, V.D. (2005). Energy problems in life evolution. *Biochemistry (Moscow)* 70:246–250.
5. Mubarakshina, M., Khorobrykh, S., and Ivanov, B. (2006). *Biochim. Biophys. Acta* 1757:1496–1503.

Antioxidant Molecules and Redox Cofactors

- 2.1. Glutathione
 - 2.1.A. Biological Functions
 - 2.1.B. Biosynthesis
 - 2.1.C. Degradation
 - 2.1.D. Other Thiol-Based Redox Buffers
- 2.2. Ascorbate
 - 2.2.A. Ascorbate Chemistry
 - 2.2.B. Ascorbate Biosynthesis
 - 2.2.C. Ascorbate Recycling
 - 2.2.D. Ascorbate Transport
 - 2.2.E. Importance of Ascorbate in Stress and Disease
- 2.3. Other Antioxidants
 - 2.3.A. Lipid-Soluble Antioxidants
 - 2.3.B. Water-Soluble Antioxidants
 - 2.3.C. Antioxidants and Human Health
- 2.4. Redox Coenzymes
 - 2.4.A. Flavin
 - 2.4.B. NAD
 - 2.4.C. Quinones
 - 2.4.D. Pterins and Molybdopterins
 - 2.4.E. Folic Acid

2.1 GLUTATHIONE

JOSEPH J. BARYCKI

Redox Biology Center and Department of Biochemistry, University of Nebraska, Lincoln, Nebraska

The tightly controlled maintenance of the intracellular redox environment is essential for normal cellular function. Oxidative stress (i.e., in the form of increased ROS), which is generated by essential metabolic reactions such as mitochondrial

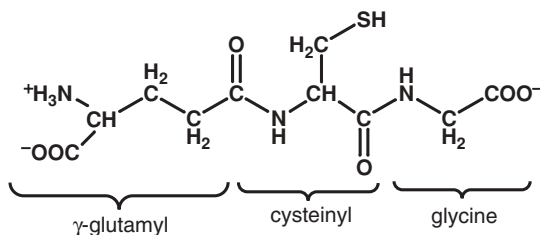


Figure 2.1. Structure of GSH.

energy production and oxidation of toxins by cytochrome P450, is dissipated by the concerted efforts of antioxidants that help buffer the redox environment. This section focuses on the major nonprotein thiol-based redox buffer of the cell. Glutathione (GSH) is a tripeptide comprised of glutamate, cysteine, and glycine (γ -glutamylcysteinylglycine) and is vital for normal cellular function (Fig. 2.1). Its homeostasis is modulated to a large extent by two enzymes: glutamate cysteine ligase, which catalyzes the committed step in GSH biosynthesis, and γ -glutamyltranspeptidase, which initiates GSH reclamation (Fig. 2.2). Since GSH can potently modulate cell signaling in an oxidation-dependent fashion, it is critical for the cell to have efficient ways of replenishing reduced levels. Reduced GSH pools are maintained by glutathione reductase, a pyridine nucleotide disulfide reductase that transfers electrons from NADPH to oxidized GSH. This enzyme provides the crucial direct link between the pool of electron-rich metabolic intermediates, like NADPH, and the array of cysteine-containing proteins that depend on thiol regeneration for sustained activity.

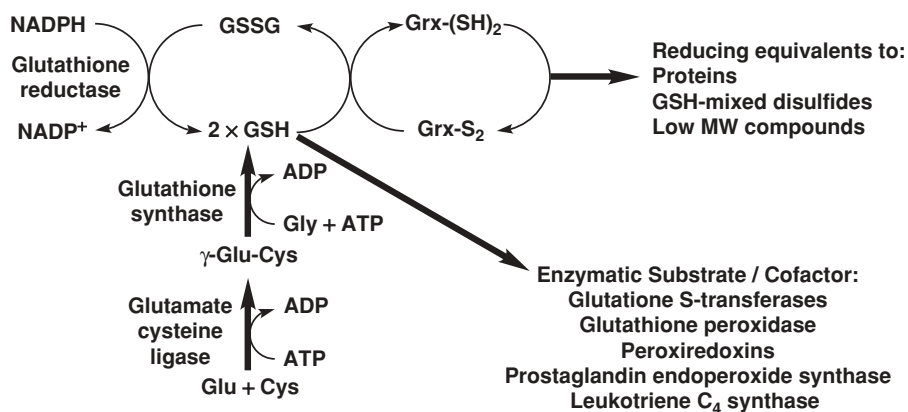


Figure 2.2. The dithiol/disulfide redox couple of reduced and oxidized glutathione is the major thiol-based redox buffer in many organisms. Grx-(SH)₂ and Grx-S₂ denote reduced and oxidized glutaredoxin, respectively.

2.1.A Biological Functions

GSH is found primarily in eukaryotes and gram-negative bacteria, although a select number of gram-positive bacteria have also been shown to utilize it. In eukaryotic systems, approximately 90% of the intracellular GSH pool resides in the cytoplasm, with the remainder in organelles such as the mitochondria, the endoplasmic reticulum, and the nucleus. However, the biosynthesis of GSH appears to occur exclusively in the cytosol. Cellular GSH concentrations are estimated to range from 0.5 to 10 mM in most cell types with the vast majority of GSH being in the reduced form. The predominant oxidized form of GSH, GSSG, results from the cross-linking of two molecules of GSH via a disulfide bond. The ratio of GSH to GSSG is often used to express the redox status of a cell. Typically, the GSH:GSSG ratio is >10:1 in the cytosol and mitochondria and as low as 1:1 in the endoplasmic reticulum. The lower GSH:GSSG ratio in the endoplasmic reticulum facilitates formation of disulfide bonds during folding of secretory and membrane proteins.

GSH is involved in numerous biological processes. These functions include the storage and transport of cysteine, leukotriene and prostaglandins biosynthesis, maintenance of protein structure and function, and the regulation of enzyme activity through the reduction of disulfide bonds or by glutathionylation. However, its primary function appears to be in the maintenance of intracellular redox homeostasis by affording protection against reactive oxygen and nitrogen species as well as electrophilic xenobiotics. As an introduction to these diverse functions, several GSH-dependent processes have been highlighted.

Protection against ROS generated as a result of aerobic metabolism is largely afforded by the combined efforts of several enzyme systems that will be discussed in detail in Chapter 3. Superoxide dismutases catalyze the conversion of two superoxide ($O_2^{\cdot-}$) molecules into hydrogen peroxide (H_2O_2) and oxygen. H_2O_2 can then be converted to water by catalase, glutathione peroxidases, or peroxiredoxins. Glutathione peroxidases are a family of selenocysteine-containing enzymes that can convert H_2O_2 to water or lipid peroxides to their corresponding alcohols concomitant with the generation of GSSG (Eqs. (2.1) and (2.2)).



Peroxiredoxins catalyze the same molecular transformations albeit by a different catalytic mechanism. The GSSG generated by glutathione peroxidases and peroxiredoxins is rapidly reduced by an NADPH-dependent glutathione reductase. Under normal cellular conditions, glutathione reductase can maintain a high GSH:GSSG ratio. However, in cases of extreme oxidative stress, GSSG can rapidly be exported to help preserve the GSH:GSSG ratio. In addition, increased GSSG levels can lead to formation of mixed disulfides between GSH and protein thiols, thus lowering GSSG levels while protecting free sulfhydryls within proteins.

Members of the glutathione transferase enzyme family can also convert organic peroxides to their corresponding alcohols and water and generate GSSG. However,

the primary function of this enzyme family is to catalyze the conjugation of GSH to electrophilic substrates. Glutathione transferases have broadly been classified as cytosolic, mitochondrial, and microsomal. The latter class is now referred to as membrane-associated proteins in eicosanoid and GSH metabolism. Cytosolic and mitochondrial glutathione transferases are distantly related and share common structural features, whereas the microsomal enzymes appear to be evolutionarily distinct. Glutathione transferases activate the free sulfhydryl of GSH by lowering its apparent pK_a , thus making it a better nucleophile. The activated GSH can then attack nonpolar compounds that contain an electrophilic carbon, nitrogen, or sulfur atom. In addition to reducing the reactivity of the electrophilic compound, conjugation to GSH can increase solubility. GSH conjugates can then be exported out of the cell by transmembrane multidrug resistance-associated proteins. In addition to detoxification, glutathione transferases are important in the biosynthesis of leukotrienes and prostaglandins and their diverse functions will be discussed in Chapter 3, Section 3.5B.

GSH can nonenzymatically form complexes with a variety of heavy metals, including mercury, lead, arsenic, gold, silver, zinc, and copper. Its free sulfhydryl is the main coordination site for metal binding but additional favorable interactions can be made with other functional groups within the tripeptide. GSH has been implicated in the storage and transport of metals, and as a cofactor in redox reactions involving metals. Glutathione can also reduce dehydroascorbate to ascorbate, another cellular antioxidant discussed in Chapter 2, Section 2.2. Glutathione-dependent dehydroascorbate reductase activity has been assigned to members of the glutaredoxin and glutathione transferase enzyme families. In addition, glutaredoxin can accept electrons from GSH and transfer reducing equivalents to a variety of proteins, low molecular weight compounds, and glutathione-mixed disulfides, thus expanding the impact of the GSH:GSSG redox system.

2.1.B Biosynthesis

GSH is synthesized from its constituent amino acids by the successive action of two ATP-dependent enzymes (Fig. 2.2): glutamate cysteine ligase and glutathione synthetase. Glutamate cysteine ligase catalyzes the rate-limiting step in GSH biosynthesis, conjugating glutamate via its γ -carboxylate to cysteine. The proposed catalytic mechanism proceeds via the phosphorylation of the γ -carboxylate of glutamate by ATP. The amino group of cysteine, serving as a nucleophile, attacks the γ -glutamyl phosphate intermediate to yield γ -glutamylcysteine. Based on sequence analysis, three distinct groups of glutamate cysteine ligases have been identified (γ -proteobacteria; nonplant eukaryotes; α -proteobacteria and plants) that may have evolved from a distant common ancestor. Although strong sequence conservation is observed within a group, insignificant sequence homology exists between these three groups. Despite these differences, all three groups of glutamate cysteine ligases are predicted to have similar catalytic mechanisms and likely have common structural motifs.

As the committed step to GSH biosynthesis, the reaction catalyzed by glutamate cysteine ligase is tightly regulated. GSH biosynthesis is often limited by free cysteine

availability and glutamate cysteine ligase is feedback regulated by the end product, GSH. Transcriptional regulation, as well as post-translational modifications of the enzyme, ensures exquisite control of intracellular GSH levels. In several eukaryotic systems, additional regulatory control is afforded by the presence of a modifier subunit. In these systems, glutamate cysteine ligase is a heterodimer comprised of a catalytic subunit and a modifier or regulatory subunit with corresponding molecular weights of ~ 70 kDa and ~ 30 kDa, respectively. Although the catalytic subunit contains each of the substrate binding sites and is capable of catalysis alone, it exhibits a high K_m for glutamate. The addition of the modifier subunit decreases the K_m , making it a more efficient enzyme at physiological concentrations of glutamate. In addition, the formation of the complex lessens product inhibition by GSH. The expression of the catalytic and modifier subunits is not tightly coordinated and differential tissue distribution of the two subunits has been observed, which may be involved in tissue-specific regulation of GSH levels. In addition, the stimulatory effects of the modifier subunit on catalysis may depend on the presence of an intersubunit disulfide bond with the catalytic subunit, thus linking the redox state of the cell with GSH biosynthesis. However, it remains unclear if this disulfide is a requirement for activation.

Escherichia coli glutamate cysteine ligase is a monomeric enzyme and structures of the apo form of the enzyme and in complex with a transition-state analogue have been determined (Fig. 2.3). A six-stranded antiparallel β -sheet is central to the protein structure and this partial barrel comprises much of the active site. In the complex

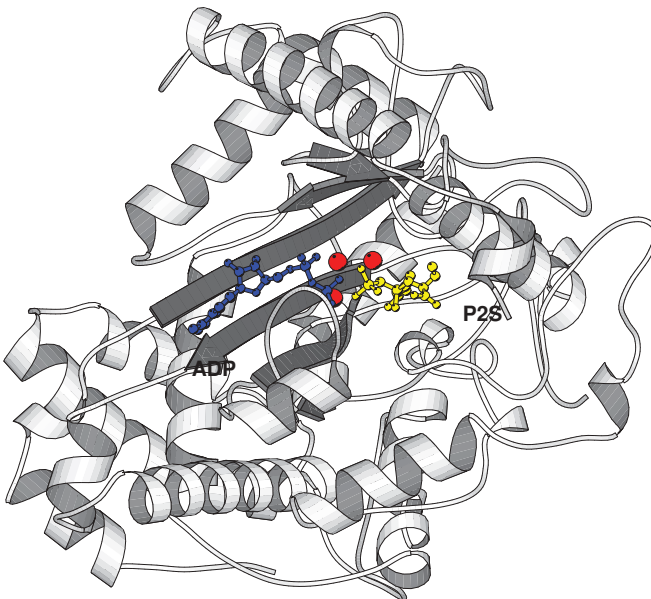


Figure 2.3. Crystal structure of *E. coli* glutamate cysteine ligase. The ribbon representation illustrates the overall fold of the monomeric enzyme. Bound in the enzyme active site are ADP, 3 Mg^{2+} ions (red spheres), and the mechanism-based inhibitor, (2*S*)-2-amino-4-[[[(2*R*)-2-carboxybutyl](phosphono)sulfon-imidoyl] butanoic acid (P2*S*). (PDB ID 1VA6)

structure, ADP is located adjacent to the inhibitor. Three magnesium ions are clustered near the phosphates of ADP and the phosphorylated transition-state analogue. It has been proposed that this magnesium cluster increases the reactivity of the γ -phosphate group of ATP and stabilizes the resulting γ -glutamylphosphate intermediate. The cysteine binding site is adjacent to the glutamate binding site and undergoes a significant conformational change upon ligand binding. Interestingly, there does not appear to be a general base located near the α -amino group of L-cysteine. Overall, the observed structure of the *E. coli* glutamate cysteine ligase is consistent with the proposed enzyme mechanism.

The resultant γ -glutamylcysteine is coupled to glycine by glutathione synthetase. Similar to the situation observed for glutamate cysteine ligase, glutathione synthetases from bacteria share limited sequence homology to eukaryotic homologs and appear to have different quaternary structures. The *E. coli* glutathione synthetase is a functional homotetramer, whereas both the human and yeast glutathione synthetases are homodimers. Despite these differences, all three homologs are members of the ATP-grasp superfamily and are thought to proceed via similar catalytic mechanisms. An acylphosphate intermediate is generated by the transfer of the γ -phosphate of ATP to the carboxylate of γ -glutamylcysteine. The α -amino group of glycine can then attack this phosphorylated intermediate, displacing the inorganic phosphate to form GSH.

Support for this mechanism has been provided by crystal structures of several glutathione synthetase complexes. Human glutathione synthetase bound to its product GSH, ADP, a sulfate ion, and two magnesium ions has been reported (Fig. 2.4). In this complex, the sulfate ion mimics the γ -phosphate of ATP and is located between the β -phosphate of ADP and the α -amino group of the glycine portion of GSH. Similar to glutamate cysteine ligase, two magnesium ions are located in the enzyme active site and likely facilitate binding of ATP, activate the γ -phosphate, and stabilize the acylphosphate intermediate. Comparisons between unliganded and ligand-bound structures of glutathione synthetase also suggest that large conformational changes accompany formation of the Michaelis complex.

Glutathione synthetase rapidly converts γ -glutamylcysteine to GSH *in vivo* and the catalytic activity of glutamate cysteine ligase is generally thought to be rate limiting in glutathione biosynthesis. The liver is the primary site of GSH biosynthesis and, in this tissue, glutathione synthetase activity is severalfold higher than glutamate cysteine ligase activity. However, in other tissues, such as skeletal muscle, the relative activities of the two enzymes are comparable, suggesting glutathione synthetase activity may affect intracellular GSH levels. As such, comparatively limited research has focused on the regulation of glutathione synthetase activity. Current studies are focused on the transcriptional regulation of glutathione synthetase, as little evidence is available to suggest glutathione synthetase activity is regulated post-translationally.

2.1.C Degradation

A significant, but overlooked, component of GSH homeostasis is precursor availability. Cysteine is often limiting in GSH biosynthesis and is obtained from the diet, the transsulfuration pathway, which converts homocysteine to cysteine, or the salvage of

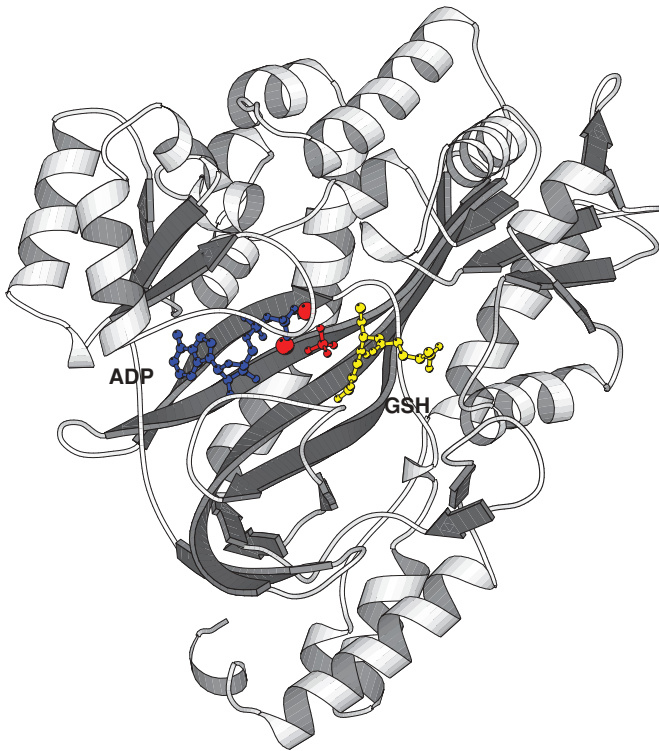


Figure 2.4. Crystal structure of human glutathione synthetase. The ribbon representation illustrates the overall fold of a single subunit of the dimeric enzyme. Bound in the enzyme active site are ADP, 2 Mg²⁺ ions (red spheres), and glutathione. (PDB ID 2HGS)

excreted GSH and its conjugates. The γ -glutamyl cycle proposed by Alton Meister and co-workers describes the reclamation of GSH (Fig. 2.5). γ -Glutamyltranspeptidase catalyzes the first step in the glutathione salvage pathway and cleaves γ -glutamyl amide bonds. The cleaved glutamate can either be transported directly into the cell or be transferred to an amino acid or peptide acceptor before import. Once inside the cell, glutamate is released from the γ -glutamyl peptide by the concerted activities of γ -glutamylcyclotransferase and 5-oxoprolinase. The cysteinylglycine is cleaved by a membrane dipeptidase to generate cysteine and glycine that can be imported into the cell. Cysteine conjugates arising from the degradation of GSH conjugates are funneled into the mercapturic acid pathway.

Mammalian γ -glutamyltranspeptidases are embedded in the plasma membrane by a single N-terminal transmembrane anchor and are heterologously glycosylated. However, the enzyme does not need to be tethered to the membrane or glycosylated to have complete activity *in vitro*. The catalytic mechanism proceeds via a γ -glutamyl-enzyme intermediate, with a conserved threonine residue serving as the nucleophile. The acyl-enzyme intermediate can be hydrolyzed to generate

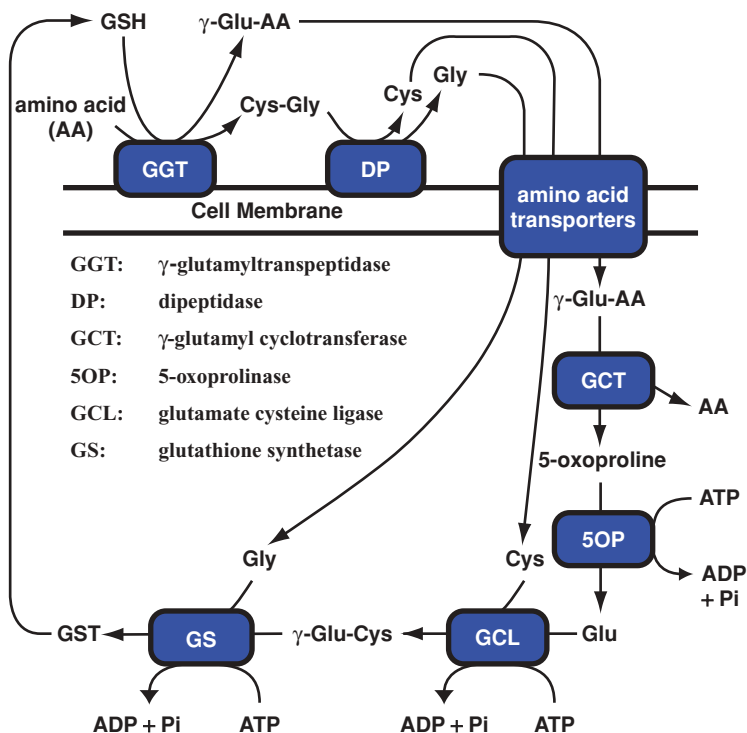


Figure 2.5. The γ -glutamyl cycle. Described by Alton Meister and co-workers, the γ -glutamyl cycle describes the salvage of GSH and GSH conjugates.

glutamate. Alternatively, the α -amino group of an amino acid or the N-terminal amino group of a small peptide can attack the acyl-enzyme intermediate, resulting in transpeptidation of the glutamate from GSH to the acceptor molecule. Bacterial γ -glutamyltranspeptidases are located in the periplasmic space and appear to have limited transpeptidase activity compared to their eukaryotic homologs. In contrast to the GSH biosynthetic enzymes, γ -glutamyltranspeptidases from these diverse species share considerable sequence homology.

γ -Glutamyltranspeptidase is synthesized as an inactive 60 kDa polypeptide and cleavage of the proenzyme yields a fully active heterodimer comprised of a 40 kDa and a 20 kDa subunit (Fig. 2.6). Processing of γ -Glutamyltranspeptidase is thought to be an intramolecular autocatalytic event. A mechanism has been proposed in which processing proceeds via an N-O acyl shift, with a conserved threonine serving as the nucleophile. The peptide bond immediately preceding the threonine residue is broken, leading to activation of the enzyme. This threonine residue at the N terminus of the newly formed 20 kDa subunit can then serve as a nucleophile in the catalytic mechanism of the enzyme as discussed previously. Based on its unique autoprocessing activity, enzymatic activity, and its structure (Fig. 2.7), γ -glutamyltranspeptidase has been identified as a member of the emerging N terminal nucleophile hydrolase

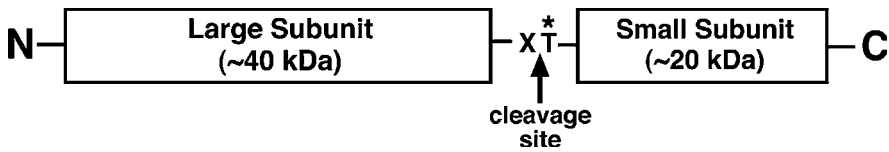


Figure 2.6. Schematic of γ -glutamyltranspeptidase. γ -Glutamyltranspeptidase is synthesized as an inactive ~ 60 kDa polypeptide. Autocleavage of the peptide bond immediately prior to a conserved threonine residue results in an active heterodimer.

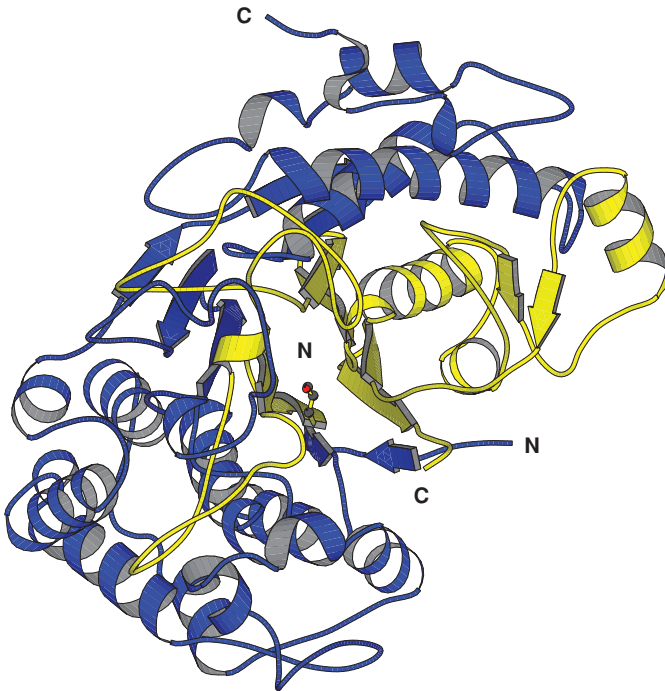


Figure 2.7. Crystal structure of *Helicobacter pylori* γ -glutamyltranspeptidase. The ribbon representation illustrates the overall fold of the active heterodimer. The 40 kDa and 20 kDa subunits are colored in blue and yellow, respectively. The conserved threonine residue at the new N terminus of the processed enzyme is shown in ball and stick representation.

superfamily. Members of this enzyme family are autocatalytically processed to yield an active enzyme, with the resulting N terminus acting as the nucleophile in amide bond hydrolysis reactions. Autoprocessing of γ -glutamyltranspeptidase leads to a large conformational change, with the loop preceding the catalytic threonine moving >35 Å, thus relieving steric constraints that likely limit substrate binding. In addition, cleavage of the proenzyme results in the formation of a threonine–threonine dyad required for efficient catalysis.

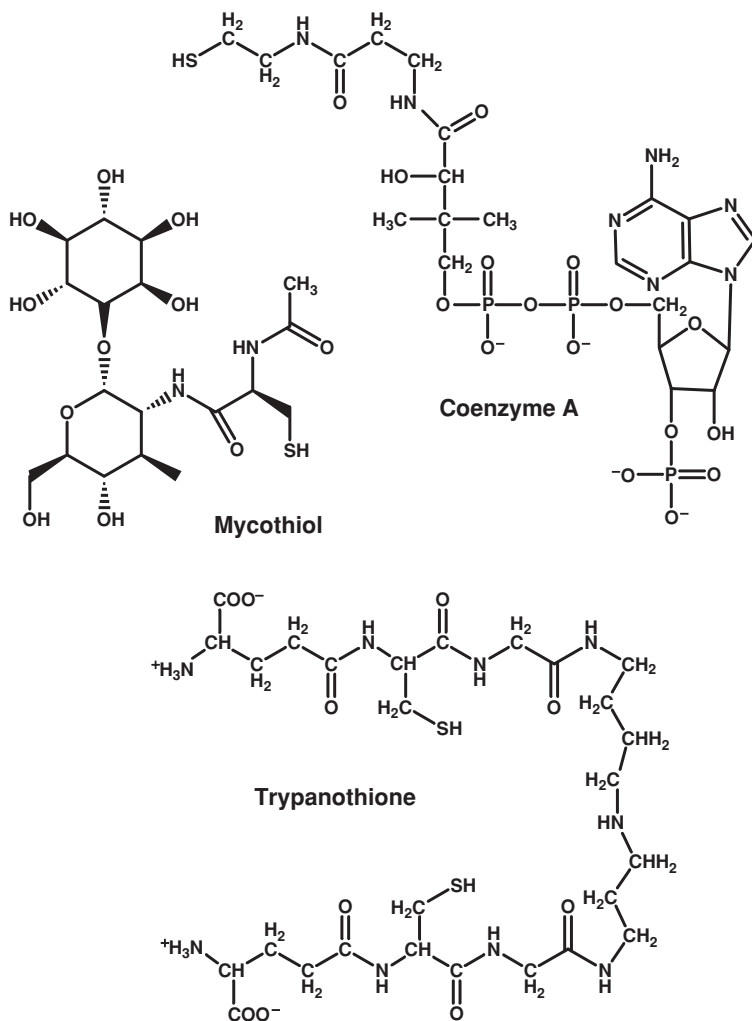


Figure 2.8. Structures of coenzyme A, mycothiol, and trypanothione.

Studies with γ -glutamyltranspeptidase-deficient mice indicate that one of the primary functions of GSH is the storage and transport of cysteine. These mice appear normal at birth, exhibit slower growth, do not mature sexually, and have shorter life spans. They are also considerably more susceptible to cataract formation and damage by ROS. Supplementation with N-acetylcysteine, a cysteine precursor, largely restores the wild-type phenotype, suggesting that the primary function of γ -glutamyltranspeptidase in normal cells is the recovery of cysteine for use in protein and GSH synthesis, which is important for growth and oxidative protection. In agreement with these findings, γ -glutamyltranspeptidase is found to be upregulated in several cancer types and has been shown to accelerate tumor growth and increase

tumor resistance to damage induced by chemotherapy and radiation treatment. This is likely due to the enhanced ability to salvage cysteine from circulating GSH.

γ -Glutamyltranspeptidase has been well characterized; however, the details of the remainder of the GSH salvage pathway are less defined. Cysteinylglycine and its conjugates are cleaved by membrane-associated dipeptidases to their constituent amino acids, which can then be transported across the membrane. In mammalian systems, aminopeptidase M and cysteinylglycinase have been reported to catalyze this reaction. Leucyl aminopeptidase, a cytosolic enzyme, also exhibits a strong preference for cysteinylglycine and its conjugates, suggesting that an unidentified cysteinylglycine transporter may contribute to GSH salvage. In addition, significant extracellular γ -glutamylcysteine arises from the transpeptidase activity of γ -glutamyltranspeptidase and a γ -glutamylcysteine transporter has been identified. Studies designed to elucidate this vital metabolic pathway remain an active area of research.

2.1.D Other Thiol-Based Redox Buffers

Although GSH is the most prevalent thiol-based redox buffer, alternative low molecular weight thiols that serve equivalent functions have been identified. Trypanothione, N^1, N^8 -bis(glutathionyl)spermidine, was initially isolated in the African trypanosome, *Trypanosoma brucei*, and is synthesized by cross-linking two molecules of GSH via spermidine (Fig. 2.8). Another variation on this strategy involves mycothiol (1D-myo-inosityl 2-(*N*-acetylcysteinyl)amido-2-deoxy- α -D-glucopyranoside), which has *N*-acetylcysteine as its redox-active thiol group. Coenzyme A, which is used as a cofactor in numerous biological processes, has also been shown to serve as a redox buffer in *Staphylococcus aureus*. Trypanothione, mycothiol, and coenzyme A can cycle between a reduced and an oxidized form, and each system has a functional reductase that is structurally related to glutathione reductase. In addition to these well characterized low molecular weight thiols, additional variations of thiol/disulfide redox systems have been identified from numerous sources.

SELECTED REFERENCES

1. Copley, S.D., and Dhillon, J.K. (2002). Lateral gene transfer and parallel evolution in the history of glutathione biosynthesis genes. *Genome Biol* 3:research0025.1-0025.16.
2. Dickinson, D.A., and Forman, H.J. (2002). Glutathione in defense and signaling: lessons from a small thiol. *Ann. NY Acad. Sci.* 973:488–504.
3. Lu, S.C. (1999). Regulation of hepatic glutathione synthesis: current concepts and controversies. *FASEB J.* 13:1169–1183.
4. Sies, H., and Packer, L. (2005). Glutathione transferases and gamma-glutamyl transpeptidases. *Methods Enzymol.* 401:408–501.
5. Wang, W., and Ballatori, N. (1998). Endogenous glutathione conjugates: occurrence and biological functions. *Pharmacol. Rev.* 50:335–356.

2.2 ASCORBATE

HAN ASARD

Department of Biology, University of Antwerp, Antwerp, Belgium

Ascorbate (vitamin C) is well known for its radical-scavenging capacity and is the most effective water-soluble antioxidant in human plasma. It is the terminal small molecule antioxidant in many biological systems and probably the most abundant free radical scavenger in many cell types.

In addition to its role as an antioxidant, the moderately positive standard redox potential of the ascorbate/monodehydroascorbate couple makes ascorbate an excellent one-electron donor to a large variety of enzymes, in particular, oxygenases and hydroxylases. Its role as a cofactor for the enzyme prolyl, hydroxylase, lies at the basis of the discovery and isolation of ascorbate in 1932 by Albert Szent-Györgyi and Charles King as the “anti-scorbutic (scurvy preventing) factor.” Soon thereafter, its chemical nature as a glucose derivative was elucidated by Walter Haworth. Major advances in understanding the importance of ascorbate in human health were made by Linus Pauling in the 1960s and 1970s. His work continues to fuel debates on the optimal daily intake of vitamin C for humans.

2.2.A Ascorbate Chemistry

Ascorbic acid (*L-threo*-hex-2-enono-1,4-lactone) is a diacid ($pK_1 = 4.2$ and $pK_2 = 11.8$), which exists almost exclusively as the monoanion at physiological pH values. The conjugated structure of the five-membered lactone ring (Fig. 2.9), containing an ene-diol group, allows stabilization of the free radical one-electron oxidation product, monodehydroascorbate, by delocalization of the unpaired electron.

Monodehydroascorbate is sufficiently stable and can be detected by electron paramagnetic resonance (EPR) in many biological samples. Increased monodehydroascorbate concentrations are considered to be a reliable marker for oxidative stress conditions. Oxidation of monodehydroascorbate yields dehydroascorbate, which is unstable at physiological pH. Hydrolysis of the O—C₁ ester bond in the lactone ring results in the generation of 2,3-diketo-L-gulonic acid and the irreversible loss of cellular ascorbate. However, the dominant mode of decay of ascorbate is through disproportionation of monodehydroascorbate (Fig. 2.9).

Ascorbate is a chain-breaking antioxidant that reacts readily with reactive species such as hydroxyl (OH[•]), alkoxy (RO[•]), and peroxy (ROO[•]) radicals, but also with tocopheroxyl (TO[•]) and urate (UH^{•-}) radicals. An important reactivity of ascorbate is its ability to reduce the tocopheroxyl radical to tocopherol. Tocopherols (vitamin E, see Section 2.3) are lipid-soluble antioxidants essential for preventing the propagative peroxidation of membrane lipids under oxidative stress conditions. A key to the regeneration of lipophilic tocopherols by hydrophilic ascorbate is the exposure of the phenolic group of tocopherol to the lipid–water interface. Consistent with the antioxidant properties of ascorbate, the standard redox potential of 0.28 V (pH 7.0)

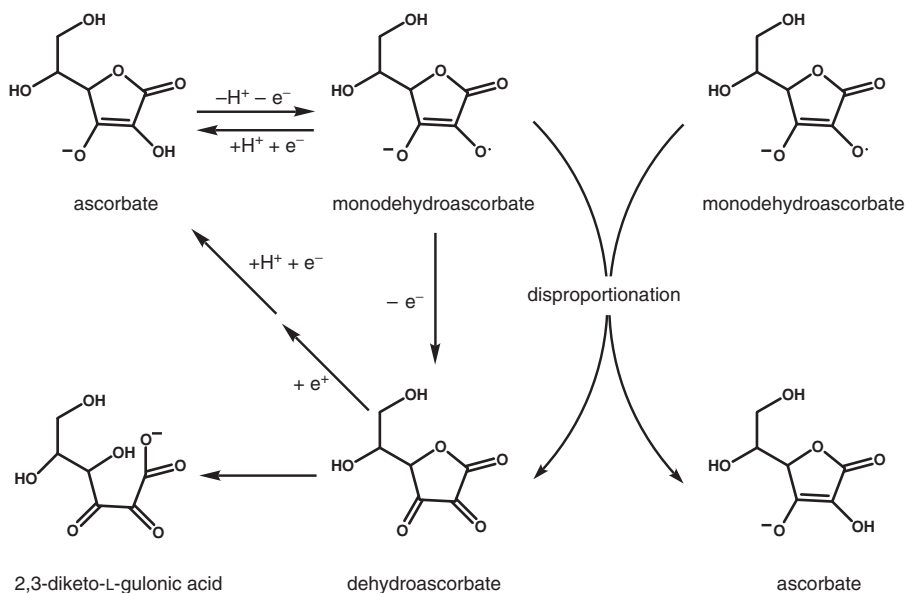


Figure 2.9. Ascorbate chemistry. Oxidation/reduction, protonation/deprotonation, and disproportionation reactions of ascorbate.

for the ascorbate/monodehydroascorbate couple is more negative than that of most common free radical redox couples.

Paradoxically, ascorbate can also function as a pro-oxidant by reducing transition metals such as Cu^{2+} and Fe^{3+} . The ascorbate mono- and dianions are readily oxidized by trace amounts of metals commonly present in buffers used in biochemical research. Ferrous iron formed by the oxidation of ascorbate can then catalyze the generation of the hydroxyl radical (OH^\cdot) from H_2O_2 in Fenton-like reactions. Because the diacid form of ascorbate is much less reactive, ascorbate is often extracted from biological samples and foodstuffs in acidic media and in the presence of metal chelators, and it is recommended to make stock solutions of ascorbate in the acid form.

2.2.B Ascorbate Biosynthesis

Although the immediate precursor for ascorbate biosynthesis is invariably an aldono-1,4-lactone, the biosynthetic pathway varies (Fig. 2.10). In mammals, the aldono-lactone is L-gulono-1,4-lactone, which is derived from UDP-glucose. L-Gulono-1,4-lactone is converted to 2-keto-L-gulono-1,4-lactone by the endoplasmic reticulum-associated L-gulono-1,4-lactone oxidase (Fig. 2.10). The keto form spontaneously converts to ascorbate, generating H_2O_2 as a by-product. Ascorbate biosynthesis occurs in the endoplasmic reticulum of the liver of most mammals and in the kidney of egg-laying mammals, reptiles, and amphibians. Loss of the lactone oxidase activity in humans and other primates, teleost fish, guinea pigs, fruit bats,

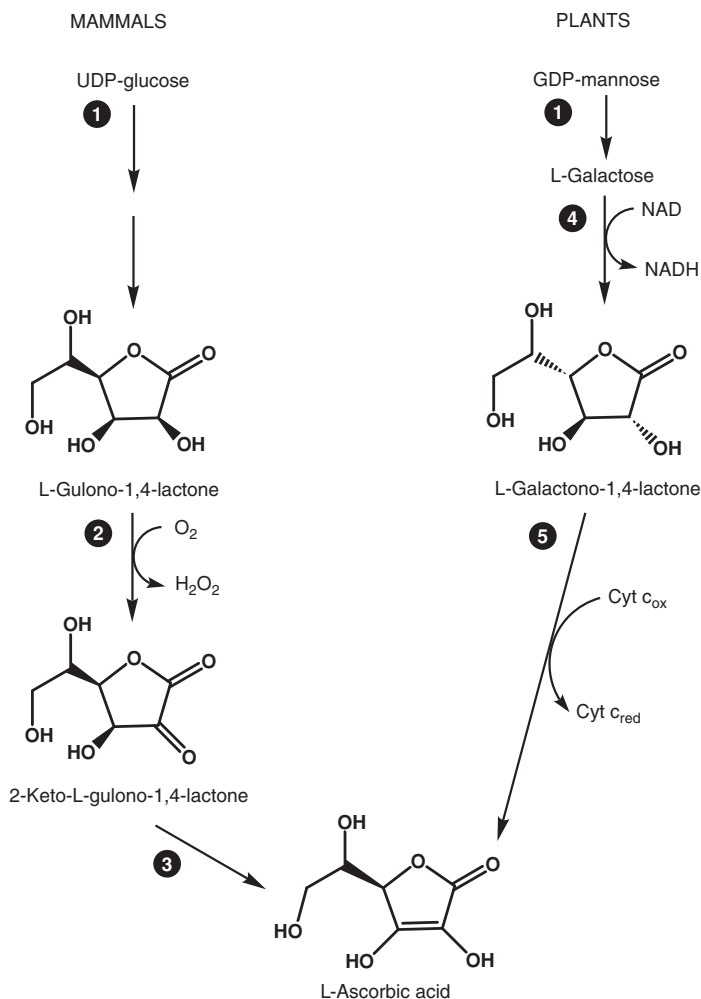


Figure 2.10. Principal ascorbate biosynthetic pathways in mammals and plants. ① Multiple conversions; ② L-gulono-1,4-lactone oxidase; ③ spontaneous reaction; ④ L-galactose dehydrogenase; and ⑤ L-galactono-1,4-lactone dehydrogenase.

and a few other groups has made them dependent on dietary vitamin C intake. The inability to synthesize ascorbate in these species may have been advantageous, in that it reduces the levels of H_2O_2 in the liver.

In plants, ascorbate is synthesized from the relatively rare sugar L-galactose via L-galactono-1,4-lactone in the so-called Smirnoff–Wheeler–Running pathway (Fig. 2.10). This two-step oxidation is catalyzed by the NAD^+ -dependent L-galactose dehydrogenase and L-galactono-1,4-lactone dehydrogenase. The latter enzyme uses

cytochrome *c* as an electron acceptor and is localized in the mitochondrial inner membrane. L-Galactose is derived from GDP-L-galactose, which itself probably originates through epimerization from GDP-mannose. A point mutation in one of the enzymes synthesizing GDP-mannose results in plants with very low ascorbate levels (*vtc1* mutants). L-Galactono-1,4-lactone can also be derived from UDP-D-galactose, and it is therefore possible that other minor biosynthetic pathways occur in plants. Obviously, engineering plants to produce higher levels of ascorbate is an attractive biotechnological target and various approaches are actively being pursued to achieve this goal. Plants respond to various oxidative stress conditions by increased levels of ascorbate.

Apart from animals and plants, the presence of ascorbate and ascorbate analogues has been documented in several other eukaryotic organisms. Most fungi synthesize the ascorbate analogue, D-erythroascorbate, and in some fungi, 6-deoxyascorbate or D-araboascorbate is found. Ascorbate, however, appears to be absent from prokaryotes.

2.2.C Ascorbate Recycling

Because ascorbate plays a pivotal role in defense against reactive free radicals, there is a redundancy in mechanisms for regenerating it from monodehydroascorbate and dehydroascorbate. Single-electron reduction of monodehydroascorbate is primarily mediated by cytochrome *b*₅-dependent monodehydroascorbate reductase, and by the thioredoxin reductase system using NADPH as the ultimate electron donor. Mammalian NADH-dependent monodehydroascorbate reductase has a high affinity for monodehydroascorbate ($K_m \sim 4 \mu\text{M}$) and is localized in the mitochondrial outer membrane and in microsomal membranes. A mutation in this enzyme is linked to type II methemoglobinemia. An alternative mechanism for reduction of monodehydroascorbate to ascorbate exists in chromaffin cells from the adrenal medulla. In these cells, a transmembrane electron shuttle provides electrons from cytosolic ascorbate to monodehydroascorbate inside chromaffin granules supporting ascorbate-dependent dopamine and norepinephrine hydroxylation. The protein responsible for this reaction is a di-heme *b*-type cytochrome (cytochrome *b*₅₆₁). Monodehydroascorbate reduction has also been detected at the surface of erythrocyte membranes, where it probably helps to maintain blood plasma ascorbate levels. New evidence suggests that a similar cytochrome *b*₅₆₁ may be involved in this reaction.

Dehydroascorbate is rapidly reduced to ascorbate in most mammalian cells. Direct reduction of dehydroascorbate by two molecules of GSH is thermodynamically feasible and has been demonstrated in cell-free systems. In addition, several GSH- and NADPH-dependent dehydroascorbate reductases have been identified in mammalian cells, including glutaredoxin, thioredoxin reductase, and protein disulfide isomerase.

Plants also contain GSH-dependent dehydroascorbate reductases and proteins with dehydroascorbate reductase activity, such as the Kunitz-trypsin inhibitor. However, the major sources of electrons for the reduction of monodehydroascorbate in plants are GSH in the so-called ascorbate–GSH pathway (or Halliwell–Foyer–Asada

pathway) and water. In the photosynthetic electron transport chain, electrons are derived from the photooxidation of water by photosystem II and are transferred to monodehydroascorbate by ferredoxin. The ascorbate–GSH cycle involves an NAD(P)H-dependent monodehydroascorbate reductase and a GSH-dependent dehydroascorbate reductase. GSH is recycled by an NAD(P)H-dependent glutathione reductase. This system is particularly well studied in the chloroplast but is also operational in other plant cell compartments such as mitochondria and peroxisomes. Increased activities of the ascorbate recycling enzymes under oxidative stress conditions suggest an important role for these reactions in regulating cellular ascorbate homeostasis.

2.2.D Ascorbate Transport

Because of its size and charge, ascorbate does not readily permeate lipid bilayers and needs to be transported from its location of synthesis at the mitochondria and endoplasmic reticulum to other cell compartments. Vitamin C redistribution in animal and plant organs is accomplished by facilitated diffusion and active transport mechanisms for ascorbate and dehydroascorbate.

The structural similarity between glucose and dehydroascorbate is sufficient for the mammalian GLUT-type facilitative glucose transporters to translocate dehydroascorbate but not ascorbate. The affinities and transport capacities of GLUT1 and GLUT3 for glucose and dehydroascorbate are similar. Hence, dehydroascorbate uptake competes effectively with glucose transport and is sensitive to regulation by insulin. In addition, glucose-insensitive dehydroascorbate uptake pathways have been demonstrated in various cell types but the transporters have not yet been identified. Less is known about dehydroascorbate transport in plant cells. Dehydroascorbate uptake has been demonstrated in tobacco cell cultures, and facilitated dehydroascorbate and glucose transport occurs in plant-derived mitochondria. Transport of ascorbate across plant plasma membranes and chloroplasts probably occurs through a glucose-insensitive system.

Ascorbate uptake in animal cells utilizes the large electrochemical sodium gradient across the cell membrane. This transport is mediated by the recently cloned sodium-dependent vitamin C transporters, SVCT1 and SVCT2. SVCT transporters are highly specific for L-ascorbate and are widespread in animal organs. Transport of ascorbate by SVCT is electrogenic and therefore very sensitive to changes in the membrane potential. For obvious reasons, there is significant interest in understanding the regulation of SVCT expression, distribution, and post-translational modifications. For example, decreased levels of SVCT expression are implied in the reduced capacity of the elderly to absorb ascorbate from the diet.

2.2.E Importance of Ascorbate in Stress and Disease

Its antioxidant capacities have raised a great deal of interest in the role of ascorbate in human health and disease. For example, oxidative damage to DNA is believed to be an

important cause underlying cancers, and increased levels of ascorbate in cell cultures have proved effective in reducing free radical-induced mutation rates. However, a large number of the physiological effects of ascorbate are actually mediated by its role as a cofactor for a variety of redox enzymes. The role of ascorbate in preventing scurvy is mainly based on its function as a cosubstrate for 2-oxoglutarate-dependent dioxygenases, which incorporate oxygen into organic substrates. Dietary deficiency of ascorbate limits hydroxylation of prolyl residues in collagen by the dioxygenase, prolyl hydroxylase, causing collagen instability and the typical scurvy symptoms. Proline hydroxylation is also essential in the post-translational modification of several other proteins such as the transcription factor hypoxia-inducible factor 1 α , responsible for oxygen sensing in mammals. Hypoxia-inducible factor 1 α controls the expression of a large number of proteins, some of which are of great importance in angiogenesis, ischemia, and cancer. This illustrates that the role of ascorbate in preventing disease clearly exceeds its function as a free radical scavenger.

SELECTED REFERENCES

1. Bánhegyi, G., Braun, L., Csala, M., Puskás, F., and Mandl, J. (1997). Ascorbate metabolism and its regulation in animals. *Free Rad. Biol. Med.* 23:793–803.
2. Smirnoff, N., and Wheeler, G.L. (2000). Ascorbic acid in plants: biosynthesis and function. *Crit. Rev. Plant Sci.* 19:267–290.
3. Wilson, J.X. (2005). Regulation of vitamin C transport. *Ann. Rev. Nutrition* 25:105–125.

2.3 OTHER ANTIOXIDANTS

JULIE M. STONE and MARK A. WILSON

Redox Biology Center and Department of Biochemistry, University of Nebraska, Lincoln, Nebraska

Antioxidant molecules can be divided into different nonmutually exclusive categories based on their functions (enzymatic or nonenzymatic), their physical properties (water-soluble or lipid-soluble), and, for humans, their sources (endogenous or exogenous). Some antioxidant molecules are enzymes (Chapter 3) or serve as cofactors for enzymes (Section 2.4). The major nonenzymatic cellular redox buffer systems rely on the water-soluble antioxidants GSH (Section 2.1) and ascorbic acid (Section 2.2). However, numerous less abundant antioxidants also serve important functions in redox homeostasis and are important for cellular function and disease prevention.

In this section, we focus on relatively common small molecule antioxidants, including some produced endogenously in animals and others that are acquired exogenously through diet. Vitamin E (tocopherols and tocotrienols) and vitamin A (or provitamin A

β -carotene and related carotenoids) are major lipid-soluble plant-derived antioxidants essential for normal growth, development, and reproduction and are described in some detail. Other antioxidant molecules are discussed only briefly. These antioxidant molecules function not only in quenching chain reactions, scavenging ROS, and preventing lipid peroxidation, but also influence cellular functions by binding to specific receptors to initiate signal transduction cascades, inhibiting or activating enzymes, and regulating gene expression.

2.3.A Lipid-Soluble Antioxidants

Some of the most abundant small molecule antioxidants, particularly GSH and ascorbic acid, are water soluble and perform their ROS scavenging activity primarily in the aqueous environment of the cytosol and within the various compartments and organelles of the cell. However, ROS can also damage lipids, particularly via free radical-mediated reactions that result in lipid peroxidation. Uncontrolled lipid peroxidation causes widespread disruptions in the cell by compromising membrane integrity and function and can lead to cell death. The threat of ROS damage to lipids requires that the cell has defense mechanisms specific to the hydrophobic environment of the cell and organelle membranes. A major part of this response is mediated by lipid-soluble small molecule antioxidants such as vitamin E and β -carotene, which quench free radicals and prevent lipid peroxidation chain reactions. We discuss the properties of some of the most important antioxidants in this section.

2.3.A1 α -Tocopherol. α -Tocopherol is the most biologically active of the eight forms of vitamin E. The name derives from the Greek *tokos*, meaning “offspring,” and *pherein*, meaning “to carry,” as vitamin E was first identified as being essential for reproductive function in rats. The other forms of vitamin E (β -, γ -, and δ -tocopherol and α -, β -, γ -, and δ -tocotrienols) are closely related in chemical structure to α -tocopherol, and all share the common two-ring (chromanol) core and the 16 carbon aliphatic side chain (Fig. 2.11). These various compounds differ from each other in the identity of the substituents on the chromanol core, and the tocotrienols are further distinguished from the tocopherols by the presence of three double bonds in their isoprenoid side chain. Adding to this complexity is the fact that α -tocopherol also contains three chiral centers, making a total of eight stereoisomers, although the most abundant naturally occurring form of the compound is the *R,R,R* form. All of the tocopherols (as this class of compounds is called) are closely related and share vitamin E activity; however, it is important to emphasize that α -tocopherol is not strictly synonymous with vitamin E.

α -Tocopherol is a potent lipid-soluble antioxidant that is synthesized exclusively by plants. The lipid solubility of α -tocopherol is a consequence of the hydrophobic phytyl side chain, which anchors the antioxidant chromanol ring to the membrane. The antioxidant function of α -tocopherol is a consequence of its ability to quench free radicals by becoming a stable radical itself, which is a common mechanism among many radical-scavenging antioxidants. α -Tocopherol forms a stable radical species

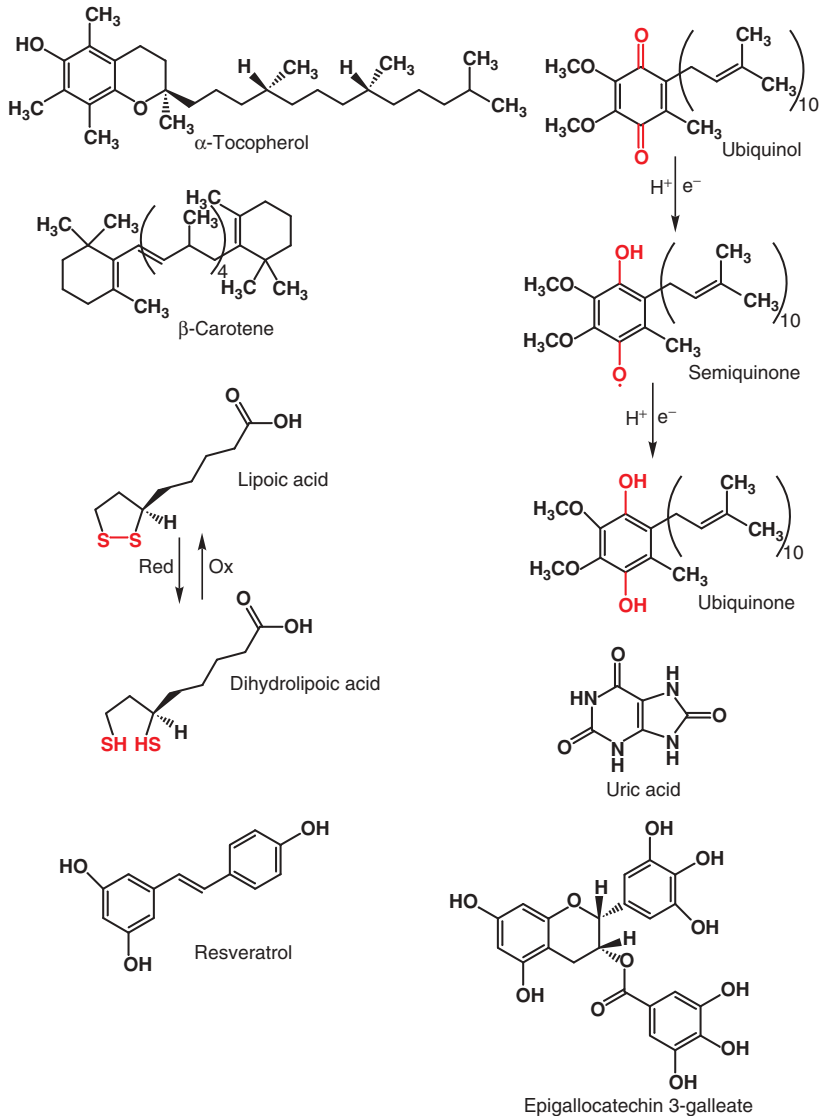


Figure 2.11. Structures for common small molecule antioxidants.

(the tocopheroxyl radical) by delocalizing the unpaired electron that is generated by hydrogen atom abstraction from the exocyclic phenolic oxygen through resonance with the aromatic moiety of the chromanol ring. By sacrificially donating the equivalent of a hydrogen atom to a reactive radical, the tocopheroxyl radical effectively sequesters the free electron in a less reactive (and therefore less damaging) form on its own chromanol moiety. The tocopheroxyl radical can be reduced to regenerate

α -tocopherol by other antioxidants, including ubiquinol, ascorbic acid, and, indirectly, dihydrolipoic acid.

2.3.A2 Carotenoids and Vitamin A. Carotenoids are the most abundant pigmented plant-derived compounds produced in photosynthetic organisms with more than 600 carotenoid compounds identified. These compounds, which impart the red and yellow colors in fruits and vegetables, are also the source of certain colors in birds, insects, and marine invertebrates. Carotenoids are isoprenoids consisting primarily of eight joined isoprene units with a rigid backbone due to the presence of 3 to 15 conjugated double bonds (Fig. 2.11). Modifications include cyclization of the carbon skeleton at one or both ends. The absorption spectrum is determined by the chromophore length, affecting the color of the molecules. A systematic nomenclature exists, but the trivial names based on their original sources are still most commonly used. For example, β -carotene was isolated from carrots and is probably the most studied carotenoid (Fig. 2.11), because of its ability to be cleaved to form retinal (vitamin A) in the animal intestine. In the human intestine, cleavage is catalyzed by the recently cloned β -carotene 15,15'-cleavage enzyme using a monooxygenase-type reaction to produce retinal. In plants, carotenoids are essential; they directly participate in photosynthesis and reactions to limit the vast amounts of ROS produced in chloroplasts. Oxygen-containing carotenoids (the xanthophylls) are integral components of photosystem II and the light-harvesting complex. Zeaxanthin is responsible for absorption of excess excitation energy and conversion to heat in a process termed thermal energy dissipation preventing formation of potentially harmful ROS. Several carotenoids also participate in protection against photoinduced damage. The relative efficiency of individual species at preventing lipid peroxidation chain reactions has been tested in liposomes and has been found to be in the order: lycopene > α -tocopherol > β -carotene > lutein. Carotenoid radicals can be reduced by both α -tocopherol and ascorbic acid, which might account for the observed synergistic interactions between these three important vitamins (A, C, and E).

2.3.A3 α -Lipoic Acid/Dihydrolipoic Acid. α -Lipoic acid is a sulfur-containing antioxidant and an essential cofactor in both the pyruvate dehydrogenase and the α -ketoglutarate dehydrogenase multienzyme complexes. α -Lipoic acid is not a vitamin, as it is synthesized in the mitochondrion, although the biochemistry of its synthesis is still incompletely understood. The general chemical architecture of α -lipoic acid is similar to many lipid-soluble antioxidants in that it contains a redox-active moiety linked to a hydrocarbon side chain that imparts lipid solubility to the molecule. Unlike most other lipid-soluble antioxidants, however, α -lipoic acid is amphipathic (soluble in both aqueous and nonaqueous environments) due to the hydrophilic carboxylic acid group at the end of its hydrocarbon side chain. α -Lipoic acid has a single chiral center, and the naturally occurring form is the *R*-enantiomer.

α -Lipoic acid contains a disulfide linkage that forms a five-membered ring, and this disulfide can be reduced to a dithiol with concomitant ring opening to form dihydrolipoic acid (Fig. 2.11). Unlike many other antioxidants, both the oxidized

(α -lipoic acid) and the reduced (dihydrolipoic acid) forms of the molecule can serve as antioxidants, albeit with different specificities for particular ROS. In general, dihydrolipoic acid is considered the superior antioxidant, because it can participate in thiol-disulfide oxidation–reduction reactions (two electron oxidation/reduction) to form α -lipoic acid. In addition, dihydrolipoic acid plays a key role in maintaining cellular redox homeostasis by reducing dehydroascorbic acid to generate lipoic acid and ascorbate.

2.3.A4 Ubiquinol/Ubiquinone. Ubiquinol and its oxidized form, ubiquinone, are so-named because they are ubiquitous in the cells of aerobic organisms. One of the major roles of the ubiquinol/ubiquinone redox pair is to shuttle electrons in the electron transport chain between mitochondrial complexes II and III during oxidative phosphorylation. In this capacity, ubiquinone accepts two reducing equivalents (hydrogen atoms) from complex II and is reduced to ubiquinol. Ubiquinol then diffuses through the lipid membrane to complex III, where it is oxidized back to ubiquinone, thus passing reducing equivalents down the electron transport chain. Consistent with the critical role of ubiquinol/ubiquinone in oxidative phosphorylation, approximately 80% of ubiquinol/ubiquinone in the cell is found in the mitochondria. Importantly, ubiquinone can also accept one electron to form a stable radical anion semiquinone. As with α -tocopherol, the formation of a stable radical is a common mechanism by which antioxidants quench reactive free radicals; thus, ubiquinone can act as a lipid-soluble antioxidant.

Like the other lipid-soluble antioxidants that we have discussed, ubiquinol contains a redox-active group (benzoquinol) attached to a hydrophobic side chain (Fig. 2.11). This hydrocarbon side chain is composed of multiple five-carbon isoprene units, and the most common form of ubiquinol in humans contains a side chain with ten isoprene units. Hence, the dominant human form of ubiquinol is sometimes called coenzyme Q₁₀, where the subscript indicates the number of isoprene units in the side chain. This long isoprenyl side chain is highly hydrophobic and anchors ubiquinol to the membrane. Unlike other more amphipathic lipid-soluble antioxidants like α -lipoic acid or α -tocopherol, the strong hydrophobicity of ubiquinol keeps the molecule completely confined in the lipid bilayer.

2.3.B Water-Soluble Antioxidants

The prevalence of so many lipid-soluble antioxidant molecules (described in Section 2.3.A) point to the importance of protecting cellular and organellar membranes from lipid peroxidation. The water-soluble antioxidant enzymes and the major redox buffers, ascorbic acid and GSH, are considered to be the primary small molecule antioxidants used in the aqueous environments of the cell. However, there are lesser known water-soluble small molecules that appear to be important as well in protecting against oxidative stress and disease, which are described in this section.

2.3.B1 Flavonoids. Plants produce a wide spectrum of secondary metabolites referred to as polyphenols. Polyphenolics are subdivided into the nonflavonoids (e.g.,

hydroxybenzoic acids, hydroxycinnamic acids, and stilbenes) and the flavonoids (flavonols, flavanols, isoflavones, and anthocyanins). The plant-derived flavonoids are composed of more than 4000 different species that have two aromatic benzene rings linked through three carbons that can form an oxygenated heterocycle. Quercetin (Fig. 2.11) is representative of the most abundant flavonoid class, the flavonols. Isoflavones (phytoestrogens), found in high abundance in legumes, are also under intense scrutiny for their potential health benefits. The antioxidant activities of flavonoids are attributed to chelation of redox-active metals to prevent peroxy radical and lipid peroxidation, scavenging of hydroxyl and peroxy radicals, and quenching of superoxide radicals and singlet oxygen.

BOX 2.1 GREEN TEA AND ANTIOXIDANT POLYPHENOLS

Green tea has been a staple beverage in Asian diets for millennia. Chinese legend claims that green tea was discovered in 2737 BC by the Emperor Shen Nung, who had the sensible habit of boiling water before he drank it. One day some leaves from a nearby tea plant fell into the emperor's boiling water, thus spontaneously brewing the first cup of green tea. The emperor was so favorably impressed with the resulting drink that he proclaimed it to have been sent from Heaven.

Though the veracity of this legend is questionable, Emperor Shen Nung would be very pleased with the subsequent success of his beverage. Tea is the second most consumed beverage in the world, the first being water. Tea was used as a currency in China, its consumption has been elevated to the level of an elaborate ritualistic ceremony in Japan, and its trade helped both finance the expansion of the British Empire and to ignite British colonial unrest that culminated in the American Revolution. Many varieties of tea exist, but they are all derived from leaves of the same plant, *Camellia sinensis*. The various types of tea differ in how the tea leaves are treated after being harvested. "Black" teas are made from processed and oxidized leaves, while "green" tea is made from freshly dried, unoxidized leaves. While both have health benefits, green tea is generally thought to have the superior effect on health, particularly in the prevention of cancer.

Researchers have identified a class of antioxidants called polyphenols that appear to be responsible for much of the health benefits of green tea. The most active of these polyphenols in green tea is (–)-epigallocatechin 3-gallate (EGCG, Fig. 2.11), although there are several other related compounds in green tea that have similar structures and some biological activity. The specific mode(s) of action of EGCG are still being investigated, but a variety of proteins that bind EGCG have been identified and include the 90 kDa heat shock protein (Hsp90), dihydrofolate reductase, DNA methyltransferases, the laminin receptor, epidermal growth factor receptor, and telomerase. This varied

and growing list of protein targets of EGCG testifies to the complex biological activity of this natural product in multifactorial diseases such as cancer, neurodegeneration, and heart disease.

BOX 2.2 THE FRENCH PARADOX AND RESVERATROL/SIRTUINS

Which diet should we follow to live long and healthy lives — Mediterranean, French, Japanese, low-fat, low-carb, or calorie-restricted? How do cultural dietary traditions impact an individual's longevity and incidence of chronic and degenerative disease? The “Free Radical Theory of Aging” purports that a healthy lifestyle and antioxidant consumption can reduce the consequences of aging. Plants produce a wide spectrum of secondary metabolites important for their own health that also function as antioxidants in humans who ingest them.

Are the foods we eat (and the antioxidants they contain) key to maintaining health and warding off disease? Perhaps. A possible molecular basis for the “French Paradox”—the low incidence of heart disease in the high-fat-diet-eating French—has surfaced only in the past few years: resveratrol (*trans*-3,5,4'-trihydroxystilbene, Fig. 2.11)—a nonflavonoid polyphenolic antioxidant produced in grape skins, soy, and peanuts to fight against plant disease and a component of an ancient oriental medicine (Ko-jo-kon) used to treat blood vessel, heart, and liver diseases—may be the key molecule. Resveratrol has received a great deal of attention in both the scientific and popular literature and has been touted to protect against a wide range of age-related diseases including Alzheimer's and heart disease. But how? The answer might lie in its ability to affect gene expression. Caloric restriction (and increased longevity) was linked to extra copies of sirtuin genes in both yeast and the nematode worm *Caenorhabditis elegans*. Sirtuins are NAD⁺-dependent protein deacetylases that can control gene expression and stabilize repetitive DNA sequences and are now implicated in aging, cell survival, and apoptosis. A screen for small molecule compounds that increase the catalytic rate of sirtuins revealed several effective plant polyphenols, including quercetin and resveratrol.

How does resveratrol solve the French Paradox? Resveratrol is abundant in grape skins and effectively extracted in red wine processing. So, washing down rich French dishes swimming in butter-laden sauces with a glass of red wine might just be the secret to longevity. Ironically, a diet high in fat may actually enhance the uptake of some important lipid-soluble antioxidants too. Discovery of “new” plant-derived antioxidants is transpiring at a staggering pace, and more “magic bullets” may be on the horizon!

2.3.B2 Uric Acid. Uric acid is a modestly water-soluble antioxidant with the ability to neutralize a broad spectrum of ROS, particularly singlet oxygen and free radicals. Uric acid is an end product of purine catabolism and is one of the most abundant circulating antioxidants, with a blood plasma concentration in humans of about 300 μM . Uric acid can accept a single electron to form a stable radical, and thereby neutralize a variety of ROS species.

Humans, apes, and certain New World monkeys have significantly higher serum uric acid levels than other primates due to an evolutionarily recent mutation that functionally inactivates urate oxidase. Urate oxidase converts uric acid to allantoin, which is more water soluble and a much poorer antioxidant than uric acid. It has been speculated that the resulting increase in serum uric acid concentrations in the hominids may contribute to their longer life span and lower age-specific cancer rates than other mammals.

2.3.C Antioxidants and Human Health

Antioxidants have diverse biochemical roles and therefore are important in human health. Vitamin E is an essential nutrient with deficiencies in humans leading to a variety of diseases including mild hemolytic anemia and spinocerebellar diseases, which usually manifest as ataxia (poorly coordinated movement) and neuropathy (nerve damage or conduction problems). Vitamin E deficiency is rare, however, as most adults receive their recommended daily allowance of vitamin E in their diet, and the majority of cases of vitamin E deficiency are diagnosed in children with congenital defects in fat absorption.

In both plants and animals, carotenoid deficiency is more detrimental than tocopherol deficiency. Vitamin A deficiency leads to various eye diseases, including xerophthalmia (childhood blindness), age-related cataract formation, and macular degeneration. Two carotenoids, lutein and zeaxanthin, accumulate in the macula of the eye, where they are thought to scavenge free radicals and protect against light-induced damage. Vitamin A deficiency remains a problem in developing countries, where humanitarian efforts to genetically engineer enhanced carotenoid content in several crop plants have met with mixed success. The major challenges that need to be addressed with crops engineered for enhanced carotenoid content are consumer distaste for “yellow” rice, the fact that retinal-forming enzymes are repressed in the guts of malnourished individuals, and the paucity of fat (to aid absorption) in their diets.

α -Lipoic acid/dihydrolipoic acid has a complex role in human health, as they are both essential enzyme cofactors and potent antioxidants. The essential role of α -lipoic acid in the pyruvate dehydrogenase and α -ketoglutarate dehydrogenase multienzyme complexes makes it vital for energy metabolism, and it is no coincidence that α -lipoic acid is synthesized in mitochondria, where these multienzyme complexes are located. The best-characterized benefit from α -lipoic acid supplements is ameliorating some of the neurological complications of diabetes, for which it is approved in Germany.

Ubiquinol/ubiquinone (coenzyme Q₁₀) can be synthesized by humans and is therefore not a vitamin by definition. Nevertheless, coenzyme Q₁₀ has enjoyed a long period of popularity as a dietary supplement. Many exaggerated claims of the sweeping

preventative and regenerative powers of coenzyme Q₁₀ should be regarded with suspicion, and there is comparatively little research that has been done to determine if coenzyme Q₁₀ supplementation has clinical value. One exception is that coenzyme Q₁₀ supplementation is generally regarded as beneficial for the treatment of congestive heart failure.

Flavonoids are reported to have antioxidant, anti-inflammatory, and estrogen hormone-like properties. Certain flavonoids, like quercetin, may protect against atherosclerosis or cardiovascular disease. Isoflavones, such as obtained from soy, are also known as phytoestrogens, because they can bind to the estrogen receptor and mimic the effects of endogenous estrogen hormones.

Uric acid is produced by the body in significant quantities, and its modest water solubility can cause serious health problems. Excess uric acid can crystallize in the body, especially in the synovial fluid in the joints of the lower extremities, causing a painful inflammatory arthritic condition known as gout. In addition, the poor water solubility of uric acid can cause problems in the kidney and urinary tract by forming kidney stones. Uric acid kidney stones represent only about 10% of the total cases of kidney stones, however, which are more commonly composed of insoluble calcium oxalate or phosphate crystals.

SELECTED REFERENCES

1. Carotenoids and Dietary Lipids (2005). Special issue *Biochimica et Biophysica—Molecular Basis of Disease* 1740(2).
2. Dellapenna, D., and Pogson, B.J. (2006). Vitamin synthesis in plants: tocopherols and carotenoids. *Annu. Rev. Plant Biol.* 57:711–738.

2.4 REDOX COENZYMES

RUMA BANERJEE

Department of Biological Chemistry, University of Michigan, Ann Arbor, Michigan

DONALD F. BECKER

Redox Biology Center and Department of Biochemistry, University of Nebraska, Lincoln, Nebraska

2.4.A Flavin

Flavin mononucleotide (FMN) and flavin adenine dinucleotide (FAD) participate in a variety of enzyme-catalyzed reactions as noncovalently or covalently bound redox cofactors. A distinguishing property of flavins is their ability to couple one-electron and two-electron transfer reactions between substrates and different electron carriers. Thus, flavins equilibrate between quinone (oxidized), semiquinone (one-electron reduced), and hydroquinone (two-electron reduced) species with reversible electron transfer occurring across the N(5) and N(1) atoms of the isoalloxazine ring of the flavin (Fig. 2.12). The redox potential of free FAD is -0.219 V

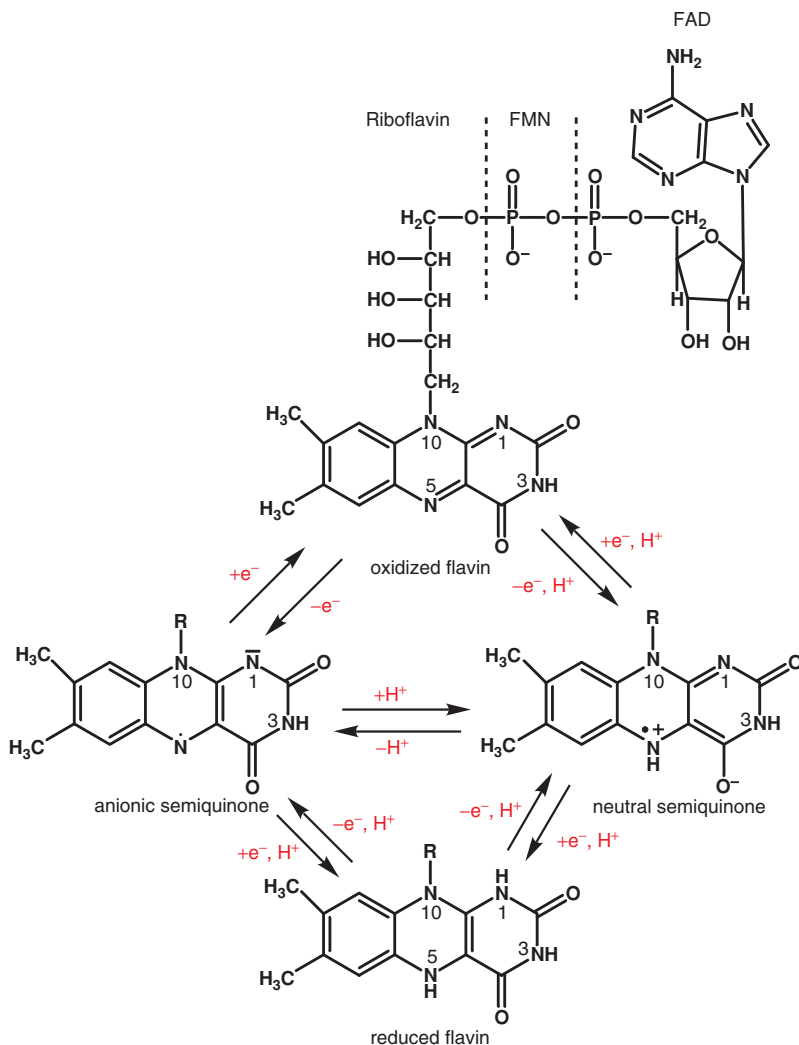


Figure 2.12. Flavin redox states.

(pH 7.0) in solution while enzyme-bound flavin has a redox potential range generally of +0.1 to -0.4 V (versus the normal hydrogen electrode), which contributes to the involvement of flavoenzymes in a remarkable variety of reactions such as dehydrogenation, electron transfer, dehalogenation, hydroxylation, luminescence, DNA repair, and disulfide reduction. Reactions catalyzed by flavoenzymes can be divided into oxidative and reductive half-reactions as shown in Fig. 2.13 for medium chain acyl-CoA dehydrogenase, which catalyzes the first step in fatty acid oxidation.

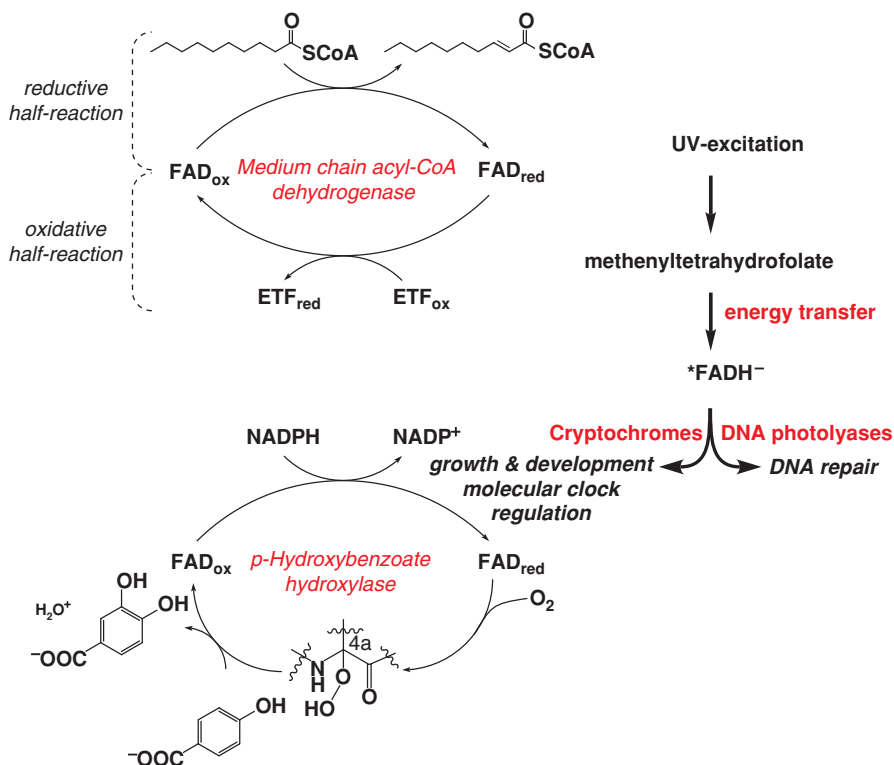


Figure 2.13. Flavin coenzyme-catalyzed reactions. Flavoenzymes shown are medium chain acyl-CoA dehydrogenase, *p*-hydroxybenzoate hydroxylase, and the cryptochrome/photolyase family.

The reductive half-reaction describes the reduction of the flavin by an electron donor such as the substrate octanoyl-CoA for medium chain acyl-CoA dehydrogenase. The oxidative half-reaction involves the oxidation of the reduced flavin by an electron acceptor such as molecular oxygen or, in the case of medium chain acyl-CoA dehydrogenase, the electron transfer flavoprotein.

The reactivity of enzyme-bound reduced flavin coenzyme with molecular oxygen is significantly influenced by the active site environment and substrate/product complexation. Reaction of reduced flavin with molecular oxygen proceeds initially through a one-electron reduction of oxygen to form a flavin semiquinone and O₂^{•-} pair. Subsequent events then lead to the formation of a flavin C(4a)-peroxide or H₂O₂/O₂^{•-} products. Monooxygenases are a group of flavoenzymes that form a C(4a)-peroxide intermediate from which one oxygen atom is inserted into the substrate while the other oxygen atom is reduced to water. A well characterized example of this class

of flavoenzymes is *p*-hydroxybenzoate hydroxylase, which utilizes NADPH as an electron donor to generate reduced flavin for subsequent hydroxylation of aromatic substrates (Fig. 2.13). Flavoenzymes that react with molecular oxygen during catalytic turnover and generate H_2O_2 are called oxidases such as D-amino acid oxidase, which directs the oxidative deamination of D-amino acids to α -keto acids and ammonia. Electron transferases such as flavodoxin react with molecular oxygen in the absence of a physiological electron acceptor to form $O_2^{\cdot-}$. Dehydrogenases also generate $O_2^{\cdot-}$ but the reactivity is considerably lower than other classes of flavoenzymes, most likely to help ensure the efficient transfer of electrons to the correct physiological acceptor such as the electron transfer flavoprotein for medium chain acyl-CoA dehydrogenase. The ability of reduced flavins to perform the one-electron reduction of molecular oxygen to $O_2^{\cdot-}$ implies that flavins generally contribute to intracellular oxidative stress.

In addition to the diverse catalytic power of flavoenzymes, several flavoenzymes are involved in regulatory and signaling pathways. An example is the programmed cell death pathway or apoptosis in which the apoptotic inducing factor is involved. The apoptotic inducing factor is a mitochondrial flavoenzyme that exhibits NADH oxidase and DNA binding activities. When localized in the inner mitochondrial membrane, the NADH oxidase function of the apoptotic inducing factor appears to enhance oxidative phosphorylation, but at the appropriate signal, the apoptotic inducing factor is trafficked to the cell nucleus, where it binds chromatin, leading to its condensation, a morphological hallmark of apoptosis. In diazotrophic bacteria, the flavoprotein NifL regulates nitrogen fixation according to the intracellular redox environment. When the flavin is oxidized, NifL inhibits NifA, the transcriptional activator of the nitrogen fixation genes, by forming a NifL–NifA complex. Under reducing conditions, NifL does not bind to NifA, allowing NifA to activate expression of the nitrogen fixation genes. Another interesting class of flavoenzymes is the structurally related cryptochromes and DNA photolyases that are activated by blue light. These flavoenzymes harvest light energy by absorbing a photon at a second cofactor, which, depending on the organism, is either 5,10-methylenetetrahydrofolate (see Fig. 2.19) or 8-hydroxy-7,8-didemethyl-5-deazariboflavin, and by transferring the excitation energy to the reduced FAD ($FADH^{\cdot-}$) (Fig. 2.13). Cryptochromes are involved in photosensitive signaling pathways that set the circadian clock and regulate plant growth and development. In bacterial DNA photolyases, light excitation of the reduced flavin triggers electron transfer to the cyclobutane pyrimidine dimer to repair the damaged thymine bases. Another group of light-sensing flavoproteins is the phototropins that help mediate adaptive responses to blue light in plants.

Riboflavin (vitamin B_2) synthesis occurs in several lower organisms and in plants but not in mammals. The biosynthesis of riboflavin originates with GTP and ribulose-5-phosphate and involves the capsid-forming enzyme lumazine synthase. Riboswitches involving flavin-binding RNA aptamers have been found in bacteria that regulate riboflavin synthesis genes in response to cellular flavin levels.

In humans, riboflavin is the precursor for the biosynthesis of FMN and FAD coenzymes. Flavokinase phosphorylates riboflavin to generate FMN, which is then adenylated by FAD synthetase to form FAD. It is generally accepted that

riboflavin deficiency results in increased oxidative stress due to lower activity of FAD-dependent glutathione reductase and xanthine oxidase resulting in lower concentrations of reduced GSH and uric acid, respectively. In fact, glutathione reductase activity is sometimes used to evaluate riboflavin nutritional status.

2.4.B NAD

The pyridine nucleotide, nicotinamide adenine dinucleotide (NAD), was originally described as a low molecular weight compound that is required for fermentation of yeast. NAD and its phosphorylated derivative, NADP, are now recognized as universal energy carriers performing reversible two-electron transfers in a variety of essential metabolic reactions. NAD^+ (oxidized form) participates primarily in oxidative reactions by accepting electrons from energy-rich substrates at the 4 position of the nicotinamide ring (ultimately leading to ATP formation), while NADPH (reduced form) serves mainly as an electron donor in reductive biosynthetic reactions (Fig. 2.14). The standard redox potentials for the two-electron reduction of the NAD^+/NADH and $\text{NADP}^+/\text{NADPH}$ couples are -0.320 V and -0.324 V (pH 7.0). However, the intracellular ratio of $\text{NADP}^+/\text{NADPH}$ is quite low, indicating that the actual cellular redox potential of the $\text{NADP}^+/\text{NADPH}$ couple is considerably more negative (≤ -0.37), favoring the principal function of NADPH as an electron donor. In addition to bioenergetics, NAD participates in signaling pathways by serving as a precursor to calcium releasing agents and as a substrate for protein modifications such as poly-ADP-ribosylation of transcription factors by poly-ADP-ribose polymerases and deacetylation of histones by sirtuins in the nucleus. NADPH has a critical role in oxidant production and antioxidant defense in mammals via the enzyme actions of NADPH oxidase and glutathione reductase, respectively (see Chapter 3, Section 3.3). In neutrophils (white blood cells), NADPH oxidase catalyzes the oxidation of NADPH

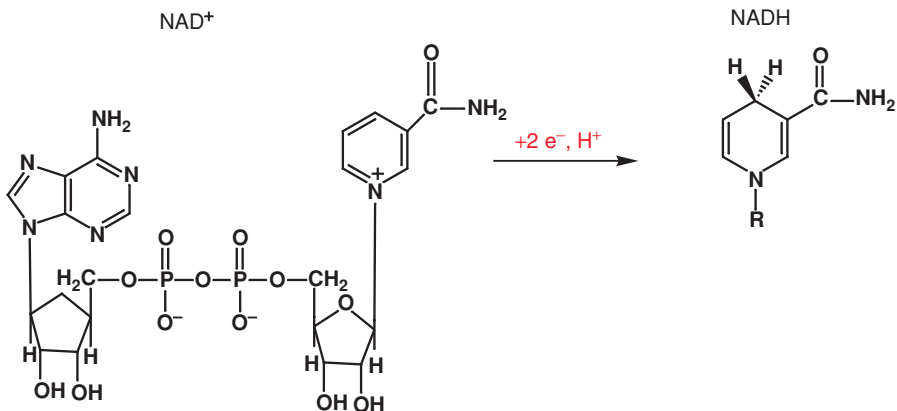


Figure 2.14. Structure of NAD^+/NADH .

by molecular oxygen to generate $O_2^{\cdot-}$, which helps kill invading microorganisms in phagocytic cells.

NAD biosynthesis in mammals can occur *de novo* from tryptophan but the salvage pathways involving either nicotinic acid (pyridine 3-carboxylic acid) or nicotinamide are the primary contributors of NAD. NAD deficiency is manifested as a disease known as pellagra, which is characterized by diarrhea, dermatitis, and dementia. Pellagra was first described in the middle of the 18th century and presently occurs mainly in developing countries and poor population groups. Niacin (vitamin B₃) is the dietary form for NAD supplements and appears useful for preventing and treating atherosclerosis. Niacin supplementation decreases lipoprotein plasma levels of LDL and VLDL while increasing HDL/HDL₂ levels.

2.4.C Quinones

Quinones were first discovered as enzymatic cofactors in the bacterial pyrroloquinoline quinone (PQQ)-dependent enzymes, glucose dehydrogenase and methanol dehydrogenase. PQQ, an *ortho*-quinone, is noncovalently bound to the enzyme through ionic interactions with its carboxylic groups. Biosynthesis of PQQ is absent in plants and animals, while in bacteria it is assembled from glutamate and tyrosine. Following the characterization of PQQ-dependent enzymes, other quinone-dependent enzymes were discovered in bacteria, yeast, plants, and animals but the structural identities of the quinone cofactors remained uncertain. Eventually, four additional quinonoid cofactors were identified but, unlike PQQ, these quinones are generated post-translationally from oxidation of side chain aromatic rings of specific tyrosine or tryptophan residues within the polypeptide chain and remain covalently bound to the enzyme. These quinone cofactors are classified according to the type of covalent linkage as topaquinone (TPQ), lysine tyrosylquinone (LTQ), tryptophan tryptophylquinone (TTQ), and cysteine tryptophylquinone (CTQ). Similar to flavins, quinone cofactors support two- or one-electron transfers and involve two half-reactions (Fig. 2.15). The reductive half-reaction involves the formation of the reduced quinone cofactor while the oxidative half-reaction is characterized by transfer of electrons from the reduced quinone cofactor to an acceptor such as ubiquinone or cytochrome *c* as in the case of alcohol dehydrogenases or molecular oxygen such as in copper amine oxidase. The redox potentials of the various quinone cofactors are generally in the range of 0.06–0.13 V (versus normal hydrogen electrode, pH 6.8–7.5).

Quinoproteins that derive their own quinone cofactor are found widely in nature. The physiological roles of these enzymes are not fully defined in mammals but copper amine oxidase (TPQ-dependent) appears to have roles in regulating glucose uptake and cell adhesion. Also in humans, LTQ-dependent lysyl oxidase helps form the extracellular matrix catalyzing the cross-linking of collagen and elastin. Diseases involving connective tissue disorders, liver fibrosis, and breast cancer have been linked to malfunctions in lysyl oxidase. In contrast to the covalently linked

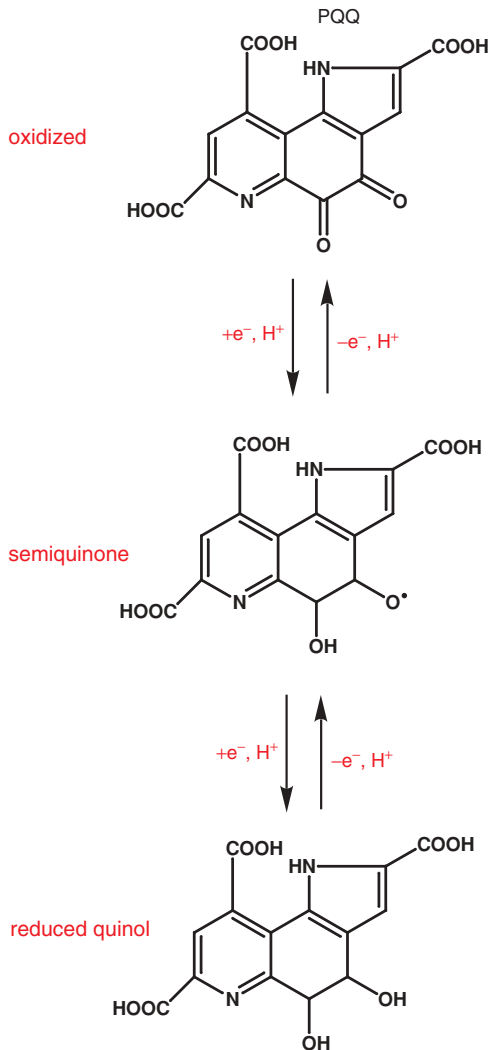


Figure 2.15. Redox states of pyrroloquinoline quinone (PQQ).

quinone cofactors, PQQ has traditionally been thought to be an essential cofactor only in bacteria. More recently, however, a PQQ-dependent dehydrogenase involved in mammalian lysine metabolism has been reported. These findings led to the proposal that PQQ should be classified as a new B vitamin but further evidence is needed to confirm whether PQQ functions as a cofactor in humans. Even so, PQQ is found in human milk and it is generally accepted that PQQ has positive nutritional effects on growth, development, and reproductive health as well as functioning as a

radical scavenger, which contribute to the antioxidant benefits of green tea that contains PQQ.

2.4.D Pterins and Molybdopterins

Pterins are redox cofactors that contain two fused heterocyclic rings, the pteridine ring, which is a structure that is also seen in folic acid and in the isoalloxazine ring in flavins. Tetrahydrobiopterin and molybdopterin serve as cofactors in hydroxylations of aromatic rings, in NO biosynthesis, and in monooxygenation reactions. Pterins can exist in multiple redox states (Fig. 2.16). The one-electron oxidation of tetrahydrobiopterin leads to formation of a radical, an intermediate that has been observed in nitric oxide synthase as discussed later. The two-electron oxidation product, dihydrobiopterin, exists as one of two tautomers and each is recognized by a different reductase. Thus, the quinonoid form generated during aromatic amino acid hydroxylation is a substrate for dihydropterin reductase, whereas 7,8-dihydrobiopterin is reduced by dihydrofolate reductase. Biopterin is the four-electron oxidized product

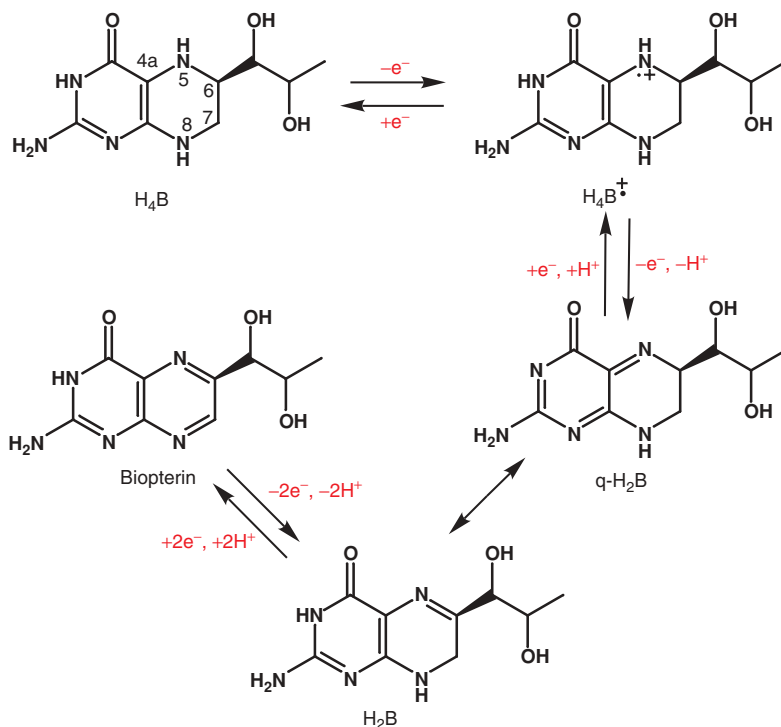


Figure 2.16. Redox states of biopterin. H_4B , H_2B , and $q-H_2B$ denote tetrahydrobiopterin, dihydrobiopterin, and quinonoid dihydrobiopterin, respectively.

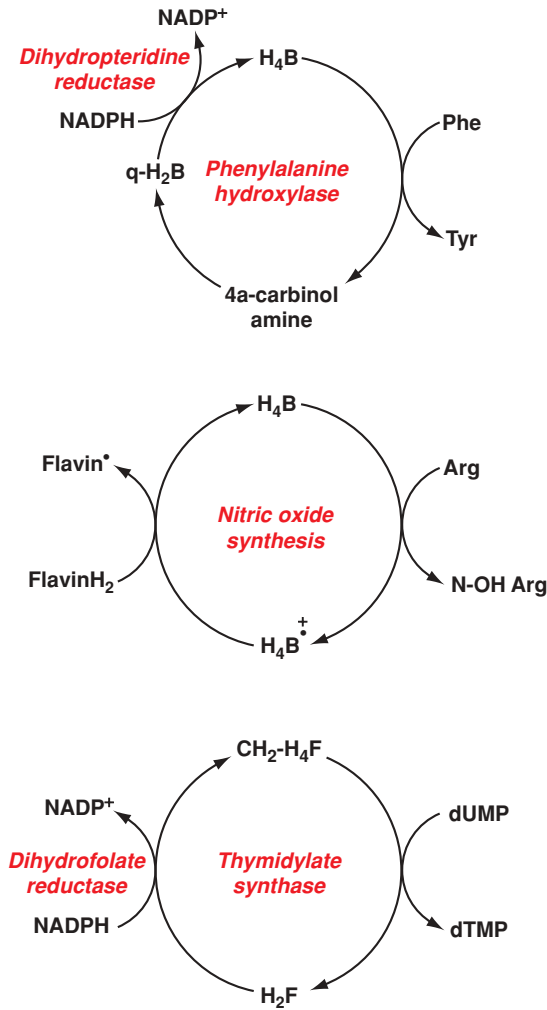


Figure 2.17. Redox reactions catalyzed by tetrahydrobiopterin and methylenetetrahydrofolate. This figure is modified with permission from Dennis Stuehr. The figure is adapted from a similar one published by C.C. Lei et al. (2003).

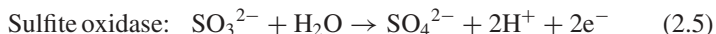
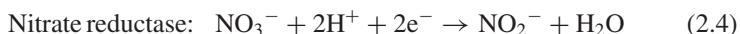
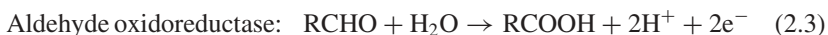
of tetrahydrobiopterin. The lability of tetrahydrobiopterin in solution to oxidation by oxygen and reactive oxygen species (viz., O₂^{•-}, peroxynitrite, and H₂O₂) has led to the suggestion that it may function as an antioxidant.

The pterin-dependent aromatic amino acid hydroxylases are monooxygenases that catalyze the addition of one oxygen atom from molecular oxygen to the substrate and reduce the other atom to water (Fig. 2.17). In addition to tetrahydrobiopterin, these

proteins require mononuclear iron, which is essential for catalysis. In analogy to the chemistry of flavin-dependent hydroxylases, in which the hydroxylating species is believed to be the 4a-peroxyflavin (see Fig. 2.13), a 4a-peroxy intermediate is postulated to form in the pterin-dependent hydroxylases. The essential role of ferrous iron in these enzymes suggests that, as in cytochrome P450-dependent hydroxylases, a high valence iron-oxo intermediate may be the actual hydroxylating agent, although this has not been established unequivocally. The product of the hydroxylase reaction is the two-electron oxidized quinonoid dihydrobiopterin, which is released and needs to be reduced by dihydropteridine reductase to tetrahydrobiopterin prior to participation in another turnover cycle. Mutations in phenylalanine hydroxylase lead to phenylketonuria, an inborn error of metabolism that is routinely screened for in all newborns in the United States and treated by a low phenylalanine-containing diet. Hyperphenylalaninemia can also result from a deficiency in dihydropteridine reductase, which is treated additionally by provision of 5-hydroxytryptophan and L-3,4-dihydroxyphenylalanine, products of the tryptophan hydroxylase and tyrosine hydroxylase reactions, respectively. These reactions also require active dihydropteridine reductase and their products are the precursors of the neurotransmitters, serotonin and norepinephrine, respectively.

A modified pterin cofactor that coordinates molybdenum or tungsten is found associated with enzymes that catalyze the transfer of an oxygen atom to or from substrates with a concomitant two-electron oxidation or reduction of the cofactor. The molybdopterin cofactor consists of a tricyclic pyranopterin with a metal-coordinating *cis*-dithiolene in the pyran ring (Fig. 2.18). In some molybdopterin enzymes, the coordination sphere of the molybdenum/tungsten can involve two molybdopterin moieties, which can be further derivatized with nucleotides (e.g., GMP).

Molybdopterin-containing enzymes catalyze important reactions in global carbon, nitrogen, and sulfur cycles, are mostly found in bacteria, and fall into two families named after representative members: (1) aldehyde oxidase/xanthine dehydrogenase and (2) nitrate reductase/sulfite oxidase. The two classes differ in the coordination environment of the molybdenum. Thus, a terminal sulfur or a strictly conserved cysteine serves as molybdenum ligands in the first and second families, respectively (Fig. 2.18). The reactions catalyzed by representative molybdopterin enzymes are shown in Eqs. (2.3)–(2.5).



The common mechanistic theme in these reactions is that the oxygen atom for “oxo transfer” is derived from water and that the molybdenum cycles between the oxidized Mo(VI) and the reduced Mo(IV) states (or the corresponding oxidation states for tungsten). Completion of the catalytic cycle requires restoration of the molybdenum to the oxidation state found in the resting enzyme. For this, additional prosthetic groups such as iron–sulfur clusters, FAD/NADH, or heme are associated

with molybdopterin-containing enzymes that restore the molybdenum to the correct oxidation state at the end of the catalytic cycle. Since iron–sulfur clusters and hemes are obligate one-electron donors/acceptors, it follows that interconversion between Mo(VI) and Mo(IV) occurs in two one-electron steps. Given the proximity of the pterin to the single-electron donors, it is possible that a pterin radical intermediate may be involved in regenerating the active form of the enzyme. In fact, a pterin radical is observed by EPR spectroscopy in purified aldehyde dehydrogenase.

Tetrahydrobiopterin is also used as a cofactor by nitric oxide synthase, which generates nitric oxide from arginine and oxygen and contains a complex array of additional cofactors: NADPH, FAD, FMN, and heme. The crystal structure of nitric oxide synthase revealed that the tetrahydrobiopterin is too remote from the substrate-binding site to be directly involved in oxygen activation for the two successive monooxygenase reactions catalyzed by this enzyme. However, kinetic and spectroscopic studies have established a role for electron transfer from tetrahydrobiopterin to the heme during oxygen activation (Fig. 2.17). The product of one-electron transfer, the tetrahydrobiopterin radical, has been observed by EPR spectroscopy

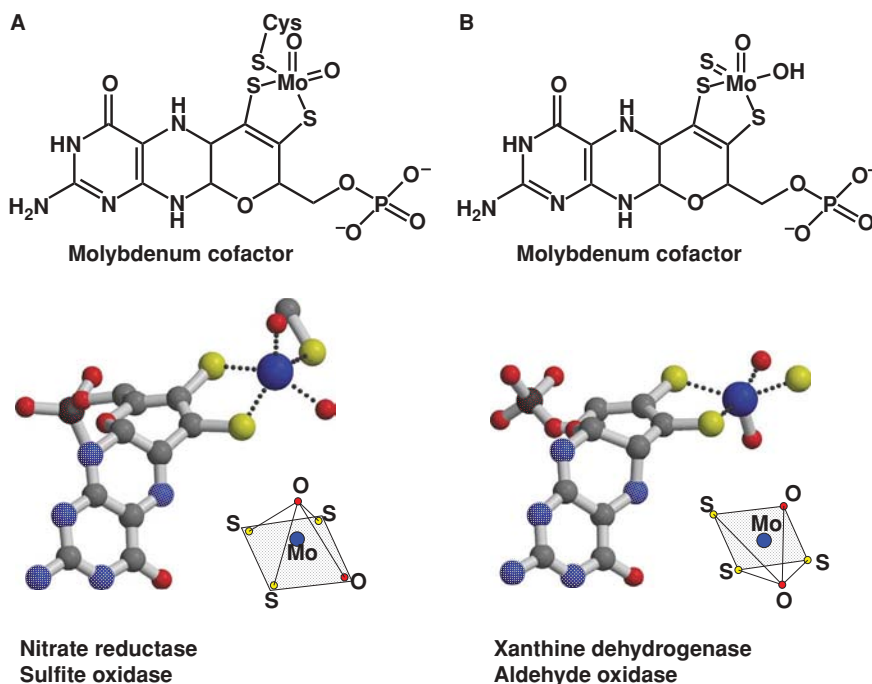


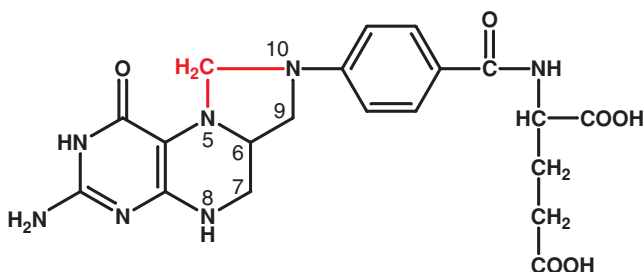
Figure 2.18. Structures of two classes of molybdopterin cofactors. In the first subclass shown in (A) the molybdenum atom is coordinated by a conserved cysteine residue, whereas in (B) it is ligated to a terminal sulfur. This figure is reproduced with permission from *Annu. Rev. Plant Biol.* (2006) 57:623. The authors thank Drs. G. Schwarts and R. Mendel for making this figure available for use.

and its formation is correlated with the disappearance of the Fe(II)–O₂ intermediate on heme and subsequent formation of the arginine hydroxylation product, *N*^ω-hydroxy-L-arginine. Thus, the role of tetrahydrobiopterin in nitric oxide synthase is in the electron relay from NADPH to heme that is required for oxygen activation.

2.4.E Folic Acid

Folic acid is a member of the B-vitamin family and represents the oxidized form of the biologically active cofactor, tetrahydrofolic acid (Fig. 2.19). The synthesis of tetrahydrofolic acid occurs in microbes and plants and involves a series of steps that bring the pterin, *p*-aminobenzoate, and glutamate moieties together in a pathway that has been heavily targeted by antibiotics including the sulfa drugs. In methanogenic bacteria, a structural variant of this cofactor, tetrahydromethanopterin, is found. The primary function of tetrahydrofolate in nature is to serve as a carrier of one-carbon units at various oxidation states, which are donated in biosynthetic reactions for generation of amino acids, purines, and pyrimidines. The one-carbon unit is carried either at the N⁵ (methyl, formimino, formyl), N¹⁰ (formyl), or between the N⁵ and N¹⁰ (methylene, methenyl) positions. In the majority of these one-carbon transfer reactions, the tetrahydrofolate carrier does not undergo a redox change. The exception is the thymidylate synthase-catalyzed reaction, which converts dUMP to dTMP. In this reaction, a one-carbon unit at the oxidation state of a methylene group is transferred from 5,10-methylene tetrahydrofolate to C5 of dUMP followed by a hydride transfer from the C6 position of the cofactor to the exocyclic methylene of the intermediate (Fig. 2.17). This leaves the coenzyme in the oxidized dihydrofolic acid state, which is not useful as a one-carbon carrier and needs to be reduced and returned to the tetrahydrofolate cycle. This reduction is catalyzed by dihydrofolate reductase.

Given the importance of the products of the thymidylate synthase and dihydrofolate reductase-catalyzed reactions to rapidly growing cells, it is not surprising that



5,10 Methylene tetrahydrofolate

Figure 2.19. Structure of methylenetetrahydrofolate. This is the tetrahydrofolate derivative that participates in the redox reactions catalyzed by photolyase and by thymidylate synthase.

these two enzymes have been heavily targeted by pharmacological agents. Hence, 5-fluorodeoxyuridylate, which is converted intracellularly to 5-fluorodeoxyuridine monophosphate, is a mechanism-based inhibitor of thymidylate synthase and is used clinically as an antitumor agent. Methotrexate, trimethoprim, and pyrimethamine are inhibitors of dihydrofolate reductase and are effective as anticancer, antibacterial, and antimalarial agents.

Tetrahydrofolate serves a novel photoantenna function in conjunction with a subclass of photolyases that repair pyrimidine dimers generated by UV light-induced damage to DNA. As shown in Fig. 2.13, photolyases contain an essential flavin, FAD, which catalyzes the photoreactivation reaction. Methylenetetrahydrofolate (Fig. 2.19) or, in some organisms, 8-hydroxy-7,8-didemethyl-5-deazariboflavin functions to increase the efficiency of the reaction, particularly under conditions of limiting light. Both photoantenna cofactors have higher extinction coefficients and absorption maxima at longer wavelengths relative to that of the two-electron reduced FAD, which is the active form of the flavin photocatalyst, making them more efficient for capturing photons. Thus, the role of methylenetetrahydrofolate in DNA photolyase is to absorb blue light photons and to transfer the excitation energy to the flavin acceptor for use in pyrimidine dimer repair.

SELECTED REFERENCES

1. Massey, V. (2000). The chemical and biological versatility of riboflavin. *Biochem. Soc. Trans.* 28:283–296.
2. Fischer, M., and Bacher, A. (2005). Biosynthesis of flavocoenzymes. *Nat. Prod. Rep.* 22:324–350.
3. Mattevi, A. (2006). To be or not to be an oxidase: challenging the oxygen reactivity of flavoenzymes. *Trends Biochem. Sci.* 31:276–283.
4. Modjtahedi, N., Giordanetto, F., Madeo, F., and Kroemer, G. (2006). Apoptosis-inducing factor: vital and lethal. *Trends Cell Biol.* 16:264–272.
5. Berger, F., Ramirez-Hernandez, M.H., and Ziegler, M. (2004). The new life of a centenarian: signalling functions of NAD(P). *Trends Biochem. Sci.* 29:111–118.
6. Dubois, J.L., and Klinman, J.P. (2005). Mechanism of post-translational quinone formation in copper amine oxidases and its relationship to the catalytic turnover. *Arch Biochem. Biophys.* 433:255–265.
7. Sancar, A. (2003). Structure and function of DNA photolyase and cryptochrome blue-light photoreceptors. *Chem. Rev.* 103:2203–2237.
8. Wei, C.-C., Crane, B.R., and Stuehr, D.J. (2003). Tetrahydrobiopterin radical enzymology. *Chem. Rev.* 103:2365–2383.
9. Schwartz, G., and Mendel, R.R. (2006). Molybdenum cofactor biosynthesis and molybdenum enzymes. *Annu. Rev. Plant Biol.* 57:623–647.
10. Mure, M. (2004). Tyrosine-derived quinone cofactors. *Acc. Chem. Res.* 37:131–139.

Antioxidant Enzymes

- 3.1. ROS-Dependent Enzymes
 - 3.1.A. A Catalase
 - 3.1.B. Superoxide Dismutase
 - 3.1.C. Peroxiredoxins
 - 3.1.D. Alkyl Hydroperoxide Reductases
- 3.2. The Thioredoxin System
 - 3.2.A. Thioredoxin
 - 3.2.B. Thioredoxin Reductase
- 3.3. The Glutathione System
 - 3.3.A. Glutathione Reductase
 - 3.3.B. Glutaredoxin (Thioltransferase)
- 3.4. Repair Enzymes
 - 3.4.A. Methionine Sulfoxide Reductases
 - 3.4.B. DNA Repair Enzymes
 - 3.4.C. Sulfiredoxins
- 3.5. Detoxification Enzymes
 - 3.5.A. Cytochrome P450 Enzymes: Structure, Function, and Mechanism
 - 3.5.B. GSH Transferases
- 3.6. Oxidative Folding
 - 3.6.A. Disulfide Bond Formation in Bacteria
 - 3.6.B. Disulfide Bond Formation in Eukaryotes
- 3.7. Other Antioxidant Enzymes
 - 3.7.A. Selenoproteins
 - 3.7.B. Heme Oxygenase

3.1 ROS-DEPENDENT ENZYMES

3.1.A Catalase

IRWIN FRIDOVICH

*Department of Biochemistry, Duke University Medical Center,
Durham, North Carolina*

3.1.A1 Formation of H_2O_2 H_2O_2 is commonly produced in aerobic cells, both as a product of the dismutation of superoxide ($O_2^{\cdot-}$), and by divalent reduction of O_2 by a variety of flavo- and metallo- oxidases; including uricase, glucose oxidase, and D-amino acid oxidase. H_2O_2 threatens the integrity of cellular macromolecules and structures. The damaging effect of H_2O_2 is primarily due to its univalent reduction, by Fe(II), to the indiscriminately reactive HO^{\cdot} . Iron is ordinarily not free to participate in this Fenton chemistry but is, rather, tightly bound within a variety of proteins. However, Fe(II) is liberated when the [4Fe-4S] clusters of dehydrases, such as aconitase, are oxidized by $O_2^{\cdot-}$ and this liberated Fe(II) is free to react with H_2O_2 . Moreover, the liberated iron would be kept reduced by cellular reductants, such as thiols, ascorbate, and leucoflavins, and would thus be able to act in a catalytic fashion. The role of iron in mediating the toxicity of H_2O_2 is revealed by the protective effect of cell permeable iron chelating agents. When the H_2O_2 -scavenging enzymes of *E. coli* are mutationally inactivated, the mutants exhibit an O_2 -dependent growth defect attributable to endogenous submicromolar H_2O_2 , and cell permeable iron chelating agents protect against this growth defect.

3.1.A2 Elimination of H_2O_2 There is a striking parallel between the ways in which $O_2^{\cdot-}$ and H_2O_2 are detoxified. Thus, for $O_2^{\cdot-}$ there are families of superoxide dismutases (SODs) and superoxide reductases; while for H_2O_2 there are hydrogen peroxide dismutases (catalases) and hydroperoxide reductases (peroxidases and periredoxins). The parallel goes on. Thus, *E. coli* contains a constitutive FeSOD and an MnSOD that is inducible as part of the SoxRS regulon. It similarly contains a catalase (HP-II) that is constitutive, but produced primarily in stationary phase, and another (HP-I) that is inducible as part of the OxyR regulon. The former (HP-II) is only a catalase, while the latter (HP-I) exhibits both catalase and peroxidase activities. Most catalases and peroxidases are ferriheme containing enzymes, but organisms such as the Lactobacillacea that cannot synthesize heme produce a dimanganic catalase when grown on heme-free media. The hemes in the heme-containing catalases and peroxidases are buried within the protein structure and are accessed via a channel. In the cases of the catalases, the channel is narrow and blocks access to molecules significantly larger than H_2O_2 ; whereas in the peroxidases, the channel is larger, allowing a variety of larger substrates to reach the heme (Fig. 3.1). In fact, even those catalases called monofunctional, because they are considered as only catalases, can act as peroxidases on small molecules such as methanol, ethanol, and azide. The restricted access to the heme distinguishes catalases from peroxidases, illustrated by the conversion of catalase to a peroxidase by partial digestion with trypsin, which increases the exposure of the heme.

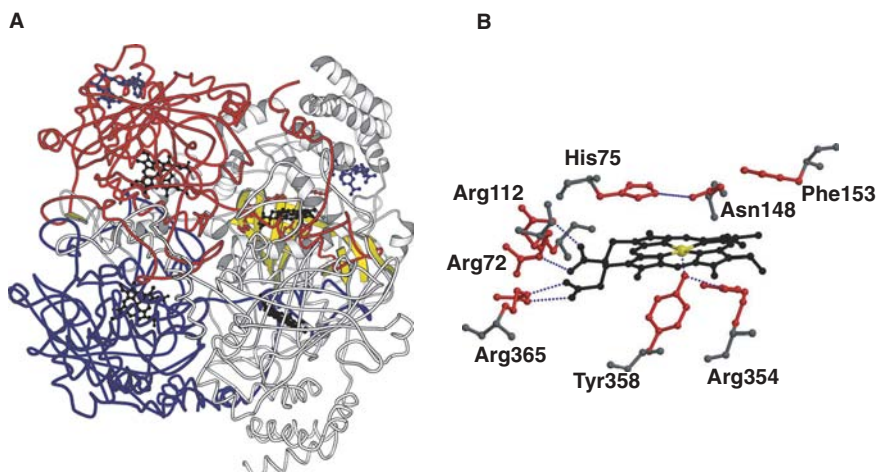
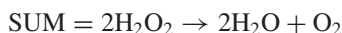
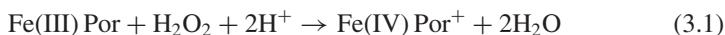
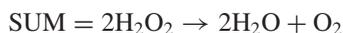
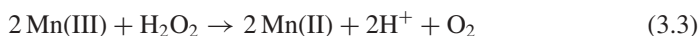


Figure 3.1. Human catalase structure (PDB ID 1DGB). (A) Tetrameric structure of human catalase. Chain A is shown as a schematic model. Chains B, C, and D are depicted as gray, red, and blue coils, respectively. Heme and NADPH are shown as a ball and stick model colored in black and blue, respectively. In chain A, β -strands are colored in yellow. (B) Active site. Fe is shown in yellow. Site chains of residues involved in hydrogen bonding to heme are shown in red, as a ball and stick model.

3.1.A3 Mechanisms The monofunctional catalases can be subdivided into three groups that appear unrelated on the basis of sequence. Two of these groups are heme containing, while the third has binuclear Mn(II) active sites. The heme-based catalases are homotetrameric, with one group having subunit weights close to 75 kDa while the other has subunit weights less than 60 kDa. The actions of the heme catalases involve divalent oxidation of the ferriheme to an Fe(IV) porphyrin cation radical, by H_2O_2 ; followed by its divalent reduction by the next H_2O_2 . This is illustrated by reactions (3.1) and (3.2.)



In the dimanganic catalases the mechanism can be written.



The dimanganic catalases were once called pseudocatalases because they are not inhibited by cyanide; but there is nothing pseudo about their action on H_2O_2 . They

are homohexameric proteins with subunit weights close to 30 kDa. Interestingly, the organisms that make these catalases will also make a heme-containing catalase when provided with heme but will make the dimanganic catalase when deprived of heme. This can be seen as an indication of the importance of detoxifying H_2O_2 .

The bifunctional catalases can also act as peroxidases by virtue of a large funnel-shaped solvent access channel to the heme. These enzymes are related by amino acid sequence to the plant peroxidases. An interesting aside is that the bifunctional catalase of *Mycobacterium tuberculosis* is responsible for the peroxidative activation of the prodrug isoniazide, and a mutational defect in this enzyme renders this pathogen insensitive to this otherwise effective treatment. The peroxidative activity of the dual function catalases begins with reaction (3.1), followed by two univalent oxidations of the electron donor substrates as depicted by reactions (3.5) through (3.7), where DH_2 is the substrate and DH^\cdot is the substrate radical, which can either dismute or dimerize, as in reaction (3.7).



3.1.A4 K_m and *in Vivo* Action The monofunctional catalases do not respond to elevation of H_2O_2 concentration in the usual Michaelis–Menten manner and the concentration of H_2O_2 at which the half maximal rate is achieved can increase as the time needed for a single assay decreases. The reason for this is that H_2O_2 can inactivate catalase so that an increase in rate with increase in H_2O_2 can be offset by increased inactivation at high levels of H_2O_2 . Very fast assays of these catalases have yielded effective K_m values for H_2O_2 as high as 1.0 M. This leads one to question how effective the monofunctional catalases can be at the submicromolar H_2O_2 concentrations encountered *in vivo*. One way around this problem is to sequester the catalase with the H_2O_2 -producing oxidases in the peroxisomes of eukaryotic cells. This allows the catalase to get at the H_2O_2 made by these oxidases before it has been diluted by diffusing into the far larger volume of the cytosol. Another possibility is that monofunctional catalases may actually act as peroxidases *in vivo* toward as yet unidentified small cellular reductants. It is the case that peroxidases do exhibit low K_m values for H_2O_2 .

3.1.A5 Inhibition by $\text{O}_2^{\cdot-}$ Catalase activity can be inhibited by univalent reduction of the Fe(IV) Por^+ to the Fe(IV) Por state since the latter oxidation state is on the peroxidative pathway, but not on the catalatic pathway. $\text{O}_2^{\cdot-}$ can cause this univalent reduction and can thus diminish catalatic activity. SOD, by removing $\text{O}_2^{\cdot-}$, can protect catalase against this type of inactivation. At the same time, H_2O_2 can inactivate the Cu, ZnSODs, and FeSODs, and catalases can, by removing H_2O_2 , protect these SODs (Fig. 3.2). This is another way in which the SODs and catalases act as an effective and mutually supportive defensive team.

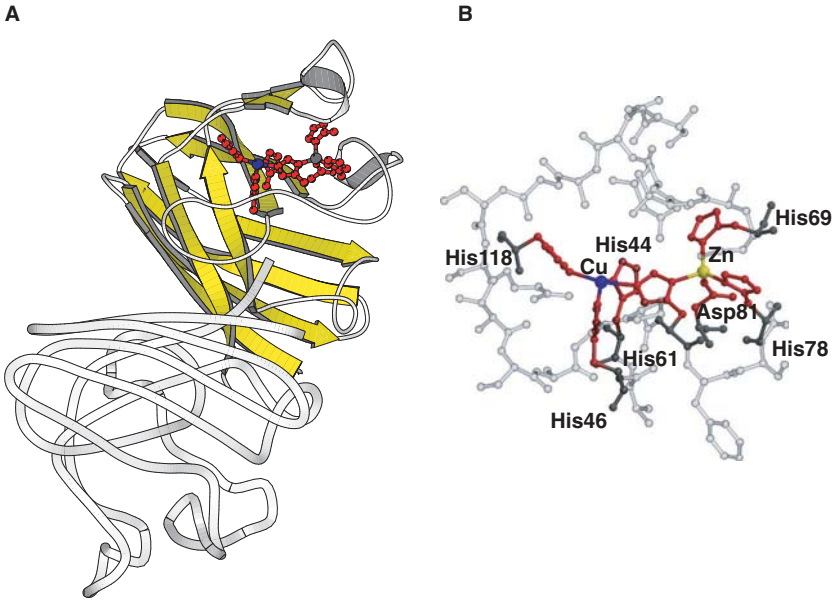


Figure 3.2. Structure of copper and zinc superoxide dismutase (PDB ID 2SOD). (A) Dimeric structure of SOD. Chains O and Y are shown as a schematic model and as coils, respectively. β -Strands in chain O are colored yellow. Copper and zinc are shown as blue and gray spheres, respectively. Residues in the active site are depicted in red, as a ball and stick model. (B) Active site of SOD. Cu and Zn are shown as blue and yellow spheres. Six histidines and one asparagine in the active site are shown in red, as a ball and stick model. Residues surrounding the active site are shown in gray.

3.1.A6 NADPH Binding Monofunctional catalases from liver, and from some bacteria, tightly bind NADPH, while other catalases do not. It has been proposed that this bound NADPH protects the catalase against inactivation, by reducing the inactive Fe(IV) Por form back to the active Fe(III) Por form. If that is the case, how do those catalases that lack a binding site for NADPH remain active? Quite possibly they utilize small reductants similar to ethanol or formate.

3.1.A7 Catalase and Life Span Transgenic mice in which catalase, targeted to mitochondria, was overproduced gained several months in average life span, while targeting the extra catalase to peroxisomes or nuclei was without effect. This result supports the view that oxidative damage to mitochondria limits the life span of aerobic eukaryotes.

The catalatic activity of the dual function catalases seems to depend on a non-peptidic covalent linkage of a methionine and a tryptophan to the phenolic ring of a tyrosine residue. When any one of the amino acids involved in this unusual troika was mutationally modified, the catalatic activity was lost, while the peroxidative activity was enhanced. The plant peroxidases, which do not display catalase activity, do not contain this structure.

3.1.A8 3-Aminotriazole Mammalian catalase is irreversibly inactivated by 3-aminotriazole; but this inactivation is dependent on the presence of H_2O_2 and the inactivated catalase contains aminotriazole covalently bound to a histidine residue. Since 3-aminotriazole is cell permeable, this inactivation has been used to measure the production of H_2O_2 in cells and to explore the consequences of elimination of catalase activity. Studies of this type demonstrated that both catalase and glutathione peroxidase are important for protecting hepatocytes against H_2O_2 .

3.1.A9 Assays Catalase activity can be assayed in terms of the disappearance of H_2O_2 followed at 230 or 240 nm. Alternatively, it can be assayed by following O_2 formation with the Clarke type of O_2 electrode. In the latter method, the buffered H_2O_2 solution is depleted of O_2 by sparging with N_2 prior to the addition of catalase. The ultraviolet assay is most convenient when working with relatively pure samples of catalase that do not have major UV-absorbing impurities. The amperometric electrode assay is insensitive to UV absorption and can be applied to crude extracts. Catalase activity on native gel electropherograms can be negatively stained by soaking gels first in horseradish peroxidase (HRP) plus H_2O_2 , followed by rinsing and then soaking in diaminobenzidine (DAB). During the soak in HRP + H_2O_2 the gel becomes impregnated with those reagents except at positions containing catalase that decomposes the H_2O_2 . During the soak in DAB, the HRP + H_2O_2 oxidizes the DAB to a pigmented product, staining all of the gel save the regions containing catalase. Since DAB inhibits catalase it is important that the DAB soak be done last.

3.1.A10 Acatlasemia Human acatalasemia, also called Takahara's disease, has been associated with ulceration of the gums and with little else. The reason for this is that the causative mutation renders the catalase somewhat unstable so that only erythrocytes, which cannot synthesize new protein, soon become catalase-negative. Bacteria that live in the oral cavity at the gum line, such as species of *Streptococcus*, produce and secrete H_2O_2 , and that H_2O_2 attacks the gums and loosens the teeth. Evidently, red cell catalase is important for protecting this well-perfused tissue against H_2O_2 .

SELECTED REFERENCES

1. Putnam, C.D., Arvai, A.S., Borne, Y., and Tainer, J.A. (2000). Active and inhibited human catalase structures: ligand and NADPH binding and catalytic mechanism. *J. Mol. Biol.* 296: 295–309.
2. Chelikani, P., Fita I., and Loewen P.D. (2004). Diversity of Structures and properties among catalases. *Cell Mol. Life Sci.* 61:192–208.
3. Wu, A.J., Penner-Hahn, J.E., and Pecorano, V.L. (2004) Structural, spectroscopic, and reactivity models for manganese catalases. *Chem. Rev.* 104:903–938.

3.1.B Superoxide Dismutase

IRWIN FRIDOVICH

Department of Biochemistry, Duke University Medical Center, Durham, North Carolina

3.1.B1 Formation of $O_2^{\cdot-}$ Molecular oxygen (O_2) contains twelve electrons. Ten of them exist as spin-opposed pairs in five orbitals; while the remaining two are in separate orbitals and have the same spin state. These two parallel electronic spins impart paramagnetism and a preference for reduction by univalent steps. The latter is readily explained. Thus, attempts to insert a spin-opposed pair of electrons from some nonradical donor would lead to violation of the Pauli exclusion principle, which points out the improbability of two parallel spins in one orbital. This is referred to as spin restriction. Spin inversion is possible but occurs on a time scale orders of magnitude slower than the lifetime of collisional complexes. Adding electrons to O_2 one at a time allows spin inversion during the intervals between electron insertions and thus circumvents the spin restriction.

Because of this preference for univalent reduction, superoxide ($O_2^{\cdot-}$) is a common, if relatively minor, product of biological O_2 reduction. $O_2^{\cdot-}$ is the conjugate base of the hydroperoxyl radical (HO_2^{\cdot}) whose pK_a is approximately 4.8). Hence, at neutral pH, somewhat less than 1% of $O_2^{\cdot-}$ will exist in its protonated form. HO_2^{\cdot} dismutates spontaneously to $O_2 + H_2O_2$ with a rate constant at 25 °C of approximately $1 \times 10^5 M^{-1} s^{-1}$. For the dismutation of HO_2^{\cdot} with $O_2^{\cdot-}$ the rate constant is approximately $1 \times 10^8 M^{-1} s^{-1}$. In contrast, for the dismutation of two $O_2^{\cdot-}$ molecules, the rate constant is vanishingly small (i.e., less than $0.3 M^{-1} s^{-1}$), undoubtedly due to electrostatic repulsion.

3.1.B2 Harmful Effects of $O_2^{\cdot-}$ $O_2^{\cdot-}$ is damaging in the biological milieu for several reasons. It oxidizes the [4Fe–4S] prosthetic group of dehydratases, such as the aconitases, with rate constants close to $10^8 M^{-1} s^{-1}$. This univalent oxidation destabilizes the [4Fe–4S] cluster such that it decomposes, releasing Fe(II) and inactivating the enzymes that depend on it. The liberated Fe(II) can reduce H_2O_2 into HO^- plus HO^{\cdot} and the latter is a very strong and indiscriminate oxidant. The liberated iron will be kept reduced by cellular reductants, such as GSH, and hence will act catalytically in the reduction of H_2O_2 . It is moreover likely that the Fe(II) will bind to nucleic acids, proteins, and membranes, causing HO^{\cdot} formation and resulting in preferential damage to these vital targets.

Nitric oxide is another radical that is commonly produced in biological systems; it acts as a neurotransmitter and smooth muscle relaxant and is one element of the offensive armamentarium of macrophages. Radical recombination reactions are usually very fast and $O_2^{\cdot-}$ reacts with NO^{\cdot} with a rate constant of approximately $1 \times 10^{10} M^{-1} s^{-1}$; producing peroxynitrite ($ONOO^-$). The latter protonates with a pK_a close to neutrality and the resultant $ONOOH$ is a powerful oxidant and nitrating agent. Clearly, $O_2^{\cdot-}$, and the species that it engenders, can damage living cells and defenses are needed.

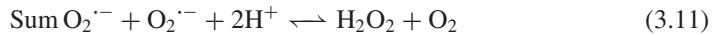
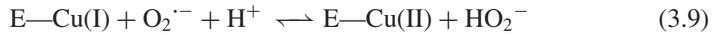
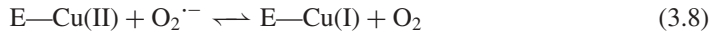
3.1.B3 Elimination of $O_2^{\cdot-}$ One way to overcome the electrostatic barrier facing the dismutation of $O_2^{\cdot-}$ is to have a redox-active metal cation act as a go-between. Thus, the metal can accept an electron from one $O_2^{\cdot-}$ and then donate it to another $O_2^{\cdot-}$, achieving the dismutation without the direct interaction between the two $O_2^{\cdot-}$ radicals. Cu(II) per se is an excellent catalyst of the dismutation of $O_2^{\cdot-}$, but free Cu(II) catalyzes many oxidations and cannot be tolerated by living cells. This problem is solved by enzymes that incorporate the catalytic metal and maximize its ability to catalyze the dismutation of $O_2^{\cdot-}$, while preventing unwanted side reactions. The enzymes that accomplish this are called superoxide dismutases or SODs. They adjust the redox potential of the catalytic metal to approximately +300 mV. This is ideal for catalysis of the dismutation reaction. Thus, the standard redox potential of the $O_2^{\cdot-}/O_2$ couple is approximately -300 mV and that for the $H_2O_2/O_2^{\cdot-}$ couple is approximately +900 mV. A redox potential of +300 mV is midway between the potentials of the two half-reactions of the catalytic cycle and thus provides equal thermodynamic driving force for both. SODs based on Cu(II), Mn(III), Fe(III), and Ni(II) exist and all exhibit metal-centered redox potentials close to +300 mV and all catalyze the dismutation of $O_2^{\cdot-}$ with catalytic rate constants of approximately $10^9 M^{-1} s^{-1}$. Moreover, they all sterically limit the access of molecules larger than $O_2^{\cdot-}$ or HO_2^- to the catalytic metal, thus minimizing side reactions. Since the reactant $O_2^{\cdot-}$ is a monovalent anion, a truly efficient catalyst should also provide electrostatic guidance, by judicious placement of charged amino acid residues, and all SODs do that too.

3.1.B4 Why There Are Multiple SODs A reactive molecule, such as O_2 , could not have been significantly present in our atmosphere prior to the advent of oxygenic photosynthesis, which is by no means a simple process. It follows that a diverse anaerobic biota must have been present prior to the oxygenation of the biosphere. A common selection pressure applied to a varied biota often calls forth multiple adaptations. It is thus understandable that multiple types of SODs evolved and persist to this day.

3.1.B5 The Cu,ZnSODs These are generally homodimeric enzymes with subunit molecular weights of approximately 16 kDa and bearing one Cu(II) and one Zn(II) per subunit. This Cu,ZnSOD is found in the cytosol as well as in many of the organelles of eukaryotic cells. In mitochondria, the Cu,ZnSOD resides in the intermembrane space. There is also an extracellular Cu,ZnSOD (EcSOD) that binds to the glycosaminoglycans of the extracellular matrix and it is a larger, homotetrameric and glycosylated molecule whose subunit molecular weight is approximately 23 kDa. EcSOD, although a different gene product, nevertheless shows considerable sequence homology to the intracellular Cu,ZnSOD.

The Cu(II) represents the catalytic center, while the Zn(II) serves a structural and facilitative role. The Cu(II) is ligated to four imidazoles from histidine residues, while the Zn(II) is ligated to three imidazoles plus one aspartate carboxylate. The Cu(II) and the Zn(II) are ligated to the same imidazole and are thus bridged by it. The reaction

cycle can be illustrated by reactions (3.8)–(3.11), where E denotes enzyme.



The protonation illustrated by reaction (3.10) occurs after the HO_2^- is released from the active site.

When the Cu(II) is reduced, as in reaction (3.8), the bridging imidazolite is released from its bond to the copper and becomes protonated to imidazole. Then, when the Cu(I) is reoxidized, as in reaction (3.9), the bridge is reestablished as the proton on the imidazole is supplied to form the nascent HO_2^- . The efficiency of this scheme of proton conduction is shown by the observation that the Cu,ZnSOD maintains full activity over the pH range of 5–10.

3.1.B6 MnSODs, FeSODs, and Cambialistic SODs MnSOD is found in the matrix of mitochondria in both animals and plants. It is also found in many bacterial species. The mitochondrial MnSOD is a homotetrameric enzyme with a subunit molecular weight of 23 kDa, while the *E. coli* MnSOD is dimeric. There is extensive sequence homology between the mitochondrial and bacterial MnSODs, supporting an endosymbiotic origin for those organelles. The *E. coli* MnSOD is upregulated by $\text{O}_2^{\cdot-}$ as a member of the SoxRS regulon. The SoxR protein is oxidized by $\text{O}_2^{\cdot-}$ and then induces synthesis of the SoxS protein, which, in turn, induces the production of MnSOD and other members of this regulon.

The FeSOD, in contrast to the MnSOD, is constitutive and is produced even when *E. coli* are grown anaerobically. We may rationalize this by considering the FeSOD to be a standby defense that allows the bacteria to survive the transition from anaerobic to aerobic conditions, while the regulated production of MnSOD allows balancing the level of defense to the level of threat. It should be noted that gram-negative bacteria, which are bounded by two membranes enclosing the periplasmic space, also contain a Cu,ZnSOD that is found in the periplasm. This enzyme is produced when cultures approach stationary phase and it protects the cells against exogenous sources of $\text{O}_2^{\cdot-}$. FeSOD has not been found in animals, but in plants it resides in the chloroplasts, along with Cu,ZnSOD.

Several groups of anaerobic bacteria, such as the Bacteriodes and the Propionibacteria, contain an SOD that can function with either Fe or Mn at the active site. This has been referred to as a cambialistic SOD and is to be contrasted with the *E. coli* MnSOD and FeSOD that can be made to bind either Mn(III) or Fe(III) but are active only with the native metal.

3.1.B7 NiSOD The most recently described SOD is one that contains Ni(III) at its active site and was found in *Streptomyces*. This is a homotetrameric enzyme with a

subunit molecular weight of approximately 13 kDa. It does not exhibit sequence homology with the other SODs. Enriching the growth medium with Ni elicits increased production of this NiSOD. Its structure has been determined by X-ray crystallography and provides for electrostatic facilitation in the catalytic mechanism as well as for a narrow solvent access channel to the metal center.

3.1.B8 SOD Knockouts Overproduction, as a means of exploring function, can yield confusing results since overproduction of an ordinarily abundant protein can cause underproduction of unrelated proteins. This potential problem is exacerbated in the case of metalloenzymes, whose overproduction can lead to a paucity of the prosthetic metal. On the other hand, ablation, or knockout, of the production of an enzyme often leads to unambiguous results. Mutational deletion of both FeSOD and MnSOD in *E. coli* imposes several phenotypic deficits including auxotrophies for branched chain, aromatic, and sulfur-containing amino acids and elevated mutagenesis—all of which are oxygen dependent and all of which are eliminated by inserting a functional gene coding for an SOD. The auxotrophies are due to inactivation, by $O_2^{\cdot-}$, of enzymes on the biosynthetic routes to these amino acids; while the mutagenesis is attributed to DNA damage by HO^{\cdot} and other oxidants engendered by $O_2^{\cdot-}$.

Murine knockouts of the MnSOD exhibit neonatal mortality with cardiomyopathy, metabolic acidosis, and other pathologies. The very short life span of the homozygous MnSOD knockouts limits the study of these animals, but heterozygous knockouts, which possess half the normal level of MnSOD, have been informative. The MnSOD^{+/-} mice exhibit decreases in capacity for exercise, flow-elicited vasorelaxation, and aconitase activity, as well as sensitivity to handling-induced seizures and severe neurodegeneration. It is thus clear that mice need all the MnSOD they normally have and do not have the ability to compensate for even a modest decrease in MnSOD.

Knockout of the Cu,ZnSOD is much better tolerated, perhaps indicating some redundant, or compensatory, defense against $O_2^{\cdot-}$ in the cytosol. Thus, Cu, ZnSOD^{-/-} mice exhibit a moderately decreased life span as well as increases in DNA damage and lipid oxidation. Interestingly, they also develop liver tumors by 9 months of age. $O_2^{\cdot-}$ can be eliminated by reduction, as well as by dismutation. Thus, desulfoferrodoxin and neelaredoxin act as $O_2^{\cdot-}$ reductases and it is possible that some compensation for the absence of the cytosolic Cu, ZnSOD can be provided by a murine $O_2^{\cdot-}$ reductase.

3.1.B9 Defense in Depth The SODs are wonderfully effective in decreasing the half-life of $O_2^{\cdot-}$ in the biological milieu. Thus, they react with $O_2^{\cdot-}$ with a rate constant of approximately $10^9 M^{-1} s^{-1}$ and that greatly exceeds the rate of spontaneous dismutation, which is approximately $10^5 M^{-1} s^{-1}$ at neutrality. Moreover, at a steady-state concentration of approximately $10^{-9} M$, $O_2^{\cdot-}$ is four orders of magnitude less abundant than SOD, which in most cells is present at approximately $10^{-5} M$. Thus, a molecule of $O_2^{\cdot-}$ would be 10,000 times more likely to encounter SOD than to encounter another $O_2^{\cdot-}$. Furthermore, its rate of reaction with the SOD is 10,000 times faster than with another $O_2^{\cdot-}$. Hence, the effective enhancement of the dismutation reaction by SOD in the cell is 10^8 -fold. Yet, eliminating $O_2^{\cdot-}$ is not the

whole story of defense against oxidative stress. An adequate defense also requires the elimination of H_2O_2 , replacement of targets sensitive to attack by $\text{O}_2^{\cdot-}$ by analogues that are not similarly sensitive, repair of the oxidative damage that is sustained in spite of the defense, replacement of the oxidatively damaged molecules that cannot be repaired, and provision of the reductants that are needed for repair. Study of the SoxRS and the OxyR regulons of *E. coli* reveals that $\text{O}_2^{\cdot-}$ and H_2O_2 induce enzymes that provide all the elements needed for such defense in depth.

SELECTED REFERENCES

1. Park, S., You, X., and Imlay, J.A. (2005). Substantial DNA damage from submicromolar intracellular hydrogen peroxide detected in Hp_x^- mutants of *Escherichia coli*. *Proc. Natl. Acad. Sci. USA* 102:9317–9322.
2. Imlay, J.A. (2003). Pathways of oxidative damage. *Annu. Rev. Microbiol.* 57:395–418.
3. Fridovich, I. (1995). Superoxide radical and superoxide dismutases. *Annu. Rev. Biochem.* 64:97–112.

3.1.C Peroxiredoxins

LESLIE B. POOLE

Department of Biochemistry and Center for Structural Biology, Wake Forest University School of Medicine, Winston-Salem, North Carolina

Peroxiredoxins are a widely distributed thiol-based group of enzymes that catalyze the reduction of H_2O_2 , organic hydroperoxides (ROOH), and peroxynitrite. The bacterial and yeast versions of peroxiredoxins, AhpC and “protector protein” (later known as thiol-specific antioxidant or TSA), respectively, were the first to be discovered and characterized. Subsequent sequence searches have demonstrated the ubiquity of these peroxidases, now known to be present in most, if not all, living organisms. Not only are the peroxiredoxins widespread in biology, but one or more peroxiredoxin family members are generally expressed at high levels in many cell types. Interestingly, at least six separate peroxiredoxin homologs are expressed in mammalian tissues, in some cases with particular subcellular distributions, although a precise understanding of the independent and overlapping functions of these various peroxiredoxins is lacking. Based on a variety of approaches and findings, peroxiredoxins are involved not just in detoxification of peroxides, but also more broadly in proliferation, differentiation, and apoptotic pathways through both known and unknown mechanisms.

3.1.C1 Mechanistic and Structural Features of Peroxiredoxins Combined structure- and sequence-based studies of peroxiredoxins support the emergence of peroxiredoxins from a thioredoxin-like ancestral protein and the classification of these enzymes into four (or in some schemes five) subgroups based on particular conserved motifs and/or mechanisms. Mechanistically, the peroxiredoxins all catalyze

the same first step in peroxide reduction, generation of the alcohol (or water) from the peroxide, and concomitant oxidation of the peroxidatic cysteine thiol (R-S_PH) to generate the sulfenic acid (R-S_POH) (Fig. 3.3A); the subsequent recycling of this oxidized cysteine can be used to differentiate among three mechanistic classes. The vast majority of peroxiredoxins possess a second reactive, conserved cysteine, the resolving cysteine (R-S_RH), which forms an intersubunit disulfide bond with the sulfenic acid form of the peroxidatic cysteine (to generate R-S_P-S_R-R) prior to reduction. In addition to these “typical 2-Cys peroxiredoxins” with the resolving cysteine on a partner subunit, there are also peroxiredoxins that use the same chemical mechanism, disulfide bond formation, for catalysis, but for which the resolving cysteine is located on the same monomer as the peroxidatic cysteine (the “atypical 2-Cys peroxiredoxins”). There are also a modest number of peroxiredoxins that function as “1-Cys peroxiredoxins,” bypassing the need for protein disulfide bond formation prior to reduction (dashed line in Fig. 3.3A). In the case of AhpC from *Salmonella typhimurium*, mutation to replace the resolving cysteine with a serine converted this typical 2-Cys peroxiredoxin into a functional 1-Cys peroxiredoxin, showing that disulfide bond formation is not essential to the mechanism of 2-Cys peroxiredoxins. The mechanism for recycling 2-Cys peroxiredoxins generally involves thioredoxin or another thioredoxin-like Cys-X-X-Cys-containing redox module or modules, and a pyridine nucleotide-dependent flavoprotein disulfide reductase; precise mechanisms for 1-Cys peroxiredoxin recycling are as yet unclear.

Structural features of the peroxide-reactive peroxiredoxin active sites are highly conserved among all the classes. In addition to the absolutely conserved cysteine (R-S_PH) required for the chemistry, a conserved Arg proximal to the active site contributes to lowering of the p*K*_a of the peroxidatic cysteine to stabilize the nucleophilic thiolate (R-S_P⁻) (Fig. 3.3B). In addition, conserved proline and threonine (with threonine sometimes replaced by serine) in a Pro-X-X-X-Thr-X-X-Cys motif (the latter being the peroxidatic cysteine) are also likely to make functional contributions to the peroxide reactivity of the peroxiredoxin active site (the proline ring closes off one side of the active site pocket, and the threonine is hydrogen bonded to the sulfur of the peroxidatic cysteine).

3.1.C2 Dimers, Decamers, and Redox-Sensitive Oligomerization of Peroxiredoxins

Although the identity of a protein named “torin” from human red blood cells studied by transmission electron microscopy in the late 1960s was not originally clear, later studies showed that this toroidal protein was one of the four typical 2-Cys peroxiredoxins expressed in mammals, PrxII, a protein and peroxiredoxin family member that is particularly abundant in erythrocytes. At the time, this protein was shown to exhibit an apparent tenfold symmetry, which was subsequently defined more precisely, using X-ray crystallographic studies, as a pentameric arrangement of intimately associated dimers ((α_2)₅); typical 2-Cys peroxiredoxins and most other 2-Cys and 1-Cys peroxiredoxins studied exist as dimers or decamers in solution and in crystal structures (Fig. 3.3C). The involvement of cysteine residues from two different subunits in each active site of typical 2-Cys peroxiredoxins makes the dimer the minimal active species in this type of peroxiredoxin.

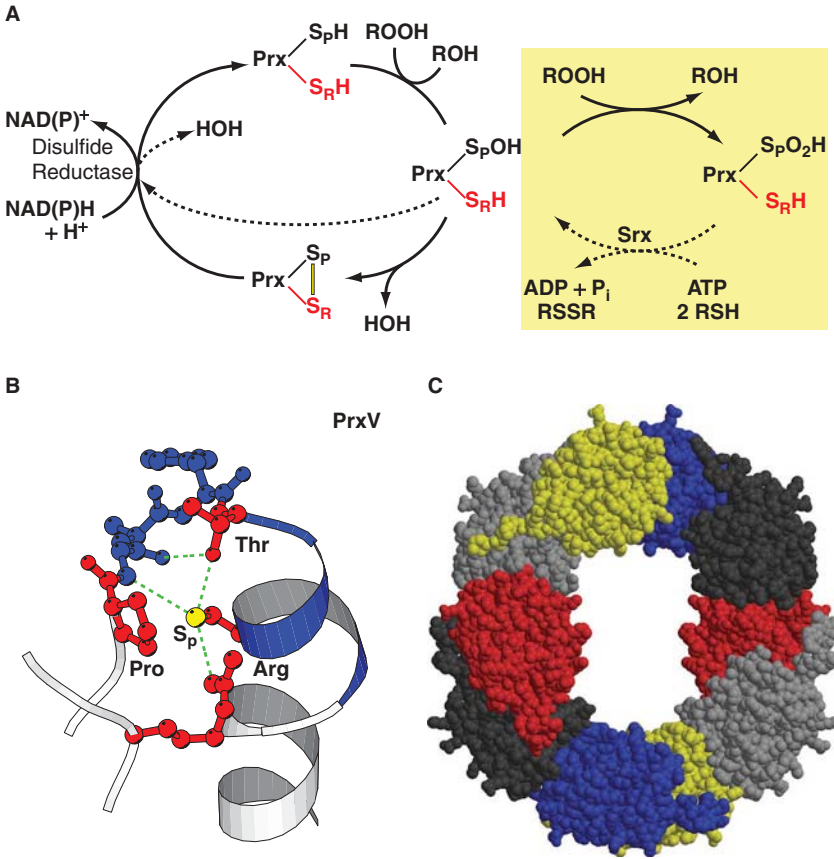


Figure 3.3. Reaction cycle and structural attributes of the peroxiredoxins. In panel (A), the peroxidatic cysteine of the peroxiredoxin (Prx) is depicted as a thiol (S_pH) or sulfenic acid (S_pOH), or in a disulfide with the resolving cysteine (S_RH). Colors distinguish the cysteine residues from different subunits of the dimer in the typical 2-Cys peroxiredoxins, and the bar between sulfurs represents the intersubunit disulfide bond (intrasubunit in the case of the atypical 2-Cys peroxiredoxins). The disulfide reductase system that regenerates the active peroxiredoxin varies with the organism and specific peroxiredoxin but is thioredoxin reductase and thioredoxin in many cases. The pathway indicated by the dashed line can be taken by 1-Cys (no resolving cysteine) or 2-Cys peroxiredoxins bypassing disulfide bond formation. The pathway in the yellow box represents regulation by oxidative inactivation (toward the right) and reactivation of hyperoxidized 2-Cys peroxiredoxins via sulfiredoxin (Srx, toward the left). Panel (B) illustrates the conserved, reduced peroxiredoxin active site (shown using the prototypic PrxV structure, PDB code 1HD2) and the conserved hydrogen bonding network (dotted lines). The active site residues conserved in all peroxiredoxins (proline, threonine, cysteine, and arginine) are colored red, and the loop–helix region is colored blue. In panel (C), the (α_2)₅ decamer (from the X-ray crystal structure of an oxidized bacterial peroxiredoxin, AhpC, solved at 2.5 Å resolution; PDB code 1YEP) is shown in a space filling representation, with each chain depicted in a different color. Panel (B) is reprinted with permission from *Trends in Biochemical Sciences*. Copyright © 2002 Elsevier Science Ltd.

Oligomeric properties of peroxiredoxins studied by gel filtration chromatography, light scattering, or analytical ultracentrifugation approaches have shown them to exist in solution as dimeric, decameric, or intermediate-sized species, with their oligomeric state influenced by such factors as ionic strength, pH, magnesium or calcium concentrations, and/or redox state. Higher order multimeric structures may also be formed under some conditions (especially seen by electron microscopy). A direct link between redox state and oligomeric state was established for a bacterial peroxiredoxin, AhpC, using analytical ultracentrifugation studies, and this linkage may apply to other typical 2-Cys peroxiredoxins as well. It should first be noted that changes in redox state during the catalytic cycle are accompanied by significant structural changes in typical 2-Cys peroxiredoxins around the two active site cysteine residues; in the absence of a disulfide bond, the respective thiol groups are pointed away from one another (sulfurs ~ 13 Å apart) in the fully folded form of the active site, requiring all regions illustrated in blue in Fig. 3.4 to rearrange to permit disulfide bond formation (where sulfurs are ~ 2 Å apart). Interestingly, reduction of the disulfide bond of AhpC stabilizes the decameric form of the protein, as do mutations or modifications that prevent disulfide bond formation. Hence, disulfide bond formation, which locally unfolds regions around the active site, promotes dissociation of the decamer

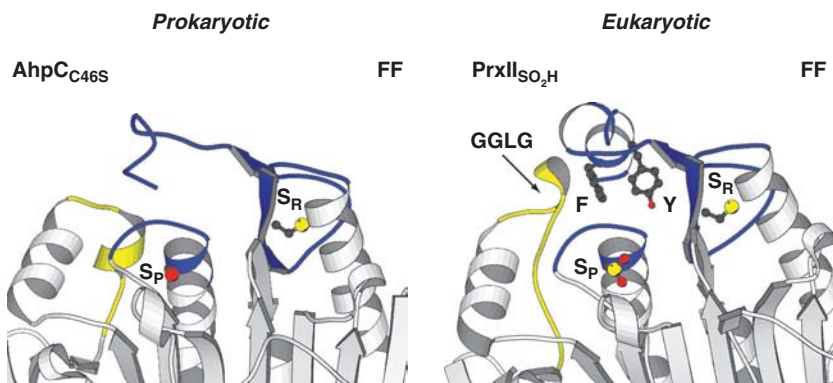


Figure 3.4. Structural differences between robust and sensitive 2-Cys peroxiredoxins. Ribbon diagrams of the peroxidatic active site region of robust (prokaryotic, PDB code 1N8J) and sensitive (eukaryotic, PDB code 1QMV) 2-Cys peroxiredoxin structures in their fully folded (FF) conformations. Shown in yellow are the 3_{10} helices followed by the conserved GGLG insertion in the eukaryotic peroxiredoxins, and identified in blue are the regions that undergo conformational rearrangements during catalysis (as the redox state of the active site changes). S_P and S_R represent the sulfur groups of the peroxidatic and resolving cysteine residues, respectively (although “ S_P ” in the left panel is actually a red oxygen in this mutant). Note the extra helix containing conserved tyrosine and phenylalanine residues in the eukaryotic peroxiredoxin. This figure depicts the increased interactions (and thus lower B-factors) in the region of the active site loop and helix of the eukaryotic peroxiredoxin (around S_P) relative to that of the prokaryotic peroxiredoxin.

into component dimers or intermediate species through its disruptive influence on the dimer–dimer interface adjacent to the active site. Recent studies have also connected the decameric arrangement of AhpC with enhanced peroxide reactivity as a result of this mutual stabilizing interaction between the reduced (fully folded) active site and the dimer–dimer interface.

3.1.C3 Roles for Peroxiredoxins in Regulating Redox-Dependent Cell Signaling: The Catalytic Sulfenic Acid (R-SOH) as a Peroxide-Sensitive Switch

In the past decade, it has become increasingly clear that H_2O_2 and other oxidants are produced not only through normal aerobic processes but also as a result of the activation of various cell-surface receptors. Thus, H_2O_2 is now recognized to be an important intracellular messenger that likely acts on reactive cysteinyl residues within a select group of proteins to modulate their function. As the catalytic activity of peroxiredoxins serves to remove H_2O_2 , these enzymes would be expected to act as regulators of H_2O_2 signaling; indeed, altered expression of peroxiredoxins in cells has been shown to affect the intracellular level of H_2O_2 produced in cells stimulated with epidermal growth factor, platelet-derived growth factor, or tumor necrosis factor- α (TNF- α). Of special interest, however, is the finding that the reverse is also true— H_2O_2 is a regulator of peroxiredoxin function; even at low micromolar levels of H_2O_2 , some eukaryotic peroxiredoxins lose activity through hyperoxidation of the active site cysteine during turnover (yellow box in Fig. 3.3A). Although this oxidation step, which produces a cysteine sulfenic acid (R-SO₂H), was originally considered to be biologically irreversible, recently identified enzymes (sulfiredoxin and sestrins) have been shown to catalyze recovery of activity for at least some of the typical 2-Cys peroxiredoxins (see Section 3.4.C). Thus, the sulfenic acid generated during normal catalysis in peroxiredoxins acts as a peroxide-sensitive switch, reversibly regulating activity of susceptible peroxiredoxins as a function of H_2O_2 concentration.

Detailed comparisons of eukaryotic and prokaryotic peroxiredoxin enzymes have elucidated the structural basis for the redox sensitivity of eukaryotic, but not so much prokaryotic, members of the peroxiredoxin family. The susceptibility of peroxiredoxins toward hyperoxidation appears to have evolved in higher organisms through the addition of two conserved structural elements in the vicinity of the active site, as illustrated in Fig. 3.4. These structural elements pack well around the peroxidatic cysteine and loop residues of the fully folded active site and may disfavor disulfide bond formation through this added stability, a factor that would also be expected to lead to the persistence of the sulfenic acid form of the peroxidatic cysteine and thus promote the inactivation pathway. The evolution of this peroxide sensitivity in eukaryotic peroxiredoxins may have been necessary to allow for H_2O_2 -linked cell signaling, as the inactivated peroxiredoxins would no longer serve to dampen the receptor-mediated “burst” in H_2O_2 concentration. This would allow peroxiredoxins to act as “floodgates” for H_2O_2 , allowing levels to rapidly increase following the initial inactivation of the abundant peroxiredoxins in the region of the signaling events. Another interpretation of the functional role for this sensitivity toward peroxide was

derived from the multimerization that was shown *in vitro* to ensue as a result of hyperoxidation, enhancing the ability of peroxiredoxins to act as chaperones to help cells recover from oxidative stress.

3.1.C4 Other Peroxiredoxin Regulatory Mechanisms and Protein-Protein Interactions PrxI and PrxII activity can also be inhibited by phosphorylation mediated by cyclin-dependent kinases (e.g., Cdc2 kinase). In the case of PrxI, phosphorylation of the protein was observed in mitotic cells, but not in interphase cells, probably because this is the stage when the nuclear envelope breaks down and Cdc2 gains access to cytosolic proteins. These results suggest that Cdc2-dependent phosphorylation of peroxiredoxins might allow for the accumulation of H₂O₂ critical to the progression of normal cell division.

Another mechanism that may regulate peroxiredoxin activity is proteolysis, observed primarily during purification procedures or as a result of *in vitro* treatment with calpain; interestingly, removal of C-terminal residues of sensitive peroxiredoxins imparts resistance toward hyperoxidation by peroxides, demonstrating the potential interplay between various regulatory mechanisms. Glutathionylation may also occur *in vivo* and affect peroxiredoxin activity. An increasing number of studies are also showing that peroxiredoxins may interact with a considerable number of other cellular proteins. Various peroxiredoxins have been demonstrated to interact with cyclophilin, c-Abl kinase, glutathione-S-transferase-pi, macrophage migration inhibitory factor, natural killer cells, Myc, and yeast signaling proteins Sty1 and Yap1, all of which may have functional consequences for the biological roles peroxiredoxins play in cells. In fact, in yeast, thiol-based peroxiredoxin and glutathione peroxidase-like peroxidases act as exquisitely sensitive peroxide sensors and oxidants of signaling proteins and transcription factors. Thus, these widespread, abundant peroxidases play diverse and important roles in controlling oxidant levels in many organisms, with a potential to contribute both protective, antioxidant activity and a complex, but fine-tuned control over cell signaling processes.

SELECTED REFERENCES

1. Hofmann, B., Hecht, H.-J., and Flohé, L. (2002). Peroxiredoxins. *Biol. Chem.* 383:347–364.
2. Wood, Z.A., Schroder, E., Harris, J.R., and Poole, L.B. (2003). Structure, mechanism and regulation of peroxiredoxins. *Trends Biochem. Sci.* 28:32–40.
3. Wood, Z.A., Poole, L.B., and Karplus, P.A. (2003). Peroxiredoxin evolution and the regulation of hydrogen peroxide signaling. *Science* 300:650–653.
4. Copley, S.D., Novak, W.R., and Babbitt, P.C. (2004). Divergence of function in the thioredoxin fold suprafamily: evidence for evolution of peroxiredoxins from a thioredoxin-like ancestor. *Biochemistry* 43:13981–13995.
5. Rhee, S.G., Chae, H.Z., and Kim, K. (2005). Peroxiredoxins: a historical overview and speculative preview of novel mechanisms and emerging concepts in cell signaling. *Free Radic. Biol. Med.* 38:1543–1552.

3.1.D Alkyl Hydroperoxide Reductases

LESLIE B. POOLE

*Department of Biochemistry and Center for Structural Biology, Wake Forest University
School of Medicine, Winston-Salem, North Carolina*

Like all living organisms exposed at least transiently to aerobic environments, bacteria require protective systems that prevent, intercept, or repair damage caused by ROS. In addition to endogenous generation of ROS through metabolic processes, pathogenic bacteria face another threat: the oxidative burst of host phagocytes. With the production of $O_2^{\cdot-}$, H_2O_2 , and hypochlorous acid to add to the arsenal of weapons, phagocytes combat invading bacteria, particularly in the battlefield of the endosome. In turn, both bacteria and the host respond to the ROS generated in order to protect themselves. In many bacteria, this response leads to the activation of several global transcriptional regulators, SoxR and OxyR, that orchestrate the enhanced expression of protective proteins. As a direct sensor of H_2O_2 through reactive cysteinyl residues, OxyR from *E. coli* or *Salmonella typhimurium* activates transcription, and thereby upregulates expression of at least nine antioxidant proteins, including glutathione reductase, glutaredoxin 1, thioredoxin 2, and HPI (KatG) catalase. Traditional bacterial genetic approaches utilizing a bacterial mutant expressing a constitutively active form of OxyR (exhibiting high tolerance to external oxidants) allowed for the majority of the targets to be identified at an early stage through comparative proteomics, and the analysis of accentuated protein spots on two-dimensional (2D) isoelectric focusing and SDS polyacrylamide gels of the bacterial proteins expressed at higher levels in the OxyR constitutive mutant.

With these and subsequent cloning approaches, two proteins have been identified among the OxyR-regulated gene products, which together are responsible for an activity that had previously been unrecognized in bacterial systems: the detoxification of alkyl or aryl hydroperoxides. These proteins, initially designated C-22 and F-52a from their approximate positions on the 2D gels, are expressed from the *ahpC* and *ahpF* genes positioned proximal to one another (designated the *ahpCF* locus) in the *E. coli* and *S. typhimurium* genomes, and located downstream of an OxyR-recognition site within the promoter region of *ahpC*.

3.1.D1 *AhpF Is a Flavoprotein Disulfide Reductase that Recycles AhpC, and AhpC Is a Protein that Reduces Peroxide Substrates*

Both components of the bacterial alkyl hydroperoxide reductase system, AhpF and AhpC, are required to catalyze the pyridine nucleotide-dependent reduction of hydroperoxide substrates (Fig. 3.5). Data from several of the better studied alkyl hydroperoxide reductase systems indicate a strong preference, in some cases absolute, for NADH over NADPH. Whereas AhpC is a prototypic representative of a very large family of enzymes (the peroxiredoxins) distributed widely across many, if not all, biological species, AhpF homologs are restricted to eubacteria (many, though not all, bacteria express them). AhpF appears to have evolved as a dedicated AhpC reductase, replacing thioredoxin reductase and thioredoxin, which recycle most other peroxiredoxin

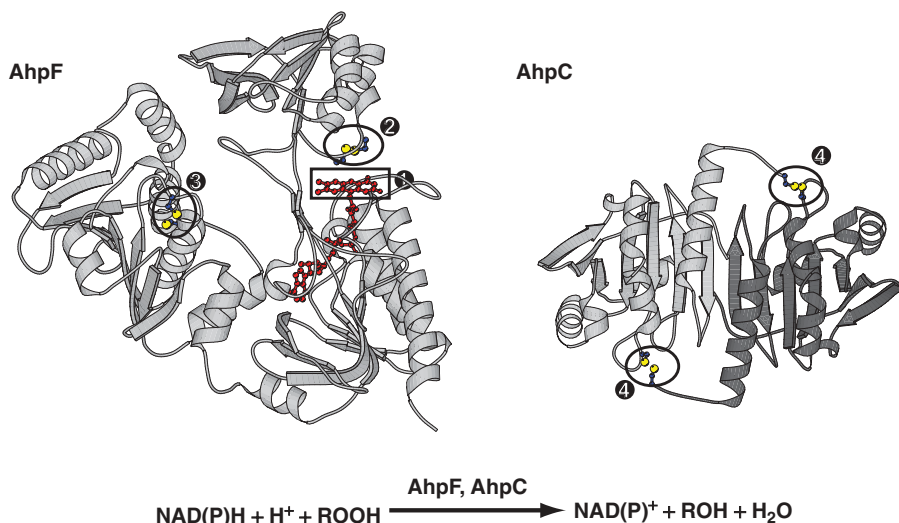


Figure 3.5. Alkyl hydroperoxide reductase proteins, AhpF and AhpC, catalyze hydroperoxide reduction through four protein-associated redox centers. Numbers indicate the location and order of reaction of redox centers in the two protein structures (depicted as ribbons, except for the ball and stick representations of atoms and bonds for the redox centers). A single monomer from the dimeric crystal structure of AhpF (PDB code 1HYU) is shown with the thioredoxin reductase-like pyridine nucleotide and flavin binding domains, and the N-terminal redox domain. A dimer of the oxidized AhpC (from the decameric structure, PDB code 1YEP, with monomers) is shown with two apparently equivalent active sites where hydroperoxide reduction occurs. The box labeled “1” highlights the isoalloxazine ring of the flavin, while circles 2 through 4 indicate the location of redox-active disulfide/dithiol centers.

homologs. As the process of AhpC recycling involves the reduction of a disulfide bond formed during its catalysis of peroxide reduction, AhpF (Section 3.1.C), like thioredoxin, possesses a disulfide/dithiol redox within a Cys-X-X-Cys center, which acts as the direct electron donor in this process. Two additional redox centers in AhpF, another disulfide/dithiol center and a tightly bound FAD cofactor, also mediate the transfer of electrons from NADH to the AhpC substrate.

Sequence-based analyses and biochemical studies of engineered truncated and chimeric forms of *S. typhimurium* AhpF, followed later by crystallographic studies, revealed the modular construction and large motions within AhpF that support its ability to reduce the disulfide bond of a large protein substrate. Like bacterial thioredoxin reductase (35% identical in amino acid sequence with the C-terminal region of AhpF), one domain of AhpF binds FAD tightly while another possesses a Cys-X-X-Cys redox center as well as a pyridine nucleotide binding site (Fig. 3.5); rotation of the pyridine nucleotide binding domain with respect to the flavin binding domain alternates the environment of the isoalloxazine ring of the flavin from a position where it can pick up electrons from the pyridine nucleotide (in a stacking interaction with the nicotinamide ring) on the one hand, to an alternative position where it can deliver

electrons to the Cys-X-X-Cys redox center (center 2 in Fig. 3.5). Also accompanying the rotation of the pyridine nucleotide domain to a position where the nicotinamide and isoalloxazine rings can interact is the movement of the now-reduced cysteinyl center to a more exposed position where, in thioredoxin reductase, it can interact with its protein substrate, oxidized thioredoxin. AhpF also has another ~200 amino acid redox domain at the N terminus containing the other Cys-X-X-Cys redox center (the direct electron donor to AhpC, center 3 in Fig. 3.5) within a double thioredoxin-like fold. This N-terminal domain thus behaves functionally like a covalently attached thioredoxin, assuming one position to pick up electrons from the more C-terminal dithiol center, then rotating to a more exposed position where it can interact with AhpC for the next step in electron transfer.

As expanded upon in the peroxiredoxin section (Section 3.1.C), AhpC is the direct electron donor to the hydroperoxide substrates, forming one water molecule and the corresponding alcohol (or a second water). This cysteine thiol-based chemistry initially generates an oxidized, sulfenic acid (R-SOH) form of the active site, peroxidatic cysteine, which then condenses to form a disulfide bond with the thiol group of the other conserved cysteine residue of a partner subunit, the resolving cysteine. This intersubunit disulfide bond is then reduced by AhpF to activate AhpC for another round of catalysis with peroxides. Because AhpC (minimally) forms head-to-tail dimers and the oxidized active site includes residues from both subunits, there are two symmetric peroxidatic active sites per dimer (Fig. 3.5).

3.1.D2 Alkyl Hydroperoxide Reductase in *E. coli* Is Essential for Maintaining Low Levels of Endogenous H₂O₂

Peroxide defense mechanisms in *E. coli* include two catalases, the AhpC/AhpF system, and two other distant relatives of AhpC—Tpx and BCP. A poorly characterized glutathione peroxidase homolog, BtuE, may also contribute to peroxide reduction in these bacteria. As shown by multiple gene knockout mutants of *E. coli*, *ahpC* is essential for maintaining low, endogenous levels of H₂O₂, whereas higher concentrations of H₂O₂ (above ~5 μM) require the presence of catalase for protection of cells. Thus, the highly expressed alkyl hydroperoxide reductase system present in many bacteria plays an important role in oxidant defense in these organisms.

SELECTED REFERENCES

1. Christman, M.F., Morgan, R.W., Jacobson, F.S., and Ames, B.N. (1985). Positive control of a regulon for defenses against oxidative stress and some heat-shock proteins in *Salmonella typhimurium*. *Cell* 41:753–762.
2. Storz, G., and Imlay, J.A. (1999). Oxidative stress. *Curr. Opin. Microbiol.* 2:188–194.
3. Seaver, L.C., and Imlay, J.A. (2001). Alkyl hydroperoxide reductase is the primary scavenger of endogenous hydrogen peroxide in *Escherichia coli*. *J. Bacteriol.* 183:7173–7181.
4. Poole, L.B. (2005). Bacterial defenses against oxidants: mechanistic features of cysteine-based peroxidases and their flavoprotein reductases. *Arch. Biochem. Biophys.* 433:240–254.

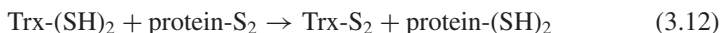
3.2 THE THIOREDOXIN SYSTEM

ARNE HOLMGREN

Department of Medical Biochemistry and Biophysics, Karolinska Institutet, Stockholm, Sweden

3.2.A Thioredoxin

Thioredoxin is a small redox protein (usually around 12 kDa) with two redox-active cysteine residues in its active site within the conserved sequence: -Cys-Gly-Pro-Cys-. Thioredoxin exists either in the reduced dithiol form or in the oxidized disulfide form. The function of thioredoxin as a superior thiol reductant is based on the fast reaction between reduced thioredoxin and disulfide substrates. This generates oxidized thioredoxin, which is reduced by NADPH and the FAD-containing enzyme thioredoxin reductase as shown in Eqs. (3.12) and (3.13):



Together, NADPH, thioredoxin reductase, and thioredoxin comprise the thioredoxin system, which is present in all living cells from unicellular prokaryotes like Archebacteria to multicellular eukaryotes like humans. Originally, thioredoxin was purified from *E. coli* in 1964 as a hydrogen (or electron) donor for ribonucleotide reductase, an enzyme that is essential for DNA synthesis by providing deoxyribonucleotides. Realization that the thioredoxin system is a general cellular protein disulfide reductase led to the identification of a large number of functions for thioredoxin in different biological systems. The thioredoxin enzyme system is responsible for maintaining a reducing environment in the cytosol of all cells with a low redox potential. A similar function is also provided by GSH, glutaredoxins, and NADPH-dependent glutathione reductase in most organisms. Other thioredoxin functions (Table 3.1) involve regeneration of reduced forms of methionine sulfoxide reductases and peroxiredoxins, light regulation of photosynthetic enzymes in plant chloroplasts, and redox regulation of enzymes and transcription factors via thiol redox status control. In mammalian cells, thioredoxin is a stress-inducible antioxidant factor and a secreted cytokine and chemokine for monocytes, macrophages, neutrophils, and T cells.

3.2.A1 Thioredoxin Isoforms Human thioredoxins exist in the cytosol/nucleus (hTrx1) and mitochondria (hTrx2) and these are encoded by separate genes. Both Trx1 and Trx2 are essential and their knockout causes embryonic lethality in mice. Cytosolic hTrx1 has three additional structural cysteine residues (Cys62, Cys69, and Cys73) apart from the active site Cys32 and Cys35 (Fig. 3.6). The additional cysteine residues control activity of hTrx1 by their redox state; for example, decreased catalytic activity accompanies the formation of an additional disulfide between Cys63 and Cys69. Glutathionylation of Cys73 as well as nitrosylation of Cys69

TABLE 3.1. Functions of Thioredoxin (Selected Examples)

Organism	Function
M13 phage infected <i>E. coli</i>	Essential for filamentous phage assembly
T7 phage infected <i>E. coli</i>	Essential for T7 phage DNA replication: reduced thioredoxin in complex with phage T7 DNA polymerase gives high activity and processivity
Bacteria, yeast, plants, mammals	Electron donor for ribonucleotide reductase: dNTPs → DNA synthesis
Bacteria, yeast, plants, mammals	Electron donor for methionine sulfoxide reductase: MetSO → Met
Plants	Regulation of chloroplast enzymes via light and ferredoxin–thioredoxin reductase
Mammals	Electron donor for peroxidoredoxins: H ₂ O ₂ → H ₂ O
Mammals	Reduced thioredoxin prevents apoptosis: inactivates ASK1
Mammals	Control of NF _κ B, API, p53, and other transcription factors mediated by APE/Ref-1 in nucleus
Mammals	General thiol redox control of protein activity via reversible disulfide formation
Mammals	Secreted cocytokine and chemokine for immune cells
Mammals	Secreted anti-inflammatory factor in oxidized form
Mammals	Secreted as Trx80 or truncated thioredoxin: a monocyte growth factor yielding a Th1 response via IL12

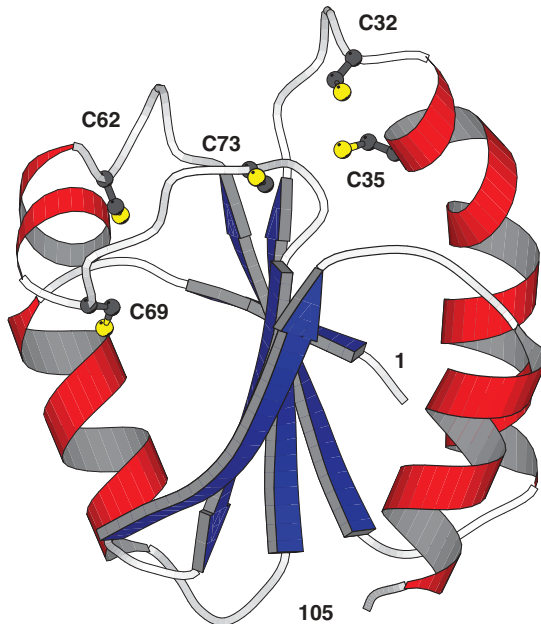


Figure 3.6. Structure of human thioredoxin 1 in reduced form. The active site cysteines (Cys32 and Cys35) are shown as well as the structural cysteine residues Cys62, Cys69, and Cys73. The N-terminal Met is residue 1 and the C terminus is residue 105. Figure generated from PDB file 1ERT.

have been reported to affect activity. Oxidative stress leads to induction of Trx1 synthesis and is followed by secretion by a leaderless pathway. Monocytes/macrophages generate a truncated form of thioredoxin (Trx80) by proteolytic cleavage at position 80 or 84. Levels of hTrx1 and Trx80 are detected in plasma. Secreted hTrx1 was discovered and cloned as ADF (adult T-cell leukemia derived factor required for growth of virally transformed T-cell leukemia cells). Human Trx1 was also purified as a T-T'cell hybridoma factor required for growth of B-cell tumor cells. Inflammation, virus infection, and cancer lead to a marked increase in the normal level of hTrx1 (around 25 ng/mL) in plasma. Trx80, identified as an eosinophilic cytotoxicity enhancing factor, is also a mitogenic agent for monocytes, inducing production of IL12, which may give rise to a T helper cell 1 (Th1) type of immune response.

In most gram-negative bacteria like *E. coli*, or fungi like *S. cerevisiae*, thioredoxin is not essential for life since GSH and glutaredoxins can act as alternative electron donors for essential enzymes like ribonucleotide reductase. In contrast, in gram-positive organisms like *Bacillus subtilis*, which lack GSH, the thioredoxin system is essential.

3.2.A2 Thioredoxin Structure and Mechanism Three-dimensional structures of both oxidized and reduced cytosolic thioredoxin from *E. coli* and human have been determined by X-ray crystallography and multidimensional nuclear magnetic resonance (NMR) in solution. The thioredoxin fold, which is a globular $\alpha\beta$ sandwich structure, was first observed in oxidized thioredoxin from *E. coli* in 1975 and subsequently in a large number of proteins. A central β -sheet core is surrounded by three α -helices (Fig. 3.6). The active site cysteine residues are located on a protrusion of the thioredoxin molecule and in the beginning of an α -helix. In reduced thioredoxin, the sulfur atom of the N-terminally located cysteine residue (Cys32) is solvent exposed and its thiolate group is an effective nucleophile with a low pK_a value. A unique conserved *cis*-proline residue (Pro76) in *E. coli* thioredoxin is present in all thioredoxins and is adjacent to the active site, which is surrounded by a flat hydrophobic surface, required for interactions with other proteins. Thioredoxin fold proteins include protein disulfide isomerase with four thioredoxin domains, two of which have Cys-Gly-His-Cys active sites. Other members of the protein disulfide isomerase family (25 members in humans) of proteins are located in the endoplasmic reticulum or on the cell surface and are involved in protein folding and generation of native disulfide bonds in secreted proteins. Other redox-active protein members of the thioredoxin fold family are glutaredoxins, glutathione peroxidases, and glutathione *S*-transferases.

Reduced thioredoxin acts to directly reduce protein disulfides via fast thiol–disulfide interchange reactions (Eq. (3.12)). Reduced thioredoxin initially docks non-covalently to a target protein via a hydrophobic interaction surface and hydrogen bonds between thioredoxin backbone residues and the substrate protein. This is followed by nucleophilic attack of the N-terminal active site thiolate on the target disulfide in a thiol–disulfide exchange reaction, resulting in a transient protein–protein mixed disulfide intermediate. Intramolecular attack by the C-terminally located thiolate (Cys35) results in cleavage of the disulfide and formation of oxidized thioredoxin and reduced target protein. Thioredoxin can utilize its hydrophobic interaction surface to dock to

other proteins and has been shown to have molecular chaperone activity. Generally, thioredoxin reacts between four and five orders of magnitude faster than dithiothreitol with protein disulfides and is present in cells at 1–20 μM concentration.

A stable 1:1 complex between the reduced *E. coli* Trx thioredoxin and phage T7 DNA polymerase has been detected. Binding of thioredoxin endows the phage-induced DNA polymerase with high processivity (high activity by strong binding to template DNA and a large number of catalytic cycles without dissociation). In human cells, complexes between reduced thioredoxin and ASK1 (apoptosis signaling kinase) prevent this mitogen activated kinase kinase kinase from signaling the apoptosis response; however, ASK1 is released from the complex when thioredoxin becomes oxidized.

3.2.A3 Thiol Redox Control Thioredoxin may control the activity of enzymes, receptors, and transcription factors via its protein disulfide reductase activity. In plants, photosynthetic enzymes are controlled by specific thioredoxins via light and the unique chloroplast enzyme, ferredoxin–thioredoxin reductase. Isoforms of thioredoxin, Trx_m and Trx_f , are specific for target enzymes like malate dehydrogenase and fructose biphosphatase dehydrogenase, respectively. Plants have an unusually high number of thioredoxin genes involved in photosynthetic regulation. In mammalian cells, regulation of transcription factor activity in the nucleus is important via interaction of thioredoxin with the apyrimidinic-apurinic endonuclease-1-redox factor-1 (APE/Ref-1). NF_κB , AP1, and p53 are among the many important mammalian transcription factors regulated by the thioredoxin system via APE/Ref-1. Upon stimulation of cells, thioredoxin moves to the nucleus together with thioredoxin reductase to serve functions in gene regulation (Table 3.1). In cells, thioredoxin is present predominantly in the reduced form, but under oxidative stress conditions, the oxidized form may dominate, possibly promoting the reverse reactions and generating disulfides.

3.2.B Thioredoxin Reductase

Thioredoxin reductase is an FAD-containing enzyme, which catalyzes the reduction of oxidized thioredoxin to its reduced form by NADPH (Eq. (3.14)).



Thioredoxin reductase exists in all living cells and is part of the thioredoxin system. Thioredoxin reductase is the only enzyme able to reduce thioredoxin by NADPH. Thioredoxin, in turn, has numerous essential functions in cells (see Section 3.2.A). There is a remarkable diversity in structure and mechanism between thioredoxin reductases from prokaryotes like bacteria, eukaryotes like yeast or plants on the one hand, and vertebrates and mammals on the other hand. The first have a low molecular weight dimeric enzyme with an M_r of 70 kDa. This enzyme has been best characterized from *E. coli* and is typically highly specific for its homologous

TABLE 3.2. Substrates for Mammalian Thioredoxin Reductase

Trx-S ₂ from many species
Protein disulfide isomerase
Ebselen
NK-lysin
Lipoic acid
Selenite
Selenocystine
Selenodiglutathione
Glutathione peroxidase
H ₂ O ₂
15-HPETE
S-nitrosoglutathione
Dehydroascorbic acid
Ascorbic acid radical
Mitochondrial glutaredoxin (Grx2)

oxidized thioredoxin and will not react with, for example, human thioredoxin. In contrast, thioredoxin reductases from mammals, which are encoded by three separate genes, are much larger in size, have broad substrate specificity, and are selenoenzymes (Section 3.7.A). They are all homologous to glutathione reductase with a C-terminal extension containing 16 residues with the active site sequence -Cys-Sec-Gly-OH. The penultimate selenocysteine (Sec) residue in the enzyme is essential for its function and encoded by a TGA stop codon in DNA. The mammalian thioredoxin reductases have a wide range of substrates (Table 3.2) including lipid hydroperoxides. Knockout experiments show that both the mitochondrial and the cytosolic enzymes are essential for embryonic development in mice.

A special ferredoxin–thioredoxin reductase is found in the chloroplasts of plants and uses electrons from light and ferredoxin, which are transferred to reduce thioredoxins, which are target-enzyme specific. The reduced thioredoxin controls the activity of specific photosynthetic enzymes like fructose biphosphatase and malate dehydrogenase by light using strategically placed disulfides. These enzymes are active as dithiol forms and inactive in disulfide form in the dark.

3.2.B1 Low Molecular Weight Thioredoxin Reductase This enzyme, best characterized from *E. coli*, has a low K_M value of 1.2 μM for thioredoxin and, upon reduction by NADPH, undergoes a domain rotation to expose the -Cys-Ala-Thr-Cys- active site located in the FAD domain. Electrons are transferred to FAD and to the redox-active disulfide generating a dithiol. The enzyme is NADPH-specific and has one FAD per 35 kDa subunit.

3.2.B2 High Molecular Weight Thioredoxin Reductases from Mammals Mammalian thioredoxin reductases are strikingly different from the smaller bacterial enzymes and are selenoproteins encoded by three different genes. Apart from separate

enzymes in the cytosol (TrxR1) and mitochondria (TrxR2) with a very complex pattern of splice variants, a third enzyme, thioredoxin glutathione reductase (TGR) containing thioredoxin reductase with an N-terminal monothiol glutaredoxin domain extension, is present predominantly in testis. The selenocysteine residue is conserved in all enzymes, which are structurally built from a glutathione reductase scaffold and with a C-terminal extension of 16 residues (Fig. 3.7). The terminal residues are -Gly-Cys-Sec-Gly, where Sec is selenocysteine that is absolutely conserved. The mechanism of the enzyme is very different from the bacterial thioredoxin reductases and involves electron transfer from NADPH via FAD to the N-terminal redox-active disulfide and then transfer to the opposite subunit, where a Cys-Sec selenenylsulfide bridge in the oxidized protein is reduced to a selenolthiol (Fig. 3.7). This C-terminal selenolthiol is also in the active site, where thioredoxin and other substrates are reduced. Replacement of the selenocysteine residue with cysteine yields an enzyme with a 100-fold lower catalytic rate. Human and mammalian thioredoxin reductase substrates (Table 3.2) include not only thioredoxins but also selenium derivatives, protein disulfide isomerase, lipid hydroperoxides and H_2O_2 , *S*-nitrosoglutathione, as

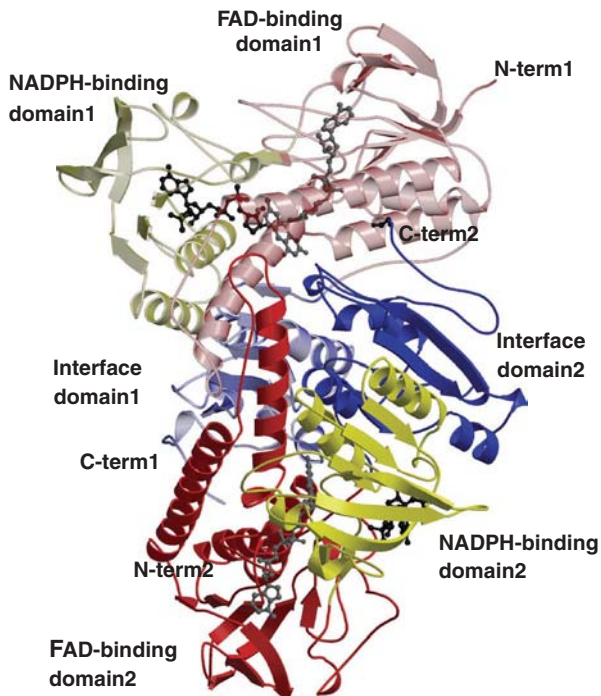


Figure 3.7. Three-dimensional structure of rat thioredoxin reductase 1 determined by X-ray crystallography. Ribbon representation of TrxR1 dimer. The two subunits are shown in light and dark color, respectively. The Sec residue is located in the C terminus (C-term1 and C-term2). Bound FAD and NADP shown as ball and stick models. Reproduced from *Proc. Natl. Acad. Sci. USA* 98: 9533–9538, (2001) with permission.

well as dehydroascorbic acid and ascorbic acid radical. The thioredoxin reductase enzymes are of central importance to the role of selenium in biology, since they both catalyze reduction of selenium compounds like selenite and are themselves dependent on selenium for essential functions in DNA synthesis or redox regulation via thioredoxin.

Clinical drugs used to treat cancer or inflammatory disorders often target the highly reactive selenocysteine residue in the C terminus of the enzyme. Such drugs include nitrosourea compounds, gold thioglucose, *cis*-platinum derivatives, and other clinically used drugs. The modified thioredoxin reductase or selenium-compromised thioredoxin reductase may directly induce apoptosis in cancer cells by yet not completely understood mechanisms.

SELECTED REFERENCES

1. Holmgren, A. (1985). Thioredoxin. *Annu. Rev. Biochem.* 54:237–271.
2. Arner, E.S.J., and Holmgren, A. (2000). Physiological functions of thioredoxin and thioredoxin reductase. *Eur. J. Biochem.* 267:6102–6109.
3. Masutani, H., Oeda, S., and Yodoi, J. (2005). The thioredoxin systems in retroviral infection and apoptosis. *Cell Death and Differentiation* 12:991–998.
4. Holmgren, A., and Björnstedt, M. (1995). Thioredoxin and thioredoxin reductase. *Methods Enzymol.* 252:199–208.
5. Arnér, E.S.J., Sarioglu, H., Lottspeich, F., Holmgren, A., and Böck, A. (1999). High level expression in *Escherichia coli* of selenocysteine-containing rat thioredoxin reductase utilizing gene fusions with engineered bacterial-type SECIS elements and co-expression with SelA, SelB and SelC genes. *J. Mol. Biol.* 292: 1003–1016.
6. Sun Q.-A. and Gladyshev, V.N. (2002). Redox regulation of cell signaling by thioredoxin reductases. *Methods Enzymol.* 47: 451–461.

3.3 THE GLUTATHIONE SYSTEM

MARJORIE F. LOU

*Redox Biology Center and Department of Veterinary and Biomedical Sciences,
University of Nebraska, Lincoln, Nebraska*

GSH is one of the most important antioxidants that occur in almost all organisms. This low molecular weight thiol-containing compound is abundantly present in the tissues vulnerable to oxidative stress, such as red blood cells, the lens, and the lung tissues. A major function of GSH is to protect cells from oxidative stress. It works with GSH peroxidase to efficiently remove intracellular H₂O₂. This process protects cellular components from oxidative modifications and GSH is converted in the process to its oxidized product, GSSG. A specific enzyme called glutathione reductase can reduce GSSG to GSH using NADPH as its electron donor, thus replenishing the GSH pool.

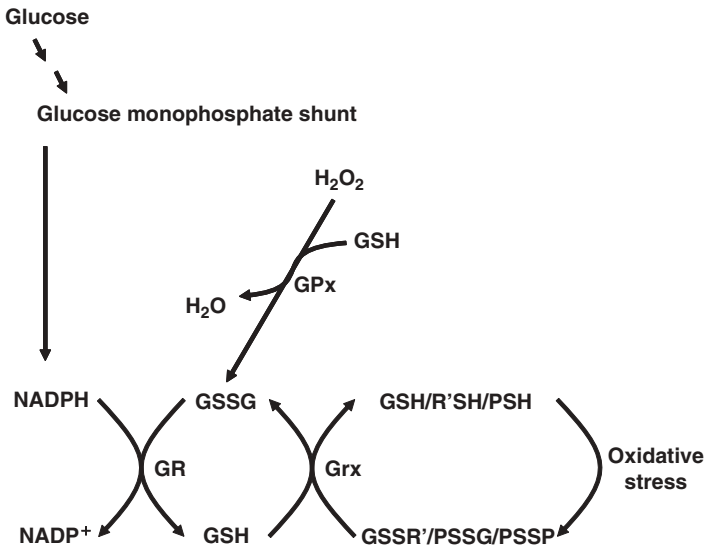
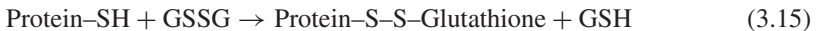


Figure 3.8. The glutathione system. Cells are protected from oxidative damage using GSH to detoxify H₂O₂ via glutathione peroxidase (GPx), using GSH-dependent glutaredoxin (Grx) to dethiolate protein disulfides or glutathionylated proteins or nonprotein thiols (R'). The decreased GSH pool is enriched by glutathione reductase (GR) with NADPH as the electron donor generated from the glucose monophosphate shunt. Used with permission from Lou (2003), *Prog. Retin. Eye Res.* 22:657–682.

GSSG can react with protein thiols to form protein–glutathione mixed disulfides in a process known as glutathionylation or protein thiolation (Eq. (3.15)). A GSH-dependent enzyme called thioltransferase, or glutaredoxin, is responsible for the de-thiolation reaction. Glutathionylation can either inactivate or activate enzymes. This regulated and reversible process is used by cells to modulate certain metabolic pathways and in cell signaling.



The glutathione system, depicted in Fig. 3.8, often functions in parallel with the thioredoxin system in regulating redox homeostasis in the cell. The two systems may work synergistically and the possibility of crosstalk between them has received a lot of attention.

3.3.A Glutathione Reductase

Glutathione reductase is an enzyme belonging to the flavoprotein disulfide oxidoreductase family. It reduces GSSG to GSH at the expense of NADPH, which is provided via the glucose monophosphate shunt. The reaction of converting GSSG to GSH is

fast and irreversible, thus the enzyme can provide cells with a high intracellular GSH/GSSG ratio (see Eq. (3.16)). Glutathione reductase was first discovered in 1930s in erythrocytes and yeast.



3.3.A1 Structure and Reaction Mechanism Glutathione reductases from different organisms all display a high affinity for their substrates (i.e., GSSG) or mixed glutathione disulfides. All glutathione reductases are homodimeric enzymes with the active site being formed by both subunits. Alignment of the deduced amino acid sequences of glutathione reductases shows a conserved sequence, and the enzymes are structurally and functionally very similar. The crystal structure of the native enzyme and the complexes of oxidized and reduced forms with NADPH and GSSG, respectively, have been determined. These structural analyses have provided important insights into the mechanism of glutathione reductase function. Figure 3.9 illustrates the homodimeric human glutathione reductase, in which each monomer of 50 kDa can be divided into three domains—the FAD domain, the NADP⁺ domain, and the interface domain. FAD and NADP⁺ are bound in an extended form, with the nicotinamide ring of NADP⁺ and isoalloxazine ring of FAD located adjacent to each other. The GSSG binding site is bridged between the interface domain of one subunit and the FAD domain of the other subunit. The reaction mechanism of glutathione reductase involves the following steps (see Fig. 3.10): first, it receives two electrons from NADPH to a tightly bound FAD; followed by transferring the reducing equivalents to the disulfide formed by two cysteine residues in the active site of the same subunit; next, the electrons are transferred to GSSG, which interacts directly with the

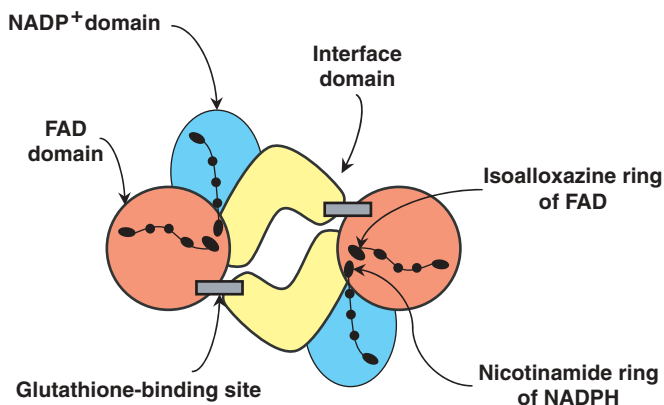


Figure 3.9. Schematic diagram of the domain structure of glutathione reductase. Each subunit in this dimeric enzyme consists of an NADP⁺ domain, an FAD domain, and an interface domain. Glutathione is bound to the FAD domain of one subunit and the interface domain of another. Used with permission from Schultz, Schirmer, Sachsenheimer, and Pai (1978), *Nature* 273:123.

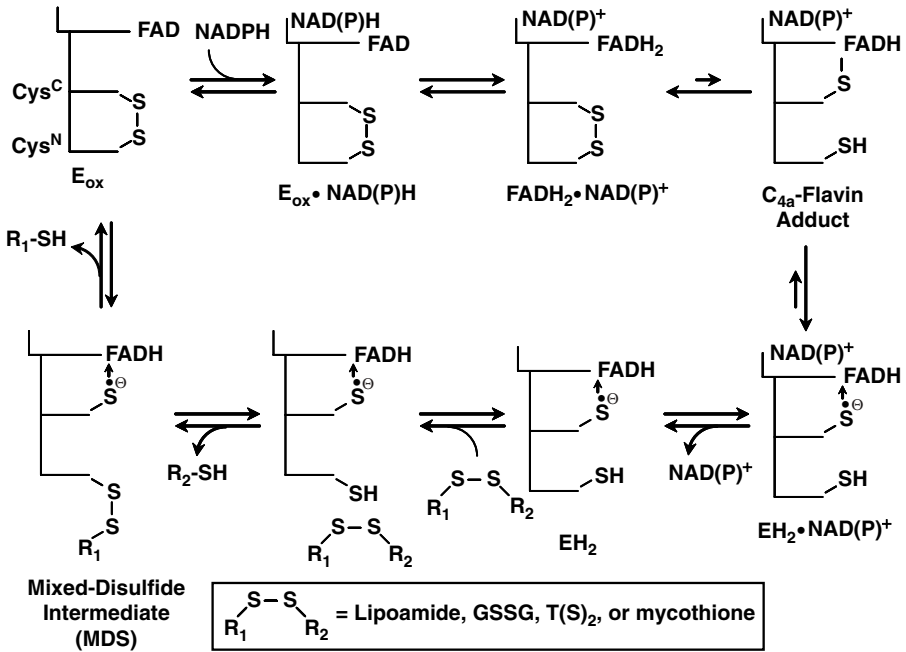


Figure 3.10. General mechanism of glutathione reductase catalysis. Adapted from Argyrou and Blanchard (2004), *Prog. Nucleic Acid Res. Mol. Biol.* 78:89–142 with permission.

newly reduced cysteine residues; finally, the enzyme releases two GSH molecules, completing the catalytic cycle. Therefore, the cascade of electron transfer involves $\text{NADPH} \rightarrow \text{FAD} \rightarrow \text{redox-active disulfide} \rightarrow \text{GSSG}$.

3.3.A2 Gene Regulation of Glutathione Reductase Human glutathione reductase is encoded by a single-copy gene of *Gr*, which has been mapped to chromosome 8. The *Gr* gene is inducible and is known to produce 1.5- to 2.5-fold higher levels of *Gr* mRNA in the cells that are under oxidative stress. The regulation of GR expression in different organisms subjected to stress could occur either at the transcriptional, translational, or post-translational levels. In yeast, the *GLR1* gene encoding glutathione reductase is inducible under oxidative stress conditions by AP1, a transcription factor analogous to mammalian AP1.

3.3.A3 Therapeutic Potential and Physiological Function Glutathione reductase can be inhibited by some metals, such as Zn^{2+} , and by sulfhydryl-targeting reagents. Glutathione reductase is very sensitive to several anticancer drugs. For instance, it can be inactivated by carmustine, or 1,3-bis(2-chloroethyl)-1-nitrosourea. Human glutathione reductase is also a good antimalarial target as the parasite *Plasmodium falciparum* is very sensitive to oxidative stress; it needs the proper functioning of glutathione reductase in its host erythrocytes for survival. Therefore, antimalarial

agents, such as methylene blue, designed to inactivate erythrocyte glutathione reductase, have been used as therapy. However, there are clinical effects of decreased glutathione reductase activity resulting from genetic impairment, enzymal inhibition, or nutritional deficiency of riboflavin. The genetic disorder is rare, but it is known that lowered glutathione reductase activity causes decreased life span of erythrocytes, shortened respiratory burst in leukocytes, cataract, and early onset of deafness. The importance of glutathione reductase in GSH metabolism has clearly been demonstrated in yeast, in which a mutation in the *GLR1* gene results in accumulation of GSSG. The yeast mutant is overly sensitive to oxidative stress. These studies strongly indicate that cells depend on the glutathione reductase/NADPH recycling pathway to maintain a high intracellular GSH pool. Therefore, the enriched GSH pool can be used by various GSH-dependent oxidation defense systems for maintaining redox homeostasis in cells.

SELECTED REFERENCES

1. Argyrou, A., and Blanchard, J.S. (2004). Flavoprotein disulfide reductase: advances in chemistry and function. *Prog. Nucleic Acid Res. Mol. Biol.* 78:89–142.
2. Dickinson, D.A., and Forman, H.J. (2002). Glutathione in defense and signaling: lessons from a small thiol. *Ann. N. Y. Acad. Sci.* 973:488-504.
3. Dym, O., and Eisenberg, D. (2001). Sequence–structure analysis of FAD-containing proteins. *Protein Sci.* 10:1712–1728.
4. Schulz, G.E., Schirmer, R.H., Sachsenheimer, W., and Pai, E.F. (1978). The structure of the flavoenzyme glutathione reductase. *Nature* 273:120–124.

3.3.B Glutaredoxin (Thioltransferase)

Glutaredoxin, also known as thioltransferase, is a member of the thiol-disulfide oxidoreductase enzyme family and an important component of the GSH system. It is a small, heat-stable protein of 10–24 kDa. Glutaredoxin catalyzes the reduction of proteins that are thiolated by GSH, or the reduction of protein *S-S*-glutathione (PSSG). The reaction proceeds as shown in Eqs. (3.17 and 3.18):



where R and R' represent protein/nonprotein thiols, respectively. The reduction of PSSG is carried out by GSH, which is oxidized to GSSG and recycled to GSH via the recycling system of NADPH and glutathione reductase. Therefore, the electron transfer path is as follows: NADPH → glutathione reductase → GSH → glutaredoxin. It has been established that glutaredoxin can reduce protein disulfides via a dithiol mechanism, or GSH *S*-conjugated with protein (PSSG), or low molecular weight thiol (GSSR') via either a monothiol or dithiol mechanism.

3.3.B1 Historical Background Glutaredoxin was first discovered in *E. coli* as a GSH-dependent electron donor for ribonucleotide reductase, and later it was realized that this enzyme was identical to mammalian thioltransferase, also known as thiol-disulfide transhydrogenase, found in rat liver. In recent years, glutaredoxin has been detected in most prokaryotes and eukaryotes, in plants, and even in viruses.

3.3.B2 Classification and Structure of Glutaredoxin Glutaredoxin reduces intracellular disulfides and has a unique CXXC motif at its active site, similar to its sister enzyme, thioredoxin. To date, many isoforms of glutaredoxin have been identified from various sources. In *E. coli* alone, there are four isoforms, designated Grx1–4. In mammalian cells, glutaredoxin is represented by two isozymes: the cytosolic Grx1 and a recently identified mitochondrial and nuclear Grx2. The mammalian Grx1 has 105 amino acids and is extended at both the N and C termini as compared to the *E. coli* Grx1 containing 85 amino acids. Furthermore, mammalian Grx1 has two additional cysteines toward the C terminus with no known function.

The three-dimensional structures of several Grx in their reduced, mixed disulfide, and oxidized forms have been obtained by NMR and X-ray crystallography (Fig. 3.11). Grx has three characteristic regions: the active site (Cys22–Cys25), the GSH binding site, and a hydrophobic site. Glutaredoxin can be classified into three categories. The first is the classical glutaredoxin of ~10 kDa molecular mass in which a CPYC motif is present in the active site, and with a thioredoxin/glutaredoxin fold. This includes *E. coli* Grx1 and Grx 3, and mammalian Grx1; all are electron donors for ribonucleotide reductase. The second category is structurally similar to glutathione *S*-transferase, with the characteristic two domains of the thioredoxin/glutaredoxin fold and an α -helical structure (Fig. 3.11). The dithiol CPYC motif is located in

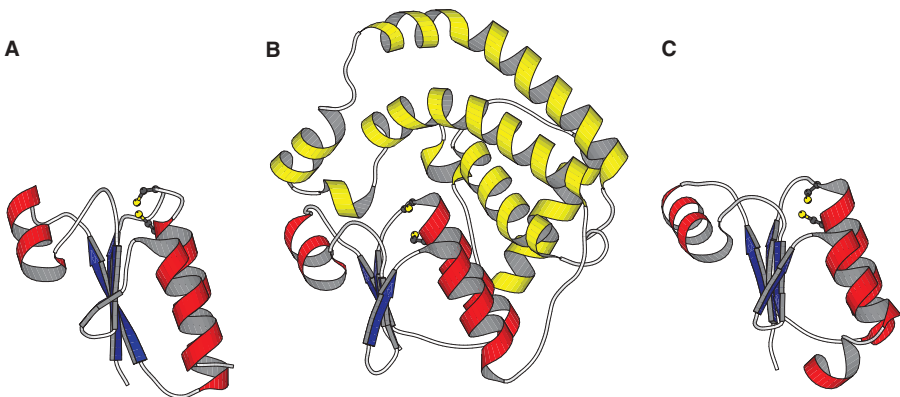


Figure 3.11. Three-dimensional structures of the *E. coli* glutaredoxins. (A) Oxidized *E. coli* Grx1 (PDB file 1EGO). (B) Reduced *E. coli* Grx2 (PDB file 1G7O). (C) Oxidized *E. coli* Grx3 (PDB file 1FOV). The active site cysteines are displayed as sticks. β -Sheets are displayed in blue, α -helices belonging to the thioredoxin/glutaredoxin fold in red, and the α -helices of the C-terminal domain of Grx2 in yellow. Adapted from Fernandes and Holmgren (2004) (Ref.1) with permission.

TABLE 3.3. Summary of *E. coli* Glutaredoxins

Gene	Protein	Molecular Mass (kDa)	Regulation	Sensitivity	Substrate Specificity	
					Protein Disulfides	Mixed Disulfides
<i>Gor</i>	Glutathione reductase (GR)		OxyR, ppGpp	H ₂ O ₂ , CHP, tBHP, diamide		GSH
<i>grxA</i>	Glutaredoxin 1 (Grx1)	9.7	OxyR	Diamide, H ₂ O ₂	RR, OxyR, PAPS reductase, ArsC (MSR)	ArsC, PAPS reductase
<i>grxB</i>	Glutaredoxin 2 (Grx2)	24.3	Acid stress, osmosis, RpoS, ppGpp, cyclic, AMP	Diamide, H ₂ O ₂	ArsC	ArsC, PAPS reductase
<i>grxC</i>	Glutaredoxin 3 (Grx3)	9		Menandione, CHP	(RR), ArsC	ArsC, PAPS reductase

Abbreviations: CHP, cumene hydroperoxide; MSR, methionine sulfoxide; RR, ribonucleotide reductase; tBHP, *tert*-butyl hydroperoxide.

Source: Adapted from Fernandes and Holmgren (2004) (Ref. 1) with permission.

the glutaredoxin domain; thus, it has only glutaredoxin activity and no glutathione *S*-transferase activity. The *E. coli* Grx2, with molecular mass of 24 kDa, belongs to this group. The third category is the N-terminal monothiol-containing glutaredoxin with an active site CGFS sequence. This group includes yeast yGrx3, yGrx4, and yGrx5 and similar proteins in most other organisms containing glutaredoxin. Apparently, the monothiol glutaredoxins are functionally distinct from the dithiol glutaredoxins, and their functions cannot be interchanged. The three-dimensional structures of *E. coli* glutaredoxins are depicted in Fig. 3.11 and their properties are summarized in Table 3.3.

3.3.B3 Human Glutaredoxin Humans have two glutaredoxins with the Grx1 gene located on chromosome 5q14, and the Grx2 gene on chromosome 1q31.2-31.3. Glutaredoxins from various sources show high amino acid sequence homology, particularly in the conserved active site containing the CXXC motif. Grx1 is a 12 kDa cytosolic protein with 70–80% sequence homology to Grx1 in other species but only 25% homology to the *E. coli* Grx1. The 18 kDa Grx2 is a newly discovered protein located in the mitochondrion and nucleus. It contains an active site of CSYC motif but has only 34% sequence homology to Grx1 and is present at low levels. However, Grx2 is the only glutaredoxin known to date to contain an iron–sulfur cluster and its oxidized form is a substrate for thioredoxin reductase. Grx2 catalyzes protein

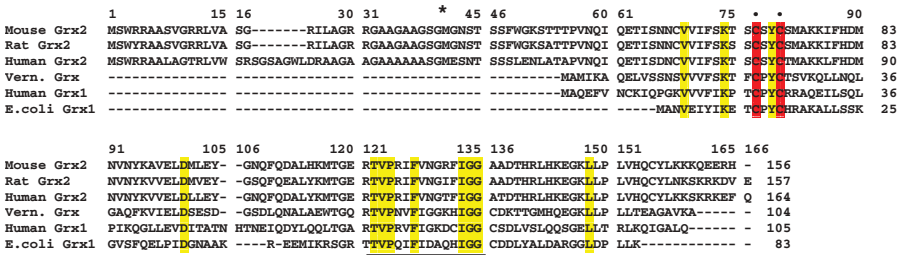


Figure 3.12. Multiple sequences alignment of human, mouse, rat Grx2, human Grx1, *E. coli* Grx1, and *V. fordii* (higher plant) Grx. The rat Grx2 sequence was compiled from ten unique ESTs. Two conserved cysteines that are located in the N-terminal portion of the protein and form a redox active center are shown by a solid circle above the sequence. Residues identical in all six sequences are highlighted in yellow. The asterisk above the sequences indicates a conserved methionine residue that is translated from the second in-frame ATG codon. The line below the sequences indicates a conserved region that is involved in GSH binding. Adapted from Gladyshev et al. (2001), *J. Biol. Chem.* 276 (32):30374–30380 with permission.

deglutathionylation efficiently via a monothiol mechanism, including such targets as complex I and other proteins in the inner mitochondrial membrane. The alignment of amino acid sequences of Grx1 and Grx2 is shown in Fig. 3.12.

3.3.B4 Catalytic Reaction Mechanism Although both thioredoxin and glutaredoxin are oxidoreductases with related functions and a common structural fold, glutaredoxin differs from thioredoxin in its distinctive dethiolating activity toward protein-S-S-glutathione mixed disulfides, which is lacking in thioredoxin. The reaction mechanism of glutaredoxin has been studied extensively with the mammalian and microbial proteins. A two-step reaction mechanism for the mammalian Grx1 is described in Fig. 3.13. In the first step, the substrate PSSG is dethiolated by the dithiol at the active site of Grx1 to form a Grx-S-SG mixed disulfide intermediate and release of protein-SH. In the second step, which is rate limiting, GSH transfers electrons to the Grx-SSG intermediate to release Grx and GSSG, which in turn can be reduced by NADPH via glutathione reductase.

Cys22 in glutaredoxin has an unusually low pK_a of 3.5, which contributes to the high reactivity of the protein. Because of this special feature of Cys22, it was hypothesized that reduction of PSSG could occur more effectively when Cys25 is absent to avoid intramolecular disulfide formation in glutaredoxin during the reaction. Indeed, quadruple Cys to Ser mutations at Cys7, Cys25, Cys78, and Cys82 results in an enzyme that catalyzes deglutathionylation as efficiently as the wild-type protein. Therefore, Cys25 is not required for the catalytic function of glutaredoxin, which is another distinction from the dithiol requirement of thioredoxin.

It is believed that glutaredoxins can reduce protein disulfides or protein-GSH mixed disulfides using a dithiol mechanism (see Fig. 3.14) and the monothiol glutaredoxins can reduce protein-GSH mixed disulfide, using the monothiol mechanism as

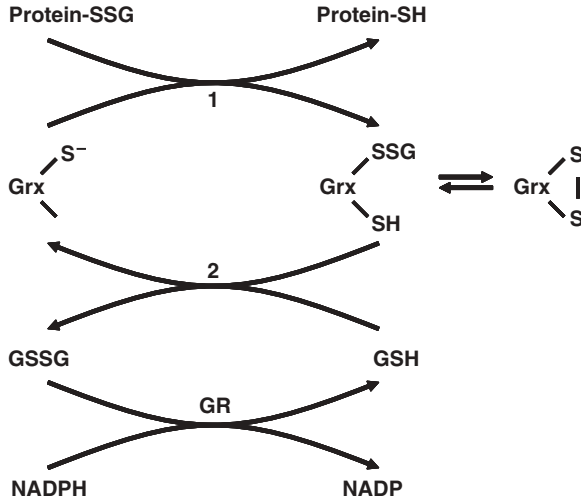


Figure 3.13. The mechanism of glutaredoxin (Grx) action. This scheme depicts the mechanism of glutaredoxin-catalyzed deglutathionylation of protein–SSG mixed disulfides, coupled to glutathione reductase (GR). Adapted from Shelton et al. (2005) (Ref. 3) with permission.

shown in Fig. 3.15. In the monothiol reaction, glutaredoxin first attacks the GSH moiety of PSSG, releasing PSH and forming the Grx–SSG mixed disulfide intermediate. Free GSH subsequently reduces Grx–SSG and is itself oxidized to GSSG.

In addition to dethiolation of protein–GSH mixed disulfides and protein–protein disulfides, glutaredoxin from pig liver, human placenta, the lens, and red blood cells has been shown to catalyze a GSH-dependent reduction of dehydroascorbate (oxidized vitamin C). This unique catalytic activity with a nondisulfide substrate is not observed for thioredoxin.

3.3.B5 Physiological Function Since the physiological state of the intracellular milieu is predominately reduced (GSH/GSSG > 100), careful modulation of the thiol/disulfide balance is crucial to the health of the cells. Glutaredoxin is known to

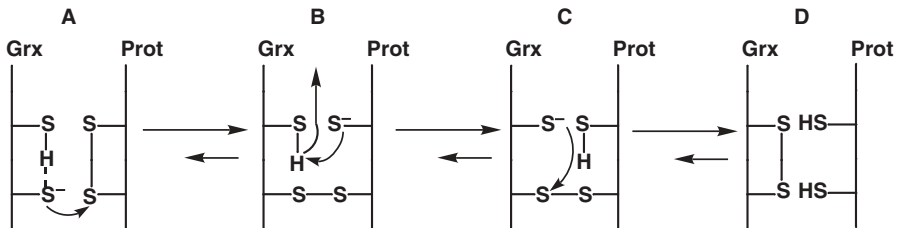


Figure 3.14. The mechanism of glutaredoxin-dependent reduction of protein disulfides. Adapted from Fernandes and Holmgren (2004) (Ref. 1) with permission.

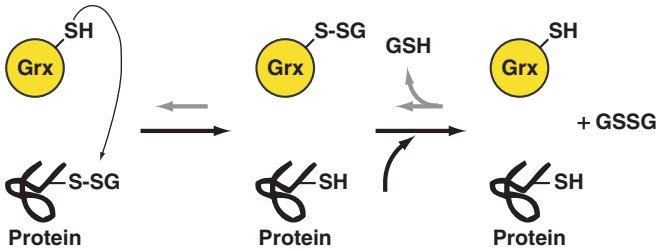


Figure 3.15. The monothiol mechanism of glutaredoxins targeted at protein–GSH mixed disulfide. Reduction of protein–GSH mixed disulfides (black arrows) and the generation of glutathionylated protein (gray arrows) by the reverse reaction are shown. Adapted from Fernandes and Holmgren (2004), (Ref. 1) with permission.

be involved in DNA synthesis by reducing the essential ribonucleotide reductase, and in reduced sulfur production by reducing 3'-phosphoadenylylsulfate. Furthermore, glutaredoxin repairs oxidatively damaged proteins by reducing protein disulfides or glutathionylated proteins (protein–GSH mixed disulfides). This unique glutathionylated substrate requirement allows glutaredoxin to regulate the activities of many metabolic enzymes. For example, phosphofructokinase, a rate-limiting enzyme in the glycolytic pathway, is glutathionylated and inactivated during oxidative stress but can be reactivated by glutaredoxin. In recent years, a more sophisticated role of glutaredoxin has been revealed. Thus, the dethiolation activity of glutaredoxin on key S-glutathionylated proteins involved in cellular signaling has been linked to activation of phosphatases. To date, the well-studied target proteins in this category include protein tyrosine phosphatase-1B, Ras, and actin, all of which are regulated by S-glutathionylation. The process of glutathionylation of proteins is still not well understood and is an area of intense research.

Glutaredoxin contributes to defense against oxidative stress; for instance, recombinant *E. coli* Grx2 is shown to be a strong antioxidant against dopamine-induced oxidative stress and cell death in rat cerebral granule neurons. Additionally, glutaredoxin can be induced under oxidative stress conditions. The *E. coli* Grx1 is upregulated by H₂O₂ in an OxyR-dependent manner. Similarly, human Grx1 can be transiently induced two-fold by H₂O₂ via the AP1 transcription factor in cultured human lens epithelial cells.

SELECTED REFERENCES

1. Fernandes, A.P., and Holmgren A. (2004). Glutaredoxins: glutathione-dependent redox enzymes with functions far beyond a simple thioredoxin backup system. *Antioxid. Redox Signal.* 6:63–74.
2. Holmgren, A., Johansson, C., Berndt, C., Lonn, M.E., Hudenmann, C., and Lillig, C.H. (2005). Thiol redox control via thioredoxin and glutaredoxin systems. *Biochem. Soc. Trans.* 33:1375–1377.

3. Shelton, M.D., Chock, P. Boon, and Mieyal, J.J. (2005). Glutaredoxin: role in reversible protein-S-glutathionylation and regulation of redox signal transduction and protein translocation. *Antioxid. Redox Signal.* 7:348–366.
4. Yang, Y., Jao, S., Nanduri, S., Starke, D.W., Mieyal, J.J., and Qin, J. (1998). Reactivity of the human thioltransferase (glutaredoxin) C7S, C25S, C78S, C82S mutant and NMR solution structure of its glutathionyl mixed disulfide intermediate reflect catalytic specificity. *Biochemistry* 37:17145–17156.

3.4 REPAIR ENZYMES

3.4.A Methionine Sulfoxide Reductases

VADIM N. GLADYSHEV

Redox Biology Center and Department of Biochemistry, University of Nebraska, Lincoln, Nebraska

3.4.A1 Methionine Residues May Be Oxidized to Methionine Sulfoxide

Sulfur-containing amino acids, cysteine and methionine, are particularly susceptible to oxidation by ROS. Cysteines can be oxidized to disulfides, sulfenic acids, sulfinic acids, and sulfonic acids. This section describes the consequences of oxidation of methionine residues, which are converted to methionine sulfoxide. A diastereomeric mixture of methionine-*S*-sulfoxide (Met-*S*-SO) and methionine-*R*-sulfoxide (Met-*R*-SO) is generated by ROS because of the presence of a chiral sulfur in methionine sulfoxides. This oxidation may result in structural and functional changes in proteins. However, in contrast to many other forms of oxidative damage, oxidation of methionines is reversible, and this pathway is thought to be part of an important process that protects cells against oxidative stress, regulates protein function, and delays the aging process (Fig. 3.16).

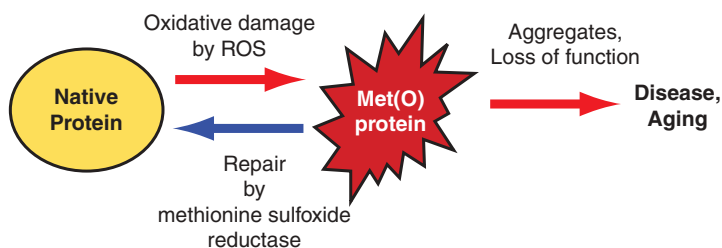


Figure 3.16. Methionine sulfoxide reduction pathway. Methionine residues in proteins are susceptible to oxidation by various ROS. The damaged proteins containing oxidized methionine can form aggregates and their functions can be compromised. Methionine sulfoxide reductases can repair the oxidized methionine residues in proteins by converting them back to methionine. When this repair system does not function properly or is inactivated, the consequence may involve disease and shortened life span.

3.4.A2 Methionine Sulfoxides Can Be Repaired by Methionine Sulfoxide Reductases

Methionine sulfoxide reduction is catalyzed by proteins known as methionine sulfoxide reductases. *In vivo*, the electron donors for this process are thioredoxins, whereas in *in vitro* assays, dithiothreitol is often used. Since methionine sulfoxides occur in the form of Met-S-SO and Met-R-SO, two distinct stereospecific enzymes, MsrA and MsrB, have evolved to repair these isomers. MsrA can only reduce Met-S-SO and MsrB is specific for Met-R-SO (Fig. 3.17). Almost all organisms from bacteria to humans contain MsrA and MsrB, indicating the importance of this repair process. However, some organisms living at high temperatures, including many Archaea, do not have these enzymes. In addition, some intracellular parasites lack these proteins and likely utilize the corresponding host enzymes. Because MsrA and MsrB carry out essentially the same function, genes coding for these enzymes are often coordinately expressed and, in bacteria, they are clustered in the same operon. In addition, the two proteins may occur in the form of fusion proteins, sometimes together with thioredoxin, such that a single protein can reduce both Met-S-SO and Met-R-SO.

Prokaryotes and unicellular eukaryotes typically have single MsrA and MsrB genes, whereas some organisms, such as plants and vertebrates, have multiple forms of MsrA and MsrB, which are targeted to different cellular compartments. Human and mouse genomes contain a single MsrA gene and three MsrB genes. Mammalian MsrA has an N-terminal mitochondrial signal peptide, but besides mitochondria, it also occurs in the cytosol and nucleus. Mammalian MsrBs are also differentially localized in cells, with MsrB1 residing in the cytosol and nucleus, MsrB2 in mitochondria, and MsrB3 in the endoplasmic reticulum. Multiple locations of MsrA and MsrB indicate that various cellular compartments independently maintain the system for repair of oxidized methionine residues.

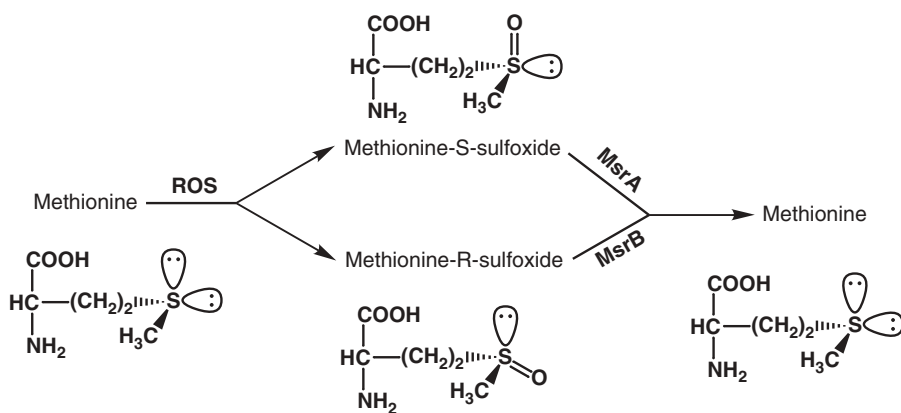


Figure 3.17. The sulfur atom in methionine is susceptible to oxidation by ROS. The oxidized form of methionine occurs in the form of two diastereomers, methionine-S-sulfoxide and methionine-R-sulfoxide, which are reduced by MsrA and MsrB, respectively.

3.4.A3 Properties of Methionine Sulfoxide Reductases The primary function of MsrA and MsrB is to repair protein-based methionine sulfoxides. However, these enzymes can also reduce, albeit inefficiently, free methionine sulfoxides. Most MsrBs also contain a single zinc atom. It is coordinated by four cysteines and serves a structural role in these proteins. Some bacterial MsrBs have lost zinc during evolution, yet preserved methionine sulfoxide reductase function.

3.4.A4 Physiological Functions of Methionine Sulfoxide Reductases Due to their function in reducing methionine sulfoxides, MsrA and MsrB have been implicated in the repair of damaged proteins, antioxidant defense by scavenging ROS, and regulation of protein function. In addition, these enzymes are thought to regulate the aging process. For example, it was reported that deletion of the MsrA gene in mice decreases the life span by 40%, whereas overexpression of MsrA in fruit flies extends it by 70%. Both MsrA and MsrB could also extend life span in yeast. In addition to regulating life span, methionine sulfoxide reductases have been directly implicated in aging-related neurodegenerative diseases, including Alzheimer's and Parkinson's diseases.

3.4.A5 Selenoprotein Forms of Methionine Sulfoxide Reductases MsrA and MsrB contain catalytic, redox-active cysteine residues. Interestingly, one of these cysteines may be replaced with selenocysteine. Selenoprotein forms are known for both MsrA and MsrB, but these forms occur in different organisms. Selenocysteine provides catalytic advantages over cysteine in these enzymes. The major MsrB in mammals is MsrB1, a selenoprotein. Expression of this protein is regulated by dietary selenium. Thus, efficient methionine sulfoxide reduction is one reason why adequate dietary selenium is needed to maintain optimal health.

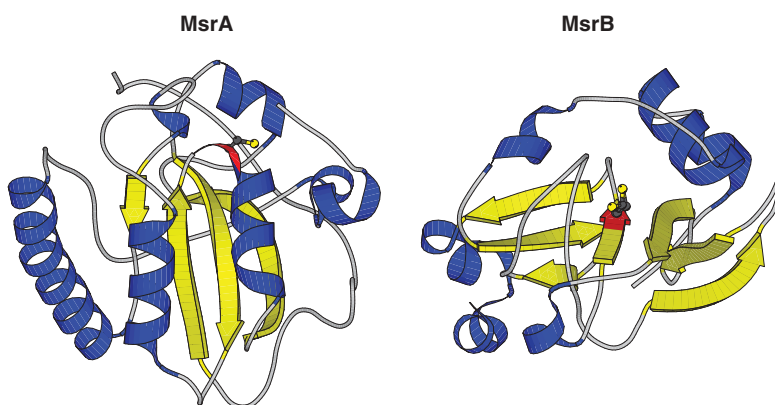


Figure 3.18. Crystal structures of MsrA and MsrB. Although the catalytic mechanisms of both MsrA and MsrB are similar, they exhibit different structural folds. Bovine MsrA (PDB file 1FVG) and *Neisseria gonorrhoeae* MsrB (PDB file 1L1D) structures are shown. The catalytic cysteines are shown in red.

3.4.A6 Catalytic Mechanisms of MsrB and MsrA Three-dimensional structures have been determined for both MsrA and MsrB (Fig. 3.18). These proteins have different folds, yet their active sites resemble mirror images of each other. Consistent with this observation, MsrA and MsrB share a similar reaction mechanism, which proceeds in the following order: (1) the catalytic cysteine thiolate (located in the N-terminal portion of MsrA and the C-terminal portion of MsrB) attacks the sulfoxide, releasing methionine and forming a sulfenic acid intermediate on the cysteine; (2) a second, resolving cysteine attacks the sulfenic acid intermediate to form an intramolecular disulfide bond; and (3) the disulfide is reduced by thioredoxin or other electron donors. Interestingly, mammalian selenoprotein MsrB1 requires a unique resolving cysteine, whereas some MsrA and MsrB sequences lack any resolving cysteines, suggesting that the sulfenic acid intermediate may be directly reduced by protein or low molecular weight reductants.

SELECTED REFERENCES

1. Weissbach, H., Resnick, L., and Brot, N. (2005). Methionine sulfoxide reductases: history and cellular role in protecting against oxidative damage. *Biochim. Biophys. Acta* 1703: 203–212
2. Kim, H.Y., and Gladyshev, V.N. (2005). Different catalytic mechanisms in mammalian selenocysteine- and cysteine-containing methionine-*R*-sulfoxide reductases. *PLoS Biol.* 3: e375.
3. Lowther, W.T., Weissbach, H., Etienne, F. Brot, N. and Matthews, B.W. (2002). The mirrored methionine sulfoxide reductases of *Neisseria gonorrhoeae* pilB. *Nat. struct. Biol.* 9:348–352

3.4.B DNA Repair Enzymes

SHEILA S. DAVID

Department of Chemistry, University of California, Davis, California

3.4.B1 Oxidative Stress and DNA Damage Of the various types of cellular damage, ROS can lead to modifications of the structure of DNA, which constitutes DNA damage. The types of DNA damage mediated by ROS include base lesions, strand breaks, and DNA–protein cross-links. Of the DNA bases, guanine is the most susceptible to oxidation, producing primarily the lesion 7,8-dihydro-8-oxo-2'-deoxyguanosine (OG). Indeed, the presence of OG is used as a biomarker for oxidative stress levels in cells. Guanine is the most susceptible to oxidation due to its low redox potential. The redox potentials for the relevant nucleosides versus NHE at pH 7 are as follows: rG, 1.29 V; rA, 1.42 V; dC, 1.6 V; and dT, 1.7 V. In addition to OG, a plethora of oxidized guanine base lesions have been identified, as well as oxidation products of other bases (Fig. 3.19). Interestingly, OG has an even lower redox potential (rOG, 0.58 V vs. NHE) than G and therefore is readily further oxidized to products such as guanidinohydantoin (Gh) or spiroiminodihydantoin

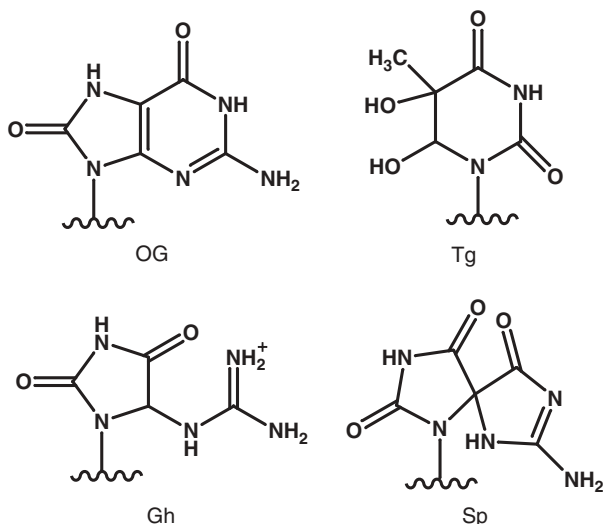


Figure 3.19. Examples of oxidized base lesions in DNA. 7,8-Dihydro-8-oxo-2'-deoxyguanosine (OG) arises from oxidation of guanine, while guanidinohydantoin (Gh) and spiroiminodihydantoin (Sp) arise either directly from oxidation of guanine or from further oxidation of OG. Thymine glycol (Tg) arises from oxidation of thymine. All of these base lesions are repaired by the base excision repair pathway.

(Sp) (Fig. 3.19). The other DNA bases also produce a variety of products. For example, oxidized products of thymine, such as thymine glycol are quite common (Fig. 3.19).

3.4.B2 DNA Repair Enzymes Modifications of DNA compromise the integrity of the genome, often leading to mutations that may fuel the progression toward carcinogenesis. Damage to the DNA bases is particularly problematic since this compromises the informational content of DNA. For example, the installation of the 8-oxo group into OG results in creating a hydrogen-bonding face on OG that mimics T. Replication of a strand containing OG results in misincorporation of A opposite OG to form a stable OG:A base pair. Subsequent replication of the A containing strand produces a normal T:A base pair. Thus, the end result of oxidation of guanine to form OG is that the genome now contains a T where a G should be located and therefore the coding properties have been potentially altered. Fortunately, there are a myriad of DNA repair pathways to reverse the harmful consequences of oxidative DNA damage. The base excision repair pathway is the primary mechanism that facilitates the repair of damaged bases. This pathway is initiated by a damage-specific glycosylase that hydrolyzes the base from the sugar. Subsequent processing of the resulting apurinic-apyrimidinic (AP) site by an AP endonuclease and a deoxyribosephosphate lyase creates the proper ends for a DNA polymerase that reinstalls the appropriate undamaged nucleotide at the site using the identity of the base on the other strand of

the duplex as a guide. A DNA ligase enzyme puts on the finishing touches by sealing the DNA backbone. The oxidatively damaged base OG is removed by a variety of OG glycosylases, including the *E. coli* OG glycosylase, Fpg, or the human OG glycosylase, hOGG1. In some cases, the glycosylase may remove a variety of different base lesions. For example, Fpg removes a variety of lesions in addition to OG, including the further oxidation products of OG, Gh, and Sp. A variety of glycosylases and the damaged bases that they target are listed in Table 3.4. Fpg and hOGG1 are often used as “reagents” to detect OG since they catalyze both removal of the base and an associated strand scission reaction. Quantitation of DNA strand breaks generated by treatment with Fpg conveniently reports on the amount of oxidized guanine lesions present in a DNA sample.

3.4.B3 [4Fe–4S] Cluster-Containing DNA Glycosylases Due to the fact that DNA glycosylases catalyze a hydrolysis reaction, it was surprising when the common redox [4Fe–4S] cluster cofactor was found in the base excision repair (BER) glycosylase, *E. coli* endonuclease III (endo III). This glycosylase removes oxidized pyrimidine bases such as thymine glycol from duplex DNA. The MutY glycosylase that prevents mutations associated with OG by removing A from OG:A base pairs was also found to contain a [4Fe–4S]²⁺ center and has high sequence homology to endo III. However, the presence of this cofactor is limited not only to glycosylases that facilitate repair of oxidative damage but also to glycosylases that target alkylation damage and UV damage (Table 3.4). Due to the similarity of these glycosylases to endo III, these enzymes are often referred to as the endo III-like family of glycosylases. Importantly, homologs to endo III and MutY are found in many organisms, including humans. The [4Fe–4S]²⁺ cofactor is coordinated within the proteins of the endo III-like subfamily by thiolates provided by four cysteine residues that are contiguously spaced (Cys-X₆-Cys-X₂-Cys-X₅-Cys) within a short stretch of the polypeptide backbone. This spacing is unusual and unique to the endo III-like family. Recently, a new family of uracil–DNA glycosylases primarily found in thermophilic organisms has been discovered that contain a [4Fe–4S]²⁺ cluster: the Family 4 uracil–DNA glycosylases (4UDGs). The [4Fe–4S]²⁺ cluster in 4UDGs is coordinated by four cysteines with spacing Cys-X₂-Cys-X_n-Cys-X_(14–17)-Cys, where *n* ranges from 70 to 100. This spacing is quite distinct from the endo III-like family and does not appear to be similar to any other Fe–S containing protein.

The unifying feature of an iron–sulfur cluster cofactor in a subset of BER glycosylases possessing widely varied substrate specificities suggests a common function. A structural role for the cluster in *E. coli* endo III was accepted based on *in vitro* work, which showed the cluster to be resistant to reduction and susceptible to degradation upon oxidation. X-ray structures of endo III and the catalytic N-terminal domain of MutY demonstrated a remote location of the cluster with relation to the putative active sites, providing additional support against the direct involvement of the cluster in the base excision reaction catalyzed by these glycosylases (Fig. 3.20). Studies on MutY have shown that although the cluster does not promote folding or contribute to the overall thermal stability of the protein, its presence is essential for DNA binding and enzymatic activity. This idea is consistent with the structural studies of endo III and

TABLE 3.4. Examples of Base Excision Repair Glycosylases

Enzyme	Organisms	Representative Substrate	Harbors [4Fe–4S] ²⁺ Cofactor
Uracil–DNA glycosylase (Family 1 or UNG)	Bacterial, mammals, viruses, yeast	Uracil	No
Family 4 uracil–DNA glycosylases (4UDG)	Thermophilic and archaeobacteria (e.g., <i>Thermatoga maritima</i> , <i>Aracheoglobus fulgidus</i>)	Uracil	Yes
AlkA	<i>Escherichia coli</i>	3-Methyladenine	No
Methylpurine glycosylase (MPG)	Mammals	3-Methyladenine	No
MPGII	<i>Thermatoga maritima</i>	3-Methyladenine	Yes
Endonuclease III	<i>Escherichia coli</i>	Thymine glycol	Yes
hNth	Human	Thymine glycol	Yes
T4-endonuclease V	Bacteriophage T4	<i>Cis-syn</i> thymidyl (3′-5′)thymidine	No
UV-endonuclease	<i>Micrococcus luteus</i>	<i>Cis-syn</i> thymidyl (3′-5′)thymidine	Yes
FPG (MutM)	Bacterial	OG	No
hOGG1	Human	OG	No
MutY	Bacterial	OG:A mismatches (adenine is removed)	Yes
MutYH	Human	OG:A mismatches (adenine is removed)	Yes
Endonuclease VIII (Nei)	Bacterial	Thymine glycol, hydantoin lesions	No
hNEIL1	Human	Hydantoin lesions	No
Thymine–DNA glycosylase	<i>Methanobacterium thermoautotrophicum</i>	G:T mismatches (thymine is removed)	Yes
hTDG	Human	G:T mismatches (thymine is removed)	No
Repressor of silencing 1 (ROS1)	<i>Arabidopsis thaliana</i>	5-Methylcytosine	Yes

MutY that revealed a solvent-exposed loop formed by the first two cysteine ligands, termed the iron–sulfur cluster loop (FCL) motif, which contains a high density of positively charged residues perfectly positioned to interact with the anionic DNA backbone (Fig. 3.20). The role of the FCL motif in mediating DNA binding that is coupled to catalysis has been established by kinetic analysis of mutated forms of these enzymes within the FCL and iron–sulfur cluster binding domain. Structures of

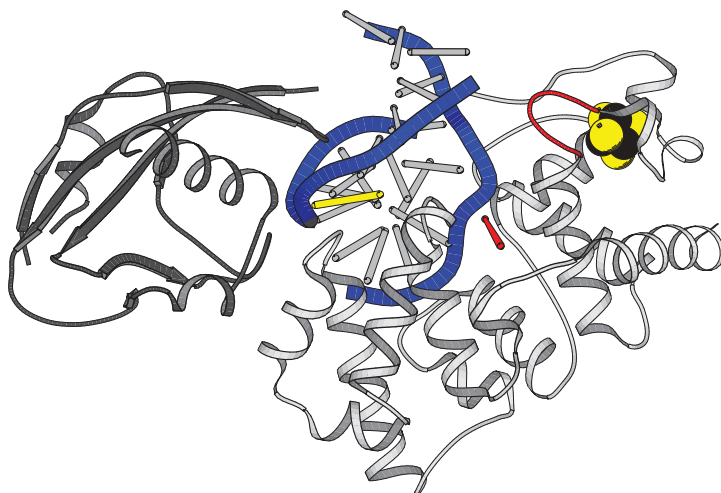


Figure 3.20. X-ray structure of an inactive variant of *Bacillus stearothermophilus* MutY bound to DNA containing an OG:A mismatch (PDB file 1RRQ). This view is end-on of the DNA helix axis (DNA bases, grey; phosphate backbone, blue). It should be noted that the enzyme unwinds and bends the DNA helix. The adenine that is excised is flipped out of the helix (red) while the OG remains in the helix (yellow). MutY has two domains: the N-terminal domain (light grey) is similar to endo III, the C-terminal domain (dark grey) is unique to MutY. The $[4\text{Fe}-4\text{S}]^{2+}$ cluster is shown in yellow and black balls, while the iron-sulfur cluster loop (FCL) DNA binding motif is shown in red. Note that the FCL is interacting with the DNA phosphate backbone at the juncture where the DNA is severely bent.

Bacillus stearothermophilus endo III and MutY bound to their respective substrate DNA duplexes have revealed considerable DNA distortion and bending. The FCL is in proximity to the DNA backbone in both structures, consistent with the proposed role of providing DNA distortion needed to facilitate extrusion of the target base out of the DNA helix for cleavage. The crystal structure of the *Thermus thermophilus* 4UDG demonstrated that the $[4\text{Fe}-4\text{S}]^{2+}$ cluster is located about 10 Å from the putative active site, suggesting that its direct participation in catalysis is unlikely (Fig. 3.21). However, based on this structure, it seems plausible that the large loop formed between two of the cysteine ligands may participate in damaged DNA recognition in a manner analogous to the FCL in MutY and endo III (Figure 3.21).

3.4.B4 Redox Properties of the $[4\text{Fe}-4\text{S}]^{2+}$ Cluster in Base Excision Repair Glycosylases The $[4\text{Fe}-4\text{S}]^{2+}$ clusters of MutY and endo III are resistant to reduction with sodium dithionite or oxidation with ferricyanide. However, the fact that the region around the $[4\text{Fe}-4\text{S}]^{2+}$ cluster contacts DNA hinted that the redox properties of the cluster may be modulated by the presence of DNA. Indeed, the redox properties of the $[4\text{Fe}-4\text{S}]^{2+}$ cluster in MutY were observed using electrochemistry with DNA-modified gold electrodes. The observed midpoint potential was +90 versus NHE. This redox potential is typical of the high potential iron-sulfur cluster proteins

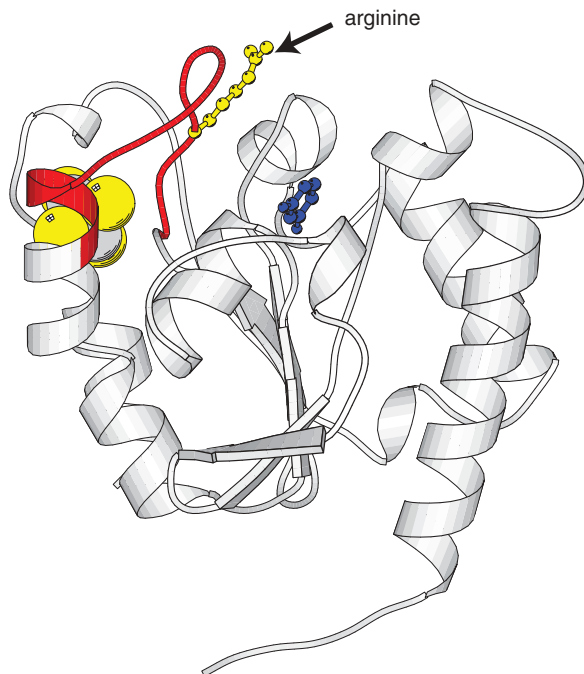


Figure 3.21. Structure of *Thermus thermophilus* 4 uracil–DNA glycosylase (PDB file 1UIO). The cluster is shown in yellow and red spheres. A free uracil base, which was soaked into the crystals, is shown in blue; this site likely is where the base is excised from DNA. A pseudo-FCL motif (red) contains an arginine (yellow) that may be positioned well to interact with the DNA phosphate backbone. The DNA likely binds in the cleft at the top face in this view of the enzyme.

(HiPIPs) that redox cycle between the $[4\text{Fe-4S}]^{2+}$ and $[4\text{Fe-4S}]^{3+}$ states. This is in contrast to the more common ferredoxins, where the cluster cycles between the $[4\text{Fe-4S}]^{2+}$ and $[4\text{Fe-4S}]^{1+}$ states. The ability to observe the redox potential in the presence of DNA shows, when bound to DNA, the 3+ oxidation state of the cluster is accessible. Similar potentials for endo III and 4UDG from *Archaeoglobus fulgidus* (AFUDG) of 59 mV and 95 mV, respectively, have also been observed. In all three proteins, the ability to access the 3+/2+ redox couple is sensitive to perturbations in DNA structure, such as introduction of a baseless site, indicating that the redox chemistry is mediated by DNA. EPR studies using $[\text{Co}(\text{phen})_3]^{3+}$ also have shown that the presence of DNA enhanced oxidation of the cluster in these three proteins. In EPR experiments with AFUDG, signals were observed consistent with the presence of $[4\text{Fe-4S}]^{3+}$ and $[3\text{Fe-4S}]^{1+}$ clusters, while with endo III and MutY only signals for the $[3\text{Fe-4S}]^{1+}$ were observed. The $[3\text{Fe-4S}]^{1+}$ cluster results from hydrolysis of the $[4\text{Fe-4S}]^{3+}$ cluster. Interestingly, the oxidation of the cluster in these proteins when bound to DNA is considerably less efficient when using ferricyanide even though its redox potential is

similar to $[\text{Co}(\text{phen})_3]^{3+}$; this is likely due to the negatively charged DNA phosphate backbone that prevents close approach of a negatively charged oxidant. These studies showed that binding of DNA activates the cluster in the protein toward oxidation. Notably, $[\text{4Fe-4S}]^{2+}$ clusters in HiPIPs are usually buried deep within the interior of the protein and this is thought to prevent degradation of the oxidized cluster. In these glycosylases, the clusters appear close to the surface of the protein but would indeed be buried in the complex with DNA. Thus, the presence of DNA likely not only shifts the redox potential of the cluster but also protects the $[\text{4Fe-4S}]^{3+}$ cluster from hydrolysis to the $[\text{3Fe-4S}]^{1+}$ form. By using highly oriented pyrolytic graphite electrodes, the redox potential of endo III in the absence and presence of DNA could be measured owing to the larger potentials that could be accessed in this system. These studies showed that DNA binding lowers the reduction potential for endo III by ~ 200 mV.

There are a variety of mechanisms to form OG; however, a common mechanism is by direct oxidation of guanine to form a guanine cation radical, which is intercepted by water and then, upon loss of a second electron, generates OG. Interestingly, if G cation radicals are generated in the presence of MutY, the $[\text{4Fe-4S}]^{2+}$ is oxidized to $[\text{4Fe-4S}]^{3+}$. These experiments were performed by photolysis of $[\text{Ru}(\text{phen})_2\text{dppz}]^{2+}$, where dppz = dipyrrophenazine, in the presence of DNA, to transiently generate the potent oxidant Ru(III) that is able to directly oxidize guanine. This observation suggests that repair enzymes like MutY may be able to directly repair radicals formed in DNA, in addition to excising out damaged bases as part of base excision repair.

On the basis of the DNA-mediated redox behavior of the $[\text{4Fe-4S}]^{2+}$ cluster containing glycosylases, it has been suggested that the affinity of the enzyme for DNA may be modulated by the redox state of the cluster. In fact, there were hints of differences in DNA affinity in the reduced and oxidized states in the electrochemistry data. The oxidized form is expected to have a higher affinity for DNA and remain localized on DNA, while the reduced state may more easily dissociate from DNA. This would serve as a mechanism to modulate the scanning of the DNA helix by these enzymes. The redox state of the cell may potentially be used as a mechanism to regulate DNA binding and glycosylase activity. In fact, the DNA itself may serve as the medium to modulate the redox properties of the cluster in these enzymes, since an oxidized DNA base could in turn oxidize the Fe-S cluster. The next step will be determining whether the redox behavior of these glycosylases is used *in vivo* for locating DNA damage and modulating their activity. Clearly, more interesting properties of these unique and intriguing enzymes are likely to be uncovered.

SELECTED REFERENCES

1. Burrows, C.J., and Muller, J.G. (1998). Oxidative nucleobase modifications leading to strand scission. *Chem. Rev.* 98:1109–1151.
2. David, S.S., and Williams, S.D. (1998). Chemistry of glycosylases and endonucleases involved in base-excision repair. *Chem. Rev.* 98:1221–1261.

3. Lukianova, O.A., and David, S.S. (2005). A role for iron–sulfur clusters in DNA repair. *Curr. Opin. Chem. Biol.* 9:145–151.
4. Klauning, J.E., and Kamnedulis, L.M. (2004). The role of oxidative stress in carcinogenesis. *Annu. Rev. Pharmacol. Toxicol.* 44:239–67

3.4.C Sulfiredoxins

LESLIE B. POOLE

Department of Biochemistry and Center for Structural Biology, Wake Forest University School of Medicine, Winston-Slem, North Carolina

Mammalian peroxiredoxins, which normally function as cysteine-based peroxide reductases to reduce H_2O_2 , alkyl hydroperoxides, and/or ONOO^- , are susceptible to hyperoxidation by excess oxidizing substrate at the peroxidatic cysteine; this produces, from the cysteine sulfenic acid, R-SOH, formed during the catalytic cycle, the two-electron more oxidized cysteine sulfinic acid, R-SO₂H (Fig. 3.22A). Generation of the inactive, hyperoxidized form of peroxiredoxin is associated with a shift in the *pI* of the protein toward a more acidic species as can be detected by two-dimensional gel electrophoresis. Cellular conditions under which this hyperoxidation occurs include oxidative stress imparted by the extracellular addition of peroxides or paraquat, or prolonged treatment with tumor necrosis factor- α (TNF- α) or, potentially, other cytokines or growth factors where signal transduction pathways leading to transcription activation have a redox-dependent component. The ability of peroxiredoxin activity to be regulated by this hyperoxidation pathway may have evolved in higher organisms to provide for the ability to achieve a localized burst in H_2O_2 concentration during the course of receptor-mediated, redox-dependent signaling processes. Another theory posits that peroxiredoxin hyperoxidation leads to generation of a high molecular weight, multimeric form of peroxiredoxins that exhibits chaperone activity to aid in cell recovery from oxidative stress.

Although cysteine sulfinic acid formation has long been considered to be biologically irreversible, studies since 2003 have shown that, at least for some typical 2-Cys peroxiredoxins, this type of oxidative damage can be reversed enzymatically. Initially, metabolic ³⁵S labeling of cells followed by exposure to H_2O_2 was shown to result in the shifting of PrxI and PrxII to their hyperoxidized forms, then a slow recovery of the lower *pI* forms of these proteins even in the absence of new protein synthesis (blocked by the addition of cycloheximide). The enzyme responsible for this recovery was subsequently identified in yeast and other lower and higher eukaryotes and named sulfiredoxin. Another less well studied group of enzymes, known as sestrins, may also catalyze the repair of hyperoxidized peroxiredoxins.

3.4.C1 Proposed Catalytic Mechanism of Sulfinic Acid Reduction by Sulfiredoxins The best studied sulfiredoxin enzymes, those from yeast and humans, reduce hyperoxidized peroxiredoxins in the presence of Mg^{2+} and ATP, and it has been suggested that phosphoryl transfer from ATP to the peroxiredoxin sulfinic acid to generate a sulfinic phosphoryl ester is an initial step required for activation

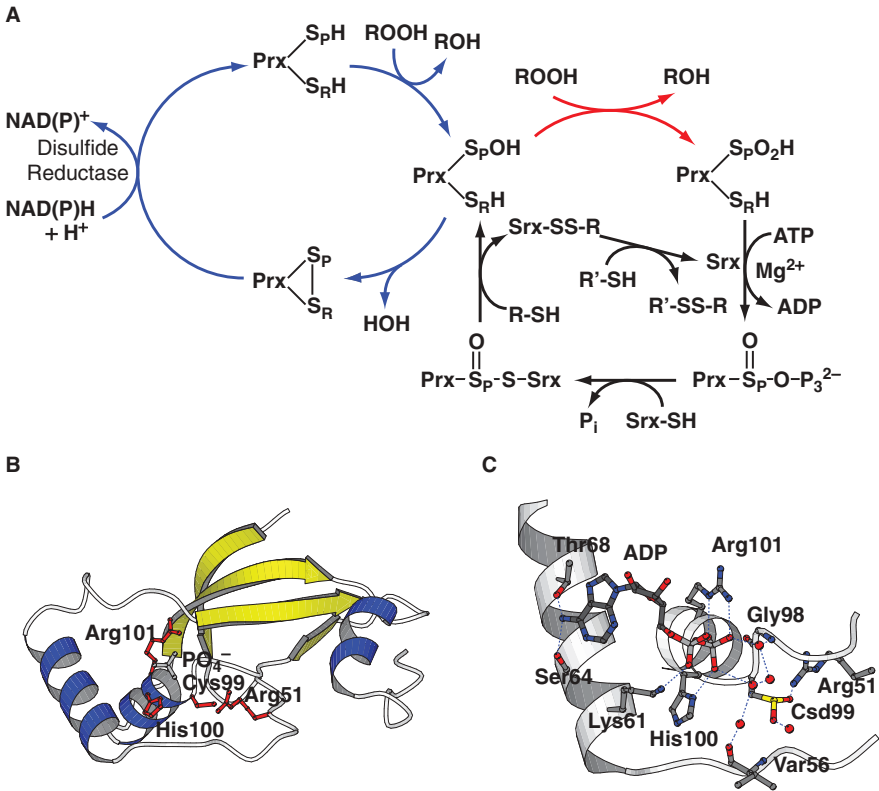


Figure 3.22. Pathways of catalysis and inactivation of peroxidases and the proposed mechanism of sulfiredoxin, and structural characteristics of human sulfiredoxin. In panel (A), catalysis of peroxide reduction by typical 2-Cys peroxidases (blue arrows) proceeds through the intermediate formation of an oxidized form of the peroxidatic cysteine, the sulfenic acid (R-S_POH). This form is susceptible to oxidation by another molecule of substrate (red arrow), resulting in the formation of a sulfinic acid at this site, and inactivation of the peroxidase molecule. The proposed mechanism of sulfiredoxin (black arrows) begins with the activation of the sulfenic acid group (R-S_PO₂H) by reaction with ATP, and proceeds through the thiol-dependent (R-SH) resolution of sulfinic phosphoryl ester (R-S_PO₂PO₃²⁻) and thiosulfinate (R-S_PO-S-R') intermediates. For clarity, the second subunit and the resolving cysteine (R-S_RH) of the peroxidase dimer are not shown in the sulfiredoxin mechanism. Panel (B) shows the overall fold of human sulfiredoxin (PDB code 1XW3) as a ribbon diagram, with stick representations of Arg51, Cys99, His100, Arg101, and a phosphate molecule to emphasize the location of the active site structures within this novel protein fold. Panel (C) depicts the structure of human sulfiredoxin with ADP bound (PDB code 1XW4). Putative hydrogen bonding interactions are shown as dotted blue lines. In this structure the active site Cys99 (which has been adventitiously oxidized to sulfinic acid) interacts with Arg51 and a water molecule; the adenine ring of ADP interacts with Ser64 and Thr68, and the β-phosphate oxygens interact with His100, Arg101, and two water molecules.

of this species (Fig. 3.22A). Evidence for the involvement in catalysis of the conserved cysteine of sulfiredoxin (Cys84 of yeast sulfiredoxin, or Cys99 of human sulfiredoxin) includes the absolute conservation of this and flanking residues among divergent sulfiredoxins, the lack of activity for the cysteine-to-serine mutant of the yeast sulfiredoxin, and the apparent catalytically relevant generation of a covalently linked form of the enzyme and substrate proteins, sulfiredoxin and peroxiredoxin, which is reducible by dithiothreitol treatment. A working hypothesis for this catalytic mechanism thus includes the nucleophilic attack on the sulfinic phosphoryl ester by the active site cysteine thiolate of sulfiredoxin to generate the thiosulfinate linkage between the two proteins (also known as a disulfide monooxide), and breakdown of the complex by reaction with another attacking thiol(ate) group (Fig. 3.22A). It appears that either dithiothreitol or thioredoxin, or possibly GSH, can serve as reductants in the repair process. While molecular details for this novel chemical reaction remain to be worked out, clues regarding the positions and roles of sulfiredoxin residues, which participate in the reaction mechanism, have been obtained from the determination of the crystal structure of human sulfiredoxin.

3.4.C2 Crystal Structures of Human Sulfiredoxin Human sulfiredoxin not only participates in novel sulfur chemistry in carrying out sulfinic acid reduction but also exhibits a new protein fold and a unique nucleotide binding motif and contains the conserved Gly98-Cys99-His100-Arg101 sequence at the N terminus of an α -helix (Fig. 3.22B). Based on the two crystal structures of human sulfiredoxin, one with the active site Cys99 thiol group intact and containing a bound phosphate anion (Fig. 3.22B), and the other with a hyperoxidized Cys99 sulfinic acid at the active site and an ADP molecule bound (Fig. 3.22C), a model of the ATP-bound form of the enzyme could be constructed. The γ -phosphate of ATP and the essential active site cysteine residue are located adjacent to large surface invaginations containing additional conserved residue, which may participate in specific interactions between human sulfiredoxin and typical 2-Cys peroxiredoxins, although more structural and mechanistic information will be required to further dissect the details of the sulfiredoxin – peroxiredoxin interaction and catalytic mechanism.

3.4.C3 Specificity of Sulfiredoxins Toward Sulfinic Acid-Containing Proteins Oxidation of cysteine thiol groups to sulfinic acids has been observed in multiple different classes of peroxiredoxins and can occur as well in other proteins with reactive cysteinyl residues. The oxidation of cysteine residues to generate sulfenic acids, and their further oxidation to sulfinic acids, may represent two steps or types of regulatory oxidation reactions that can act as functional switches for protein activities, particularly if the modifications are reversible. Thus, there is a need to determine whether or not sulfiredoxin or other enzymes can act as broad spectrum sulfinic acid reductases to reverse biologically relevant sulfinic acid formation in target proteins. Several lines of investigation indicate that sulfiredoxins have differential reactivities toward different hyperoxidized peroxiredoxin targets; replacement of active forms of some hyperoxidized peroxiredoxins relies more heavily, or exclusively, on *de novo* synthesis rather than repair by sulfiredoxins. Several other proteins

that undergo regulatory hyperoxidation to sulfinic acid, such as glyceraldehyde-3-phosphate dehydrogenase and DJ-1, were not substrates for mammalian sulfiredoxin. Thus, there exists no evidence as yet that sulfinic acid reduction can act as a reversible regulatory mechanism for proteins other than a subset of the peroxiredoxin enzymes.

SELECTED REFERENCES

1. Woo, H.A., Chae, H.Z., Hwang, S.C., Yang, K.S., Kang, S.W., Kim, K., and Rhee, S.G. (2003). Reversing the inactivation of peroxiredoxins caused by cysteine sulfinic acid formation. *Science* 300:653–656.
2. Biteau, B., Labarre, J., and Toledano, M.B. (2003). ATP-dependent reduction of cysteine–sulphinic acid by *S. cerevisiae* sulphiredoxin. *Nature* 425:980–984.
3. Chang, T.S., Jeong, W., Woo, H.A., Lee, S.M., Park, S., and Rhee, S.G. (2004). Characterization of mammalian sulfiredoxin and its reactivation of hyperoxidized peroxiredoxin through reduction of cysteine sulfinic acid in the active site to cysteine. *J. Biol. Chem.* 279:50994–51001.
4. Jönsson, T.J., Murray, M.S., Johnson, L.C., Poole, L.B., and Lowther, W.T. (2005). Structural basis for the retroreduction of inactivated peroxiredoxins by human sulfiredoxin. *Biochemistry* 44:8634–8642.
5. Rhee, S.G., Chae, H.Z., and Kim, K. (2005). Peroxiredoxins: a historical overview and speculative preview of novel mechanisms and emerging concepts in cell signaling. *Free Radic. Biol. Med.* 38:1543–1552.

3.5 DETOXIFICATION ENZYMES

3.5.A Cytochrome P450 Enzymes: Structure, Function, and Mechanism

ROBERT L. OSBORNE and JOHN H. DAWSON

Department of Chemistry and Biochemistry, University of South Carolina, Columbia, South Carolina

Oxidation–reduction reactions are vitally important to all biological systems and are involved in energy storage as well as numerous biosynthetic reactions. Perhaps most intriguing are the more than 200 redox enzymes that react directly with oxygen, especially the monooxygenases. These enzymes are named monooxygenases because they catalyze the insertion of one oxygen atom into substrates while reducing the second oxygen atom to water (Eq. (3.19)).



The best characterized and most scrutinized superfamily of monooxygenases are the heme-containing cytochrome P450 enzymes, which are ubiquitous throughout the plant, animal, and microorganism kingdoms. Many members of the P450 superfamily

are currently known, and the numbers of P450s continue to increase as more genomes are identified. With over 5000 genes reported, P450 is one of the most important and versatile enzymes in nature. In general, there are two primary functional roles of mammalian P450. The most important function of these enzymes is the metabolic detoxification of xenobiotics (non-energy-yielding compounds exogenous to an organism). P450 metabolizes foreign compounds by solubilizing them in preparation for excretion from an organism. A second broad role is the involvement of P450 in the biosynthesis of critical signaling molecules that maintain homeostasis and control development.

More specifically, the types of reactions catalyzed by P450 are quite diverse and include the hydroxylation of unactivated alkanes, conversion of alkenes to epoxides, arenes to phenols, and sulfides to sulfoxides and further to sulfones. In human health, P450 isozymes are responsible for the metabolism of drugs and xenobiotics as well as critical biosynthetic transformations of steroids, eicosanoids, and vitamin D. The processes of hormone biosynthesis and herbicide degradation in plants are catalyzed by P450. Insects utilize P450 for developmental control by synthesizing hormones as well as for resistance against insecticides. P450 enzymes can also convert certain, otherwise inert compounds into carcinogens, making P450 enzymes attractive targets for cancer-related drug design and development (e.g., P450 EpoK).

The majority of P450 enzymes are membrane bound, and they are connected to either the inner mitochondrial or endoplasmic reticulum (microsomal) membranes. The membrane-bound nature of most P450s has presented a challenge to scientists due to their minimal solubility. However, bacterial P450 enzymes are generally not membrane bound and can therefore serve as structural models for eukaryotic systems. Many soluble P450 isozymes have been cloned and sequenced, which has allowed for detailed mechanistic, spectroscopic, and crystallographic analyses. The important metabolic roles, along with the unique physical and chemical properties, of P450 have made this one of the most interesting enzymes to researchers. Challenges still remain to understand how such a versatile set of substrate specificities and metabolic processes are supported by the precise nature of the protein structure and heme-iron active site.

3.5.A1 P450 Molecular Structure P450 enzymes share a common three-dimensional, protein fold despite less than 20% sequence identity across the gene superfamily. P450-CAM (CYP101) was the first P450 protein to have its structure solved. The protein is composed of 12 α -helices and five anti parallel β -sheets and the overall protein has an asymmetrical triangular shape (Fig. 3.23). The conserved P450 active site is deeply embedded into the interior of the protein and protected by a four-helix bundle composed of three parallel helices labeled D, L, and I and one antiparallel helix E. The prosthetic heme group, protoporphyrin IX, is located between the distal I helix and the proximal L helix. The universally conserved cysteine residue is the proximal ligand to the heme iron, and this sulfur ligand is anionic in nature and thus termed thiolate.

Crystallization and structural analyses of various P450 enzymes and mutants have revealed two regions of sequence similarity. One area of conserved residues includes

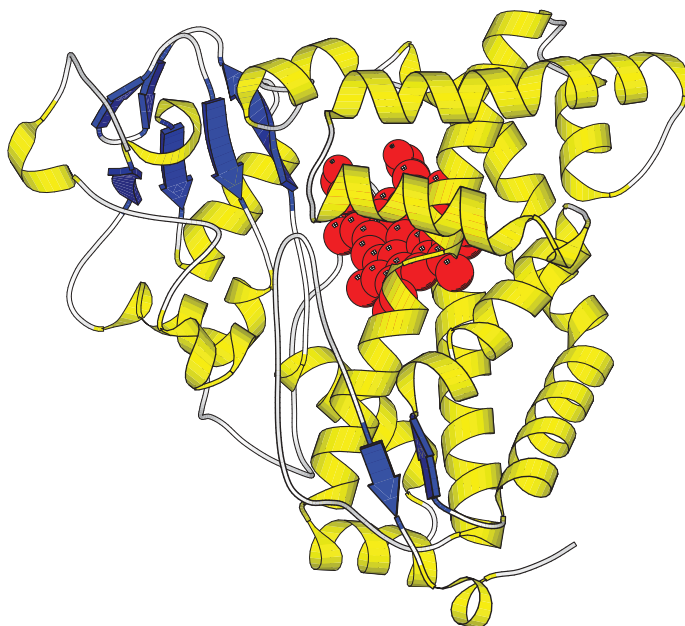


Figure 3.23. Crystal structure of O₂ ferrous cytochrome P450 (P450-CAM, PDB file 2A1M).

the cysteine thiolate ligand and the amino acids encompassing its proximal, binding pocket. The second region is located on helix I, which includes residues that interact directly with the bound dioxygen molecule of the oxyferrous P450 complex (i.e., Thr252 of P450-camphor). Since the spatial organization of the heme binding site is highly conserved throughout the P450 superfamily, differences in the primary, secondary, and tertiary structures of the proteins likely contribute to the diversity of substrate and redox partner interactions involved in P450-catalyzed reactions.

3.5.A2 Electron Transport Systems Two electrons originating from pyridine nucleotides, NADH or NADPH, participate in each cycle (turnover) of monooxygenation. The purpose of the P450 electron transport redox partners is to accept two electrons from NAD(P)H and subsequently transfer them one at a time to P450 during the monooxygenase reaction cycle. Classes of P450 are distinguished based on their electron transport components. Class I P450s include most bacterial and mitochondrial P450 enzymes and utilize the flavin moiety from FAD and FMN cofactors as well as an iron–sulfur protein for electron transfer from NAD(P)H. First, FAD is reduced by accepting two electrons from NAD(P)H, which are then independently transferred to an iron–sulfur protein (putidaredoxin, adrenodoxin) by the FAD-containing reductase. The iron–sulfur protein is a one-electron carrier and thus receives and delivers electrons one at a time. Microsomal systems utilize Class II P450 enzymes and require a single NADPH-specific P450 reductase that contains both FAD and FMN as cofactors, which are reduced by two electrons and then transfer one electron at a time to P450. Some microsomal P450s can accept the second electron from NADH

by utilizing cytochrome *b*₅ reductase and cytochrome *b*₅. Class III P450 enzymes, like bacterial P450-BM3, are unusual in that the entire system is composed of one large, soluble protein with a P450 reductase domain and a cytochrome P450 domain, making this system self-sufficient. P450_{nor} is a Class IV P450 from *Fusarium oxysporum*, which appears to accept electrons directly from reduced pyridine nucleotides without the assistance of electron transfer proteins to catalyze the reduction of nitric oxide to nitrous oxide.

3.5.A3 The P450 Reaction Cycle and Intermediates P450 cytochromes have unusual spectral properties, and studies in numerous laboratories first led to a detailed reaction cycle (Fig. 3.24) for P450-CAM, which is likely shared by most members of the P450 superfamily. This common catalytic cycle illustrates the roles of the core components involved in monooxygenation turnover. All P450 enzymes utilize a cysteine thiolate-ligated, heme-iron active site to catalyze their respective monooxygenase chemistry. The P450 reaction cycle involves four extensively studied

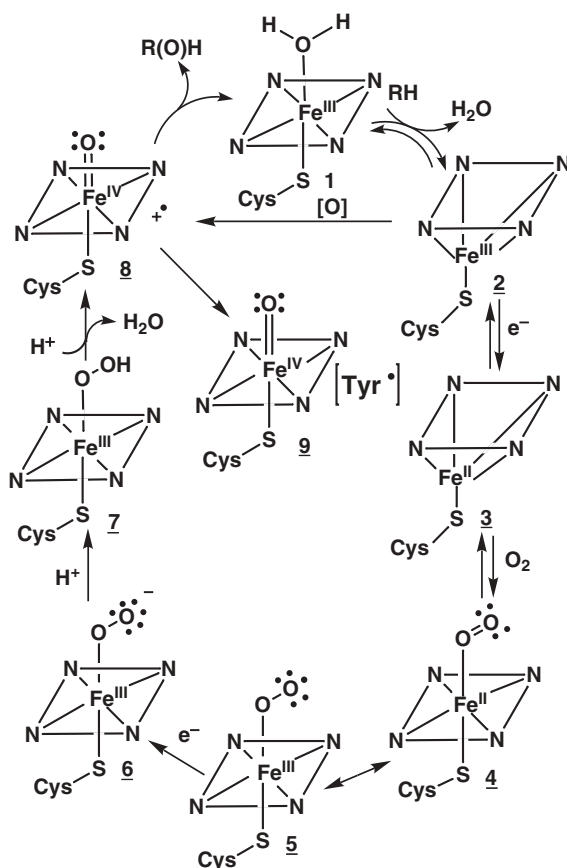


Figure 3.24. Scheme 1 of the P450 reaction cycle.

and isolable complexes (1–4). The substrate-free resting state (1) is six-coordinate low-spin with a proximal cysteine residue from the protein and a distal water molecule from the solvent serving as axial ligands. Addition of substrate to low-spin ferric P450 displaces the water molecule, yielding a five-coordinate, substrate-bound high-spin ferric complex (2) with a vacant coordination site on the distal side of the heme active site for subsequent oxygen binding. The shift in ferric iron spin state (from low-spin to high-spin) upon addition of substrate with concomitant displacement of the water ligand results in an increase in heme–iron reduction potential, making reduction to the ferrous state easier. Reduction of high-spin ferric P450 (2) results in the ferrous (deoxyferrous) state of the protein (3). Oxygen binds to the ferrous heme iron yielding oxyferrous P450 (4 ↔ 5), the last relatively stable intermediate in the cycle. The structure of oxyferrous P450 (4) can also be represented as ferric superoxide P450 (5), and the autoxidation of this resonance structure yields one equivalent of the superoxide anion and returns the enzyme to the ferric resting state (1). Addition of carbon monoxide to adduct 3 yields a carbon monoxide ferrous P450 complex (not shown), which has a Soret absorbance peak at 450 nm, the origin of the unusual name for the enzyme superfamily.

Addition of a second electron from NADH to 4 ↔ 5 produces the ferric peroxide complex (6). Transfer of the second electron is generally the rate-limiting step in the P450 catalytic cycle. The ferric peroxide complex can then be protonated to yield the ferric hydroperoxide species (7), which has recently been shown to be a catalytically active P450 intermediate for epoxidation reactions. Additional protonation of the outer oxygen atom facilitates heterolytic cleavage of the O—O bond, generating a molecule of water and an oxoiron(IV) porphyrin π -cation radical (8). Intermediate 8 is equivalent to the oxoiron intermediate of peroxidase enzymes known as Compound I. P450 Compound I is believed to be the “active oxygen” intermediate responsible for hydroxylating inert hydrocarbons. The P450 reaction cycle is highly coupled in that it accepts two electrons for each hydroxylated substrate molecule. However, there are three uncoupling reactions that can take place during the P450 cycle. The first, already mentioned, is the autoxidation of oxyferrous P450 (4 ↔ 5). A two-electron uncoupling reaction involves protonation of 7 followed by release of H₂O₂ and generation of the five-coordinate ferric state (2) without incorporation of oxygen into substrate. A four-electron uncoupling reaction occurs following the input of two electrons and two protons to the oxygen atom of the oxoiron(IV) of Compound I (8), yielding a molecule of water and complex 2.

The mechanism of hydrocarbon hydroxylation is thought to involve abstraction of a hydrogen atom from the substrate by 8 to produce a substrate carbon radical and hydroxyl radical bound to the heme iron. A radical rebound mechanism yields the hydroxylated product with concomitant regeneration of the ferric resting state of the enzyme (1). The P450 reaction cycle can also be turned over by reaction of alternative oxygen atom donors ([O]) such as H₂O₂, peracids, and iodosobenzene. The oxygen atom donors react directly with 2 to generate oxygenated products likely via Compound I (8). The use of H₂O₂ presumably results in Compound I (8) formation through the ferric hydroperoxide species (7). Additionally, in the absence of substrate, the porphyrin π -cation radical generated by the peroxide shunt can oxidize an adjacent tyrosine residue by one electron to generate an [oxoiron(IV)/Tyr[•]] derivative that has

recently been characterized and termed Compound ES (9). Addition of one electron to P450 Compound I/ES should generate P450 Compound II [oxoiron(IV)], a well-established intermediate for the peroxidase catalytic cycle.

3.5.A4 Oxygen Activation: Thiolate Push A distinguishing feature of monooxygenases and peroxidases compared to oxygen transport heme-containing proteins like myoglobin and hemoglobin is the ability of the former two classes of enzymes to heterolytically cleave the peroxide O—O bond, whereas globins utilize homolytic cleavage of H_2O_2 resulting in Compound II and a hydroxyl radical (Fig. 3.25). After years of investigation, the following mechanism has been proposed for the formation of P450 Compound I. Over 25 years ago, it was posited that the P450 proximal cysteine thiolate ligand serves as a strong internal, electron donor—“the thiolate push”—that facilitates O—O bond cleavage, generating the “active oxygen” species, Compound I (Fig. 3.25). In addition, it has been proposed that P450 Compound I formation requires the input of two protons provided by a distal charge relay (see Section 3.5.A5). Hydrogen bonding to the cysteine thiolate ligand of P450s is believed to be a significant factor in stabilizing thiolate ligation to the heme iron. The importance of the hydrogen bonding network to the cysteinyl proximal ligand has been demonstrated using site-directed mutagenesis to change critically important amino acid residues. For example, the Leu358Pro P450-CAM mutant, which has one less hydrogen bond to the proximal cysteine, has properties consistent with a greater “thiolate push.”

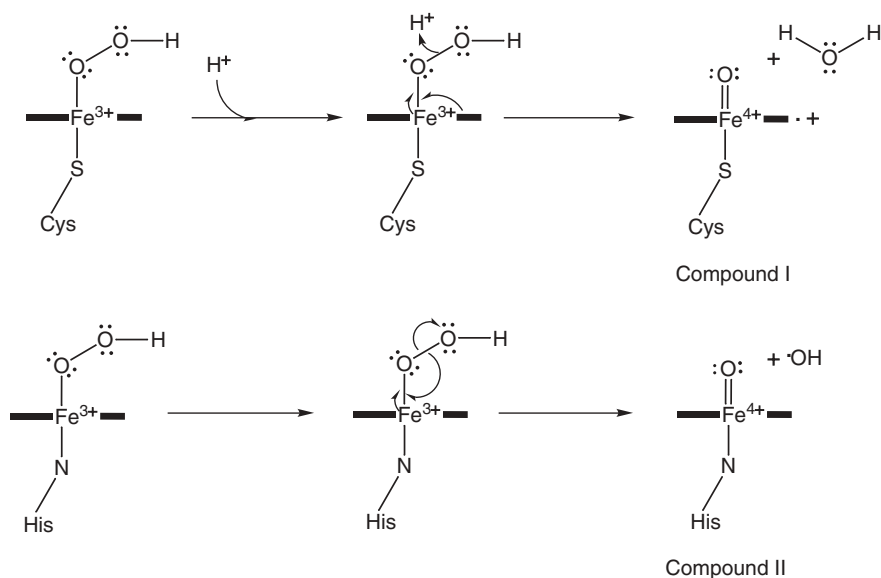


Figure 3.25. Heterolytic O—O bond cleavage (i.e., Compound I formation) and homolytic bond cleavage (i.e., Compound II formation).

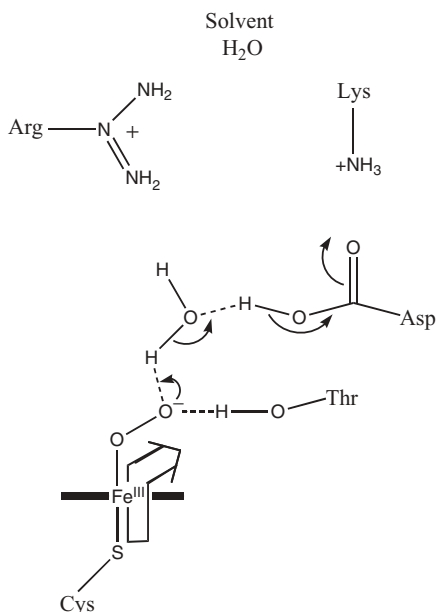


Figure 3.26. Thiolate push and distal charge relay.

3.5.A5 Oxygen Activation: Distal Charge Relay The “thiolate push” alone is insufficient to achieve heterolytic cleavage of the O—O bond because a source of two protons is also required to break the O—O bond and form Compound I (Fig. 3.26). The initial protonation of the outer oxygen significantly weakens the O—O bond, whereas addition of the second proton facilitates cleavage of the dioxygen bond resulting in Compound I and a water molecule. Extensive examination of the P450-CAM active site has identified two possible routes for the distal charge relay, the first involving two highly conserved residues, Thr252 and Asp251. It has been proposed that Thr252 and Asp251 form a proton relay network that works together with two other charged amino acids in the distal pocket to contact the surface solvent, and tested by mutagenesis of Thr252 and Asp251 to alanine and asparagine, respectively. Thr252Ala produces little hydroxylated product without a decrease in NADPH and oxygen consumption, suggesting that it does not form much Compound I (i.e., a highly uncoupled process producing H₂O₂). In P450-BM3, replacement of the corresponding threonine residue (Thr268) with alanine (Thr268Ala) results in an 85% decrease in substrate hydroxylation. However, replacing Thr252 with serine or an O-Me-Thr residue in P450-CAM yields an enzyme that retains high hydroxylation activity (i.e., a coupled process). The mechanistic implications derived from studies with these mutants suggest that the role of Thr252 is to provide a hydrogen bond during the hydroxylation reaction rather than a proton during turnover. The crystal structure of oxyferrous P450-CAM (Fig. 3.23) displays Thr252 within hydrogen bonding distance to the bound dioxygen molecule as well as water 901, which is

possibly a catalytic solvent molecule involved with the distal charge relay. Replacing Asp251 with asparagine resulted in a decrease in the rate of hydroxylation by two orders of magnitude, but the reaction remains coupled, which has been interpreted as evidence that Asp251 plays a role in stabilization of water 901.

SELECTED REFERENCES

1. Sono, M., Roach, M.P., Coulter, E.D., and Dawson, J.H. (1996). Heme-containing oxygenases. *Chem. Rev.* 96:2841–2887.
2. Ogura, H., Nishida, C.R., Hoch, U.R., Perera, R., Dawson, J.H., and Ortiz De Montellano, P.R. (2004). EpoK, a cytochrome P450 involved in biosynthesis of the anticancer agents epothilones A and B. Substrate-mediated rescue of a P450 enzyme. *Biochemistry* 43:14712–14721.
3. Nagano, S., and Poulos, T.L. (2005). Crystallographic study on the dioxygen complex of wild-type and mutant cytochrome P450cam: implications for the dioxygen activation mechanism. *J. Biol. Chem.* 280:31659–31663.
4. Jin, S., Makris, T.M., Bryson, T.A., Sligar, S.G., and Dawson, J.H. (2003). Epoxidation of olefins by hydroperoxo-ferric cytochrome P450. *J. Am. Chem. Soc.* 125:3406–3407.
5. Denisov, I.G., Makris, T.M., Sligar, S.G., and Schlichting, I. (2005). Structure and chemistry of cytochrome P450. *Chem. Rev.* 105:2253–2277.

3.5.B GSH Transferases

SHELLEY D. COPLEY

University of Colorado, Boulder, Colorado

Glutathione transferases catalyze the nucleophilic attack of GSH upon an electrophilic substrate as part or all of the reaction mechanism. These enzymes were formerly called glutathione *S*-transferases, and the abbreviation GSTs is commonly used. A reaction catalyzed by most GSTs is the replacement of a chlorine substituent on 1-chloro-2,4-dinitrobenzene (Fig. 3.27) with GSH to form a GSH conjugate (a compound containing covalently bound GSH). GSTs also attack a number of other electrophiles; some additional examples are shown in Fig. 3.27.

GSTs are best known for their role in detoxification of environmental carcinogens. However, they also catalyze specific reactions in a number of biosynthetic and catabolic pathways and play an important role in defense against oxidative stress by reducing peroxides and dehydroascorbate. Some GSTs modulate signaling pathways as well, by catalyzing attack of GSH upon signaling molecules such as 15-deoxy- $\Delta^{12,14}$ -prostaglandin J₂ and 4-hydroxynonenal. The physiological roles of some GSTs, particularly the bacterial and plant enzymes and the membrane-bound enzymes, are not well understood.

3.5.B1 The Three GST Superfamilies GSTs cluster into three superfamilies, each of which has a distinct structural fold. Two of the three superfamilies contain

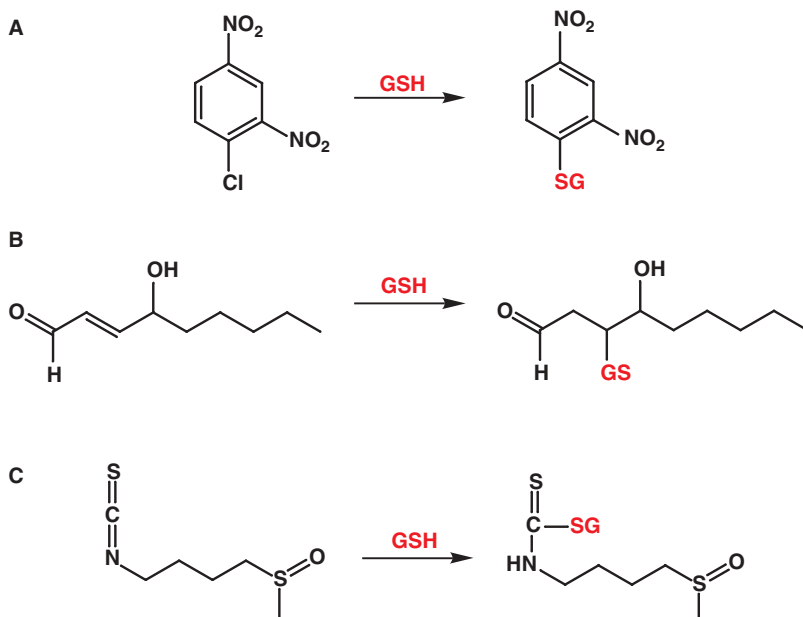


Figure 3.27. Formation of GSH conjugates from GSH and (A) 1-chloro-2,4-dinitrobenzene, (B) 4-hydroxynonenal, and (C) sulforaphane.

a rich variety of enzymes, nearly all of which have retained the ancestral ability to activate GSH for nucleophilic attack on an electrophilic substrate. In many cases, this comprises the entire reaction. However, in some cases, additional steps have been added before or after this characteristic step, allowing more complex transformations to occur.

3.5.B1a Cytoplasmic GSTs Numerous GSTs are found in the cytoplasm of eukaryotes and bacteria that have GSH, but not in Archaea, which generally lack GSH. The cytosolic GSTs are dimeric enzymes. Each subunit contains an N-terminal domain consisting of a thioredoxin fold, and a C-terminal domain consisting of 4–6 α -helices. The active site in each subunit is located in a cleft at the interface between the two domains (Fig. 3.28). The GSH binding site (the G-site) is located primarily in the N-terminal domain, while the binding site for the electrophilic substrate is located primarily in the C-terminal domain. Since the electrophilic substrates are generally hydrophobic, this binding site is termed the H-site.

When GSH binds to the G-site, its pK_a is decreased from 8.5 to about 6–7 due to selective stabilization of the thiolate form. In most cytosolic GSTs, this is accomplished by a hydrogen bond between the thiolate and a hydroxyl group of a nearby tyrosine or serine. Since thiolates are orders of magnitude more reactive than thiols, much of the catalytic power of GSTs is due to their ability to increase the concentration of the thiolate form of GSH at the active site.

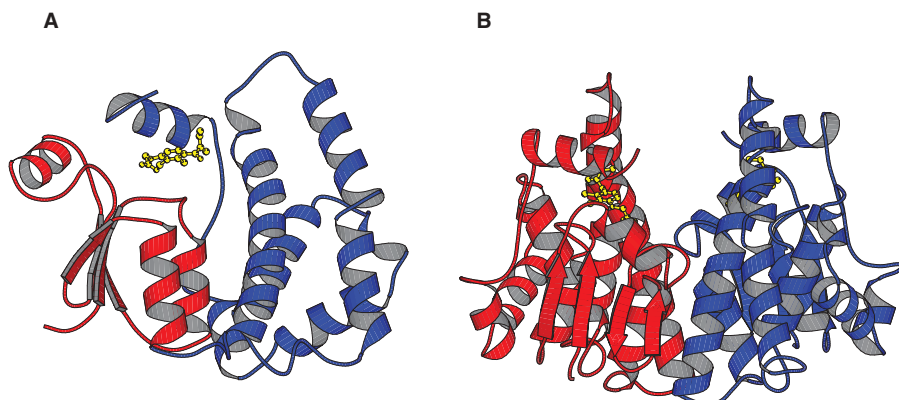


Figure 3.28. Architecture of a typical cytosolic GST. (A) One subunit of the human alpha GST A1-1 (PDB 1GSF), showing the thioredoxin domain in red, the α -helical domain in blue, and ethacrynic acid binding to the H-site in yellow; (B) the dimeric alpha GST A1-1, showing one subunit in red and the other in blue. Ethacrynic acid (shown in yellow) is visible in only one active site in this view.

The cytosolic GST superfamily is divided into several classes (Table 3.5). Enzymes within a class generally share more than 40% sequence identity, while enzymes in different classes share less than 25% sequence identity. Although all of these enzymes share the same overall fold, there are subtle structural differences between classes. For example, Mu class enzymes have an extra loop near the active site that results

TABLE 3.5. Classes of Cytosolic GSTs

Class	Found in	Known Functions
Alpha	Eukaryotes	Detoxification, peroxide reduction
Beta	Bacteria	Haloalkane conjugation
Delta	Insects	Detoxification, insecticide resistance
Epsilon	Insects	Detoxification, insecticide resistance
Zeta	Bacteria and eukaryotes	Maleylacetoacetate and maleylpyruvate isomerases, tetrachlorohydroquinone dehalogenase
Theta	Bacteria and eukaryotes	Detoxification, peroxide reduction, haloalkane conjugation
Mu	Eukaryotes	Detoxification
Pi	Eukaryotes	Detoxification
Sigma	Insects and animals	Detoxification, prostaglandin D synthesis, lens crystallins in cephalopods
Tau	Plants	Anthocyanin synthesis
Phi	Plants	Anthocyanin synthesis
Omega	Bacteria and eukaryotes	Thiol transferase, dehydroascorbate reduction

in a deeper than usual active site, and Alpha class enzymes have an extra α -helix in the C-terminal domain that packs into the active site, resulting in a smaller and more hydrophobic active site. The subunit interface and the size of the cleft between the subunits, which appears to act as a catalytically inert ligand binding site, also vary between classes. Various classes also use different means to stabilize the thiolate of GSH at the active site. Some utilize a hydrogen bond with a tyrosine residue, while others utilize a serine residue. Some classes lack a corresponding serine or tyrosine residue but may use a cysteine for the same purpose.

3.5.B1b Mitochondrial GSTs Mitochondria of eukaryotic cells have a distinct GST called the kappa class GST. The structure of the kappa class GSTs is reminiscent of those of cytosolic GSTs. However, in the kappa class GSTs, the α -helical domain is inserted in the middle of the thioredoxin-fold domain, rather than being added at its C terminus. Its structure is quite similar to that of the disulfide isomerase, DsbA. Thus, it appears that GSTs arose by insertion or addition of an α -helical domain into a thioredoxin fold in two different evolutionary events. Like the cytoplasmic GSTs, the kappa class GST also lowers the pK_a of GSH at the active site to potentiate its reactivity. The kappa class GST has a high level of activity with 1-chloro-2,4-dinitrobenzene, but its physiological role has not been established. A role in protection against oxidative stress seems likely given its mitochondrial location.

3.5.B1c The MAPEG Superfamily A third type of GST is found in the MAPEG superfamily, the acronym deriving from the term “membrane-associated proteins in eicosanoid and GSH” metabolism. (Eicosanoids are compounds derived from 20-carbon fatty acids and include prostaglandins, prostacyclins, and leukotrienes.) Less is known about these membrane-bound GSTs than about the cytosolic GSTs because of the lack of high resolution structural information. The best characterized enzyme, MGST1, is a trimer; each subunit appears to be a left-handed four-helix bundle embedded in the membrane. This is likely to be the common structure for subunits of all members of the superfamily. However, there appears to be variability in quaternary structure. Various members of the superfamily exist as monomers or trimers or have multiple aggregation states.

Enzymes in this superfamily are found in eukaryotes and some bacteria, but not Archaea. There are six families of MAPEG proteins, including three families of microsomal GSTs (MGST1, MGST2, and MGST3), leukotriene C4 synthase, prostaglandin E synthase, and 5-lipoxygenase activating protein (FLAP). Notably, FLAP does not have a known catalytic function. It is required for activation of 5-lipoxygenase, which catalyzes the first step in leukotriene synthesis, the conversion of arachidonic acid into leukotriene A4.

3.5.B2 Roles of GSTs in Detoxification In mammals, GSTs play an important role in detoxification of harmful electrophilic compounds of both endogenous or exogenous origin. The liver, which receives toxins absorbed in the intestine

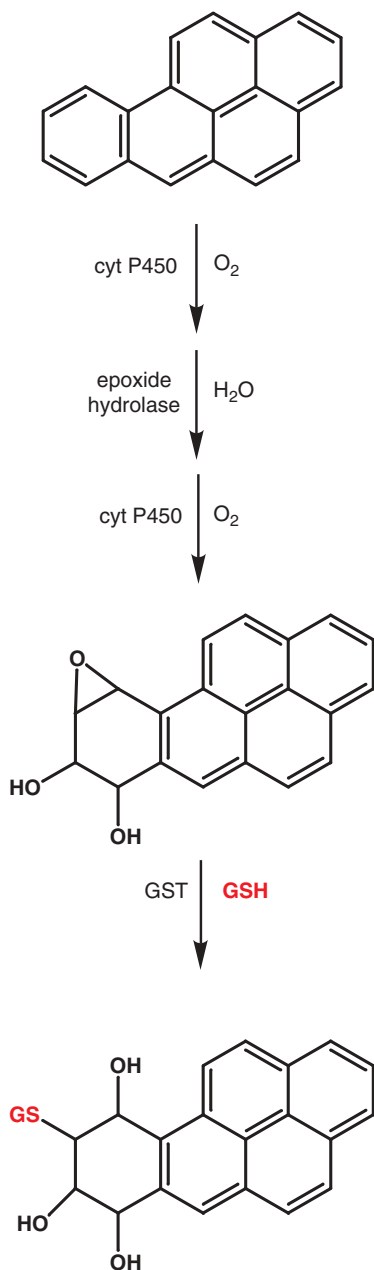


Figure 3.29. An example of the role of GSTs in Phase II detoxification reactions.

directly through the portal vein, is the primary site for such detoxification reactions—cytosolic GSTs comprise up to 10% of the soluble protein in liver cells. However, GSTs are involved in detoxification in other cell types as well. The MAPEG superfamily GSTs also provide detoxification functions. MGST classes 1–3 are active with a wide range of electrophilic substrates and have both GSH transferase and GSH-dependent peroxidase activity.

Many harmful compounds, including carcinogens, pesticides, and drugs, are attacked in the liver by cytochrome P450 enzymes in what is referred to as Phase I of detoxification. Oxidation of such compounds results in addition of a functional group that can be attacked by Phase II enzymes, which catalyze conjugation of highly polar groups to the newly added functional groups. GSTs are the most important of the Phase II enzymes. GSH conjugates may be exported or undergo further processing to remove the glutamate and glycine moieties and acetylate the amino group of the remaining cysteine moiety before export. An example of the role of a GST in detoxification of a xenobiotic compound is shown in Fig. 3.29. Benzo[*a*]pyrene is a procarcinogen formed by incomplete combustion of organic materials. It is converted by cytochrome P450 and epoxide hydrolase to the potent carcinogen (7*R*,8*S*)-dihydroxy-(9*S*,10*R*)-epoxy-7,8,9,10-tetrahydrobenzo[*a*]pyrene. Attack of GSH upon the epoxide moiety of this molecule destroys its ability to alkylate DNA and allows it to be exported from the cell.

Many cytosolic GSTs display considerable substrate promiscuity, reacting with a range of electrophilic substrates, although with different catalytic efficiencies. This is an advantage for enzymes involved in detoxification, since such enzymes need to be able to act upon a large number of toxins that may be encountered in the environment. Furthermore, it is not surprising from a mechanistic point of view, since production of the reactive thiolate form of GSH in proximity to any electrophile in the active site will provide substantial acceleration over the rate of the uncatalyzed reaction. The range of substrates that can be dealt with is further expanded by the presence of multiple isozymes of some classes of GSTs. Humans have five genes for Mu class GSTs, four for alpha class GSTs, and two for the theta and omega class GSTs. These isozymes often differ in substrate specificity. For example, the human theta class T1-1 isozyme has highest activity with dichloromethane, 1,2-epoxy-3-(*p*-nitrophenoxy)propane, and 4-nitrobenzyl chloride, while the T2-2 isozyme has highest activity with 1-menaphthyl sulfate.

3.5.B3 Roles of GSTs in Protection Against Oxidative Stress In addition to their ability to catalyze formation of GSH conjugates, many GSTs also reduce peroxides (Fig. 3.30). Although the specific activities for reduction of peroxides are generally lower than those for reaction with substrates such as 1-chloro-2,4-dinitrobenzene, high levels of GSTs, particularly in liver, result in a high capacity for peroxide reduction. Such reduction reactions result in cleavage of the O—O bond of the peroxide, forming an alcohol and water. Two molecules of GSH are oxidized to GSSG in this process. Similar reactions are carried by the selenium-dependent GSH peroxidases (see Section 3.7.A).

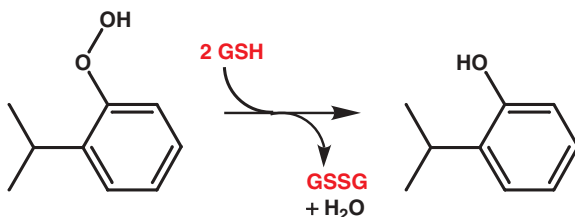


Figure 3.30. Reduction of cumene hydroperoxide by GSTs.

An additional contribution to protection against oxidative stress is provided by the omega class GSTs, which reduce dehydroascorbate, the oxidized form of vitamin C. These GSTs have both thioltransferase and dehydroascorbate reductase activity, but little or no activity with electrophilic substrates that undergo typical conjugation reactions with most GSTs.

3.5.B4 Specific Enzymatic Roles of GSTs Although GSTs involved in detoxification have evolved to be catalytically promiscuous to allow reaction with a wide range of electrophilic compounds, certain GSTs catalyze specific reactions in metabolic pathways. The examples of such reactions catalyzed by cytosolic GSTs in Fig. 3.31 illustrate the remarkable versatility of this superfamily. In nearly every case, nucleophilic attack of GSH upon an electrophilic form of the substrate is part of the reaction, and additional steps have been added before and/or after this step. An interesting exception is the isomerization of the steroids Δ^5 -androstene-3,17-dione and Δ^5 -pregnene-3,20-dione in the pathways leading to testosterone and progesterone, respectively, which are catalyzed by several human GSTs, and especially the alpha class GST A3-3. In this reaction, the thiolate of GSH is proposed to act as a base, removing a proton from the substrate, rather than serving as a nucleophile.

The MAPEG superfamily also includes enzymes that catalyze specific reactions (Fig. 3.32). Leukotriene C_4 synthase catalyzes the typical nucleophilic attack of GSH upon an electrophilic substrate, leukotriene A_4 , to produce the GSH conjugate, leukotriene C_4 . Prostaglandin E_2 synthase catalyzes the more complex isomerization of prostaglandin H_2 to prostaglandin E_2 . Note that this MAPEG superfamily enzyme catalyzes a reaction almost identical to that catalyzed by the cytosolic prostaglandin D_2 synthase (Fig. 3.31A), differing only in the disposition of the hydroxyl and carbonyl moieties in the reaction product.

3.5.B5 Importance of GST Polymorphisms in Human Health Because GSTs detoxify electrophilic compounds that damage cellular macromolecules, protect cells from oxidative stress, and contribute to the metabolism of therapeutic drug molecules, they are expected to play important roles in human health. Many GST genes are polymorphic. Both null alleles and single nucleotide polymorphisms have been identified in genes for many of the cytosolic and MAPEG superfamily GSTs. For example, 50% of the human population lacks the gene for the mu class GST isozyme 1 and 10–38% lack the gene for the theta class GST isozyme 1.

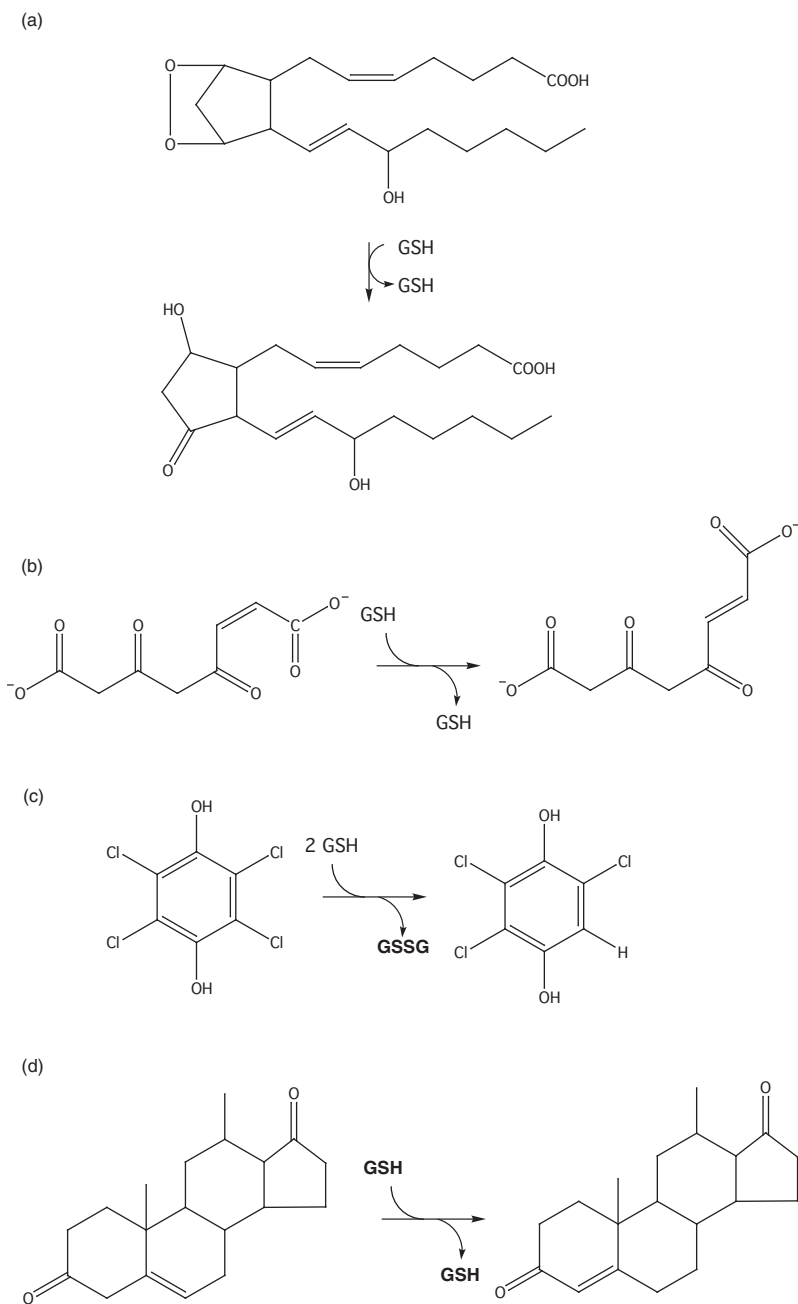


Figure 3.31. Roles of cytosolic GSTs in specific reactions. Each reaction involves nucleophilic attack of GSH upon an electrophilic substrate, although additional steps before or after that step may result in a more complex overall transformation. (A) Synthesis of prostaglandin D_2 from prostaglandin H_2 ; (B) isomerization of maleylacetoacetate to fumarylacetoacetate; (C) dehalogenation of tetrachlorohydroquinone; (D) isomerization of Δ^5 -androstene-3,17-dione to Δ^4 -androstene-3,17-dione.

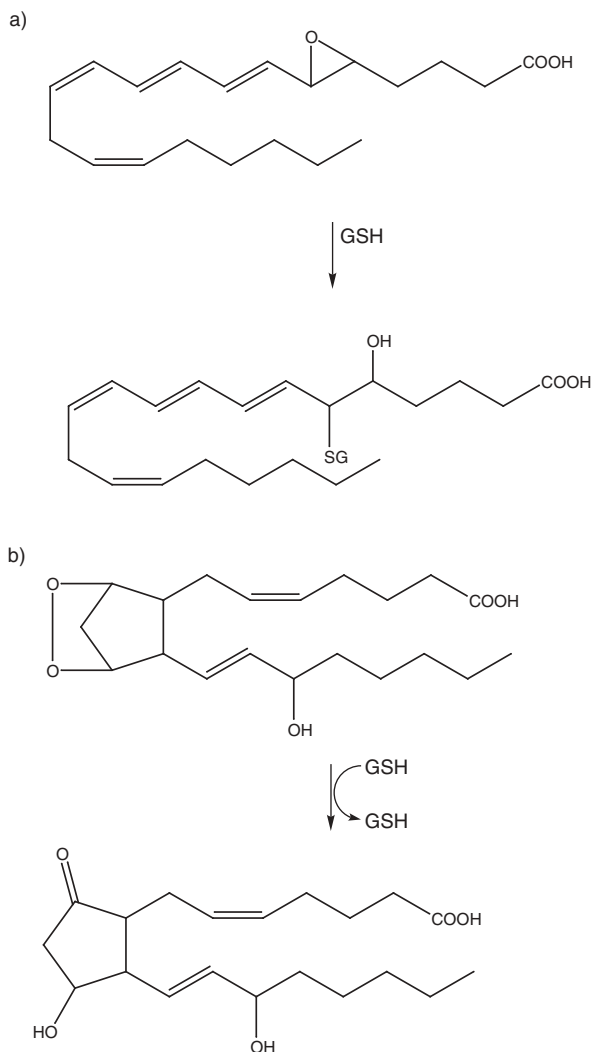


Figure 3.32. Roles of MAPEG superfamily GSTs in specific reactions: (A) leukotriene C_4 synthase and (B) prostaglandin E_2 synthase.

Considerable effort has been directed at deciphering relationships between particular alleles and susceptibility to disease. However, significant linkages between particular GST alleles and susceptibility to cancer have not been found in most cases, possibly because the overlapping functions of many broad-specificity GSTs minimize the effects of lack of function or diminished function in any one GST. It is also possible that such effects are difficult to find because the data are confounded by polymorphisms in other genes, including GSTs and cytochrome P450s, as well as unexamined interactions between variations in genes and other environmental exposures. However, there is a modest effect of the null alleles of GST M1 and GST T1 on the incidence

of head and neck cancer, and a somewhat larger effect of the null allele of GST M1 on the incidence of gastric cancer in smokers.

GSTs play a role in the metabolism of therapeutic drugs, raising the possibility that polymorphisms in GSTs may also influence response to chemotherapy. GST pi is often overexpressed in tumor cells and appears to play an important role in resistance to drugs used to treat tumors. Selective inhibitors of GST pi show promise for use in enhancing the efficacy of chemotherapeutic agents.

SELECTED REFERENCES

1. Hayes, J.D., Flanagan, J.U., and Jowsey, I.R. (2005). Glutathione transferases. *Annu. Rev. Pharmacol. Toxicol.* 45:51–88.
2. Sheehan, D., Meade, G., Foley, V.M., and Dowd, C.A. (2001). Structure, function and evolution of glutathione transferases: implications for classification of non-mammalian members of an ancient enzyme superfamily. *Biochem. J.* 360:1–16.
3. Ladner, J.E., Parsons, J.F., Rife, C.L., Gilliland, G.L., and Armstrong, R.N. (2004). Parallel evolutionary pathways for glutathione transferases: structure and mechanism of the mitochondrial class kappa enzyme rGSTK1-1. *Biochemistry* 43:352–361.
4. Bresell, A., Weinander, R., Lundqvist, G., Raza, H., Shimoji, M., Sun, T.-H., Balk, L., Wiklund, R., Eriksson, J., Jansson, C., Persson, B., Jakobsson, P.-H., and Morgenstern, R. (2005). Bioinformatic and enzymatic characterization of the MAPEG superfamily. *FEBS J.* 272:1688–1703.
5. Mahajan, S., and Atkins, W.M. (2005). The chemistry and biology of inhibitors and prodrugs targeted to glutathione *S*-transferases. *Cell. Mol. Life Sci.* 62:1221–1233.

3.6 OXIDATIVE FOLDING

3.6.A Disulfide Bond Formation in Bacteria

HIROSHI KADOKURA and JON BECKWITH

Department of Microbiology and Molecular Genetics, Harvard Medical School, Boston, Massachusetts

Disulfide bonds contribute to the stability, activity, and folding of secretory proteins or extracytoplasmic domains of membrane proteins. It had long been assumed that the oxidation of two cysteines to form a disulfide bond was a spontaneous process *in vivo* and *in vitro*. However, disulfide bond formation in proteins *in vitro* often requires hours or even days of incubation, whereas disulfide bond formation in a cell is a much more rapid process, occurring within seconds or minutes after the synthesis of proteins. In the early 1990s, genetic studies led to the discovery of the gene *dsbA* in the gram-negative bacterium *Escherichia coli*. DsbA, a thioredoxin-like protein, was shown to promote disulfide bond formation, thus establishing that, *in vivo*, this process is catalyzed. Since then, enzymes dedicated to disulfide bond formation have been identified in many organisms.

Disulfide bond formation commonly occurs in noncytoplasmic compartments such as the periplasm of gram-negative bacteria and the endoplasmic reticulum of eukaryotes. In this section, we discuss the catalytic systems that form disulfide bonds in proteins in *E. coli*, where it has been most thoroughly studied.

3.6.A1 The Pathway for Oxidative Protein Folding

3.6.A1a DsbA, the Disulfide Bond Forming Enzyme Mutants of *E. coli* that have lost DsbA are severely defective in disulfide bond formation in many extracytoplasmic proteins. Accordingly, *dsbA* null mutants show pleiotropic phenotypes such as loss of motility and increased sensitivity to dithiothreitol and metal ions like Cd^{2+} and Hg^{2+} .

DsbA has a Cys-Xaa-Xaa-Cys (CXXC) active site motif embedded in a thioredoxin-like fold (Fig. 3.33A). These two cysteines are kept oxidized (disulfide bonded) *in vivo*. When a newly translocated protein appears in the periplasm, DsbA introduces its disulfide bond directly into a pair of cysteines of the substrate (Fig. 3.34). This process is thought to occur via formation of an unstable mixed disulfide complex between DsbA and its substrate (Fig. 3.35A). Recently, complex formation was demonstrated *in vivo* using a mutation in DsbA that slows down the resolution step of this reaction.

DsbA, with a standard redox potential of -120 mV, is one of the most oxidizing proteins known. This enzyme oxidizes its substrates very quickly *in vitro* and *in vivo*. This is in contrast to thioredoxin, which has a much lower standard redox potential of -270 mV and reduces disulfide bonds in the cytoplasm.

The ability of DsbA to act as a strong oxidant derives in part from its biophysical properties. Cys30 of DsbA, the first cysteine of the CXXC motif, has an unusually low pK_a value of 3.5 (the normal pK_a of cysteine residues is ~ 9). Thus, Cys30 is in the thiolate anion state at physiological pH. Structural studies suggest how the thiolate anion of Cys30 is stabilized. First, Cys30 is located at the N terminus of an α -helix, where a partial positive charge from the helix dipole can stabilize the thiolate. Second, this thiolate is also maintained by an electrostatic interaction with His32 in the reduced DsbA. These features result in the reduced form of the protein being more stable than the oxidized form, thus providing a thermodynamic driving force for the transfer of disulfide bonds from DsbA to its substrates.

While DsbA catalyzes disulfide bond formation in a wide variety of proteins, it apparently avoids interaction with a subset of proteins containing potentially oxidizable cysteines (e.g., DsbC and DsbD, see below). These latter interactions may be avoided because DsbA is able to interact only with unfolded or partially folded proteins in which hydrophobic regions are exposed. NMR studies of complexes between DsbA and a bound peptide indicate that DsbA binds substrates in a hydrophobic manner, perhaps utilizing a hydrophobic groove near its active site.

3.6.A1b DsbB, the Enzyme that Maintains DsbA in the Oxidized State After DsbA transfers its disulfide bonds to substrates, its active site must be reoxidized to repeat another catalytic cycle. The isolation of a second class of mutants that were defective in protein disulfide bond formation led to the discovery of DsbB, a

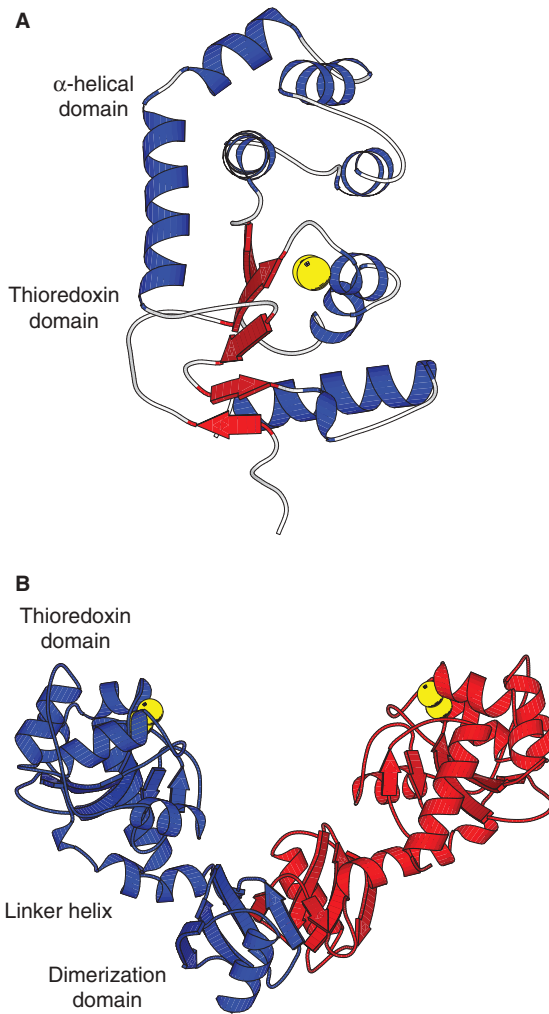


Figure 3.33. The crystal structures of DsbA (A) and DsbC (B). DsbA has a thioredoxin-like fold with the insertion of an α -helical domain. DsbC is a V-shaped homodimer, where each arm is a monomer containing an N-terminal dimerization domain and a C-terminal thioredoxin domain. The two domains are connected by a linker helix. The yellow spheres represent the sulfurs of active site cysteines.

cytoplasmic membrane protein. Normally, DsbA is found exclusively in the oxidized form. Mutations of the *dsbB* gene cause accumulation of DsbA in the reduced form and exhibit the same phenotype as *dsbA* mutants.

Previously, we saw that the oxidizing nature of DsbA derives in part from the instability of its oxidized form. However, most thioredoxin-like proteins can catalyze, *in vitro*, both oxidation and reduction depending on the redox state of their active site.

An important factor determining the role of DsbA *in vivo* is that it is maintained in the oxidized state. Indeed, when the cytoplasmic reducing enzyme thioredoxin was exported into the periplasm using a signal sequence, it also acted, albeit weakly, as an oxidant of proteins because it was oxidized by DsbB. This result shows that the redox partner enzymes play a vital role in determining the physiological property of a protein of this family.

DsbA is oxidized by DsbB. Then, what regenerates oxidized DsbB? Depletion of the respiratory chain components, quinones or heme, caused DsbA and DsbB to accumulate in their reduced forms, indicating that the respiratory chain is necessary for the oxidation of DsbB. Later, an *in vitro* system with purified components revealed that ubiquinone and menaquinone serve as direct recipients of electrons from DsbB. Thus, aerobically, DsbB is oxidized by ubiquinone, which is then reoxidized by terminal oxidases that pass electrons to O₂. Anaerobically, DsbB is reoxidized by menaquinone, which then passes electrons to acceptors other than O₂ (Fig. 3.34). This mechanistic switch allows DsbB to work under both aerobic and anaerobic conditions.

DsbB spans the membrane four times and has two periplasmic loops, each containing a pair of essential cysteines (Cys41–Cys44 and Cys104–Cys130). These cysteine

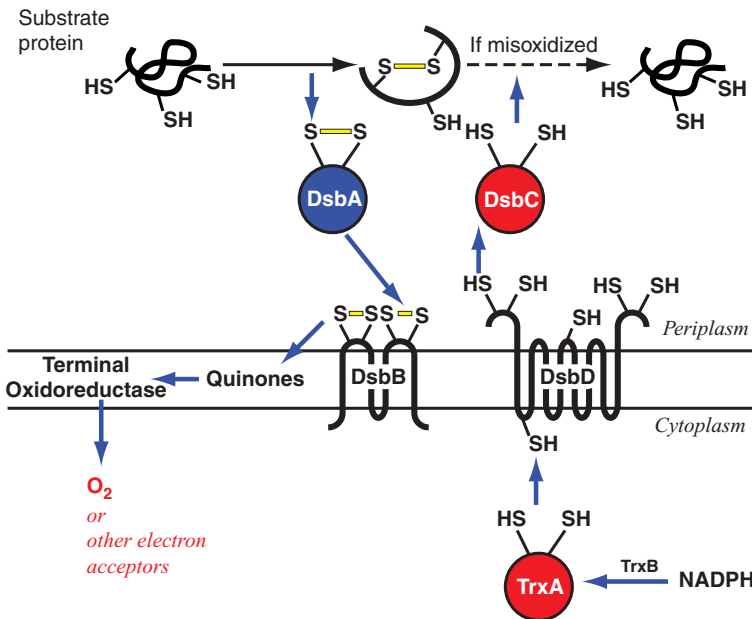


Figure 3.34. Models for disulfide bond formation in the periplasm of *E. coli*. The solid black arrow indicates the oxidative folding reaction catalyzed by DsbA. In the instance where the first folding reaction resulted in a misoxidized protein, DsbC may repair it by acting as a reductase (dotted arrow) or an isomerase (not shown in this figure) of the incorrect disulfide bond. The blue arrows indicate the flow of reducing equivalents. See text for details.

pairs are redox-active and found in the oxidized state *in vivo*. The *in vivo* and *in vitro* analyses of mutants in which these cysteines are altered provided insights into DsbB's action. First, the Cys104–Cys130 pair interacts directly with reduced DsbA. Second, oxidation of the Cys104–Cys130 pair requires the Cys41–Cys44 pair. Finally, the Cys41–Cys44 pair is directly oxidized by quinones. Thus, electrons from DsbA flow first to the Cys104–Cys130 pair, then to the Cys41–Cys44 pair, and from there to quinones in the respiratory chain.

Interesting questions remain concerning the mechanism of DsbB action. For example, paradoxically, on the basis of standard redox potentials, the Cys104–Cys130 pair of DsbB is less oxidizing (-267 mV) than the cysteine pair of DsbA (-120 mV). Consistently, the oxidized Cys104–Cys130 pair in a DsbB lacking the Cys41–Cys44 pair could not oxidize DsbA *in vitro*. If the Cys104–Cys130 pair alone cannot oxidize DsbA, how does DsbB utilize these cysteines to directly oxidize DsbA? How quinone oxidizes the Cys41–Cys44 pair of DsbB is another exciting question. Although some models have been proposed, there are no definitive answers to these questions.

3.6.A2 Protein Disulfide Bond Isomerization Pathway

3.6.A2a DsbC, the Protein Disulfide Bond Isomerase For a protein with two cysteines, there is only one possible disulfide bond that can form. However, in a protein with three or more cysteines, two cysteines could be joined in a disulfide bond that does not appear in the native structure. In *E. coli*, the periplasmic protein DsbC repairs such “misoxidized” proteins (Fig. 3.34). DsbC was discovered by searching for a mutation or a gene on a multicopy plasmid that altered the sensitivity of cells to dithiothreitol. Studies *in vivo* and *in vitro* established that DsbC repairs incorrect disulfide bonds, earning it the name disulfide isomerase. The *in vivo* function of a second periplasmic isomerase, DsbG, is not understood.

DsbC is a homodimeric molecule with V-shaped structure (Fig. 3.33B). Each arm of the dimer is a monomer (23 kDa) consisting of a C-terminal thioredoxin domain with a CXXC active site and an N-terminal dimerization domain. Two cysteines (Cys98 and Cys101) in the active site face the inside of V-shape from each monomer and are in the reduced state *in vivo*. DsbC has a standard redox potential of -130 mV, which is slightly lower than that of DsbA.

How does DsbC repair incorrect disulfide bonds? Two models have been proposed (Fig. 3.35B,C). In both cases, the process starts with the nucleophilic attack by Cys98 of DsbC on the incorrect disulfide bond. This reaction results in the formation of a mixed disulfide between DsbC and its substrate. After this event, the two possible pathways diverge. In the first, the mixed disulfide is attacked by a third cysteine of the substrate, resolving the complex, allowing a more stable disulfide bond to form in the substrate and restoring a reduced DsbC. In this case, DsbC is acting as an isomerase (Fig. 3.35B). In the second, the mixed disulfide is attacked by Cys101 of DsbC, generating a reduced substrate and an oxidized DsbC. The reduced substrate could then be oxidized again by DsbA to give the correct disulfide bond. In this model, DsbC is acting as a reductase (Fig. 3.35C). An important feature of both pathways is

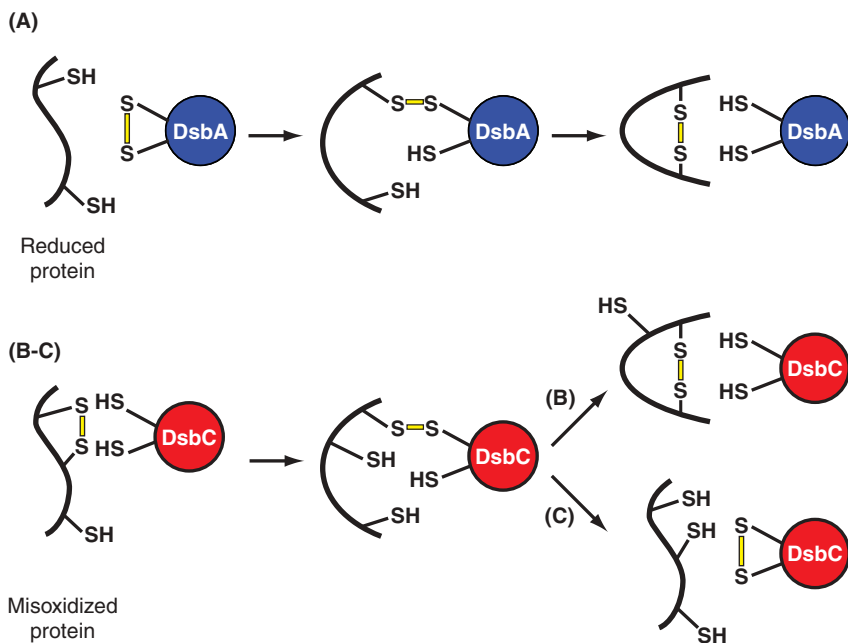


Figure 3.35. Disulfide bond formation (A), isomerization (B), and reduction (C). Because the mixed disulfide intermediate is formed by the attack on the disulfide by a thiolate anion, the thiol of the attacking cysteine must be deprotonated (not shown). Following the reduction of the substrate protein in sequence (C), DsbA can reoxidize the substrate, potentially generating the correct disulfide bond.

that the active site of DsbC must be in the reduced state for this enzyme to repair a nonnative disulfide bond.

While DsbA, which is monomeric, is oxidized by DsbB, DsbC is protected from such unwanted oxidation by its dimeric state. However, a mutation that results in the inability of DsbC to form a dimer allows DsbB to oxidize DsbC. The oxidized mutant DsbC can now act as an oxidant of exported proteins in the periplasm.

How does DsbC recognize its misoxidized substrates and why does it not attack disulfide bonds in properly oxidized proteins? In addition to its role as an isomerase of disulfide bonds, DsbC has chaperone activity, which allows it to assist the folding of proteins without disulfide bonds. For this activity, the cysteine residues of the active site of DsbC are not required. The possession of the dual activity may allow DsbC to efficiently recognize proteins with nonnative disulfide bonds (chaperone activity) and repair the disulfide bonds (isomerase or reductase activity), but not recognize properly folded proteins.

The recognition site in DsbC for the misfolded protein probably resides in a cleft formed by the inside of the V-shape (Fig. 3.33B). This cleft is large enough ($40 \text{ \AA} \times 40 \text{ \AA} \times 25 \text{ \AA}$) to bind small proteins. Furthermore, the inner surface is covered

with uncharged and hydrophobic residues, a feature often seen in domains that bind misfolded or unfolded proteins.

3.6.A2b DsbD, the Enzyme Responsible for Maintaining DsbC in the Reduced State As we have seen earlier, DsbC must be maintained in the reduced state for it to be active. This task is carried out by a membrane protein DsbD. In *dsbD* null mutants, DsbC (and its homolog DsbG) fails to be reduced and thus cannot act as an isomerase or reductase. In addition, *dsbD* mutant strains are unable to synthesize *c*-type cytochromes since DsbD also transfers electrons to CcmG, a membrane-tethered thioredoxin-like protein involved in keeping the cysteines of the heme attachment site of *c*-type apocytochromes in the reduced state, a prerequisite for the binding of heme to the apocytochromes.

As a result of reducing DsbC, DsbD becomes oxidized. Oxidized DsbD is reduced by cytoplasmic thioredoxin (TrxA). Thereby, DsbD transfers electrons from TrxA in the cytoplasm to DsbC in the periplasm. Oxidized TrxA is in turn reduced by thioredoxin reductase (TrxB), which uses NADPH as a source of electrons. Thus, reducing power to maintain DsbC in the reduced state originates from NADPH (Fig. 3.34).

DsbD (59 kDa) consists of three domains: an N-terminal periplasmic domain (DsbD α) with an immunoglobulin-like fold, a hydrophobic core domain that spans the membrane eight times (DsbD β), and a C-terminal periplasmic domain (DsbD γ) with a thioredoxin-like fold. Each of these domains has a pair of cysteines that are essential for the protein's activity.

Surprisingly, these three domains, when expressed as separate polypeptides, restore DsbD activity *in vivo*. This finding facilitated the analysis of the protein's mechanism. By examination of the effect of mutating cysteines of one domain on the redox state of the other two domains and detection of mixed disulfide complexes between thioredoxin and DsbD β and between DsbC and DsbD α , it was concluded that DsbD α directly reduces oxidized DsbC; oxidized DsbD α , thus generated, is then reduced by DsbD γ ; likewise, oxidized DsbD γ is reduced by DsbD β ; and finally oxidized DsbD β is reduced by thioredoxin. This cascade model was validated later using an *in vitro* system with purified components.

The standard redox potentials of DsbD α and DsbD γ are -229 mV and -241 mV, respectively, which, as predicted, are lower than that of DsbC (-130 mV) but higher than that of thioredoxin (-270 mV). Thus, DsbC reduction by DsbD appears to be thermodynamically favored, unlike the oxidation of DsbA by the second periplasmic domain of DsbB.

Among the reactions catalyzed by DsbD, most intriguing perhaps is the transmembrane electron transfer by DsbD β . If this step proceeds via stepwise thiol–disulfide exchanges, the two essential cysteines of DsbD β need to interact with both thioredoxin in the cytoplasm and DsbD γ in the periplasm. One of the models proposed for electron transfer by DsbD β predicts that, like the lactose permease, DsbD β alternates in conformation between an opening of its membrane-embedded portion, including its active site cysteines, to the periplasm and an opening to the cytoplasm. In the

oxidized state, DsbD β would open to the cytoplasm to interact with reduced thioredoxin; upon reduction, it would open to the periplasm for interaction with DsbD γ , which would allow the passage of electrons across the membrane without perturbing the function of the membrane as a permeation barrier.

Both oxidative (DsbA–DsbB) and reductive (DsbC–DsbD) pathways coexist in the periplasm (Fig. 3.34). The collision of two pathways (e.g., oxidation of DsbC by DsbB) would cause a futile cycle of oxidation and reduction, leading to the loss of both oxidative and reductive powers. To prevent such a wasteful collision, each protein appears to have evolved features that allow it to interact only with its expected redox partners. For example, the α -helical domain of DsbA is thought to protect the active site of DsbA from misreduction by DsbD (Fig. 3.33A). Furthermore, in addition to its role in preventing misoxidation of DsbC by DsbB, the dimeric structure of DsbC appears to be required for DsbC to be reduced by DsbD. Moreover, the rate of electron transfer between reduced DsbC and oxidized DsbA is very small. This fact can be explained by assuming that both proteins can bind only unfolded or misfolded proteins.

SELECTED REFERENCES

1. Bader, M.W., Hiniker, A., Regeimbal, J., Goldstone, D., Haebel, P.W., Riemer, J., Metcalf, P., and Bardwell, J.C.A. (2001). Turning a disulfide isomerase into an oxidase: DsbC mutants that imitate DsbA. *EMBO J.* 20:1555–1562.
2. Bardwell, J.C., McGovern, K., and Beckwith, J. (1991). Identification of a protein required for disulfide bond formation in vivo. *Cell* 67:581–589.
3. Kadokura, H., Tian, H., Zander, T., Bardwell, J.C.A., and Beckwith, J. (2004). Snapshots of DsbA in action: detection of proteins in the process of oxidative folding. *Science* 303:534–537.
4. Katzen, F., and Beckwith, J. (2000). Transmembrane electron transfer by the membrane protein DsbD occurs via a disulfide cascade. *Cell* 103:769–779.
5. Kobayashi, T., Kishigami, S., Sone, M., Inokuchi, H., Mogi, T., and Ito, K. (1997). Respiratory chain is required to maintain oxidized states of the DsbA–DsbB disulfide bond formation system in aerobically growing *Escherichia coli* cells. *Proc. Natl. Acad. Sci. USA* 94:11857–11862.

3.6.B Disulfide Bond Formation in Eukaryotes

HIRAM F. GILBERT

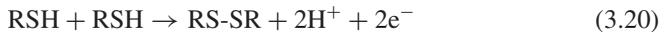
Department of Biochemistry and Molecular Biology, Baylor College of Medicine, Houston, Texas

Disulfide bond formation between two cysteine residues represents a reversible post-translational modification that can be introduced into proteins to increase stability in an oxidizing external environment or to modulate protein function in a reducing

environment. Disulfide bond formation and the reduction of disulfide bonds occur by a simple chemical exchange of thiols and disulfides that is catalyzed by thiol/disulfide oxidoreductases. In both prokaryotic and eukaryotic organisms, the electrons derived from disulfide bond formation flow through a series of carriers and are eventually delivered to a flavoprotein oxidase. Secreted eukaryotic proteins contain a larger number of disulfides than bacterial proteins and, consequently, have a more active quality control system to ensure that the correct disulfides are formed as the protein matures. Because most disulfides occur in extracellular proteins, the eukaryotic endoplasmic reticulum (ER) provides a redox environment that encourages disulfide bond formation and a network of chaperones and folding catalysts to ensure that the correct disulfides are formed prior to exiting the ER.

3.6.B1 General Characteristics of Disulfides in Proteins Appreciating the overall mechanisms that govern protein disulfide formation in eukaryotes (and prokaryotes) requires a brief introduction to the chemistry and biochemistry of disulfide bond formation.

3.6.B1a Chemistry of Disulfide Bond Formation Disulfide bond formation is formally a two-electron chemical oxidation in which two cysteines (RSH) are covalently bonded (RS-SR) with the formation of two protons and two electrons (Eq. (3.20)).



The two cysteines to be connected may reside in the same polypeptide chain (intramolecular disulfide) or in different polypeptide chains within the same complex (intermolecular disulfide). The two cysteines in an intramolecular disulfide may be close to each other in primary sequence or far away; however, to form a disulfide, the two cysteines must be able to approach each other closely enough to form a covalent bond and an electron acceptor must be able to remove electrons, a process that is additive with other interactions in the folding protein. The sequence cues that determine which cysteines will pair as disulfides are not understood; however, disulfide formation is linked to the overall folding of the protein and the same side chain interactions that stabilize secondary and tertiary structure will also direct which cysteines will pair and how stable the disulfide will be.

Metal-catalyzed oxidation using oxygen as an electron acceptor can produce disulfides, but the chemistry of “spontaneous” disulfide formation is generally too slow to accommodate the requirements for producing disulfide-containing proteins *in vivo*. In the cell, disulfide bond formation (and the reverse, reduction of disulfides) occurs through catalyzed thiol–disulfide exchange involving donor disulfides and acceptor dithiols resulting in the transfer of disulfides between proteins (Fig. 3.36).

3.6.B1b Disulfide Stability The cellular oxidation of protein thiols to protein disulfides generally occurs through thiol–disulfide exchange. Thiols are oxidized to

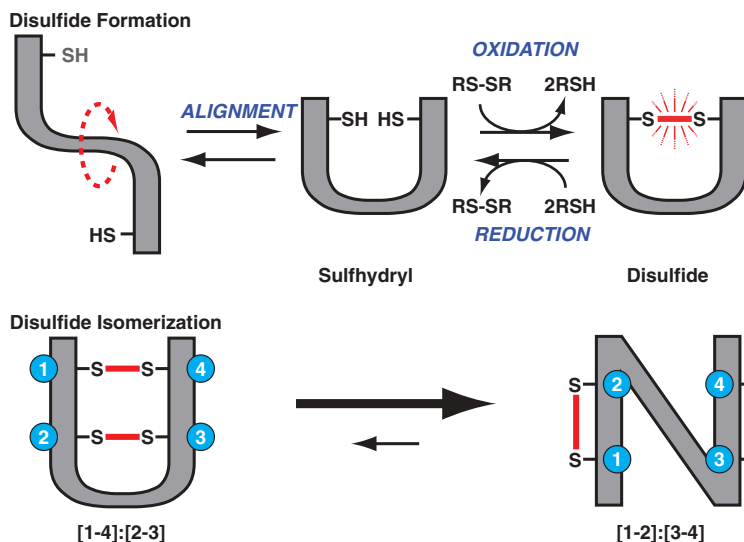
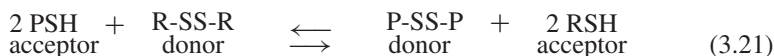


Figure 3.36. Protein disulfide formation and isomerization. Used with permission from Gilbert, H.F. (2004), Protein disulfide formation. In *The Encyclopedia of Biological Chemistry*, Elsevier, New York, pp. 598–602.

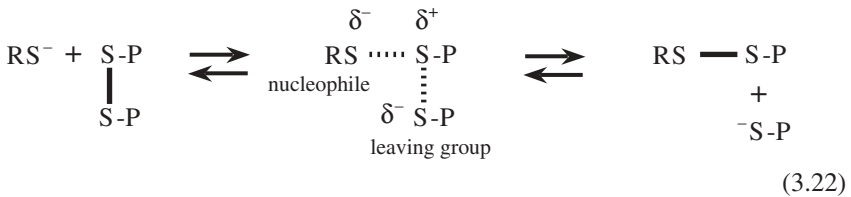
disulfides by an exchange of electrons and protons with a donor disulfide in a reversible chemical reaction (Eq. (3.21)).



The equilibrium position will depend on the properties of the individual thiols and disulfides and their concentrations. At equilibrium, the more stable disulfide will form (lowest reduction potential). Structural factors in the protein (secondary and tertiary structure) that stabilize a disulfide will favor its formation. All disulfides in proteins are not equally stable and their stabilities may span a range of at least 10^5 in equilibrium stability (~ 6.8 kcal/mol). The ratio of concentrations of the donor disulfide and its dithiol form will also influence how much acceptor disulfide will form. For example, in the eukaryotic cytosol, the high concentration of GSH ($\sim 2\text{--}10$ mM) and the low concentration of GSSG (GSH/GSSG = 100–400), make it more difficult to form disulfides in cytosolic proteins; however, the eukaryotic cell provides a more oxidizing environment in the ER with GSH/GSSG of 2–5. This more oxidizing environment accommodates the formation of the relatively unstable disulfides, which can form during protein folding.

3.6.B1c Disulfide Reactivity The thiol–disulfide exchange reaction occurs by the attack of a thiolate anion (the nucleophile) on one of the sulfurs of the disulfide (the central sulfur) resulting in the expulsion of a thiolate anion (the

leaving group) from the original disulfide and the formation of a new disulfide (Eq. (3.22)).



The pK_a of the SH group of cysteine (8.6) is higher than cellular pH; consequently, protein structural factors (i.e., nearby positive charge and hydrogen bonding) that lower the pK_a of a thiol will result in more thiolate anion at neutral pH and cause the reaction to occur faster (this effect disappears when the pK_a of the thiol is sufficiently low to be completely ionized at cellular pH). However, the ability of the sulfur to act as a leaving group will continue to improve as the SH pK_a drops below solution pH. Consequently, the pK_a values of catalysts of thiol–disulfide exchange in the cell are often low, compared to the pK_a of the SH of cysteine itself, making them more reactive and better leaving groups.

3.6.B2 Pathways for Disulfide Formation

3.6.B2a The Endoplasmic Reticulum Disulfide-containing proteins are largely extracellular, where the disulfide is introduced to stabilize the structure (note that there are other ways to stabilize structure and, in fact, proteins from thermophiles have few disulfides). There are few disulfides in the cytosol because of its highly reducing environment. The nature of disulfide-containing proteins places some requirements on their formation. Because disulfide formation is a chemical oxidation, eukaryotic cells require an electron transfer pathway to remove electrons from proteins as they form disulfides. This must also occur in an environment that is oxidizing enough to accommodate disulfide formation during the synthesis and processing of extracellular proteins. Too reducing an environment would prevent formation of disulfides, particularly the ones that form early in the folding pathway that may not be particularly stable. Spontaneous disulfide formation is slow, so catalysts will also be needed to accelerate disulfide exchange reactions. In eukaryotic cells, this specialized intracellular environment is the ER. During translation, extracellular proteins are translocated into this compartment, processed to a correctly folded form (or degraded), and released to the Golgi for further processing (Fig. 3.36). Disulfide formation, coupled to the correct folding of the protein, is generally complete before leaving the ER. The ER environment is also significantly more oxidizing than the cytosol, allowing disulfides to accumulate during protein folding. The ER also contains proteins that set up electron transfer pathways to remove the electrons produced by disulfide formation. In addition, there are catalysts for disulfide exchange and a quality control system that monitors disulfides to ensure the correct disulfide is formed.

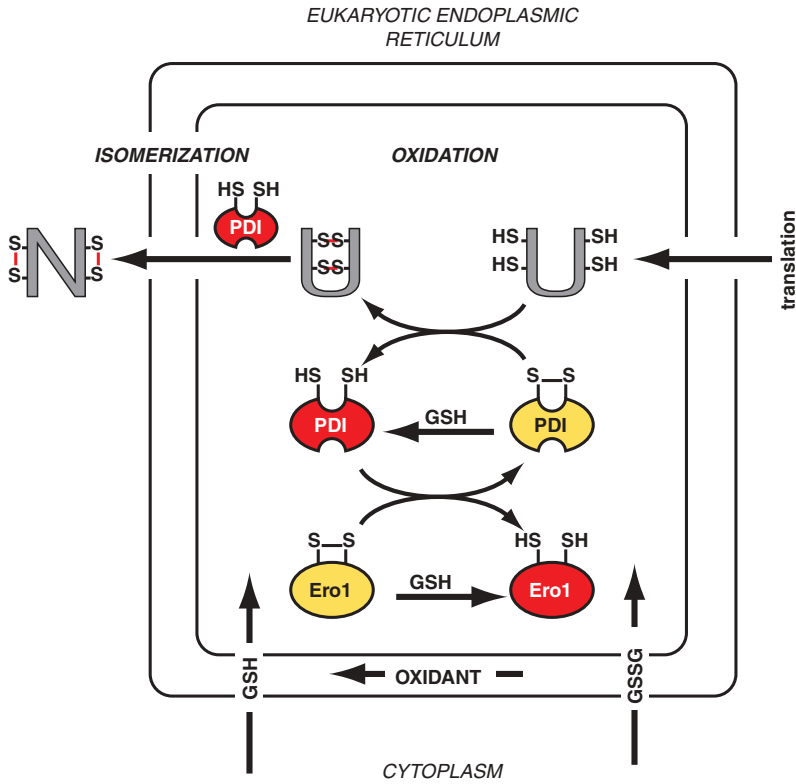


Figure 3.37. Protein disulfide formation and isomerization in the eukaryotic endoplasmic reticulum. Used with permission from Gilbert, H.F. (2004), Protein disulfide formation. In *The Encyclopedia of Biological Chemistry*, Elsevier, New York, pp. 598–602.

3.6.B2b Electron Flow in the ER Newly synthesized, extracellular proteins enter the ER from ribosomes directed to the ER membrane by the ER secretion signal (Fig. 3.37). During synthesis, the new polypeptide chain is cotranslationally inserted into the ER lumen with the cysteines in the reduced (SH) state. Because of the complexity of the intermediates during disulfide formation, it has been difficult to obtain a great deal of detail about disulfide formation in individual proteins *in vivo*. However, disulfide formation has been detected on nascent chains, still attached to the ribosome. In other cases, disulfide formation is observed significantly after the completion of synthesis. The determinates that specify the initial order of disulfide formation in the ER are not understood.

As the newly synthesized proteins enter the ER lumen, a catalyst—protein disulfide isomerase (PDI)—utilizes disulfides in its active sites to introduce disulfides into the substrate protein. To recycle the PDI back to its disulfide form, an ER oxidase(s)—Ero1p—oxidizes PDI (Fig. 3.37).

Ero1 and Erv2P Independently, the Kaiser and Weissman laboratories discovered an ER oxidase (Ero1p) in eukaryotic cells (*Saccharomyces cerevisiae*) by screening for mutations that made yeast sensitive to reductive stress from dithiothreitol. Ero1p is a conserved flavoprotein oxidase that uses a covalently bound flavin to introduce disulfides into its substrate, PDI, which, in turn, introduces those disulfides into newly synthesized proteins. In yeast, *ERO1*, like *PDII*, is an essential gene, so that disulfide formation in secreted proteins is essential to the viability of yeast. The structure of Ero1p (and the structure of the related Erv1p) show a dithiol–disulfide pair near the flavin and another pair near the active site that is involved in shuttling electrons between the flavin cofactor and PDI.

In yeast, there are two ER oxidases. Ero1p, which is the essential oxidant for PDI, is the major oxidant, although Erv2p rescues the deletion of Ero1p when overexpressed. In humans, there are also two ER thiol oxidases. Ero1-L α is expressed constitutively, while Ero1-L β is induced under conditions of ER stress during the Ero1-catalyzed oxidation of protein substrates. H₂O₂ is produced, and the suggestion has been made that this may contribute significantly to the cellular load of H₂O₂. Although oxygen can serve as the terminal electron acceptor *in vitro*, the specific pathway of electron transfer is not known *in vivo*.

PDI as an Oxidase/Isomerase The spontaneous formation of disulfides during protein folding in even small proteins like ribonuclease and lysozyme is much too slow (hours to days) to be biologically relevant. Searching for an enzyme that might speed up disulfide formation, the Anfinsen group found PDI, a 55 kDa protein localized in the ER and responsible for introducing disulfide bonds into proteins. During disulfide formation (Fig. 3.36), two cysteines must be correctly aligned and oxidized. The catalyst for this reaction, PDI, is a multidomain protein with four thioredoxin domains linked in tandem with a C-terminal anionic tail. The two catalytic domains (a and a') are located in the N- and C-terminal thioredoxin domains, separated by the two noncatalytic thioredoxin domains (b and b') (Fig. 3.38). The two active sites both contain a CGHC sequence in which the cysteine nearer the N terminus is exposed and able to react with substrate cysteines. The more C-terminal cysteine is buried and only forms a disulfide bond with its N-terminal neighbor. The structure of PDI reveals a C-shaped molecule arranged about the noncatalytic domains, similar to that observed for the prokaryotic isomerase, DsbC.

In its disulfide form, the PDI active site is an exceptionally good oxidant, approximately 500-fold more reactive than the disulfide of GSSG. The multidomain structure of PDI is not really necessary for PDI to act as an oxidant; the individual a and a' domains each exhibit about 50% of the disulfide-forming ability of full-length PDI. *In vitro*, when presented with an unfolded protein substrate, PDI places disulfides



Figure 3.38. The domain structure of protein disulfide isomerase. Each of the ~ 10 kDa domains has sequence and structural similarity to thioredoxin.

indiscriminately, resulting initially in a large collection of disulfide isomers, many of which are incorrect. The early steps in oxidative protein folding, at least *in vitro*, are prone to error, and the mispairing of cysteines is commonplace. PDI has the ability to correct these errors through a process of disulfide isomerization (Fig. 3.36). For example, PDI will efficiently transform scrambled ribonuclease, which is oxidized under denaturing conditions to generate a near-random collection of mispaired disulfides, into the native structure. Unlike its disulfide-forming activity, the isomerase activity of PDI requires a multidomain structure, including the b' domain, which most likely mediates a rather nonspecific interaction with unfolded and partially folded substrates. To catalyze isomerization, the reduced (dithiol) form of PDI is also required. Thus, PDI appears to catalyze isomerization simply by reducing incorrect disulfides and allowing another opportunity to form a correct disulfide. This continues until a connection of disulfides is sufficiently stable that it is no longer a substrate for the isomerase activity of PDI. Thus, PDI-catalyzed disulfide formation and isomerization may be considered a trial-and-error process rather than one specifically guided by PDI.

In yeast, *PDI1* is an essential gene. Of the two enzyme activities (oxidase and isomerase), the oxidase activity is the essential feature of the molecule, at least under normal growth conditions. The PDI a' catalytic domain will, under the control of the *PDI1* promoter (and with comparable expression levels), rescue the lethal *PDI1* gene deletion. The isolated a' domain has <5% of the isomerase activity of PDI but retains about half of the oxidase activity when measured *in vitro*. The a' domain also rescues the *PDI1* deletion even in strains where all of the ER homologs of PDI have been deleted. This suggests that normal growth is not highly dependent on the ability of the yeast ER to isomerize incorrect disulfides. Although the growth rate of yeast strains that are deficient in isomerase activity is near wild-type, PDI does exhibit isomerase activity *in vivo*, accelerating the maturation of the extracellular protein CPY, which requires isomerization to mature. Also consistent with its role as both an oxidase and isomerase *in vivo*, the redox state of PDI in the yeast ER maintains a significant amount of reduced PDI (about 40% of the two active sites are reduced). The balance of Ero1p oxidation, protein substrate oxidation, and reduction/oxidation by any ER GSH results in an active site redox state that is capable of catalyzing disulfide formation and disulfide reduction.

GSH and GSSG In addition to the redox cycle provided by Ero1p, PDI, and substrate thiols, the ER contains GSH. Few details are available about the specific function of GSH in the ER. Mutation of the *GSH1* gene allows yeast cells with an otherwise lethal mutation in *ERO1* to survive. This suggests that GSH may be imported into the ER to oppose the oxidase activity of Ero1 and maintain an appropriate redox balance in the ER.

The formation of disulfides in eukaryotic cells bears many similarities to disulfide formation in prokaryotes, including similarities in the basic mechanisms for transferring electrons and the utilization of thioredoxin-motif proteins to catalyze thiol–disulfide exchange reactions. In general, eukaryotic extracellular proteins have more disulfides and with more complex arrangements. The disulfide formation and quality control system of the eukaryotic ER is clearly able to cope with this increased

complexity through a series of catalysts and other ER chaperones to assist the folding protein in reaching its correct arrangement of disulfides.

SELECTED REFERENCES

1. Tu, B.P., and Weissman, J.S. (2004). Oxidative protein folding in eukaryotes: mechanisms and consequences. *J. Cell. Biol.* 164:341–346.
2. Schwaller, M.F., Wilkinson, B., and Gilbert, H.F. (2003). Reduction/reoxidation cycles contribute to catalysis of disulfide isomerization by protein disulfide isomerase. *J. Biol. Chem.* 278:7154–7159.
3. Xiao, R., Wilkinson, B., Solovyov, A., Lundstron-Ljung, J., Winther, J.R., Holmgren, A., and Gilbert, H.F. (2004). Protein disulfide isomerase is an oxidase and isomerase in the *S. cerevisiae* endoplasmic reticulum. *J. Biol. Chem.* 279:49780–49786.

3.7 OTHER ANTIOXIDANT ENZYMES

3.7.A Selenoproteins

VADIM N. GLADYSHEV

Redox Biology Center and Department of Biochemistry, University of Nebraska, Lincoln, Nebraska

Selenium is an essential trace element in many life forms. It is present in proteins in the form of selenocysteine, the 21st amino acid in the genetic code. Selenocysteine is encoded by the TGA codon and found in all domains of life (e.g., Eubacteria, Archaea, and Eukarya). Selenocysteine differs from cysteine and serine by a single atom, but has some unique chemical and biological properties (Fig. 3.39). It is clear that the essential role of selenium in biology, as well as its role in human health, are due to its presence in selenoproteins in the form of selenocysteine. In contrast to the other 20 genetically encoded amino acids found in proteins, selenocysteine

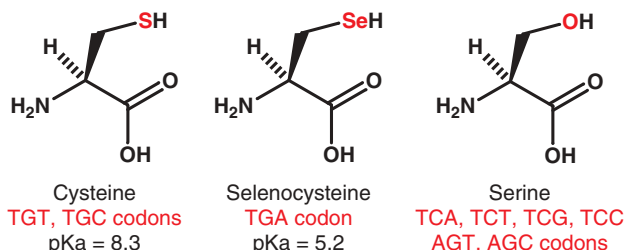


Figure 3.39. Cysteine, selenocysteine, and serine. These three amino acids differ by a single atom (S versus Se versus O) and are encoded by unique codons. Selenocysteine and cysteine have similar chemical properties, but selenocysteine is more reactive. Its low pK_a (5.2) ensures that it is ionized under physiological conditions, whereas the pK_a for cysteine (8.3) is such that many cysteines are protonated.

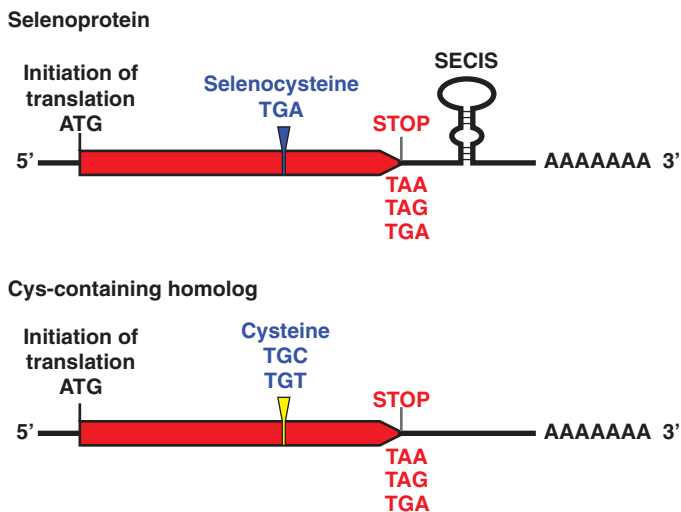


Figure 3.40. Comparison of selenoproteins and their cysteine-containing homologs. For TGA to code for selenocysteine, selenoprotein mRNAs utilize SECIS element, a stem–loop structure present in their 3'-untranslated regions. Many proteins with redox-active cysteines have homologs that contain selenocysteine in place of cysteine. Likewise, most selenoproteins have homologs in which the redox-active selenocysteine is replaced with cysteine.

is utilized only when it is required for protein function. In selenoproteins with established function, selenocysteine is a key catalytic group that is used for redox catalysis.

Selenoprotein genes have two characteristic features: selenocysteine-encoding TGA codon and a stem–loop structure known as the selenocysteine insertion sequence (SECIS) element (Fig. 3.40). These genes are difficult to spot in sequence databases, because the normal function of TGA triplets is to terminate translation and therefore gene annotation tools recognize TGA only as stop signals. Although the TGA triplets that code for Sec do not provide sufficient information for their identification in sequences, SECIS elements are amenable to computational analyses as these structures are highly specific for selenoprotein genes, have areas of sequence conservation, and possess a sufficiently complex secondary structure. In fact, searches for SECIS elements have been performed in various sequence databases, including entire genomes, and information is currently available on the composition of entire sets of selenoproteins (selenoproteomes) in many organisms, including humans, which have 25 such proteins. Some of the major selenoproteins and their functions are discussed.

3.7.A1 Selenoproteins with Known Functions

Glutathione Peroxidase Glutathione peroxidase 1 (GPx1) was the first selenoprotein to be discovered in animals and is perhaps the best characterized. It is expressed in essentially all tissues and accounts for the majority of body selenium in mammals. It catalyzes GSH-dependent H_2O_2 reduction and is one of the

major antioxidant enzymes in mammals. As such, GPx1 is a component of the GSH system, and the reduction of hydroperoxides is ultimately coupled to the oxidation of NADPH via glutathione reductase and GSH. GPx1 is a homotetramer of ~23 kDa subunits, each containing a single selenocysteine residue in the active site. During catalysis, selenocysteine attacks the hydroperoxide substrate, reducing it to water, and itself oxidizes to selenenic acid. In the second step, GSH reacts with the selenenic acid, generating a mixed selenenylsulfide between GPx1 and GSH. Finally, a second GSH molecule attacks the selenenylsulfide, resulting in the reduced GPx1 and GSSG. The selenocysteine-containing GPx1 is a highly efficient catalyst compared to its cysteine-containing homologs and other thiol peroxidases, such as peroxiredoxins.

Humans have five selenoprotein glutathione peroxidases, including GPx1, gastrointestinal GPx2, plasma GPx3 and its close homolog GPx6, and phospholipid hydroperoxide glutathione peroxidase, known as PHGPX or GPx4. Although all GPx1 homologs are known as glutathione peroxidases, the functions of some of these proteins are not clear. For example, mammalian plasma does have sufficient levels of GSH to support the glutathione peroxidase activity of GPx3, and GPx4 lacks the GSH-binding site that is present in GPx1 and GPx2, exists as a monomer, and can be regenerated by thioredoxins. Studies have shown that deletion of the GPx4 gene leads to early embryonic lethality in mice, whereas mouse GPx1, GPx2, or GPx3 genes are dispensable for life. Nevertheless, these proteins become important during stress and metabolic disorders. In addition to the five selenoprotein GPxs, humans have several cysteine homologs of unknown function.

Thioredoxin Reductases Mammalian thioredoxin reductases are discussed in Section 3.2. These proteins have a selenocysteine residue within their C-terminal tetrapeptide. Mammals contain three thioredoxin reductases (cytosolic, mitochondrial, and testis-specific), and all three are selenoproteins. Therefore, the entire thioredoxin system in mammals is dependent on selenium.

Methionine-R-Sulfoxide Reductases (MsrBs) These proteins occur as selenoproteins only in vertebrates and are discussed in detail in Section 3.4.A.

Methionine-S-Sulfoxide Reductases (MsrAs) The proteins of another family of methionine sulfoxide reductases, MsrAs, may also exist in the form of selenoproteins. As discussed in Section 3.4.A, MsrA is distinct from MsrB: both catalyze methionine sulfoxide reduction, but they have different structural folds, do not have sequence homology, and each utilizes only one of the two diastereomers of methionine sulfoxide.

Selenophosphate Synthetase Selenophosphate synthetases in some bacteria, Archaea, and animals are also selenoproteins. These enzymes catalyze the formation of selenophosphate, a selenium donor needed for biosynthesis of selenocysteine.

Protein Disulfide Isomerases (PDIs) Some eukaryotes contain selenocysteine-containing PDIs, which are homologs of the enzymes discussed in Section 3.6.B.

Thyroid Hormone Deiodinases Mammals have three deiodinases, DI1, DI2, and DI3, which activate or inactivate thyroid hormones by reductive deiodination of these compounds.

Formate Dehydrogenases (FDHs) FDH is a widely distributed selenoprotein family in prokaryotes. In these enzymes, selenocysteine is directly coordinated to molybdenum and involved in the oxidation of formate to carbon dioxide. In many bacteria, FDH is the only selenoprotein, which may be responsible for maintaining the selenocysteine trait in these organisms.

Formylmethanofuran Dehydrogenases (FMDHs) FMDH is a distant homolog of FDH and catalyzes a similar reaction using formylmethanofuran as a substrate.

Hydrogenases Several selenocysteine-containing hydrogenases are known. In these enzymes, selenocysteine directly binds nickel and is involved in redox catalysis.

Selenoproteins A (GrdA) and B (GrdB) These proteins are components of the glycine reductase complex. GrdA may also form complexes with other substrate-specific GrdBs and be involved in the reduction of sarcosine, betaine, and other substrates.

Peroxiredoxins (Prxs) Peroxiredoxins are abundant cysteine-containing proteins that are discussed in Section 3.1.C. Some peroxiredoxins occur as selenocysteine-containing proteins, in which this residue replaces the catalytic cysteine.

Thioredoxins (Trxs) As discussed in Section 3.2.A, thioredoxin is the major intracellular protein disulfide reductant. Some bacterial thioredoxins are selenoproteins.

Glutaredoxins (Grxs) Grx is discussed in Section 3.3.B and it may also exist in the form of selenocysteine-containing proteins.

3.7.A2 Selenoproteins with Unknown Functions Several selenoproteins have no known function. However, structural analogies of many selenoproteins to thioredoxin-fold proteins suggest their roles in redox catalysis. These include mammalian selenoproteins Sep15, H, M, T, V, and W, and selenoproteins U and Fep15 in fish. There are additional selenoproteins, for which no functional information is available, such as mammalian selenoproteins I, K, N, O, and S. An additional selenoprotein is selenoprotein P (SelP), the only such protein having multiple selenocysteines. For example, the mouse SelP has 10 selenocysteine residues. It is synthesized in the liver, secreted into plasma, and delivers selenium to other organs.

3.7.A3 Selenoprotein Functions From this brief discussion of selenoprotein functions, it is apparent that all functionally characterized selenoproteins are redox proteins. In these enzymes, selenocysteine serves as the catalytic residue and is employed because of its strong nucleophilicity and low pK_a as compared with cysteine. Like redox-active cysteine, selenocysteine reversibly changes its redox state during catalysis. Although the functions of many selenoproteins are not known, it is likely that the majority of these selenoproteins will be found to serve a redox function as well.

Many selenoproteins have homologs that contain cysteine in place of selenocysteine (Fig. 3.40). In these homologs, cysteine is the catalytic residue. Such selenocysteine–cysteine pairs in homologous sequences can be used to identify both selenoproteins and cysteine-containing thiol-based oxidoreductases.

SELECTED REFERENCES

1. Kryukov, G.V., Castellano, S., Novoselov, S.V., Lobanov, A.V., Zehrab, O., Guigo, R., and Gladyshev, V.N. (2003). Characterization of mammalian selenoproteomes. *Science* 300:1439–1443.
2. Stadtman, T.C. (2005). Selenoproteins—tracing the role of a trace element in protein function. *PLoS Biol.* 3:e421.
3. Driscoll, D.M., and Copeland, P.R. (2003). Mechanism and regulation of selenoprotein synthesis. *Annu. Rev. Nutr.* 23:17–40.
4. Berry, M.J. (2005). Knowing when not to stop. *Nat. Struct. Mol. Biol.* 12:389–390.

3.7.B Heme Oxygenase

Stephen W. Ragsdale

Department of Biological Chemistry, University of Michigan, Ann Arbor, Michigan

Heme oxygenase catalyzes the conversion of heme to biliverdin, CO, and iron (Fig. 3.41). The reaction is coupled to cytochrome P450 reductase and biliverdin reductase. During the course of the reaction sequence, purple-colored heme converts to the green pigment biliverdin, which then transforms to yellow bilirubin, a color sequence that is observed in bruising. Heme oxygenase plays an important role in heme and iron homeostasis and is present in nearly all classes of Eukarya and Bacteria. Heme oxygenase is linked to various signaling pathways and is important in the response to oxidative stress. In cyanobacteria, algae, and plants, heme oxygenase is involved in generating the chromophores for photosynthesis. The two forms of heme oxygenase (HO-1 and HO-2) share similar physical and kinetic properties but exhibit different physiological roles and organ locations.

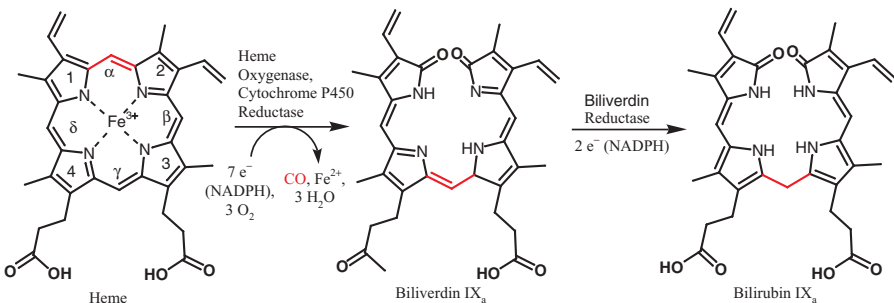


Figure 3.41. Heme oxygenase catalyzes the conversion of heme to biliverdin, CO, and iron.

3.7.B1 *The Heme Oxygenase Reaction and Generation of Three Redox-Active Signal Molecules*

The substrates and products of the heme oxygenase reaction have important regulatory and metabolic roles. Heme is the prosthetic group of many electron transfer proteins and redox enzymes and regulates genes involved in oxygen utilization in lower eukaryotes and prokaryotes and in higher eukaryotes through interactions with transcription factors (e.g., Bach1 and NPAS2). Excess or deficiency of iron is pathological; therefore, iron homeostasis is tightly regulated. Iron is required for all heme-dependent processes and serves as a prosthetic group for a variety of nonheme metalloenzymes and as the effector for transcriptional regulators. Bilirubin is an antioxidant and biliverdin reductase, which produces bilirubin from biliverdin, also plays a key role in gene regulation as a transcription factor and in metabolic signaling as a kinase in the insulin receptor/MAP kinase pathway. CO also acts as a signaling molecule by its role as an activator of guanylate cyclase. CO also is involved in controlling respiration as a function of blood oxygen levels.

The mammalian HO-1 or HO-2 cleaves heme at the α -meso carbon (red lines in Fig. 3.41), while some bacterial heme oxygenases attack at the β position. The heme oxygenase reaction mechanism involves several cycles of reaction with oxygen and NADPH and is coupled to NADPH:cytochrome P450 reductase for input of electrons and to NADPH:biliverdin reductase for reduction of the product biliverdin to bilirubin. The heme oxygenase catalytic mechanism is similar to that of cytochrome P450 (Section 3.5.A), in which ferric iron reduction to the ferrous state precedes oxygen binding, followed by one-electron reduction to generate a peroxy-Fe³⁺ intermediate. However, in HO, the peroxy-Fe³⁺ directly reacts with the α -meso carbon of the heme to form a hydroxy-heme intermediate. Then, after another round of oxygen addition, carbon monoxide is liberated and ferric verdoheme is generated. After NADPH-dependent reduction of the iron and binding of a third mole of oxygen, biliverdin is formed and iron is released. Biliverdin reductase then reduces the C10 γ bridge of biliverdin to generate bilirubin.

3.7.B2 *HO-1 and HO-2 Compared*

HO-1 and HO-2 share a high level of sequence homology (55% identity, 76% similarity) (Fig. 3.42A). These isozymes bind heme within a novel helical structure that sandwiches the heme between the distal helix and the proximal helix and donate a histidine ligand to the heme iron (His25 in HO-1 and His45 in HO-2). The structure of HO-1 has been determined (Fig. 3.43). HO-1 and HO-2 have similar molecular masses (HO-1 is 33 kDa and HO-2 is 36 kDa), comparable enzymatic activities, and related stretches of 20 hydrophobic residues at their C termini to anchor them to the microsomal membrane.

HO-1 is the ancient form of heme oxygenase and is present in nearly all organisms from bacteria to mammals, yet appears to be absent in the Archaea. HO-2 is present in all Amniota, perhaps reflecting a response to the selective pressure of organisms moving from water onto dry land. What distinguishes the sequence of HO-1 from that of HO-2 is the occurrence of heme-responsive motifs in HO-2 (Fig. 3.42B). A more primitive HO-2, containing a single heme-responsive motif, may be present in fish and amphibians. The interaction of heme with heme-responsive motifs has been proposed to control the activity of many regulatory proteins. The role of heme-responsive motifs

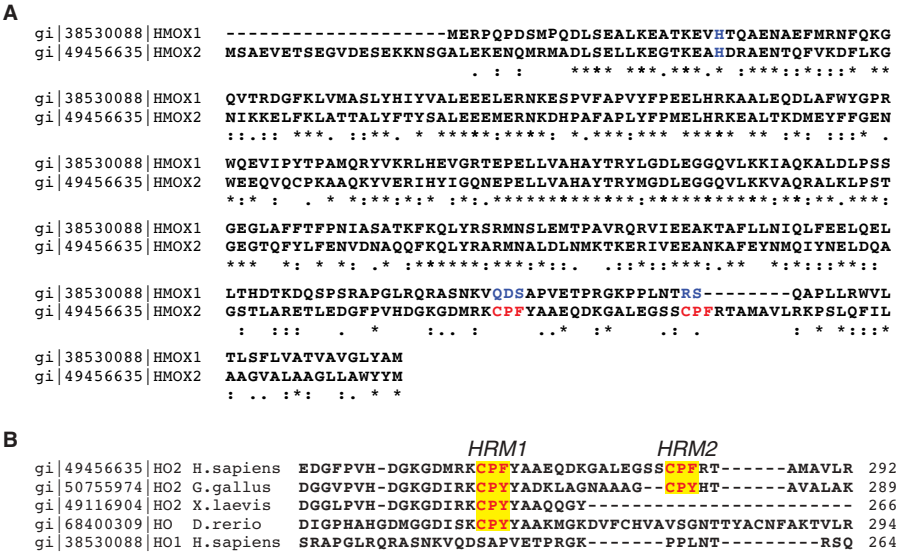


Figure 3.42. Alignments of animal heme oxygenases. (A) Comparison of human heme oxygenase-1 and heme oxygenase-2. (B) Comparison of the heme-responsive motif (HRM) of disparate heme-oxygenase-2-like proteins with this region in human heme oxygenase-1.

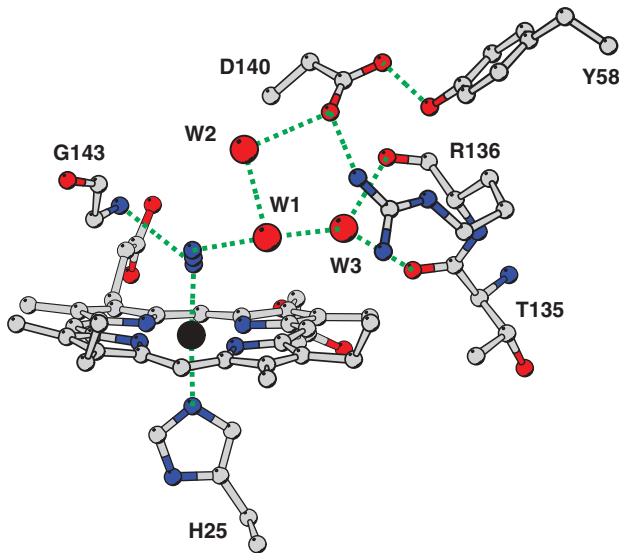


Figure 3.43. Heme oxygenase-1 (PDB file 1ILV) structure generated using MolScript.

in proteins has not yet been determined, though various authors have proposed that the heme-responsive motif per se can bind heme.

HO-1 is induced by various stress conditions and is found in most tissues with particularly high levels in spleen and liver. On the other hand, HO-2 is constitutively expressed and has a narrow tissue distribution, with high levels in the brain and in testes. HO-2 has recently been implicated in oxygen sensing in the carotid body.

3.7.B3 Control of Gene Expression of HO-1, HO-2, and Biliverdin Reductase The existence of inducible HO-1 and constitutive HO-2 parallels the two forms of nitric oxide synthase, iNOS and cNOS (see Chapter 4.2). This analogy extends to the complexity of multiple cycles of redox chemistry and the generation of diatomic signaling molecules by both classes of enzymes.

Expression of HO-1, which also is known as heat shock protein 32, is regulated by heat shock and various oxidative stress conditions such as ischemia, hypoxia, hyperoxia, and alteration of GSH levels. These conditions are relayed to the transcriptional machinery by the many cis-acting regulatory elements proximal to the HO-1 gene, which interact with various trans-acting factors, including heat shock factor, AP-1, NF κ B, and metals. Expression of HO-1 is also controlled by biliverdin reductase through the hypoxia-induced transcription factor Bach 1. The only effectors that have been shown to regulate expression of HO-2 are adrenal glucocorticoids, which bind to a glucocorticoid response element in the promoter region of the gene encoding HO-2.

Biliverdin reductase, which is functionally linked to both HO-1 and HO-2, is involved in various regulatory networks. Biliverdin reductase activity is regulated by phosphorylation at serine/threonine and tyrosine, and by binding adenosine dinucleotide and zinc, while its ability to interact with other proteins is regulated through leucine zipper and SH2 domains and by dithiol/disulfide redox interchange. Expression of the biliverdin reductase gene is repressed by a zinc finger transcription factor (GATA1) and derepressed by heme. Biliverdin reductase itself activates a variety of genes involved in cell–cell signaling, in the immune response, and in oxidative stress (including HO-1). Many of these regulatory functions may be linked to translocation of biliverdin reductase to the nucleus.

SELECTED REFERENCES

1. Maines, M.D. (2004). The heme oxygenase system: past, present, and future. *Antioxid. Redox Signal.* 6:797–801.
2. Hantke, K. (2001). Iron and metal regulation in bacteria. *Curr. Opin. Microbiol.* 4:172–177.
3. Baranano, D.E., and Snyder, S.H. (2001). Neural roles for heme oxygenase: contrasts to nitric oxide synthase. *Proc. Natl. Acad. Sci. USA* 98:10996–1002.
4. Williams, S.E., Wootton, P., Mason, H.S., Bould, J., Iles, D.E., Riccardi, D., Peers, C., and Kemp, P.J. (2004). Hemoxygenase-2 is an oxygen sensor for a calcium-sensitive potassium channel. *Science* 306:2093–2097.
5. Montellano, P.R. (2000). The mechanism of heme oxygenase. *Curr. Opin. Chem. Biol.* 4:221–227.

Redox Regulation of Physiological Processes

- 4.1. Reactive Oxygen, Nitrogen, and Thiol-Based Signal Transduction
 - 4.1.A. Nitric Oxide Signaling
 - 4.1.B. Carbon Monoxide Signaling
 - 4.1.C. Superoxide and Hydrogen Peroxide
 - 4.1.D. Other Novel Redox Molecules
- 4.2. Role of Nitric Oxide Synthases in Redox Signaling
 - 4.2.A. Characterization of the Nitric Oxide Synthases
 - 4.2.B. Regulation of Nitric Oxide Synthases by Intrinsic Elements
 - 4.2.C. Extrinsic Regulation of Nitric Oxide Synthases
 - 4.2.D. Interactions of NO with Other Proteins and Enzymes
- 4.3. Redox Regulation of Genes
 - 4.3.A. MAP Kinase/Cell Cycle
 - 4.3.B. Redox Control of Gene Expression
 - 4.3.C. Peptide Editing and Thiol-Mediated Redox Regulation
- 4.4. Redox Regulation of Apoptosis
 - 4.4.A. Apoptotic Pathways
 - 4.4.B. Reactive Oxygen Species and Apoptosis
- 4.5. Metal Homeostasis
 - 4.5.A. Physiological Significance of Metal Metabolism
 - 4.5.B. Metal Uptake from the Extracellular Environment
 - 4.5.C. Intracellular Metal Distribution by Target-Specific Chaperones
 - 4.5.D. Subcellular Membrane Metal Transporters
 - 4.5.E. Heme and Iron–Sulfur Cluster Synthesis
 - 4.5.F. Cellular Storage
 - 4.5.G. Metal Export
 - 4.5.H. Regulation of Metal Metabolism
 - 4.5.I. Genetic Disorders in Metal Metabolism
 - 4.5.J. Perturbation of Metal Homeostasis and Degenerative Disorders
- 4.6. Redox Enzymology

- 4.7. Circadian Clock and Heme Biosynthesis
 - 4.7.A. Cyclic Expression of Heme Binding Proteins
 - 4.7.B. Circadian Clock Mechanism
 - 4.7.C. PAS Is a Heme Binding Domain
 - 4.7.D. Expression of *Npas2* Is Controlled by mPER2
 - 4.7.E. NPAS2 Regulates Expression of Aminolevulinate Synthase 1

4.1 REACTIVE OXYGEN, NITROGEN, AND THIOL-BASED SIGNAL TRANSDUCTION

ILSA I. ROVIRA AND TOREN FINKEL

Cardiology Branch, NHLBI NIH, Bethesda, Maryland

I have learned in the school of life and experience that moderation is the most valuable virtue a citizen can possess

—From *An Enemy of the People* by Henrik Ibsen, 1882

In Henrik Ibsen's famous play *An Enemy of the People*, the town physician Dr. Stockmann realizes that his small Swedish town's medicinal mineral baths, a source of the town's considerable wealth and fame, are actually contaminated and unhealthy. The local townspeople, rather than reacting with encouragement and support, attack the good physician/scientist and drive him out of town. The mayor, in an effort to convince the doctor of the folly of his ways, argues that "moderation" is the secret, and that those things viewed initially as harmful, when taken in moderation, are naturally beneficial.

The lessons of Ibsen's play are of some relevance to the study of oxidant signaling. In many cases the progress of the last decade stands as the mirror image of Dr. Stockmann's travails. Indeed, for many years physicians/scientists were convinced that reactive species such as $O_2^{\cdot-}$, H_2O_2 , and carbon monoxide were toxic substances that caused numerous diseases and pathological states. That view has been altered by the growing realization that in low doses (i.e., moderation) these potentially toxic moieties actually play a beneficial role in normal signal transduction pathways. The list of such species includes nitric oxide, carbon monoxide, H_2O_2 , and even hydrogen sulfide. Here, we review the evidence that these molecules are regulated within cells and that they function in a specific and reversible fashion to transmit downstream signals.

4.1.A Nitric Oxide Signaling

The discovery of nitric oxide (NO) as a signal transduction molecule provided the intellectual framework for many of the other subsequent discoveries in redox biology. Like many great discoveries, the discovery of NO was, however, partly accidental.

Furchgott and colleagues were studying the ability of vascular rings to relax or vasodilate in response to an external stimulus such as acetylcholine. When the individual who normally prepared the vascular rings was absent, a substitute technician was enlisted for the experiments. Fortunately or unfortunately, this substitute appeared unable to get vascular ring preparations that would dilate in response to acetylcholine. Curious as to why this was, Furchgott eventually realized that these new ring preparations lacked the normal thin endothelial cell layer. Presumably the new substitute technician failed to carefully prepare the rings, which in turn led to the loss of the normal endothelial layer. This led Furchgott to realize that the endothelium, rather than being a passive barrier, was actually involved in a paracrine signaling process. It was subsequently appreciated by others that NO was the molecule that endothelial cells secrete in response to stimuli such as acetylcholine. These discoveries led to the Nobel Prize being awarded in 1998 to Furchgott, Ignarro, and Murad.

The biochemical basis of nitric oxide synthesis was significantly accelerated by the discovery and cloning of the enzyme responsible for NO production. This family of enzymes, nitric oxide synthase (NOS), has a unique structure and is encoded by three separate genes. All three enzymes use the common substrate L-arginine to generate NO in addition to L-citrulline. Historically, the first enzyme cloned was neuronal NOS (also termed NOS1). The structure of the cloned gene demonstrated predicted binding sites for multiple potential regulatory cofactors including NADPH, flavin adenine dinucleotide (FAD), flavin mononucleotide (FMN), heme, tetrahydrobiopterin, and calmodulin. Similar motifs were found in the other two NOS genes termed endothelial NOS (NOS3) and inducible/calcium independent NOS (NOS2). The regulation of enzymatic activity as well as the actual production of NO differs considerably between the various NOS family members. In particular, when NOS2 is activated in immune regulatory cells such as macrophages, large amounts of NO are produced. Activation of this gene product is predominantly through transcriptional mechanisms. In contrast, both NOS1 and NOS3 tend to produce lower amounts of NO and the activity of these enzymes is regulated by a rise in intracellular calcium leading to calmodulin–NOS interaction.

While it is impossible to summarize all the information regarding the regulation of NOS enzymatic activity, we would like to briefly discuss one aspect that has particularly important clinical applications. The NOS3 isoform is expressed in the vascular endothelium and is responsible for vasorelaxation of the underlying vascular smooth muscle cells. This is the enzyme Furchgott and colleagues were studying in their original physiological observations. A variety of animal and human evidence suggests that, in patients with atherosclerosis, the biological activity of NO is reduced within the vessel wall. The physiological result of this NO deficiency is a clinical syndrome termed endothelial dysfunction. Characteristics of endothelial dysfunction include an inappropriate vasodilatory response to pharmacological agonists such as acetylcholine or physiological stimuli such as increased shear stress. The development of endothelial dysfunction is thought to precede the development of visible atherosclerotic plaque and a variety of evidence suggests that patients who develop endothelial dysfunction are at significantly increased risk for subsequent cardiovascular events. An increase in $O_2^{\cdot-}$ production is thought to be the mechanism by which endothelial

dysfunction develops in the preatherosclerotic individual. It is well known that $O_2^{\cdot-}$ and NO can interact to produce the potentially harmful reactive species peroxynitrite. The increase in $O_2^{\cdot-}$ therefore reduces NO levels through a direct chemical reaction and in turn produces a state characterized by impaired vasodilation.

Clinically, individuals with atherosclerosis or risk factors for atherosclerosis are often put on agents to lower serum cholesterol. The most commonly used agents are the family of 3-hydroxy-3-methylglutaryl-coenzyme A (HMG-CoA) reductase inhibitors often termed "statins." These drugs have revolutionized the care of patients with hypercholesterolemia and have significantly reduced cardiovascular mortality and morbidity. While the long term effects of these agents are dramatic, reduction of serum cholesterol takes time. Interestingly, careful kinetic studies in animals and patients suggest that statins can reverse endothelial dysfunction and appear to do so before there is a measurable drop in serum cholesterol. These and other observations have led to the idea of cholesterol-independent effects of statins. Molecular studies have subsequently delineated a plausible explanation for the observed quick reversal of endothelial dysfunction by these agents. This explanation involves an understanding of the post-translational modification that occurs on a family of important signaling molecules, the family of small GTPases. This family includes proteins such as Ras, Rac, RhoA, and numerous other similar proteins that regulate a host of intracellular processes. In particular, as discussed later, members of this family are crucial for ligand-stimulated H_2O_2 production. While a review of the small GTPases is not our intention, a useful framework is to view these molecules as molecular switches that turn pathways on or off based on which nucleotide (GDP or GTP) is bound to the GTPase. The small GTPases undergo post-translational modification including the addition of isoprenoid intermediates to their carboxyl tail. The addition of these lipid moieties allows for the insertion of the small GTPases into a variety of biological membranes (Fig. 4.1). The synthesis of isoprenoids, like that of cholesterol, is inhibited by HMG-CoA reductase inhibitors. One effect of this statin inhibition is that the Rho subfamily of small GTPases is less abundant in the plasma membrane because of its reduced post-translational modification. An immediate effect of blocking Rho activity is that the activity of a downstream kinase, Akt, appears to be increased. The precise mechanism for Akt activation in this scenario is incompletely understood. It is well known that Akt can directly phosphorylate NOS3 on a particular serine residue and this phosphorylation leads to increased NO production. Similarly, Rho inhibition also results in increased NOS3 mRNA stability, leading to increased NOS3 expression. Therefore, statins appear to quickly reverse endothelial dysfunction by modulating Rho activity that, in turn, increases NO bioavailability through effects on NOS3 phosphorylation and protein levels.

The biological response to NO is often viewed as being two independent arms with both cGMP-dependent and cGMP-independent modes of action (Fig. 4.2). Soluble guanylyl cyclase (sGC) exists in the cytosol and the active enzyme is composed of an α and β subunit. This heme-containing enzyme is responsible for converting GTP into cGMP. The ensuing production of cGMP is transduced by a variety of important downstream effectors including cGMP-dependent kinases and cyclic nucleotide-gated channels. Interaction of NO with the heme moiety of sGC leads to activation of the

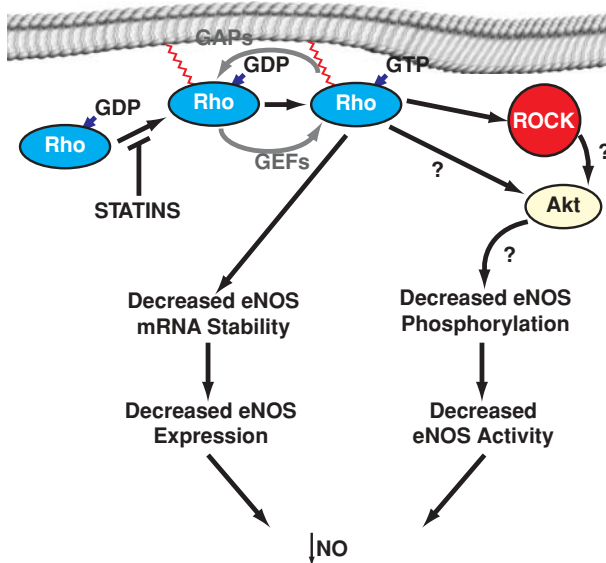


Figure 4.1. Statins regulate NO availability. The production of NO is regulated at both transcriptional and post-translational levels. The commonly used drug family, the HMG-CoA reductase inhibitors (statins), blocks the post-translational addition of lipid groups to the Rho family of small GTPases. Rho GTPases negatively regulate endothelial NOS (eNOS) message stability as well as activity. The latter regulation is by altering the phosphorylation of eNOS protein. Negative regulation of Rho activity by statin treatment leads to more NO bioavailability and a reversal of endothelial dysfunction. Interestingly, another small GTPase, Rac1, appears essential for $O_2^{\cdot-}$ production, suggesting a critical role for this family of molecules in overall redox regulation. GAPs are GTPase activating proteins and GEFs are GTP exchange factors.

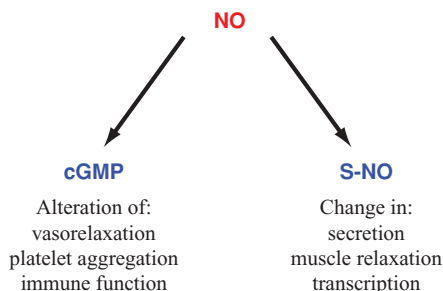


Figure 4.2. NO-dependent signaling. NO regulates numerous important physiological processes. There are at least two major arms of this regulation. The classical arm is through the activation of cGMP-dependent signaling. Alternatively, NO can directly modulate protein function through S-nitrosylation (S-NO).

enzyme and a subsequent rise in cGMP levels within target tissues. It is believed that the majority of vasodilation induced by NO is due to the rise in cGMP within the underlying vascular smooth muscle cells.

In addition to its effects on sGC, NO can directly modify a number of target proteins through a process sometimes called S-nitrosylation. This post-translational modification results in the reversible, covalent modification of target proteins when NO interacts with a reactive cysteine thiol to form an S-NO protein. A number of proteins appear capable of forming S-NO intermediaries including caspases, phosphatases, signaling molecules (e.g., small GTPases, Src, Ask1), and channels. Some of the S-nitrosylated proteins have a subsequent increase in their enzymatic activity, while in other cases, the reverse is true. The biological importance of this modification is underscored by the regulatory role that a number of target proteins play. Indeed, everything from oxygen delivery by hemoglobin, to the transcriptional regulation of gene expression, to overall muscle contraction appears to be modulated in part by NO-protein intermediates. One cell biology example will hopefully underscore this importance. Exocytosis depends on the fusion of membrane-bound intracellular vesicles with the plasma membrane. One important component of the exocytosis machinery is the *N*-ethylmaleimide (NEM) sensitive factor (NSF). The fact that this factor displays NEM sensitivity suggests that reactive thiols may play an important role in the underlying biology. NSF is an ATPase involved in the regulation of two critical components of the exocytosis machinery termed SNAPs and SNAREs. Interestingly, NO treatment appears to block exocytosis and this intervention is associated with the S-nitrosylation of NSF. It was subsequently shown that exocytosis could be restored to previously NO-treated cells when native but not S-nitrosylated NSF was added back. The blocking of exocytosis from endothelial and immune cells may be one way that NO exerts its powerful anti-inflammatory effect.

Finally, the intersection of NO with other ROS is an important area of research. As previously mentioned, NO and $O_2^{\cdot-}$ can form the reactive peroxynitrite and this species is generally viewed as a harmful by-product. Another pathway in which NO may interact with other ROS is through the regulation of mitochondrial activity. Since the majority of intracellular $O_2^{\cdot-}$ and H_2O_2 derives from mitochondrial activity, regulation of mitochondrial biology by NO represents an important potential overlap between ROS species. There is a variety of evidence that NO can bind to cytochrome *c* present in mitochondria as the terminal electron acceptor. This binding results in an NO-dependent inhibition of electron transport. Less clear is whether the NO that regulates mitochondrial activity is derived from a mitochondrial-specific isoform of NOS. Evidence supporting a mitochondrial NOS (mtNOS) does exist but is not uniformly accepted. By using knockout animals, it would appear that mtNOS shares the most similarity with neuronal NOS. There is also growing evidence that NO is an important regulator of the number of mitochondria within cells, a program called mitochondrial biogenesis. Treatment of cells with NO was demonstrated to increase mitochondrial number through a cGMP-dependent pathway. Interestingly, in mice that underwent caloric restriction, there was an overall increase in eNOS expression. This rise in eNOS was shown to trigger a series of events including mitochondrial biogenesis that appear essential for the longevity-associated benefits of caloric restriction.

4.1.B Carbon Monoxide Signaling

The production of carbon monoxide occurs in a continuous fashion and predominantly results from the enzymatic degradation of heme by the family of heme oxygenase enzymes discussed previously in Chapter 3, Section 3.7.B. High levels of carbon monoxide are toxic. This toxicity results primarily from tissue hypoxia, since the affinity of carbon monoxide for hemoglobin is more than two orders of magnitude higher than the corresponding affinity of oxygen for hemoglobin. Binding of carbon monoxide to hemoglobin that contains four heme iron centers produces carboxyhemoglobin and the allosteric nature of oxygen dissociation ensures that carbon monoxide binding to hemoglobin inhibits both oxygen binding and release. Besides hemoglobin, the heme-containing mitochondrial enzyme cytochrome *c* oxidase might also play a role in carbon monoxide poisoning.

While clearly toxic at high doses, there is a growing appreciation that, like other small reactive molecules, production of carbon monoxide at lower levels might have a signaling function. Perhaps in a counterintuitive fashion, numerous studies have suggested that this low level of carbon monoxide production might provide protection to a number of cellular and organismal stresses. The connection between stress and carbon monoxide production was first appreciated by analyzing heme oxygenase expression. Two different heme oxygenase enzymes have been isolated. Both HO-1 and HO-2 stimulate the degradation of heme to produce biliverdin, Fe^{2+} , and CO. This reaction also requires the presence of molecular oxygen and NADPH. While HO-2 is constitutively expressed especially in the brain and vascular tissues, HO-1 is generally inducible and only seen after exposure to certain stresses. Indeed, the discovery of HO-1 was a result of experiments that sought to identify a common 32 kDa protein that was induced after fibroblasts were stressed by either UV radiation, H_2O_2 , or sodium arsenite. This protein turned out to be HO-1 and subsequent analysis has solidified the notion that HO-1 expression protects cells from a diverse array of cellular stresses.

A number of putative protein targets for carbon monoxide have been identified; however, for the sake of brevity, we discuss only a handful that are the most illustrative. Perhaps the most studied target is sGC. Activation of this heme target induces vasorelaxation and is of course the major basis through which NO regulates vascular tone. On a mole per mole basis, compared to NO, carbon monoxide is a much weaker inducer of sGC. Its physiological role remains incompletely defined although it may be most important under circumstances where there is an absolute or relative NO deficiency. Application of carbon monoxide directly to vessels as well as increased expression of HO-1 in the vessel wall both result in increased vasorelaxation. Interestingly, the application of carbon monoxide to vascular smooth muscle cells results in a cGMP-dependent inhibition of smooth muscle cell growth. These results raise the possibility that carbon monoxide might be in part responsible for maintaining VSMC quiescence. Deregulation of this pathway may contribute to disease states such as atherosclerosis, which involve smooth muscle proliferation.

Another interesting example of HO-2 and carbon monoxide-dependent signal transduction comes from some recent studies on the molecular basis of oxygen sensing. It has been known from elegant physiological studies that the carotid body, a

small specialized locus of cells in the neck, contains the main arterial chemoreceptors that sense changes in arterial oxygen, carbon dioxide, and pH. The carotid body, when activated, releases a number of transmitters that in turn regulate the central respiratory centers in the brain. In particular, a fall in arterial oxygen saturation triggers the carotid body, which in turn stimulates an increase in the rate of breathing. The ability of the carotid body to respond to low oxygen resides within a specialized cell called a glomus cell. Electrophysiological analysis of isolated glomus cells has demonstrated that hypoxia inhibits cell-surface K^+ channels. Inhibition of these channels results in a surge of Ca^{2+} entry and subsequent transmitter release. One of the K^+ channels responsible for regulating glomus cell membrane potential is itself calcium activated. This channel is often referred to as BK_{Ca} , and physiological studies have suggested that the channel opening is decreased under hypoxic conditions. Nonetheless, relatively little was known regarding how the oxygen sensitivity of channel opening was regulated. A recent study, however, has implicated the ubiquitous enzyme HO-2 as a candidate oxygen sensor. As mentioned previously, the enzymatic reaction of HO-1 and HO-2 enzymes with heme requires oxygen. Interestingly, HO-2 appears to form a complex with BK_{Ca} and carbon monoxide donating compounds appear to significantly activate the channel (Fig. 4.3). Similarly, knockdown of HO-2 resulted in reduced channel activity. These results support a model where, in the presence of oxygen, HO activity is present and the subsequent generation of carbon monoxide modifies the BK_{Ca} channel. In contrast, hypoxia inhibits the activity of the channel by the loss of HO-2 generated carbon monoxide production. This inhibition is therefore a direct result of the oxygen dependence of HO-2. Since the initial description of this pathway, a subsequent report has indicated that the alpha subunit of BK_{Ca} contains

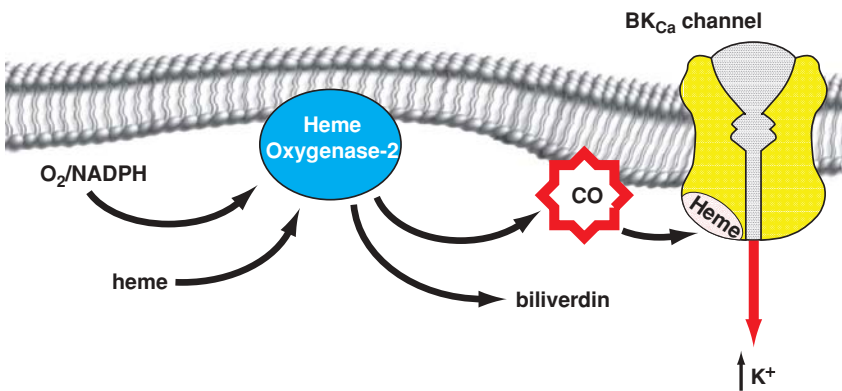


Figure 4.3. Carbon monoxide is an important regulator of hypoxic sensing of the carotid body. Glomus cells in the carotid body respond to low oxygen levels by altering the opening of specialized channels such as BK_{Ca} on their cell surface. Channel activity regulates potassium entry and subsequent neurotransmitter release. The activity of the BK_{Ca} channel is sensitive to oxygen concentrations and recent evidence suggests that the oxygen-dependent production of carbon monoxide by HO-2 may be part of the overall hypoxic sensing system.

a heme binding domain, suggesting that the effects of carbon monoxide on channel activity may be direct.

Another intriguing aspect of carbon monoxide signaling involves the transcription factor, NPAS2. This protein binds to DNA along with another protein partner, BMAL1. Together, these transcription factors have been implicated in circadian rhythms. For instance, knockout of NPAS2 in mice destroys the day–night cycle of expression of the circadian regulated gene *Per2*. One conserved motif in NPAS2 is the PAS domain and evidence suggests that in simple organisms this domain senses oxygen and does so through the requisite binding of a prosthetic heme group. The ability to bind heme is also seen in NPAS2 although the transcription factor can bind to DNA in both the apo (heme-free) and holo (heme-loaded) state. Interestingly, low micromolar concentrations of carbon monoxide appear to selectively inhibit DNA binding of the holo-NPAS2 form. In contrast, NO did not appear to have such effects at physiological concentrations of the gas. These results raise the possibility that carbon monoxide might regulate circadian rhythms by directly modulating NPAS2 binding. In this regard it is of interest that elevated HO-2 expression is localized to the same regions of the brain that abundantly express *Per2*. In addition, heme synthesis appears to be regulated in a circadian fashion. Finally, the requirement for NADPH in the heme oxygenase reaction might allow a connection between metabolism, carbon monoxide production, and the circadian clock.

Finally, there is growing interest in the therapeutic application of low dose carbon monoxide. A number of *in vitro* and *in vivo* studies have suggested that carbon monoxide may have anti-inflammatory, antiproliferative, and antiapoptotic effects. Some of these effects may be mediated through cGMP-dependent pathways. In addition, there is considerable evidence that carbon monoxide may affect certain arms of the mitogen activated protein kinase (MAPK) family. In particular, activation of p38 MAPK by carbon monoxide appears to be important in numerous contexts. The precise mechanism by which these effects are transduced is not known, nor is it clear whether heme sensing plays a prominent role. Similarly, a number of animal models involving both ischemia-reperfusion and solid organ transplantation have suggested that carbon monoxide might provide significant therapeutic benefit. In addition, HO-1 deficient mice appear to have increased mortality following ischemia-reperfusion induced injury and inhaled carbon monoxide appears to at least partially correct this susceptibility. It remains unclear how these beneficial effects are actually modulated and in particular what the relative contribution is for carbon monoxide's effects on p38 MAPK versus cGMP-dependent pathways.

4.1.C Superoxide and Hydrogen Peroxide

Long believed to be merely toxic by-products of aerobic metabolism, both superoxide ($O_2^{\cdot-}$) and H_2O_2 have emerged in the last decade as bona fide signaling molecules. At present, because of limitations with *in vivo* detection, it is often difficult to determine whether $O_2^{\cdot-}$ and H_2O_2 represent distinct signaling molecules. $O_2^{\cdot-}$ is relatively short-lived and can rapidly dismutate to H_2O_2 either spontaneously or with the aid of the enzyme superoxide dismutase. Questions remain therefore as to whether these

two ROS have shared or different protein targets as part of their signaling pathways. In this regard it is of some interest to note that, in *E. coli*, different sensing and effector pathways exist for $O_2^{\cdot-}$ and H_2O_2 . In this organism, a rise in H_2O_2 is sensed by the OxyR transcription factor while $O_2^{\cdot-}$ is sensed by the SoxRS pathway. The activation of these two pathways leads to the induction of two distinct transcriptional pathways including a nonoverlapping set of genes involved in DNA repair and antioxidant defenses. The basis for sensing these different ROS lies in the primary structure of the OxyR and SoxS proteins. For the case of OxyR, the ability to sense changes in H_2O_2 is secondary to two reactive cysteine residues within the molecule. Some controversy exists regarding the activation of OxyR, as two slightly different models have been proposed. Both involve the oxidation of one reactive cysteine residue from the thiolate anion state (S^-) to a sulfenic form ($S-OH$). In one model, this oxidation is sufficient to induce the full transcriptional activity of OxyR, while in the other model this sulfenic residue is rapidly converted to a disulfide bond by reacting with a neighboring reactive cysteine residue. The ability of cysteine residues to undergo a series of reversible oxidation and reduction steps represents a critical aspect of H_2O_2 signaling mechanisms (Fig. 4.4). For the case of the SoxS system, the ability to sense and respond to $O_2^{\cdot-}$ comes from the prosthetic Fe-S cluster found in the molecule. Oxidation of the iron moiety provides a metal-based $O_2^{\cdot-}$ detection system. As such, it would appear that evolutionary simple organisms such as bacteria have evolved to be capable of detecting either $O_2^{\cdot-}$ or H_2O_2 and responding to each of these different ROS with distinct genetic programs. It would seem likely that such discrimination would be maintained in higher organisms, although the proof of this is still not conclusive. Nonetheless, the use of Fe-based $O_2^{\cdot-}$ detection and cysteine-based H_2O_2 detection appears to be a common theme from bacteria to mammalian cells.

Interest in H_2O_2 as signaling molecules was sparked by the observation that the addition of peptide growth factors such as PDGF and EGF rapidly (e.g., within seconds) induces a burst of production of this oxidant. It was known for many years that phagocytic cells such as the neutrophil could produce large amounts of $O_2^{\cdot-}$ and H_2O_2 after stimulation, but the production of these ROS in nonphagocytic cells was not well studied. Perhaps more intriguing than the actual production was the observation that inhibiting the rise in H_2O_2 resulted in a blunted response to the peptide growth factors. For instance, both EGF and PDGF stimulate the rapid tyrosine phosphorylation of

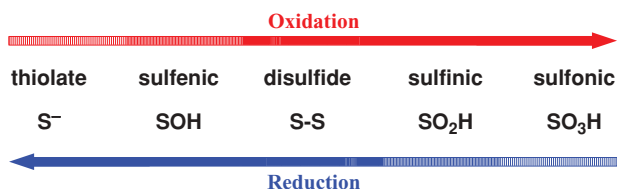


Figure 4.4. Oxidation of cysteine residues as the basis for H_2O_2 signaling. Certain reactive cysteine residues are capable of forming a thiolate anion (S^-) at physiological pH. These residues can be further oxidized depending on the strength of ROS. Generally, the sulfenic and sulfonic forms are viewed as nonreversible modifications, although there is at least one example of the reversibility of a sulfinic-modified protein.

numerous downstream molecules. Interestingly, blocking the rise in ROS appears to block this burst of tyrosine phosphorylation, while the addition of exogenous H_2O_2 stimulates tyrosine phosphorylation. Numerous questions arose from these initial studies including what was the source of ligand-stimulated ROS production and how did a rise in ROS result in increased downstream phosphorylation.

Subsequent studies have provided some preliminary answers to these questions. For instance, it now appears that, similar to professional phagocytic cells, nonphagocytic cells also have purposeful ROS generators. In the neutrophil, a multisubunit NADPH oxidase has been described that contains multiple membrane-bound as well as cytosolic-recruited proteins. Activation of the NADPH oxidase in phagocytes also requires a small GTPase protein called Rac2. Once activated, the neutrophil NADPH oxidase produces large amounts of $O_2^{\cdot-}$ that is essential for the host defense functions of this cell type. Recent evidence suggests that the neutrophil oxidase is part of a family of related oxidases now termed NOXs that appear to be widely expressed in a variety of tissues. Molecular studies are still relatively preliminary at this point, but most evidence suggests that the general mode of regulation of various NOXs may be similar between nonphagocytic and phagocytic cells. In particular, there appears to be an essential role for Rac family members in regulating ROS levels in different cell types (Fig. 4.5). In contrast, the molecular makeup of the oxidase may be tissue specific, especially with regard to the major cytochrome, which in the neutrophil is the protein originally termed gp91phox. A number of gp91phox-related proteins have now been isolated that appear to be expressed outside the neutrophil and appear to produce a regulated burst of $O_2^{\cdot-}$. Levels of ROS are thought to be several orders of magnitude lower in these newer oxidases when compared to the neutrophil complex. This lower amount has been viewed as more compatible with normal signaling. These novel oxidases also have the potential to contribute to cellular transformation and may play an important role in tumorigenesis. It is interesting to note that the production of high or low amounts of $O_2^{\cdot-}$ by the various NADPH oxidases is reminiscent of the previous example for the various NOS isoforms. In both cases, professional immune cells appear to produce large amounts of either NO or $O_2^{\cdot-}$ as part of their host defense function. In contrast, in other cell types, another form of the enzyme system, be it NOS or NOX, is assembled to produce the same species of oxidant but at significantly lower amounts. These lower amounts presumably function in normal signaling pathways in these various nonimmune cell types.

Similar to the progress that has been made in understanding the potential sources of ligand-stimulated ROS production, there has been considerable progress made in identifying potential specific cellular protein targets of H_2O_2 . Again, here the characteristic that has emerged from an analysis of these target molecules is the common theme of reactive cysteine modification. One class of molecules that is of particular recent interest is the family of protein tyrosine phosphatases and the related family of dual-specific phosphatases. These families of molecules have at their active site a reactive cysteine residue and have long been viewed as potential targets of oxidants. Subsequent in-depth analysis has confirmed and extended this hypothesis, and it now appears likely that ROS represent an important method of phosphatase regulation. Careful kinetic analysis suggests that, for the tyrosine phosphatase PTP1B, oxidation of the

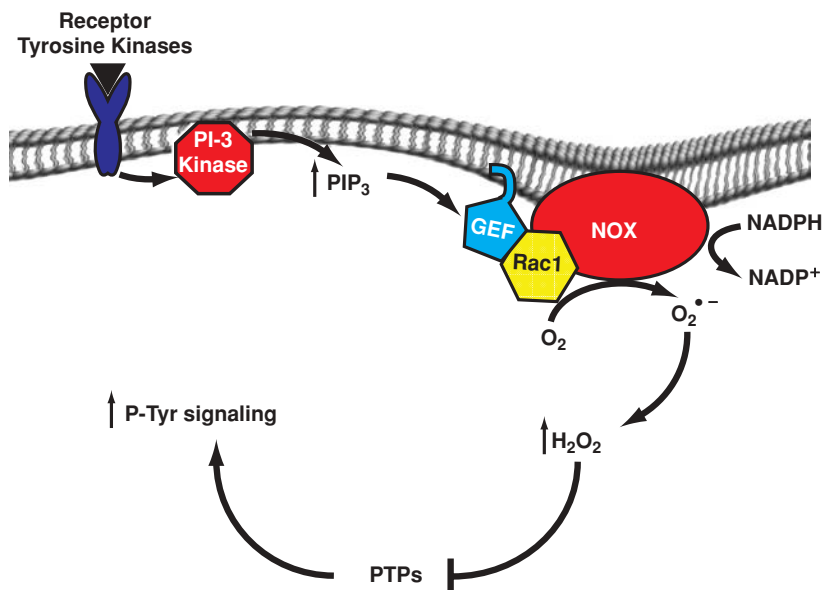


Figure 4.5. Signaling by H_2O_2 . Activation of receptor tyrosine kinases (e.g., PDGFR or EGFR) leads to the activation of PI-3 kinase and the subsequent stimulation of the activity of guanine exchange factors (GEFs). These GEFs can activate small GTPases such as Rac1, leading to the production of H_2O_2 by the NOX family of oxidases. One class of targets for H_2O_2 includes the phosphotyrosine phosphatases (PTPs) and the dual specific phosphatases that contain reactive cysteines in their active sites. Inhibition of these phosphatases leads to increased phosphotyrosine signaling (p-Tyr).

catalytic and reactive cysteine first produces the sulfenic intermediate (Cys-S-OH). Interestingly, evidence then suggests that this moiety reacts with a nitrogen atom in a neighboring serine residue to produce a five-membered cyclic sulfenyl amide species. It will be interesting to know whether other phosphatases also go through the unusual intermediate following their oxidation. In addition to PTP1B, there are a number of other important phosphatases that appear to undergo reversible oxidation and inactivation including PTEN and Cdc25C. Since the observed level of phosphorylation represents the balance between kinase and phosphatase activity, these results suggest that the basis for oxidant-induced tyrosine phosphorylation may have less to do with actually stimulating kinase activity and more to do with inhibiting phosphatase action.

Another emerging area related to ROS signaling is the regulation of protein function by a process termed glutathiolation. GSH is present in millimolar concentrations in cells and provides an essential role in maintaining a reducing environment within the cell. It represents an important H_2O_2 scavenging system, where two molecules of GSH can interact with H_2O_2 to produce two molecules of water and one molecule of GSSG. The GSSG can then be reduced back to GSH by the action of glutathione reductase with NADPH being consumed in the reaction (see Chapter 3, Section 3.3.A). GSSG can directly react with the thiolate anion of reactive cysteine residues in proteins. Alternatively, GSH can directly react with cysteine sulfenic intermediates (S-OH)

to also produce a glutathiolated intermediate. In both cases, a glutathiolated protein is produced. A number of proteins appear to undergo such modifications following physiological or pathological stress, and new methods to more readily detect such intermediaries have emerged. The list of glutathiolated proteins includes transcription factors, metabolic enzymes, and structural proteins. Relatively little is known regarding how the cysteine residue of glutathiolated proteins is reduced back to the original thiolate anion, although such reversibility would appear essential if glutathiolation is to emerge as a means of signaling rather than merely a protective response to oxidative stress.

Taken together, these results suggest that cells purposely produce $O_2^{\cdot-}/H_2O_2$ both to fight infection in the case of phagocytes and to transmit signals in other cell types. Many questions remain regarding how specificity is achieved with ROS-dependent signaling, although the spatial confinement of the oxidant signal may be important. In this regard, it was recently noted that, following ligand addition, the reactive cysteine of the PTP1B located in the plasma membrane was oxidized while the larger cytoplasmic pool of the phosphatase remained reduced and enzymatically active. Presumably this difference in oxidation status and corresponding activity reflects how near the source of oxidant production a specific PTP1B molecule was.

4.1.D Other Novel Redox Molecules

The discovery that NO, carbon monoxide, $O_2^{\cdot-}$, and H_2O_2 all can act as intracellular messengers has suggested that other small molecules and gases might also be important for biological signaling. In plants, for instance, the gas ethylene plays a major role in growth, ripening, development, and stress resistance. Similarly, less well characterized gases may also be important in mammals. One such molecule whose physiology remains incompletely understood is the molecule hydrogen sulfide (H_2S). Formation of this gas is thought to result from the action of either of two different enzymes, cystathionine β -synthase or cystathionine γ -lyase. Both these enzymes are capable of catalyzing multiple enzymatic reactions including producing H_2S . Once produced, H_2S is a colorless but certainly not odorless gas that readily diffuses across plasma membranes. Similar to both NO and carbon monoxide, H_2S is produced abundantly in the brain. This appears to be secondary to the action of cystathionine β -synthase, which is highly expressed especially in the hippocampus and the cerebellum. The neuronal actions of H_2S have been reported to include regulation of memory and long term potentiation (LTP). This effect is thought to occur through regulation of NMDA receptor activity. Interestingly, both NO and carbon monoxide also regulate LTP although H_2S does not appear to regulate cGMP levels like these two other gases. Again, in an analogous fashion to carbon monoxide and NO, H_2S can act as a vasoregulatory molecule. The mechanisms underlying this vasodilatation are unclear, although some have speculated that K_{ATP} channels are involved. One fascinating application of H_2S has recently been reported in mice. Inhalation of H_2S resulted in a slowing down of metabolism by approximately an order of magnitude. This effect was completely reversible, suggesting that certain nonhibernating mammals could be induced to undergo a state that was metabolically equivalent to hibernation. The ability of H_2S to induce mice to revert to a quasihibernating state was presumably

related to the ability of H₂S to reversibly bind to cytochrome *c* oxidase. This binding, a property also shared by both carbon monoxide and NO, potently downregulates mitochondrial oxidative phosphorylation. The controlled use of such a strategy in patients with ischemia, trauma, or undergoing prolonged surgery may potently reduce tissue injury in these settings.

The last two decades have witnessed an enormous growth in our understanding regarding the biological activity of reactive nitrogen and oxygen species. Although oxidants have long been implicated in the development and progression of various diseases, as well as in organismal aging, the prevailing prejudice was that ROS contribute to these processes through random and nonspecific damage to DNA and/or proteins. The discovery that oxidants act as normal signaling molecules raises doubts about whether our previously held prejudices were correct or complete. The next several decades should provide more insight into this question and should provide significantly more information on how small diffusible molecules regulate such complex biological systems.

SELECTED REFERENCES

1. Hess, D.T., Matsumoto, A., Kim, S.O., Marshall, H.E., and Stamler, J.S. (2005). Protein S-nitrosylation: purview and parameters. *Nat. Rev. Mol. Cell Biol.* 6:150–166.
2. Kim, H.P., Ryter, S.W., and Choi, A.M. (2006). CO as a cellular signaling molecule. *Annu. Rev. Pharmacol. Toxicol.* 46:411–449.
3. Kimura, H., Nagai, Y., Umemura, K., and Kimura, Y. (2005). Physiological roles of hydrogen sulfide: synaptic modulation, neuroprotection, and smooth muscle relaxation. *Antioxid. Redox Signal.* 7:795–803.
4. Sundaresan, M., Yu, Z.X., Ferrans, V.J., Irani, K., and Finkel, T. (1995). Requirement for generation of H₂O₂ for platelet-derived growth factor signal transduction. *Science* 270:296–299.
5. Tonks, N.K. (2005). Redox redux: revisiting PTPs and the control of cell signaling. *Cell* 121:667–670.

4.2 ROLE OF NITRIC OXIDE SYNTHASES IN REDOX SIGNALING

BETTIE SUE MASTERS

Bettie Sue Masters.

Department of Biochemistry, The University of Texas Science Center at San Antonio, San Antonio, Texas

The vast number of proteins containing prosthetic groups, such as iron protoporphyrin IX (heme) or FAD or FMN, that facilitate electron transfer, continue to fascinate investigators due to their ability to function in a variety of redox reactions. As demonstrated in multienzyme systems, such as the mitochondrial respiratory system, a number of proteins containing such prosthetic groups can interact in a carefully orchestrated manner to transfer electrons serially from an electron donor prosthetic group of more negative potential in one protein to an electron acceptor prosthetic group of

higher potential in another protein. Enzymes have also been discovered that contain several different prosthetic groups of differing redox potentials, enabling them to act as miniature electron transfer systems in a single polypeptide chain.

The nitric oxide synthases (NOSs) represent such an electron transport system within a single polypeptide chain. The components of these enzymes—so-named because the isoforms produced by three genes in mammalian systems are expressed in various tissues to produce NO for a specific physiological purpose—are addressed. Inducible or macrophage NOS (iNOS) is found in phagocytic cells in which NO is produced for cytotoxic purposes by combining with $O_2^{\cdot-}$ to produce peroxynitrite. Endothelial NOS (eNOS) is located in endothelial cells in blood vessels, where NO serves as a vasodilator. Neuronal NOS was first isolated from rat brain neuronal cells and is involved in neurotransmission. The characterization of these isoforms and the reactions catalyzed are discussed in order to understand how each of them is regulated and performs its specific function.

4.2.A Characterization of the Nitric Oxide Synthases

Figure 4.6 shows the linear arrangement of the flavin- and heme-containing domains of all three nitric oxide synthases. It can be seen that these enzymes are divided by a calmodulin binding site roughly into a C terminus, containing an NADPH binding site and both FAD and FMN binding domains, and an N terminus containing the heme and tetrahydrobiopterin binding sites, as well as a zinc tetrathiolate.

The existence of such a bidomain structure was discovered by using protease digestion techniques that proved that the enzymes could be separated into distinct domains and later by heterologous expression of the separate genes in *E. coli* for the flavin and heme binding domains that could transfer electrons and bind ligands, respectively. The ability to isolate, purify, and crystallize these separate domains has permitted researchers to determine differences among the three isoforms of NOSs.

Nitric oxide synthases were first characterized as flavoproteins and were shown to be 50–60% sequence identical to NADPH-cytochrome P450 reductase, an

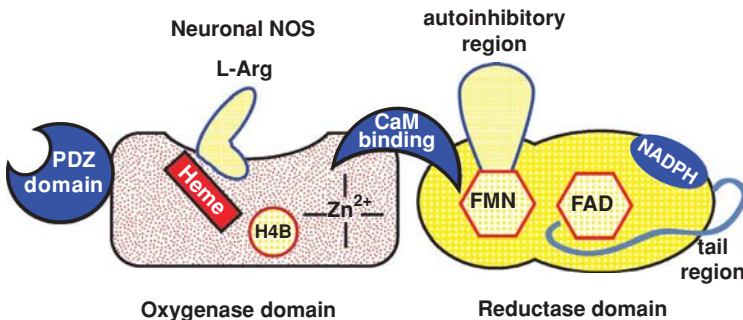


Figure 4.6. Linear arrangement of the flavin- and heme-containing domains applies to all three nitric oxide synthases. (Adapted with permission from Figure 11.16 of *Textbook of Biochemistry with Clinical Correlations*, 6th ed., edited by Thomas M. Devlin. Copyright © 2006 Wiley-Liss.)

endoplasmic reticulum flavoprotein, also containing both FAD and FMN, essential for electron transfer from NADPH to the cytochromes P450 in a multienzyme system that metabolizes therapeutic drugs, steroids, fatty acids, and carcinogens (polycyclic aromatic hydrocarbons). With the ability to express the genes in both mammalian and prokaryotic cells, it became possible to purify sufficient quantities of protein to characterize the NOS isoforms as flavin- and heme-containing proteins that could bind tetrahydrobiopterin in the heme domain. Spectroscopic techniques determined that these enzymes were heme proteins that exhibited a reduced, CO-bound difference spectrum that absorbed visible light at approximately 450 nm, similar to the cytochromes P450.

With this discovery, investigators began to make comparisons between the mechanisms involved in electron transfer within NADPH–cytochrome P450 reductase and neuronal NOS. Later studies confirmed the mechanistic similarities between the flavo-protein moieties of cytochrome P450 reductase and the NOS isoforms and it has been shown that both enzymes produce stable neutral blue semiquinone forms upon reoxidation of flavin hydroquinone forms by either artificial electron acceptors (such as heme-Fe³⁺) or molecular oxygen (Fig. 4.7).

Thus, catalysis by both cytochrome P450 reductase and NOS appears to involve redox cycling between one-, two-, and three-electron reduced states of these flavo-protein moieties in order to permit the reduction of the protoporphyrin-bound Fe³⁺, which is a one-electron acceptor.

4.2.B Regulation of Nitric Oxide Synthases by Intrinsic Elements

The real puzzle, yet to be solved, is the conformational changes that must occur in order to accommodate these redox events during catalysis by the NOS isoforms, since

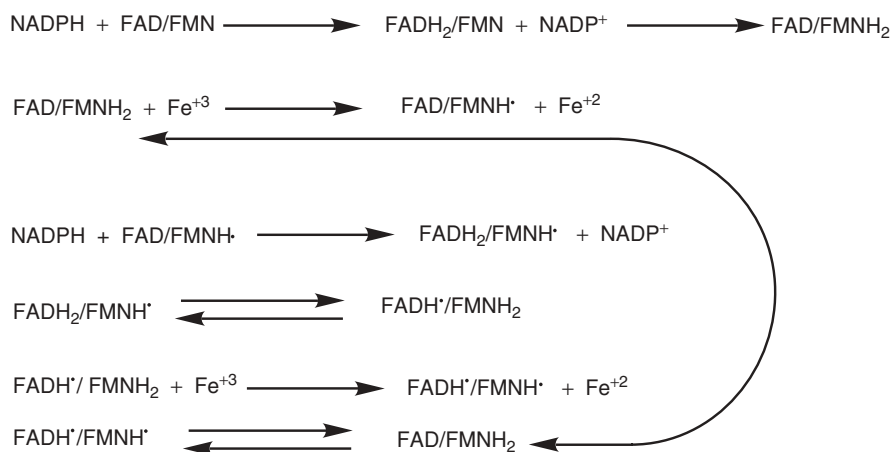


Figure 4.7. The formation of stable neutral blue semiquinone forms by reoxidation of flavin hydroquinone by artificial electron acceptors or molecular oxygen.

they function as dimers. Although no full-length X-ray structures are yet available, structural studies have thus far revealed that the expressed heme domains are dimeric in themselves, featuring over 3000 Å of dimer interface and a single Zn tetrathiolate involving identical cysteine residues from each monomer (Fig. 4.8A). A recent X-ray structure of the flavoprotein domain of nNOS also shows a dimeric conformation (Fig. 4.8B), although solution techniques, such as analytical ultracentrifugation of these constructs, have not yet verified this structure. It is probable that until a full-length structure of one of the NOS isoforms is obtained, the overall relationship of the domains within the holoenzyme dimer will remain unsolved.

The discovery, through sequence alignments of the NOS isoforms with cytochrome P450 reductase and other diflavin (FAD- and FMN containing) enzymes, indicated that autoregulatory inserts exist within the flavoprotein domains of constitutive isoforms (nNOS and eNOS) of NOS, thus shedding new light on their functional characteristics. It is important to point out that iNOS from phagocytic cells is regulated at the transcriptional level, while the constitutive NOS isoforms are regulated at the post-translational level. Therefore, the existence of additional residues (~50) in nNOS and eNOS within the FMN binding domain, compared to cytochrome P450 reductase and iNOS, raised the possibility that these flexible loops play a role in the regulation of these enzymes. Originally, it was shown that the addition of Ca^{2+} /calmodulin, required for the interaction of the flavoprotein domain with the heme domain and subsequent electron transfer, caused significant conformational changes in nNOS and eNOS. Also, peptides derived from the autoregulatory insert of eNOS, when applied to either nNOS or eNOS, produced dramatic, titratable inhibition of the electron

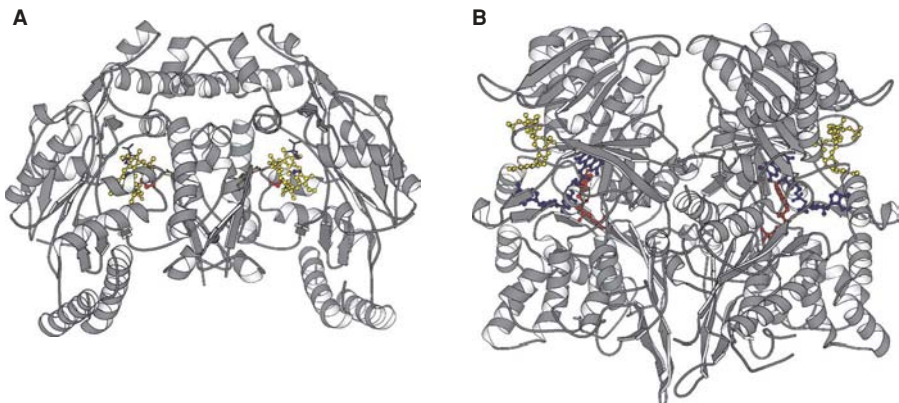


Figure 4.8. Structures of the heme and reductase domains of rat nNOS. (A) The heme domain structure was generated from the PDB file 2G6K. Heme, NO, and the axial Cys415 ligand are shown in ball and stick representation in yellow, blue, and red, respectively. Tetrahydrobiopterin and arginine are shown in stick representation in yellow and blue, respectively. The Zn ion is shown as a black sphere. (B) The reductase domain was generated from the PDB file 1TLL. FMN, FAD, and NADP are shown in ball and stick representation in red, blue, and yellow, respectively.

transfer activities, including NO formation, and this inhibition was reversed by the addition of Ca^{2+} /calmodulin.

Furthermore, examination of the three NOS isoforms revealed that the C termini of all three isoforms were between 21 and 42 residues longer than cytochrome P450 reductase, suggesting a functional role for these residues.

The production of mutants of all three NOS isoforms, which did not contain these C-terminal “tails,” showed a dramatically increased electron transfer to all artificial electron acceptors through the flavoprotein domain in the absence of Ca^{2+} /calmodulin. Interestingly, the addition of Ca^{2+} /calmodulin, required for electron transfer from the flavoprotein domain to the heme domain for the production of NO, the rate-limiting step for the overall reaction, reduced this increased activity to the level of wild-type enzyme. These results alone strongly indicate that the C termini exert a negative modulatory influence on NOS activity and that, in the case of the constitutive NOS isoforms, the addition of Ca^{2+} /calmodulin relieves this inhibition. Additional studies indicate that these actions occur in concert with conformational changes involving the autoregulatory insert in the FMN binding domain, Ca^{2+} /calmodulin binding to the connecting domain between the flavoprotein and heme domains, and the C termini in constitutive NOS isoforms. In the case of iNOS, the C terminus is also involved in negative modulation but this is independent of Ca^{2+} /calmodulin binding since iNOS is expressed with tightly bound Ca^{2+} /calmodulin.

These intrinsic mechanisms provide regulatory control of NO production within the physiological milieu as influenced by the influx of Ca^{2+} into neuronal or endothelial cells in the case of nNOS and eNOS. This influx of Ca^{2+} also influences other extrinsic interactions, such as phosphorylation, particularly in the case of eNOS, by specific kinases. Since cytokines and interleukins control the induction of iNOS at the transcriptional level, extrinsic factors play a major role in the regulation of this NOS isoform.

4.2.C Extrinsic Regulation of Nitric Oxide Synthases

The most studied NOS isoform with respect to post-translational modification is eNOS. These studies, which showed the involvement of protein kinase B (Akt/PKB) in the regulation of eNOS, revealed residues in the flavoprotein domain that were modified by phosphorylation. The C terminus is most likely involved in the “masking” of the potential phosphorylation site and Ca^{2+} binding influences both the binding of calmodulin and the interaction of NOSs with kinases, which also require Ca^{2+} .

4.2.D Interactions of NO with Other Proteins and Enzymes

The first implication of an interaction of NO, produced by chemical means, with a biological entity was published by Ferid Murad, who was awarded the Nobel Prize in 1998 for this discovery. His two fellow Nobelists, Robert F. Furchgott and Louis J. Ignarro,

were recognized for their later identification of NO as the endothelium-derived relaxing factor. These findings were profound in discovering one of the physiological consequences of NO in biological systems through its binding to the heme prosthetic group of an enzyme known as guanylyl cyclase. For example, NO causes vasodilation following a rise in Ca^{2+} concentration due to ligand binding (i.e., acetylcholine, bradykinin, histamine, or insulin) to a specific receptor or shear stress in the blood vessel. Binding of Ca^{2+} to calmodulin and subsequent binding to and activation of eNOS stimulates NO production. NO then diffuses across the endothelial cell membrane to a smooth muscle cell, where it binds to and activates soluble guanylyl cyclase (sGC), which makes cGMP. In turn, cGMP activates protein kinase G (PKG), which phosphorylates a variety of channels and receptors. Activation of these channels and receptors leads to inhibition of Ca^{2+} influx into the smooth muscle cell, thus decreasing contraction and causing vasodilation. cGMP levels are regulated by sGC activity, activated by NO binding, and phosphodiesterases, particularly cGMP-specific phosphodiesterase 5, which hydrolyzes cGMP to 5'-GMP resulting in termination of the vasodilation signal.

Contrastingly, iNOS from macrophages is either present and functional or absent. It is induced by cytokines and interleukins upon immune challenge and is responsible for the major portion of NO production in mammalian systems. While it is an important function to produce cytotoxic agents, such as peroxynitrite, for the destruction of bacterial, fungal, and cancerous cells, the overproduction of NO by this isoform is also responsible for endotoxic shock marked by a precipitous drop in blood pressure that can be life-threatening.

Nitric oxide synthases are prime examples of redox enzymes with newly discovered functions involving cellular signaling. The hierarchy of controlling factors involved in the function of these enzymes makes them extremely important targets for drug design, as a number of pathologies are associated with abnormal NOS regulation.

SELECTED REFERENCES

1. Sheta, E.A., McMillan, K., and Masters, B.S.S. (1994). Evidence for a bidomain structure of constitutive cerebellar nitric oxide synthase. *J. Biol. Chem.* 269:15147–15153.
2. McMillan, K., and Masters, B.S.S. (1995). Prokaryotic expression of the heme- and flavin-binding domains of rat neuronal nitric oxide synthase as distinct polypeptides: identification of the heme-binding proximal thiolate ligand as cysteine-415. *Biochemistry* 34:3686–3693.
3. Salerno, J.C., Harris, D.E., Irizarry, K., Patel, B., Morales, A.J., Smith, S.M.E., Martásek, P., Roman, L.J., Masters, B.S.S., Jones, C.L., Weissman, B.A., Lane, P., Liu, Q., and Gross, S.S. (1997). An autoinhibitory control element defines calcium-regulated isoforms of nitric oxide synthase. *J. Biol. Chem.* 272:29769–29772.
4. Fulton, D., Gratton, J.-P., McCabe, T.J., Fontana, J., Fujio, Y., Walsh, K., Franke, T.F., Papapetropoulos, A., and Sessa, W.C. (1999). Regulation of endothelium-derived nitric oxide production by the protein kinase Akt. *Nature* 399:597–601.

5. Roman, L.J., Martásek, P., Miller, R.T., Harris, D.E., De la Garza, M.A., Shea, T.M., Kim, J.-J.P and Masters, B.S.S. (2000). The C termini of constitutive nitric oxide synthases control electron flow through the flavin and heme domains and affect modulation by calmodulin. *J. Biol. Chem.* 275:29225–29232.
6. Lane, P., and Gross, S.S. (2002). Disabling a C-terminal autoinhibitory control element in endothelial nitric oxide synthase by phosphorylation provides a molecular explanation for activation of vascular NO synthesis by diverse physiological stimuli. *J. Biol. Chem.* 277:19087–19094.
7. Roman, L.J., Martásek, P. and Masters, B.S.S. (2002). Intrinsic and extrinsic modulation of nitric oxide synthesis. *Chem. Rev.* 102:1179–1189.

4.3 REDOX REGULATION OF GENES

MARTIN B. DICKMAN

*Institute for Plant Genomics and Biotechnology, Texas A&M University,
College Station, Texas*

A number of studies have shown that the oxidative burst, induced by stress or developmental cues as well as by alteration of antioxidant defenses, is associated with specific changes in gene expression. There have been an increasing number of reports where gene/protein expression is influenced by cellular redox status and redox changes. Modification of specific amino acid residues of proteins is fundamental for modulation of gene expression. In particular, modulation of the redox states of cysteine residues has emerged as a widespread mechanism in cell regulation and signaling pathways. Cysteine residues play ubiquitous roles in mediating cellular responses to redox status through their ability to both detect changes in the redox environment and transduce a change in protein structure and function. Emerging evidence has also shown that several transcription factors are modulated by redox-regulated DNA binding activity. In addition, mitogen activated protein kinase (MAPK) pathways not only represent crosstalk between redox-mediated signaling and protein phosphorylation cascades, but also are a prime example of ROS activation for induction of signal transduction pathways.

4.3.A MAP Kinase/Cell Cycle

A number of important signaling pathways are activated when cells are treated with oxidants. The association between MAPK signaling and oxidative stress is well documented. The MAPKs are modules of three successive protein kinases that are central for regulation of many cellular processes and are modulated, in part, by redox regulation. Depleting cellular GSH causes transient increases in ROS, leading to the activation of ERK2, a classic MAPK. This activation is prevented by *N*-acetyl cysteine (NAC) treatment. Stress-activated protein MAP kinases (SAPK) are also sensitive to redox modulation. Activation of p38 SAPK by tumor growth factor β requires free radical production. Similarly, protein phosphatases, particularly protein tyrosine phosphatases, need to be tightly controlled for maintenance of mitogenic signaling. Under basal conditions, ROS levels are low and protein tyrosine phosphatase activity is

high; following growth factor stimulation, ROS increases leading to transient inactivation of protein tyrosine phosphatases, and a concomitant burst of kinase activity, until ROS returns to basal levels and protein tyrosine phosphatase activity is restored. Both protein tyrosine phosphatases and serine/threonine phosphatase are redox sensitive. The active sites of protein tyrosine phosphatases include cysteine and arginine residues separated by five amino acids, creating a low pK_a , rendering cysteine residues more susceptible to oxidation. Oxidation of the cysteine residue results in protein tyrosine phosphatase inactivation. Several oxidative stressors, including $O_2'^{-}$, H_2O_2 , and peroxynitrite, activate receptor tyrosine kinases following downstream signaling including MAPK.

The multifunctional p53 tumor suppressor gene encodes a transcription factor involved in cell cycle arrest. Reduced cysteines are essential for p53 DNA binding activity; mutations involving these residues are associated with many cancers. Several studies have shown that the cell cycle can be arrested in response to ROS and/or reactive nitrogen species (RNS). Alteration of cellular redox state by GSH depletion (increasing ROS) results in delayed progression through G1 and S phases as well as G2 arrest; thus, cycling ceases or can induce programmed cell death.

4.3.B Redox Control of Gene Expression

Among the possible targets of redox signaling pathways are redox-regulated transcription factors. Redox alteration of transcription factor activity can occur via (1) oxidative modification of the DNA binding motif of the transcription factor by ROS, or (2) a phosphorylation/dephosphorylation switch as a result of redox-regulated signaling. It is known that the DNA binding activity of a number of transcription factors

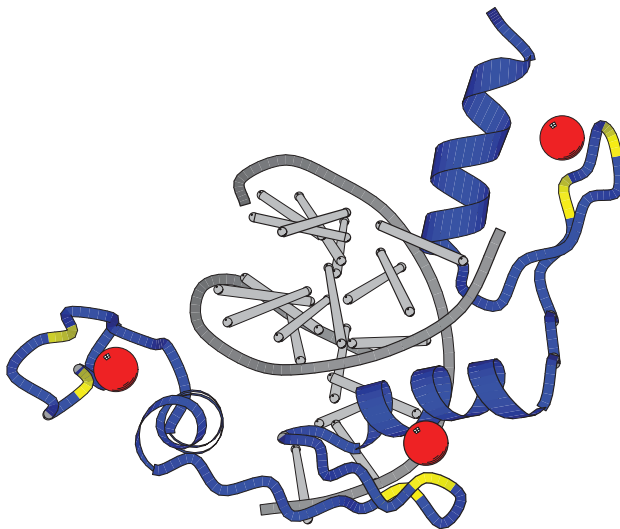


Figure 4.9. Crystal structure of Zif268 protein–DNA complex (from RCSB PDB 1AAY) showing thiol groups (yellow) and Zn^{2+} (red). Blue γ -helices represent the zinc fingers with the GGCGT nucleic acid binding finger in the lower left corner.

is abolished by oxidizing conditions *in vitro*. Zinc finger motifs, a common DNA binding domain, are particularly sensitive to redox changes; the thiol group of cysteine residues in the zinc finger protein Sp1 confers redox sensitivity (Fig. 4.9).

Oxygen sensing in bacteria offers a number of particularly instructive examples illustrating the importance of the redox state for cellular metabolism and maintaining redox homeostasis. Bacteria have developed specific sensors that detect redox imbalance and trigger gene expression to generate an appropriate cellular response. For example, recent work with the human pathogen *Staphylococcus aureus* has shown that a global regulator, MgrA, is both an important virulence determinant and functions as an oxygen sensor to regulate antibiotic/oxidative stress resistance. Using a genetic approach with transposon mutants, pathogenicity-related functions for MgrA were established. To elucidate regulatory mechanisms, the crystal structure for MgrA was solved. A potentially key cysteine residue was identified and experimentally tested. Oxidation of this cysteine regulates MgrA binding to DNA. MgrA DNA binding normally occurs under oxidative stress; MgrA binding induces several pathways regulating antibiotic resistance as well as other defense-related genes. Thus, these bacteria utilize a single protein that is oxidatively regulated, to activate a number of stress-responsive pathways that serve as a general strategy for responding to numerous environmental cues involving oxidative stress.

4.3.C Peptide Editing and Thiol-Mediated Redox Regulation

The mechanism for distinguishing and selecting peptides by MHC Class 1 molecules during antigen processing is a result of thiol-based redox regulation. This was determined from mechanistic studies evaluating how MHC Class 1 molecules select peptides from a complex background of self versus nonself proteins in the ER. Peptide loading complexes were purified and components identified by tandem mass spectrometry. Among the proteins identified, protein disulfide isomerase was established as a member of the antigen processing loading complex. This enzyme is necessary for the correct formation of disulfide bonds and is involved in disulfide bond oxidation and reduction as well as isomerization. Functional studies determined the specificity of the protein disulfide isomerase in this complex and the role for this enzyme MHC Class 1 antigen presentation. RNA knockdown of protein disulfide isomerase demonstrated the physiological relevance of this enzyme in MHC Class 1 processes. Coupling the enzymatic function of protein disulfide isomerase and the knockdown experiments suggested that redox regulation of MHC Class 1 molecules is important. It is believed this redox switch might provide a checkpoint for protein quality control of complex assembly, and permit rapid and sustained responses to pathogens as well as deterring unwanted immune responses.

It is evident that cells employ redox status to regulate a wide variety of physiological functions. Although there are gaps in our knowledge of ROS and signaling, it is known that ROS are produced continuously in the cell during normal growth and development. All cells harbor an efficient suite of antioxidant systems that protect against perturbations that increase ROS (see Chapter 2). ROS can propagate signals to multiple subcellular pathways, thus influencing a variety of cellular processes

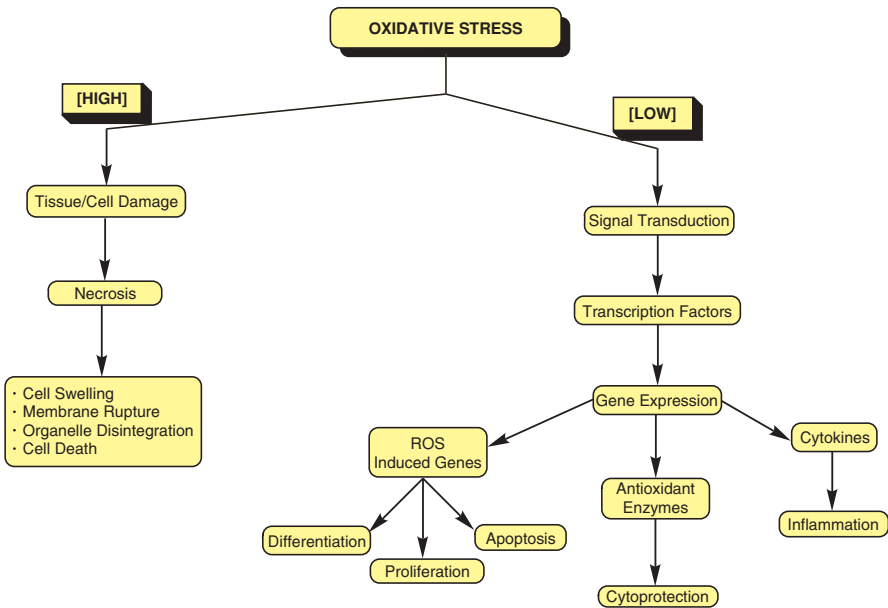


Figure 4.10. Generalized view of ROS-mediated signal transduction. At low concentrations, ROS can indirectly trigger signaling leading to proliferation, differentiation, or death (apoptosis). At high concentrations, excess ROS leads directly to death (necrosis).

(Fig. 4.10). Since the cell has an efficient anti-ROS system, how do basal (nontoxic) concentrations of ROS exist? This is an issue often faced with signaling and gene regulation. Possibly, basal ROS and the antioxidants are located in different cellular compartments, thus enabling ROS to affect its target prior to being affected by the cells' antioxidant system.

The sensitivity of reactive cysteine residues to oxidation builds redox switches into proteins that can respond to changes in cellular redox status. The thiolate anion can be stabilized by proximity to hydrogen bond donors, basic residues, and metal ions. Thus, the reactivity of cysteine residues toward ROS can influence the selectivity of the response. The capacity of redox-sensitive cysteine residues to both detect and affect a response to changes in redox status provides a relatively simple and rapid mechanism to elicit regulation of biological responses.

SELECTED REFERENCES

1. Green, J., and Pagar, M.S. (2004). Bacterial redox sensors. *Nature* 2:954–966.
2. Finkel, T. (2003). Oxidant signals and oxidative stress. *Curr. Cell Biol.* 15:247–254.
3. Guyton, K.Z., Lin, Y., Gorospe, M., Xu, O., and Holbrook, N.J. (1996). Activation of mitogen-activated protein kinase by H_2O_2 . *J. Biol. Chem.* 271:4138–4142.

4. Chen, P.R., Bae, T., Williams, W.A., Duguid, E.M., Rice, P.A., Schneewind, O., and He, C. (2006). An oxidation-sensing mechanism is used by the global regulator MgrA in *Staphylococcus aureus*. *Nat. Chem. Biol.* 2:591–595.
5. Park, B., Lee, S., Kim, E., Cho, K., Riddell, S.R., Cho, S., and Ahn, K. (2006). Redox regulation facilitates optimal peptide selection by MHC Class I during antigen processing. *Cell* 127:369–382.

4.4 REDOX REGULATION OF APOPTOSIS

MARTIN B. DICKMAN

*Institute for Plant Genomics and Biotechnology, Texas A&M University,
College Station, Texas*

Multicellular organisms eliminate redundant, damaged, or unnecessary cells by a gene-directed death process. Programmed cell death or its morphological equivalent, apoptosis, is a genetically encoded cellular suicide that is essential for normal growth, development, and tissue homeostasis in all multicellular eukaryotes. In humans and other animals, dysregulation of this natural cell death pathway significantly contributes to a number of major diseases. Defects of genes that control death pathways that save cells normally destined to die can underlie both cancer and autoimmune diseases, while defects that promote cell death that do not normally occur can contribute to stroke, AIDS, Alzheimer's, Parkinson's, and other neurodegenerative diseases. In addition, most viruses and intracellular bacteria, as well as plant pathogenic fungi, control the cell death pathways in the host cells, thus linking apoptosis to infectious diseases.

Morphological and biochemical features associated with this cell death process include cell shrinkage, membrane blebbing, chromatin condensation, DNA cleavage and fragmentation (resulting in a characteristic “ladder”), and externalization of the inner membrane lipid phosphatidylserine. A group of dedicated cysteine-directed proteases, termed caspases, are activated during this process and cleave major structural proteins during the orderly dismantling of the cell. These proapoptotic caspases are present as inactive zymogens and are induced and activated following an apoptotic stimulus. These proteases are divided into two groups: initiator or upstream caspases and executioner caspases. The net result of apoptosis is the clean removal of cells without an inflammatory response, which is in contrast to necrotic or accidental cell death, where the cell does not actively participate in the process and inflammation occurs.

4.4.A Apoptotic Pathways

In mammalian systems, apoptosis proceeds by at least two major pathways, extrinsic and intrinsic (Fig. 4.11). As is often the case with complex signaling pathways, the lines of distinction between these “independent” pathways can be obscured by crosstalk. The extrinsic or death receptor pathway is typified by members of the tumor necrosis factor family of receptors. Following binding of specific “death” ligands,

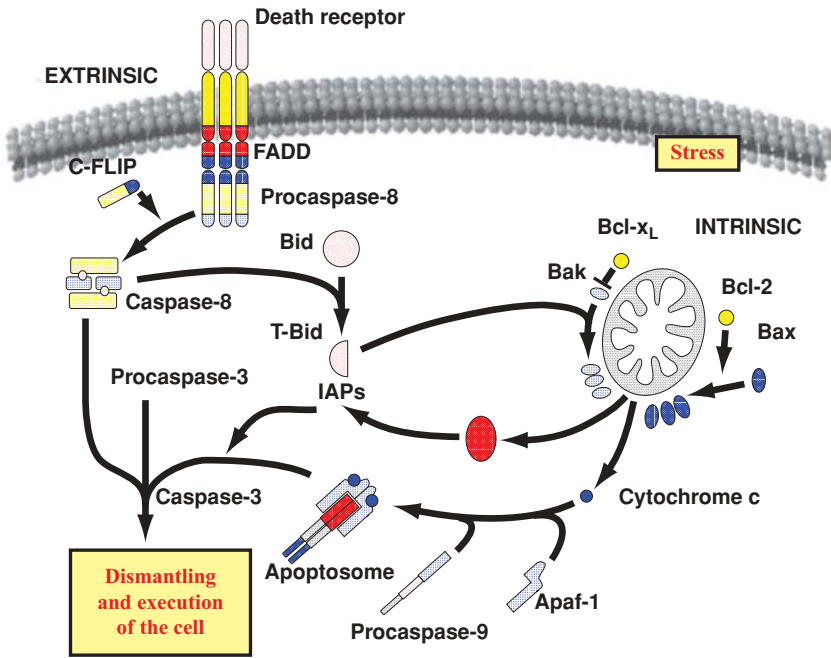


Figure 4.11. Major apoptotic pathways in mammalian cells. Proapoptotic proteins include caspases, Bak, Bic, Bax, cytochrome, Apaf-1, and Smac. Antiapoptotic proteins include IAPs, Bcl-2, and Bcl-xl.

receptors aggregate, forming a death-inducing signaling complex that results in the activation of a caspase 8, an initiator caspase. Caspase 8 then proteolytically activates downstream “executioner” caspases (e.g., caspase 3, 6, or 7), which cleave structural and other proteins for the orchestrated dismantling of the cell.

The intrinsic pathway can be triggered by numerous stimuli, including growth factor withdrawal, DNA damage, and oxidative stress. This pathway generally involves mitochondria, which, when stimulated by an apoptotic signal, release several apoptotic regulators, including cytochrome *c* and other proteins normally sequestered between the inner and outer mitochondrial membranes. Upon release, cytosolic cytochrome *c* binds to an adaptor protein (Apaf-1), resulting in the dATP-dependent formation of the “apoptosome” comprised of oligomers of cytochrome *c*, Apaf-1, and procaspase 9. This high molecular weight complex results in the proteolytic activation of caspase 9. Caspase 9, in a manner similar to caspase 8, activates downstream caspases for cellular demise.

4.4.B Reactive Oxygen Species and Apoptosis

Many redox-sensitive proteins are involved in regulating apoptotic pathways, suggesting that the redox environment of the cell is important. The production of ROS, in particular, has been associated with programmed cell death in many pathological

contexts including stroke, inflammation, ischemia, lung edema, and neurodegeneration. Several chemical and physical treatments capable of inducing apoptosis are also known to generate oxidative stress. The major physiological source of ROS in mammals is the mitochondrion, where oxygen is reduced to water. A crucial event associated with the intrinsic pathway is the uncoupling of oxidative phosphorylation in the mitochondria and the dissipation of mitochondrial transmembrane potential, a decrease in ATP, and an increase in ROS. The Bcl-2 family of apoptotic regulators contains both pro- and antiapoptotic proteins that localize to the outer mitochondrial membrane. The sensitivity of cells to apoptotic stimuli often is dependent on the balance between pro- and antiapoptotic Bcl-2 family member proteins. Under conditions of oxidative stress, cytoprotective proteins like Bcl-2 prevent the ability of ROS to induce apoptosis. Conversely, Bad and Bax, proapoptotic Bcl-2 family members, act as sensors of cellular damage, translocate to the mitochondria following such stress, increase the generation of ROS, and disrupt the ability of antiapoptotic proteins to inhibit death; caspases are activated and death ensues. The resultant phenotypes are concentration dependent; at relatively low levels, ROS function as signaling molecules promoting proliferation and survival, whereas higher levels of ROS are apoptotic while even higher levels are necrotic. ROS-mediated apoptosis causes disruption of the mitochondrial membrane potential and permeability transition leading to cellular dysfunction; ATP synthesis is blocked, redox molecules including NADH, NADPH, and GSH are oxidized, and ROS levels increase. In the death receptor pathways, ROS accumulates prior to all morphological and biochemical alterations associated with apoptosis. Antioxidant treatments prevent death-receptor-mediated apoptosis.

In most cases, ROS triggers programmed cell death by oxidatively altering cellular proteins and other components or by directly activating the mitochondrial pathway. Apoptotic effectors, particularly caspases, are redox sensitive. All caspases harbor a QACXG motif, which contains the active site cysteine. This cysteine residue is sensitive to redox changes. Both thioredoxin and GSH are required for caspase 3 activity and in regulating apoptosis signal-regulating kinase-1 (ASK-1), a mitogen active protein kinase kinase kinase (MAPKKK) that regulates the activation of c-Jun N-terminal kinase (JNK) that is involved in stress signal transduction pathways, including apoptosis. Cells therefore require a reducing environment for caspases to function properly. ASK-1 is a redox sensor kinase involved in oxidative stress-induced activation of JNK, which leads to apoptosis. Thioredoxin has been shown to be a negative regulator of the ASK-1/JNK pathway, thus functioning essentially as a cytoprotectant. JNK is maintained at low levels in nonstimulated cells, and its enzymatic activity is inhibited by interaction with glutathione *S*-transferase. Following apoptotic stimuli, such as H₂O₂ or UV radiation, this complex dissociates and JNK is activated via phosphorylation by ASK-1. The identification of thioredoxin and glutathione *S*-transferase as modulators of ASK-1 and JNK suggests a mechanistic model for how redox-mediated signaling events can result in programmed cell death (Fig. 4.12).

Other important factors contributing to redox regulation of apoptosis include heat shock proteins (HSPs). HSPs can directly interact with various apoptotic proteins at key points along the pathway. Hsps have antiapoptotic functions by providing

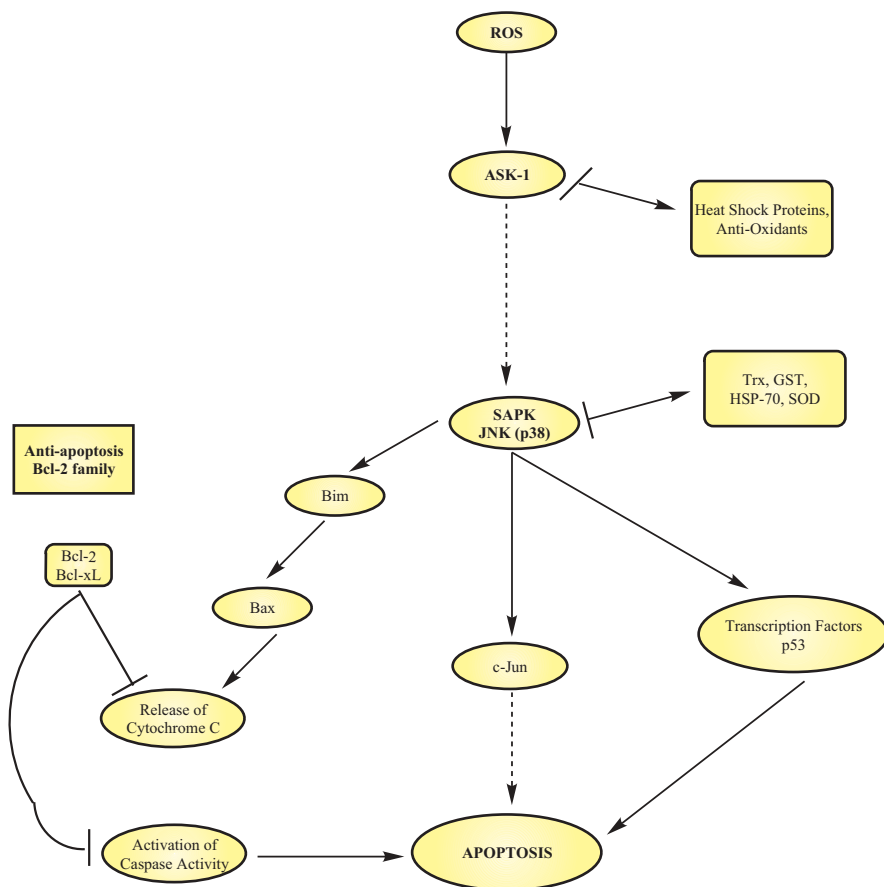


Figure 4.12. Oxidative stress-induced apoptosis and MAP kinases. ASK-1, a MAPKKK, is activated by ROS. Activated ASK-1 induces kinase activity of JNK and/or p38 SAPKs. Several antioxidants (enzymes, heat shock protein) negatively regulate kinase activation. SAPK activation phosphorylates several downstream targets including the transcription factor c-Jun or p53, which indirectly or directly cause programmed cell death. SAPKs appear to also affect oxygenation of Bcl-2 family members, inhibiting Bcl-2 and activating Bax.

time for cellular adaptation during conditions that are otherwise lethal. For example, several apoptotic stimuli induce HSP27 overexpression. HSP27 can be cytoprotective in several ways including decreasing ROS levels and neutralizing the toxic effects of oxidized proteins. HSP27 can inhibit caspases and prevent oligomerization of Apaf-1. Control of programmed cell death by Hsps is dependent on the nature of the stimulus and cell type.

In terms of reactive nitrogen species, NO can function as a cell killer or protector depending on its concentration. At relatively high concentrations, NO can induce

programmed cell death or necrosis. The cytotoxicity of NO is primarily due to interaction with $O_2^{\cdot-}$ to form peroxynitrite. At relatively low concentrations, NO inhibits programmed cell death due to its reactivity with thiol groups. NO can block catalytic cysteine residues by S-nitrosylation of caspases and can also increase the concentration of Bcl-2, thus indirectly preventing programmed cell death at several points in the pathway.

Due to its high concentration, the GSH:GSSG redox couple usually mirrors the intracellular redox environment. The concentration of GSH and/or the ratio of GSH/GSSG are crucial in processes leading to programmed cell death under conditions of oxidative stress. For example, the release of cytochrome *c*, a major component of the intrinsic cell death pathway mentioned previously, is significantly affected by a decrease in GSH.

While the precise mechanisms by which ROS regulate apoptosis is not entirely clear, modification of important cysteine residues may account for regulation of the redox balance in cells undergoing programmed cell death. Cysteine redox status can influence protein structure leading to an activation or inhibition of function. Antioxidants such as superoxide dismutase, catalase, and GSH peroxidase also influence redox status by scavenging ROS. Although questions remain, redox regulation of oxidative stress is central to the modulation of programmed cell death.

SELECTED REFERENCES

1. Hengartner, M.O. (2000). The biochemistry of apoptosis. *Nature* 407:770–776.
2. Shen, Y., and Shenk, T.E. (1995). Viruses and apoptosis. *Curr. Opin. Gen. Dev.* 5:105–111.
3. Kannan, K., and Jain, S.K. (2000). Oxidative stress as a mediator of apoptosis. *Pathophysiology* 7:153–163.
4. Brune, B. (2005). The intimate relation between nitric oxide and superoxide in apoptosis and cell survival. *Antioxid. Redox Signal.* 7:497–507.
5. Filomeni, G., and Ciriolo, M.R. (2006). Redox control of apoptosis: an update. *Antioxid. Redox Signal.* 8:2187–2192.

4.5 METAL HOMEOSTASIS

JAEKWON LEE

Redox Biology Center and Department of Biochemistry, University of Nebraska, Lincoln, Nebraska

The inorganic chemistry of metals is widely utilized in various biological processes such as enzyme reactions, signal transductions, electron transfer, and oxygen transport. Transition metal ions in particular play critical roles as electron transfer intermediates in various redox reactions. Organisms must acquire metals from the environment and incorporate them into metalloproteins by the post-translational addition

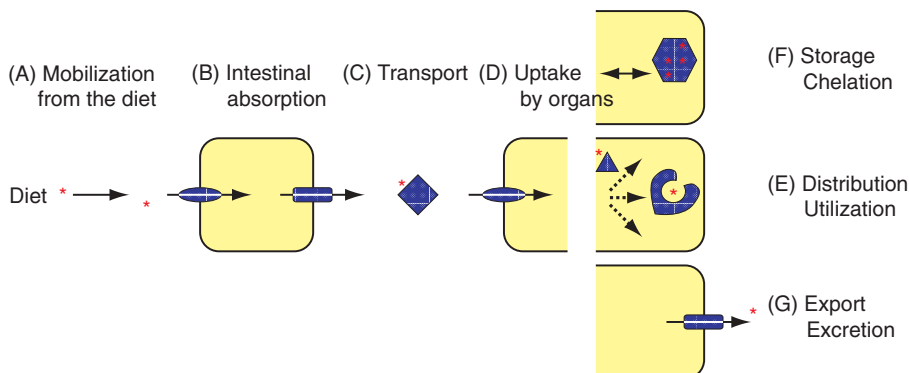


Figure 4.13. Metal metabolism is comprised of many steps. (A–C) Metals are absorbed in the intestine from the diet and transported to the organs and tissues. Membrane metal transporters and carriers are involved in the absorption and transport steps. (D) Metal-specific transporters at the cell surface take up metals at the peripheral organs and tissues. (E) Cytoplasmic metal carrier molecules and metal transporters at the subcellular organelles play critical roles in intracellular metal trafficking, compartmentalization, and utilization. (F) Mechanisms for metal storage and mobilization have been characterized. (G) Metals accumulate in excess or nonphysiological metals are excreted from the body. Expression, localization, and/or activities of the proteins involved in metal metabolism are regulated by several different delicate mechanisms to maintain optimal levels of metals in the body.

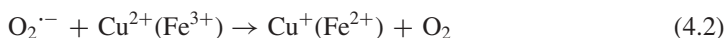
of metal or metal-containing prosthetic groups. However, excess metal accumulation and their release in free reactive forms can be toxic. Since both deficiency and excess lead to serious problems in organisms, regulation of metal metabolism, including uptake, trafficking, assembly into metalloproteins, and detoxification, is clearly important. Recent progress in elucidating mechanisms for metal homeostasis has revealed underlying principles of metal metabolism and implicates metals in development, growth, and disease. Since disorders in metal metabolism are linked to a number of health problems, studies on metal metabolism can have important clinical implications. This section summarizes the fascinating mechanisms for metabolism of copper (Cu) and iron (Fe) in mammals and the implication of defects in metal metabolism in disease (Fig. 4.13).

4.5.A Physiological Significance of Metal Metabolism

Redox-active metals mediate electron transfers in various biochemical reactions. The catalytic centers of many enzymes contain Cu, Fe, heme, or iron–sulfur clusters that are essential for function. For example, energy generation by mitochondrial oxidative phosphorylation depends on Cu and heme incorporation into proteins, such as cytochrome *c* oxidase. Cu- and zinc-containing superoxide dismutase (Cu,ZnSOD) utilizes Cu in the detoxification of $O_2^{\cdot-}$ (see Chapter 3, Section 3.1.B). Aconitase in mitochondrial citric acid cycle is an Fe–S center enzyme. Cu-containing

enzymes play essential roles in the synthesis of catecholamine, a neurotransmitter. Furthermore, hemoglobin in red blood cells carries a major portion of Fe in mammals, and oxygen transport by heme in red blood cells is essential for respiration. Nutritional metal deficiency and genetic diseases of metal metabolism have further provided striking evidence that metals are critical trace elements in a number of other physiological processes.

While metals are essential nutrients, their excess accumulation is toxic. Transition metal ions readily catalyze reactions that result in the production of hydroxyl radicals through the Fenton and Haber–Weiss reactions [reactions (4.1) and (4.2)].



The highly reactive oxygen intermediates are responsible for lipid peroxidation, oxidation of proteins, and cleavage of nucleic acids. These cellular damages are believed to be major contributing steps to various diseases in humans.

4.5.B Metal Uptake from the Extracellular Environment

Organisms obtain metals from the diet and the environment through specific transporters at the cell membrane. Although Cu and Fe are abundant in the earth's crust, these metals are not readily bioavailable due to limited solubility. Cell-surface metalloreductases containing two hemes as prosthetic groups for transmembrane electron transport have been identified in yeast and plant. They play critical roles in enhancing uptake of oxidized metals. Although a potential mammalian Fe reductase has been proposed, its role in Fe absorption has not been firmly established. The gene encoding Cu reductase remains to be identified.

Several high and low affinity Cu and Fe membrane transport systems have been characterized. The Ctr1 (copper transporter 1) family of proteins, conserved in eukaryotes from yeast to mammals, is generally accepted as a Cu transporter (Fig. 4.14). Members of the Ctr1 family have no apparent homology to known proteins. Although the overall sequence similarity between yeast Ctr1 and human Ctr1 is low, Ctr1 family members have common structural features. In fact, both human and plant Ctr1 function in yeast cells. This suggests that the mechanism of Ctr1-mediated Cu transport is conserved among eukaryotes. Evidence that Ctr1 is critical for cellular Cu transport is accumulating. For example, Ctr1 overexpression stimulates cellular Cu uptake, and Ctr1 gene knockout in yeast and mice reduces Cu levels. However, its precise role in Cu transport is not currently defined. It is uncertain whether Ctr1 is a Cu transporter, a Cu receptor, or a component of Cu transporter.

The mammalian Fe uptake system is comprised of several components, including Fe-binding transferrin in serum, cell membrane transferrin receptors, and Fe transporter (DMT1/DCT1/Nramp2) (Fig. 4.15). Transferrin-bound transferrin receptor

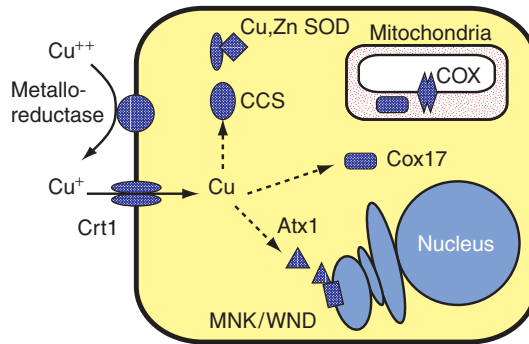


Figure 4.14. Copper transport and distribution. Ctr1 is an integral membrane protein that is an essential component of cellular copper uptake. Two Cu carriers (CCS, Atx1) in the cytoplasm deliver Cu in a target-specific manner. Copper-transporting CP_X -type ATPases (MNK and WND) at the membrane of the post-Golgi compartment transport Atx1-delivered Cu for incorporation of Cu into secretory proteins. CCS directly interacts with Cu,ZnSOD for Cu relay. Cox17 plays a critical role in Cu insertion into cytochrome *c* oxidase.

undergoes endocytosis. The acidic environment in the endosome causes Fe to be released from transferrin, and Fe is transported to the cytoplasm through DMT1 by a proton cotransport mechanism. DMT1 also plays a role in nonheme Fe uptake in the intestine. Since oxidized Fe forms insoluble complexes, Fe^{3+} reductase is required for Fe uptake in the intestine. Dcytb, a cytochrome *b*-like protein, was identified as an Fe reductase. However, gene knockout in mice revealed that Dcytb is not essential for intestinal nonheme Fe absorption. Thus, an alternative Fe reductase must exist, since Fe reduction appears to be an essential step for Fe absorption from the diet. Dietary heme is also a significant source of Fe for humans and carnivorous animals and a heme transporter has been cloned. Several other Fe uptake systems that are specific for substrate, cell, or developmental stage have been identified in mammals and other eukaryotes.

4.5.C Intracellular Metal Distribution by Target-Specific Chaperones

Once metals are transported into the cell, they must reach their appropriate destination efficiently and are incorporated into metal-requiring proteins without participating in harmful side reactions. The mechanism for cytoplasmic Cu distribution to Cu-requiring proteins or to cellular compartments by target-specific Cu carrier molecules (Cu chaperones: Atx1/Atox1, Cox17, and CCS) have been identified (Fig. 4.14). Atx1 delivers Cu to the secretory compartment, where Cu is loaded into Cu-containing proteins. Another Cu chaperone, Cox17, has been shown to play an essential role in the delivery of Cu to the mitochondria. The delivery of Cu to cytoplasmic Cu,ZnSOD is mediated through a soluble factor identified as CCS that directly interacts with Cu,ZnSOD to transfer Cu. Since free Cu is toxic and virtually no free Cu appears

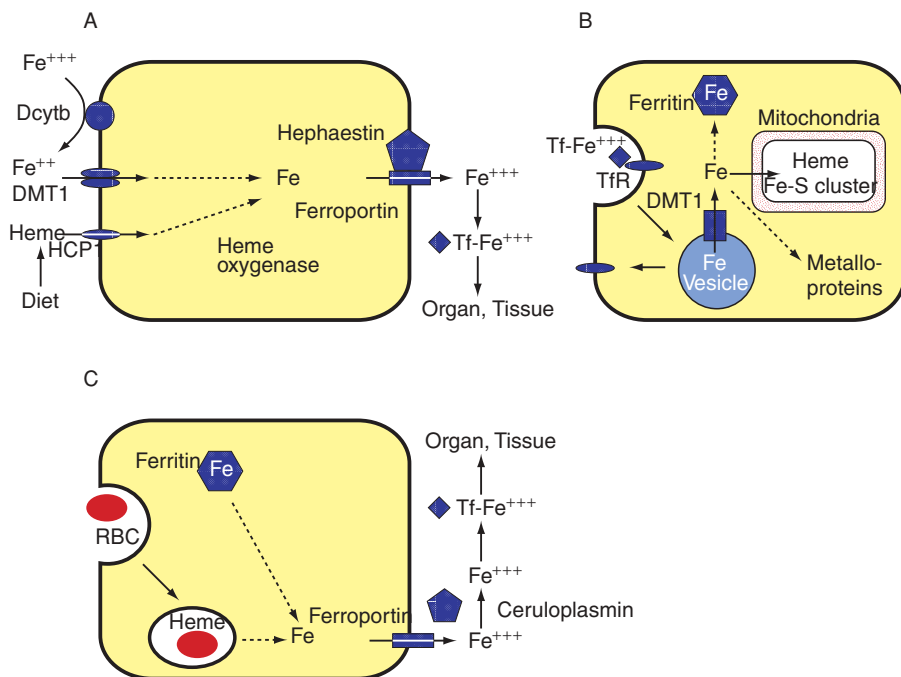


Figure 4.15. Iron transport and distribution. (A) Intestinal Fe transport. DMT1 transports Fe at the apical side of the intestinal epithelial cell layer. HCP1 has been identified as a heme transporter. Iron exported by ferroportin is oxidized by hephaestin, a Cu-containing ferroxidase, and binds to transferrin (Tf). (B) Fe uptake by organs and tissues. The Tf and transferrin receptor (TfR) complex undergoes endocytosis. Fe is released from Tf in the acidic endosome and transported to the cytoplasm through DMT1. The majority of the Fe is utilized for the synthesis of heme and iron–sulfur (Fe–S) clusters. Excess Fe is stored in ferritin. (C) Fe mobilization from storage cells. Ferroportin exports Fe from hepatocytes and reticuloendothelial macrophages that engulf senescent red blood cells (RBCs). Ceruloplasmin, a Cu-containing ferroxidase in serum, oxidizes Fe for incorporation into Tf.

to be present in the cell, it is reasonable to predict that the Cu chaperones acquire Cu directly from a plasma membrane Cu transporter. However, although it has been demonstrated that Ctr1-mediated Cu uptake is necessary for Cu distribution by chaperones, the interaction between Ctr1 and Cu chaperones has not been demonstrated. Cu chaperones may transiently bind with Ctr1, or there may be other components that are required for the Cu relay between Ctr1 and Cu chaperones. Chaperone-mediated intracellular Cu distribution is a new concept in metal metabolism. Most intracellular Fe is moved to the mitochondria for the synthesis of heme and Fe–S clusters. It is unlikely that free Fe is released in the cytoplasm following uptake from the outside of the cell. However, specific carrier molecules that transfer Fe to the mitochondria have not been identified.

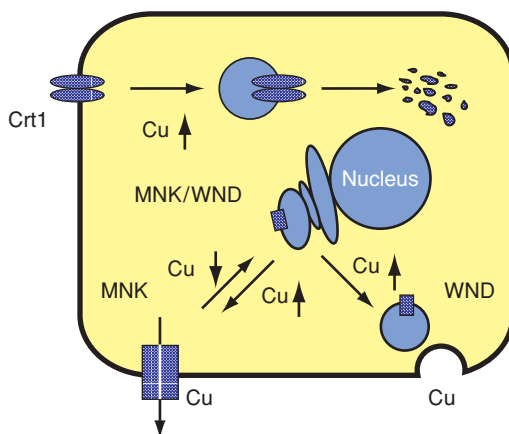


Figure 4.16. Regulation of Cu metabolism. MNK localizes at the post-Golgi compartment and the plasma membrane depending on cellular copper levels. MNK exports copper at the plasma membrane. Copper-dependent localization of WND at the vesicles is implicated in excretion of excess copper into bile from the liver, which is an essential step for systemic copper homeostasis in mammals. Ctr1 cell-surface expression appears to be controlled in a copper-dependent manner, which may be a critical mechanism for the regulation of copper uptake.

4.5.D Subcellular Membrane Metal Transporters

The Menkes (MNK, ATP7a) and Wilson (WND, ATP7b) disease genes encode P-type ATPases localized in the trans-Golgi network, where they deliver Cu to proteins that traverse the secretory pathway (Fig. 4.16). The observations of Cu hyperaccumulation in MNK-defective fibroblasts and intestinal epithelial cells and the trafficking of MNK protein to the plasma membrane under conditions of high Cu indicate that MNK plays a role in cellular Cu efflux. The MNK gene is strongly expressed in many organs and tissues, including intestinal mucosal cells, but only in a trace amount in the liver. WND expression is seen almost exclusive to hepatic and brain tissue. This expression pattern is consistent with the requirement of WND for incorporation of Cu into ceruloplasmin, an Fe oxidase, in the liver, and for biliary excretion of Cu. Mitochondria represent another membrane-bound compartment into which Cu needs to be transported for incorporation into cytochrome *c* oxidases. It is now apparent that Cu homeostasis in the mitochondrion is considerably more complex than previously thought. Recently, the role of the Cu chaperone, Cox17, as the main mitochondrial Cu shuttle has come into question. Cox17, tethered to the mitochondrial inner membrane by fusion with the N-terminal transmembrane domain of an inner membrane protein, complemented the respiratory deficiency of Δcox17 cells. Thus, the role of Cox17 appears to be confined to the mitochondrial intermembrane space, where Cu(I) is translocated to the inner membrane proteins Sco1 and Cox11 that play critical roles for incorporation into the Cu_A and Cu_B sites of cytochrome *c* oxidase, respectively. Evidence also exists for a

nonprotein pool of Cu in the mitochondrial matrix. If Cox17 does not supply Cu to the mitochondria, then how does it get there? One possibility is that Cu transporters exist within the mitochondrial outer and inner membranes. Such transporters have remained elusive.

Mitochondria are the major organelles utilizing Fe for the synthesis of heme and Fe–S clusters. However, the mechanisms for uptake and export of Fe in the mitochondria and regulation of these steps are not well understood. This is a key question that remains to be answered in cellular Fe metabolism.

4.5.E Heme and Iron–Sulfur Cluster Synthesis

Heme in hemoglobin of red blood cells is a major form of Fe in mammals. The pathway for heme biosynthesis, including the roles and compartmentalization of the enzymes, has been established. Fe–S clusters are also important Fe-containing prosthetic centers that are essential for electron transport, enzymatic catalysis, and gene regulation. The scaffolding proteins required for the assembly of Fe–S clusters have been identified. The mechanisms of action of these proteins need to be fully elucidated to understand the molecular details of Fe–S cluster assembly. Synthesis and export of Fe–S clusters from the mitochondria play important roles in cellular Fe homeostasis. It has been proposed that cytoplasmic Fe–S cluster levels are sensed by a regulatory system to control Fe import into mitochondria and Fe homeostasis.

4.5.F Cellular Storage

Excess intracellular Cu and Fe are sequestered in cells. The biological significance of this mechanism appears to be both in detoxification and storage. Metallothionein is a well-characterized chelator of various metals such as Cu, Zn, and Cd. Mammalian metallothionein is a 60–61 amino acid peptide containing 20 cysteines. Metal reconstitution *in vitro* demonstrated that metallothionein coordinates up to 12 atoms of Cu through thiolate bonds to cysteine residues. Sensitivity to metal toxicity in metallothionein gene disruption in mice and in yeast strongly supports a role for metallothionein in metal detoxification. However, it is not clear whether metallothionein-bound Cu plays a significant role in Cu storage. The yeast vacuole is involved in sequestration of metals, and metal-specific transporters (e.g., Ctr2 Cu exporter, CCC1 Fe importer, Fth1 and Fet5 Fe export complex) at the vacuolar membrane have been identified. Ferritin is an Fe storage multimeric protein that is composed of 24 light and heavy chain subunits (Fig. 4.15B) that sequesters up to 4500 Fe atoms in the ferrihydrite form. Ferroxidase activity of the H subunit is required for Fe sequestration. Various stimuli, including cellular Fe deficiency, degrade ferritin to mobilize stored Fe.

4.5.G Metal Export

Cu-dependent trafficking of Cu-transporting P-type ATPase from the secretory compartment to the plasma membrane is an important step for Cu export. This appears to be particularly important for Cu absorption from the intestine. WND Cu-transporting

ATPase-mediated Cu excretion into bile from the liver is a major mechanism for systemic Cu homeostasis in mammals (Fig. 4.14).

Ferroportin, an integral membrane protein, mediates Fe export at the basolateral membrane of enterocytes, which is critical for Fe absorption (Fig. 4.15A). Ferroportin-mediated export of Fe from macrophages that engulf senescent erythrocytes also plays a critical role in recycling Fe (Fig. 4.15C). The mechanism of Fe excretion from the body has not been identified. Only a minimal amount of Fe is excreted from the body through loss of hair and skin cells. It appears that systemic Fe homeostasis relies on regulation of Fe absorption from the diet and mobilization from intracellular stores.

4.5.H Regulation of Metal Metabolism

Regulation of metal homeostasis basically leads to maintenance of optimal levels of bioavailable metals in cells, organs, and whole organisms. This is achieved by controlling the expression levels and/or localization of the components involved in metal uptake, distribution, storage, and excretion. Cu and Fe homeostasis is maintained by several regulatory mechanisms that include metal binding to transcriptional and post-transcriptional regulators, metal-mediated interactions between components involved in metal metabolism, communication between organs, and/or signals from metabolic pathways in which metals are required. Some of the systems are unique, providing new paradigms for gene regulation.

4.5.H1 Transcriptional Regulation. With the exception of the metallothionein gene, transcriptional regulation of genes encoding components of Cu metabolism has not been characterized in mammalian cells. However, transcriptional regulation is a major mechanism for Cu homeostasis in yeast. The Cu-sensing Mac1 transcription regulator plays a critical role in Cu homeostasis in yeast by regulation of transcription of the genes encoding Cu uptake proteins. Ace1 is another transcription factor that responds to toxic levels of Cu to regulate the Cup1 gene encoding metallothionein. Both regulators appear to bind Cu directly, which controls their activities.

Aft1 and Aft2 regulate Fe metabolism in yeast. The two transcription factors have significant sequence homology with each other. Interestingly, they have overlapping but independent functions in their target gene regulation. The mechanisms of sensing Fe status by Aft1 and Aft2 have not been elucidated, but Fe–S cluster levels in cytoplasm are implicated in Aft1/2 regulation. In mammals, cytokines (e.g., TNF- α , interleukin, IFN- γ) regulate expression of several components of Fe metabolism (e.g., ferritin, transferrin receptor 1, ferroportin, hepcidin). Cytokine-induced regulation of Fe metabolism seems to be linked to host defense mechanisms by limiting availability of Fe to invading pathogens.

4.5.H2 Post-transcriptional Regulation. Iron regulatory proteins (IRPs) 1 and 2 play major roles in the regulation of expression of proteins involved in Fe metabolism (Fig. 4.17A). IRP binds to an iron response element (IRE), which is a conserved hairpin structure in the untranslated regions (UTRs) of mRNAs encoding proteins involved in Fe metabolism (Fig. 4.17B). IRP binding to IRE located at the 5' UTR inhibits

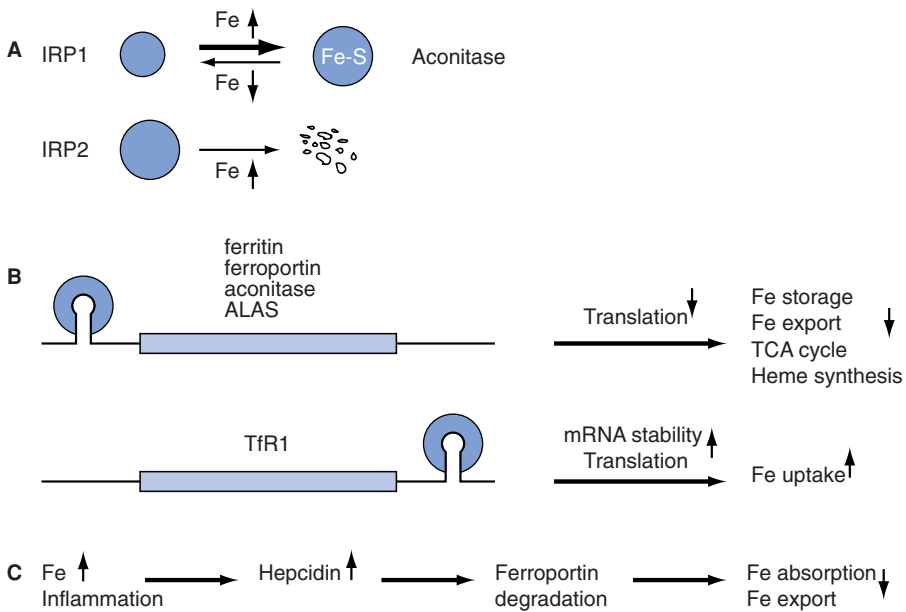


Figure 4.17. Regulation of Fe metabolism. (A) Regulation by iron regulatory protein 1 (IRP1) and iron regulatory protein 2 (IRP2). IRP1 is a cytoplasmic aconitase containing a 4Fe-S cluster. Lack of Fe-S cluster assembly into IRP1 due to Fe deficiency converts it into an iron regulator. Excess Fe induces IRP2 degradation, which controls cellular IRP2 levels. (B) Regulation of translation by Fe regulatory proteins. IRP1 and IRP2 bind to iron response element (IRE) in the 5' or 3' untranslated regions of their target mRNAs to control translation efficiency of their targets. (C) Regulation of Fe metabolism by hepcidin. Excess Fe levels and inflammation induce transcription of hepcidin, a systemic regulator of Fe metabolism. Hepcidin circulates in the blood and binds to ferroportin to induce its endocytosis and degradation. This reduces Fe absorption from the intestine and mobilization of Fe from storage proteins.

translation of target mRNAs encoding ferritin, mitochondrial aconitase, ferroportin, and aminolevulinic acid synthase, the first enzyme in the heme synthesis pathway. The 3' UTR of transferrin receptor 1 carries multiple IREs. Binding of IRP to the 3' UTR enhances mRNA stability and leads to increased translation of transferrin receptor 1. IRP1 is a cytoplasmic Fe-S cluster-containing aconitase that is converted to an mRNA binding protein depending on cellular Fe status and other signals that perturb the Fe-S cluster in IRP1. For example, reduced Fe-S cluster synthesis resulting from Fe deficiency leads to defective Fe-S cluster assembly in IRP1. The Fe-S cluster of the IRP1 is also sensitive to reactive oxygen and nitrogen species (e.g., H_2O_2 , NO). The Fe-S cluster-defective form of IRP1 loses aconitase activity and serves as an IRE binding regulator. Thus, Fe deficiency inhibits translation of Fe storage molecules, mitochondrial citric acid cycle, Fe export, and heme synthesis. At the same time, binding of IRP to the 3' UTR of transferrin receptor 1 stabilizes the mRNA and enhances its translation, which leads to increased Fe uptake into cells. Fe transport

and Fe-S cluster incorporation into IRP1 converts it to aconitase. This is a feedback mechanism for controlling IRP1 activity. The mode of regulation of IRP2 by Fe is different from that of IRP1. Fe stimulates the proteosomal degradation of IRP2. It appears that direct binding of Fe to IRP2 is a signal for its degradation. IRP gene knockout in mice suggested that IRP2 dominates the Fe-deficiency responses in mice. It is not clear yet why mammals utilize two IRPs in Fe regulation and whether the IRPs have distinct role(s) in Fe homeostasis.

It was recently discovered that a Fe-responsive post-transcriptional regulatory process controls metabolic reprogramming in yeast. Under Fe deficiency, yeast Cth2 protein specifically downregulates mRNAs encoding proteins that play roles in many Fe-dependent physiological processes. mRNA turnover requires the binding of Cth2 to specific AU-rich elements in the 3' UTRs of genes targeted for degradation. Identification of Cth2 target genes suggested that Cth2-mediated acceleration of mRNA decay could be an important mechanism for coordinated remodeling of cellular metabolism during Fe deficiency.

4.5.H3 Post-translational Regulation. Cu-mediated regulation of trafficking and turnover of Cu transporters have been characterized (Fig. 4.16). In low Cu medium, the human MNK (ATP7a) and WND (ATP7b) are localized in the trans-Golgi network, where they transport Cu for its incorporation into secretory proteins. When Cu levels are elevated, MNK is mobilized to the plasma membrane in a reversible manner. The biological significance of this trafficking event is that MNK may participate in Cu extrusion at the plasma membrane to export Cu from intestinal cells into blood for circulation and to protect cells from Cu toxicity in other organs. Excess Cu mobilizes WND from the trans-Golgi network to a cytoplasmic vesicle-like compartment in the liver. This appears to be an important mechanism for excretion of excess Cu into bile to maintain systemic Cu homeostasis. While the regulation of Cu excretion is relatively well characterized in mammals, Cu-induced regulation of Cu absorption has been reported only recently. Elevated extracellular Cu triggers the endocytosis as well as degradation of human Cu transporter Ctr1. Further studies will define the physiological significance of the modes of Ctr1 regulation in Cu metabolism.

Several lines of evidence have demonstrated that hepcidin is a master regulator of systemic Fe homeostasis (Fig. 4.17C). Systemic Fe status, inflammation, and hypoxia regulate hepcidin gene expression. Hepcidin (84 amino acids) is secreted from the liver and is then cleaved to small peptides (20, 22, or 25 amino acids) that circulate in blood and are excreted in urine. Recent studies showed that hepcidin regulates cellular Fe efflux in the intestine and from macrophages and hepatocytes by binding to ferroportin and induces its internalization and degradation. Consequently, this post-translational regulation of ferroportin by hepcidin completes the Fe regulatory loop in mammals.

4.5.I Genetic Disorders in Metal Metabolism

Consistent with the essential roles of Cu and Fe and their complex metabolism, many of the proteins involved in Cu and Fe homeostasis have been linked to human

genetic disorders. X-linked Menkes disease and autosomal recessive Wilson disease are well-characterized genetic diseases of Cu deficiency and toxicity, respectively. Patients with Menkes disease die in the first year of life due to defects in the function of Cu-requiring enzymes. The onset of Wilson disease in humans is variable as is the severity of symptoms, which suggests environmental and/or genetic factors modulate progression of the disease.

Although the Ctr1-mediated Cu uptake system and intracellular Cu chaperones have been identified, no genetic disorders have been linked to defects in Cu uptake and cytoplasmic distribution. Recent studies on knockout mice lacking the genes encoding Ctr1, Cox17, or Atx1 demonstrate their critical role in embryonic development. Thus, it is possible that humans possessing nonfunctional Ctr1 may die during development in utero.

Hereditary hemochromatosis is the most common inherited disease among Caucasians. It is estimated that as many as one in eight individuals of northern European descent are carriers of a faulty allele. Hereditary hemochromatosis is characterized by Fe overload, resulting in cirrhosis of the liver, diabetes, and heart failure, presumably due to Fe toxicity in the organs. Regulation of Fe absorption in the intestine is defective in hereditary hemochromatosis patients. Four different types of hemochromatosis based on the mutated gene have been characterized: (1) Missense mutations in the HFE gene encoding an atypical major histocompatibility class I protein is linked to type 1 hemochromatosis. Although the function of HFE is not known, it forms a complex with transferrin receptor 1 and inhibits transferrin binding. This interaction between HFE and transferrin receptor 1 leads to reduction of cellular Fe uptake. (2) HFE2 gene mutation is linked to type 2 hemochromatosis. HFE2 may play a role in regulation of hepcidin expression. (3) Transferrin receptor 2 mutations that disrupt complex formation with HFE lead to type 3 hemochromatosis. (4) Heterozygosity for mutations in ferroportin leads to an autosomal dominant type 4 hemochromatosis. Interestingly, ferroportin forms a dimeric complex and the mutant forms interfere with plasma membrane trafficking of the wild-type monomer and/or hepcidin-induced degradation of mutant and normal monomer complex at the plasma membrane.

Many other relatively rare Fe-related genetic diseases have been identified in humans and/or animals. Ceruloplasmin is a Cu-containing ferroxidase in plasma that is required for Fe export and binding to transferrin. Aceruloplasminemia patients exhibit Fe accumulation in cells such as hepatocytes and macrophages. Lack of transferrin in atransferrinemia patients induces severe defects in mobilization of Fe from stores for its utilization (e.g., in hemoglobin synthesis). This leads to hypoxia-induced upregulation of Fe uptake from the intestine and excess Fe accumulation in Fe storage tissues. Defects in frataxin affect Fe-S cluster synthesis in mitochondria. Fe accumulation in mitochondria results in mitochondrial damage and progressive neurodegeneration.

4.5.J Perturbation of Metal Homeostasis and Degenerative Disorders

Aberrant Cu and/or Fe metabolism is implicated in multifactorial human disorders such as neurodegenerative diseases, cardiovascular diseases, and cancer. For example, Cu has been implicated in the etiology of Alzheimer's disease, which is characterized

by accumulation of β -amyloid ($A\beta$), a proteolytic product of the amyloid precursor protein (APP). APP binds Cu to reduce Cu(II) to the more reactive Cu(I). The binding of Cu to $A\beta$ elevates $A\beta$ aggregation. Cu is highly concentrated within senile plaques, the histopathologic hallmarks of Alzheimer's disease that are generated by the deposition of $A\beta$. Deposition of Fe in the brain is also a common feature of neurodegenerative diseases such as Alzheimer's disease and Parkinson's disease. Although it is not known whether Fe and Cu deposition is a cause or consequence of these diseases, Fe and Cu toxicity likely plays an important role in progression of neuronal damage observed in these diseases.

SELECTED REFERENCES

1. Pena, M.M., Lee, J., and Thiele, D.J. (1999). A delicate balance: homeostatic control of copper uptake and distribution. *J. Nutr.* 129:1251–1260.
2. O'Halloran, T.V., and Culotta, V.C. (2000). Metallochaperones, an intracellular shuttle service for metal ions. *J. Biol. Chem.* 275:25057–25060.
3. Schaefer, M., and Gitlin, J.D. (1999). Genetic disorders of membrane transport. IV. Wilson's disease and Menkes disease. *Am. J. Physiol.* 276(2 Pt 1):G311–314.
4. Hentze, M.W., Muckenthaler, M.U., and Andrews, N.C. (2004). Balancing acts: molecular control of mammalian iron metabolism. *Cell* 117:285–297.
5. Kaplan, J. (2002). Strategy and tactics in the evolution of iron acquisition. *Semin. Hematol.* 39:219–226.

4.6 REDOX ENZYMOLOGY

STEPHEN W. RAGSDALE

Department of Biological Chemistry, University of Michigan, Ann Arbor, Michigan

This section describes the study of redox enzymes, which either catalyze oxidation–reduction reactions or depend on oxidation or reduction for activity. It excludes electron transfer proteins, like cytochrome *c* or ferredoxin, that transfer electrons but do not catalyze reactions. Some oxidation–reduction reactions involve the net uptake or donation of electrons (e.g., carbon monoxide oxidation), while others involve an internal redox reaction, for example, the uptake/release of an electron that is returned during the overall reaction.

All redox enzymes require a redox-active prosthetic group, either a metallocofactor or an organic cofactor (FAD, NAD^+ , etc.). Since there are hundreds of redox enzymes, Table 4.1 cannot be exhaustive, but includes representative examples covering most of the known redox cofactors. A collection of reviews describing the mechanisms of a number of redox enzymes is available.

Redox enzymes catalyze reactions that are central to the metabolic processes that sustain life. Most metabolic pathways are either net redox processes (Table 4.2) or

TABLE 4.2. Examples of Redox Pathways

Photosynthesis (O ₂ evolution)	Methanogenesis
Respiration	Acetogenesis
Oxidation of fats, sugars, nucleic acids	Sulfate reduction
Fermentations (glycolysis, fatty acid oxidation, nucleotide oxidation)	Sulfur oxidation
	Metal oxidation and metal reduction

involve redox reactions that are regulated by the redox state of the cell by transcriptional, translational, and enzyme-level control mechanisms. For example, in *E. coli*, the global FNR (fumarate, nitrate reduction) transcriptional regulator of the cellular redox state regulates nearly 300 genes in over 180 operons, including nearly all metabolic pathways.

Redox reactions can involve the transfer of one or two electrons during the transformation. The overall enzymatic reaction can involve a few elementary steps like glutathione reductase with five component steps. Alternatively, the reaction may be much more complex as in the pyruvate:ferredoxin oxidoreductase reaction, which involves at least 15 steps, including binding of two substrates (pyruvate and CoA), the formation of a series of pyruvate-derived intermediates including a hydroxyethylthiamine pyrophosphate radical, multiple steps of electron transfer through the protein's three [4Fe–4S] clusters, and the release of two products (carbon dioxide and acetyl-CoA).

Many enzymes undergo internal redox reactions. For example, the isomerase class of adenosylcobalamin-dependent enzymes catalyze 1,2 rearrangement reactions (Fig. 4.18). In these reactions, (i) the cobalt–carbon bond of deoxyadenosylcobalamin is cleaved to form a cobalt- and a carbon-centered adenosyl radical that (ii) abstracts a hydrogen atom from the substrate to generate a substrate radical and deoxyadenosine. (iii) The substrate radical then rearranges to form a product radical that (iv) reabstracts the hydrogen atom from adenosine to yield the product and reform the deoxyadenosyl radical (v). Finally, the deoxyadenosyl radical recombines with cobalt to regenerate deoxyadenosylcobalamin (v).

A number of enzymes undergo *redox activation*. Some enzymes require *oxidative* activation. For example, some enzymes like protein kinase C γ require two specific cysteine residues to be in a disulfide state before catalysis can progress. Other enzymes require *reductive* activation. For example, a common theme among metal-containing hydroxylases, oxidases, and oxygenases is the requirement for reduction of a metal ion (Fe³⁺, Cu²⁺) to its low valent (Fe²⁺, Cu¹⁺) state before oxygen can bind. Accordingly, cobalamin-dependent methyltransferases, which do not catalyze overall redox reactions, can suffer inactivation to the Co²⁺ state under oxidative conditions. Thus, reductive activation of the cobalt ion is required before these enzymes can undergo methylation via a nucleophilic substitution reaction (Fig. 4.19). In some methyltransferases, a redox system directly reduces the Co²⁺ enzyme to the active Co¹⁺ state (Fig. 4.19A). In the case of methionine synthase (Fig. 4.19B), reduction is coupled

to activation and involves a reductive methylation in which *S*-adenosyl-L-methionine reacts with the Co^{2+} form of the cofactor to generate the methyl- Co^{3+} state of the enzyme.

The enzymes (Table 4.1) and pathways (Table 4.2) that catalyze redox processes or require redox activation are being studied at different levels. Many laboratories are attempting to develop an enhanced understanding of the details of the catalytic cycles of redox enzymes and experimental approaches for uncovering such information are described in Chapter 6. Some laboratories are attempting to understand how redox enzymes and pathways are regulated at the transcriptional, translational, and enzyme levels. Many of these regulatory systems themselves are subject to redox control as described in Section 4.3. Redox enzymology is a vast field that comprises enzymes with major significance to life's processes.

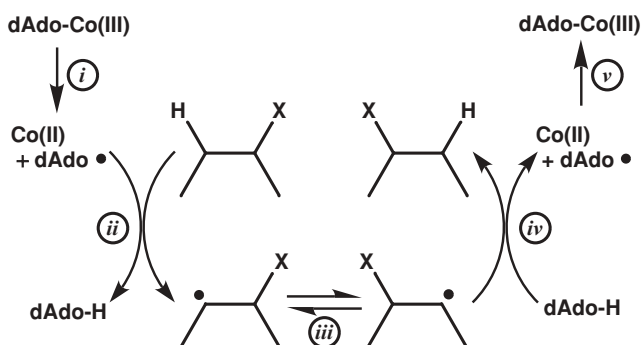


Figure 4.18. Internal redox reactions catalyzed by adenosylcobalamin-dependent isomerases.

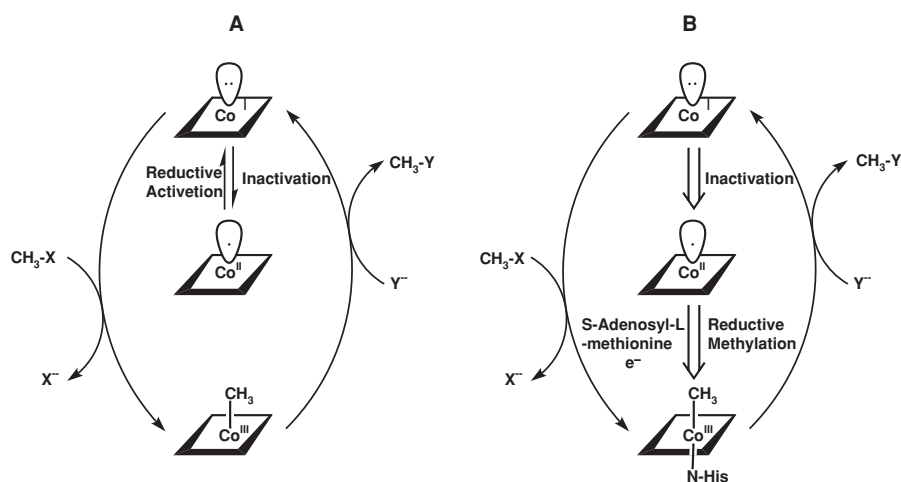


Figure 4.19. Reductive activation is required for cobalamin-dependent methyltransferases. X designates a variety of methyl donors like hydroxide, tetrahydrofolate, thiolates, and amines and Y specifies various methyl acceptors like homocysteine and coenzyme M.

SELECTED REFERENCES

1. Kang, Y., Weber, K.D., Qiu, Y., Kiley, P.J., and Blattner, F.R. (2005). Genome-wide expression analysis indicates that FNR of *Escherichia coli* K-12 regulates a large number of genes of unknown function. *J. Bacteriol.* 187:1135–1160.
2. Ragsdale, S.W. (2003). Pyruvate:ferredoxin oxidoreductase and its radical intermediate. *Chem. Rev.* 103:2333–2346.
3. Banerjee, R., and Ragsdale, S.W. (2003). The many faces of vitamin B₁₂: catalysis by cobalamin-dependent enzymes. *Annu. Rev. Biochem.* 72:209–247.

4.7 CIRCADIAN CLOCK AND HEME BIOSYNTHESIS

CHENG CHI LEE

Department of Biochemistry and Molecular Biology, University of Texas, Houston Medical School, Houston, Texas

In response to daily environmental cues, endogenous circadian oscillators control the behavior of many living organisms. The endogenous clock is characterized by a self-sustaining cycle of approximately 24 hours in duration that acts as a pacemaker for cellular and behavioral processes such as the sleep–wake rhythm. Fundamentally, the circadian clock regulates a range of physiological and biochemical processes necessary to maintain metabolic homeostasis. How the circadian clock accomplishes this task is of great biological interest.

4.7.A Cyclic Expression of Heme Binding Proteins

It has been observed that activities of many hemoproteins such as nitric oxide synthase, guanylyl cyclase, and catalase, prostaglandin synthase, cytochrome oxidases/P450 display a diurnal pattern. Gene expression studies suggest that the transcription of these genes is under circadian regulation *in vivo*. These hemoproteins are often the rate-limiting regulators of their respective biochemical cascades. Essential for their biochemical function is the prosthetic moiety heme. Heme is necessary for electron flow, as in cytochrome-mediated electron transport in mitochondria, and for sensing gaseous signals, as in guanylate cyclase. At the cellular level, these observations raise the question of how temporal production of these rate-limiting biological regulators and the heme prosthetic moiety are coordinated.

Heme biosynthesis starts and ends in the mitochondrion and requires multiple enzymatic steps. The first enzyme in this pathway is aminolevulinate synthase 1 or, unique to erythrocytes, aminolevulinate synthase 2, which catalyzes condensation of glycine and succinyl-CoA into aminolevulinic acid. Cells incubated with varying glycine and succinyl-CoA concentrations do not produce proportional levels of heme in contrast to those treated with aminolevulinic acid, indicating that aminolevulinic acid is the rate-limiting step. Free heme is known to negatively regulate aminolevulinic acid synthase 1 expression but the exact feedback mechanism remains

unclear. Gene expression analysis revealed that both aminolevulinate synthase 1 and aminolevulinate synthase 2 display a robust 24 hour temporal profile indicating that they are under circadian control *in vivo* (Fig. 4.20). This conclusion is consistent with the observation that the diurnal pattern of aminolevulinate synthase 1 gene expression is deregulated in circadian deficient genetically altered mice. Other studies also demonstrate circadian control of aminolevulinate synthase expression in fruit flies, indicating that the temporal regulation is evolutionarily very ancient. To illustrate the relationship between heme biosynthesis and circadian control, an understanding of the current circadian clock mechanism is necessary.

4.7.B Circadian Clock Mechanism

Our current knowledge of the mammalian clockwork has been aided in part by genetic studies with the fruit fly, *Drosophila melanogaster*. The fruit fly clock is based on a transcription/translation autoregulatory mechanism. Mammalian homologs to the *Drosophila* circadian regulators include the bHLH PAS transcription factors CLOCK and BMAL. The mammalian CLOCK has a paralog known as NPAS2. CLOCK or NPAS2 will heterodimerize with BMAL1 to form the core transcriptional complex whose activity is modulated by feedback regulators such as cryptochrome (mCRY1 and mCRY2) and Period (mPER1 and mPER2). Other modulators of the circadian mechanism include casein kinases (epsilon and delta) that regulate phosphorylation of circadian regulators that in turn control its stability and degradation. In addition, the orphan nuclear receptors Rev-Erb α and ROR α regulate transcription of *Bmal1* gene that in turn controls the availability of BMAL1 level. Mutations in genes encoding these regulators in the mouse affect, to varying degrees, the temporal expression of cellular functions and animal behavior such as sleep–wake rhythm. The loss of function mutations of *Bmal1* and *mPer2* severely impact the mouse circadian clock rhythm. One view is that mPER2 may be a rate-limiting modulator of the mammalian circadian clock mechanism. Mice carrying double mutations of either *mCry1/mCry2* or *mPer1/mPer2* display no circadian rhythm in sleep–wake behavior. While there are similarities in function between the circadian homologs in fruit fly and mouse, there are also significant differences in their respective roles in the clock mechanism. For example, it remains unclear whether the mouse *Timeless* homolog is a circadian regulator. In addition, multiple mammalian homologs of the respective fruit fly gene were observed. In fruit fly and zebrafish, cryptochromes serve as the circadian photosensor, but mouse cryptochromes have apparently lost this photoreception function. Instead, the circadian photoreception is regulated in part by melanopsin, a member of the opsin photosensor family. The *cryptochromes* are FAD binding proteins belonging to the plant blue light receptor family. They have peptide sequence homology to DNA photolyase but have no DNA repair function. That mCRY plays a negative modulating role on the core transcriptional complex activity is supported by key observations. First, expression of *mPer1* is elevated in genetically modified mice deficient in cryptochromes. Second, reporter assay studies demonstrate mCRYs are potent inhibitors of the BMAL1/CLOCK or BMAL1/NPAS2 circadian transcription complex activity. While early reporter assay studies suggested mPER2, like its fruit fly counterpart dPER, is a negative regulator, other studies showed that mPER2 did not significantly

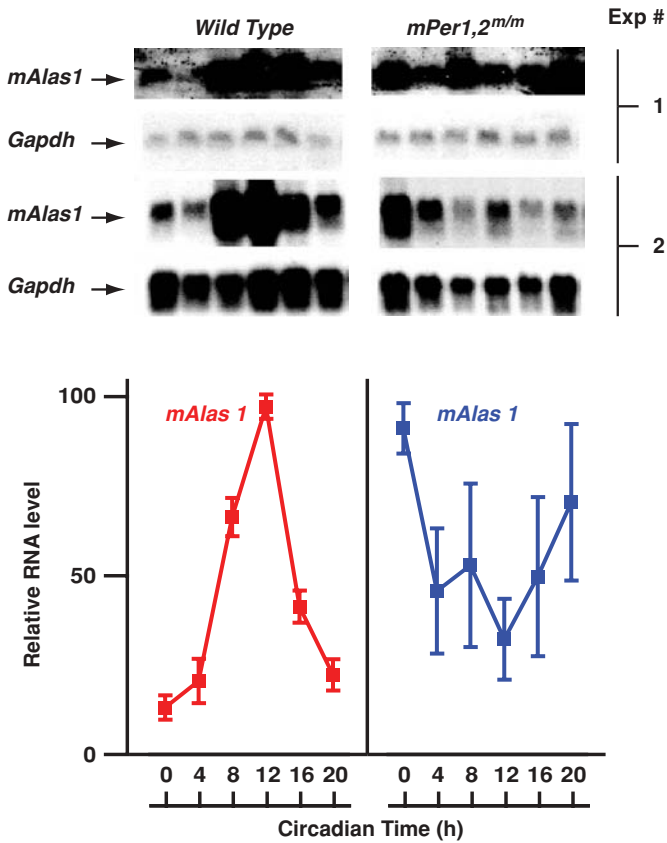


Figure 4.20. Circadian expression of mouse aminolevulinic acid synthase 1 (*mAlas*) gene during a daily cycle. The analysis of gene expression was carried out by Northern blotting of liver mRNA obtained from mouse livers at the indicated time points with radiolabeled cDNA probes. A duplicated set of experiments is shown to illustrate the lack of temporal regulation of *Alas1* expression in circadian deficient animals carrying a mutation of *mPer1* and *mPer2* genes. Levels of glyceraldehyde 3-phosphate dehydrogenase (*Gapdh*) mRNA were used as an internal control. The lower panel shows the quantification of the band intensity of the Northern blot with respect to the mRNA of *Gapdh*.

inhibit BMAL1/CLOCK transcription complex activity. Critically, the loss of mPER2 function in mice dampened expression of *Bmal1*, *mPer1*, or *mCry1*, implicating it as a positive regulator *in vivo*. Thus, the molecular target and function of mPER2 was an enigma.

4.7.C PAS Is a Heme Binding Domain

Important insight into the role of heme in circadian clock function came from analysis of the PAS domain structure shared among circadian regulators including CLOCK,

BMAL1, NPAS2, mPER1, and mPER2. In mammals, the PAS domains are two conserved 51 amino acid repeats known as PAS-A and PAS-B. The PAS domain has three-dimensional folds that are highly conserved from bacteria to mammals. The PAS domain of proteins such as A_xPDEA1, DOS, FIX, and NPAS2 is the heme binding motif. PAS proteins such as FIXL bind one heme molecule whereas NPAS2 binds two heme molecules, one each to the PAS-A and PAS-B. *In vitro* studies with reconstituted peptides have demonstrated that NPAS2/BMAL1 does not bind DNA in the presence of carbon monoxide and heme. However, carbon monoxide or heme alone does not affect the ability of NPAS2/BMAL1 to bind DNA. Thus, these *in vitro* studies demonstrate that heme could control BMAL1/NPAS2 transcription complex activity by DNA binding inhibition in response to carbon monoxide.

The effects of free heme on the expression of key clock regulators further illustrate its importance in the circadian clock mechanism *in vivo*. Heme injected into mice enhanced *mPer1* but dampened *mPer2* expression. In contrast, expression of *Bmal1*, *Npas2*, *mCry1*, and *Clock* were apparently unaffected *in vivo*. Since the BMAL1/NPAS2 transcription complex regulates expression of *mPer1* and *mPer2*, the findings that heme modulates the circadian transcriptional activity is consistent with the *in vitro* observations.

4.7.D Expression of *Npas2* Is Controlled by mPER2

A finding that revealed key insight into the circadian mechanism was that the loss of mPER2 function resulted in the loss of *Npas2* but not *Clock* expression *in vivo*. The observation suggests that the molecular target of mPER2 is NPAS2 rather than CLOCK. Reporter assay studies demonstrate mPER2 positively activates BMAL1/NPAS2 transcription complex activity but not that of BMAL1/CLOCK. The finding would also be consistent with observations that implicate mPER2 as a positive regulator of the clock transcription mechanism *in vivo*. Together, these findings indicate that mPER2 is a major regulator of NPAS2 and not CLOCK *in vivo*. Recent studies have revealed that mice carrying a loss of function mutation of CLOCK displayed circadian behavior similar to wild-type animals. It raises the possibility that the phenotype of the original *Clock* mutant mice was a gain of function. Recent mouse genetic studies showed that NPAS2 is a redundant homolog of CLOCK in the mammalian circadian mechanism.

4.7.E NPAS2 Regulates Expression of Aminolevulinate Synthase 1

Given that aminolevulinate synthase 1 expression is under circadian control, it raises the question whether NPAS2 is a key regulator. Mice deficient in NPAS2 function display reduced expression of aminolevulinate synthase 1, confirming that NPAS2 is a major transcriptional regulator of its expression. Therefore, BMAL1/NPAS2 transcription complex control of aminolevulinate synthase 1 expression closes the loop on a reciprocal regulation between circadian clock regulation of heme biosynthesis and heme control of circadian clock complex regulated transcription. A model (Fig. 4.21) illustrates the expression of aminolevulinate synthase 1 is dependent on

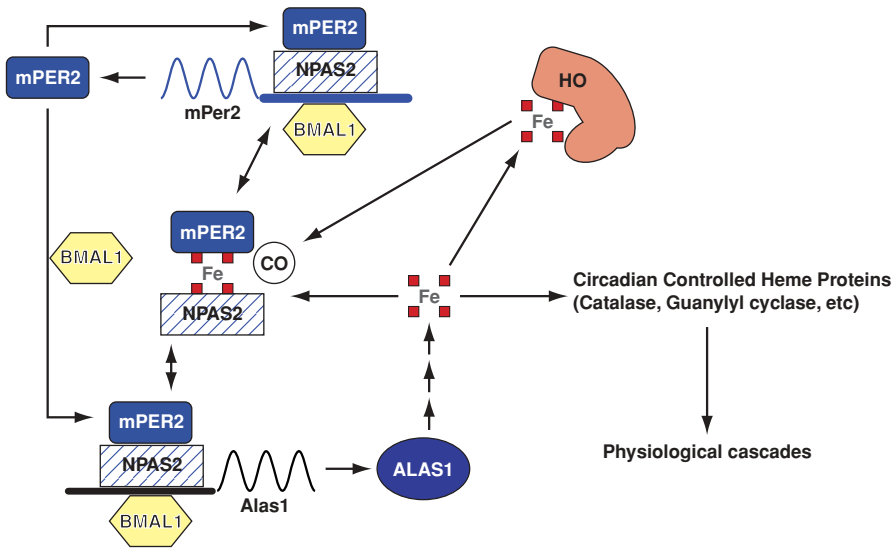


Figure 4.21. A model for reciprocal regulation between the circadian clock and heme biosynthesis: mammalian Period protein 2 (mPER2), neuronal PAS domain protein 2 (NPAS2), brain-muscle-ARNT-like protein 1 (BMAL1), heme-oxygenase (HO), aminolevulinatase synthase 1 (ALAS1), carbon monoxide (CO), and heme (four red squares with Fe).

BMAL1/NPAS2 transcription activity under positive regulation by the mPER2 protein. Via biosynthesis, the level of heme is controlled by the level of aminolevulinatase synthase 1 expressed. Heme then binds to NPAS2 and mPER2 proteins via the PAS domains to activate their function. In addition, heme biosynthesis is coordinated with the expression of circadian controlled genes that encode hemoproteins such as nitric oxide synthase, catalase, guanylyl cyclase, and others that are key regulators of various biochemical and physiological cascades. Increased levels of heme eventually induce its own degradation via heme oxygenase enzymes whose gene expression is induced by free heme. Degradation of heme by heme oxygenases results in the formation of carbon monoxide, biliverdin, and free iron. In the presence of carbon monoxide, heme bound to the BMAL1/NPAS2 transcription complex stops DNA binding and, by extension, gene transcription. The decline in transcription complex activity is further amplified by a decreased level of mPER2. The consequence is lower aminolevulinatase synthase 1 expression leading to a decreased heme level. The released transcription complex components are then presumably targets for degradation. The decline in heme level eventually reaches a trough that in turn allows a basal level BMAL1/NPAS2 transcription complex to bind DNA, thus restarting the feedback cycle. Additional evidence of the heme role in regulating the circadian mechanism has come from independent studies. The transcription of *Bmal1* gene is regulated by the orphan nuclear receptors Rev-Erb α . Mutation of Rev-Erb α in mouse or its *Drosophila* homolog E75 affects circadian behavior. Recent studies

demonstrate that E75 is a heme binding protein. Thus, the role of heme in the circadian mechanism is likely to be broad. In conclusion, the reciprocal regulation between heme biosynthesis and the circadian clock mechanism allows output signals from the cellular/subcellular environment to provide feedback regulation on the core clock mechanism.

SELECTED REFERENCES

1. Bunger, M.K., Wilsbacher, L.D., Moran, S.M., Clendenin, C., Radcliffe, L.A., Hogenesch, J.B., Simon, M.C., Takahashi, J.S., and Bradfield, C.A. (2000). Mop3 is an essential component of the master circadian pacemaker in mammals. *Cell* 103:1009–1017.
2. Gilles-Gonzalez, M.A., and Gonzalez, G. (2004). Signal transduction by heme-containing PAS-domain proteins. *J. Appl. Physiol.* 96:774–783.
3. Kaasik, K., and Lee, C.C. (2004). Reciprocal regulation of haem biosynthesis and the circadian clock in mammals. *Nature* 430:467–471.
4. Kume, K., Zylka, M.J., Sriram, S., Shearman, L.P., Weaver, D.R., Jin, X., Maywood, E.S., Hastings, M.H., and Reppert, S.M. (1999). mCRY1 and mCRY2 are essential components of the negative limb of the circadian clock feedback loop. *Cell* 98:193–205.
5. Zheng, B., Albrech, U., Kaasik, K., Sage, M., Lu, W., Vaishnav, S., Li, Q., Sun, Z.S., Eichele, G., Bradley, A., and Lee, C.C. (2001). Non-redundant roles of the *mPer1* and *mPer2* genes in the mammalian circadian clock. *Cell* 105:683–694.

Pathological Processes Related to Redox

- 5.1. Protein Modification
 - 5.1.A. Protein Oxidation and Aging
 - 5.1.B. Mechanisms of Protein Oxidation
 - 5.1.C. Peptide Bond Cleavage
 - 5.1.D. Oxidation of Amino Acid Residue Side Chains
 - 5.1.E. Beta Scission of Amino Acid Side Chains
 - 5.1.F. Generation of Protein Carbonyl Derivatives
 - 5.1.G. Formation of Protein Cross-Linked Derivatives
 - 5.1.H. Role of Protein Oxidation in Aging
- 5.2. Oxidative Stress in the Eye: Age-Related Cataract and Retinal Degeneration
 - 5.2.A. Oxidative Stress and Cataract
 - 5.2.B. Oxidative Stress and Retinal Pathology
- 5.3. Redox Mechanisms in Cardiovascular Disease: Chronic Heart Failure
 - 5.3.A. Excitation–Contraction Coupling in Cardiac Myocytes
 - 5.3.B. Role of Oxidative Stress in Chronic Heart Failure
 - 5.3.C. Redox Modulation of Ca^{2+} Handling Proteins
 - 5.3.D. Hypertrophy and Cell Death
 - 5.3.E. Extracellular Matrix Remodeling
- 5.4. Role of Reactive Oxygen Species in Carcinogenesis
 - 5.4.A. ROS Act as Growth Signaling Messengers
 - 5.4.B. Phosphatases are Prime Targets for ROS During Growth Stimulation
 - 5.4.C. Uncontrolled Production of ROS is Carcinogenic
 - 5.4.D. ROS Can Induce Carcinogenic DNA and Protein Adducts
 - 5.4.E. ROS Can Affect DNA Methylation and Gene Expression
 - 5.4.F. Mitochondrial DNA Mutations Are Induced by ROS
 - 5.4.G. Clinical Trials on Antioxidant Supplementation Against Cancer
- 5.5. Oxidative Stress and the Host–Pathogen Interaction
 - 5.5.A. Neutrophils and the Innate Immune Response
 - 5.5.B. Bacterial Targets of Oxidative Damage

5.5.C. Regulating the Oxidative Stress Response

5.5.D. The Oxidative Stress Response

5.5.E. Evasion of the Innate Immune Response

5.1 PROTEIN MODIFICATION

EARL R. STADTMAN

Laboratory of Biochemistry, National Heart, Lung, and Blood Institute, National Institutes of Health, Bethesda, Maryland

5.1.A Protein Oxidation and Aging

Organisms are continually exposed to a number of ROS and reactive nitrogen species (RNS) that react with intracellular lipids, proteins, and nucleic acids, leading to loss of biological function. As illustrated in Fig. 5.1, various forms of ROS/RNS are present as pollutants in the atmosphere, are formed during exposure to irradiation, or occur as by-products of normal metabolic processes. The reactive species formed by these processes are shown in Table 5.1. Whereas organisms contain numerous antioxidants (listed in Table 5.2) that can convert ROS/RNS to inactive derivatives, their antioxidant efficiency is dependent on their intracellular concentrations and on the rates of ROS/RNS generation, which depends on the magnitude of the oxidative stress. In addition, as shown in Fig. 5.1, the oxidation of proteins targets them for degradation by the 20S proteasome and several other proteases.

5.1.B Mechanisms of Protein Oxidation

Basic mechanisms involved in the oxidation of proteins were elucidated by the pioneering studies of Garrison, Swallow, Schuessler, and Schilling, who exposed free amino acids, peptides, and proteins to ionizing radiation under conditions where $\cdot\text{OH}$, $\text{O}_2^{\cdot-}$, or a mixture of these were formed (Fig. 5.2, reaction *a*). The studies demonstrated that reaction with $\cdot\text{OH}$ leads to abstraction of a hydrogen atom from the protein polypeptide backbone to form a carbon-centered radical (reaction *c*), which under aerobic conditions reacts with free oxygen to form a protein peroxy radical derivative (reaction *d*). The protein peroxy radical is readily converted to the protein peroxide by reaction with the protonated form ($\text{HO}_2^{\cdot-}$) of superoxide anion (reaction *e*) or by abstraction of a hydrogen atom from another molecule (RH) to form another radical (R^{\cdot}) derivative (reaction *g*). Upon reaction with another molecule of $\text{HO}_2^{\cdot-}$, the protein peroxide is converted to its alkoxy radical derivative (reaction *h*), which can react with another HO_2^{\cdot} molecule to form a stable protein hydroxyl derivative and oxygen (reaction *j*). Alternatively, the alkoxy radical may undergo peptide bond cleavage by diamide or α -amidation pathways (Eq. (5.1)). Whereas ionizing radiation was used to generate the $\cdot\text{OH}$ used in these early studies, it was subsequently shown that $\cdot\text{OH}$ is formed by metal ion (Fe^{2+} or Cu^{1+}) cleavage of H_2O_2 (Eq. (5.1)).



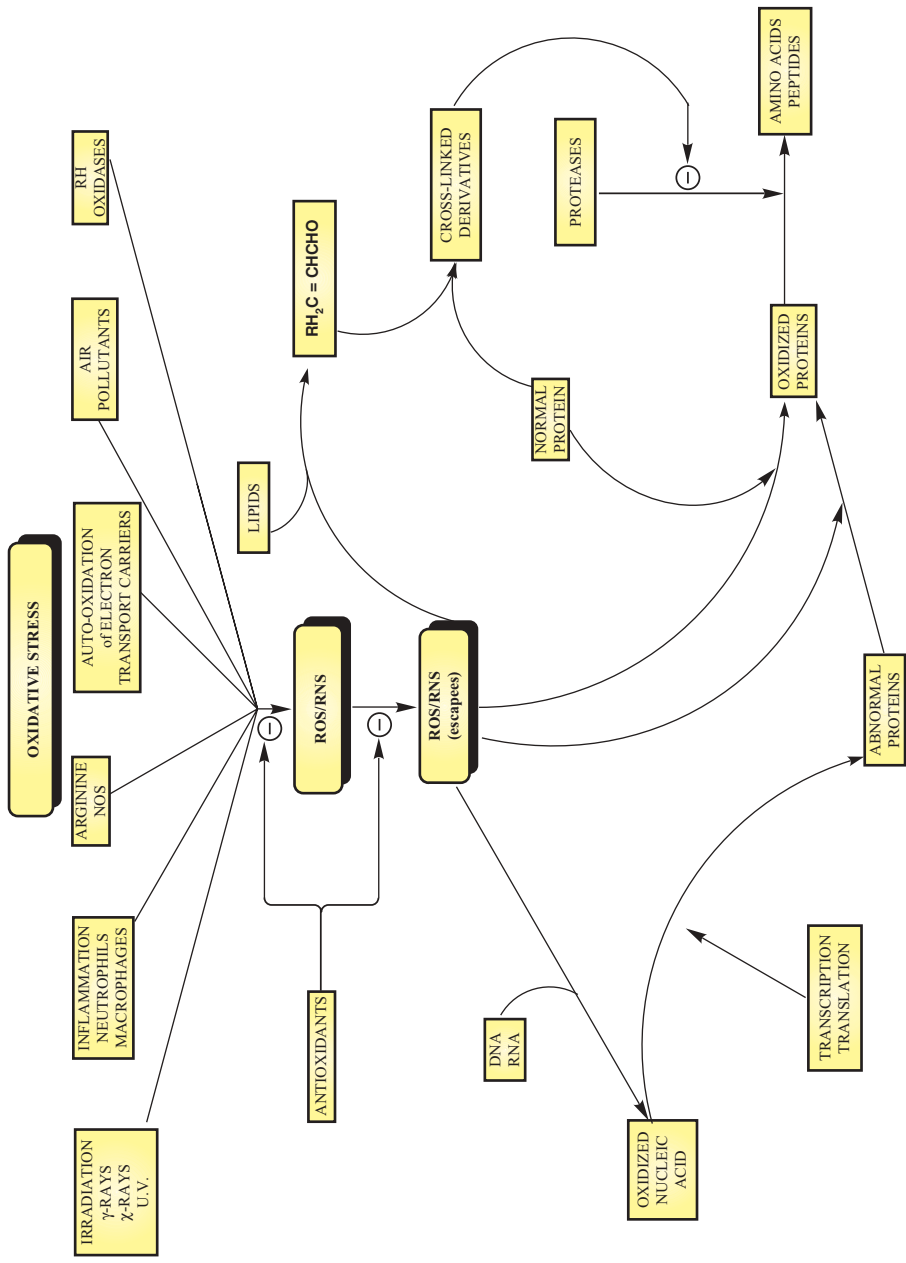


Figure 5.1. Role of oxidative stress-induced oxidation of proteins, lipids, and nucleic acids on protein degradation.

TABLE 5.1. Origin of Reactive Oxygen Species

Source	ROS
Atmosphere pollution	CO, Ozone, NO ₂ , N ₂ O ₂
By-products of electron transport	O ₂ ^{·-}
Irradiation (X-, γ-, UV)	O ₂ ^{·-} , ·OH, ¹ O ₂
Metal-catalyzed oxidation	·OH, H ₂ O ₂ , ferryl ion
Inflammation (neutrophils, macrophages)	OCl ⁻ , H ₂ O ₂ , O ₂ ^{·-} , NO, ONOO ⁻
Oxidases	H ₂ O ₂
Arginine metabolism	NO

TABLE 5.2. Antioxidants

Proteins	Metabolites Vitamins
Superoxide dismutase	—
Catalase	Vitamins A, E, C
Glutathione peroxidase	Bilirubin
Glutathione transferase	GSH/GSSG
Glutathione reductase	Ubiquinol
Methionine sulfoxide reductase	NADP/NADPH
Ceruloplasmin	Lipoic acid
Ferritin	Mn ²⁺ , Mg ²⁺ , Zn ²⁺
Thioredoxin	—
Thioredoxin reductase	—
Peroxidoxins	—

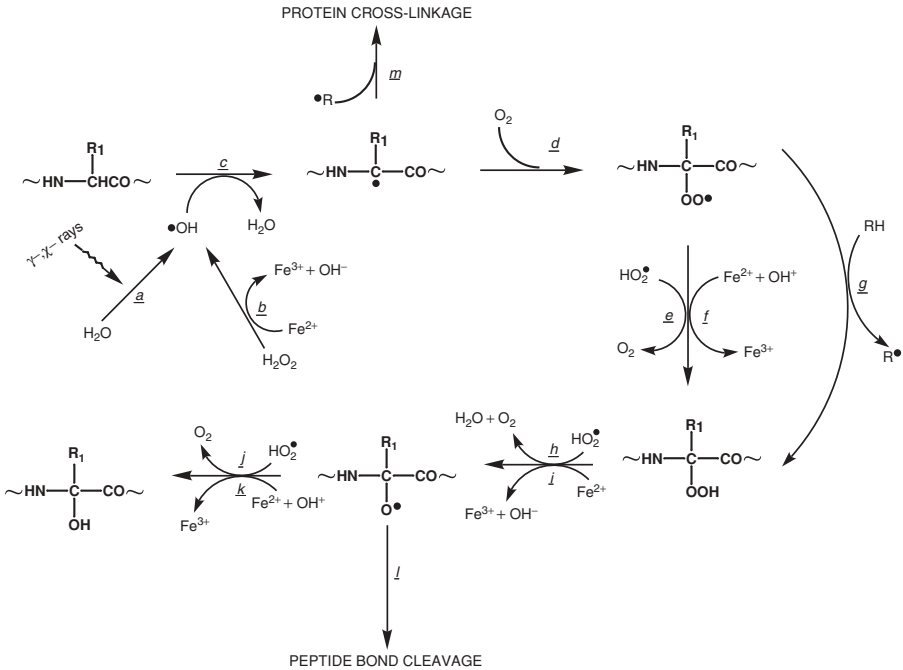


Figure 5.2. Mechanisms of protein oxidation.

Thus, Fe(II)- or Cu(I)-mediated cleavage of H_2O_2 provides another, more physiologically relevant, pathway for the generation of $\cdot\text{OH}$ involved in the initiation of protein oxidation (Fig. 5.2, reaction *b*). Significantly, Fe(II) can also replace $\text{HO}_2^{\cdot-}$ in other reactions as illustrated by reactions *f*, *i*, and *k* in Fig. 5.2.

5.1.C Peptide Bond Cleavage

As mentioned previously, alkoxy radical derivatives of proteins are susceptible to peptide bond cleavage by either of two pathways. As illustrated in Fig. 5.3A, cleavage

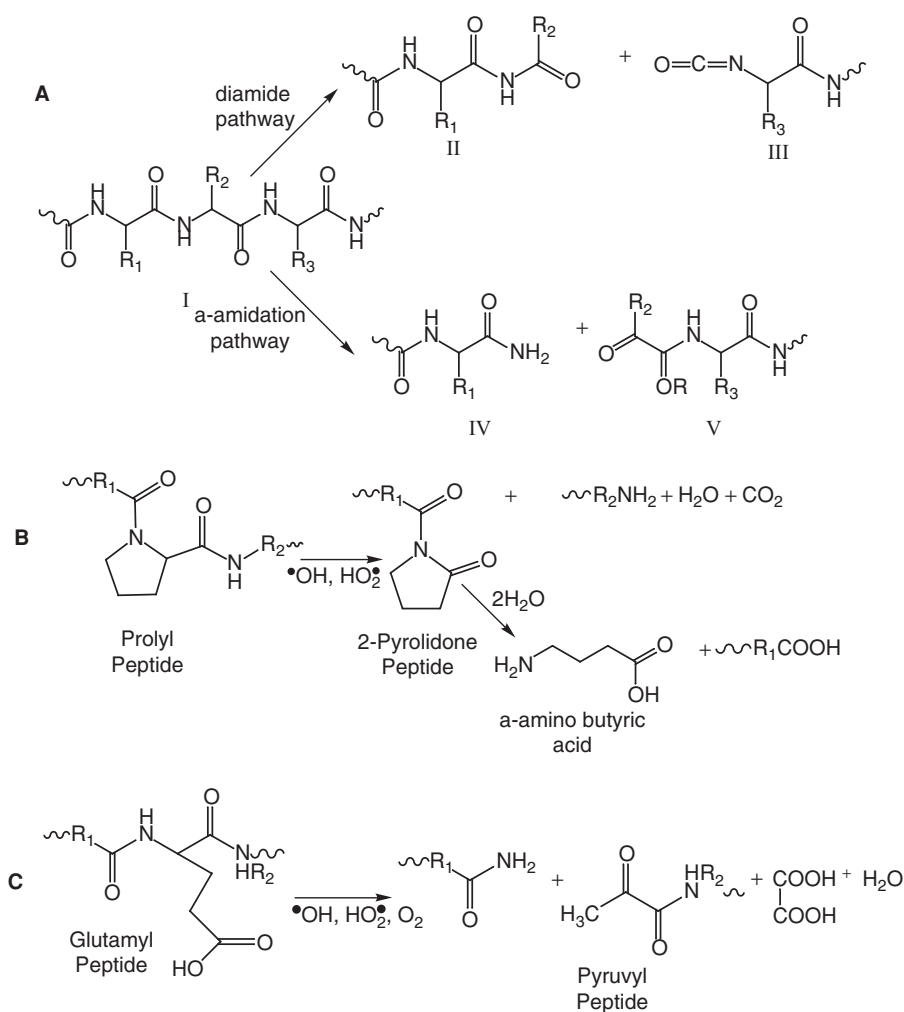


Figure 5.3. Oxidative cleavage of the polypeptide chain.

by either pathway leads to formation of two peptides. Upon cleavage by the diamide pathway, the peptide derived from the N-terminal portion of the protein contains a diamide derivative at its C-terminal end and the peptide derived from the C-terminal portion of the protein contains an isocyanate moiety at its N-terminal end. Upon cleavage by the α -amidation pathway, the peptide derived from the N-terminal portion of the protein contains an amide group at the C-terminal end and the peptide derived from the C-terminal portion contains an α -ketoacyl group at its N-terminal end. Peptide bond cleavage occurs also as a consequence of hydroxy radical attack on prolyl and glutamyl residues of proteins (Fig. 5.3B, C).

5.1.D Oxidation of Amino Acid Residue Side Chains

Side chains of all amino acid residues of proteins are susceptible to oxidation by hydroxyl radicals. The aromatic amino acids are particularly sensitive to oxidation. As shown in Table 5.3, oxidation of phenylalanine residues yields 2-, 3-, and 4-monohydroxy derivatives and the 2,3-dihydroxy derivative. Hydroxy radical-mediated oxidation of tyrosine residues leads to formation of dityrosine, (2,2'-biphenyl derivatives) DOPA, whereas reaction with RNS leads to 3-nitrotyrosine and reaction with HOCl leads to the generation of 3-chlorotyrosine and 3,5-dichlorotyrosine derivatives. Oxidation of tryptophan residues leads to *N*-formylkynurenine, 3-hydroxykynurenine, and either 2-, 4-, 5-, 6-, or 7-hydroxytryptophan. Histidine residues are major targets of oxidation by metal-catalyzed systems that can convert histidine to 2-oxo-histidine, 4-hydroxyglutamate,

TABLE 5.3. Amino Acid Residue Modification

Amino Acid Residue	Products Formed ^a
Arginine	Glutamic semialdehyde
Cysteine	Disulfides: Cys-S-S-Cys, Cys-S-S-R
Glutamate	4-Hydroxyglutamate, pyruvate, α -ketoglutarate
Histidine	2-Oxo-histidine
Leucine	3- and 4-Hydroxyleucine
Lysine	2-Aminoadipic-semialdehyde, 3-, 4-, and 5-hydroxyllysine
Methionine	Methionine sulfoxide, methionine sulfone
Phenylalanine	2-, 3-, and 4-Hydroxyphenylalanine
Proline	Glutamic semialdehyde, pyroglutamic acid, 2-pyrrolidone 4-hydroxyproline
Threonine	2-Amino-3-ketobutyric acid
Tryptophan	<i>N</i> -Formyl-kynurenine, kynurenine, 2-, 4-, 5-, 6-, and 7-hydroxytryptophan
Tyrosine	3- and 4-Dihydroxyphenylalanine (DOPA), Tyr-Tyr cross-linked proteins, 3-nitrotyrosine, 3,5-dichlorotyrosine
Valine	3- and 4-hydroxyvaline

^aFor references see Headlam and Davies (2002) (Ref. 2).

asparagines, or aspartate derivatives. As shown in Table 5.3, proline and arginine residues are oxidized to glutamic semialdehyde derivatives. In addition, proline residues are also oxidized to pyroglutamic acid, 2-pyrrolidone, and 4- or 5-hydroxy derivatives. Lysine residues are oxidized to α -aminoadipicsemialdehyde and *N* γ -(carboxymethyl)lysine derivatives. Methionine residues are readily oxidized to methionine sulfoxide derivatives by many different ROS and RNS. But, in contrast to oxidation of other amino acid residues (except cysteine residues), the oxidation of methionine can be repaired by the action of reductases that catalyze the thioredoxin-dependent reduction of methionine sulfoxide residues back to methionine residues (Chapter 3). Significantly, the cyclic oxidation and reduction of methionine residues constitutes an important antioxidant mechanism. As shown in Table 5.3, oxidation of cysteine residues leads to a number of derivatives, including disulfides (RSSR), sulfenic acid (RSOH), sulfinic acid (RSOOH), and sulfonic acid (RSOOH) derivatives. All of these derivatives, except sulfonic acid, can be reduced back to cysteine residues.

5.1.E Beta Scission of Amino Acid Side Chains

In addition to preferential attack of α -hydrogen atoms at the peptide bond backbone of proteins, amino acid residues are also subject to β -oxidation by hydroxyl radicals generated during irradiation. Such oxidations lead to cleavage of the side chains and their conversion to low molecular weight carbonyl derivatives. For example, β -oxidation of alanine, valine, leucine, and aspartic acid side chains leads to the formation of formaldehyde, acetone, isobutyraldehyde, and glyoxylic acid, respectively, and in each case, cleavage of the side chain leads to formation of a carbon-centered radical derivative of the polypeptide (NH'CO) identical to that obtained by hydroxyl radical attack of a glycine residue.

5.1.F Generation of Protein Carbonyl Derivatives

Carbonyl derivatives of proteins are generated by many different mechanisms, illustrated in Fig. 5.4. Thus, carbonyl derivatives are formed by metal-catalyzed oxidation of arginine, proline, and lysine residues to aldehyde derivatives (Fig. 5.4, reactions *a,b,c*). Metal-catalyzed oxidation of threonine residues leads to formation of 2-amino-3-ketobutyric acid derivatives (reaction *d*). Cleavage of alkoxy radicals by the α -amidation pathway leads to formation of a peptide that is N-acylated by a pyruvyl group (reaction *e*). Oxidation of glutamyl residues of proteins leads to cleavage of the peptide bond and generation of a peptide in which the N-terminal residue is alkylated by a pyruvyl group (reaction *f*). Reaction of the lysyl amino group of a protein with just one of the two aldehyde groups of malondialdehyde leads to formation of an aldehyde derivative (reaction *g*). Aldehyde derivatives are also formed by the interaction of cysteine, lysine, and histidine residues with α - β unsaturated aldehydes formed during lipid peroxidation (reaction *h*). In addition, products of glycation reactions lead to formation of intermediates containing a carbonyl

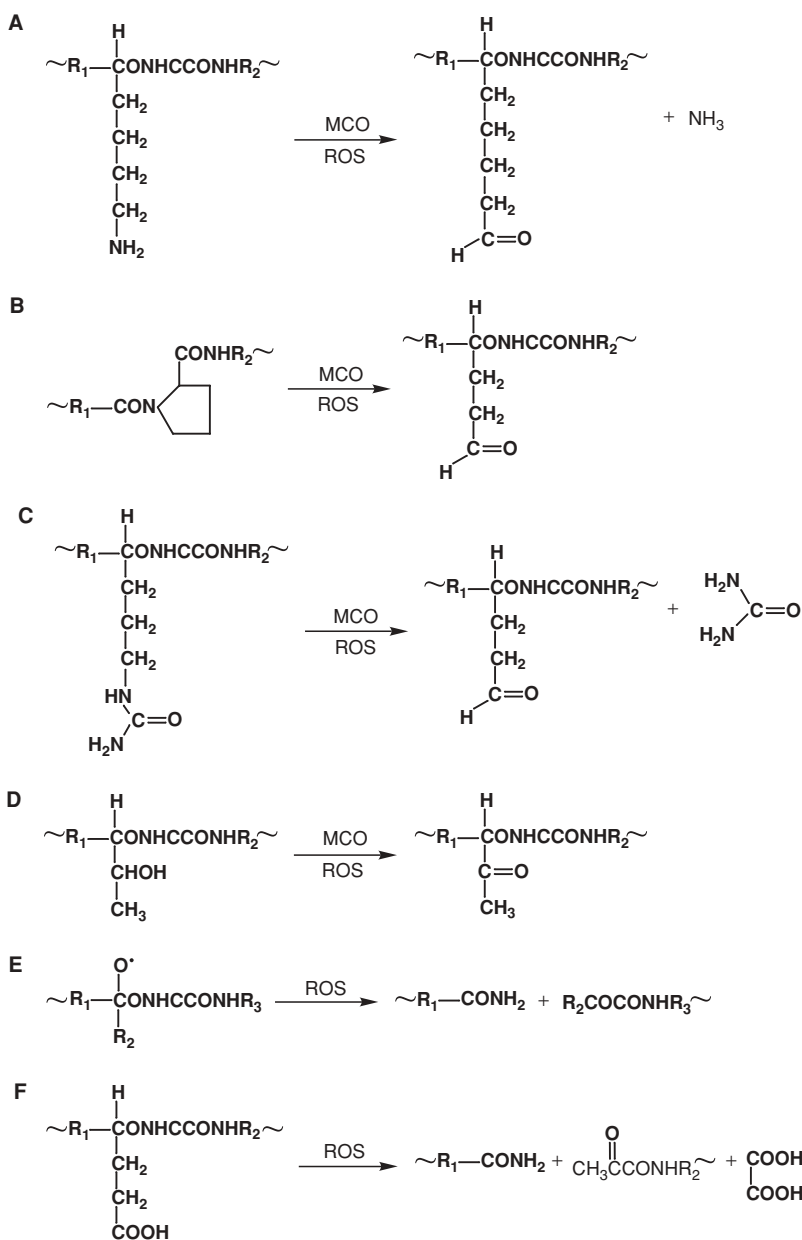


Figure 5.4. Generation of protein carbonyl derivatives. (a) Oxidation of lysyl residues to aldehyde derivatives (metal-catalyzed oxidation is abbreviated as MCO). (b) Oxidation of prolyl residues to aldehyde derivatives. (c) Oxidation of arginyl residues to aldehyde derivatives. (d) Oxidation of threonyl residues to keto derivatives. (e) Cleavage of protein alkoxyl radicals by the α -amidation pathway. (f) Peptide bond cleavage associated with oxidation of glutamyl residues to pyruvyl peptide derivatives. (g) Reaction of malondialdehyde with lysyl amino groups. (h) Michael addition reactions of L-lysine, histidine, and cysteine residues with 4-hydroxy-2-nonenol and other α - β -unsaturated aldehydes formed during oxidation of polyunsaturated fatty acids. (i) Glycation.

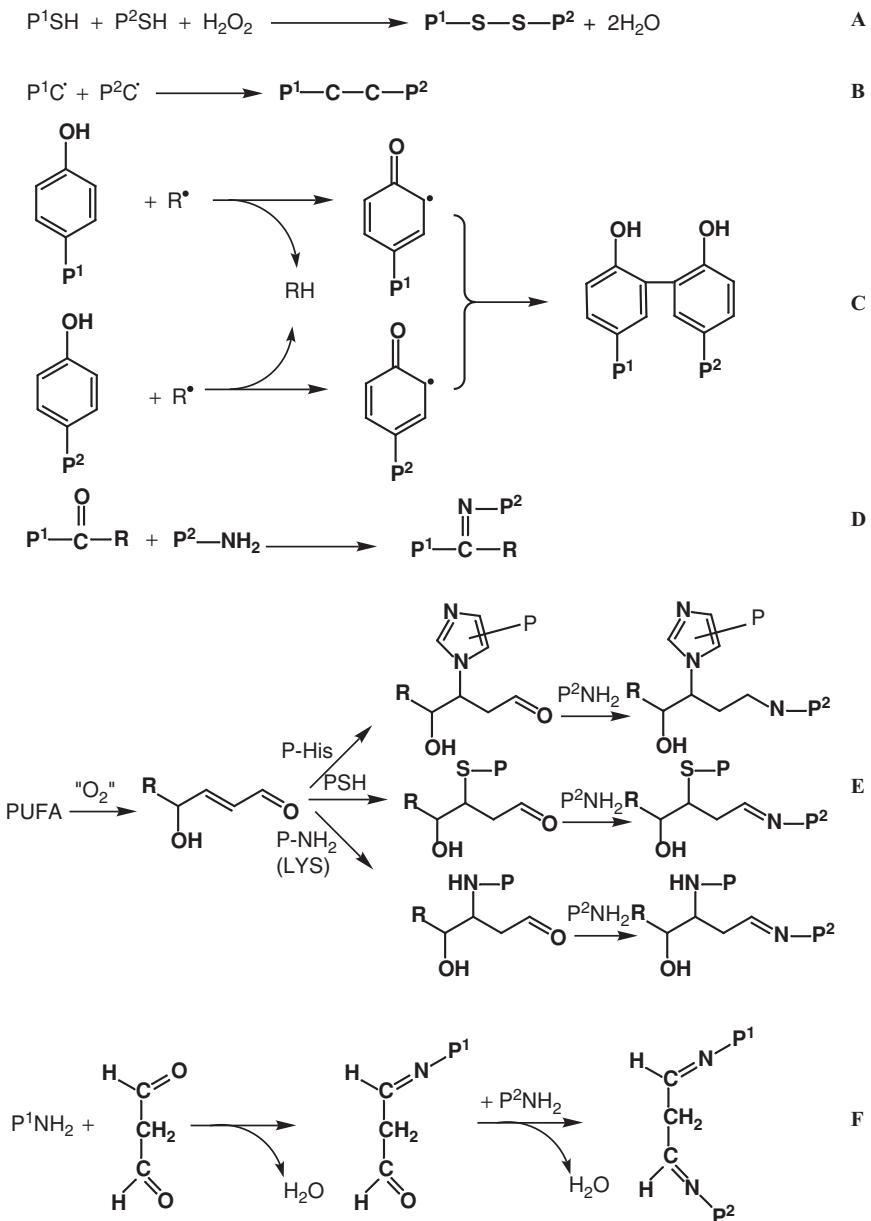


Figure 5.5. Protein oxidation-dependent formation of protein-protein cross-linkages.

5.1.G Formation of Protein Cross-Linked Derivatives

Oxidation of proteins can lead to the generation of inter- or intra- protein–protein cross-linked derivatives by any one of several different mechanisms as illustrated in Fig. 5.5. These include (a) oxidation of cysteine sulfhydryl groups to disulfide derivatives; (b) reaction of two different carbon-centered radicals (see also Fig. 5.2, reaction *m*); (c) bridging of two different tyrosine residues following their oxidation to carbon-centered radicals; (d) reaction of the free amino group of a protein lysine residue with the protein carbonyl group of an oxidized protein to form a Schiff-base adduct; (e) reaction of lysine amino groups with aldehydes obtained by Michael addition of lysine, histidine, or cysteine residues with 4-hydroxy-unsaturated aldehydes formed during oxidation of polyunsaturated fatty acids; or (f) reaction of two different lysine amino groups with aldehyde groups of the fatty acid oxidation product malondialdehyde to form Schiff-base derivatives.

5.1.H Role of Protein Oxidation in Aging

The possibility that protein oxidation is implicated in the aging process is suggested by observations that the intracellular levels of oxidized proteins increase with age and in some age-related diseases, and also because conditions that lead to an increase in the life span of organisms also lead to a decrease in the accumulation of oxidatively damaged protein molecules and vice versa. The age-related accumulation of oxidized proteins reflects the balance between a multiplicity of factors that govern: (1) the levels of ROS and RNS formation (Fig. 5.1), (2) the levels and activities of numerous antioxidant systems (Table 5.2), and (3) the concentrations and activities of proteases that exhibit a preference for the degradation of oxidized proteins. Although moderate oxidation of proteins makes them susceptible to proteolytic degradation, excessive oxidation increases the tendency of proteins to form aggregates that are not only resistant to proteolysis but can inhibit the ability of the proteases to degrade other oxidatively modified proteins. All of these factors may vary from one individual to another due to genetic differences, and also as to the kind and magnitude of oxidative stress they are exposed to.

In summary, oxidation of proteins by ROS leads to (1) peptide bond cleavage, (2) oxidative modification of amino acid residues, (3) β -scission of amino acid side chains, (4) generation of protein–protein cross-linkages, and (5) conversion of some amino acid residues to carbonyl derivatives. These oxidative modifications render proteins susceptible to proteolytic degradation by the 20S proteasome and other proteases. Accumulation of oxidized proteins is associated with aging in animals and a number of age-related diseases.

SELECTED REFERENCES

1. Garrison, W.M. (1987). Reaction mechanisms in the radiolysis of peptides, polypeptides, and proteins. *Chem. Rev.* 87:381–398.

2. Headlam, H.A., and Davies M.J. (2002). Beta-scission of side-chain alkoxy radicals on peptides and proteins results in the loss of side-chains as aldehydes and ketones. *Free Radc. Biol. Med.* 32:1171–1184.
3. Levine, R.L., and Stadtman, E.R. (2001). Oxidative modification of proteins during aging. *Exp. Gerontol.* 36:1495–1502.

5.2 OXIDATIVE STRESS IN THE EYE: AGE-RELATED CATARACT AND RETINAL DEGENERATION

MARJORIE F. LOU

*Redox Biology Center and Department of Veterinary and Biomedical Sciences,
University of Nebraska, Lincoln, Nebraska*

JOHN W. CRABB

Cole Eye Institute, Cleveland Clinic Foundation, Cleveland, Ohio

The visual process of the eye involves the collective contributions of cornea, lens, and retina (Fig. 5.6). The cornea, which covers the anterior segment of the eye globe, is a transparent tissue with high refractive power. Light that passes through the cornea is collected and focused by the lens, another transparent tissue in the anterior segment that, like the cornea, is bathed with aqueous humor. The lens focuses the incoming light onto the neural retina, where the light is absorbed and visual signal transduction is initiated. These neural signals are transmitted from the retina through the optic nerve to the brain for visual readout of images. Figure 5.6 depicts a cross section of a typical human eye. Both the lens and retina can develop pathological conditions leading to vision loss associated with aging. The lens loses its transparency, a condition called cataract, while the retina slowly degenerates and loses its function, a condition often associated with age-related macular degeneration. Because of the

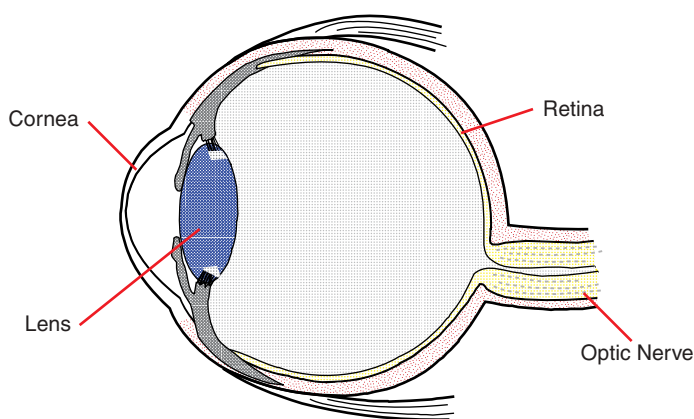


Figure 5.6. Schematic illustration of a human eye.

anatomical locale of the eye, and its constant exposure to light, it is very vulnerable to external environmental changes, in particular, oxidative stress. Mounting evidence indicates that oxidative stress is one of the major risk factors for age-related cataract and age-related macular degeneration. This section reviews some of the evidence supporting oxidative stress as a risk factor for cataract and some types of retinal degeneration.

5.2.A Oxidative Stress and Cataract

5.2.A1 The Lens and Age-Related Cataract The eye lens is an oval shaped, avascular, and transparent organ whose major function is to collect and focus light on the retina for proper vision. The lens has an active monolayer of epithelial cells at the anterior side, and the cells at both equatorial regions elongate and differentiate into fiber cells, which eventually lose their nuclei and other organelles, and lay down concentrically under the epithelial layer. Thus, this process allows the lens to increase in weight and thickness throughout life, with older cells continuously compressed toward the center of the lens and newly formed fibers building up layers on the outside. Therefore, the lens nucleus represents the oldest lens fibers, and is the oldest tissue in the animal body, while the region of cortical fibers between the epithelial monolayer and the nucleus is younger and metabolically more active. This unique feature of the lens makes it a good research model to study aging and developmental biology. A schematic diagram of the lens is depicted in Fig. 5.7.

Another unique feature of the lens is its high protein content, which is about 35% of its own wet weight and can be 65–70% in the central region. The lens contains mostly structural proteins called crystallin, which are packed in a short-range spatial order to provide a smooth gradient of refractive index, allowing the lens to be transparent and to have the necessary refractive power. The lens accumulates post-translationally

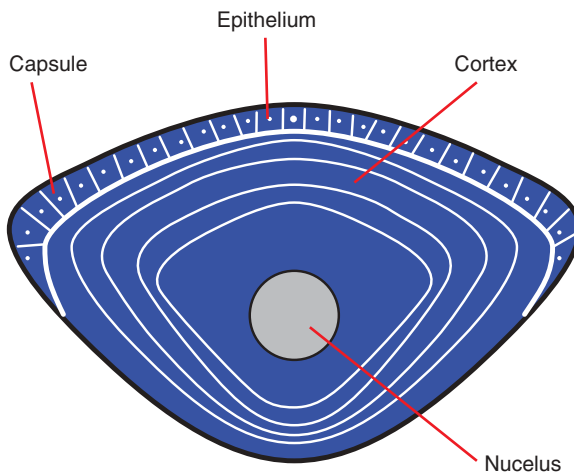


Figure 5.7. Schematic diagram of a human lens.

modified proteins throughout its lifetime; however, most lens proteins have a slow turnover rate, with half-lives calculated in decades.

Increased protein insolubility, triggered by protein modification and high molecular weight aggregate formation, is the major reason for the lens to progressively lose transparency during aging. Other basic metabolic changes also occur during aging, and the reason for such age-associated degeneration is unclear. Transparency loss due to protein aggregates, or opacity of the lens, causes light scattering and compromises vision and eventually causes blindness. This pathological condition is known as cataract.

Cataract is a complex disease. Based on the anatomic location of the lens opacity, it can be classified into cortical, nuclear, and mixed cataracts. Based on the etiology, it can be divided into senile or age-related cataract, congenital cataract, or cataract associated with systemic diseases, such as diabetes. Of these, age-related cataract is most common and is the leading cause of blindness worldwide. In the United States alone, cataract afflicts nearly 50% of the population over 65 years of age. However, blindness due to cataracts is readily treatable by surgical replacement of the cataractous lens with an artificial lens. The association between oxidation and cataract formation is summarized next.

5.2.A2 Association Between Oxidation and Cataract Human senile cataract is a multifactorial disease. Several risk factors are deemed important in cataractogenesis, including oxidative stress, hyperglycemia, ultraviolet light exposure, cigarette smoking, and genetic factors. Of these, oxidative stress is considered to be the most important risk factor. Studies in many laboratories have shown convincing results connecting oxidation with cataract. For instance, in human senile cataractous lens, the thiol-containing antioxidant GSH has been drastically depleted, and the thiol groups in proteins are extensively oxidized to form protein–nonprotein or protein–protein disulfide bonds. In some severe cases, extensive conjugation between water-insoluble proteins in the cytosol and the membrane has been found. In addition, a high percentage of lipids in the membrane are oxidized. Several epidemiological reports indicate that fishermen or people working outdoors without proper protection, or residents in regions with high ultraviolet light exposure have a higher incidence of cataract and a younger age of onset for this disease. Table 5.4 summarizes the evidence for oxidation associated with the changes found in cataracts.

5.2.A3 Source of Oxidants In mammals, ROS, such as $O_2^{\cdot -}$ can be generated from incomplete reduction of molecular oxygen in the mitochondrial electron transport chain, and during cellular response to inflammation. Superoxide can be dismutated nonenzymatically or by superoxide dismutase enzymes to produce the relatively stable H_2O_2 , which easily diffuses into cells, causing oxidative damage. Because of the anatomical locale, the lens can receive ROS from both the anterior and posterior sides. ROS generated from the iris, ciliary body, or corneal endothelial cells can be collected in the anterior chamber as H_2O_2 and diffuse into the lens while the ROS (such as lipid peroxide) generated from the retina and collected in the vitreous body can diffuse posteriorly into the lens. Therefore, the lens is accessible and vulnerable

TABLE 5.4. Evidence for Oxidative-Related Biochemical Changes in Human Cataract

-
- A. Changes in lens protein and nonproteins
 - 1. Decrease in total protein thiols
 - 2. Increase in protein–thiol mixed disulfides, including protein-S-S-glutathione (PSSG) and protein-S-S-cysteine (PSSC) conjugates
 - 3. Increase in protein–protein disulfides
 - 4. Formation of high molecular weight protein aggregates
 - 5. Thiol modification and inactivation of Na/K-ATPase
 - 6. Prevalence of methionine sulfoxide and cysteic acid in lens proteins
 - 7. Formation of cytosolic and membrane protein disulfide linkage
 - 8. Oxidation of GSH and ascorbate
 - B. Changes in lens membrane lipids
 - 1. Lipid peroxidation with malondialdehyde accumulation
 - 2. Increase in membrane rigidity
 - C. Changes in DNA
 - 1. DNA strand break
 - D. Other evidence
 - 1. Elevated H₂O₂ in aqueous humor of cataract patients
 - 2. Epidemiological studies associate outdoor lifestyle and UV exposure to higher incidence of cataract
-

to oxidative stress, and often cataract formation is the final pathological outcome. The other major contributor to oxidative stress is light, in particular, ultraviolet light. This photooxidative stress results from light absorption by the chromophores of the lens.

5.2.A4 Antioxidants and Oxidation Defense Systems in the Lens

The lens has a very high GSH content, which is among the highest in all tissues in the body. The level of GSH averages 4–6 mM, depending on the animal. The lens uses GSH to counteract oxidative stress and to protect proteins from oxidative damage. The lens also uses other antioxidants such as ascorbate, vitamin E, and carotenoids for protection. Similar to other organs, the lens has well-developed enzymatic systems for oxidation defense and oxidation damage repair of proteins and nucleic acids. It is enriched in glutathione reductase, glutathione peroxidase, catalase, and superoxide dismutase (see Chapter 3). The GSH-dependent thioltransferase (or glutaredoxin) system and the NADPH-dependent thioredoxin/thioredoxin reductase systems have recently been found in the lens. The former specifically reduces protein–GSH mixed disulfides, while the latter reduces protein–protein disulfides. Methionine sulfoxide reductase has recently been identified in the lens. All these thiol repair enzymes are important in maintaining the thiol/disulfide homeostasis in the lens, and in keeping a reducing environment in the lens. Under oxidative stress conditions, some of the above enzymes are upregulated to offset the influx of oxidants. Catalase is known to increase nearly 50-fold, while thioltransferase, thioredoxin, and thioredoxin reductase are all transiently upregulated approximately twofold. The redox homeostatic system and its potential role in preventing cataract formation are depicted in Fig. 5.8. The lens also uses proteases and the proteasome to remove oxidatively damaged proteins.

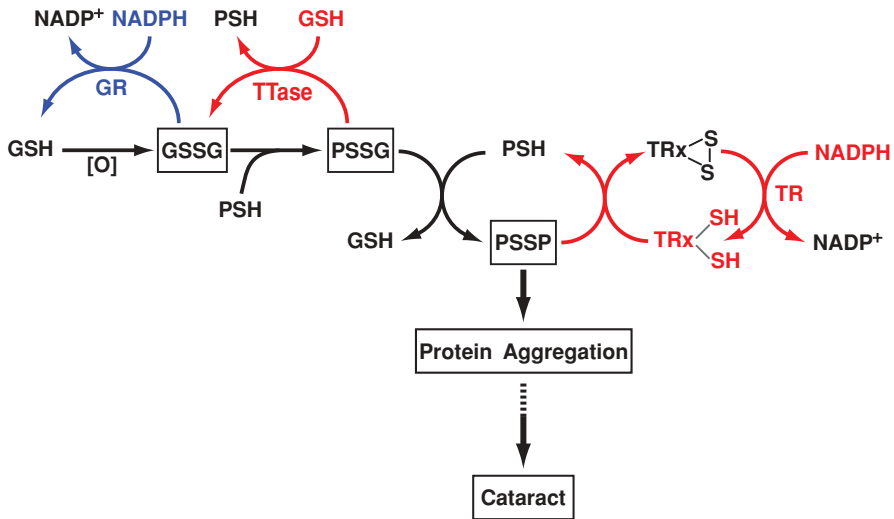


Figure 5.8. Thiol modification and repair of lens proteins. GSH, glutathione; GSSG, oxidized glutathione; GR, glutathione reductase; PSH, protein thiol; PSSG, protein-S-S-glutathione conjugates; TTase, thioltransferase (glutaredoxin); PSSP, protein-protein disulfides; TR, thioredoxin reductase.

Similarly, damaged DNA can be repaired by a series of direct and excision-repair mechanisms, including poly(ADP-ribose) polymerase.

5.2.A5 Specific Damages in the Lens Related to Oxidation

5.2.A5a The Lens Membrane The severity of the opacity in human cataractous lenses is associated with the presence of malondialdehyde, a product of lipid peroxidation. Malondialdehyde can further damage the lens by forming cross-links with nucleic acid, proteins, and phospholipids. Lipids with a higher number of double bonds, such as glycerolipids, are selectively oxidized over the more saturated lipids, such as sphingolipids, leading to enhanced membrane rigidity that may contribute to light scattering, and impair functioning of membrane-associated transport ion pumps.

5.2.A5b Lens Proteins Mass spectrometric analyses have revealed little or no protein oxidation in young and normal lens, but extensive protein oxidation is observed in older lenses (especially of the membrane proteins). Lenses older than 60 years have nearly double the amount of protein disulfides as lenses from infants. However, cataractous lenses have more extensive disulfide cross-links in lens proteins, particularly in the structural proteins: the α -, β - and γ -crystallins. α -Crystallin, which has only two thiols, can lose its chaperone-like function, thus exacerbating insolubility of lens proteins. Indeed, intramolecular disulfide bonds in α -crystallin have been found in all cataractous lenses.

In a normal lens, mixed disulfide bonds with protein are present in only trace amounts. Conjugates of proteins with glutathione (PSSG) and protein with cysteine (PSSC) increase gradually with the age of the lens and are highly elevated in cataractous lenses. Both PSSG and PSSC are increased in proportion to the degree of lens opacity, and the lens color from light yellow to dark brown. In advanced brunescence (dark brown) nuclear cataracts, the PSSG content can be four- or fivefold higher than the GSH content of the same lens. In older or opaque lenses, protein conjugates with γ -glutamylcysteine are often present at the same levels as PSSG and PSSC. Accumulation of γ -glutamylcysteine indicates impairment of GSH synthesis machinery in advanced cataracts. In some nuclear cataracts, the number of protein thiol groups is less than 10% of that found in normal lens. Protein thiols may be oxidized to cysteic acid and the extensive oxidation of cysteine residues may be responsible for shifting the lens proteins from a water-soluble to highly water-insoluble state. Furthermore, in some isolated polypeptides, over 50% of methionine and nearly all cysteine moieties are oxidized. Most of these disulfides are present in high molecular weight aggregates, containing proteins and membrane particles with sizes $>1 \times 10^6$ Da, which can lead to light scattering.

5.2.A5c Damage to the Oxidation Defense Systems Two of the earliest changes in aging and cataractous lenses are the loss of the primary antioxidant molecules (GSH, ascorbate) and the decreased activity of antioxidant defense enzymes. GSH decreases by 50–60% in lenses older than 70 years and decreases further in cataractous lenses. There is little or no accumulation of GSSG in the same lens, since most of the GSSG is used to form protein conjugates. The concentration of cysteine is 3–5% of that of GSH in a normal lens and also decreases with aging and lens opacity. The activity of glutathione reductase decreases with aging and to a greater extent in cataractous lenses. The epithelium of cataractous lenses has little or no glutathione reductase activity. Both superoxide dismutase and glutathione peroxidase exhibit lower activity in the cataractous lens, but interestingly, the activity of catalase is not changed.

5.2.B Oxidative Stress and Retinal Pathology

5.2.B1 Structure and Function of the Retina The neural retina is the complex, multicell type tissue in the posterior segment of the eye responsible for converting light into neural signals directed to the brain (Fig. 5.9). Proteins like rhodopsin in rod photoreceptor cells and blue, green, and red opsins in cone photoreceptor cells absorb light via their retinoid chromophore 11-*cis*-retinal, triggering visual signal transduction (i.e., phototransduction). These light-absorbing proteins are integral membrane proteins located in the outer segments of photoreceptor cells. The small, central portion of the retina responsible for high acuity vision is called the macula. Additional cells in the retina, including bipolar and ganglion cells, relay the signal from the photoreceptor cells through the nerve fiber layer to the optic nerve, modulated in part by horizontal and amacrine cells and supported by Müller cells, astrocytes, and microglia. The neural retina has an internal vasculature; however, the principal blood

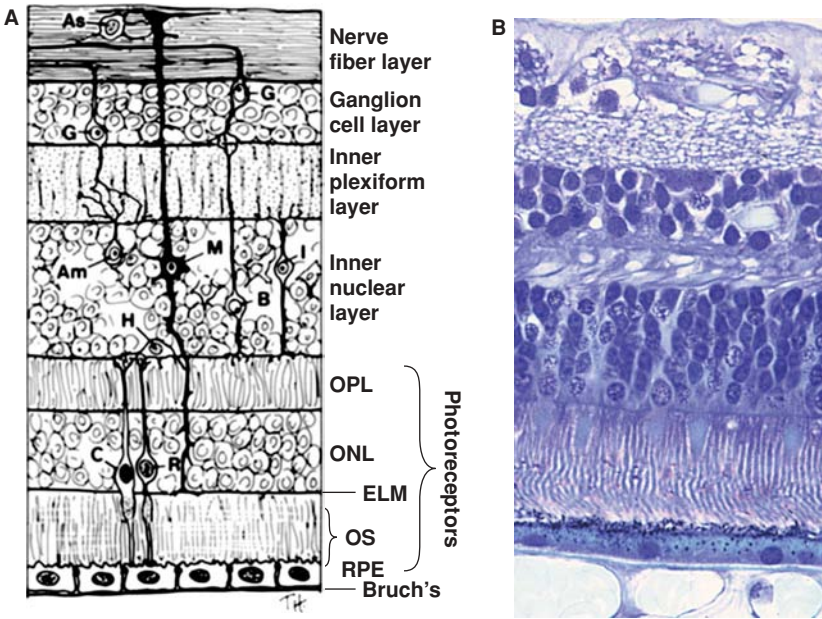


Figure 5.9. Cell layers of a retina. (A) Schematic drawing of the cell layers of the retina (AS, astrocyte; G, ganglion cell; Am, amacrine cell; M, Müller glial cell; I, interplexiform cell; B, bipolar cell; H, horizontal cell; C, cone photoreceptor; R, rod photoreceptor; OPL, outer plexiform layer; ONL, outer nuclear layer; ELM, external limiting membrane; OS, photoreceptor outer segments; RPE, retinal pigment epithelium) and (B) histological section of peripheral retina showing the cell layers as well as blood vessels in the choriocapillaris below the RPE and Bruch's membrane. Panels (A) and (B) compliments of A.H. Milam and S.K. John from *The Human Retina in Health and Disease*, Scheie Eye Institute, Philadelphia, PA.

supply for the photoreceptor cells is the choroid cell layer of the eye. The choroid and photoreceptor cells are separated by the retinal pigment epithelium, a polarized single-cell layer that plays key roles in retinal physiology. Intense research effort continues toward a better understanding of retinal physiology, including regulation of visual sensitivity and dark adaptation, regeneration of 11-*cis*-retinal for cone visual pigments (the visual cycle), neuronal transmission, and retinal pathology.

5.2.B2 Oxidative Stress in the Retina The retina is particularly susceptible to oxidative damage because of its exposure to light, oxygen, and a high polyunsaturated fatty acid content. As described previously in Section 5.2.A3, ROS are readily generated in mammalian cells. However, the outer segments of the photoreceptors, where photons are absorbed and visual signal transduction is initiated, contain lipid-rich membrane disks with approximately 50% of the lipids being docosahexaenoate, the most oxidizable fatty acid in humans. Furthermore, the light-absorbing retinoid chromophore carried by the visual pigments (e.g., rhodopsin) is another highly conjugated structure readily susceptible to oxidation. Accordingly, significant

macromolecular turnover is required to maintain functional photoreceptors. In the healthy retina, approximately 10% of the photoreceptor outer segment disks are replaced daily with newly synthesized outer segment disks and the “spent” disks are phagocytosed by the retinal pigment epithelium. Interestingly, the retinal pigment epithelium is the most active phagocytic tissue in humans, with each epithelial cell phagocytizing shed outer segment tips from about 50 photoreceptor cells. In addition to phagocytosis, the retinal pigment epithelium is responsible for vectorial transport of nutrients to the photoreceptors, removal of waste products to the blood, and absorption of scattered light, and functions in the retinoid visual cycle and regeneration of 11-*cis*-retinoid and visual pigments. Accordingly, the retinal environment and associated physiological processes provide an excellent source of ROS. In addition, the waste products in the retinal pigment epithelium and components from the blood provide a ready source of substrates for oxidative modifications.

With age, the retinal pigment epithelium often accumulates fluorescent intracellular debris and extracellular deposits may form between the retinal pigment epithelium and the blood-bearing choroid. Retinal pigment epithelium intracellular debris known as lipofuscin and extracellular deposits termed drusen have been associated with the major retinal degenerative disease “age-related macular degeneration.” Exposure to bright light can also damage the retina. Oxidative stress-related retinal pathology from exposure to intense light and associated with age-related macular degeneration are addressed in the following sections.

5.2.B3 Retinal Light Damage Acute light-induced photoreceptor cell degeneration has been studied for over 40 years as a model of visual cell loss arising from genetic and age-related disease. Age, diet, genetics, and environmental light history all influence the extent and type of retinal injury from light exposure and appear to involve both apoptosis and necrosis. Both the photoreceptor and retina pigment epithelial cell layers are susceptible to degeneration with the extent of damage dependent on the wavelength, the intensity, and the duration of light exposure. Retinal light damage appears to be initiated by oxidative stress since antioxidants such as ascorbate and dimethylthiourea provide protection. However, the damaging reactive oxygen and reactive nitrogen species and the pathways of oxidative damage are still under investigation. The similarity in the action spectrum of retinal light damage and the absorption spectrum of rhodopsin (~500 nm maximum) suggests that injury may be initiated by rhodopsin bleaching and involve retinoids. Other evidence also supports a role for retinoids. For example, blue light induces apoptosis in retinal pigment epithelial cells in culture in proportion to the amount of retinoid compound lipofuscin A2E, and vitamin A deficient rats or mice unable to regenerate 11-*cis*-retinal, the light-absorbing chromophore bound to visual pigment proteins like rhodopsin, are resistant to retinal light damage.

Nitration of tyrosine is one of several protein modifications that can occur as a result of oxidative stress and proteomic analyses of rat retina after light exposure have shown that light modulates tyrosine nitration. Several inflammatory and neurodegenerative disorders have been associated with tyrosine nitration including Parkinson’s disease, Alzheimer’s disease, and Huntington’s disease. Nitrotyrosine is formed from the reaction of free or protein-bound tyrosine with reactive nitrogen oxide species.

The actual species responsible for tyrosine nitration *in vivo* continue to be debated; however, free radical nitrogen dioxide ($\cdot\text{NO}_2$) and peroxynitrite (ONOO^-) have both been implicated.

5.2.B4 Age-Related Macular Degeneration Age-related macular degeneration is the most common cause of blindness in the elderly in Western populations and is characterized by the breakdown of the macula, the small, central portion of the retina responsible for high acuity vision. It is a progressive, multifactorial, polygenic disease and its etiology remains poorly understood. Both genetic and environmental risk factors are contributory. An association between variants in complement component genes and susceptibility to age-related macular degeneration has been found, implicating inflammatory processes in the pathophysiology of the disease. Cumulative oxidative damage contributes to aging and has long been suspected of contributing to the pathogenesis of age-related macular degeneration. Indirect evidence that oxidative damage plays a role comes from epidemiological studies showing that smoking significantly increases the risk of age-related macular degeneration and that, for select individuals, disease progression can be slowed by dietary supplementation with antioxidant vitamins and zinc.

The intracellular accumulation of lipofuscin in the retinal pigment epithelium appears to correlate with the progression of age-related macular degeneration. Lipofuscin is a heterogeneous group of lipid/protein aggregates, which have characteristic yellowish-green fluorescence emission when excited with ultraviolet light. Oxidative modification of cellular components through lipoxidation and glyoxidation is thought to play a role in lipofuscin formation. At least ten fluorophores have been detected in retinal pigment epithelial lipofuscin and two of these have been identified, namely, retinyl palmitate and A2E, a pyridinium bisretinoid occurring as a Schiff base reaction product derived from two molecules of vitamin A and one of phosphatidylethanolamine. Lipofuscin appears to be a photoinducible generator of ROS that can compromise lysosomal and DNA integrity, induce lipid peroxidation, and cause retina pigment epithelial cell atrophy.

The discovery of elevated oxidative protein modifications in individuals with age-related macular degeneration has revealed a direct molecular link between oxidative damage and this disease. Specifically, carboxyethylpyrrole modifications, a unique protein modification derived from the oxidation of docosahexaenoate-containing lipids, are elevated in ocular tissues and plasma in those with age-related macular degeneration, as are autoantibodies that recognize this adduct (Fig. 5.10). Notably, docosahexaenoate is highly susceptible to ROS and is abundant in the retina. Carboxyethylpyrrole adducts have been shown to stimulate angiogenesis and may also play a role in the most advanced stage of the disease, namely, choroidal neovascularization, where abnormal blood vessel growth into the retina from the choroids causes irreversible vision loss.

5.2.B5 Antioxidant Defense Systems in the Retina As in other tissues, the retina also has well-developed enzymatic systems for protection from oxidative damage including, for example, glutathione reductase, glutathione peroxidase,

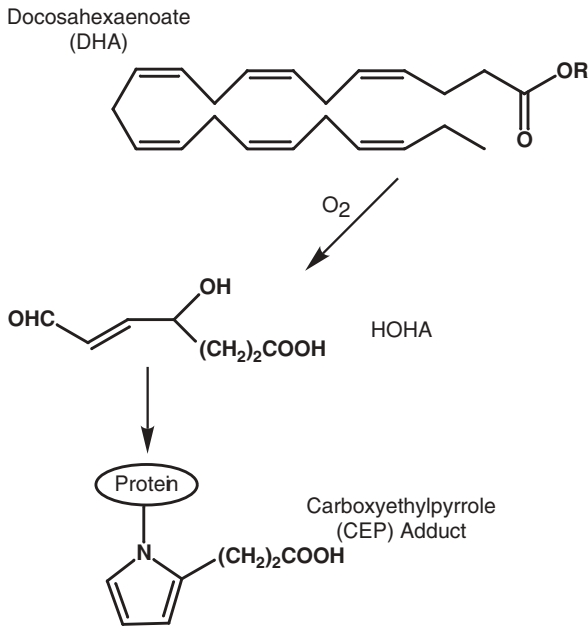


Figure 5.10. Carboxyethylpyrrole (CEP), an oxidative protein modification, is elevated in light-damaged retina and in ocular tissues and blood from donors with age-related macular degeneration. ROS attack of docosahexaenoate (DHA)-containing phospholipids uniquely yields 4-hydroxy-7-oxohept-5-enoic acid (HOHA), a reactive lipid fragment that combines with primary amino groups to yield CEP adducts. A common R group in the above structure would be phosphatidylcholine.

glutaredoxin, catalase, and superoxide dismutase. The superoxide dismutase (SOD) isozymes that catalyze dismutation of O_2^- are a particularly noteworthy antioxidant defense system in the retina. SOD1 (Cu,Zn-SOD) scavenges O_2^- in the cytosol, SOD2 (Mn-SOD) provides protection from oxidative stress in mitochondria and SOD3, a secretory form of the enzyme, functions in extracellular regions of the retina. Mice genetically engineered to be deficient in SOD1 develop features of retinal pathology similar to age-related degeneration, including drusen, thickened Bruch's membrane, and choroidal neovascularization. Mice with targeted disruption of SOD2 expression in the retinal pigment epithelium also develop pathological changes in the outer retina resembling age-related macular degeneration.

SELECTED REFERENCES

1. Spector, A. (1984). The search for a solution to senile cataracts: Proctor lecture. *Invest. Ophthalmol. Vis. Sci.* 25:130–146.
2. Crabb, J.W., Miyagi, M., Gu, X., Shadrach, K., West, K.A., Sakaguchi, H., Kamei, M., Hasan, A., Yan, L., Rayborn, M.E., Salomon, R.G., and Hollyfield, J.G. (2002). Drusen

- proteome analysis: an approach to the etiology of age-related macular degeneration. *Proc. Natl. Acad. Sci. USA* 99:14682–14687.
3. Gu, X., Meer, S.G., Miyagi, M., Rayborn, M.E., Hollyfield, J.G., Crabb, J.W., and Salomon, R.G. (2003). Carboxyethylpyrrole protein adducts and autoantibodies, biomarkers for age-related macular degeneration. *J. Biol. Chem.* 278:42027–42035.
 4. Ebrahem, Q., Renganathan, K., Sears, J., Vasanji, A., Gu, X., Lu, L., Salomon, R.G., Crabb, J.W., and Anand-Apte, B. (2006). Carboxyethylpyrrole oxidative protein modifications stimulate neovascularization: implications for age-related macular degeneration. *Proc. Natl. Acad. Sci. USA* 103:13480–13484.

5.3 REDOX MECHANISMS IN CARDIOVASCULAR DISEASE: CHRONIC HEART FAILURE

GEORGE J. ROZANSKI

Department of Cellular and Integrative Physiology, University of Nebraska Medical Center, Omaha, Nebraska

Chronic heart failure is a clinical condition characterized by the inability of the heart to pump blood at a sufficient flow rate to meet the metabolic demands of the body. Currently, about 5 million U.S. residents have been diagnosed with chronic heart failure and more than 500,000 are diagnosed with this condition each year. In this section, the determinants of contractile dysfunction in the failing heart are discussed at the level of the cardiac myocyte with emphasis on regulatory proteins that are modulated by redox mechanisms.

5.3.A Excitation–Contraction Coupling in Cardiac Myocytes

There is clear evidence that Ca^{2+} is essential for contraction of cardiac muscle. Within physiological limits, mechanisms that increase the free Ca^{2+} concentration in the cytoplasm of cardiac myocytes increase force development whereas factors that decrease Ca^{2+} levels reduce contractile force. The normal cycle of cardiac contraction and relaxation is controlled by a complex interplay of cellular proteins that regulate cytosolic Ca^{2+} concentration from approximately 10^{-7} M under resting conditions to near 10^{-6} M during active contraction. The contractile event in cardiac muscle depends on a preceding electrical excitation, a process termed excitation–contraction coupling (Fig. 5.11). During the cardiac action potential, Ca^{2+} enters the myocyte from the extracellular space through voltage-gated Ca^{2+} channels that in turn triggers the release of Ca^{2+} from the intracellular stores in the sarcoplasmic reticulum (SR) by binding to Ca^{2+} release channels called ryanodine receptors (RyR2). The Ca^{2+} that leaves the SR through RyR2 elicits a rapid and large increase in cytosolic free Ca^{2+} , which binds to the protein troponin C and elicits a conformational change allowing crossbridge cycling and sliding of the myofilaments to elicit contraction. The cellular events that raise cytosolic Ca^{2+} and lead to contraction are followed by processes that remove cytosolic Ca^{2+} and cause relaxation. A major protein that achieves this

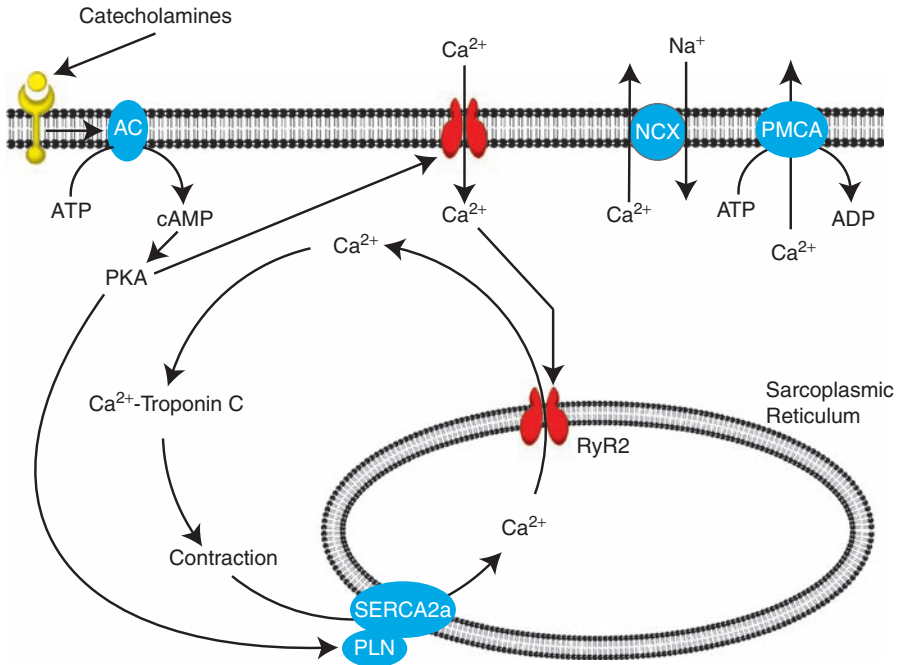


Figure 5.11. Excitation–contraction coupling in cardiac myocytes. During the propagated action potential in cardiac myocytes, voltage-gated Ca²⁺ channels open, allowing the entry of Ca²⁺ from the extracellular space to trigger the release of Ca²⁺ from the sarcoplasmic reticulum through ryanodine receptors (RyR2). Released Ca²⁺ binds to troponin C, which causes a conformational change in the troponin complex and the sliding of thick and thin filaments to cause contraction. Removal of Ca²⁺ from the cytoplasm is achieved mainly by a sarco(endo)plasmic reticulum calcium ATPase (SERCA2a), which pumps Ca²⁺ back into the sarcoplasmic reticulum. The activity of this ATPase is negatively modulated by the protein phospholamban (PLN). Cytosolic Ca²⁺ is also removed by a Na⁺/Ca²⁺ exchanger (NCX) and a plasma membrane Ca²⁺-ATPase (PMCA), which extrude Ca²⁺ to the extracellular space. As the cytoplasmic Ca²⁺ concentration falls, Ca²⁺ dissociates from troponin C and causes relaxation. Modulation of excitation–contraction coupling occurs through β -adrenergic activation of adenylyl cyclase (AC) and cAMP-dependent PKA, which phosphorylates Ca²⁺ channels and PLN.

function is the sarco(endo)plasmic reticulum calcium ATP-ase (SERCA2a), which actively pumps the released Ca²⁺ back into the SR at the expense of ATP hydrolysis. The trigger Ca²⁺ that entered the cell from the extracellular space is removed from the cytoplasm by a Na⁺/Ca²⁺ exchange transporter and a plasma membrane Ca²⁺-ATPase that extrudes Ca²⁺ back into the extracellular space. Thus, the kinetics of relaxation and the degree of SR Ca²⁺ loading are largely controlled by SERCA2a, the Na⁺/Ca²⁺ exchange transporter, and to a lesser degree the plasma membrane Ca²⁺-ATPase. Finally, myocyte Ca²⁺ handling and contractile force are modulated by several mechanisms, one of the most important of which is mediated by

catecholamines binding to β -adrenergic receptors and activation of adenylyl cyclase. The resulting increase in cAMP activates cAMP-dependent protein kinase A (PKA), which phosphorylates Ca^{2+} channels and elicits a greater influx of Ca^{2+} into the cell to augment SR Ca^{2+} release and contractile force. Activated PKA also phosphorylates the regulatory protein phospholamban, which removes inhibition of SERCA2a activity and increases the rate of Ca^{2+} uptake into the SR. Thus, the result of cAMP-dependent PKA phosphorylation is an increase in contractile force and an increase in the speed of both contraction and relaxation.

5.3.B Role of Oxidative Stress in Chronic Heart Failure

Experimental and clinical evidence suggests that the pathogenesis of chronic heart failure involves increased production of ROS and RNS that overwhelm cellular antioxidant defenses and elicit oxidative stress. In the failing heart, ROS/RNS are generated from multiple sources and affect several protein targets involved in regulating cardiac contraction (Fig. 5.12). An important stimulus for ROS/RNS production is the physiological activation of neuronal and hormonal systems that compensate for the decreased pumping capacity of the heart. This activation is manifest as increased circulating levels of catecholamines, vasoactive substances such as angiotensin II and endothelin, and inflammatory mediators such as tumor necrosis factor- α . These neurohumoral factors increase $\text{O}_2^{\cdot-}$ production by the myocardium through increased expression and activity of a phagocyte-like NAD(P)H oxidase and autooxidation of plasma catecholamines to form cyclized *o*-quinones (aminochromes, dopachrome, adrenochrome, noradrenochrome). Other major sources of ROS in chronic heart failure include the uncoupling of the electron transport chain in mitochondria and enhanced breakdown of cellular ATP, which can generate $\text{O}_2^{\cdot-}$ via xanthine oxidase.

Increased RNS production in chronic heart failure mainly involves nitric oxide synthase (NOS), which exists as constitutive and inducible isoforms that are expressed in myocytes, endothelial cells, and intramyocardial nerve fibers. The NO generated by NOS is by itself not toxic to cardiac myocytes but it can combine with $\text{O}_2^{\cdot-}$ to generate the powerful oxidant peroxynitrate or with GSH to form *S*-nitrosoglutathione. With depletion of the substrate L-arginine or a lack of the cofactor tetrahydrobiopterin, NOS may paradoxically produce $\text{O}_2^{\cdot-}$ instead of NO. Thus, multiple sources of ROS and RNS in the failing heart elicit a complex array of reactive molecules that are capable of modifying proteins involved in cardiac contraction and that contribute to the ventricular dysfunction characteristic of chronic heart failure.

5.3.C Redox Modulation of Ca^{2+} Handling Proteins

Experimental measurements of evoked Ca^{2+} transients in myocytes from failing hearts are characterized by markedly smaller amplitudes with slower kinetics of Ca^{2+} increase and decay compared to normal. Thus, depressed force development and prolonged relaxation that are characteristic of chronic heart failure can be due to (1) impaired Ca^{2+} influx through voltage-gated Ca^{2+} channels, (2) decreased Ca^{2+}

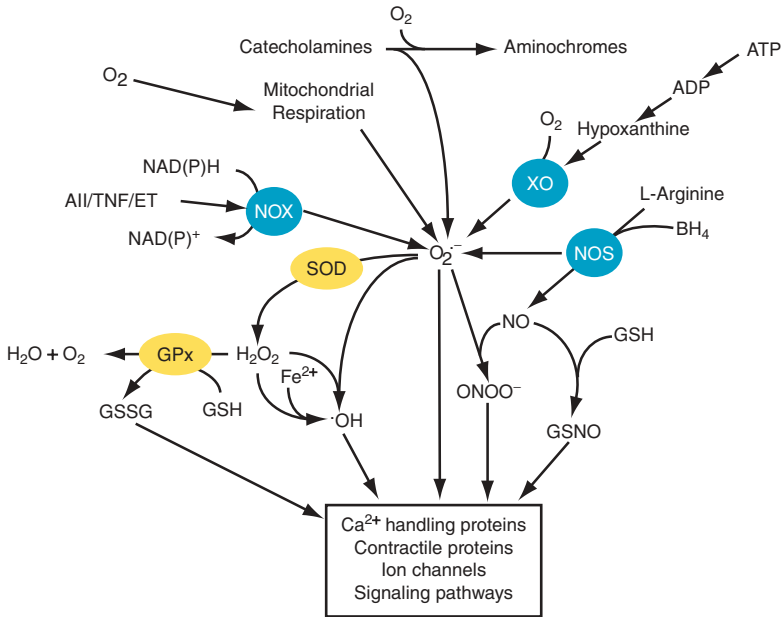


Figure 5.12. Sources of ROS and RNS in the myocardium during the development of chronic heart failure. $O_2^{\cdot-}$ is at the center of a complex network of reactive molecules that are capable of modulating key cellular proteins involved in excitation–contraction coupling. Increased production of $O_2^{\cdot-}$ by the myocardium is stimulated in part by increased levels of neurohumoral effectors such as angiotensin II (AII) and endothelin-1 (ET), and cytokines such as tumor necrosis factor- α (TNF- α), which increase activity of NAD(P)H oxidase (NOX). Increased $O_2^{\cdot-}$ production mediated by xanthine oxidase (XO) also occurs during the breakdown of cellular ATP. NO formed by nitric oxide synthase (NOS) generates several RNS such as peroxynitrite (ONOO $^-$) and S-nitrosoglutathione (GSNO). In the absence of the cofactor tetrahydrobiopterin (BH_4), NOS can produce $O_2^{\cdot-}$ instead of NO.

release from the SR, (3) decreased Ca^{2+} reuptake by the SR, or (4) decreased Ca^{2+} efflux from the cell.

5.3.C1 Ca^{2+} Influx It is proposed that reduction in the amount of Ca^{2+} entering the myocyte through voltage-gated Ca^{2+} channels contributes to depressed contractile performance in the failing heart by decreasing the stimulus for SR Ca^{2+} release through RyR2. The pore-forming subunit of the human Ca^{2+} channel appears to be inhibited by hypoxia and thiol-reactive agents, and is reversed by reducing agents such as dithiothreitol. This suggests that Ca^{2+} channels are sensitive to redox regulation, raising the possibility that oxidative stress contributing to chronic heart failure reversibly impairs Ca^{2+} channel function. However, more direct evidence of redox control of Ca^{2+} channels by changes in the GSH/GSSG ratio or other redox systems is lacking.

Other sarcolemmal ion channels, in particular, K^+ channels that indirectly modulate Ca^{2+} influx, may also contribute to contractile dysfunction in chronic heart failure. Downregulation of K^+ channels is correlated with a significant decrease in the GSH/GSSG ratio, reflecting a shift in the ambient redox state toward oxidation. Importantly, this electrophysiological phenotype of myocytes from failing hearts is reversed by exogenous activators of glucose flux through the pentose pathway and this effect is mediated by the thioredoxin system.

5.3.C2 Ca^{2+} Release The tetrameric RyR2 channel has approximately 80 cysteine residues whose thiol groups are accessible to oxidizing or nitrosylating molecules. Some of these residues are modified by oxidation or nitrosylation under physiological conditions and are important for normal Ca^{2+} release function of RyR2. Under conditions associated with small increases in intracellular levels of thiol-reactive molecules such as $O_2^{\cdot-}$, H_2O_2 , or GSSG, the probability of RyR2 opening in response to free Ca^{2+} increases, which in the intact myocyte is associated with increased Ca^{2+} release and increased contractile force. However, at pathophysiological levels of oxidizing molecules, the RyR2 activity decreases, which is in keeping with depressed contraction. Indeed, in the failing heart, RyR2 activity is significantly less than normal and this phenotype is reversed by GSH or dithiothreitol, suggesting a redox mechanism. The biphasic responsiveness of RyR2 to thiol-reactive molecules (i.e., activation at low concentrations, inhibition at high concentrations) is proposed to be related to the extent of thiol modification of RyR2. That is, thiol modification of a relatively small number of sensitive cysteine residues leads to channel activation whereas modification of more residues causes inactivation. Thus, while RyR2 function is well known to be redox sensitive, the molecular basis for the divergent sensitivity to ROS and other thiol-reactive agents is unclear.

5.3.C3 SERCA2a and Na^+/Ca^{2+} Exchange Transporter The characteristically prolonged decay of Ca^{2+} transients in myocytes from failing hearts is consistent with prolonged relaxation in the intact ventricle and is likely mediated by changes in SERCA2a and/or Na^+/Ca^{2+} exchange transporter activity. ROS decrease SR Ca^{2+} uptake by decreasing SERCA2a activity, possibly by modifying or blocking access of ATP to its binding site. However, more direct evidence for redox control of SERCA2a activity is lacking and it is not clear whether this type of post-translational modification is responsible for the decreased SR Ca^{2+} uptake that is observed in the failing myocardium. Delayed Ca^{2+} transients can also be expected from changes in the activity of the Na^+/Ca^{2+} exchange transporter (Fig. 5.11), but experimental studies generally show that transporter activity in the failing heart is increased compared to normal, possibly a compensatory alteration in response to depressed SERCA2a activity. A possible redox mechanism for this alteration in Na^+/Ca^{2+} exchange transporter function has been suggested by studies showing that biochemical systems generating $O_2^{\cdot-}$, H_2O_2 , or $\cdot OH$ increase transporter activity, and that this modulating effect is prevented or reversed by reducing agents.

Additional explanations for decreased SERCA2a activity in chronic heart failure involve the small, regulatory phosphoprotein phospholamban (Fig. 5.11). Molecular studies suggest that oxidation of a critical methionine residue on phospholamban

to methionine sulfoxide prevents its dissociation from SERCA2a, effectively locking SERCA2a in an inhibited state. Protein methionine sulfoxide is a substrate for thioredoxin-dependent reduction by methionine sulfoxide reductases, implying that direct redox modulation of phospholamban in the failing heart may play a role in depressed SR Ca^{2+} uptake. A second possible mechanism contributing to abnormal phospholamban function in chronic heart failure is decreased phosphorylation resulting from depressed β -adrenergic signaling. Indeed, recent studies of PKA show that this critical kinase is inactivated by disulfide bond formation between cysteines 199 and 343 in the catalytic subunit and that this effect is reversed by dithiothreitol. Therefore, experimental evidence suggests that redox mechanisms play a role in depressed β -adrenergic signaling in the failing heart that influences the function of Ca^{2+} handling proteins such as voltage-gated Ca^{2+} channels and phospholamban.

5.3.D Hypertrophy and Cell Death

Chronic pathophysiological conditions impose a variety of stress factors on the heart that cause increased generation of ROS/RNS, which in turn elicit cellular responses facilitating the progression to chronic heart failure. An increase in cardiac myocyte size (i.e., hypertrophy), is one cellular stress response that is an early adaptive mechanism in the intact heart to compensate for increased cardiac workload or deficiencies in excitation–contraction coupling. Cardiac stressors acting via ROS/RNS are also potent stimuli activating pathways involved in programmed cell death (i.e., apoptosis). Indeed, specimens from failing human hearts show an increased percentage of apoptotic cells compared with normal hearts. The loss of functional myocytes due to apoptosis would be predicted to decrease ventricular performance and promote slippage of muscle bundles, dilatation, and wall thinning, all hallmarks of the failing ventricle.

In relation to ROS/RNS as initiators of cell stress responses, several key proteins in apoptotic and hypertrophic pathways are redox sensitive, such as apoptosis signal-regulated kinase 1 (ASK1) which initiates programmed cell death through activation of c-Jun N-terminal kinase (JNK) and p38 MAP kinase (see Chapter 4.4). As in other cell types, reduced thioredoxin and glutaredoxin are negative regulators of ASK1 under physiological conditions. However, under pathogenic conditions of increased ROS production, oxidation of thioredoxin and glutaredoxin causes their dissociation from ASK1 and activation of downstream, proapoptotic targets. Thus, the negative regulation of ASK1 in the heart by reduced thioredoxin and glutaredoxin underscores the redox control of the apoptosis signal transduction pathway and helps explain the effects of antioxidants against stress-induced apoptosis.

5.3.E Extracellular Matrix Remodeling

The extracellular matrix contains fibrillar collagens that maintain the normal structural and geometric alignment of myocytes important for overall pump function. In the failing heart, the myocardial tissue undergoes profound structural changes (i.e., remodeling) that are manifest as a deterioration of the extracellular matrix causing slippage of myocardial fiber bundles and chamber dilatation. These structural changes, in addition to intrinsic alterations in myocyte excitation–contraction coupling, contribute

significantly to the contractile phenotype of chronic heart failure. The process of structural remodeling in chronic heart failure is mediated by an imbalance of proteases and protein synthesis that lead to net breakdown of the extracellular matrix. This imbalance is caused by the increased activity of matrix metalloproteinases (MMPs), which are a family of Zn^{2+} -dependent endopeptidases that are secreted by cardiac myocytes and fibroblasts, and that degrade specific components of the extracellular matrix. Most MMPs are secreted as proenzymes (pro-MMPs), which are subsequently activated in the extracellular space. MMP activation involves the breakage of a sulfhydryl bond between a cysteine residue in the autoinhibitory domain of the propeptide and Zn^{2+} in the catalytic center, a process referred to as the cysteine switch mechanism. With the breakage of the sulfhydryl bond, the enzyme is accessible to its substrates in the extracellular matrix. Although pro-MMPs can be activated by proteolytic cleavage of the propeptide, most activation conditions in pathological states involve excess ROS/RNS, which can also suppress endogenous tissue inhibitors of MMPs to further increase net proteolytic activity. Therefore, in the failing heart, increased production of ROS/RNS is a major stimulus for the net activation of MMPs and remodeling of the extracellular matrix.

Pro-MMPs are activated through S-glutathiolation of the autoinhibitory domain of the pro-MMP protein. This redox modification is elicited through the generation of different thiol-reactive intermediates such as GSSG, S-nitrosoglutathione, and S-nitroglutathione, but not all MMP isoforms are activated by the same intermediates, suggesting specificity of action. Under physiological conditions, extracellular GSH, which is present in micromolar concentrations, scavenges ROS/RNS and suppresses MMP activation. In pathophysiological states, excess ROS/RNS production leads to decreased GSH levels and increased levels of thiol-reactive intermediates that activate pro-MMPs. Thus, the redox balance of extracellular GSH plays a critical role in the remodeling of the myocardial extracellular matrix.

While redox mechanisms are important for activation of MMPs, they also play a role in controlling the expression of MMP isoforms in cardiac myocytes and fibroblasts under pathophysiological conditions. For example, the promoter region of certain MMP genes contains a putative binding site for the redox-sensitive transcription factor activator protein-1 (AP-1). The binding of AP-1 to its target gene and its subsequent activation is regulated by the redox state of the accessory protein redox factor-1, which itself is activated by reduced thioredoxin. Similarly, the expression of some MMPs is controlled by the redox-sensitive transcription factor NF- κ B. Although thioredoxin in the cytoplasm acts to inhibit translocation of NF- κ B to the nucleus, the binding of NF- κ B to its target gene is facilitated by reduced thioredoxin and inhibited by oxidized thioredoxin. Therefore, transcriptional activation of MMPs that contribute to structural remodeling of the heart during the transition to failure is controlled by the interplay of reduced thioredoxin with key regulatory proteins such as redox factor-1, AP-1, and NF- κ B.

The clinical manifestation of chronic heart failure is elicited by diverse pathophysiological states that affect the heart and blood vessels through the generation of ROS and RNS (Fig. 5.13). Increased production of ROS/RNS by the myocardium is stimulated by several neurohumoral factors and inflammatory cytokines that are part of

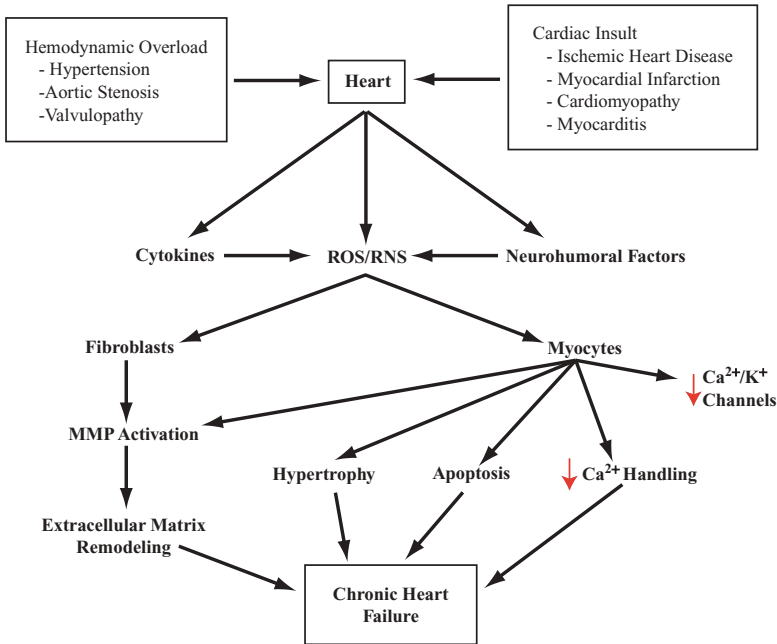


Figure 5.13. Multiple cellular factors underlying the development of chronic heart failure. Pathogenic changes in myocyte and fibroblast function are mediated by increased production of ROS/RNS through the activation of neurohumoral and cytokine networks affecting the heart. Changes in the extracellular matrix are mediated by the activation of matrix metalloproteinases (MMPs).

a network of cellular signals that initially compensate for the decrease in ventricular performance. Over time, these compensatory mechanisms and the chronic production of ROS/RNS they create affect a wide array of redox-sensitive proteins in several different cell types that together cause abnormal ventricular function and that contribute to the development of chronic heart failure.

SELECTED REFERENCES

1. Shannon, T.R., and Bers, D.M. (2004). Integrated Ca^{2+} management in cardiac myocytes. *Ann. NY Acad. Sci.* 1015:28–38.
2. Dhalla, N.S., Temsah, R.M., and Netticadan, T. (2000). Role of oxidative stress in cardiovascular diseases. *J. Hyperten.* 18:655–673.
3. Foo, R.S.-Y., Mani, K., and Kitsis, R.N. (2005). Death begets failure in the heart. *J. Clin. Invest.* 115:565–571.
4. Spinale, F.G. (2002). Matrix metalloproteinases. Regulation and dysregulation in the failing heart. *Circ. Res.* 90:520–530.

5.4 ROLE OF REACTIVE OXYGEN SPECIES IN CARCINOGENESIS

SURESH VEERAMANI and MING-FONG LIN

Department of Biochemistry and Molecular Biology and Eppley Institute for Cancer Research, University of Nebraska Medical Center, Omaha, Nebraska

5.4.A ROS Act as Growth Signaling Messengers

Since many of the cell signaling proteins are susceptible to oxidation, redox regulation of these proteins can be an excellent method to potentially initiate or block a signaling pathway. An important advantage of having ROS molecules over conventional protein signaling messengers is that ROS molecules have a very short half-life and thus could be more easily controlled. Furthermore, ROS, such as H_2O_2 , diffuse easily through the membrane, so that intercellular communication becomes easily achievable.

The generation of ROS by growth factor treatment and the inhibition of growth factor signaling by antioxidants suggest that crosstalk does exist between ROS and growth signaling pathways. For example, treatment of murine fibroblast cell line NIH/3T3 with H_2O_2 leads to increased tyrosine phosphorylation of platelet-derived growth factor receptor (PDGFR) and subsequent cell growth. Conversely, antioxidants, for example, *N*-acetyl cysteine (NAC), interfere with growth factor-induced cell proliferation, such as in skin fibroblasts and vascular smooth muscle cells. Binding of growth factors, such as epidermal growth factor (EGF) and platelet-derived growth factor (PDGF), to their cognate receptors has been shown to stimulate the production of ROS in responsive cells, such as HeLa cervical carcinoma cells and Rat-1 fibroblasts, respectively. In this regard, membrane-bound NAD(P)H oxidases play an important role in the production of ROS in that stimulation of PDGFR by PDGF leads to increased NAD(P)H oxidase activity via Rac1 activation and correlates with increased ROS production as seen in hepatic stellate cells. A representative scheme for ROS generation by growth factors, for example, PDGF, is shown in Fig. 5.14. Recent data also indicate that steroid hormones that can alter the intracellular level of calcium can induce the production of ROS by altering the phosphorylation status of cytochrome *c* oxidase present in mitochondria. Dephosphorylation of cytochrome *c* oxidase correlates with increased mitochondrial membrane potential and $O_2^{\cdot-}$ generation. Thus, steroid hormones might alter the mitochondrial membrane potential to generate ROS.

5.4.B Phosphatases Are Prime Targets for ROS During Growth Stimulation

Considering the high specificity of ligand-induced receptor activation through ROS production and the short half-life of ROS, it is apparent that ROS molecules inactivate a set of phosphatases in the vicinity of receptors; that is, the receptor-bound phosphatases may be the prime target. This has become evident from the studies on oxidation of protein tyrosine phosphatases, including RPTP- α , SHP-2, MKPs, and PTP-1B, which have been reported to be inactivated upon treatment of cells with H_2O_2 . Treatment of NIH3T3 cells with growth factors, such as EGF and PDGF, or oxidants, such as H_2O_2 , leads to inactivation of PTP-1B (Fig. 5.14) through formation

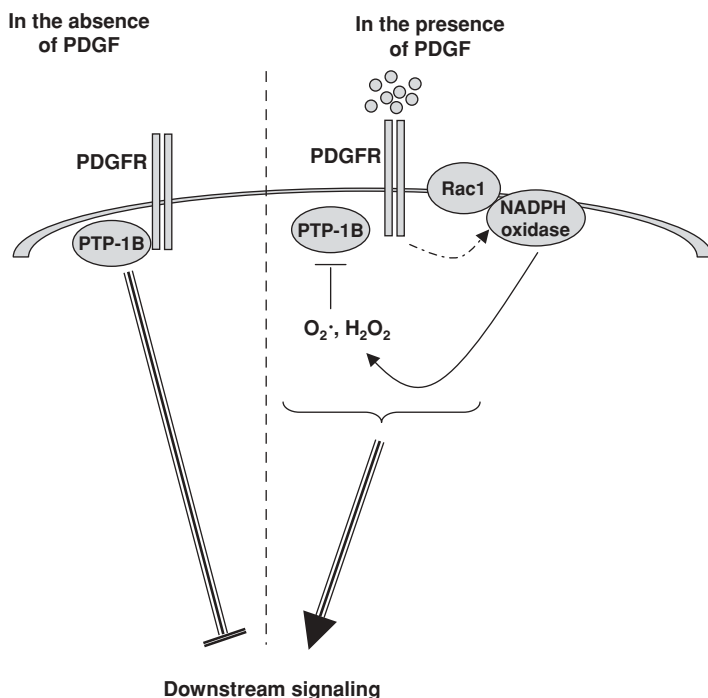


Figure 5.14. The role of ROS molecules in growth factor signaling through phosphatase inactivation is schematically represented. In the absence of growth factors such as PDGF, phosphatases such as PTP-1B are bound to PDGFR, resulting in its inactivation by dephosphorylation. Binding of PDGF to PDGFR leads to activation of membrane-bound NAD(P)H oxidase associated with Rac1. Activation of this complex leads to increased production of ROS molecules, such as $O_2^{\cdot-}$ and H_2O_2 that oxidize PTP-1B, leading to its inactivation. This results in activation of PDGFR by increased phosphorylation and subsequent flow of growth stimulatory signals.

of cysteine sulfenic acid in its active site. Interestingly, this reaction is reversed through GSH-mediated reduction of oxidized phosphatases, ensuring a regulatory mechanism for controlling growth factor receptor signaling. Many electron-rich amino acids, such as cysteine, methionine, histidine, tryptophan, and tyrosine, which are present in the active sites of many phosphatases, are easily susceptible to oxidation that leads to the inactivation of these phosphatases, impairing their ability to bind and/or dephosphorylate target receptors.

Another way by which ROS can interfere with cell signaling is through the oxidation of antioxidant proteins, such as thioredoxin and peroxiredoxin, which are normally bound to kinases, such as apoptosis signaling kinase 1 (ASK1). Binding of ASK1 by thioredoxin inhibits the activity of the kinase. When thioredoxin is oxidized, its binding to ASK1 is disrupted, which results in ASK1 activation. Induction of dimerization of phosphatases by oxidation, such as RPTP- α that leads to its inactivation, also represents a mechanism of phosphatase inactivation by ROS. Thus,

it could be envisaged that in a given cell where ROS molecules favor cell proliferation, accumulation of ROS due to their overproduction or reduced degradation could inactivate the growth-inhibitory phosphatases and, thus, activate the growth-stimulatory kinases.

5.4.C Uncontrolled Production of ROS Is Carcinogenic

In general, carcinogenesis is a multistep process that includes initiation, promotion, and progression as observed in many animal experiments using chemical and physical carcinogens. Initiation includes formation of a mutated, precancerous cell that possesses one or many of the altered genes coding critical tumor suppressive mechanisms. Promotion involves the clonal expansion of the precancerous cell to form a localized microneoplasia that slowly expands into the surrounding tissues. These clonal cells progress into macrolesions due to uncontrolled growth, which then move to other areas of the tissue by a process called metastasis. The diversity of the cancerous tissue arises from the fact that the initiation process can occur at many genes at the same time and in different cells. Furthermore, changes in the expression of many genes can occur at any of the three stages, making the cancerous cells more heterogeneous.

Excessive generation of ROS in cells can occur by stimulation of the otherwise tightly regulated NAD(P)H oxidases on the cell membrane. For example, in prostate cancer tissue specimens, H_2O_2 level was higher in the cancerous areas compared to the noncancerous areas, which correlated with the increased expression of NAD(P)H oxidase 1. Since activated receptor protein tyrosine kinase (RPTK) can increase the production of ROS through Rac1-associated NAD(P)H oxidase, aberrant levels of NAD(P)H oxidases and activation of RPTKs due to overproduction of their ligands or RPTK per se or down regulation of its regulatory phosphatases could play a key role in this aspect of carcinogenesis. Additional sources of ROS are the electron transport chain in mitochondria and other cellular oxidases, such as xanthine oxidase. In certain cases, mitochondrial production of $\text{O}_2^{\cdot-}$ can reach very high levels, up to $10 \mu\text{M}$. Furthermore, in the case of reduced antioxidant activities that degrade $\text{O}_2^{\cdot-}$ and H_2O_2 , such as superoxide dismutase, glutathione peroxidase, and catalase, increased ROS molecules induce mitochondrial and nuclear DNA damages. However, the molecular mechanism by which uncontrolled production of ROS is initiated in cells that leads to their transformation is currently unknown. Therefore, aberrant regulation of ROS production may result in excess cellular growth leading to malignant transformation.

Apart from the activation of RPTKs, ROS can also have an effect on other signaling proteins, including transcription factors and apoptotic signaling mediators, which are discussed in Chapter 4. ROS has been shown to increase the transcriptional activities of transcription factors, for example, NF- κ B or AP-1 complexes. These transcription factors are closely linked to both cell survival and cell growth whose activation could lead to carcinogenesis. Accumulating evidence further suggests that oxidative stress is equally important in the initiation and in the progression of cancer; however, the involvement of ROS in either step may depend on the cell type. Further studies are needed to address these issues.

5.4.D ROS Can Induce Carcinogenic DNA and Protein Adducts

In a respiring cell, accumulation of ROS is inevitable, despite its tightly regulated production and clearance, and this causes increased production of DNA and protein adducts. DNA and protein adducts are formed by the reaction of reactive products, such as hydroxy radical or lipid peroxidation products, including malondialdehyde, crotonaldehyde, and 4-hydroxy-2-nonenal, to DNA and protein molecules as discussed in Chapter 3 Section 3.4.B and in Section 5.2. Formation of DNA adducts favors DNA mutations that are passed on at a high rate to daughter cells in a highly proliferative cell population. Over 100 DNA modifications have been identified in cells, including DNA breakage, cross-links, purine and pyrimidine modifications, and alterations in deoxyribose, which all can lead to inhibition of transcription, activation of aberrant or altered signaling pathways, genomic instability, and errors in DNA replication.

The best characterized DNA and protein adducts in relation to cancer are 8-hydroxy guanosine (OH8dG) and 4-hydroxy nonenal adducts (Table 5.5). OH8dG favors a high mutation rate, for example, C to A and G to T transversions. The presence of G to T transversions in the coding sequences of functional genes in many cancers correlates with the dose-dependent induction of transformation *in vitro* by OH8dG. Malondialdehyde–DNA adducts, such as methyl nucleosides including M1G, M2G, M1dA, M3dA, M1dC, and M3dC, can induce mutations and promote tumorigenesis and are frequently seen in liver, pancreas, breast, and leukocyte tissues and the association of these adducts with cancer risk is almost 40%.

Most commonly identified aldehyde–protein adducts in many epithelial cancers, including prostate and breast cancers, are 4-hydroxy nonenal adducts. Malondialdehyde–acetaldehyde hybrid–protein adducts have also been suggested to be associated with higher cancer risk. For example, malondialdehyde–protein adducts are found to be twofold higher in normal breast epithelia from women with cancerous breast tissue compared to normal breast epithelia from women with healthy breast tissues. Immunohistochemical analysis of protein adducts and other biochemical and enzymatic assays in normal versus cancerous tissues have also opened up the possibility of protein adducts serving as markers for identifying patients with a high risk of cancer.

TABLE 5.5. DNA and Protein Adducts in Different Cancerous and Inflammatory Lesions

Adducts	Related Diseases
8-Hydroxy guanosine	Breast, lung, colorectal, prostate, and pancreatic cancers
1-Methyl guanosine	Lung, breast, colorectal, and prostate cancers
2-Methyl guanosine	Colorectal cancer
5-Methyl uridine	Colorectal cancer
Malondialdehyde–acetaldehyde	Liver injuries, alcohol-induced muscle injuries
4-Hydroxy nonenal	Renal, prostate, and breast carcinomas
4-Amino-biphenyl–hemoglobin	Higher in respiratory tract of smokers than in nonsmokers
3-Nitro-L-tyrosine	Colorectal cancer

A relation between adduct formation due to ROS and carcinogenesis can be found in hormone-induced epithelial cancers. Hormones that can affect mitochondrial membrane potential and enzyme activities governing redox reactions are proposed to play a critical role in the initiation of cancer. For example, androgens and estrogens are considered to be important etiological factors for prostate and breast cancer, respectively. Apart from their role in RPTK activation and cell proliferation through ROS production, as described earlier, DNA or protein adducts induced by steroid hormones through increased production of ROS could also play a key factor in cancer initiation.

5.4.E ROS Can Affect DNA Methylation and Gene Expression

Apart from induction of different mutations by DNA adducts, ROS can also affect the methylation pattern of different genes that are closely linked to cell growth. Methylation of DNA is a major mechanism for regulating gene expression in cells. The promoter is either hypomethylated or hypermethylated to turn on or turn off gene expression. In other words, DNA methylation inversely correlates with gene expression. Increased ROS in cells is associated with hypomethylation of promoter elements of many genes. Formation of DNA adducts, such as OH8dG, can interfere with the ability of methyltransferases to methylate DNA. Thus, it is foreseeable that increased ROS production in cells may favor promoter hypomethylation of an oncogene that codes for a growth-stimulatory kinase or a transcription factor. This, in addition to the mutational silencing of tumor suppressor genes, may trigger the development of cancer and favor progression.

5.4.F Mitochondrial DNA Mutations Are Induced by ROS

Most studies have focused on nuclear DNA damage and mutations as a predisposing event for carcinogenesis. Nevertheless, results of several studies have implied that mitochondrial DNA (mtDNA) mutations may also contribute to the outcome of carcinogenesis. In fact, mtDNA is extremely susceptible to ROS-induced mutations. The absence of histones in the mitochondrial genome, the close proximity of mtDNA to the ROS-producing machinery, and the limited DNA proofreading ability in mitochondria together make mtDNA vulnerable to adduct formation and mutations. This is consistent with the observation that the prevalence of mutations in mtDNA is twofold higher than in nuclear DNA. Mutations in the mtDNA encoding electron transport chain complexes have been reported in many human cancers. Such mutations may contribute to the aberrant production of ROS, which could either accelerate mutagenesis in nuclear DNA by adduct formation or activate the transcriptional factors and/or kinases that affect cell survival and growth, resulting in the formation of cancer.

5.4.G Clinical Trials on Antioxidant Supplementation Against Cancer

Large scale clinical trials conducted in the past decade have reached different conclusions on the effectiveness of antioxidants toward cancer prevention. These studies have concluded that antioxidants, for example, β -carotene, have different effects,

depending on the population. The first large scale Chinese Cancer Prevention Study on antioxidants and cancer risk was published in 1993 and showed that a combination of β -carotene, selenium, and vitamin E significantly decreased the incidence of gastric cancer in Chinese men and women who were at the risk of developing cancer. However, in 1994, it was reported that in Finnish male smokers, the lung cancer rate is increased with β -carotene treatment. The 1999 Women's Health Study on the effect of β -carotene in the prevention of cancer and cardiovascular diseases among women of age 45 years or more reported no benefit or harm in apparently healthy subjects. These studies are further complicated by the fact that some antioxidants, depending on the conditions, can function as prooxidants (i.e., favor the generation of ROS).

These studies make it difficult to recommend an appropriate combination of antioxidants to patients undergoing cancer treatment or prevention regimen. Nevertheless, it is evident that the use of antioxidants may reduce the efficacy of cancer therapeutic protocols that induce apoptosis through high levels of ROS production in cancer cells, such as radiation and chemotherapy. Based on our current knowledge, it is premature to generalize about the use of antioxidants for cancer prevention and treatment. Several large scale clinical trials are currently underway. For example, a Phase III randomized selenium and vitamin E cancer prevention trial (SELECT) with 32,400 participants for prostate cancer is in progress. Similar large scale clinical trials are being undertaken for other types of cancer including colorectal, breast, and lung cancers. Results from these trials are expected to provide valuable data that will contribute to our understanding of the role of antioxidants in cancer prevention and treatment (See Box 5.1).

BOX 5.1 ANTIOXIDANT SUPPLEMENTS—ARE THEY EFFECTIVE IN CANCER PREVENTION?



Antioxidants have become commonly used dietary supplements in American diets. Antioxidants can be defined as any dietary chemical that can decrease

the adverse effect of reactive oxygen or nitrogen species on normal physiological processes. Some well-known dietary antioxidants occur naturally in fruits, vegetables, and even in meat, including poultry, and fish. β -carotene (carrots and other orange foods), selenium (meat), vitamin A (liver, egg yolks, and milk), vitamin C (citrus fruits), vitamin E (nuts, fish, and corn oil), genistein (soybean), and epigallocatechin-3-gallate (green tea) are some of the most commonly known antioxidants.

Epidemiological studies indicate that the intake of diets rich in antioxidant molecules, especially the Mediterranean diet, inversely correlates with cancer incidence. It is thus intriguing to ask whether antioxidant supplementation can really function as a valuable preventive measure against cancer. According to the National Cancer Institute, cell culture and animal studies suggest that antioxidants may slow down or possibly prevent the development and progression of cancer. This is supported by many *in vitro* studies that dietary antioxidants, such as vitamin E, selenium, vitamin C, and β -carotene, have a potential value against various cancers, including prostate and colon cancer. Clinical trials based on antioxidants for cancer prevention have been conducted and many are still in progress.

SELECTED REFERENCES

1. Tonks, N.K. (2005). Redox: revisiting PTPs and the control of cell signaling. *Cell* 121:667–670.
2. Klaunig, J.E., and Kamendulis, L.M. (2004). The role of oxidative stress in carcinogenesis. *Annu. Rev. Pharmacol. Toxicol.* 44:239–267.
3. Howes, R.M. (2006). The free radical fantasy: a panoply of paradoxes. *Ann. NY Acad. Sci.* 1067:22–26.

5.5 OXIDATIVE STRESS AND THE HOST–PATHOGEN INTERACTION

GREG A. SOMERVILLE

*Redox Biology Center and Department of Veterinary and Biomedical Sciences,
University of Nebraska, Lincoln, Nebraska*

The philosophy of Taoism holds that a single great principle governs the universe, the Tao, which can be divided into two opposing, yet balanced, forces; yin and yang. Much like the Tao, an infectious disease can be divided into two balanced but opposing forces; the host and the pathogen. The first line of defense in the host is a physical barrier created by the skin; however, once this barrier is breached the innate immune response is critical to overcoming the infection. Central to the innate immune response are professional phagocytic cells, the most abundant of which are neutrophils. Neutrophils are highly motile polymorphonuclear white blood cells that phagocytose, kill, and digest bacteria. In addition to neutrophils, the innate immune

system contains a second professional phagocytic cell, the macrophage, which serves to bridge the innate immune response and the humoral immune response. As with yin and yang, there is balance; some bacteria have evolved and/or acquired genetic elements allowing them to evade the host immune response and survive the host's killing mechanisms. Due to the importance of the innate immune response in bacterial pathogenesis, the first part of this section focuses on the role of redox biology in the innate immune response to bacterial pathogens, while the remainder of the section is devoted to the bacterial response to host defenses.

5.5.A Neutrophils and the Innate Immune Response

The innate immune system is chiefly comprised of complement, macrophage, and neutrophils. Activation of the complement system initiates a proteolytic cascade producing chemoattractants that recruit proinflammatory and phagocytic white cells to the site of infection. Phagocytic cells engulf, kill, and digest bacteria, and in the case of macrophage, they display the digested products in class I or II major histocompatibility complexes to activate cells of the humoral immune system. Of the professional phagocytic cells, neutrophils constitute 50–70% of circulating white blood cells and are a critical component of the innate immune response—a point easily observed in neutropenic individuals. People with neutropenia have abnormally low numbers of neutrophils in their blood, resulting in frequent and severe bacterial infections. Neutrophil-mediated killing of bacterial pathogens is a multistep process, involving attachment, phagocytosis, killing, and digestion.

Attachment of a neutrophil to a bacterium is usually mediated by a receptor for either complement (C3b), the Fc portion of an antibody, lipopolysaccharide, or other opsonin. Following attachment, the neutrophil cell membrane rapidly invaginates around the bacterium, resulting in the encapsulation of the bacterium into an intracellular phagosome. Granules (azurophil, specific, or gelatinase) in the neutrophil cytosol fuse with the phagosome releasing their contents into the phagosomal compartment (Fig. 5.15) creating a bactericidal environment. A fundamental constituent of this bactericidal environment are ROS produced by NADPH oxidase. NADPH oxidase is a multicomponent enzyme complex comprised of cytosolic proteins (p40^{phox}, p47^{phox}, p67^{phox}, and Rac 1 or Rac 2) and the membrane-associated cytochrome *b* (p22^{phox} and gp91^{phox}) that catalyzes the conversion of O₂ into O₂^{•-}. Upon phagocytosis of a bacterium, NADPH oxidase assembles at the phagosomal membrane and transports electrons from NADPH on the cytoplasmic side of the phagosomal membrane to oxygen inside the phagosomal compartment to produce large amounts of O₂^{•-}, a process requiring both FAD and heme (Fig. 5.16). It is thought that the low pH of the phagolysosome facilitates the rapid dismutation of the O₂^{•-} into the more stable H₂O₂; however, the presence of superoxide dismutase in the neutrophil cytosol and bacterial derived superoxide dismutase may also contribute to this reaction. H₂O₂ undergoes a halogenation reaction to produce hypochlorous acid (HOCl), a reaction catalyzed by myeloperoxidase. Myeloperoxidase is a major constituent of the azurophil granule and is released into the phagolysosome during granular fusion. Native myeloperoxidase is a heterodimer composed of two identical heavy–light protomers derived from

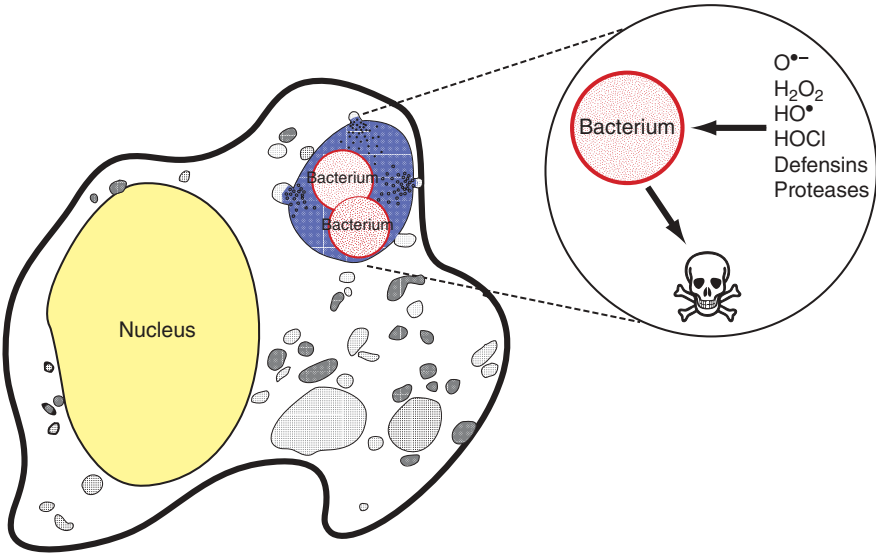


Figure 5.15. A schematic representation of neutrophil-mediated killing of bacteria.

a single gene. The mature protein consists of the two heterodimers (heavy α subunit (57 kD) and light β subunit (12 kD)) linked via a disulfide bond between the heavy subunits, two heme molecules, and mannose-rich side chains. It is this mature form of myeloperoxidase that catalyzes the oxidation of chloride with H_2O_2 to generate the bactericidal HOCl . Of note, HOCl can react with the $\text{O}_2^{\cdot-}$ to form the highly reactive hydroxyl radical ($^{\cdot}\text{OH}$); however, the significance of this reaction is debatable due to its extreme reactivity and very low concentration in activated neutrophils.

5.5.B Bacterial Targets of Oxidative Damage

Bacteria ingested into a phagosome are rapidly exposed to an oxidizing environment capable of killing them; hence, considerable effort has focused on targets of and mechanisms by which ROS damage bacterial macromolecules. Ostensibly, all

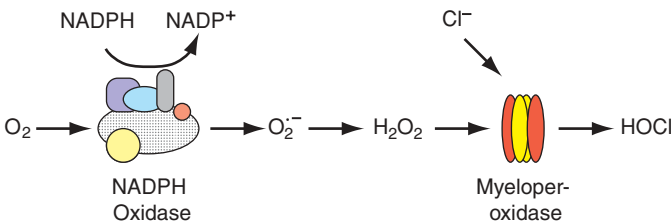


Figure 5.16. NADPH-dependent pathway for the generation of antimicrobial ROS and hypochlorous acid.

oxidizable moieties in a bacterium are potential targets of ROS; however, certain structures are more prone to oxidative inactivation than others. A brief summary of some of the targets of oxidative damage are discussed in the following section.

5.5.B1 Iron–sulfur Clusters The observation that aerobic growth of bacterial superoxide dismutase mutants required supplemental amino acids to grow suggested oxidative stress inhibited amino acid biosynthesis. This oxidative inactivation of amino acid biosynthesis led investigators to focus on a class of dehydratase enzymes containing iron–sulfur clusters in their active sites. In these iron–sulfur cluster-containing enzymes, three conserved cysteinyl residues bind three of the iron atoms and the fourth iron atom is held in place by a molecule of substrate or water. Because the fourth iron atom is not bound to a cysteinyl residue and is exposed in the catalytic site, it is highly susceptible to oxidative inactivation. Oxidation of the fourth iron atom creates an unstable cluster, resulting in the reversible decomposition of the iron–sulfur cluster center and loss of enzymatic function. Two iron–sulfur cluster-containing enzymes are involved in the tricarboxylic acid (TCA) cycle: aconitase and fumarase. One function of the TCA cycle is to supply biosynthetic intermediates for amino acid synthesis (i.e., oxaloacetate, α -ketoglutarate, and succinyl-CoA); therefore, inactivation of iron–sulfur cluster-containing proteins can account for some of the amino acid auxotrophies in the superoxide dismutase mutants.

5.5.B2 DNA Damage Oxidative stress-induced release of iron from iron–sulfur clusters creates an intracellular environment permissive to Fenton chemistry. The Fenton reaction generates the highly reactive $\cdot\text{OH}$ from ferrous iron and H_2O_2 . The $\cdot\text{OH}$ will react with virtually any molecule that it encounters; hence, to induce damage it must be in close proximity to its cellular target. DNA is a negatively charged molecule that attracts positively charged molecules, like Fe^{2+} ; hence, charge–charge interaction brings iron in close proximity to DNA and increases the local concentration of $\cdot\text{OH}$ generated by the Fenton reaction that can react with DNA, inducing lethal and nonlethal mutations.

5.5.B3 Sulfhydryl Groups Thiolate anions can be oxidized to sulfenic acid by H_2O_2 . Sulfenic acid reacts with free sulfhydryls to form disulfide bonds. In nonoxidatively stressed bacteria, disulfide bond formation does not present a significant problem due to the presence of the GSH and thioredoxin systems that effectively reduce disulfide bonds (discussed in Chapter 3). However, a large oxidative burst can overwhelm bacterial defense mechanisms, resulting in the formation of disulfide bonds, loss of protein function, and/or protein aggregation. Because of the potential deleterious effects of intracellular disulfide bond formation, bacteria have evolved sensing mechanisms that detect disulfide bond formation to modulate the oxidative stress response.

5.5.C Regulating the Oxidative Stress Response

A consequence of the rapid growth rate of bacteria is that they must adapt quickly to changing environmental conditions or risk death; hence, bacteria have evolved very

sensitive mechanisms to detect environmental changes. Interestingly, the mechanisms that bacteria have evolved to sense oxidative stress often utilize the targets of oxidative stress as the molecular switches. For instance, iron–sulfur clusters are targets of oxidative inactivation but are also critical for sensing oxidative stress by SoxR; similarly, oxidative stress induces disulfide bond formation, yet intraprotein disulfide bonds are thought to be essential for sensing by OxyR. In addition to these proteins, many others exist to regulate the response of bacteria to oxidative stress, including BosR, PerR, Sigma S, and Sigma B.

5.5.C1 SoxR One component of the enteric bacterial oxidative stress-sensing network is the $O_2^{\cdot -}$ response regulator SoxR. SoxR is a transcriptional activator of the *soxS* gene, which encodes a transcriptional regulator of more than 60 genes involved in the bacterial response to oxidative stress, such as superoxide dismutase (*sodA*), aconitase A (*acnA*), and fumarase (*fumC*). *In vitro*, SoxR forms a homodimer, with each monomer possessing a [2Fe–2S] iron–sulfur cluster. *In vivo* studies have demonstrated that the [2Fe–2S] iron–sulfur cluster is in a reduced state; however, upon treatment of whole cells with methyl viologen, the two iron–sulfur clusters are oxidized to $[2Fe-2S]^{2+}$. The SoxR dimer binds immediately upstream of the *soxS* gene but will only activate transcription of *soxS* when the iron–sulfur clusters are in the oxidized state. Upon removal of the oxidative stress, the iron–sulfur clusters rapidly revert to the reduced state (presumably due to the action of an unknown reductase), inactivating SoxR and repressing transcription of *soxS*.

5.5.C2 OxyR While SoxR detects $O_2^{\cdot -}$ and NO, OxyR is primarily responsible for regulating the bacterial response to H_2O_2 . Similar to SoxR, the mechanism OxyR utilizes to detect H_2O_2 relies on a target of oxidative damage, in this case it is oxidation of cysteinyl sulfhydryls. OxyR is a 34 kDa protein with six cysteine residues, which forms a DNA binding homotetramer regulating more than 20 genes involved in the response to H_2O_2 (e.g., catalase, alkyl hydroperoxide reductase, and Dps (DNA-binding protein from starved cells)). While the mechanism of OxyR activation remains controversial, it is known that one cysteine residue (Cys199) is critical for detecting H_2O_2 stress. One proposed mechanism of OxyR activation involves oxidative stress inducing intraprotein disulfide bond formation between Cys199 and Cys208, resulting in a conformational change that permits binding to DNA. Upon removal of H_2O_2 stress, GSH or glutaredoxin reduces the protein–glutathione mixed disulfide bond, converting OxyR to the inactive state. A second proposed mechanism for OxyR activation relies solely on the oxidative state of Cys199. In this mechanism, activation of OxyR requires oxidation of Cys199 to a sulfenic acid or to a mixed disulfide state with GSH. The mechanism of reversion to an inactive state is the same as in the first model, in that it requires reducing the sulfenic acid to a thiol.

5.5.C3 Aconitase Aconitase is a TCA cycle enzyme catalyzing the reversible isomerization of citrate to isocitrate. The enzymatic activity of aconitase is mediated by an essential [4Fe–4S] cluster that is highly susceptible to inactivation by oxygen radicals. Oxidative loss of the fourth Fe atom results in the reversible inactivation of

aconitase and the TCA cycle. The remaining iron atoms in the iron–sulfur cluster can be lost or removed, generating the apoconitase form of the enzyme. Eukaryotic organisms have mitochondrial and cytoplasmic aconitase activity. The cytoplasmic aconitase activity is caused by the iron-responsive protein-1 (IRP-1), an mRNA binding protein that post-transcriptionally regulates the synthesis of iron-regulated proteins. Thus, cytosolic aconitase is a bifunctional protein. Similarly, it has been demonstrated that aconitase from *Bacillus subtilis* and *E. coli* bind, in an iron-dependent fashion, to structural elements in mRNAs. These observations established bacterial aconitase, like eukaryotic cytosolic aconitase/IRP-1, as a bifunctional protein. Of interest, one post-transcriptionally regulated target in *E. coli* is the mRNA encoding superoxide dismutase; hence, aconitase creates a direct link between the bacterial metabolic status and the oxidative stress response.

5.5.D The Oxidative Stress Response

Bacteria respond to oxidative stress by synthesizing ROS scavenging enzymes and small molecules. Mutants lacking ROS scavenging enzymes (i.e., catalase, superoxide dismutase, alkyl hydroperoxide reductase, or glutathione peroxidase) are attenuated in virulence, more susceptible to neutrophil killing, and/or have decreased resistance to antibiotics and stress.

5.5.E Evasion of the Innate Immune Response

Neutrophils and macrophages attach to, phagocytose, kill, and digest bacteria that breach the physical barrier of the skin. Therefore, if bacteria can interrupt this sequence of events, they can circumvent a major component of the innate immune response and potentially establish an infection. The mechanisms that bacterial pathogens use to circumvent the host innate immune system are as varied as the pathogens themselves; hence, this section can only provide a limited number of examples of these mechanisms.

5.5.E1 Blocking Attachment Neutrophils and macrophages attach to a bacterium via a receptor for either complement (C3b), the Fc portion of an antibody, lipopolysaccharide, or other opsonin. Activation of the complement system occurs when factor C3 is cleaved by C3 convertase into C3a and C3b. Factor C3b covalently attaches to the surface of an invading bacterial pathogen, creating a ligand on the bacterial surface that is recognized by a C3b receptor on a professional phagocytic cell. Attachment of the phagocytic cell to the bacterium induces phagocytosis and killing of the pathogen; therefore, it is not surprising that bacteria have evolved mechanisms to prevent complement activation. *Staphylococcus aureus* secretes a 9.8 kDa protein (staphylococcal complement inhibitor) that stabilizes C3 convertase, preventing the deposition of C3b onto the bacterial surface and inhibiting phagocytosis. In addition to C3b, binding of antibodies to bacterial surface components can target bacteria for phagocytosis. The Fab portion of an antibody binds to bacterial-associated antigens exposing the Fc portion of an antibody to receptors on the surface of macrophages and

neutrophils. Binding of the phagocytic cell Fc receptor to the Fc portion of an antibody induces phagocytosis and subsequent killing of bacterial pathogens. To counter this, *S. aureus* produce a cell wall-anchored protein known as protein A that binds to the Fc portion of antibodies, preventing the interaction of the Fc receptor with its ligand.

5.5.E2 Inhibiting Phagocytosis Attachment of a professional phagocytic cell to a bacterial or host-derived ligand on the surface of a bacterium induces the phagocytic cell to engulf that bacterium. This is a regulated, active process requiring energy and cytoskeletal rearrangements, providing pathogenic bacteria many potential targets with which to interrupt this process. *Pseudomonas aeruginosa* inhibits phagocytosis by inactivating the regulatory cascade that initiates phagocytosis. Using a type III secretion system, *P. aeruginosa* directly translocates exoenzyme S (ExoS) and exoenzyme T (ExoT) into the cytoplasm of host cells. In the cytoplasm, ExoS ADP-ribosylates small GTP binding proteins (e.g., Ras, Ral, Rab, or Rac1), preventing activation of the signaling cascade and subsequent phagocytosis. Like ExoS, ExoT is translocated into the host cytosol by the type III secretion system where it ADP-ribosylates Crk, a regulator required for activation of phagocytosis.

5.5.E3 Preventing Bacterial Killing Professional phagocytic cells engulf and encapsulate bacteria into a phagosomal vacuole; however, the environment of a phagosome is not bactericidal until late endosomes or lysosomes and/or granules release their contents into the phagosome. Therefore, it is not surprising that some bacteria have evolved mechanisms to prevent the fusion of cytosolic vesicles with the phagosome. The best example of a bacterium using this strategy comes from *Mycobacterium tuberculosis*, the causative agent of tuberculosis. *M. tuberculosis* organisms are phagocytosed by macrophages but they are not killed by macrophages because *M. tuberculosis* inhibits fusion of the phagosome with lysosomes. Preventing phagosomal maturation is a complex process requiring both host components (i.e., coronin 1 and phosphatidylinositol 3-phosphate, a phospholipid) and bacterial components (i.e., mannose-capped lipoarabinomannan and mycobacterial protein kinase G). As a consequence of preventing fusion of lysosomes with the phagosome, *M. tuberculosis* creates an immunologically protected niche in which to grow. This intracellular niche complicates clearance of the bacterial infection by the immune system and hinders antimicrobial therapy, a contributing cause in the estimated 2 billion human *M. tuberculosis* infections worldwide.

SELECTED REFERENCES

1. Klebanoff, S.J. (2005). Myeloperoxidase: friend and foe. *J. Leukoc. Biol.* 77:598–625.
2. Imlay, J.A. (2002). How oxygen damages microbes: oxygen tolerance and obligate anaerobiosis. *Adv. Microb. Physiol.* 46:111–153.
3. Carlizoz, A., and Touati, D. (1986). Isolation of superoxide dismutase mutants in *Escherichia coli*: Is superoxide dismutase necessary for aerobic life? *EMBO J.* 5:623–630.

4. Greenberg, J.T., Monach, P., Chou, J.H., Josephy, P.D., and Dimple, B. (1990). Positive control of a global antioxidant defense regulon activated by superoxide-generating agents in *Escherichia coli*. *Proc. Natl. Acad. Sci.* 87:6181–6185.
5. Alèn, C., and Sonenshein, A.L. (1999). *Bacillus subtilis* aconitase is an RNA-binding protein. *Proc. Natl. Acad. Sci.* 96:10412–10417.

Specialized Methods

- 6.1. Mass Spectrometry Applications for Redox Biology
 - 6.1.A. Mass Spectrometer
 - 6.1.B. Applications of Mass Spectrometry
 - 6.1.C. Hydrogen Exchange Mass Spectrometry
- 6.2. Electron Paramagnetic Resonance (EPR) for the Redox Biochemist
 - 6.2.A. Introduction to Magnetic Resonance Spectroscopy
 - 6.2.B. Basic EPR Theory
 - 6.2.C. Appearance of the EPR Spectrum
 - 6.2.D. The EPR Experiment
 - 6.2.E. The Conventional EPR Spectrometer: detection of the Signal
 - 6.2.F. Sensitivity and Saturation in EPR
 - 6.2.G. Measuring the Concentration of Spins
 - 6.2.H. Nuclear Hyperfine and Spin–Spin Interactions
- 6.3. Redox Potentiometry
 - 6.3.A. Midpoint Potential
 - 6.3.B. Redox-Linked Processes
 - 6.3.C. Potentiometric Technique
- 6.4. Bioinformatics Methods to study Thiol-Based Oxidoreductases
 - 6.4.A. Identification of Redox-Active Cysteines in Proteins
 - 6.4.B. Cysteine-Based Redox Motifs
 - 6.4.C. Conserved Cysteines in Metal-Binding Proteins
 - 6.4.D. Secondary Structure Context of Redox-Active Cysteines
 - 6.4.E. Structure Modeling
 - 6.4.F. Comparative Sequence Analysis of Thiol-Based Oxidoreductases
- 6.5. Electrophysiology
 - 6.5.A. Ion Channel Physiology
 - 6.5.B. Electrophysiology Part Two
- 6.6. Methods to Detect Reactive Metabolites of Oxygen and Nitrogen
 - 6.6.A. Detection of the Superoxide Anion Radical
 - 6.6.B. Detection of Hydrogen Peroxide
 - 6.6.C. F2-Isoprostanes as Indicators of Lipid Peroxidation *in Vivo*

- 6.6.D. Measurement of the GSSG/GSH Redox Couple in Cells and Tissue
- 6.6.E. Methods to Detect NO and Its Oxidized Metabolites *in Vitro and in Vivo*
- 6.6.F. Detection of S-Nitrosothiols by Colorimetric and Fluorimetric Methods
- 6.4.G. Is the Presence of 3-Nitrotyrosine a Specific Footprint for Peroxynitrite?

6.1 MASS SPECTROMETRY APPLICATIONS FOR REDOX BIOLOGY

ASHRAF RAZA

Redox Biology Center and Department of Biochemistry, University of Nebraska, Lincoln, Nebraska

JOHN R. ENGEN

Department of Chemistry and Chemical Biology, Northeastern University, Boston, Massachusetts

Mass spectrometry is a technique that is used to identify and differentiate molecules on the basis of their mass. Mass spectrometry has been called the universal detector because almost all types of molecules are amenable to analysis. A few examples include determining adulteration of honey, detecting steroids in athletes, identifying unknown proteins, determining post-translational modifications in proteins, confirming mutations in proteins, quantitating drugs in biological matrices, and measuring the concentration of pollutants in the air. Depending on the application, mass spectrometers are usually coupled to a separation method, that is, gas chromatography and mass spectrometry (GC-MS) or liquid chromatography and mass spectrometry (LC-MS). In this section, the focus is on LC-MS, which is the most useful technique for biological applications, and on the applications of mass spectrometry in redox biology.

6.1.A Mass Spectrometer

There are different types of mass spectrometers for different applications. However, all mass spectrometers share several common features (Fig. 6.1), i.e., inlet, source, analyzer, and detector. Often, several kinds of interchangeable inlets and sources are coupled with an analyzer and detector. The source may operate either at atmospheric pressure or under moderate vacuum ($< 10^{-3}$ torr) but the analyzer and the detector are always under high vacuum ($< 10^{-5}$ torr). The sample is introduced into the inlet and ionized in the source region, the ionized sample molecules are separated on the basis of their mass-to-charge ratio (m/z) in the analyzer, the total ion current of the molecules with different mass-to-charge ratio is measured by the detector, and the data system generates a mass spectrum.

Inlets This part of the mass spectrometer is used to introduce the sample into the source. The sample can be introduced in different ways, for example, with a syringe pump, pico tip, or HPLC, or it may be mixed with a matrix on a probe.

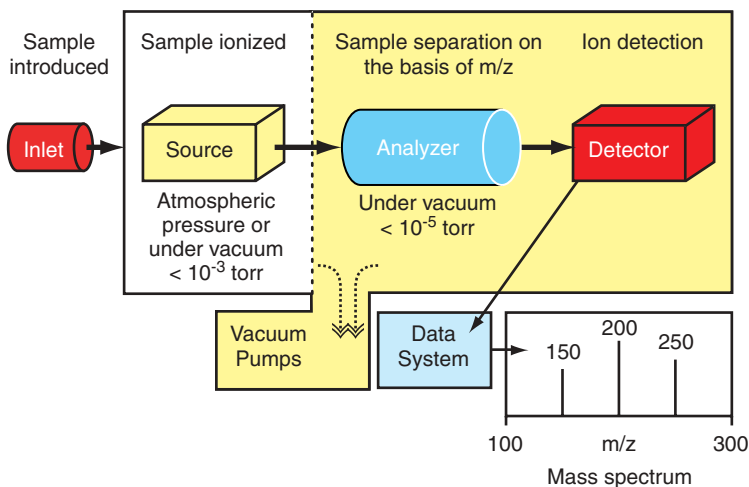


Figure 6.1. Schematic of a typical mass spectrometer.

Sources In order for the mass spectrometer to separate molecules on the basis of their mass-to-charge ratio (see below), the source ionizes and vaporizes the molecules. The choice of the source that converts the sample molecules into ions depends on the nature of the sample. Common sources include EI, CI, MALDI, ESI, APCI, and APPI.

- *Electron Ionization (EI)* This source is used primarily for small molecules. Electrons bombard the sample molecules in the gas phase, ionizing the sample at a sufficiently high energy to break the molecules into fragments. The molecular mass is deduced from the fragmentation pattern.
- *Chemical Ionization (CI)* This source is also used for small molecules but the energy imparted to the sample is much less. Electrons ionize a gas (methane, ammonia), which in turn ionizes the sample molecules.
- *Atmospheric Pressure Chemical Ionization (APCI)* This source is similar to that of regular CI except that ionization occurs at atmospheric pressure in ionized air. APCI cannot be used to ionize large peptides and proteins as it gives only one positive or negative charge to the molecules (see ESI below). APCI is useful for ionizing small molecules in complex mixtures (like biological fluids) because the small molecules undergo ionization, while the larger molecules like proteins do not.
- *Atmospheric Pressure Photo Ionization (APPI)* In this source, light is used to ionize the sample molecules. This source is good for analyzing nonpolar molecules like steroids, which are difficult to ionize with other sources.
- *Electrospray Ionization (ESI)* This source is often coupled to HPLC and uses a high electric field to deposit charge on liquid that is sprayed into a very fine mist. Proteins and peptides undergo ionization in this method and can become multiply charged. Because the mass-to-charge ratio is measured, high molecular weight molecules can be analyzed. Turbo ion spray (TIS),

micro ion spray, and nano spray are modifications of electrospray ionization sources that handle the different flow rates of solvents.

- *Matrix-Assisted Laser Desorption Ionization (MALDI)* This laser source ionizes the sample, which is enmeshed within a matrix that absorbs the energy of the laser and transfers it to the sample. MALDI is used for samples in very complex matrices, has a quick analysis time, and can directly scan tissues. Recent advances in MALDI source design make it possible to couple it directly with an HPLC.

Sources like ESI, APCI, APPI, and MALDI are more commonly used for biological analyses because of the “softer ionization” and ease of automation. Soft ionization does not break up the sample molecules during the analysis, while “hard sources” like EI and CI impart enough energy to cause fragmentation. All of the above-mentioned sources can produce negative or positive ions. Generally, proteins and peptides produce positive ions, while RNA, sugars, or fatty acids produce primarily negative ions.

Analzers Mass analyzers separate molecules on the basis of their mass-to-charge ratio (m/z) and generate the mass spectrum. The separation can occur based on the interaction of the ions with magnetic or electric fields. Some examples of analyzers are sectors, quadrupoles, ion traps, time-of-flight (TOF), or Fourier transform ion cyclotron resonance (FT-ICR). A single analyzer (MS analysis) may be used or several analyzers may be used together (called tandem mass spectrometry or MS/MS). Examples of tandem mass spectrometers include triple quadrupole, quadrupole ion trap, and quadrupole TOF. Only a few of the common analyzers are briefly discussed in this section. For more details on the theory of these analyzers, see the Selected References.

- *Quadrupole* This commonly used analyzer has fast scan speed, has a high upper limit of up to m/z 4000 mass range, is easy to maintain, and is relatively inexpensive. However, it is a low resolution analyzer with low mass accuracy. As a single quadrupole, it can only do MS analyses and not MS/MS analyses.
- *Triple Quadrupole* A combination of three quadrupoles in series, this analyzer is very successful for the quantitation of small molecules and can perform MS and MS/MS analysis. The first quad (Q1) selects the parent ion, the second quad (Q2) breaks the parent ion into several daughter ions using collision energy, and the third quad (Q3) analyzes a particular daughter ion. For the quantitation of small molecules it is most commonly used in the MRM (multiple reaction monitoring) mode, allowing different analytes and their internal standards to be quantified simultaneously. Thus, triple quadrupoles are commonly used in drug development for studying pharmacokinetics and pharmacodynamics.
- *Ion Trap* This analyzer has similar capabilities as the quadrupole in MS mode. However, ion traps can perform MS/MS multiple times (termed MSⁿ). Thus, it can break the parent ion into several daughter ions, choose and then further

fragment a particular daughter ions. This process helps differentiate between two different molecules with the same parent and daughter ion masses after the first MS/MS step. In theory, this process of MS/MS may be performed until there is no more sample left in the trap.

- *Quadruple Ion Trap* This is similar to the triple quadrupole analyzer, but the third quadrupole is replaced with a linear ion trap. In addition to the good quantitation capabilities in MRM mode, it also provides the capability of performing MS/MS on daughter ions, while the triple quad can only perform MS/MS on the parent ions.
- *Quadrupole Time of Flight (Quad TOF)* In this mass spectrometer configuration, the Q3 quad is replaced by a TOF analyzer that measures the time it takes for ions to fly a finite distance. A TOF analyzer can have a resolution of up to 20,000 with very good mass accuracy. The high resolution of this instrument allows accurate determination of the charge state of peptides (see below) and precise identification of unknown molecules. This mass spectrometer is routinely used for proteomics and metabolomics; however, it is generally poorer at quantitation and cannot perform MRM. Quadrupole ion traps and quadrupole time of flight analyzers are discussed further in Section 6.1.B.
- *Detectors* There are several different detectors to detect the ions coming from the analyzers including electron multipliers, Faraday cups, photomultiplier conversion dynodes, high energy dynode detectors, array detectors, and charge detectors. The most common detectors are photomultiplier conversion dynodes and electron multiplier detectors. Detectors transfer the signals to the data system, which in turn processes them into a mass spectrum.

6.1.B Applications of Mass Spectrometry

6.1.B1 Peptide Analysis In electrospray ionization, molecules may become multiply charged. The number of charges (called the charge state) on a peptide may be determined by analyzing the pattern of the isotopes. Because the naturally occurring isotopes all have approximately integer differences between them (e.g., carbon 12 and carbon 13 differ by one mass unit), if the mass differences is 1, the charge state is 1. Thus, if the mass difference between peaks is 0.5, then the charge state is 2 (Fig. 6.2A), while if the mass difference is 0.33, the charge state is 3 (Fig. 6.2B), and so on. For example, the molecular weight of the renin substrate peptide is 1757.93; however, the most abundant peak observed in the electrospray mass spectrum is at 586.980, a triply charged ion (Fig. 6.2B).

The molecular weight of the peptide may be calculated from the spectrum (which provides the m/z and charge state) of the +3 ion by the following equation:

$$\frac{m}{z} = \frac{MW + nH^+}{n^+} \quad (6.1)$$

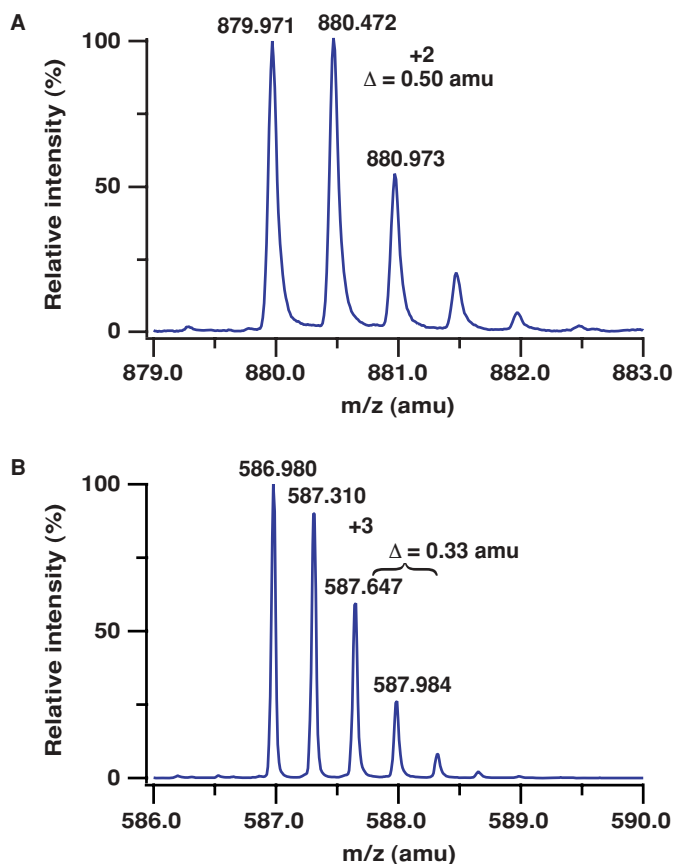


Figure 6.2. Mass spectrum of multiply charged peaks for renin substrate (molecular weight 1758). (A) The doubly charged species, monoisotopic mass m/z 879.971 amu with 0.50 Da mass differences between the isotopic peaks. (B) The triply charged species, monoisotopic m/z of 586.980 amu with 0.33 Da mass differences between the isotopic peaks.

where m/z = the mass-to-charge ratio, MW = the molecular weight of the sample, n = the integer number of charges on the ions, and H = the mass of a proton = 1.008 Da.

$$(m/z) \times 3 = MW + nH^+$$

$$586.980 \times 3 = MW + 3 \times 1.008$$

$$1760.949 = MW + 3.024$$

$$MW = 1760.949 - 3.024 = 1757.92$$

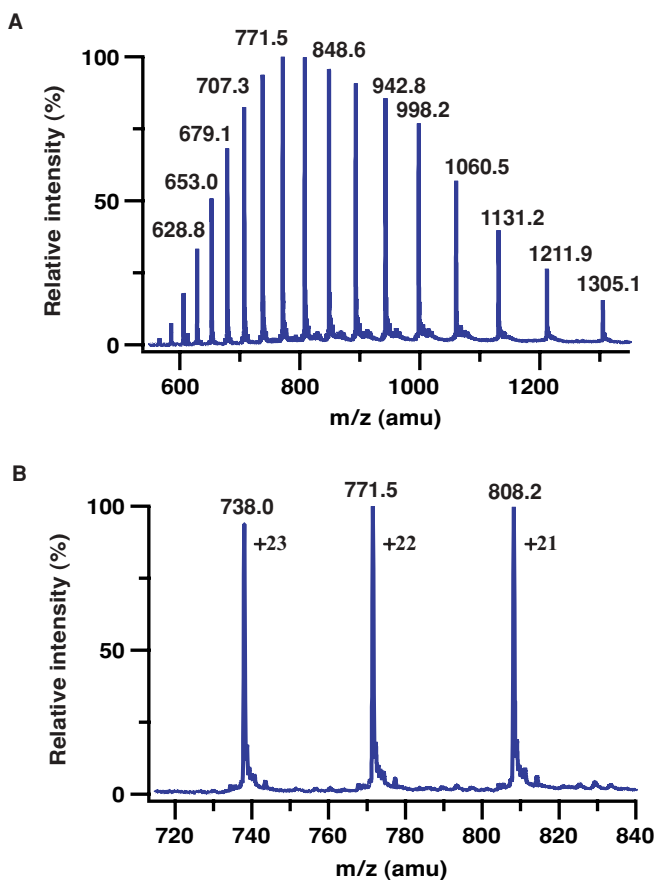


Figure 6.3. Mass spectrum of intact myoglobin. (A) The full m/z range with multiple charge state peaks. (B) The same spectrum as in (a) but zoomed on three peaks with charge states 21–23.

As shown, substituting in the values in the spectrum of renin, a molecular weight of 1758 Da is obtained.

6.1.B2 Intact Protein Analysis ESI permits intact protein analyses as it multiply charges proteins, providing a charge distribution. For example, the mass spectrum of myoglobin (MW = 16,951.0 Da) exhibits a number of peaks, each with different m/z values (Fig. 6.3A); therefore, only two charge states of a particular m/z are needed to determine the mass from the m/z relationship; a few peaks are zoomed in for charge state calculations (Fig. 6.3B). Simultaneous equations (Eq. (6.2)) are first used to determine the charge state of a single m/z . Solving these equations for myoglobin results in 21 charges for m/z 808.2. Once the charge is known for a particular m/z peak, a simple calculation yields the mass.

If m/z 808.2 in the myoglobin spectrum has n charges, then m/z 771.5 will have $n + 1$ charges:

$$808.2 = \frac{(MW + nH^+)}{n} \quad \text{and} \quad 771.5 = \frac{[MW + (n + 1)H^+]}{n + 1} \quad (6.2)$$

These simultaneous equations can be rearranged to exclude the MW term:

$$n(808.2) - nH^+ = (n + 1)771.5 - (n + 1)H^+$$

The number of charges for m/z 808.2 is $771.5/36.7 = 21$. Substituting 21 for the value of n Eq. (6.1) yields the MW of renin:

$$\begin{aligned} 808.2n &= (MW + nH^+) \\ 808.2 \times 21 &= MW + (21 \times 1.008) \\ MW &= 16972.2 - 21.2 = 16,951.0 \end{aligned}$$

6.1.B3 Quantitative Analysis Quantitative analysis is performed when the concentration of a particular compound needs to be determined. For example, pharmacokinetics and pharmacodynamics studies require determination of the exact concentration of a drug compound in a biological fluid, such as blood or urine. To study problems in redox biology, one may wish to determine the change in concentration of GSH, cysteine, and homocysteine in response to oxidative stress. Quantitation is mostly performed using ESI, as MALDI is less accurate. Triple quadrupole mass spectrometers are considered the best choice for the quantitation of compounds. Quantitation of a compound may be done with an external standard; however, the highest accuracy is obtained when the analysis is performed with an internal standard, such as an isotopically labeled (^2H , ^{15}N , etc.) version of the same molecule that is being detected. With isotopically labeled internal standards, losses of the compound during complex extraction procedures can be monitored as can fluctuations in injection volume and ESI response. If an isotopically labeled internal standard is not available, an analogue may be used as an internal standard; however, differences in the properties of the analogue versus the analyte may lead to differences in the level of extraction, ionization, and/or detection.

Quantitation of proteins is a more complicated process than quantifying small molecules and peptides. Several approaches have been used. One is to compare relative rather than absolute concentrations. Alternatively, a signature peptide approach may be used in which a protein is digested using a proteolytic enzyme (e.g., pepsin) into several peptides, one of which (the signature peptide) is isotopically labeled and spiked in all samples before the extraction step. Thus, the quantity of this signature peptide represents the quantity of the protein in the sample. Other approaches like ICAT[®] (isotope-coded affinity tags) and iTRAQ[®] (multiplexed set of four isobaric amine-specific labeling reagents) may also be used; however, they are not discussed here due to space limitations.

6.1.B4 Proteomics and Post-translational Modifications (PTMs) It is often desirable to identify the proteins present in certain cell types and to determine their post-translational modifications, such as phosphorylation, ubiquitination, and acetylation. Post-translational modifications, may be essential for signal transduction, translocation, and other important biological processes. Either in-solution or in-gel digestion of proteins with different proteases (trypsin, AspN) is used, followed by the analysis of the fragments with ESI nano-LC-MS/MS. The masses of the tryptic peptides are searched with a database and confirmed by manual interpretation. Modifications found using one protease may be confirmed by digesting the sample with different proteolytic enzymes.

A similar procedure may be used to determine the oxidation state of cysteines in proteins (Fig. 6.4A–D). In this analysis, samples are treated sequentially with two alkylating agents. The reduced cysteines are first modified with an alkylating agent (e.g., iodoacetamide), the excess alkylating agent is removed, and the oxidized cysteines are reduced with dithiothreitol and modified with a second alkylating agent (e.g., vinyl pyridine). Mass analysis of tryptic peptides of this protein indicates an increase in mass corresponding to the mass of the modifying agent in all cysteine-containing peptides. The iodoacetamide-modified cysteines represent residues that were in the reduced cysteine thiol state, whereas the vinyl pyridine-modified cysteines were present in the oxidized disulfide form in the protein.

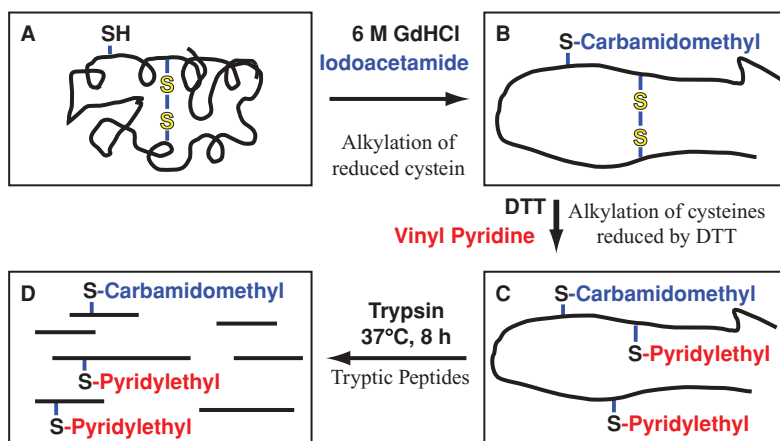


Figure 6.4. Schematic of the double alkylation procedure for determining the oxidation states of cysteines. (A) Intact protein with 1 free (reduced) and 2 oxidized cysteines. (B) The protein is denatured using 6 M guanidinium hydrochloride (GdHCl) and the free cysteine was labeled with iodoacetamide. (C) Oxidized cysteines are then reduced by dithiothreitol (DTT), and then alkylated with vinyl pyridine. (D) Protein is digested with trypsin to get tryptic peptides. LC-MS/MS analysis of these tryptic peptides will locate the positions of reduced (cysteine with carbamidomethyl) and oxidized (cysteine with pyridylethyl) cysteines in protein.

6.1.B5 Metabolomics Small molecules such as antioxidants, enzyme cofactors, cellular metabolites, and vitamins are responsible for the maintenance of routine physiological functions. Disease or oxidative stress may change the level of these molecules, which may serve as useful biomarkers. For example, to monitor the change in levels of general metabolites (of unknown identity) in response to oxidative stress, a fingerprinting approach may be applied. In this approach, mass spectra of controls and experimental samples are acquired and compared in a desired mass range with high mass accuracy (ideally <5 ppm). When the peak intensities for the two samples differ, those selected masses are submitted to a database search engine to identify the metabolite. The structural assignment may be confirmed by analyzing the fragmentation pattern by MS/MS. One may also monitor the changes in the concentration of known compounds using MRM with a triple quadrupole instrument.

If the small metabolites of interest are thiol-containing compounds, they can be captured and identification may be performed by derivatization with alkylating agents such as GSH, N-ethylmaleimide, or iodoacetic acid. First, the daughter ion fragments of the selected alkylating agent alone are generated in the mass spectrometer. A precursor ion scan is then performed for the compounds that were treated with this alkylating agent. The precursor ion scan looks for the precursor ions that generate the same daughter ion fragments as were generated by the alkylating agent alone. Using this method, the precursor mass of the unknown compounds that were modified by that particular alkylating agent can be determined. By subtracting the mass of the alkylating agent from the mass of the precursor ion of the unknown compounds, the molecular masses of the unknowns can be determined. In separate experiments, the identity and characterization of the unknown compounds can be performed with the aid of standards of the suspected compounds.

6.1.C Hydrogen Exchange Mass Spectrometry

Hydrogen exchange (HX) and mass spectrometry (MS) may be used to determine conformational changes of proteins. For example, conformational changes caused by modification of the oxidation state of cysteine residues may be determined by HX MS. For example, the structural differences in native human α -lactalbumin between the oxidized and reduced state have been determined by this method. Stabilization of the C-terminal domain was found to be important for the compact molten globule structure of the protein. HX MS has also been used to determine the location of a peptide in human cystathione β -synthase that was correlated with the transmission of intrasteric inhibition and allosteric activation.

SELECTED REFERENCES

1. Castro-Perez1, J., Plumb, R., Liang, L., and Yang, E. (2005). A high-throughput liquid chromatography/tandem mass spectrometry method for screening glutathione conjugates using exact mass neutral loss acquisition. *Rapid Commun. Mass Spectrom.* 19:798–804.

2. Hirose, M., Takahashi, N., Oe, H., and Doi, E. (1988). Analyses of intramolecular disulfide bonds in proteins by polyacrylamide gel electrophoresis following two-step alkylation. *Anal. Biochem.* 168(1):193–201.
3. Engen, J.R., and Smith, D.L. (2000). Investigating the higher order structure of proteins: Hydrogen exchange, proteolytic fragmentation, and mass spectrometry. *Methods Mol. Biol.* 146:95–112.
4. Tolstikov, V.V., Lommen, A., Nakanishi, K., Tanaka, N., and Fiehn, O. (2003). Monolithic silica-based capillary reversed-phase liquid chromatography/electrospray mass spectrometry for plant metabolomics. *Anal. Chem.* 75(23):6737–6740.
5. Korfmacher, W.A. (2005). Principles and applications of LC-MS in new drug discovery. *Drug Discov. Today* 10(20): 1357–1367.

6.2 ELECTRON PARAMAGNETIC RESONANCE (EPR) FOR THE REDOX BIOCHEMIST

STEPHEN W. RAGSDALE

Department of Biological Chemistry, University of Michigan, Ann Arbor, Michigan

JAVIER SERAVALLI

Redox Biology Center and Department of Biochemistry, University of Nebraska, Lincoln, Nebraska

6.2.A Introduction to Magnetic Resonance Spectroscopy

Electron paramagnetic resonance (EPR), which is also known as electron spin resonance (ESR), is a spectroscopic technique used to observe species containing unpaired electrons. In general, materials or species in solution can be classified as (1) diamagnetic if they lack unpaired electrons or have a closed electron shell configuration, (2) ferromagnetic when they have a large number of aligned unpaired electrons like conventional magnets, or (3) paramagnetic if they have a small number of unpaired electrons. Only paramagnets are observable in an EPR experiment because only paramagnets orient in the same direction as an external applied magnetic field (ferromagnets orient in the opposite direction).

There are two types of paramagnetic species: organic free radicals and transition metals. Many sections in this book focus on free radicals and transition metals because of their importance to redox biology. Thus, EPR has become a routine tool in the redox biochemistry laboratory. EPR, which detects unpaired electron spins, is often described by comparing it to nuclear magnetic resonance (NMR) spectroscopy, which observes unpaired nuclear spins (^1H , ^{13}C , etc.), because these methods have many common features. Since they are both resonance-based spectroscopies, they require two forms of radiation: a magnetic field (in the 1–70 kG range) and waves in the radiofrequency range for NMR or in the microwave frequency range for EPR. A given nucleus (for NMR) or paramagnet (for EPR) resonates at a defined position, which is called the chemical shift in NMR or the g -value in EPR, that is independent (in most cases) of the frequency or the magnetic field used in the experiments. Finally, the quantum mechanical explanations for NMR and EPR are both based

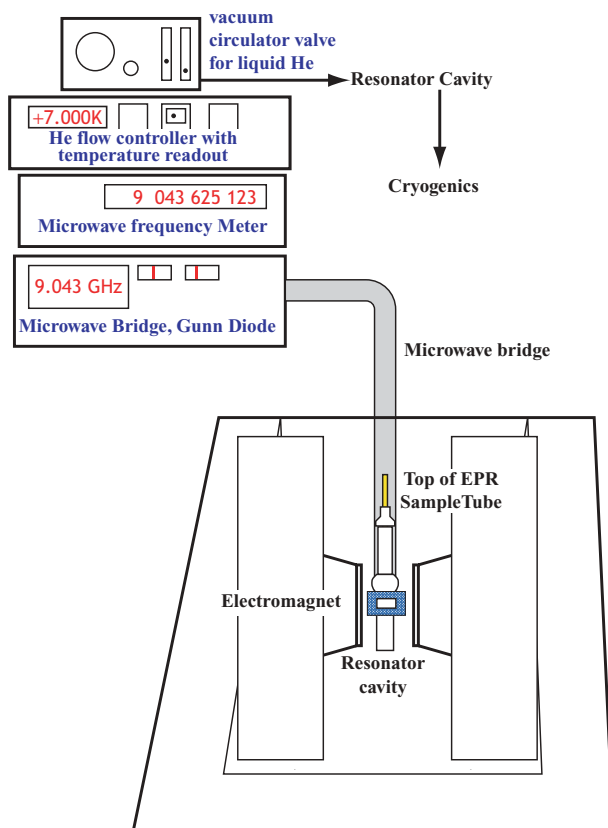


Figure 6.5. Schematic representation of the EPR spectrometer.

on the interaction of the unpaired spin with an external field through the Zeeman effect (Fig. 6.5).

There are some significant differences both in the scope and the experimental design of EPR and NMR spectroscopy. First, while most biological molecules contain nuclei with magnetic moments and therefore are NMR-active, almost all atoms are EPR-inactive (“EPR-silent”) because they are diamagnetic. Second, since the electron has a mass that is 1860 times smaller than the smallest nucleus (^1H), weaker magnetic fields (<1 tesla for X-band EPR versus 5–12 tesla for NMR) and higher frequencies (1–100 GHz or microwaves for EPR compared to 100–1000 MHz or radiowaves for ^1H -NMR) are required. Third, while the NMR experiment is carried out by broadband pulse irradiation at a constant magnetic field, most EPR experiments use a fixed microwave frequency and variable magnetic field. The reasons for this are explained later. However, these continuous wave EPR experiments (CW-EPR) are augmented by pulsed EPR in which frequency is varied at a single field setting. Since most components of the biological system under study are diamagnetic and do not produce

EPR signals, the researcher can obtain valuable information on the few paramagnetic sites without interference from buffers, ligands, and even many metals (like Ca^{2+} , Mg^{2+} , and Zn^{2+}).

The four types of biological samples that EPR can be used to study include (1) transition metals and rare earth atoms or complexes containing such atoms, (2) stable radicals such as 1,1'-diphenyl-2-picryl-hydrazyl (DPPH) and 2,2,6,6-tetramethyl-1-piperidinyloxy (TEMPO), (3) transient reactive organic radicals that must be trapped during a reaction often by freezing and studying at temperatures below the freezing point of water (273.15 K), and (4) triplet organic radicals and biradical species.

6.2.B Basic EPR Theory

An extensive set of monographs is available on the theory underlying an EPR experiment. EPR spectra are sensitive to a number of interactions between the unpaired spin and the environment: (1) the Zeeman interaction between the unpaired spin and the external magnetic field, (2) the spin orbit coupling, (3) the electron spin–nuclear spin interactions, and (4) the interaction with other unpaired electrons (spin–spin interaction). The largest interaction in most cases and the one on which EPR is based is the Zeeman effect (Fig. 6.6), which is the splitting of energy levels and the associated spectral lines by an external magnetic field. The most characteristic value that describes an EPR spectrum is the g -value, which is very close to 2.0 ($g_e = 2.0023193$) for the free electron. If the electron has a nonzero orbital angular momentum (L), the g -value will deviate from that for the free electron. For example, for transition metals, the ligand environment strongly affects the g -value through its electric and magnetic fields. An additional factor is that a large number of biological transition metals (^{57}Co , ^{63}Cu , ^{65}Cu , ^{55}Mn) as well as other common nuclei (^1H , ^{14}N , ^{31}P) have nuclear moments that split the EPR signal into a defined number of lines through electron spin–nuclear spin coupling, which is described in more detail (see Section 6.2.H). The number of lines (#) is related to the number of coupled nuclei (N) and

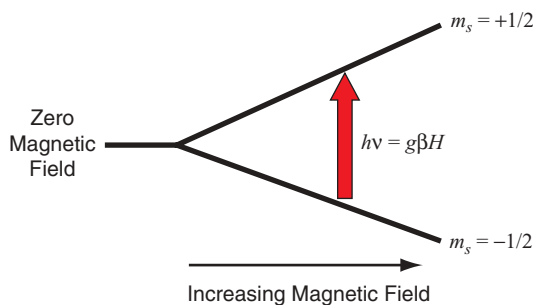


Figure 6.6. The Zeeman effect. An increasing magnetic field is applied in the presence of a fixed microwave frequency. When the resonance condition is reached (position of the arrow), an absorption occurs between the lower energy level ($m_s = -\frac{1}{2}$) and the upper energy level ($m_s = \frac{1}{2}$). The energy difference is quantized and equivalent to the term $g\beta H$.

its nuclear spin (I_N) as shown in Eq. (6.3). Although these lines complicate the appearance of the EPR spectrum, they are extremely useful in diagnosing the nature of the paramagnetic center. For example, when an electron spin is coupled to an ^{14}N ($I_N = 1$) nucleus, each of the lines in the spectrum will split into 3 lines.

$$\# \text{ of lines} = 2NI_N + 1 \quad (6.3)$$

6.2.C Appearance of the EPR Spectrum

The EPR spectrum in CW mode is a derivative spectrum, which can nevertheless be integrated to produce the absorption spectrum of intensity versus magnetic field (Fig. 6.7). The position of the absorption peak occurs at the crossover point with the baseline in the derivative spectrum as shown in Fig. 6.7A. The interaction of the unpaired electron with other electrons in the same atom is usually treated as a coupling of the unpaired electron spin with its orbital momentum. Such coupling produces a splitting of the signal into three separate transitions with characteristic g -values. This is almost always the case for transition metal species. There are three possible g -values as there are three vectors describing the orientation of the g -tensor with the magnetic field. The observed g -values are not the actual values of g_x , g_y , and g_z because EPR spectra are usually obtained in a frozen powder state, so they should be called g_1 , g_2 , and g_3 . They are generally reported in order of increasing energy ($g_1 > g_2 > g_3$). If all three g -values are identical, the spectrum is said to be isotropic (Fig. 6.8A); if two of them are identical, it is said to be axial (Figs. 6.8B, C), and if all three g -values are different, the spectrum is said to be rhombic (Fig. 6.8D).

6.2.D The EPR Experiment

During a CW-EPR experiment, the microwave frequency is maintained constant and the magnetic field (B) is varied. When the field reaches a value that satisfies the condition given in Eq. (6.4), the resonance condition is achieved and an absorption peak is observed due to the absorption of microwave energy (Fig. 6.6). In this equation, h is Planck's constant, ν is the microwave frequency, g is the g -value, and β is a constant known as the electron Bohr magneton (9.2740×10^{-24} J/T). Since h , ν , and β are constants, when ν is given in GHz and B in gauss, Eq. (6.5) relates the g -value and the magnetic field.

$$B = h\nu/g\beta \quad (6.4)$$

$$g = \frac{714.48 \times \nu}{B} \quad (6.5)$$

Knowledge of the g -value to high precision is important for correctly assigning the identity of the radical and for characterizing the environment (ligands, polarity, etc.) in which the spin resides. In the EPR experiment, the frequency ν is generally fixed

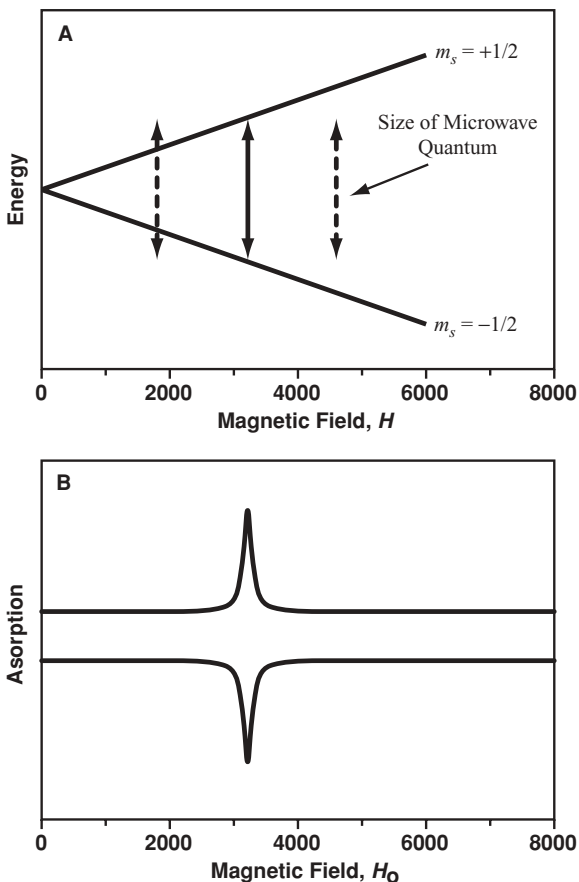


Figure 6.7. The quantum mechanical resonance phenomenon. The effect of varying magnetic field (H) and the resonance conditions are plotted in (A). Observation of absorption (or emission) when the resonance is reached is plotted in (B). For an X-band experiment (9–10 GHz), for an organic radical with a g -value of 2.0, the resonance condition is achieved at ~ 3400 gauss.

and highly stable and can be measured with a high degree of accuracy. Generally, the frequency is known with an accuracy of at least six significant figures. The magnetic field (B) must also be known and can be precisely measured with a gaussmeter to an accuracy of below 0.1 gauss.

6.2.E The Conventional EPR Spectrometer: Detection of the Signal

To understand why conventional EPR spectra are presented in a derivative mode, it is necessary to examine the instrumental setup (Fig. 6.5). The EPR experiment is conducted at constant microwave frequency and variable oscillating magnetic field.

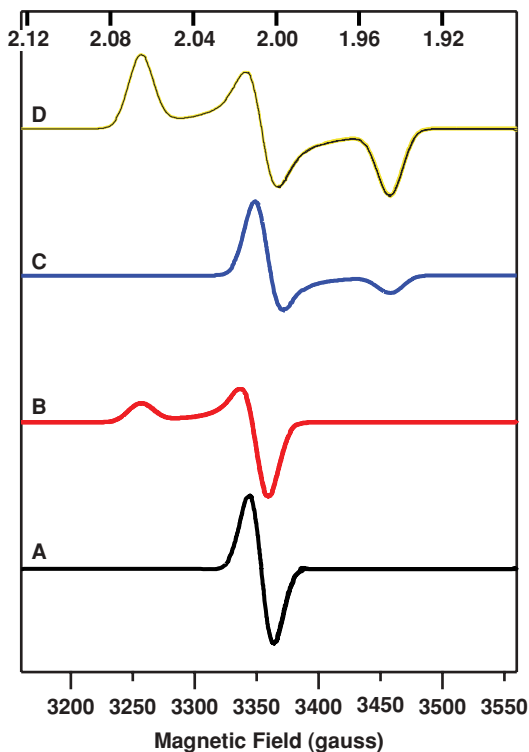


Figure 6.8. Anisotropy of the g -value. If all three g -values in the tensor are identical, the signal is isotropic ($g_1 = g_2 = g_3 = 2.00$ for this case) (A). If $g_2 = g_3$ (2.00 for spectrum B) or $g_1 = g_2$ (2.00 for spectrum C), an axial spectrum is observed, with the S shape at higher energy (B) or lower energy (C), respectively. If all three g -values are quite different, then a rhombic spectrum is observed (spectrum D). The spectra were simulated with the program Simfonia from Bruker using a frequency of 9.389 GHz, a linewidth of 20 G, modulation amplitude of 10 G, and g -value of 2.06, 2.00, and 1.94.

The magnet operates in the range that covers g -values from infinity to ~ 1 (3400 gauss for X-band EPR). In an EPR instrument, the sample is mounted in a microwave cavity, which must have a length equal to the wavelength of the microwave radiation (3.3 cm for X-band). In the middle of the cavity, the sample sits where the electrical field is at a minimum but the magnetic field is at a maximum. The typical X-band instrument is capable of achieving a maximum power of 200 mW (if the attenuation is set to zero).

The microwaves are generated by two types of electronic devices known as Klystron tubes or Gunn diodes. Both devices contain solid state electronics that generate the microwaves along with a certain amount of electronic noise. The frequencies at which EPR instruments operate are in the range of 3–190 GHz. Since the frequency is usually fixed, EPR instruments are classified in “band” according to the frequency range of operation. Thus, instruments operating in 9–10 GHz range are

X-band EPRs, while instruments operating in the 30–35 GHz are Q-band EPRs. Other common bands are S-band (3 GHz), K-band (23 GHz), and W-band (95 GHz). The main advantage of higher frequencies is that the separation of the spin levels is higher (Fig. 6.6). This results in a higher population of spins in the ground state and therefore higher signal intensity. However, because the resonator cavities have to be smaller at higher frequency, the required sample size must decrease proportionally; thus, there are fewer spins present in the cavity, resulting in a compensating decrease in signal intensity.

To acquire an EPR spectrum, the operator increases the magnetic field intensity by increasing the current that travels through the electromagnet. In order to increase sensitivity, an additional oscillating magnetic field is applied at a frequency much smaller (100 kHz) than the resonant frequency (9–10 GHz). The amplitude of the oscillating radiation (known as modulating field) creates an oscillation of the magnetic field (δB) along the magnetic field axis (i.e., at each point as the magnetic field is being swept). Meanwhile, the diode detector operates at the same oscillating frequency (the modulation frequency) as the sample and reference beams of the microwave generator. This hard-wired protocol acts as a filter that removes any current variations that have a different modulation frequency than that of the diode detector. This results in a tremendous increase in the signal-to-noise ratio, with a corresponding increase in sensitivity. The trade-off is that the resulting spectrum displays the variation of signal intensity with the magnetic field (denoted also by $d\chi/dB$). Thus, the EPR spectrum appears as a first derivative, as shown in Fig. 6.7. For a typical instrument operating at X-band (9–10 GHz) or Q-band (30–35 GHz), the limit of detection (and therefore sensitivity) for free radicals is $\sim 10^{11}$ spins, which corresponds to a spin concentration as low as 1×10^{-9} M.

Small variations in the sample composition and size will cause variations in the frequency of the resonator cavity. For that reason, the resonator or cavity needs to be tuned to the resonant frequency transmitted by the waveguide by means of a small screw known as the iris screw (Fig. 6.9), which brings the sample cavity (resonator) to the same frequency as the incident radiation traveling the waveguide. Frequency

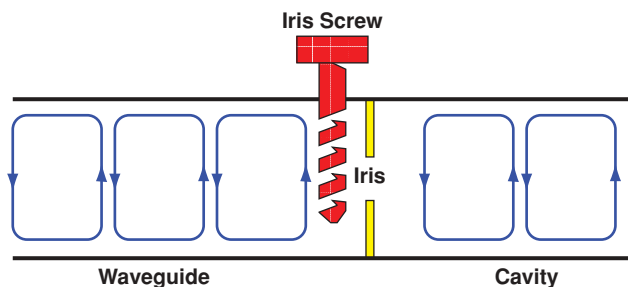


Figure 6.9. Coupling between the waveguide and the resonator cavity. The iris screw changes the size of the iris hole by a small amount so that the frequency of the waveguide matches that of the resonator.

meters are part of a standard EPR instrument, which provides highly accurate (at least 1 part in 10^5) values of the resonant frequency.

6.2.F Sensitivity and Saturation in EPR

In an EPR experiment, the sensitivity is also inversely proportional to the square of the linewidth. Increasing the microwave power will promote more spins to the higher state. At high microwave power, the populations will eventually become identical, resulting in a decrease in intensity. This phenomenon is called *saturation*, a point at which the spins cannot relax faster to the lower state than they are promoted back to the higher state. The spin relaxation mechanism is with the surrounding environment, or spin–lattice relaxation (rate constant = $1/T_1$). Slow relaxing spin systems (long T_1) saturate easily, while fast relaxing systems require higher microwave power and/or lower temperatures to saturate. Another mechanism of relaxation is through spin–orbit coupling, which is very common in transition metal complexes. Such fast relaxing systems are much harder to saturate. On the other hand, rapidly relaxing systems are difficult to observe at high temperatures because $1/T_1$ increases with temperature. This is the reason why the observation of organic radicals usually requires liquid nitrogen temperatures (77 K) while transition metal-based paramagnetic states require liquid He temperatures (20 K and below).

EPR signals for slow relaxing radicals in the liquid state typically have a Lorentzian shape (Fig. 6.10). For biological samples in the frozen state, the effective magnetic field varies slightly among each apparently identical paramagnetic molecule present in the sample, resulting in inhomogeneous broadening. In this case, the signal exhibits a Gaussian lineshape. In contrast, when the intensity of the magnetic field does not vary among radicals but varies rapidly with time, homogeneous broadening occurs, producing a Lorentzian lineshape. The linewidths for transition metal ions are within the range of 10–100 G and exhibit Gaussian lineshapes (Fig. 6.10, Gaussian with 10 G linewidth), due mainly to the fast relaxing ($T_1 \sim 10^{-9}$ s) nature of spin–orbit coupling.

6.2.G Measuring the Concentration of Spins

To determine the spin concentration, the derivative EPR spectrum should be integrated two times and compared with the double integral of the spectrum of a paramagnet of known spin concentration. The spectra of the unknown and the standard should be measured under similar conditions of temperature, gain, modulation amplitude, and power and at a power that is not saturating. Under non saturating conditions, the intensity is proportional to the square root of the power. Sometimes it is not possible to use exactly the same instrument parameters, especially when the sample is a fast relaxing transition metal and you wish to use a slow relaxing system as a standard. The estimation of the spin concentration requires knowledge of the temperature, field modulation amplitude, spectrometer gain, the scan width, and microwave power (Eq. (6.6)). Since the integration is done digitally, the density of data points must be

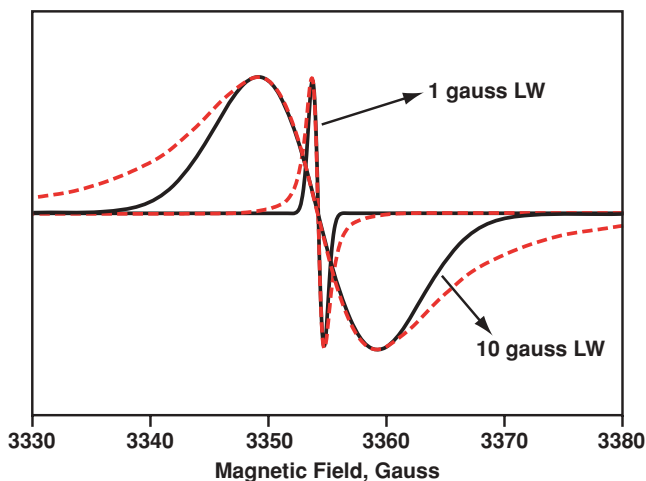


Figure 6.10. Effect of broadening on the EPR signal shape. A species that does not exhibit broadening or unresolved couplings should actually show a broader signal in the derivative spectrum since it follows a Gaussian lineshape (shown by the red dashed lines). The solid black lines show hypothetical isotropic Lorentzian EPR signals with $g = 2.0$ with linewidths of 1 gauss (expected for free radicals) and 10 gauss (homogeneous broadening). The dashed lines show the corresponding Gaussian EPR signals (powder spectra of a radical plus inhomogeneous broadening).

identical for both sample and standard.

$$[S]_{\text{Unk}} = \frac{[S]_{\text{Std}} \iint \text{Unk} \times \sqrt{P_{\text{Std}}} \times \text{Gain}_{\text{Std}} \times Bm_{\text{Std}}}{\iint \text{Std} \times \sqrt{P_{\text{Unk}}} \times \text{Gain}_{\text{Unk}} \times Bm_{\text{Unk}}} \quad (6.6)$$

In this equation, $[S]$ is the concentration of spins, P is the power, Bm is the field modulation, and the integration is the value of the double integrals for the sample (Unk) or standard (Std). The concentration of the standard must be known beforehand. Another term that needs to be included is the g ratio term. It corresponds to the ratio between the g -values of the standard and unknown, $g_{\text{std}}/g_{\text{unk}}$. These g -values are not the normal ones, but the intensity factors, or g_p , that are calculated from the g -values according to Eq. (6.7):

$$g_p = \frac{2}{3} \times [(g_x^2 + g_y^2 + g_z^2)/3]^{1/2} + \frac{1}{3} \times (g_x + g_y + g_z)/3 \quad (6.7)$$

This correction is usually negligible for $S = 1/2$ systems, but it is extremely important for $S > 1/2$ systems. Good standards for integration are $\text{Cu}^{2+}(\text{EDTA})$, $\text{Fe}^{3+}(\text{EDTA})$, and $\text{Cu}(\text{ClO}_4)_2$. The EDTA complexes are relatively stable and provide strong signals

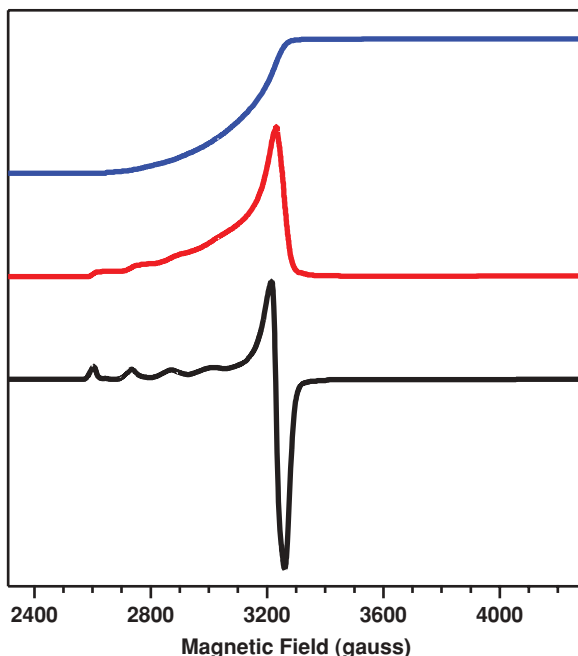


Figure 6.11. Spectrum of a $\text{Cu}(\text{ClO}_4)_2$ -containing solution (black), the single integrated absorption (red), and double-integrated spectra (blue), obtained after baseline correction. Note that the resolution of the hyperfine couplings is better appreciated in the derivative spectrum. The area under the double-integrated spectrum is proportional to the amount of Cu^{2+} spins in the sample.

in the $g \approx 4$ (Fe^{3+}) and $g \approx 2$ (Cu^{2+}) regions of the spectrum, but the $\text{Cu}(\text{ClO}_4)_2$ complex (Fig. 6.11) is more stable, albeit easily saturable at low temperatures.

6.2.H Nuclear Hyperfine and Spin–Spin Interactions

Association of the unpaired electron with a magnetic nucleus (e.g., ^1H , ^{13}C , ^{63}Cu) causes the EPR spectrum to be split (called electron–nuclear coupling). The magnitude of this interaction is much smaller than the electron Zeeman splitting ($\frac{1}{768}$ for the ^1H). Since the nuclear and electron magnetic moments are not necessarily collinear, A_I is not just a number but a tensor composed of at least three different values (corresponding to the couplings with g_x , g_y , and g_z). The nuclear splitting of an electron spin transition is referred to as the nuclear hyperfine interaction and described by the nuclear hyperfine constant A . If more than one equivalent nucleus interacts with an electron spin transition, it will follow a Pascal triangle pattern. Usually the splittings by nuclei are not equivalent, so the number of lines observed in the spectrum follows Eq. (6.1). So for an unpaired electron in Cu^{2+} , the two most abundant Cu isotopes (^{63}Cu and ^{65}Cu) both have $I_N = \frac{3}{2}$, so four lines are expected (Fig. 6.11). For $^{59}\text{Co}^{2+}$, $I_N = \frac{7}{2}$, so a total of eight lines are expected.

SELECTED REFERENCES

1. Aasa, R., and Vanngard, T. (1975). EPR signal intensity and power shapes: a reexamination. *J. Magnet. Resonance* 19:308–315.
2. Beinert, H., Orme-Johnson, W., and Palmer, G. (1978). *Methods Enzymol.* 54:111–132.
3. Cammack, R., and Cooper, C.E. (1993). Electron paramagnetic resonance spectroscopy of iron complexes and iron-containing proteins. *Methods Enzymol.* 227:353–384.

6.3 REDOX POTENTIOMETRY

DONALD BECKER

Redox Biology Center and Department of Biochemistry, University of Nebraska, Lincoln, Nebraska.

Common redox centers in proteins include transition metals, organic cofactors, iron–sulfur clusters, and cytochromes. To understand the mechanisms of electron transfer, bioenergetics, and redox-linked processes in biological systems, it is necessary to characterize the electrochemical properties of these centers. Methods for determining the midpoint potential (E_m) of a redox center in a protein at ambient pH include mediated and direct electrochemistry techniques. Mediated electrochemistry is readily accessible with most proteins and is described here. Direct electrochemistry is a powerful technique; however, it often cannot be used with proteins because of its strict requirement for a suitable arrangement of the redox centers relative to the protein surface. Although direct electrochemistry is not discussed here, interested students are encouraged to read how voltammetric methods can be used in redox chemistry questions.

6.3.A Midpoint Potential

The midpoint potential (E_m) for the half-reaction in Eq. (6.8) characterizes the thermodynamic tendency of the redox center to accept or donate an electron(s).



The role that a redox center has in an electron transfer reaction depends on the relative electrochemical properties of its partner(s). For electron transfer between two species to be thermodynamically favorable, the electromotive force must be positive (i.e., $\Delta E > 0$). Therefore, redox centers with the most positive E_m values in an electron transfer reaction will act as electron acceptors while redox centers with the most negative E_m values will act as electron donors.

The E_m value for a half-reaction involving a redox center in a protein can be determined using the Nernst equation (Eq. (6.9)),

$$E_{\text{meas}} = E_m + (2.3RT/nF) \log \frac{[\text{ox}]}{[\text{red}]} \quad (6.9)$$

where E_{meas} is the measured equilibrium potential at each point in a potentiometric titration, E_{m} is the midpoint potential, R is the gas constant ($8.314 \text{ J K}^{-1} \text{ mol}^{-1}$), F is the Faraday constant ($96485 \text{ J V}^{-1} \text{ mol}^{-1}$), n is the number of electrons transferred, and $[\text{ox}]$ and $[\text{red}]$ are the concentrations of the oxidized and reduced species at each point in the titration.

The number of protons coupled with an electron transfer reaction (Eq. (6.10)) can be evaluated by determining the pH dependence of E_{m} . A plot of E_{m} versus pH reveals the number of protons transferred with each electron using Eq. (6.11).



$$E_{\text{m}(\text{pH } X)} = E_{\text{m}(\text{pH } 0)} - (2.3RT/nF) \times \text{pH} \quad (6.11)$$

In simple cases, this plot will be linear over the pH range.

6.3.B Redox-Linked Processes

In addition to determining the E_{m} value of a redox center, potentiometry can be used to study properties of the protein that are influenced by reduction of the redox center (i.e., redox linked). For example, a nonlinear pH dependence of the E_{m} value may indicate that the $\text{p}K_{\text{a}}$ of a nearby amino acid is affected by reduction of the redox center. Subsequent characterization of site-directed mutants can identify the residue responsible for the pH-sensitive behavior in E_{m} . Other redox-linked interactions may include binding of ligands and large macromolecules, like other proteins, nucleic acids, and phospholipids. These interactions can be important for regulating electron transfer reactions and redox-dependent protein functions. For example, in acyl-CoA dehydrogenase, binding of the fatty acyl-CoA substrate increases the E_{m} of the enzyme-bound flavin cofactor, thereby favoring electron transfer from the substrate to the flavin. Thus, the electrochemical properties of redox centers are determined by the immediate protein environment as well as by interactions with other molecules.

The influence of a molecule (L) on the electrochemical properties of a redox center in a protein can be evaluated by establishing a thermodynamic relationship between the oxidized and reduced forms of a protein. Differences in the potential of the redox center in the presence ($E_{\text{m}(\text{bound})}$) and absence ($E_{\text{m}(\text{free})}$) of the ligand can be evaluated using a thermodynamic box as shown in Fig. 6.12. The difference in E_{m} between the ligand-complexed and ligand-uncomplexed states can infer the change in binding affinity that occurs upon reduction of the redox center if $K_{\text{d}(\text{ox})}$ is already known using Eq. (6.12). The greater the influence of the ligand on the E_{m} of the redox center, the more sensitive the protein–ligand interaction is to the redox state of the protein, implying a highly redox regulated association.

$$E_{\text{m}(\text{bound})} = E_{\text{m}(\text{free})} + (2.3RT/nF) \log \frac{K_{\text{d}(\text{ox})}}{K_{\text{d}(\text{red})}} \quad (6.12)$$

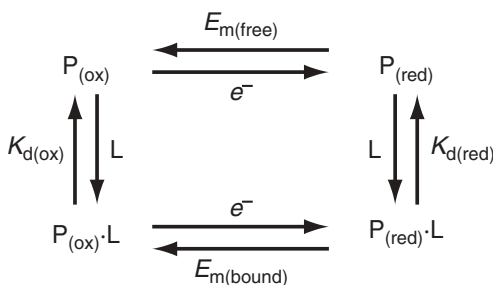


Figure 6.12. Thermodynamic relationship of ligand binding to the oxidized and reduced forms of a protein (P).

6.3.C Potentiometric Technique

The fundamental problem in the accurate determination of n and E_m values of redox centers in proteins is the slow heterogeneous electron transfer between the protein and a working electrode. This sluggish behavior prevents many redox proteins from being studied by direct electrochemical methods. The redox center is surrounded by a polypeptide coat, which often results in slow electron transfer, especially in large proteins. Furthermore, proteins can also adsorb onto the electrode surface, resulting in irreversible electrochemical behavior. These problems are circumvented by adding one or more electroactive species, called redox mediators, to the protein solution, which act as “electron carriers” by coupling electron transfer between the working electrode and the protein redox center. Thus, the redox center achieves equilibrium with the working electrode via the mediators. These redox mediator dyes have well defined optical and electrochemical properties and, as a general guideline, should be used within a 0.1 to 10 ratio of [oxidized]:[reduced] dye. Therefore, based on the Nernst relationship, the mediators must have a redox potential that is ± 0.06 V ($n = 1$) from the E_m of the protein redox center.

The general method for measuring the E_m of redox cofactors in proteins involves measuring the ambient potential of the protein–mediator solution within the cell while monitoring a property of the redox cofactor, such as changes in the UV–visible, EPR, or circular dichroism spectrum. Initially, the protein solution is in the fully oxidized state. Reducing equivalents are then added to the protein solution by bulk electrolysis using a potentiostat and a three electrode system involving an auxiliary electrode (Ag/AgCl). Alternatively, the protein solution can be titrated with chemical reducing agents such as sodium dithionite or titanium(III) citrate. Photoreduction using 5-deaza-flavin is also another method for introducing reducing equivalents. After each addition of reducing equivalent, the protein solution is monitored until no further change in the spectroscopic signal is observed, indicating that the solution has reached equilibrium. At equilibrium, the potential between the reference (e.g., Ag/AgCl) and working electrodes (e.g., gold or platinum) is recorded. The protein solution is then reduced further and equilibrated at a different measured cell potential. This process is repeated until the redox center is fully reduced. At each potentiometric measurement, the distribution of oxidized and reduced species is determined from

the spectral changes and a Nernst plot is generated. The measured potentials are reported in reference to the normal hydrogen electrode (versus NHE) by calibrating the reference electrode using a potassium ferricyanide/ferricyanide standard solution. Quantifying the oxidized and reduced forms of the protein-bound redox cofactor sometimes requires subtracting out the mediator dye spectra at each corresponding measured potential. This requires a separate potentiometric titration of the mediator dyes prior to analyzing the protein–mediator dye mixture.

Ideally, the E_m value should be the same whether approached from a reductive or oxidative direction. Oxidative potentiometric measurements are performed identically to reductive potentiometric titrations except that the fully reduced protein solution is oxidized by applying an oxidative current or by titrating with a chemical oxidant (e.g., potassium ferricyanide). It is a good practice to apply oxidative changes periodically during a reductive titration and vice versa, thus simultaneously performing reductive and oxidative titrations and ensuring that the protein is at equilibrium.

Because of its high reactivity with most redox mediators, oxygen must be excluded from potentiometric experiments and maintained at <10 ppm. Thus, potentiometric experiments require an anaerobic chamber or an anaerobic electrochemical cell

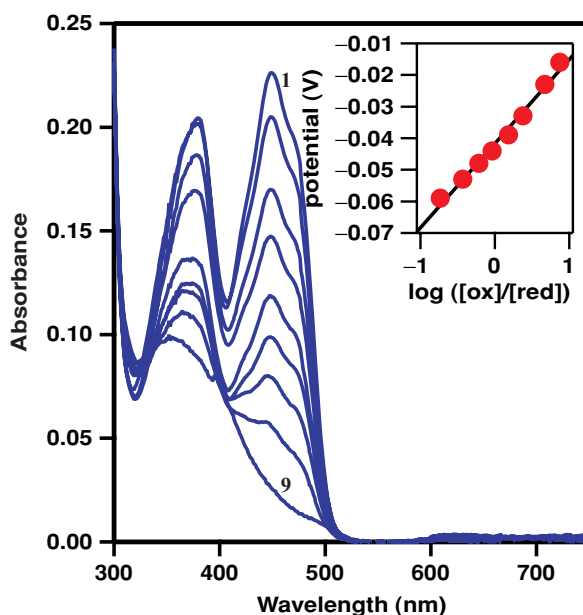


Figure 6.13. Example of a potentiometric titration of an enzyme-bound flavin cofactor ($17.2 \mu\text{M}$) in the proline dehydrogenase domain of the PutA protein from *E. coli*. Titration was performed in 50 mM potassium phosphate buffer (pH 7.0 at 25°C). Curves 1–9: fully oxidized, -0.016 , -0.033 , -0.039 , -0.044 , -0.048 , -0.053 , -0.059 V, and fully reduced, respectively. The inset is a Nernst plot of the potentiometric data from which an E_m value of -0.042 V with a 27 mV slope was determined. (Reprinted from *Biochim Biophys. Acta* 1701, B.A. Baban et al., Probing a hydrogen bond pair and the FAD redox properties in the proline dehydrogenase domain of *Escherichia coli* PutA, 49–59, 2004, with permission from Elsevier.)

designed specifically for the experimental application (e.g., UV-visible or EPR). The atmosphere of an electrochemical cell is replaced with an inert gas such as nitrogen or argon and the protein solution is degassed by carefully applying cycles of vacuum and positive gas pressure. Various electrochemical cells have been designed for potentiometric experiments.

An example of a potentiometric titration of an enzyme-bound flavin cofactor is shown in Fig. 6.13. Here, the proline dehydrogenase domain of the PutA flavoprotein from *E. coli* is electrochemically titrated and the potential is recorded at different stages in the titration. The spectral contributions from mediators have been subtracted to generate the final spectral changes of the noncovalently bound flavin cofactor in PutA. From the Nernst plot, an E_m value of -42 mV was calculated. Thus, the flavin cofactor bound to PutA displays an E_m value that is significantly shifted in the positive direction relative to free flavin in solution ($E_m = -219$ mV, pH 7.0).

SELECTED REFERENCES

1. Dutton, P.L. (1978). Redox potentiometry: determination of midpoint potentials of oxidation-reduction components of biological electron-transfer systems. *Methods Enzymol.* 54:411–435.
2. Fultz, M.L., and Durst, R.A. (1982). Mediator compounds for the electrochemical study of biological redox systems: a compilation. *Anal. Chim. Acta* 140:1–18.
3. Lenn, N.D., Stankovich, M.T., and Liu, H.W. (1990). Regulation of the redox potential of general acyl-CoA dehydrogenase by substrate binding. *Biochemistry* 29:3709–3715.
4. Stankovich, M.T. (1980). An anaerobic spectroelectrochemical cell for studying the spectral and redox properties of flavoproteins. *Anal. Biochem.* 109:295–308.

6.4 BIOINFORMATICS METHODS TO STUDY THIOL-BASED OXIDOREDUCTASES

DMITRI E. FOMENKO and VADIM N. GLADYSHEV

Redox Biology Center and Department of Biochemistry, University of Nebraska, Lincoln, Nebraska

As discussed in Chapter 3, thiol-dependent oxidoreductases are involved in a variety of biological functions, such as oxidative stress defense, redox regulation, signal transduction, and protein folding. A large number of these proteins have been extensively characterized, but the identities and functions of many other thiol-based oxidoreductases are unknown. This section describes the application of bioinformatics methods to study these proteins.

6.4.A Identification of Redox-Active Cysteines in Proteins

By definition, all thiol-based oxidoreductases contain cysteine or, in the rare case, selenocysteine residues in their active sites; therefore, identification of these redox

residues is key to studying these enzymes. The major property of redox-active cysteines is their conservation. They are expected to occur even in very distant homologs, provided that the overall oxidoreductase function is preserved. Conservation of amino acids can be determined by collecting sequences of homologs and building multiple sequence alignments. One of the most popular sequence analysis tools is BLAST (Basic Local Alignment Search Tools). BLAST is a set of specialized sequence comparison programs that can be used to search sequence databases for optimal local alignments to a query sequence. These programs exist as standalone versions for most computer platforms, and as web versions at <http://www.ncbi.nlm.nih.gov/BLAST/>. NCBI sequence databases are updated every day and contain most publicly available protein and nucleotide sequences. Among the BLAST programs, PSI-BLAST should be noted as being among the most relevant to the subject of this section. This tool is useful for identification of evolutionary relationships between distantly related proteins.

Occurrence of conserved cysteines in a protein sequence suggests that these residues may be functionally important. Some of the common functions of conserved cysteines include:

- 1. Catalytic redox-active cysteine residues.** These cysteines are directly involved in catalysis and occur in thiol-based oxidoreductases. As discussed in Chapter 3, these residues undergo oxidation to form transient disulfides or sulfenic acids and are regenerated by specialized enzymes or other reducing systems. Redox cysteines are highly conserved in protein sequences. Examples of such proteins discussed in this book are thioredoxin, glutaredoxin, glutathione peroxidase, peroxiredoxin, and methionine sulfoxide reductase.

- 2. Regulatory cysteines.** Protein activity may be regulated by the redox state of regulatory cysteine residues. Such residues may occur in transcription factors, kinases, redox sensors, and other regulatory proteins. The most frequent modifications are glutathionylation and S-nitrosylation, but other reversible modifications may also occur. Regulatory cysteine residues have a lower level of conservation than catalytic redox-active cysteines. Examples of such proteins are transcription factors OxyR and Yap1, the chaperone Hsp33, and mitochondrial branched chain aminotransferase.

- 3. Structural cysteines.** Occurring in numerous proteins in all of life's kingdoms, these cysteines form intramolecular and intermolecular disulfide bonds following oxidative folding. The structures of many secreted proteins are stabilized by disulfide bonds (e.g., alkaline phosphatase).

- 4. Metal-coordinating cysteines.** These residues are involved in the coordination of certain metal ions and represent the majority of conserved cysteines in proteins. Examples include proteins containing iron-sulfur clusters, zinc fingers, and calcium ions.

- 5. Catalytic cysteines that do not change their redox state during catalysis.** This diverse class of enzymes utilizes the nucleophilic properties of cysteine for catalysis. Examples are cysteine proteases and glyceraldehyde-3-phosphate dehydrogenase.

- 6. Other functions.** Cysteines may have additional functions, such as targeting proteins to a particular cellular compartment or a membrane, being sites of irreversible

post-translational modifications, and maintaining functions (e.g., hydrogen bonding) that are not specific to cysteine.

6.4.B Cysteine-Based Redox Motifs

Many thiol-based oxidoreductases have a characteristic catalytic CXXC (i.e., two cysteines separated by two amino acids) motif. In some proteins, one cysteine could be replaced by serine or threonine; for example, the CXX(C|S|T) motif occurs in glutaredoxins, glutathione peroxidases, and arsenate reductases, and the (C|S|T)XXC motif occurs in peroxiredoxins and several selenoproteins.

6.4.C Conserved Cysteines in Metal-Binding Proteins

In addition to their role as redox residues, cysteines in the CXXC motif may be engaged in metal ion coordination. How can these residues be distinguished from redox-active residues? Metal-binding proteins can be identified using PROSITE database profiles and patterns (<http://ca.expasy.org/prosite/>). Patterns and profiles of amino acid sequences that are directly involved in metal coordination are based on prior experimental data, such as protein structures and the results of site-directed mutagenesis experiments. The PROSITE database currently contains 1416 entries that describe 1948 different patterns and profiles and can be used for identification of metal-binding proteins with good sensitivity and selectivity. Information on the new metal-binding proteins increases coverage of these proteins in the database; therefore, its predictive power is expected to grow as more proteins are identified and their functions and metal content are determined. Some cysteine residues involved in metal coordination are sensitive to oxidation, leading to disulfide bond formation and release of the metal ion. This mechanism represents an important aspect of redox regulation, such as regulation of activity of certain zinc-binding transcription factors.

6.4.D Secondary Structure Context of Redox-Active Cysteines

Analysis of the secondary structure context of candidate thiol-based redox motifs may help in their functional analysis. The major representatives of thiol-based oxidoreductases are proteins of the thioredoxin-fold superfamily. More than 90% of known thiol-based oxidoreductases belong to this superfamily. In these and many other oxidoreductases, the CXXC motifs, or the N-terminal cysteine in this motif, are located in a loop between a β -strand and an α -helix (Fig. 6.14). The downstream α -helix may stabilize the reactive thiolates of the CXXC motif and could assist in prediction of an oxidoreductase function of these motifs. In contrast, most metal-binding CXXC sequences lack this structural feature. Recent progress in structural bioinformatics led to an increased accuracy of secondary structure prediction, which for thioredoxin-fold proteins exceeds 80%. There are numerous secondary structure prediction tools available on the Web (<http://ca.expasy.org/tools/#secondary>). For example, PSIPRED (<http://bioinf.cs.ucl.ac.uk/psipred/>) is a simple and a reliable secondary structure prediction method, which is based on sequence alignment outputs obtained from PSI-BLAST.

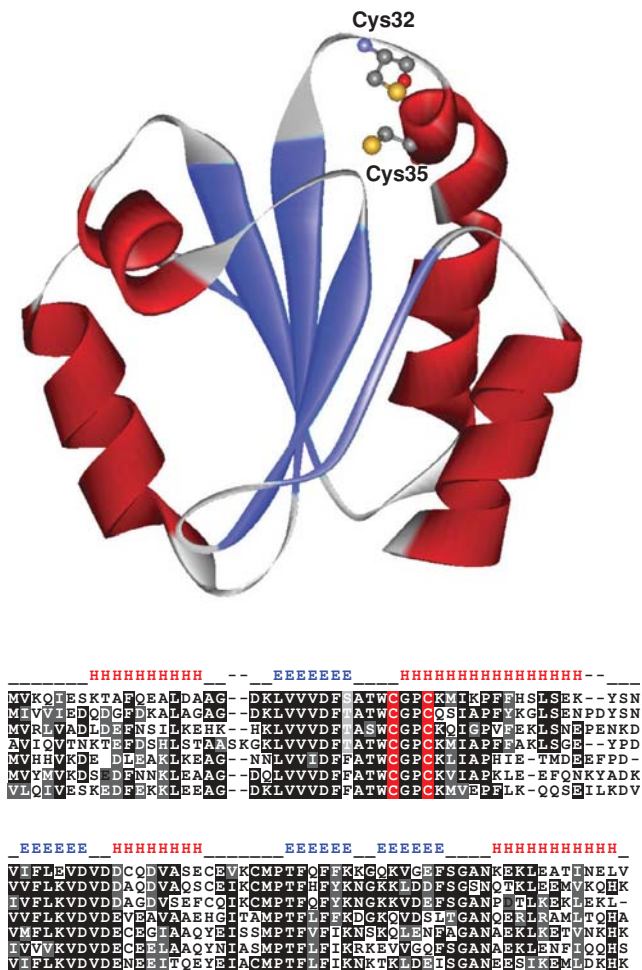


Figure 6.14. The three-dimensional structure of human thioredoxin and a multiple alignment of thioredoxins. The predicted secondary structure of thioredoxins is shown above the sequences. α -Helices are shown as red stretches of H, and β -strands as stretches of blue E. The CXXC-like motif (highlighted in red in the sequences) is located in the loop and corresponds to Cys32 and Cys35 in the structure of human thioredoxin. This motif is also close to the surface of the protein and is accessible to substrates.

6.4.E Structure Modeling

The current version of the Protein Data Bank (<http://www.rcsb.org>) contains a redundant set of 39,678 protein structures, covering most known protein families. One of the requirements for thiol-based catalysis is accessibility of redox cysteines for substrate binding, and structure modeling may help examine this property (Fig. 6.14). One of the popular and reliable 3D structure prediction services is the Structure Prediction Meta Server (<http://bioinfo.pl/meta/>). It combines various fold recognition and local

structure prediction programs from independent international projects. There is also a powerful and fast standalone tool, MODELER (<http://www.salilab.org/modeller/>), which is based on primary sequence similarity to proteins with known structures. An additional advantage of structure modeling, as applied to thiol-based oxidoreductases, is the ability to filter out the proteins with structural cysteines. Finally, one method, known as Fuzzy Functional Forms (FFF), has been applied successfully to identify thiol-based oxidoreductases by searching for structural similarity to the active site residues of thioredoxins.

6.4.F Comparative Sequence Analysis of Thiol-Based Oxidoreductases

Identification of conserved domains in candidate oxidoreductases containing catalytic cysteines is an additional powerful method of functional analysis. An RPS-BLAST program, coupled with a frequently updated NCBI Conserved Domains database, can be used for this purpose. The use of CDART (Conserved Domain Architecture Retrieval Tool, <http://www.ncbi.nlm.nih.gov/Structure/lexington/lexington.cgi?cmd=rps>) allows identification of domains and their combinations in proteins of interest. An additional useful tool for protein function prediction is STRING (<http://string.embl.de/>). This precalculated database of functional associations currently contains 1,513,782 proteins from 373 species. STRING combines information derived from gene neighborhoods in completely sequenced genomes, domain fusion, and protein co-occurrence (phylogenetic profiles), and integrates information from these methods. The user may also take advantage of built-in tools for literature search and data from high throughput functional analyses.

Identification of specific functions of cysteine residues has been limited to case-by-case experimental approaches. Recently, a procedure was developed for high-throughput identification of catalytic redox-active cysteine in proteins by searching for sporadic selenocysteine-cysteine pairs in sequence databases. This method is independent of protein family, structure, and taxon, and identifies the majority of known thiol oxidoreductases. Rapid accumulation of sequence information should lead to detection of additional oxidoreductase families.

SELECTED REFERENCES

1. Martin, J.L. (1995). Thioredoxin—fold for all reasons. *Structure* 3:245–250.
2. Giles, N.M., Watts, A.B., Giles, G.I., Fry, F.H., Littlechild, J.A., and Jacob, C. (2003). Metal and redox modulation of cysteine protein function. *Chem. Biol.* 10:677–693.
3. Fomenko, D.E., and Gladyshev, V.N. (2003). Identity and functions of CxxC-derived motifs. *Biochemistry* 42:11214–11225.
4. Fetrow, J.S., Siew, N., Di Gennaro, J.A., Martinez-Yamout, M., Dyson, H.J., and Skolnick, J. (2001). Genomic-scale comparison of sequence- and structure-based methods of function prediction: Does structure provide additional insight? *Protein Sci.* 10:1005–1014.
5. Fomenko, D.E. Xing, W., Adair, B.M., Thomas, D.J., and Gladyshev, V.N. (2007). High-throughput identification of catalytic redox-active cysteine residues. *Science* 315:387–389.

6.5 ELECTROPHYSIOLOGY

6.5.A Electrophysiology Part I: Ion Channel Physiology

MARK P. THOMAS

School of Biological Sciences, University of Northern Colorado, College of Natural and Health Sciences, Greeley, Colorado

Ion channels play roles in all tissues and mediate functions as diverse as cell volume regulation, water balance, cell migration and shape changes, and metabolite uptake. These functions share a common feature: the use of ion gradients as a source of energy to move water, ions, and other solutes between compartments. The other basic function of ion channels is to use ion gradients as a source of information in the transduction of signals between and within cells. This section begins with a discussion of the essential properties of ion channels that account for their diversity and adaptation to varied physiological roles. To help the student interpret and critically evaluate the electrophysiological literature, a short primer on electrical terminology and diffusion potentials is then provided. Following a general description of the factors that modulate ion channel function, specific examples of the interactions between ion channels and cellular redox state are discussed.

6.5.A1 Properties of Ion Channels Large arrays of ion channel proteins exist in biological membranes, with each cell type expressing a unique pattern of proteins that render a distinct electrical phenotype. However, the differences between channel proteins that account for their functional diversity can be accounted for by a small number of essential characteristics. Thus, ion channels are characterized by three major properties: their relative permeability to different ionic species (*selectivity*), the manner in which their opening and closing is regulated (*gating*), and the rate at which permeable ions are able to transit the pore structure (*single-channel conductance*). A brief survey of these major properties is discussed here.

6.5.A1a Ionic Selectivity The primary characteristic of an ion channel is its relative permeability to different ion species. Channels are grouped into families based on their ionic selectivity, and thus there are families of Na^+ , Ca^{2+} , K^+ , and Cl^- selective channels. In addition, there are also less selective groups of pores that are permeable to a broader range of ionic species, for example, monovalent cations (Na^+ and K^+) or all cations (effectively, Na^+ , K^+ , and Ca^{2+}). Ion selectivity is determined by the amino acid sequence in the region of the membrane-spanning portion of the protein known as the selectivity filter. This region is located where the aqueous channel narrows to a minimum diameter and consists of amino acids with charged side chains that define the electrostatic environment that ions “see” as they diffuse into the water-filled pore. The dimensions and valence of this region constrain the effective electrical diameter of the pore, thus determining which ionic species are able to pass through the channel. In addition to determining permeant ionic species (e.g., Na^+ or K^+), the selectivity filter also determines which ions are able to block the channel pore (e.g., Mg^{2+} or Pb^{2+}).

6.5.A1b Channel Gating A second fundamental characteristic of ion channels is the manner in which the opening and closing of the pore is regulated. This property is referred to as channel gating and serves to subdivide ion channels further into three general groups; thus, channels are gated by (1) changes in the transmembrane electrical potential, (2) mechanical forces impinging on the pore, or (3) allosteric binding of a “ligand,” which can be an ion, a small molecule, or another protein molecule. Regardless of the mechanism, all ion channels are gated by conformational changes that affect ion transit through the pore region. For voltage-gated channels, the conformational change is mediated by movement of charged moieties (usually specific amino acid side chains) within the protein in response to changes in the electrical field across the membrane. For mechanically gated channels, the change in conformation results from forces transmitted through associated proteins (usually cytoskeletal elements) in response to mechanical deformation of the cell membrane. For ligand-gated channels, the conformational change results from binding of the gating agent to a specific binding site on the channel protein. This category of channel is the most diverse, due to the many different types of ligand–channel interactions that have evolved to regulate channel function.

Ion flow through channel pores occurs in an all-or-none fashion: the channel is either in a “closed” state or an “open” state and the probability that the channel is in a given state is determined by the gating factor(s) for that channel type. For example, the binding of a neurotransmitter ligand to its cognate receptor channel leads to an increase in the probability that the channel will be in an “open” state.

6.5.A1c Single-Channel Conductance The third important property of an ion channel is a quantitative measure of its ability to transport charge across the membrane, the single-channel conductance. The rate of flow of a particular ion is proportional to the potential energy difference for that ion species across the biological membrane in which the pore is situated. This proportionality is expressed as a conductance and is generally a fixed, invariant characteristic of a given ion channel type. The total flow of ions through a population of ion channels on the surface of a cell is thus regulated by (1) the total number of channels present in the membrane and (2) the amount of time that individual channels are open, a function of the channel’s “open probability.” In order to understand and quantify this process, a review of electrical terminology and diffusion potentials is discussed next.

6.5.A2 Ohm’s Law, Diffusion Potentials, and Current–Voltage Relationships The relationship between charge flow and electrical potential is described by Ohm’s law (Eq. (6.13)):

$$I = \frac{V}{R} \quad \text{or} \quad I = g V, \quad \text{where} \quad g = \frac{1}{R} \quad (6.13)$$

where I is current or charge flow per unit time, V is the electrical potential or “pressure” exerted on the charged species, and their proportionality is expressed as either R (resistance) or its reciprocal, g (conductance). For biological membranes, it is more intuitive to refer to conductance, since this parameter can be associated with

the permeability or “leakiness” of the membrane. The unit of current is an ampere or amp (symbol A); in biomembranes and channels current magnitudes range from nanoamps to picoamps. The unit of potential is the volt (symbol V), with transmembrane potentials measured in millivolts. The unit of resistance is the ohm (Ω ; typically megohms ($M\Omega$; 1×10^6 ohms) or gigohms ($G\Omega$; 1×10^9 ohms)) and conductance is expressed as siemens (typically nanosiemens (nS; 1×10^{-9} siemens) or picosiemens (pS; 1×10^{-12} siemens)).

Across cell membranes, there are two sources of potential energy that exert motive forces on ionic species: differences in ion concentrations and differences in charge distribution (i.e., charge separation, which creates an electrical force on all charged species). From thermodynamic theory, we can derive an equation that quantifies the energy difference between ions on opposite sides of a biomembrane. The energy stored in a concentration gradient is quantified as (Eq. (6.14)):

$$\Delta G_{\text{chem}} = -RT \times \ln \frac{[\text{ion}]_{\text{out}}}{[\text{ion}]_{\text{in}}} \quad (6.14)$$

where ΔG_{chem} = chemical energy difference inside the cell with respect to the outside, R = gas constant = $8.314 \text{ J/mol} \cdot \text{K}$, and T = temperature in (K). Whereas the energy stored in an electrical gradient is quantified as (Eq. (6.15)):

$$\Delta G_{\text{elec}} = zF \times \Delta V \quad (6.15)$$

where ΔG_{elec} = electrical energy difference inside the cell with respect to the outside, z = valence of the ion, F = Faraday’s constant = $\sim 10^5$ coulomb/mol, and ΔV = potential difference inside the cell with respect to the outside (note: volt = joule/coulomb). Now, at equilibrium ($\Delta G = 0$), these quantities must sum to zero; rearranging yields the Nernst equation (Eq. (6.19)):

$$\Delta G_{\text{chem}} + \Delta G_{\text{elec}} = 0 \quad (6.16)$$

$$\Delta G_{\text{elec}} = -\Delta G_{\text{chem}} \quad (6.17)$$

$$zF \times \Delta V = RT \times \ln \frac{[\text{ion}]_{\text{out}}}{[\text{ion}]_{\text{in}}} \quad (6.18)$$

$$\Delta V = V_{\text{ion}} = \frac{RT}{zF} \times \ln \frac{[\text{ion}]_{\text{out}}}{[\text{ion}]_{\text{in}}} \quad \text{or} \quad V_{\text{ion}} = 2.3 \frac{RT}{zF} \times \log \frac{[\text{ion}]_{\text{out}}}{[\text{ion}]_{\text{in}}} \quad (6.19)$$

where V_{ion} is defined as the Nernst potential for that ion species. The Nernst equation is a very useful tool for the electrophysiologist; knowing the concentrations of an ion on both sides of a membrane, this equation predicts the transmembrane potential where no net forces are exerted on the ion. The Nernst potential is a theoretical parameter.

Currents through ion channels can be recorded using two different configurations. In whole-cell recordings, the current flowing across the entire cell membrane is measured as a function of membrane potential. In single-channel recordings, the

current through a single channel is measured as a function of membrane potential. When currents are measured as a function of varying potential, the reversal potential is the transmembrane voltage where no net current flow is observed across the cell membrane (in a whole-cell recording) or through the single pore (in a single-channel recording). The reversal potential (V_{rev}) is thus an empirical parameter. Importantly, when a channel is permeable to a single ion species, the reversal potential for the channel is equal to the Nernst potential for that ion. Thus, measuring the current flow through a single channel over a range of potentials enables the investigator to determine (1) the single-channel conductance and (2) the permeability characteristics of the channel, by using the measured reversal potential in comparison with the predicted V_{ion} for candidate ions.

To illustrate this concept, we need a new form of Ohm's law for diffusion potentials (Eq. (6.20)):

$$I = g(V_m - V_{\text{rev}}) \quad (6.20)$$

where I = current (whole cell or single channel), g = conductance (whole cell or single channel), V_m = transmembrane potential ($V_{\text{in}} - V_{\text{out}}$), and V_{rev} = reversal potential for conductance or channel type. Figure 6.15 shows a current–voltage plot for recordings from a single K^+ -selective pore that has a single-channel conductance of 5 nS. Also shown is a diagram of the forces on the K^+ ion (the electrical force (F_e), the chemical force (F_c) and the net force (F_{net}) at three different transmembrane potentials. Note that the chemical force does not change as the membrane potential is altered, since the ion concentrations do not change significantly during the experiment. Note also that the net force, and thus net current flow, is zero when the membrane potential is -98 mV (the K^+ equilibrium potential, V_K , calculated using typical concentrations of intracellular and extracellular K^+ ion). This is shown on the current–voltage

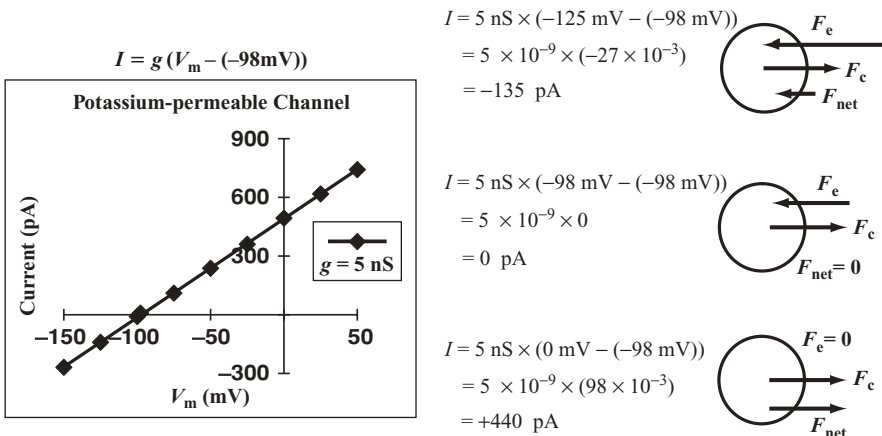


Figure 6.15. A current–voltage plot for a K^+ permeable channel ($V_{\text{rev}} = V_K = -98$ mV).

plot as the x-intercept point, where $I = 0$. The force diagrams also show the direction of net ion flow; from this it is seen that inward currents have a negative sign and outward currents are positive. This is due to our formulation of Ohm's law for ionic diffusion potentials, and thus a characteristic of all current–voltage plots and a convention used in traces of ionic currents versus time. Note that, for a negatively charged ion such as Cl^- , the inward movement of Cl^- is an “outward” (positive) current.

6.5.A3 Role of Ion Channels in Redox Regulation Redox reaction in cells can modulate their electrical properties. As an example, here we outline the consequences of the production of free oxygen radicals by the major cellular element of the innate immune system, the mononuclear phagocyte or macrophage. These cells, present in all tissues, play a major role in the phagocytosis of debris from damaged and dying cellular elements. The process of phagocytosis is accompanied by a respiratory burst (increase in oxygen consumption) and the production of ROS such as $\text{O}_2^{\cdot-}$ and H_2O_2 . ROS production, which occurs in all cells to some extent as a consequence of oxidative metabolism, is mediated in phagocytes by the electrogenic enzyme complex, NADPH-oxidase. The activity of the membrane-bound NADPH-oxidase results in the release of $\text{O}_2^{\cdot-}$ into the phagocytic compartment of the macrophage (the phagosome) and release of protons into the cytosol (Fig. 6.16). The generation of ROS by macrophages is thus accompanied by plasma membrane depolarization and cytosolic acidification. Since macrophages are capable of producing large quantities of $\text{O}_2^{\cdot-}$ during a respiratory burst, this sustained ROS production requires a continuous compensatory movement of positive charge outward across the plasma membrane. Based on studies using human neutrophils or eosinophils, it has been hypothesized that the voltage- and pH-dependent proton conductance present in all phagocytes may play a role in compensating for ROS production in all macrophages (Fig. 6.16).

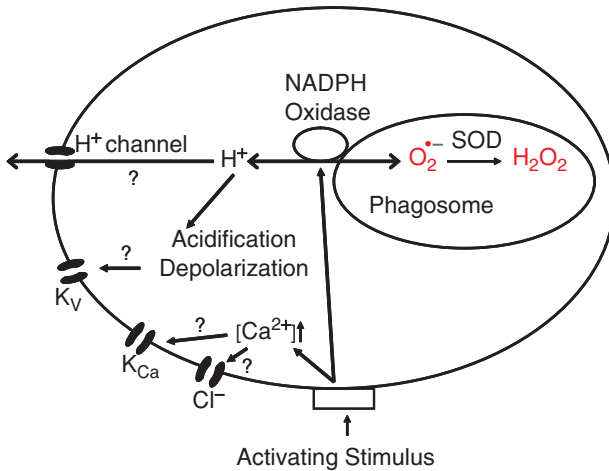


Figure 6.16. Oxidative burst in a macrophage.

However, other ion currents mediated by channels permeable to potassium, chloride, or nonspecific cations may also play a role. It is especially interesting to note that chloride channels activated by NADPH oxidase-derived H_2O_2 have recently been identified. It is possible that the story may be complicated by the fact that, in addition to charge compensation, another function of these ionic conductances may be to compensate for or regulate pH changes or volume changes that accompany the respiratory burst. Nevertheless, this cellular process represents a mechanism whereby redox activity is intimately linked to ion channel activity. A complete understanding of this association may provide therapeutic avenues for the control of free radical production, which plays a crucial role in all inflammatory processes.

6.5.A4 Modulation of Ion Channels by Redox State Given the importance of cellular redox state in cell function, it is not surprising that ion channels, like other cellular proteins, are affected by their redox environment. However, the modulation of channel activity by redox state represents a relatively novel and understudied area of research. Two interesting examples of the redox modulation of ion channels are described next.

6.5.A4a NMDA-Type Glutamate Channels A major family of ligand-gated ion channels present in vertebrate brains is activated by the amino acid glutamate. These channels mediate rapid communication between nerve cells at excitatory (depolarizing) synapses. A subgroup of glutamate-gated channels, named for the exogenous agonist *N*-methyl-D-aspartate (NMDA), play a vital role in the changes in synaptic efficacy that underlie learning and memory (i.e., information storage and retrieval) in the vertebrate brain. Their functional role in this synaptic “plasticity” stems from two properties inherent to the ion pore: a voltage-dependent blockade of the pore by Mg^{2+} at “resting” membrane potential that is alleviated by membrane depolarization, and a substantial permeability to Ca^{2+} in addition to the monovalent cations Na^+ and K^+ . The former property accounts for the associative characteristics of NMDA receptor-mediated synaptic responses that determine the manner in which synaptic activity shapes information storage at the synapse. The Ca^{2+} permeability of the pore enables the coupling of channel activation to a Ca^{2+} signaling cascade that induces the synaptic alterations.

The same properties of NMDA-type glutamate channels that support normal synaptic transmission and plasticity can also lead to neuronal injury and death in pathological states such as epilepsy, traumatic brain injury, and neurodegenerative disorders. Thus, neuronal hyperexcitability induced in these disease conditions can lead to prolonged membrane depolarization and excessive activation of NMDA channels, resulting in Ca^{2+} -mediated neurotoxicity. In the normal brain, many homeostatic mechanisms exist to protect against overactivation of NMDA channels; among these it appears that redox-sensitive sites on the channel may play a role. Thus, one or more redox-sensitive thiol groups are present on the extracellular domain of the channel that affect channel activation. It has been proposed that, under physiological conditions, small changes in redox potential that accompany changes in neural activity may feed back to regulate NMDA receptor activity within a controlled range. However,

the larger changes in redox potential that accompany many pathological states may overwhelm this feedback system, leading to enhanced activation of NMDA receptors and exacerbation of neuronal damage. Hence, redox modulation of NMDA receptor activity may lead to novel therapies for alleviating neural damage under pathological conditions.

6.5.A4b ATP-Sensitive K^+ Channels in Dopaminergic Neurons Neurons in the ventral midbrain of vertebrate brains that produce and release dopamine as the primary neurotransmitter play a vital role in the regulation of behavior, including motor control, habit learning, and cognitive functions. The progressive loss of dopaminergic neurons, which may be especially sensitive to oxidative stress due to oxidative products of dopamine metabolism, is responsible for the severe motor impairment and cognitive disabilities characteristic of Parkinson's disease.

The sensitivity of dopaminergic neurons to oxidative damage suggests that homeostatic mechanisms might exist in these cells linking metabolic state to cellular excitability. Indeed, these neurons contain very high levels of a K^+ channel that is closed by allosteric binding of ATP to the cytosolic region of the pore. Thus, when ATP levels drop as a result of low energy availability, these channels open, leading to cell hyperpolarization and a decrease in firing rate, which represents an elegant mechanism for coupling metabolic state to cellular excitability. Furthermore, it has been demonstrated that these same channels are modulated by intracellular redox state. Thus, elevation of cytosolic H_2O_2 levels leads to ATP-sensitive K^+ channel activation. This example demonstrates how a single ion channel species can “monitor” both the energy status (ATP/ADP ratio) and redox potential of a cell to regulate energy balance. While these channels are highly expressed in dopaminergic neurons of the midbrain, they are present throughout brain and in other redox-sensitive tissues such as cardiac muscle and kidney, suggesting a universal role in linking energy homeostasis to membrane excitability.

The modulation of ion channel function by cellular redox potential represents a relatively unexplored area of electrophysiological research. The growing awareness of the role that oxidative stress and redox imbalances may play in disease states such as neurodegenerative disorders, stroke, and cardiac myopathies promises to stimulate research into the modulation of electroexcitable properties of brain and cardiac tissue by redox status. Conversely, studying the role that ion channels play in regulating redox balance may lead to insights into the homeostatic mechanisms that link cellular energy metabolism and excitability.

SELECTED REFERENCES

1. Avshalumov, M.V., Chen, B.T., Koos, T., Tepper, J.M., and Rice, M.E. (2005). Endogenous hydrogen peroxide regulates the excitability of midbrain dopamine neurons via ATP-sensitive potassium channels. *J. Neurosci.* 25(17):4222–4231.
2. Gozlan, H., and Ben-Ari, Y. (1995). NMDA receptor redox sites: Are they targets for selective neuronal protection? *Trends Pharmacol. Sci.* 16:368–374.

6.5.B Electrophysiology Part II

HAROLD D. SCHULTZ

Department of Cellular and Integrative Physiology, University of Nebraska College of Medicine, Omaha, Nebraska

Changes in the redox state of proteins play an important role in many cellular functions including ion channel function. For example, reduction of disulfide bonds in proteins that form the ion-traversing pore of a channel may alter the conformation of the protein and impair or enhance the ability of ions to flow through the pore, and thus alter the ionic conductance across the cell or organelle membrane. Section 6.5.A on ion channel physiology summarizes the basic concepts governing the movement of ions through membrane channels. Fundamentally, the movement of ions through channels generates a current flow and generates electrical potential differences across membranes which can be measured. The characteristics of currents through ion channels provide important information about the function and regulation of ion channels and their influence on membrane properties and cell function. This section describes basic techniques for assessing the electrophysiological characteristics of ion channels from the level of the whole animal to the isolated channel itself. These techniques can be combined with biochemical and genetic manipulations of redox states and systems in cells to assess the redox regulation of ion channels and its role in cell and tissue function.

6.5.B1 An Introduction to Electrophysiological Techniques Electrophysiology pertains to the study of the cellular and molecular mechanisms that regulate the flow of ions in single cells or tissues and, in particular, to the electrical recording techniques that enable the measurement of this flow or current. These currents are generated by the passive diffusion of ions such as Na^+ , K^+ , Ca^{2+} , and Cl^- through highly selective molecular pores or ion channels in the cell surface membrane. Electrophysiological techniques have been devised to record the electrical potential difference (voltage) maintained by these ions across a cell membrane, to record the currents generated as ions move through channels across a cell membrane, or (with extracellular recording) to record changes in macroscopic current densities created within regions of tissue.

There are two major types of electrophysiological techniques: extracellular and intracellular recordings. Extracellular recording includes single unit recording (e.g., action potentials from a “single” axon or nerve soma), field potential recording, and amperometry. Intracellular recording techniques encompass two major subdivisions: passive measurement of the transmembrane potential and voltage/current clamp techniques.

Because voltage and current changes across cell membranes are normally very small in magnitude (mV and pA range, respectively), the signal output must be enhanced (often by >1000-fold) by an amplifier for recording and display purposes. Due to the large amplification of the signal intensity, modern computer-controlled

amplifiers incorporate analog and digital filters and series resistance and capacity compensation to provide stable and reliable outputs with high signal-to-noise ratios.

6.5.B2 Extracellular Voltage Recording An easily applied technique used in electrophysiological research is extracellular voltage recording. Single- and multiunit (a unit can be a nerve soma or an axonal fiber, which can be discriminated by the characteristic size and shape of its action potential) recordings of action potentials are commonly performed in brain, brain slice, and peripheral nerve preparations. Field potentials (the voltage vectors created by the activity of large numbers of electrically excited cells within a tissue) are recorded by placing recording leads at various points on the surface of the tissue or of the body. Typical examples of field potentials are electrocardiograms, myograms, and encephalograms. The recording electrodes and the specific techniques themselves vary considerably depending on the application. The major advantage of this technique is that *in vivo* measurements can be obtained from working tissues. Recordings of multiunit and field potentials often can be obtained from conscious animals, and with the use of modern telemetric devices, such signals even can be obtained from freely moving animals over long periods of time.

Recordings of extracellular potentials from intact single cells in tissues, termed single-unit recordings, typically are performed by positioning a sharp metal (platinum, tungsten, etc.) or glass microrecording electrode with a micromanipulator, such that the tip of the electrode records extracellular potentials from a nearby nerve or muscle cell. This technique can be used to record single-unit nerve activity from functioning neurons in the intact brain or peripheral nerves, or from isolated brain slices for more precise control of cellular influences.

6.5.B3 Intracellular Recording Intracellular recording, sometimes known as transmembrane recording, measures the voltage across the membrane of a single cell or a single ion channel (patch clamp, see Section 6.5.B4). This requires the insertion of a recording electrode into a cell so that the intracellular potential can be measured against the extracellular or ground potential. The recording of this transmembrane voltage is the basic measurement made in all intracellular recordings.

Due to the constraints required for visualization and control of electrode insertion into a single cell (entailing the use of a microscope and micromanipulator), intracellular recordings are most successfully applied to isolated cells or tissue slices, where vibration and disruption of the preparation can be minimized.

The properties of the recording electrode vary according to the requirements of a particular recording. The most common electrophysiological recording techniques use a glass electrode to establish electrical contact with the inside of a cell. Such an electrode is made by heating and pulling out a fine capillary glass pipette to form an even finer tip. The tips of these electrodes are about 0.1 micron in diameter for intracellular “sharp electrode” recording or 1 micron in diameter for patch-clamp recording (see Section 6.5.B4). For intracellular recording, a sharp glass electrode is filled with a salt solution, and a chloride-coated silver wire is inserted to establish an electrochemical junction with the pipette fluid and the tissue or cell into which the

pipette is inserted. This electrode salt solution typically is composed of a high concentration (2–3 M) of potassium chloride, potassium acetate, or potassium methylsulfate. Potassium is used since it is the predominant intracellular ion.

Current-clamp is a method of intracellular recording involving measurement of the voltage difference across the cellular membrane while injecting constant positive or negative current (as “square” DC pulses) into the cell. By using appropriate “bridge” methods to balance out the resistance of the recording micropipette, the resistance (R , or its inverse, conductance, g) of the membrane can be obtained by Ohm’s law ($I = gV$). If a drug or test solution is applied to the cell, a change in the response to the current pulse indicates a change in ionic conductance. By incrementally varying the amplitudes of the current steps over a wide range (typically from 0.1 to 1 nA for neurons), a family of voltage–current (V – I) curves is obtained, where voltage is typically plotted as a function of injected current. This curve reveals much about the “macroscopic” currents, that is, the aggregate currents flowing through many ionic channels passing through the cell membrane at different membrane potentials. Any experimental treatment that alters ionic conductance (e.g., a redox perturbation) will also alter the slope and shape of the V – I curve. Thus, a reduction in the slope of the V – I curve (with voltage as the dependent variable) indicates increased ionic conductance, whereas a steeper slope indicates decreased conductance. A disadvantage of this technique, however, is that the measurements do not allow one to discern which ion(s) are responsible for the conductance change. In addition to V – I curves, other cellular voltage responses that can be recorded by this technique include neuronal postsynaptic potentials (excitatory or inhibitory) in response to activation of synaptic inputs and rebound voltage responses to strong hyperpolarizing (or depolarizing) current steps.

Voltage-clamp recording is another common method of intracellular recording in which the investigator measures the current required to hold a cell at a constant voltage, that is, the inverse to the current-clamp technique explained previously. Voltage commands or “clamps” are typically applied as steps or as a steady voltage, termed “holding potential”. A major advantage of this method over current-clamp recording is that the investigator can directly measure ionic currents. In addition, by using abrupt voltage-command jumps, one can measure the rapid changes in the currents and their kinetics as the channels adjust (open or close) to the new potential. Thus, with this method, voltage-dependent and time-dependent ionic conductances can be monitored directly, and the effects of drugs, such as oxidizing and reducing agents, or other manipulations on these conductances can be assessed.

Voltage-clamp recording involves the same experimental setup and data analysis methods as those used in current-clamp recording; thus, most high-performance commercial headstage amplifiers allow switching between the two modes. Typically, one usually penetrates a cell with the micropipette in the current-clamp mode to determine if the cell exhibits a normal resting membrane potential and is viable. Then after the cell stabilizes, a series of adjustments of the recording characteristics can allow switching to the voltage-clamp mode. Because sharp glass microelectrodes have the unfortunate features of high electrical resistance, high thermal noise, and thus a limited ability to pass the current necessary for voltage clamping, the preferred method

of voltage clamping involves inserting two pipettes into a cell—one to inject current to maintain the holding potential and the other to record the transmembrane voltage. This technique can be used for large cells such as the *Xenopus* oocyte or some invertebrate neurons, but it is technically limited for small cells such as mammalian neurons.

For small cells, a “switch-clamp” or discontinuous voltage-clamp method is used in which a single pipette is switched rapidly (at about 5 kHz) between current injection and voltage measurement modes and the measured voltage is compared to a desired voltage (the “holding” or “command” potential). This current-injection cycle is repeated iteratively. Disadvantages of the switch-clamp method include the loss of high fidelity recordings of rapid changes in membrane conductance because of the slow time constant of the electrode as it switches between injecting and measuring modes, the difficulty of keeping the pipette resistance and capacitance to a minimum (usually 50–70 megohms or less), and the difficulty in clamping remote membrane areas (e.g., dendrites), which can lead to “space-clamp” artifacts; thus, frequent finetuning of the bridge circuit is required to minimize microelectrode resistance drifts.

6.5.B4 The Patch-Clamp Technique The limitations of intracellular patch-clamp techniques led Sakmann and Neher in the 1970s to explore the idea that one could use a glass electrode with a larger tip diameter and, by juxtaposing the tip at the cell surface, isolate a small area of the membrane surface itself (a patch) to allow measurement of currents across the isolated membrane patch. The patch-clamp method requires fabricating and fire-polishing of specific types of glass micropipettes with large tip (1 micron) diameters that can form a high resistance (gigohm) seal with the cell membrane while maintaining a low internal resistance. The gigohm seal is essential to allow the high current gain and low noise amplification necessary for recording the small, brief currents passing through single ionic channels. The low internal resistance of the tip allows the microelectrode to simultaneously and continuously control membrane voltage across the membrane patch while recording the ionic conductance across the membrane at that command voltage. For this reason, the patch-clamp is sometimes referred to as the continuous single electrode voltage-clamp technique. In patch-clamp configurations, the salt solution in the recording pipette is the bathing solution for one side of the cell membrane; thus, the composition of the pipette solution should mimic the normal ionic environment exposed to the membrane surface.

6.5.B5 Single Channel Patch-Clamp Configurations Patch-clamp methods can be applied in at least five configurations, giving the technique formidable adaptability for testing the molecular mechanisms of ion channel function. Three of these configurations (cell-attached patch, inside-out patch, and outside-out patch) allow study of individual ion channels under different conditions (Fig. 6.17). In the cell-attached configuration, after formation of the gigaohm seal between the electrode and the membrane, recording of single channels is made without further disruption of the cell membrane. In the other two patch-clamp preparations, the membrane patch

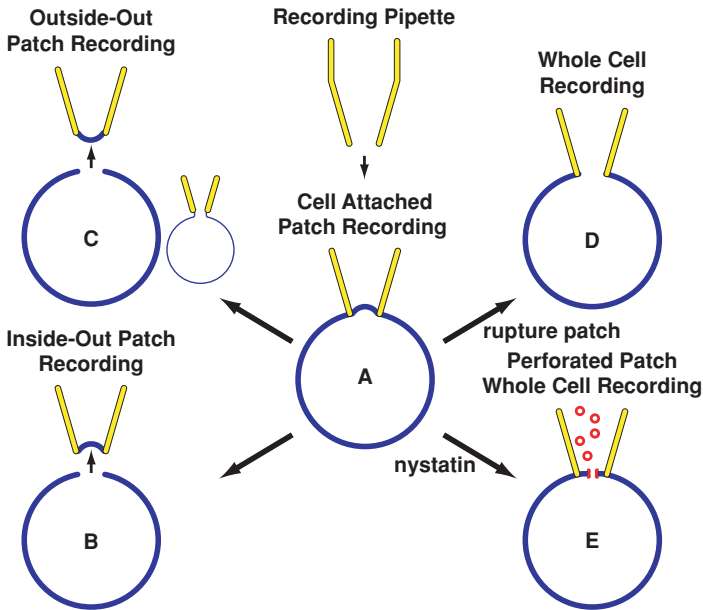


Figure 6.17. Schematic representations of patch-clamp configurations. The same patch pipette and amplifier setup can be used to record in five different configurations (see text for details). Single channel recordings can be taken from three of the five configurations: cell-attached (A), inside-out (B), and outside-out patches (C). Breaking the patch under the pipette (by suction) allows whole-cell voltage or current recording (D). Addition of a pore-forming compound (e.g., nystatin) to the pipette solution will allow whole-cell recording while preventing dialysis of large molecular cytosolic constituents into the pipette (E).

is detached from the cell after a gigohm seal is formed, and single channel activity is recorded from the membrane patch in isolation from the cell.

In the inside-out configuration, the patch of membrane is gently pulled away from the cell, and the patch remains attached to the pipette with its cytoplasmic surface now exposed to the bathing solution. Preparation of the outside-out patch begins by making a whole-cell configuration (see Section 6.5.B6) whereby, after forming the gigohm seal, the membrane patch under the pipette is ruptured by applying a strong vacuum through the recording pipette. Then the pipette is gently pulled away from the cell, carrying a piece of membrane with it. The detached membrane seals over the pipette tip during this maneuver, in favorable cases forming a membrane patch in which the extracellular membrane surface is exposed to the bathing solution.

From these types of recordings, it is now known that virtually all ion channels exhibit stochastic fluctuations between states that are closed and open to the flow of ions, and that the current carried by this flow of ions is fixed and does not vary for a specific channel (e.g., Fig. 6.18, single channel recording). This single channel conductance is an intrinsic property of the channel and differs with different

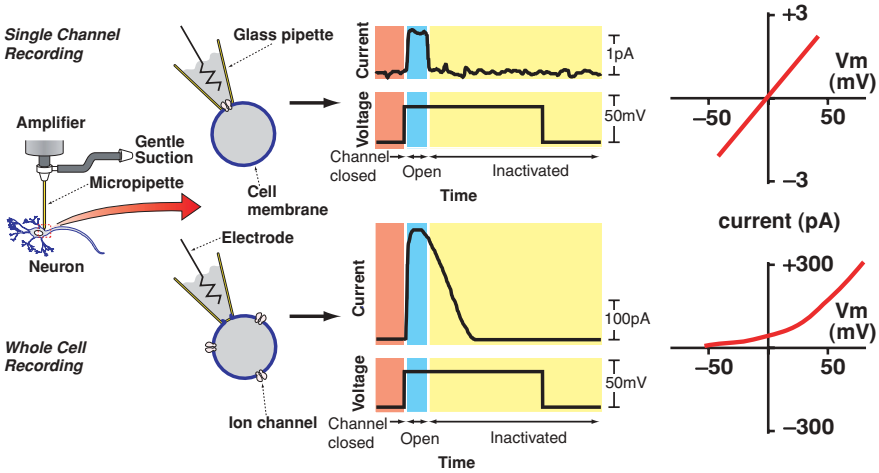


Figure 6.18. Schematic illustration of a patch-clamp electrode attached to a neuron with recordings obtained from either the cell-attached single channel patch configuration (top) of the whole-cell configuration (bottom). Examples of current traces obtained from these configurations are shown to the right of the illustrations. In single channel recording (top), current is generated as specific ions (such as K^+) move through the ion-selective channel in response to a voltage gradient across the patch membrane. In this example the channel remains open only momentarily and then closes (inactivated) due to a conformational change in the channel pore. In the bottom example, the same channels are recorded, but the current output is the sum of all of the individual currents generated by these channels in the open state at any given voltage. The peak current taken from the current trace is then plotted as a function of the voltage change for each voltage step applied (far right graphs). The slope of the current–voltage relationship for a single channel recording represents the conductance of that channel (top graph), represented as a linear relationship between current and voltage. The magnitude of the current generated in the whole-cell configuration (bottom far right graph) is a function of both the conductance of the channels and the number of channels in the open state at any given voltage. The nonlinear characteristic of this whole-cell recording would suggest that the open state of the channels is influenced by the voltage gradient, indicating that ion movement through the channel is voltage gated.

channels and ions used but is independent of the voltage or ion gradient. This observation has led to the concept of the unit conductance, one of several physical parameters by which ion channels can be distinguished (other parameters would be ion selectivity and pharmacological profile). The contribution of individual ion channels to total membrane conductance is not dependent on variations in current carried through each channel, but by the gating characteristics of the channel that determine the relative times spent in open and closed states. Therefore, single channel recordings are analyzed by measuring the durations of the closed and open times and determining their statistical properties, such as the probability density function of the closed and open durations, and the statistical correlations between those durations,

as indices of the channel's gating characteristics. This topic is further discussed in Section 6.5.A.

6.5.B6 Whole-Cell Patch-Clamp Configurations The fourth adaptation of the patch technique, called the whole-cell patch-clamp configuration, is a bit of a misnomer, since the technique does not measure conductance through ion channels of a discrete “patch” of cell membrane, but rather the total or macroscopic current across the whole-cell membrane. The whole-cell clamp uses the same pipette type and gigohm seal method described earlier for the cell-attached isolated membrane patch configuration; however, after the pipette is sealed to the membrane, another slightly stronger vacuum is applied to the pipette tip (via the tube attached to the pipette holder) to rupture the membrane under the tip without disrupting the gigohm seal or cell viability. The membrane under the tip is ruptured, allowing recording of the “macroscopic” or summed currents flowing through all channels in the entire cellular membrane (Fig. 6.18, whole-cell recording). In this configuration, the diffusible contents of the pipette then exchange over time with those of the cell cytoplasm, which imparts specific advantages and disadvantages to the usefulness of the technique (see Section 6.5.B7). A procedure can be used to prevent dialysis of cellular constituents into the recording pipette.

The fifth configuration, called the perforated whole-cell patch technique, involves inclusion of a pore-forming protein (such as antibiotics, nystatin, or amphotericin B) in the pipette solution. After a seal is formed on the cell, the antibiotic channels insert in the patch of membrane under the electrode tip, thereby providing electrical continuity between the pipette and the cell interior. The nystatin pores in the pipette tip allow passage of small monovalent ions (for current flow) but prevent the diffusion of most divalent and large nonionic constituents (e.g., protein buffers and cytosolic components of phosphorylation systems) from the cell.

The total current measured across the whole-cell membrane can be influenced by the area of the membrane (i.e., a larger cell with larger membrane surface may have more conducting ion channels and thus larger macroscopic currents). To compensate for this effect, the capacitance of the cell membrane is measured and used as an index of membrane surface area; thus, whole-cell currents are generally expressed as pA/pF, termed “current density.” Another limitation to the measurement of whole-cell currents is that it is often difficult to discern whether a change in current density is due to a change in the kinetics of the channels or due to a change in the number of active channels in the membrane. On the other hand, it is difficult to discern how the properties of single channel activities derived from the isolated patch techniques impact whole-cell currents and potentials. Thus, often both single channel and whole-cell patch techniques are used in tandem to assess channel function at the molecular and cellular levels.

6.5.B7 Advantages and Disadvantages of the Patch-Clamp Technique

The patch-clamp methods have major advantages over other conventional electrophysiological techniques to assess ion channel function. Some of the advantages of this method include the ability to directly test the gating mechanism(s) governing the

opening and closing of specific channels. In addition, selective ions, second messengers, neurochemicals, and other pharmacological agents can be applied easily and quantitatively (either in the bath or in the pipette) to both the external and internal surfaces of the membrane.

The single channel cell-attached, and inside-out patch-clamp methods are well suited for the study of second messenger systems, particularly for those systems (such as G-protein-mediated events) that are “membrane-delimited.” These methods are also well suited for use of molecular and genetic techniques. For example, one can measure the effects of site-specific substitutions in an ion channel or in any of the components coupled to that channel. Thus, one can pinpoint where in a channel molecule or subunit an antagonist or drug acts, or how protein phosphorylation or other modifications can modulate channel ionic conductance and function.

A disadvantage of the single channel patch-clamp method is the necessity to use cultured cells, or cells freshly isolated from tissue; these cells allow formation of better gigohm seals, probably because the relative lack of overlying supporting tissue facilitates close apposition and seal of the pipette to the cell membrane. In addition, compared to cells within a tissue preparation, an isolated single cell reduces the capacitance in the recording system and allows better recording characteristics for the small-current signals generated by single channels. Therefore, most single channel studies to date have been limited to cultured or isolated cells. However, new refinements have allowed whole-cell patch (and some single channel) recording in brain slices and other tissue, and even *in vivo*.

A major disadvantage of the whole-cell method usually stems from the same properties that confer the advantages. Thus, because it is usually not possible to know the exact ionic or second messenger composition of the normal resting cell, there is always the risk that essential cell constituents (e.g., cyclic AMP) will diffuse out of the cell into the pipette, which constitutes a much larger volume than that of the cell. It is thought that such diffusion accounts for the slow “run-down” in some cells of certain currents such as the L-type Ca^{2+} current. Attempting to replace such lost constituents (e.g., cyclic AMP, ATP, GTP) by adding them to the pipette solution can help alleviate some of these problems. Another approach is to use the perforated patch technique described earlier (Section 6.5.B6)

6.5.B8 Application to the Study of Redox Regulation of Ion Channel Function

This section provides a brief overview of the various types of electrophysiological techniques that are available to analyze the properties of ionic conductances across biological membranes that range in applicability from the whole animal (field potentials), to tissue (extracellular recordings), cellular (intracellular and whole-cell patch-clamp), and molecular (single channel patch-clamp) techniques. Although each experimental approach has certain limitations, one can generally minimize the limitation of one approach by combining more than one technique to address the question.

A variety of approaches can be incorporated into these techniques to assess whether the electrophysiological characteristics of ion channels are redox sensitive. These approaches include pharmacological (application of oxidizing and reducing agents,

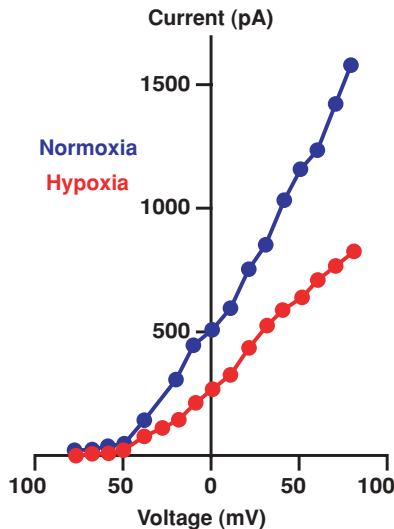


Figure 6.19. Whole-cell K^+ currents recorded from a carotid body type I cell superfused with normoxic ($PO_2 = 100$ torr) and hypoxic ($PO_2 = 40$ torr) and media. Hypoxia inhibited peak outward current at any given voltage.

activation or inhibition of redox enzymes, etc.), molecular (amino acid substitutions of cysteines in channel proteins), and genetic (knockout and knockin of genes for redox enzymes or protein subunits of channels).

Several examples of redox-sensitive ion channels are discussed in Chapter 5, Section 5.4 and Section 6.5A. Another classic example of how these techniques can be used to study the redox sensitivity of ion channels can be given by the phenomenon of inhibition of K^+ channels by hypoxia. These channels are known to play an important role in the ability of specialized sensory neurons in the carotid body to detect a depletion of oxygen in arterial blood. In response to hypoxia, these cells depolarize and send action potential signals to the brain to evoke an increase in ventilation and restore oxygen uptake into the bloodstream. Measurement of whole-cell currents across the membranes of these neurons reveals that K^+ channels are inactivated when the cells are exposed to hypoxic media (Fig. 6.19). Because K^+ currents are an outward (positive) hyperpolarizing current, inhibition of K^+ channels will allow depolarization of the plasma membrane potential above the threshold to activate action potentials. Thus, hypoxic inhibition of K^+ channels can explain the ability of the carotid body type I cells to depolarize in response to hypoxia.

The mechanism by which oxygen inhibits these channels is not known, but because oxygen is central to the function of many redox enzymes in cells, a number of ongoing studies are investigating the role of redox mechanisms in the gating properties of these channels. In particular, studies have used specific pharmacological inhibitors of certain redox enzymes such as NADPH-oxidase and heme-oxygenase, and the study

of cells from transgenic animals with knockout of redox enzymes, to illustrate that products from these reactions such as $O_2^{\cdot-}$ or carbon monoxide interact with the channel protein to regulate gating of these channels. Such evidence is obtained from open probability analysis from single channel current recordings and the magnitude of whole-cell K^+ currents. These types of studies from patch-clamp recordings in isolated neurons are further substantiated by extracellular recordings of action potentials evoked from functioning carotid body neurons *in vivo* using the extracellular recording techniques described earlier. The observation that similar manipulation of redox pathways evokes the expected change in nerve impulses arising from the carotid body provides supportive evidence for the functional implications of these redox systems on K^+ channel activity.

From this example, it is evident that patch-clamp techniques, by combining isolated patch recordings of single channels and whole-cell recordings of macroscopic currents, have become the most useful and powerful approaches for addressing questions of ion channel function at the cellular and molecular levels. Nevertheless, classical electrophysiological techniques applied to tissue and whole animals provide an additional layer of important information about the functional implications of altered ion channel activity revealed from patch-clamp studies.

SELECTED REFERENCES

1. Heinemann, S.H., and Hoshi T. (2006). Multifunctional potassium channels: electrical switches and redox enzymes, all in one. *Science* 350:1–3.
2. Kemp, P.J. (2006). Detecting acute changes in oxygen: Will the real sensor please stand up? *Exp. Physiol.* 91:829–834.
3. Morad, M. and Suzuki, Y.J. (2000). Redox regulation of cardiac muscle calcium signaling. *Antioxid. Redox Signal.* 2:65–71.

6.6 METHODS TO DETECT REACTIVE METABOLITES OF OXYGEN AND NITROGEN

MATTHEW B. GRISHAM

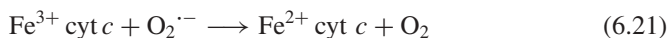
Department of Molecular and Cellular Physiology, LSU Health Sciences Center, Shreveport, Louisiana

ROS and RNS play important roles in mediating cytotoxicity through alterations in protein, lipid, and nucleic acid structure and function with resultant disruption of cellular homeostasis. This direct toxicity is due primarily to large increases (orders of magnitude) in steady-state fluxes of reactive species. However, more subtle changes in the rates of production of reactive species may impact cellular homeostasis initiating signaling cascades. Thus, sensitive, specific, and reliable methods to detect changes in reactive species are essential to understanding the roles that these substances play in normal and diseased states. However, measurement of the

in situ production of reactive species is difficult because of their rapid enzymatic and nonenzymatic decomposition. This section presents the common approaches used to detect specific reactive oxygen and nitrogen species using methods and instrumentation found in most research laboratories. Particular attention is given to those approaches that utilize methods for the *in vivo* determinations of these reactive species.

6.6.A Detection of the Superoxide Anion Radical

6.6.A1 Cytochrome *c* Reduction The reduction of ferricytochrome *c* (cyt *c*) to ferrocyanochrome *c* is one of the most widely used methods to measure rates of formation of $O_2^{\cdot-}$ by enzymes, whole cells, and vascular tissue (Eq. (6.21)). The rate constant for this reaction (at pH 8.5 and room temperature) is $\sim 1.5 \times 10^5 \text{ M}^{-1} \text{ s}^{-1}$.



The reaction may be followed spectrophotometrically at 550 nm using a difference extinction coefficient of $2.1 \times 10^4 \text{ M}^{-1} \text{ cm}^{-1}$. Besides $O_2^{\cdot-}$, other cellular reducing agents (e.g., ascorbate and GSH) will reduce ferricytochrome *c* and reductases, thereby necessitating the use of exogenous superoxide dismutase to determine the specificity of ferricytochrome *c* reduction by $O_2^{\cdot-}$. An additional complication is that reduced cytochrome *c* can be reoxidized by cytochrome oxidases, cellular peroxidases, and oxidants (e.g., H_2O_2 , peroxynitrite), requiring the use of enzyme inhibitors or scavengers of reactive species. The specificity of the cytochrome *c* assay for $O_2^{\cdot-}$ may be enhanced substantially by acetylation or succinylation of cytochrome *c*.

While the use of the cytochrome *c* reaction is considered the “gold standard” for the detection of $O_2^{\cdot-}$, particularly with *in vitro* assays and activated leukocytes, its relative insensitivity as well as interference by a variety of endogenous reductants limits its applicability for *in vivo* detection.

6.6.A2 Oxidation of Hydroethidine by Superoxide Hydroethidine (dihydroethidium, HE) is a membrane-permeable compound that can undergo two-electron oxidation to form the DNA-binding fluorophore ethidium bromide or a structurally similar product. The reaction is relatively specific for $O_2^{\cdot-}$, with minimal oxidation induced by H_2O_2 or hypochlorous acid (HOCl). However, there are limitations to the use of hydroethidine conversion to ethidium as a quantitative marker for $O_2^{\cdot-}$ production. For example, cytochrome *c* can oxidize hydroethidine. Furthermore, use of high concentrations of hydroethidine can result in $O_2^{\cdot-}$ -independent fluorescence. Finally, as with the use of any fluorophore for tissue localization of the compound of interest, the potential for autofluorescence must be addressed.

6.6.A3 Inhibition of Aconitase Activity by Superoxide Aconitase is found in the cytosol and the mitochondria and catalyzes the conversion of citrate to isocitrate. $O_2^{\cdot-}$ inactivates aconitase via the oxidation and reversible loss of an Fe from its

active site [4Fe–4S] cluster. The rate constant for this reaction is 10^6 – 10^7 $M^{-1} s^{-1}$. Alterations in aconitase activity have been used as a sensitive index of changes in steady-state levels of $O_2^{\cdot-}$ *in vitro* and *in vivo*. Using this method, steady-state $O_2^{\cdot-}$ concentrations have been estimated to be ~81–130 pM in A549 lung epithelial cells under normal conditions (86% active aconitase) and 50–200 pM under conditions of oxidative stress (50% inactive aconitase).

Aconitase activity in cell or tissue homogenates is measured spectrophotometrically by recording the conversion of isocitrate to *cis*-aconitate at $A_{240\text{ nm}}$. A coupled assay has been developed where the isocitrate product is then converted to α -ketoglutarate by NADP⁺-dependent isocitrate dehydrogenase and NADPH formation at $A_{340\text{ nm}}$ is monitored. Reactivation of aconitase activity can be accomplished by addition of the reducing agent dithiothreitol, ferrous ammonium sulfate, and Na₂S to cellular extracts and remeasuring aconitase activity. One limitation is that other oxidants such as NO, ONOO⁻, and, to a lesser extent, H₂O₂ can oxidize aconitase.

6.6.A4 Use of Chemiluminescence Reactions to Measure Superoxide Generation

Different chemiluminescent methods for the detection of $O_2^{\cdot-}$ have frequently been employed over the past ten years primarily because of the potential for access to intracellular sites of $O_2^{\cdot-}$ generation, the alleged specificity of reaction of the chemiluminescent probe with $O_2^{\cdot-}$, minimal cellular toxicity, and increased sensitivity when compared with chemical measurements. The most widely used chemiluminescent compound for $O_2^{\cdot-}$ detection is lucigenin. However, some concerns have been raised about using this probe for quantifying rates of $O_2^{\cdot-}$ formation including redox cycling of lucigenin and artifactual generation of $O_2^{\cdot-}$.

Another chemiluminescent probe for $O_2^{\cdot-}$ is coelenterazine, (2-(4-hydroxybenzyl)-6-(4-hydroxyphenyl)-8-benzyl-3,7-dihydroimidazo[1,2- α]pyrazin-3-one). While the intensity of light emitted from the interaction of coelenterazine with superoxide is greater than lucigenin-dependent chemiluminescence, coelenterazine-dependent chemiluminescence is not entirely specific for $O_2^{\cdot-}$, as ONOO⁻ will also promote luminescence in the presence of coelenterazine. Coelenterazine-dependent chemiluminescence has been used in cultured cells, neutrophils, vascular tissues, and isolated mitochondria. Structural analogues, CLA (2-methyl-6-phenyl-3,7-dihydroimidazo[1,2- α]pyrazin-3-one), and MCLA (2-methyl-6-(4-methoxyphenyl)-3,7-dihydroimidazo[1,2- α]pyrazin-3-one), have also been used to assess $O_2^{\cdot-}$ formation in a variety of conditions, including neutrophil and macrophage activation, cultured cells, and vascular tissue.

6.6.B Detection of Hydrogen Peroxide

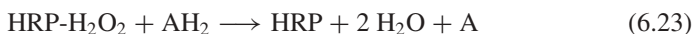
6.6.B1 Oxidation of Dihydrodichlorofluorescein The oxidation of 2'-7'-dihydrodichlorofluorescein (DCFH) to the fluorescent compound 2'-7'-dichlorofluorescein (DCF) has been used extensively in the detection of H₂O₂ produced by activated phagocytes, cell lysates or in intact cells using flow cytometry.

The diacetate form of DCFH (DCFH-DA) is taken up by cells, where DCFH-DA is metabolized by intracellular esterases to form DCFH, which is said to trap it within the intracellular compartment. However, some DCF can diffuse outside the cell and react with extracellular oxidants. In the presence of H_2O_2 , DCFH is oxidized to DCF and the fluorescence measured has an excitation wavelength of 498 nm and an emission wavelength of 522 nm. Limitations to the use of DCF fluorescence as a specific marker for intracellular H_2O_2 formation include stimulation of DCF formation by redox-active metals such as iron and copper, hematin, peroxidases, or cytochrome *c*. Peroxidases are also capable of promoting DCFH oxidation in the absence of H_2O_2 . Furthermore, ONOO^- , HOCl , and lipid peroxides can induce DCF fluorescence.

A structurally related cell permeant analogue of DCFH is dihydrorhodamine 123 (DHR 123), which can be oxidized to the fluorophore rhodamine 123 by H_2O_2 in the presence of heme-containing peroxidases such as horseradish peroxidase or other heme compounds, including cytochrome *c*. However, several other cell-derived oxidants such as ONOO^- and HOCl are also capable of directly oxidizing DHR 123.

Because of the various biologic substances that can lead to DCF and rhodamine fluorescence, and the inherent uncertainty relating to endogenous versus artifactual oxidant generation, these fluorescent assays are probably best applied as *qualitative markers* of cellular oxidant stress, rather than as quantitative measures of rates of H_2O_2 formation.

6.6.B2 Horseradish Peroxidase (HRP)-Coupled Assays In order to circumvent the limitations with the use of DCF and DHR, a number of assays based on the H_2O_2 - and HRP-dependent oxidation of a detector compound have been developed. These assays utilize the specific interaction of H_2O_2 with the hemoprotein horseradish peroxidase to generate a potent oxidizing intermediate (Compound I) that is capable of oxidizing a number of different hydrogen donor detectors (AH) (Eqs. (6.22) and (6.23))

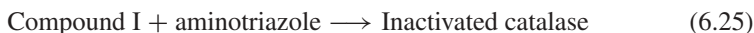
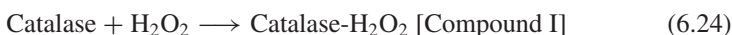


The amount of H_2O_2 present may be estimated by following the decrease in fluorescence of initially fluorescent probes such as scopoletin (7-hydroxy-6-methoxycoumarin) or by monitoring the increase in fluorescence from previously nonfluorescent hydrogen donors such as diacetyldichlorofluorescein, *p*-hydroxyphenylacetate, homovanillic acid (3-methoxy-4-hydroxyphenylacetic acid), or Amplex Red (*N*-acetyl-3,7-dihydroxyphenoxazine). Certain reductants such as thiols and ascorbate may serve as substrates for horseradish peroxidase and thus compete with the detector molecule for oxidation, leading to an underestimation of H_2O_2 formation. Competition with horseradish peroxidase by endogenous catalase for H_2O_2 can also lead to underestimation of H_2O_2 . Another potential problem is that quenching of the

fluorescence by cell and tissue components can lead to overestimation of H_2O_2 in the case of scopoletin or underestimation when using homovanillic acid.

Oxidation of tetramethylbenzidine or phenol red can be followed spectrophotometrically using the same principle. Limitations of this method include direct reduction of the oxidized detector molecule by electron transport components for the tetramethylbenzidine assay and the exquisite pH dependence and low sensitivity of the phenol red method. Taken together, the HRP-linked assays represent a particularly useful method for the quantification of H_2O_2 levels in cultured cells, organ cultures, and isolated buffer-perfused tissue preparations. However, these methods are not suitable for determination of H_2O_2 in plasma or serum since many reducing agents present in extracellular fluid (e.g., GSH, ascorbate) will react with Compound I and interfere with the assay.

6.6.B3 H_2O_2 -Dependent Inhibition of Catalase by Aminotriazole A major pathway by which H_2O_2 is broken down in cells and tissues is through its reaction with catalase. In much the same way as it interacts with peroxidases, H_2O_2 interacts with catalase to generate Compound I, which will oxidize and bind aminotriazole resulting in the irreversible inhibition of catalase (Eqs. (6.24) and (6.25)).



Therefore, catalase is inhibited by aminotriazole only in the presence of H_2O_2 . Because of this relationship, intracellular rates of H_2O_2 production can be estimated by determining the half-time of aminotriazole-dependent inactivation of catalase. Steady-state H_2O_2 concentrations can be approximated according to the expression

$$[\text{H}_2\text{O}_2] = \frac{k_{\text{cat}}}{k_1} \quad (6.26)$$

where $\frac{0.5}{t_{1/2}} = -k_{\text{cat}}$ and $k_1 = 1.7 \times 10^7 \text{ M}^{-1} \text{ s}^{-1}$.

This method has been used to assess rates of H_2O_2 formation in numerous isolated cell types as well as *in vivo*. However, under conditions that glutathione peroxidase-reductase significantly contributes to H_2O_2 metabolism, this method will underestimate the actual H_2O_2 concentrations.

6.6.C F2-Isoprostanes as Indicators of Lipid Peroxidation *In Vivo*

Lipid peroxidation remains one of the most widely used indicators of oxidant/free radical formation *in vitro* and *in vivo*. Unfortunately, many of the methods used to detect lipid peroxidation in urine, blood plasma, or tissue are nonspecific. In 1990, Roberts, Morrow, and co-workers discovered that nonenzymatic, free radical-induced lipid peroxidation produced F2-isoprostanes (IsoP). Oxidants such as $\bullet\text{OH}$, peroxy radicals, nitrogen dioxide, ONOO^- , and higher oxidation states of heme and

hemoproteins (ferryl heme) are capable of initiating lipid peroxidation to produce F2-like prostanoid derivatives of arachidonic acid called F2-isoprostanes. The measurement of F2-isoprostanes represents an attractive method for assessing oxidative stress *in vivo* because: (1) these compounds are stable and not produced by any known enzymatic pathways; utilizing arachidonate such as the cyclooxygenase or lipoxygenase pathways; and (2) levels of F2-isoprostanes can be quantified in extracellular fluids such as plasma and urine making this a relatively noninvasive approach and particularly useful for human and whole animal studies. The major drawbacks of this method are that samples must be partially purified and mass spectrometry is required for definitively detecting/quantifying the different F2-isoprostanes, making this an expensive and time-consuming endeavor.

6.6.D Measurement of the GSSG/GSH Redox Couple in Cells and Tissue

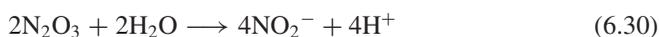
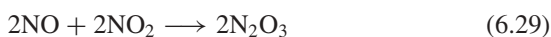
The steady-state concentrations of GSH and GSSG represent a dynamic indicator of the redox state of cells and tissues *in vivo*. Quantification of redox state of the GSH/GSSG pool in tissue and/or plasma that takes into account the correct stoichiometry of two GSH oxidized per GSSG formed may be determined by the redox potential (E_h), which is calculated according to the Nernst equation:

$$E_h(\text{mV}) = E^0 + 30 \log ([\text{GSSG}]/[\text{GSH}]^2) \quad (6.27)$$

where GSH and GSSG are *molar* concentrations and E^0 is -264 mV at pH 7.4. GSH and GSSG may be determined biochemically or by HPLC. In order to avoid over- or underestimation of plasma GSH and GSSG, one must avoid hemolysis and inhibit the GSH degrading ectoenzyme γ -glutamyltranspeptidase. Because thiols may be oxidized very rapidly upon tissue disruption, it is critical that tissue be rapidly excised and snap-frozen in liquid nitrogen prior to disruption.

6.6.E Methods to Detect NO and Its Oxidized Metabolites *In Vitro* and *In Vivo*

NO is associated with a multitude of physiological processes ranging from modulation of cardiovascular and neurological functions to the regulation of immune responses. NO is relatively unstable in the presence of molecular oxygen and will rapidly and spontaneously auto-oxidize to yield a variety of nitrogen oxides (Eqs. (6.28) to (6.30)):



NO_2 , N_2O_3 , and NO_2^- represent nitrogen dioxide, dinitrogen trioxide, and nitrite, respectively. The only stable product formed by the spontaneous autooxidation of NO

in metal-free oxygenated solutions is NO_2^- . However, when one analyzes physiological fluids such as urine or plasma, a mixture of NO_2^- and nitrate (NO_3^-) is found with the latter comprising the large majority of oxidized nitrogen species. The mechanisms by which NO is converted to NO_3^- *in vivo* are not entirely clear; however, it has been proposed that NO may interact directly with oxyhemoproteins to yield NO_3^- . The methods outlined next describe approaches to quantify NO_2^- and NO_3^- in extracellular fluids such as plasma, urine, and/or lymph. The same methods may also be used for other extracellular fluids (e.g., saliva, tears), cell culture fluid, and/or organ culture supernatants.

6.6.E1 Quantification of nitrate and nitrite using the griess reaction

One of the easiest and most popular methods to indirectly measure NO utilizes the spectrophotometric determination of its stable decomposition products NO_3^- and NO_2^- . This method requires that NO_3^- be reduced to NO_2^- and then NO_2^- determined by the Griess reaction (Fig. 6.20A). For quantification of NO_3^- and NO_2^- in extracellular or tissue culture fluids as well as in tissue homogenates or organ cultures, NO_3^- can be quantitatively reduced to NO_2^- using a commercially available preparation of nitrate reductase from *Aspergillus* (Eq. (6.31)):



Following incubation, any unreacted NADPH should be oxidized by addition of lactate dehydrogenase and pyruvic acid because reduced pyridine nucleotides (NADPH, NADH) strongly inhibit the Griess reaction. An alternative method for oxidizing any unreacted NADPH is to replace the lactate dehydrogenase /pyruvate system with 1 mM potassium ferricyanide. A known volume of premixed Griess reagent is then added to each incubation mixture and incubated for 10 min, and the absorbance of each sample is determined at 543 nm. One drawback of the Griess reaction is its low sensitivity (2–3 μM).

6.6.E2 Determination of NO Using Fluorescence Spectroscopy

6.6.E2a Diaminonaphthalene Assay To enhance the sensitivity of measuring NO_2^- or NO generated under physiological conditions, several different fluorimetric methods have been developed that exploit the ability of NO to produce N-nitrosating agents. One of these methods utilizes the aromatic diamino compound 2,3-diaminonaphthalene, which is relatively nonfluorescent and reacts rapidly with the NO-derived N-nitrosating agent (N_2O_3). The latter is generated by reaction of NO with oxygen or from the acid-catalyzed formation of NO_2^- to yield the highly fluorescent product 2,3-naphthotriazole (Fig. 6.20B). The specificity, sensitivity, and versatility of this assay offers an attractive alternative or additional method for the determination of NO and its decomposition products. This assay can detect as little as 10–30 nM naphthotriazole and by continuously monitoring the reaction spectrophotometrically, one can quantify the flux of NO generation using physiologically relevant

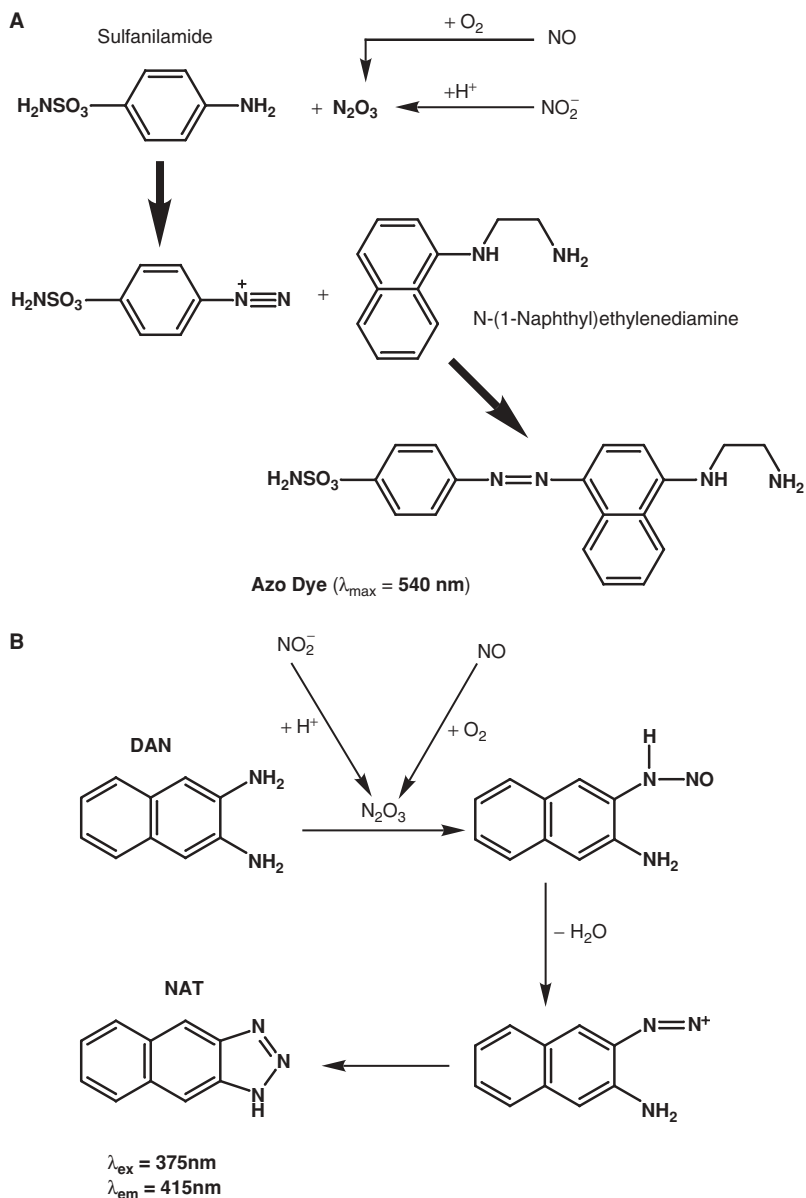


Figure 6.20. Detection of oxidized metabolites of NO. (A) The nitrosating agent dinitrogen trioxide (N_2O_3) generated from the autoxidation of NO or from the acidification of nitrite (NO_2^-) reacts with sulfanilamide to yield a diazonium derivative. This reactive intermediate will interact with *N*-1-naphthylethylenediamine to yield a colored diazo product that absorbs strongly at 540 nm. (B) Fluorimetric detection of NO or NO_2^- using diaminonaphthalene. The nitrosating agent dinitrogen trioxide (N_2O_3) generated from the autoxidation of NO or from the acidification of NO_2^- reacts with diaminonaphthalene (DAN) to yield the highly fluorescent product naphthotriazole (NAT). From Tarpey et al. (2004) (Ref. 1) with permission.

conditions (e.g., neutral pH, ionic strength) with minimal interference from nitrite decomposition. As with the Griess reaction, the 2,3-diaminonaphthalene assay can be used to quantify NO production under physiological conditions and/or stable decomposition products of NO in physiological fluids, tissue culture media, and organ culture supernatants.

6.6.E2b Diaminofluoroscein-2 Assay Diaminofluoroscein-2 (DAF-2), another fluorometric substrate, is used to detect intracellular levels of NO. The diacetate salt of DAF-2 diffuses into cells and tissue, where nonspecific esterases hydrolyze the diacetate residues thereby trapping DAF-2 within the intracellular space. NO-derived nitrosating agents (such as N_2O_3) nitrosate DAF-2 to yield its highly fluorescent product DAF-2 triazole in a manner similar to 2,3-diaminonaphthalene nitrosation (Fig. 6.21). The advantages of this compound are that wavelengths associated with fluorescein can be used making equipment currently used for other bioassays as well as cell and tissue imaging easily adapted to detect NO *in vitro* and *in vivo*.

Although DAF-2 has been thought to be an indicator of NO, nitroxyl (HNO/NO) also reacts with DAF-2 giving even higher yields of triazole than NO. In light of the potential for HNO in biological systems, it could be interesting to entertain the possibility that some of the NO detected by DAF-2 is in fact HNO. One cautionary note is that use of powerful light sources such as lasers can result in photochemistry that can lead to false-positives. It should be noted that controls need to be performed to ensure that it is the NO-derived chemistry and not some artifact of the photochemistry.

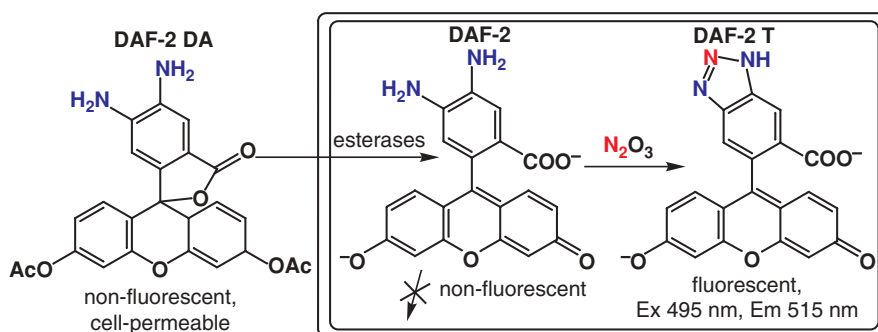
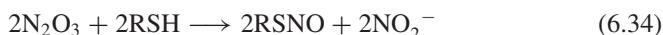


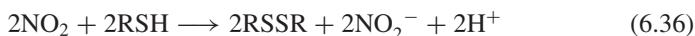
Figure 6.21. Fluorimetric detection of NO using diaminofluoroscein-2 diacetate (DAF-2 DA). DAF-2 DA diffuses into cells and tissue, where nonspecific esterases hydrolyze the diacetate residues thereby trapping DAF-2 within the intracellular space. NO-derived nitrosating agents such as N_2O_3 nitrosate DAF-2 to yield its highly fluorescent product DAF-2 triazole (DAF-2T). From Tarpey et al. (2004) (Ref. 1) with permission.

6.6.F Detection of S-Nitrosothiols by Colorimetric and Fluorimetric Methods

S-nitrosothiols (RSNOs) play an important part of the biology of NO. Different RSNOs are known to promote vasorelaxation, enhance oxygen delivery by hemoglobin, and mediate cell signaling. Here we describe methods for the colorimetric and fluorimetric detection of RSNOs. It is well appreciated that autoxidation of NO in the presence of thiols (RSH) generates RSNOs via one or both of the following mechanisms (Eq. (6.32) to (6.37)).



or



Historically, the detection of RSNO has employed the Saville reaction, which involves the displacement of the nitrosonium ion (NO^+) from the RSNO by mercury salts. The resulting nitrite or NO is detected by chemiluminescence or HPLC. Other methods for the detection of RSNO employ colorimetric methods such as the Griess reaction to measure the NO_2^- formed from the treatment of RSNO with mercuric chloride. However, samples, that contain large amounts of NO_2^- can interfere with and limit the detection range of these methods under acidic conditions. To circumvent these problems, two methods have been developed to detect RSNO-derived nitrosating species at neutral pH. The colorimetric method uses the components of the Griess reaction. NO^+ interacts with sulfanilamide to form a diazonium ion, which reacts with naphthylethylenediamine to form the colored azo complex (Fig. 6.22A). The fluorimetric method utilizes the reaction of 2,3-diaminonaphthalene with NO^+ liberated from RSNO following mercuric chloride addition to yield a primary nitrosamine, which is converted rapidly to a fluorescent triazole (Fig. 6.22B). These methods may be conducted at neutral rather than acidic pH, which eliminates the interference of contaminating nitrite and allows the detection of nitrosation mediated by the presence of NO.

The colorimetric assay has a detection range of 0.5–100 μM , while the fluorimetric assay is effective in the range of 50–1000 nM RSNO. The combination of the two assays provides a detection range from 50 nM to 100 μM RSNO, required for most biological experiments. Variations of these methods have been used successfully to quantify high and low molecular weight RSNOs in human and rat plasma as well as the S-nitrosated derivatives of human and rat hemoglobin.

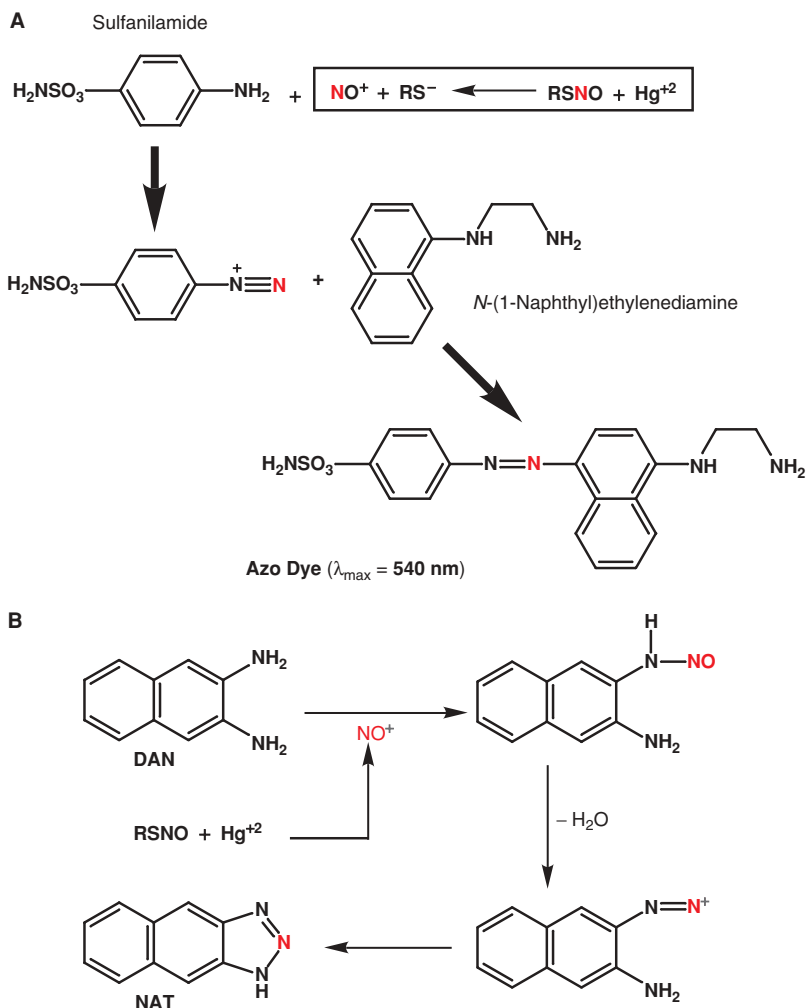
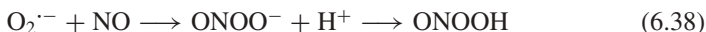


Figure 6.22. Detection of *S*-nitrosothiols (RSNOs). (A) Saville Reaction: Liberation of the nitrosating species nitrosonium (NO^+) by interaction of RSNO with mercury salts in the presence of the Griess reagent results in the formation of the same diazo product as described in Fig. 6.2 (B) Fluorimetric detection of RSNOs. Liberation of nitrosonium (NO^+) by interaction of RSNO with mercury salts in the presence of the diamionaphthalene (DAN) results in the formation of the same fluorometric triazole derivative described in Fig. 6.20. From Tarpey et al. (2004) (Ref. 1) with permission.

6.6.G Is the Presence of 3-Nitrotyrosine a Specific Footprint for Peroxynitrite?

NO rapidly interacts with $O_2^{\cdot-}$ to yield the potent oxidants $ONOO^-$ and its conjugate acid, peroxynitrous acid ($ONOOH$) (Eq. (6.38)):



It has been reported that *only* $ONOO^-$ will nitrate tyrosine residues in proteins and peptides under physiological conditions to generate 3-nitrotyrosine, and its detection has been used as evidence for $ONOO^-$ production *in vivo*. Indeed, the vast majority of studies implicating $ONOO^-$ as an important cytotoxic species have used immunohistochemical or HPLC determinations of 3-nitrotyrosine as evidence of $ONOO^-$ formation *in vivo*. In reality, 3-nitrotyrosine may be generated by multiple pathways suggesting that the presence of 3-nitrotyrosine is not a specific “footprint” for $ONOO^-$ formation *in vivo* (Fig. 6.23). For example, tyrosine can be nitrated by peroxidase or heme-catalyzed, H_2O_2 -dependent oxidation of NO_2^- to form NO_2 followed by its interaction with tyrosine to generate 3-nitrotyrosine (NT) (Eq. (6.39) to (6.41)).

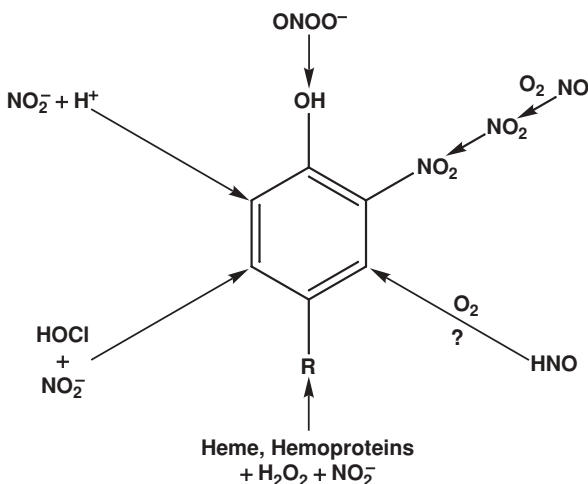
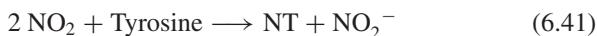
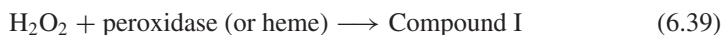


Figure 6.23. Multiple pathways for the formation of 3-nitrotyrosine. 3-Nitrotyrosine may be generated by peroxynitrite ($ONOO^-$), autoxidation of NO or nitroxyl (HNO) in the presence of oxygen, heme or hemoprotein catalyzed, H_2O_2 -dependent oxidation of NO_2^- , NO_2^- interaction with HOCl and acidified NO_2^- . From Tarpey et al. (2004) (Ref. 1) with permission.

In addition to peroxidases (e.g., horseradish peroxidase, lactoperoxidase, myeloperoxidase) and hemoproteins (e.g., hemoglobin, myoglobin, cytochromes), other compounds such as nitryl chloride (Cl-NO_2), acidified nitrite, and nitroxyl (HNO) will nitrate tyrosine to yield 3-nitrotyrosine.

SELECTED REFERENCES

1. Tarpey, M.M., Wink, D.A., and Grisham, M.B. (2004). Methods for detection of reactive metabolites of oxygen and nitrogen: *in vitro* and *in vivo* considerations. *Am. J. Physiol. Regul. Integr. Comp. Physiol.* 286:R431–R444.
2. Roberts, L.J., and Morrow, J.D. (2000). Measurement of F(2)-isoprostanes as an index of oxidative stress *in vivo*. *Free Radic. Biol. Med.* 28:505–513.
3. Jones, D.P. (2002). Redox potential of GSH/GSSG couple: assay and biological significance. *Methods Enzymol.* 348:93–112.
4. Miles, A.M., Wink, D.A., Cook, J.C., and Grisham, M.B. (1996). Determination of nitric oxide using fluorescence spectroscopy. *Methods Enzymol.* 268:105–120.
5. Eiserich, J.P., Hristova, M., Cross, C.E., Jones, A.D., Freeman, B.A., Halliwell, B., and van der Vliet, A. (1998). Formation of nitric oxide-derived inflammatory oxidants by myeloperoxidase in neutrophils. *Nature* 391:393–397.

INDEX

- Acatlasemia, 54
- Ace1 transcription factor, 169
- Aceruloplasminemia, 172
- Acetogenesis, as redox pathway, 175
- Acetylcholine, nitric oxide and, 137
- N*-Acetyl cysteine (NAC)
- growth signaling and, 212
 - in redox regulation of genes, 154–155
- Acidified nitrite, in detecting peroxynitrite, 284
- acnA* (aconitase A) gene, in immune-system oxidative stress response regulation, 222
- Aconitase, 163
- in oxidative immune-system damage to bacteria, 221, 222–223
- Aconitase inhibition, in superoxide anion detection, 273–274
- cis*-Aconitate, in aconitase activity measurement, 274
- Activation, of enzymes, 175–176
- Activator protein-1 (AP-1)
- in cardiac myocyte extracellular matrix remodeling, 210
 - uncontrolled ROS production and, 214
- Adenosylcobalamin-dependent enzymes, 175, 176
- ADP (adenosine diphosphate), in glutathione biosynthesis, 16
- Aerobic organisms, ubiquinone and ubiquinol in, 31
- Aerobic respiration, 3, 7–8
- Aft1/2 transcription factors, in iron regulation, 169
- AFUDG glycosylase, 92–93
- Age-related cataract, 196
- Age-related macular degeneration, 194–195, 201, 202, 203
- Aging. *See also* Cataract; Longevity
- eye degeneration during, 194–195
 - free radicals and, 33
 - protein modification associated with, 184, 185, 186, 193
- ahpC* gene, 65
- AhpC peroxyreductase, 59, 60, 61, 62–63
- AhpF and, 65–67
 - molecular structure of, 66
- AhpF flavoprotein disulfide reductase
- AhpC and, 65–67
 - mechanism of action of, 66–67
 - molecular structure of, 66
- ahpF* gene, 65
- Akt kinase, nitric oxide synthase and, 138
- Aldehyde derivative formation, 189, 190
- Aldehyde oxidase, 44, 45
- Aldone-1,4-lactone, as ascorbate precursor, 23
- Algae
- heme oxygenases in, 131
 - photosynthesis by, 6
- Alkoxy radical
- cleavage of, 189, 190
 - in protein oxidation, 184–187
- Alkyl hydroperoxide reductases, 65–67
- in *Escherichia coli*, 67
- α -amidation pathway, protein modification via, 187–188
- α -lipoic acid
- as antioxidant, 30–31
 - human health and, 34
- α -tocopherol
- as antioxidant, 28–30
 - molecular structure of, 29
- Alzheimer's disease, perturbed metal homeostasis and, 172–173
- α -Amidation pathway, protein modification via, 187–188

- Amino acid residues, in redox regulation of genes, 154
- Amino acid residue side chains, oxidation of, 188–189
- Amino acids
 in bioinformatics, 252
 during growth stimulation, 213
 in ionic selectivity, 256
- Amino acid sequences, of glutaredoxins, 80–81
- Amino acid side chains, beta-scission of, 189
- Aminolevulinatase synthases
 in heme biosynthesis, 177–178, 179
 NPAS2 regulation of, 180–182
- Aminotriazole, in hydrogen peroxide detection, 276
- 3-Aminotriazole, catalase inactivation by, 54
- Ammonia, from nitrogen-fixing bacteria, 4–5
- Amphibians, ascorbate biosynthesis in, 23–24
- Amplifiers, for electrophysiological recording, 263–264
- β -Amyloid ($A\beta$), perturbed metal homeostasis and, 173
- Amyloid precursor protein (APP), perturbed metal homeostasis and, 173
- Anaerobic bacteria, superoxide dismutases in, 57
- Anaerobic chamber, for potentiometry, 250–251
- Analyzers, for mass spectrometers, 228, 230–231
- Animals
 cytosolic GSTs in, 106
 quinones in, 40
- Anisotropic EPR spectra, 242
- Anoxygenic bacterial photosynthesis, 2–3
- Anthocyanins, 32
- Anticancer drugs, glutathione reductase inhibition by, 77
- Antioxidant enzymes, 49–134
 alkyl hydroperoxide reductases, 65–67
 catalases, 50–54
 detoxification by, 97–113
 DNA repair by, 87–94
 glycosylases, 87–94
 in glutathione system, 74–84
 heme oxygenase, 131–134
 methionine sulfoxide reductases, 85–87
 oxidative folding by, 113–127
 peroxyredoxins, 59–64
 repairs by, 83, 84–97
 ROS-dependent, 50–67
 selenoproteins, 127–131
 sulfiredoxins, 94–97
 superoxide dismutase, 55–59
 in thioredoxin system, 68–74
- Antioxidant molecules, 11–35
 ascorbate, 22–27
 classification of, 27
 glutathione, 11–21
 human health and, 33, 34–35
 lipid-soluble, 28–31
 water-soluble, 31–34
- Antioxidants
 in the lens, 197–198
 longevity and, 33
- Antioxidant supplements, clinical cancer trials of, 216–217
- Apoptosis
 of cardiac myocytes, 209
 flavoenzymes in, 38
 reactive oxygen species and, 159–162
 redox regulation of, 158–162
- Apoptosis signal-regulated kinase 1 (ASK1)
 apoptosis and, 160, 161
 in cardiac myocyte hypertrophy/death, 209
 during growth stimulation, 213–214
- “Apoptosome,” 159
- Apoptotic inducing factor, 38
- Aqueous humor, 194
- Archaea
 aerobic, 3–4
 glutathione *S*-transferases in, 105, 107
 heme oxygenases in, 132
- Archaeal period, atmosphere during, 3–4
- Archaeoglobus fulgidus*, glycosylases in, 92
- Arginyl residue oxidation, 189, 190
- Aromatic amino acid hydroxylases,
 pterin-dependent, 43–44
- Asard, Han, xiii, 22
- Ascorbate, 22–27. *See also* Vitamin C
 biosynthesis of, 23–25
 chemistry of, 22–23
 glutathione and, 14
 high-molecular-weight thioredoxin reductase and, 73–74

- history of, 22
- as lens antioxidant, 197, 199
- molecular structure of, 23
- recycling of, 25–26
- stress and disease and, 26–27
- transport of, 26
- Ascorbate–GSH pathway, in ascorbate recycling, 25–26
- Aspergillus*, 278
- Assays
 - catalase, 54
 - horseradish peroxidase-coupled, 275–276
 - for NO determination, 278–280
- Atherosclerosis, nitric oxide synthase and, 137–138
- Atmosphere
 - during Archaean period, 3–4
 - global redox cycling and, 4–5
 - increase of oxygen in, 4
- Atmospheric pressure chemical ionization (APCI), as mass spectrometer source, 229, 230
- Atmospheric pressure photoionization (APPI), as mass spectrometer source, 229, 230
- Atox1 copper carrier, 165
- ATP (adenosine triphosphate), in glutathione biosynthesis, 16
- ATPase
 - in cardiac myocyte expansion–contraction coupling, 205
 - in export of copper from cells, 168–169
- ATP-dependent enzymes, in glutathione biosynthesis, 14–15
- ATP synthesis, aerobic respiration and, 8
- Atransferrinemia, 172
- Atx1 copper carrier, 165
 - genetic metal-metabolism disorders and, 172
- “Atypical 2-Cys peroxyredoxins,” 60
- Axial EPR spectra, 240, 242
- Azo dye, in RSNO detection, 281, 282
- Bacillus stearothermophilus*, glycosylases in, 91
- Bacillus subtilis*, 223
 - thioredoxins in, 70
- Bacteria
 - acatalasemia and, 54
 - aerobic, 3–4
 - alkyl hydroperoxide reductases in, 65
 - cytochrome P450 enzymes in, 98
 - evasion/blocking of immune response by, 223–224
 - folic acid in, 46
 - glutathione *S*-transferases in, 105, 106
 - heme oxygenases in, 131, 132
 - in host-pathogen interaction, 219
 - immune-system oxidative stress response regulation and, 221–223
 - innate immune response and, 219–220
 - methionine sulfoxide reductases of, 85, 86
 - molybdopterins in, 44
 - as oxidative damage immune-system targets, 220–221
 - oxidative-stress response by, 223
 - oxygenic photosynthesis in, 3, 4
 - oxygen sensing in, 156
 - peroxyredoxins in, 59
 - protein disulfide bond formation in, 113–120
 - quinones in, 40
 - superoxide dismutases in, 57
 - thioredoxin reductase in, 71–72
 - thioredoxins in, 69, 70
- Bacterial amine dehydrogenase, 174
- Bacterial photosynthesis, anoxygenic, 2–3
- Bad apoptotic regulator, 160
- Banerjee, Ruma, xiii, xviii, 1, 35
- Barycki, Joseph J., xiii, 11
- Bax apoptotic regulator, 160
- Bcl-2 apoptotic regulator family, 160, 161, 162
- BCP catalase, versus hydrogen peroxide, 67
- Becker, Donald F., xiii, xvii, 35, 247
- Beckwith, Jon, xiii, 113
- Benzoquinol group, 31
- BER (base excision repair) glycosylases, 89
 - table of, 90
- β -amyloid (A β), perturbed metal homeostasis and, 173
- β -carotene
 - as antioxidant, 30
 - clinical cancer trials of, 216–217
 - molecular structure of, 29
- Beta-scission, of amino acid side chains, 189

- Bifunctional catalases, 52
- Bilirubin, 131, 132
- Biliverdin, 132
conversion of heme to, 131
- Biliverdin reductase, control of gene
expression of, 134
- Bioenergetic cycles, 6–8
- Bioinformatics, 251–255
- Biopterin, 42–43. *See also*
Tetrahydrobiopterin
redox states of, 42
- Biosynthesis
of ascorbate, 23–25
of folic acid, 46
of γ -glutamyltranspeptidase, 18–19
of glutathione, 14–16, 17
of heme, 177–182
of NAD⁺, 40
- BK_{Ca} channel, carbon dioxide and, 142–143
- BLAST (Basic Local Alignment Search
Tools) software, 252, 255. *See also*
PSI-BLAST software
- Blindness
cataract and, 195–196
via macular degeneration, 202
- Blood vessels, in retina, 199–200
- Bmal1* gene, in circadian clock, 178–179,
180, 181
- BMAL1 transcription factor, carbon dioxide
and, 143
- Bohr magneton, 240
- “Bridge” methods, for intracellular
recording, 265
- C3 factors, in innate immune system
response, 223
- C-22 protein, 65
- Ca²⁺ (calcium ion)
Ca²⁺-handling proteins and, 206–209
in cardiac myocyte expansion–contraction
coupling, 204–206
ionic selectivity for, 256, 261
- Ca²⁺/calmodulin
nitric oxide and, 153
nitric oxide synthases and, 152
- Ca²⁺-handling proteins, redox modulation
of, 206–209
- Caenorhabditis elegans*, 33
- Calcium (Ca). *See* Ca²⁺ entries
- Calmodulin
nitric oxide and, 153
nitric oxide synthases and, 152
- Cambialistic superoxide dismutases, 57
- Cambrian period, evolution of life and, 4
- Camellia sinensis*, 32
- cAMP (cyclic AMP), in cardiac myocyte
expansion–contraction coupling, 205,
206
- Cancer. *See also* Anticancer drugs;
Carcinogen-entries; Tumor necrosis
factor- α (TNF- α)
antioxidant-supplement clinical trials
against, 216–217
ascorbate and, 27
 γ -glutamyltranspeptidase and, 20–21
high-molecular-weight thioredoxin
reductase and, 74
thioredoxins and, 70
- Carbon (C), global equilibrium redox
cycling of, 4, 5
- Carbon monoxide (CO)
circadian clock and, 181
perceived toxicity of, 136
as signal transduction molecule,
141–143
- Carbonyl derivatives, of proteins, 189–191
- Carboxyethylpyrrole (CEP) adducts, in
macular degeneration, 202, 203
- Carcinogenesis
hormones in, 216
reactive oxygen species in, 212–218
uncontrolled ROS production and, 214
- Carcinogenic DNA adducts, induction by
reactive oxygen species, 215–216
- Carcinogenic protein adducts, induction by
reactive oxygen species, 215–216
- Cardiac myocytes
Ca²⁺ influx into, 207–208
Ca²⁺ release from, 208
in chronic heart failure, 206, 207
expansion–contraction coupling in,
204–206
extracellular matrix remodeling around,
209–211
- Cardiovascular disease. *See also* Heart
failure
multiple cellular factors underlying, 211
redox mechanisms and, 204–211

- β -Carotene
 as antioxidant, 30
 clinical cancer trials of, 216–217, 218
 molecular structure of, 29
- Carotenoids
 as antioxidants, 30
 as lens antioxidants, 197
- Carotid body, carbon dioxide and, 141–142
- Casein kinases, in circadian clock, 178
- Caspases, in programmed cell death, 158, 159, 160
- Catalases, 50–54
 acatalasemia and, 54
 alkyl hydroperoxide reductases and, 67
 3-aminotriazole inactivation of, 54
 assays of, 54
 bifunctional, 52
 hydrogen peroxide-dependent inhibition of, 276
 inhibition by superoxide, 52–53
in vivo action of, 52
 K_m of, 52
 as lens antioxidants, 197
 life span/longevity and, 53
 mechanisms of action of, 51–52
 monofunctional, 51–52
 NADPH binding by, 53
- Catalysis
 of protein carbonyl derivative formation, 189
 by redox enzymes, 173–175
- Catalytic cysteines, 252
- Catalytic redox-active cysteine residues, 252
- Cataract, 194
 oxidation and, 196
 oxidative stress and, 195–199
 types of, 196
- Cataractogenesis, factors in, 196, 197
- CCS copper carrier, 165
- CDART (Conserved Domain Architecture Retrieval Tool) software, 255
- Cell-attached patch configuration, for patch-clamp technique, 266–267, 268
- Cell cycle, in redox regulation of genes, 154–155
- Cell death. *See also* Apoptosis
 apoptotic versus necrotic, 158
 of cardiac myocytes, 209
- Cell membranes, cytochrome P450 enzymes in, 98. *See also* Membranes
- Cells. *See also* Cyto- entries; Endoplasmic reticulum (ER); Golgi apparatus; Macrophages; Mitochondria; Phagocytes
 catalyzed disulfide bond formation in, 121
 electrophysiological techniques for, 263–272
 glutathione system in, 75
 ion channel regulation in, 260–261
 measurement of GSH:GSSG redox couple in, 377
 metal export from, 168–169
 methionine sulfoxide reductases in, 85
 protein disulfide bond formation in, 113–114, 123–127
 in retina, 199–200
 ubiquinone and ubiquinol in, 31
- Cell signaling, redox-dependent, 63–64
- Cellular homeostasis, RNS/ROS and, 272–273
- Cellular storage, of metals, 168
- Ceruloplasmin, 172
 in intracellular iron transport, 166
- cGMP (cyclic guanosine monophosphate), nitric oxide and, 138–140, 153
- Channel gating, in ionic channels, 256, 257
- Chaperones, target-specific, 165–166
- Chemical ionization (CI), as mass spectrometer source, 229, 230
- Chemiluminescence reactions, in superoxide generation measurement, 274
- Chemistry, of ascorbate, 22–23. *See also* Redox biochemistry
- China, green tea from, 32–33
- Chinese Cancer Prevention Study, 217
- Chlorine (Cl), GSH conjugates and, 104, 105. *See also* Cl⁻ (chloride ion)
- Chlorophyll, in photosynthesis, 7
- Chloroplasts, 6
- Cholesterol, nitric oxide synthase and, 138
- Chromophores, 199
 oxidative damage to, 200–201
- Chronic heart failure, 204
 extracellular matrix remodeling in, 209–211
 multiple cellular factors underlying, 211

- Chronic heart failure (*Cont.*)
 oxidative stress in, 206, 207
 redox mechanisms and, 204–211
- Circadian clock
 heme biosynthesis and, 177–182
 mechanism of, 178–179
- cis*-aconitate, in aconitase activity
 measurement, 274
- Cl⁻ (chloride ion), ionic selectivity for, 256, 260. *See also* Chlorine (Cl)
- Clinical trials, of antioxidants versus cancer, 216–217
- Clock* gene, in circadian clock, 179–180
- Cobalamin-dependent methyltransferases, 176
- Cobalt (Co), enzyme reactions involving, 175–176
- Co dehydrogenase, 174
- Coelenterazine, in superoxide generation
 measurement, 274
- Coenzyme A, 21
 molecular structure of, 20
- Coenzyme Q, in aerobic respiration, 8
- Coenzyme Q₁₀, human health and, 34–35.
See also Ubiquinol; Ubiquinone
- Cofactors
 pterins as, 42
 for redox enzymes, 173, 174
- Collagens
 ascorbate and, 27
 fibrillar, 209
- Colorimetric methods, in RSNO detection, 281–282
- Complement system, in innate immune system response, 223–224
- Complexes
 in cytochrome P450 reaction cycle, 100–102
 glutathione in, 14
- Complexes I–IV, in aerobic respiration, 8
- Cone photoreceptor cells, in retina, 199
- Conformational change, in ionic channels, 257
- Congenital cataract, 196
- Conserved cysteines, 253
- Continuous single electrode voltage-clamp technique, for intracellular recording, 266. *See also* Patch-clamp techniques
- Continuous-wave EPR (CW-EPR), 238, 240–241
- Contraction. *See* Expansion–contraction coupling
- [Co(phen)₃]³⁺, 92–93
- Copley, Shelley D., xiii, 104
- Copper (Cu). *See also* Cu entries
 ascorbate reactions with, 23
 cellular storage of, 168
 EPR spectra of, 246
 export from cells, 168–169
 genetic disorders in metabolism of, 171–172
 intracellular distribution of, 165–166
 metabolism of, 163–164
 mitochondria and, 167–168
 perturbed metabolism of, 172–173
 post-translational regulation of, 171
 in protein oxidation, 184–187
 in superoxide dismutation, 56
 transcriptional regulation of, 169
 uptake from the extracellular environment, 164–165
- Copper amine oxidase, 174
- Copper- and zinc-containing superoxide dismutases (Cu,ZnSODs), 163, 165, 203
- Copper superoxide dismutase (CuSOD), 52
 molecular structure of, 53
- Cornea, 194
- Cox11 membrane protein, 167
- Cox17 copper carrier, 165, 167–168
 genetic metal-metabolism disorders and, 172
- Crabb, John W., xiii, 194
- Cross-linked protein derivatives, formation of, 192, 193
- Cryptochrome (mCRY1/2) regulator, in circadian clock, 178
- Cryptochromes, 38
 in circadian clock, 178
- Crystallins
 in lens, 195
 oxidation damage to, 198
- Cth2 protein, in yeast post-transcriptional iron regulation, 171
- Ctr1 (copper transporter 1) protein family, 164, 165, 166

- genetic metal-metabolism disorders and, 172
- Cu(CIO₄)-containing solution, EPR spectrum of, 246
- Cu chaperones, 165–166
- Cumene hydroperoxide, reduction of, 110
- Current-clamp method, for intracellular recording, 265
- Current density, of ion channels, 269
- Current–voltage relationships, for ion channels, 257–260, 263–264, 265–266, 268, 269
- Cu,ZnSODs, 56–57, 163, 165, 203
- CXXC site motif, 253, 254
 - of DsbA protein, 114
 - in protein disulfide bond isomerization, 117
- Cyanobacteria
 - heme oxygenases in, 131
 - photosynthesis by, 6
- Cyanobacterial-like microbe, emergence of, 2–3
- Cycles. *See also* Cell cycle; Reaction cycle
 - bioenergetic, 6–8
 - global redox, 4–5
- Cyclophilin, in peroxyredoxin regulation, 64
- CYP101 protein, molecular structure of, 98–99
- 1-Cys peroxyredoxins, 60, 61
- Cystathionine β -synthase, in H₂S biological signaling, 147
- Cysteine
 - AhpC and AhpF and, 66–67
 - apoptosis and, 160
 - in cross-linked protein derivative formation, 192, 193
 - in cytochrome P450 reaction cycle, 100
 - DNA glycosylases and, 89–90
 - DsbA protein and, 114, 115
 - in eukaryote protein disulfide bonds, 120–127
 - in γ -glutamyltranspeptidase-deficient mice, 20–21
 - glutaredoxin mechanism and, 81–82, 83
 - in glutathione, 12, 13
 - in glutathione biosynthesis, 14
 - in glutathione homeostasis, 16–17
 - glutathione reductase and, 76–77
 - in mass-spectrometry proteomics, 235
 - methionine residues and, 84
 - methionine sulfoxide reductases and, 87
 - molecular structure of, 127
 - peroxyredoxins and, 60, 61, 62, 94, 95
 - in protein disulfide bond formation, 113–114, 115, 116–117
 - in protein disulfide bond isomerization, 117–119
 - redox-active, 251–255
 - selenocysteine and, 127–128
 - sulfiredoxins and, 96
 - thioredoxin reductase and, 72, 73
 - thioredoxins and, 68, 69, 70
- Cysteine-based redox motifs, 253
- Cysteine residues
 - in bioinformatics, 251–255
 - in immune-system oxidative stress response regulation, 222
 - oxidation of, 144, 147
 - in peptide editing, 157
 - in redox regulation of genes, 154
- Cysteine sulfinic acid, peroxyredoxins and, 94, 95
- Cysteine tryptophylquinone (CTQ), 40
- Cytochrome *b₆f* complex, in photosynthesis, 6, 7
- Cytochrome *b₅₆₁*, in ascorbate recycling, 25
- Cytochrome *c*
 - in apoptosis, 159, 162
 - nitric oxide and, 140
- Cytochrome *c* oxidases, 3–4, 163, 174
 - in aerobic respiration, 8
 - carbon dioxide and, 141
 - copper transport into, 167–168
 - in H₂S biological signaling, 148
- Cytochrome *c* reduction, in superoxide anion detection, 273
- Cytochrome P450, 12, 174
 - heme oxygenases and, 131
- Cytochrome P450 enzymes, 97–104
 - classes of, 99–100
 - in detoxification by GSH transferases, 108, 109
 - distal charge relay involving, 103–104
 - in electron transport systems, 99–100
 - molecular structure of, 98–99
 - occurrence and functions of, 97–98
 - reaction cycle with, 100–102
 - “thiolate push” and, 102–103

- Cytochrome P450 reductase, nitric oxide synthases and, 149–150, 151
- Cytokines, in iron regulation, 169
- Cytoplasmic GSTs, 105–107
- Cytosol
- glutathione in, 13
 - high-molecular-weight thioredoxin reductase in, 73
 - protein disulfide bond formation in, 123–127
 - thioredoxins in, 68–70
- Cytosolic glutathione transferases (GSTs), 14, 105–107
- classification of, 106–107
 - in detoxification, 109
 - as enzymes, 111
 - in human health, 110–113
 - molecular mechanisms of, 105, 106
 - molecular structure of, 106
- Cytotoxicity, RNS/ROS mediation of, 272–273
- Databases. *See* Bioinformatics
- David, Sheila S., xiii, 87
- Dawson, John H., xiii, 97
- Dcytb reductase, 165
- Decamers, of peroxyredoxins, 60–63
- Degenerative disorders, metal homeostasis and, 172–173
- Degradation, of glutathione, 16–21
- Dehydroascorbate, 22
- in ascorbate recycling, 25–26
 - high-molecular-weight thioredoxin reductase and, 73–74
 - molecular structure of, 23
- Dehydrogenases, 38
- Denitrification, 5
- Detectors, for mass spectrometers, 228, 231
- Dethiolation, by glutaredoxin, 83
- Detoxification. *See also* Toxicity
- GSH transferases in, 107–109
 - of hydrogen peroxide, 50
 - metallothionein in, 168
 - of metals, 163, 164
 - Phase I and II of, 108, 109
 - of superoxide, 50
- Detoxification enzymes, 97–113
- cytochrome P450 enzymes, 97–104
 - GSH transferases, 104–113
- Diamagnetism, 238
- Diamide pathway, protein modification via, 187–188
- Diaminofluorescein-2 (DAF-2) assay, NO determination via, 280
- Diaminofluorescein-2 diacetate (DAF-2 DA), in NO determination, 280
- Diaminonaphthalene (DAN) assay, NO determination via, 278–280, 281, 282
- Dichlorofluorescein (DCF), in hydrogen peroxide detection, 274–275
- Dickman, Martin B., xiii, xvii, 154, 158
- Diet
- ascorbate and, 27
 - Mediterranean, 218
- Diffusion potential, for ion channels, 257–260, 263–264
- 7,8-Dihydro-8-oxo-2'-deoxyguanosine (OG)
- DNA repair and, 88–89
 - formation of, 93
- Dihydrobiopterin, 42
- Dihydrodichlorofluorescein (DCFH), oxidation of, 274–275
- Dihydrodichlorofluorescein diacetate (DCFH-DA), in hydrogen peroxide detection, 275
- Dihydroethidium, in superoxide anion detection, 273
- Dihydrolipoic acid
- as antioxidant, 30–31
 - human health and, 34
 - molecular structure of, 29
- Dihydrorhodamine 123 (DHR 123), in hydrogen peroxide detection, 275
- Dimanganic catalases, 51–52. *See also* Manganese entries
- Dimers, of peroxyredoxins, 60–63
- Dinitrogen trioxide, 277, 278, 279, 280
- Disease, ascorbate and, 26–27. *See also* Cancer; Health; Human health
- Dismutation, of superoxide, 50, 56
- Disproportionation reactions, of ascorbate, 23
- Distal charge relay, involving cytochrome P450, 103–104
- Disulfide bonds/linkage
- cataract and, 196, 197
 - characteristics of, 121, 122
 - DsbA protein and, 114, 115

- DsbB protein and, 114–117
 in eukaryote proteins, 120–127
 formation in bacteria, 113–120
 formation in endoplasmic reticulum proteins, 123–127
 formation in proteins, 113–114, 121, 122
 ion channels and, 263
 isomerization of, 117–119, 122
 in lens oxidation damage, 198–199
 in lipoic acid, 30–31
 oxidative immune-system damage to bacteria and, 221
 peroxyredoxins and, 60, 61
 reactivity of, 122–123
 stability of, 121–122
- Disulfide isomerase, in protein disulfide bond isomerization, 117–119
- Disulfide reductase system, 61
- DMT1 iron carrier, 164–165, 166
- DNA (deoxyribonucleic acid) adducts, carcinogenic, 215–216. *See also* mtDNA (mitochondrial DNA)
- DNA binding, in redox control of gene expression, 155–156
- DNA damage
 by immune system, 221
 oxidative stress and, 87–88
- DNA glycosylases, [4Fe–4S]
 cluster-containing, 89–91, 91–93
- DNA methylation, ROS effects on, 216
- DNA photolyases, 38
 folic acid and, 47
- DNA repair, enzymes for, 87–94
- DNA synthesis, glutaredoxin in, 83
- Docosahexaenoate (DHA), in macular degeneration, 202, 203
- Domains. *See also* Zinc finger motifs
 of DsbD protein, 119
 of glutaredoxin molecule, 79–80
 of glutathione reductase molecule, 76–77
 of nitric oxide synthase molecules, 149, 151
 PAS, 179–180, 181
 sequence analysis of, 255
- Dopaminergic neurons, ion channels in, 262
- Drosophila melanogaster*, circadian clock in, 178, 181–182
- Drugs. *See also* Anticancer drugs;
 Pharmacological redox regulation studies
 GSTs in therapeutic metabolism of, 113
 high-molecular-weight thioredoxin reductase and, 74
- Drusen, 201
- dsbA* gene, 113, 114, 115
- DsbA protein, 113
 crystal structure of, 115
 DsbB protein and, 114–117
 in oxidative protein folding, 114
 in protein disulfide bond isomerization, 117, 118
- dsbB* gene, 115
- DsbB protein
 DsbA protein and, 114–117
 mechanism of, 117
 in protein disulfide bond isomerization, 118
- DsbC protein
 crystal structure of, 115
 DsbD protein and, 119–120
 in protein disulfide bond isomerization, 117–119
- DsbD protein, 119–120
 molecular structure of, 119
- DsbG protein, 117
- Dual-specific phosphatases,
 superoxide/hydrogen peroxide pathways and, 145–146
- E75 protein, circadian clock and, 181–182
- Earth, evolution of life on, 1–4
- EcSODs (extracellular superoxide dismutases), 56
- EGCG ([–]-epigallocatechin 3-galleate)
 clinical cancer trials of, 218
 in green tea, 32–33
 molecular structure of, 29
- EGF peptide growth factor, 144–145, 146
- Eicosanoids, 107
- Electrochemistry, 247
- Electrodes, for intracellular recording, 264–265, 265–266, 268
- Electron acceptors, 3
- Electron Bohr magneton, 240
- “Electron carriers,” 249

- Electron flow
 in aerobic respiration, 7–8
 in endoplasmic reticulum, 124–127
 in photosynthesis, 6–7
- Electron ionization (EI), as mass spectrometer source, 229, 230
- Electron paramagnetic resonance (EPR), 237–247
 in ascorbate studies, 22
 continuous-wave, 238, 240–241
 in glycosylase studies, 92–93
 nuclear hyperfine interactions in, 246
 operation of, 237–239
 performing experiments using, 240–241
 sensitivity of, 244, 245
 spectra from, 240, 241, 242
 spectrometers using, 241–244
 spin concentration in, 244–246
 spin-spin interactions in, 239, 246
 theory of, 239–240, 241, 242
- Electron-rich amino acids, during growth stimulation, 213
- Electrons, Zeeman effect and, 239–240
- Electron spin–nuclear spin coupling, 239, 246
- Electron spin resonance (ESR), 237. *See also* Electron paramagnetic resonance (EPR)
- Electron spins, EPR and, 237, 239–240
- Electron transfer
 metallic ions in, 162
 nitric oxide synthases in, 148–149
 in potentiometry, 247–248, 249
- Electron transport
 in cytochrome P450 reaction cycle, 100, 101
 by ionic channels, 257
 redox enzymes and, 173, 175
 uncontrolled ROS production and, 214
- Electron transport systems, cytochrome P450 enzymes in, 99–100
- Electrophysiology, 256–272
 applications of, 270–272
 in redox regulation studies, 270–272
 techniques of, 263–272
- Electrospray ionization (ESI)
 as mass spectrometer source, 229–230
 in peptide analysis mass spectrometry, 231–233
 in protein analysis mass spectrometry, 233–234
 in quantitative mass spectrometry, 234
- Endo III glycosylase
 DNA and, 89–91
 redox properties of, 91–92
- Endoplasmic reticulum (ER). *See also* ER entries
 cytochrome P450 enzymes in, 98
 electron flow in, 124–127
 glutathione in, 13
 methionine sulfoxide reductases in, 85
 protein disulfide bond formation in, 121, 122, 123–127
- Endothelial dysfunction, nitric oxide synthase and, 137–138, 139
- Endothelial NOS (eNOS; NOD3), 149, 151–152. *See also* eNOS expression
 discovery of, 137
- Endothelium-derived relaxing factor, 153
- Endotoxic shock, nitric oxide and, 153
- Energy, evolution of life and, 1–4
- Engen, John R., xiii, 228
- eNOS expression, nitric oxide and, 140. *See also* Endothelial NOS (eNOS; NOD3)
- Enzymes. *See also* Antioxidant enzymes; Flavoenzymes; Redox coenzymes; Redox enzymes
 ascorbate and, 22, 23–24, 24–25, 25–26
 GSH transferases as, 110, 111–112
 lipoic acid and, 30–31
 molybdopterin-containing, 44
 nitric oxide interactions with, 152–153
 PQQ-dependent, 40, 41–42
 redox activation of, 175–176
 that repair DNA, 87–94
- Epidermal growth factor (EGF), growth signaling and, 212, 213
- Epigallocatechin 3-gallate (EGCG)
 clinical cancer trials of, 218
 in green tea, 32–33
 molecular structure of, 29
- Epithelial cells, in lens, 195
- ER lumen, 124. *See also* Endoplasmic reticulum (ER)
- ERO1 gene, 125, 126
- Ero1p ER oxidase, 125
- ER oxidases, 124, 125
 PDI, 125–126

- ER secretion signal, 124
ER thiol oxidases, 125
Erv2p ER oxidase, 125
Escherichia coli, 223, 251
 alkyl hydroperoxide reductases of, 65, 67
 glutaredoxin in, 79–80, 83
 glutathione cysteine ligase of, 15–16
 glycosylases in, 89
 protein disulfide bond formation in, 113–114, 116
 redox pathways in, 175
 superoxide dismutases in, 57
 superoxide/hydrogen peroxide pathways in, 144
 thioredoxin reductase in, 71–72
 thioredoxins in, 68, 69, 70, 71
Ethylene, in biological signaling, 147
N-Ethylmaleamide (NEM), 140
N-Ethylmaleamide sensitive factor (NSF), 140
Eukaryotes
 ascorbate biosynthesis in, 23–25
 disulfide bond formation in, 120–127
 evolution of, 3–4
 glutaredoxin in, 79
 glutathione biosynthesis in, 16
 glutathione *S*-transferases in, 105, 106, 107
 heme oxygenases in, 131
 immune-system oxidative stress response regulation in, 223
 metal uptake from the extracellular environment in, 164–165
 methionine sulfoxide reductases of, 85
 peroxyredoxins in, 63
 programmed cell death in, 158
 thioredoxins in, 68, 69
Evolution, of life, 1–4
Exocytosis, nitric oxide and, 140
Expansion–contraction coupling, in cardiac myocytes, 204–206
Extracellular environment, metal uptake from, 164–165
Extracellular matrix remodeling, in chronic heart failure, 209–211
Extracellular recording, 263, 264
Extracellular superoxide dismutase, 56
Extrinsic regulation, of nitric oxide synthases, 152
Eye
 aging and, 194–195
 anatomical structure of, 194
 oxidative stress in, 194–204
F2-isoprostanes (IsoP), in lipid peroxide detection, 276–277
F-5a protein, 65
Factors C3, C3a, C3b, in innate immune system response, 223
FAD domain, of glutathione reductase, 76–77. *See also* Flavin-containing domain
FADH₂, in aerobic respiration, 7–8. *See also* Flavin adenine dinucleotide (FAD)
Faraday constant, 248, 258
Fenton-like reactions, of ascorbate, 23
Fenton reaction, 164, 221
Fermentation, as redox pathway, 175
Ferredoxin
 in ascorbate recycling, 26
 in photosynthesis, 6
Ferredoxin–thioredoxin reductase, 72
Ferricytochrome *c* reduction, in superoxide anion detection, 273
Ferritin, in intracellular iron transport, 166
Ferroportin, 166
 in export of iron from cells, 169
Ferroportin mutations, hemochromatosis resulting from, 172
Fe–S clusters. *See* [4Fe–4S] cluster entries; Iron–sulfur (Fe–S) clusters
Fibrillar collagens, 209
Finkel, Toren, xiii, 136
FLAP (5-lipoxygenase activating protein), 107
Flavin, 35–39
 coenzyme-catalyzed reactions of, 36–39
 redox states of, 36
Flavin adenine dinucleotide (FAD), 35, 38–39, 148, 149, 150, 151. *See also* FAD entries
 cytochrome P450 and, 99–100
 glutathione reductase and, 76–77
 innate immune response and, 219
 low-molecular-weight thioredoxin reductase and, 72, 73
 molybdopterins and, 44–45

- Flavin cofactor, potentiometry of, 249, 250, 251
- Flavin-containing domain, of nitric oxide synthase molecules, 149, 151, 152. *See also* FAD domain
- Flavin-dependent hydroxylases, 44
- Flavin hydroquinone, 150
- Flavin mononucleotide (FMN), 35, 38, 148, 149, 150, 151
- cytochrome P450 and, 99–100
- tetrahydrobiopterin and, 45
- Flavodoxin, 38
- Flavoenzymes, 36–39
- Flavokinase, 38
- Flavonals, 32
- Flavonoids
- human health and, 35
- as water-soluble antioxidants, 31–32
- Flavonols, 32
- Flavoprotein disulfide oxidoreductases, 75
- Flavoprotein disulfide reductase, AhpC and, 65–67
- Flavoproteins, nitric oxide synthases as, 149–150, 151
- 5-Fluorodeoxyuridylate, 47
- Fluorescence spectroscopy, NO
- determination via, 278–280
- Fluorimetric methods, in RSNO detection, 281–282
- Fluorophores, in macular degeneration, 202
- Folding, oxidative, 113–127
- Folic acid, 46–47
- biosynthesis of, 46
- Fomenko, Dmitri E., xiii, 251
- Formate dehydrogenases (FDHs), as selenoproteins, 130
- Formylmethanofuran dehydrogenases (FMDHs), as selenoproteins, 130
- [4Fe–4S] cluster-containing DNA glycosylases, 89–91, 92
- redox properties of, 91–93
- [4Fe–4S] clusters, 273–274
- Fourier transform ion cyclotron resonance (FT-ICR) analyzer, for mass spectrometers, 230
- Frataxin, 172
- Free radicals
- aging and, 33
- as paramagnetic species, 237
- “Free Radical Theory of Aging,” 33
- “French Paradox,” 33
- Fridovich, Irwin, xiii, 50, 55
- Fumarase, in oxidative immune-system damage to bacteria, 221
- Fumarate reductase, 174
- fumC* (fumarase C) gene, in immune-system oxidative stress response regulation, 222
- Furchgott, Robert F., 137, 152–153
- Fuzzy Functional Forms software, 255
- L-Galactose, in ascorbate biosynthesis, 25
- Gas chromatography and mass spectrometry (GC-MS), 228
- Gating, in ionic channels, 256, 257
- Gaussian EPR signals, 244, 245
- GDP-L-galactose, in ascorbate biosynthesis, 25
- Gendelman, Howie, xvii
- Gene expression
- circadian enzyme regulation and, 177–178, 179
- of heme oxygenases, 134
- redox control of, 155–156
- ROS effects on, 216
- Gene regulation, of glutathione reductase, 77
- Genes
- circadian clock, 178–179
- in programmed cell death, 158
- redox regulation of, 154–158
- Genetic disorders, in metal metabolism, 171–172
- Genetic redox regulation studies, electrophysiological techniques in, 271
- Genistein, clinical cancer trials of, 218
- Gilbert, Hiram F., xiv, 120
- Gladyshev, Vadim N., xiv, xvii, 84, 127, 251
- Global FNR (fumarate, nitrate reduction), 175
- Global redox cycles, 4–5
- Glomus cells, carbon dioxide and, 142
- GLR1* gene, 77
- Glucose transport, 26
- Glutamate, in glutathione, 12
- Glutamate cysteine ligase, 12
- crystal structure of, 15
- in glutathione biosynthesis, 14–15

- γ -Glutamyl cycle, in GSH homeostasis, 17, 18
- γ -Glutamylcyclotranspeptidase, in GSH homeostasis, 17
- γ -Glutamylcysteine
in glutathione biosynthesis, 16
in lens oxidation damage, 199
- Glutamyl residue oxidation, 189, 190
- γ -Glutamyltranspeptidase, 12
biosynthesis of, 18–19
crystal structure of, 19
in GSH homeostasis, 17
in mammals, 17–18
mice deficient in, 20–21
- Glutaredoxins (Grxs), 12, 75, 78–84
amino acid sequences of, 81
catalytic mechanism of, 81–82, 83
classification of, 79–80
genetic sequences homologies of, 80–81
history of, 79
human, 80–81
in immune-system oxidative stress response regulation, 222
isoforms of, 79–80
as lens antioxidant, 197
molecular structure of, 79–80
occurrence of, 78
physiological functions of, 82–83
as selenoproteins, 130
- Glutathiolation, superoxide/hydrogen peroxide pathways and, 146–147
- Glutathione (GSH), 11–21. *See also* Glutathione system; GSH entries; GSSG (oxidized glutathione)
in ascorbate recycling, 25–26
biological functions of, 13–14
biosynthesis of, 14–16, 17
degradation of, 16–21
in immune-system oxidative stress response regulation, 222
as lens antioxidant, 197–198, 199
protein disulfide bonds and, 126–127
structure of, 12
superoxide/hydrogen peroxide pathways and, 146–147
- Glutathione peroxidase 1 (GPx1), as selenoprotein, 128–129
- Glutathione peroxidase 2 (GPx2), as selenoprotein, 129
- Glutathione peroxidases (GPxs), 13, 74, 75
in lens oxidation damage, 199
in retinal antioxidant defense systems, 202–203
- Glutathione reductase (GR), 12, 75–78, 174, 175
functions of, 75–76
gene regulation of, 77
glutaredoxin and, 78, 82
physiological function of, 77–78
in retinal antioxidant defense systems, 202–203
structure and mechanism of, 76–77
therapeutic potential of, 77–78
- Glutathione *S*-transferases (GSTs), 104. *See also* GSH transferases; GST polymorphisms
cytoplasmic, 105–107
MAPEG, 107, 110
mitochondrial, 107
- Glutathione synthetase, in glutathione biosynthesis, 14, 16, 17
- Glutathione system, 74–84. *See also* Glutathione (GSH)
functions of, 74–75
glutaredoxin in, 78–84
glutathione reductase in, 75–78
- Glutathione transferase family, 13–14
- Glutathionylation, 13, 75
by glutaredoxin, 83
in peroxyredoxin regulation, 64
- GLUT-type glucose transporters, in ascorbate transport, 26
- Glycation, 189–191
- Glycine
in glutathione, 12
in glutathione biosynthesis, 16
- Glycosylases, 89
[4Fe–4S] cluster-containing, 89–91, 91–93
- Golgi apparatus, in copper metabolism, 167, 171
- Gor* gene, 80
- Gram-negative bacteria. *See also* Bacteria
protein disulfide bond formation in, 113–114
thioredoxins in, 70
- “Great Oxygenic Event,” 3, 4
- Green bacteria, 2

- Green tea, antioxidant polyphenols in, 32–33
- Gr* gene, 77
- Griess reaction, 278
in RSNO detection, 281, 282
- Grisham, Matthew H., xiv, 272
- Growth signaling messengers, reactive oxygen species as, 212, 213
- Growth stimulation, phosphatases during, 212–214
- grxA* gene, 80
- grxB* gene, 80
- grxC* gene, 80
- GSH1* gene, 126
- GSH conjugates, 104, 105. *See also* Glutathione (GSH)
- GSH:GSSG ratio, 13, 14, 207–208. *See also* GSSG (oxidized glutathione)
- GSH:GSSG redox couple
apoptosis and, 162
measurement in cells and tissue, 377
- GSH homeostasis, 16–17
- GSH transferases, 104–113
enzymatic roles of, 110, 111–112
in detoxification, 107–109
in human health, 110–113
occurrence and functions of, 104
polymorphisms among, 110–113
three superfamilies of, 104–107
versus oxidative stress, 109–110
- GSSG (oxidized glutathione). *See also* GSH:GSSG entries
in disulfide bond stability, 122
glutaredoxin and, 78, 82, 83
glutathione reductase and, 75–76, 76–77
in glutathione system, 74–75
GSH and, 13–14
in lens oxidation damage, 199
protein disulfide bonds and, 126–127
superoxide/hydrogen peroxide pathways and, 146–147
- GST polymorphisms, importance to human health, 110–113. *See also* Glutathione *S*-transferases (GSTs)
- GTPases, nitric oxide synthase and, 138, 139
- Guanidinohydantoin (Gh), DNA damage and, 87–88
- Guanine, DNA damage and, 87–88
- Guanylyl cyclase, circadian enzyme regulation and, 177
- L-Gulono-1,4-lactone, in ascorbate biosynthesis, 23–24
- Gunn diodes, 242–243
- g*-values, for EPR spectra, 240, 241, 242
- Haber–Weiss reaction, 164
- Halliwell–Foyer–Asada pathway, in ascorbate recycling, 25–26
- Halogen gases, as electron acceptors, 3
- Haworth, Walter, 22
- Health. *See also* Disease; Human health
antioxidants and, 33
harmful superoxide effects on, 55
- Heart failure, 204. *See also* Cardiac myocytes; Cardiovascular disease
extracellular matrix remodeling in, 209–211
multiple cellular factors underlying, 211
oxidative stress in, 206, 207
redox mechanisms and, 204–211
- Heat shock proteins (HSPs), apoptosis and, 160–161
- Heavy metal complexes, glutathione in, 14
- Helicobacter pylori*,
 γ -glutamyltranspeptidase of, 19
- Heliobacteria, 2
- Heme, 148
carbon dioxide and, 141, 143
in catalases, 50, 51
conversion to biliverdin, 131
in detecting peroxynitrite, 283–284
incorporation into proteins, 163–164
innate immune response and, 219
iron–sulfur cluster synthesis and, 168
in peroxidases, 50
tetrahydrobiopterin and, 45
- Heme-binding proteins
cyclic expression of, 177–178
PAS domain structure in, 179–180, 181
- Heme biosynthesis, 177–178
circadian clock and, 177–182
- Heme compounds, in hydrogen peroxide detection, 275
- Heme-containing domain, of nitric oxide synthase molecules, 149, 151
- Heme oxygenase 1 (HO-1), 132–134, 141, 142

- Heme oxygenase 2 (HO-2), 132–134, 141, 142
- Heme oxygenases (HOs), 131–134, 174, 271
 carbon dioxide and, 141
 control of gene expression of, 134
 functions of, 132
 human, 132–134
 molecular structures of, 132–133
- Hemochromatosis, 172
- Hemoglobin, carbon dioxide and, 141
- Hemoproteins, 177–177
 in detecting peroxynitrite, 283–2848
- Hepcidin, in post-transcriptional iron regulation, 170, 171
- Hephaestin, 166
- Heterolytic O–O bond cleavage, in cytochrome P450 “thiolate push,” 102–103
- HFE2 gene mutations, hemochromatosis resulting from, 172
- High-molecular-weight thioredoxin reductase, 72–74
- HMG-CoA inductase inhibitors (statins), nitric oxide synthase and, 138, 139
- HOHA (4-hydroxy-7-oxohept-5-enoic acid), in macular degeneration, 203
- Holmgren, Arne, xiv, 68
- Homocysteine, in GSH homeostasis, 16–17
- Homolytic O–O bond cleavage, in cytochrome P450 “thiolate push,” 102–103
- Hormones, in carcinogenesis, 216
- Horseradish peroxidase (HRP)-coupled assays, in hydrogen peroxide detection, 275–276
- Host–pathogen interaction, oxidative stress and, 218–225
- Human acatalasemia, 54
- Human glutathione reductase, malaria and, 77–78
- Human glutathione synthetase, 16
 crystal structure of, 17
- Human health. *See also* Disease; Health
 antioxidant molecules and, 33, 34–35
 GST transferases in, 110–113
- Humankind, global redox cycling and, 4, 5
- Humans
 cytochrome P450 enzymes in, 98
 genetic metal-metabolism disorders in, 171–172
 quinoproteins in, 40–41
 riboflavin in, 38–39
 sulfiredoxins in, 94–96
 thioredoxins in, 68–70
 ubiquinone and ubiquinol in, 31
- Human thioredoxin 1, molecular structure of, 69
- Hydroethidine (HE) oxidation, in superoxide anion detection, 273
- Hydrogen (H), global equilibrium redox cycling of, 4, 5. *See also*
 Protonation/deprotonation reactions
- Hydrogenases, 174
 as selenoproteins, 130
- Hydrogen donors, in hydrogen peroxide detection, 275. *See also*
 Protonation/deprotonation reactions
- Hydrogen exchange (HX) mass spectrometry, 236
- Hydrogen peroxide (H₂O₂)
 acatalasemia and, 54
 alkyl hydroperoxide reductases versus, 67
 in catalase assays, 54
 catalase detoxification of, 51–52
 cataract and, 196
 in cytochrome P450 “thiolate push,” 102–103
 detection of, 274–276
 elimination of, 50
 formation of, 50
 glutathione and, 13
 in immune-system oxidative stress response regulation, 222
 innate immune response and, 219
 in ion channel regulation, 261
 in photosynthesis, 6
 in protein oxidation, 184–187
 perceived toxicity of, 136
 peroxyredoxins versus, 59
 as signal transduction molecule, 143–147
 sulfenic acid and, 63–64
 superoxide and, 55
- Hydrogen peroxide dismutases, 50
- Hydrogen sulfide (H₂S), in biological signaling, 147–148
- Hydroperoxide reductases, 50

- 4-Hydroxy-7-oxohept-5-enoic acid (HOHA), in macular degeneration, 203
- p*-Hydroxybenzoate hydroxylase, 37, 38
- 8-Hydroxyguanosine (OH8SdG), ROS induction of, 215, 216
- Hydroxylases, flavin-dependent, 44
- 4-Hydroxy nonenal adducts, ROS induction of, 215
- Hyperfine interactions, in EPR, 246
- Hyperoxidation, of peroxyredoxins, 94, 95
- Hyperphenylalaninemia, 44
- Hypertrophy, of cardiac myocytes, 209
- Hypochlorous acid (HOCl), innate immune response and, 219–220
- Hypoxia, inhibition of K⁺ channels by, 271–272
- Hypoxia-inducible factor 1 α , ascorbate and, 27
- Ibsen, Henrik, 136
- Ignarro, Louis J., 137, 152–153
- Immune system, in host–pathogen interaction, 218–219. *See also* Innate immune response
- Inducible/calcium independent NOS (NOS2), discovery of, 137
- Inducible NOS (iNOS), 149, 151–152, 153
- Inlets, for mass spectrometers, 228
- Innate immune response. *See also* Immune system
- bacterial evasion of, 223–224
 - neutrophils and, 219–220
- Insects
- cytochrome P450 enzymes in, 98
 - cytosolic GSTs in, 106
- Inside-out patch configuration, for patch-clamp technique, 266–267
- Intact protein analysis, mass spectrometry for, 233–234
- Interface domain, of glutathione reductase, 76–77
- Intermediates, in cytochrome P450 reaction cycle, 100–102
- Intermolecular disulfide bond, 121
- Intracellular recording, 263, 264–266
- Intracellular redox environment, 11–12
- Intramolecular disulfide bond, 121
- Intrinsic regulation, of nitric oxide synthases, 150–152
- In vitro* NO detection methods, 277–280
- In vitro* protein disulfide bond formation, 113, 115–116, 125–126
- In vivo* lipid peroxidation, 276–277
- In vivo* NO detection methods, 277–280
- In vivo* protein disulfide bond formation, 113, 115–116
- Ion channels
- ATP-sensitive K⁺, 262
 - channel gating in, 256, 257
 - in dopaminergic neurons, 262
 - ionic selectivity of, 256
 - NMDA-type glutamate, 261–262
 - Ohm's Law, diffusion potentials, and current–voltage relationships for, 257–260
 - physiology of, 256–262
 - properties of, 256
 - redox modulation of, 261
 - in redox regulation, 260–261, 270–272
 - single-channel conductance by, 256, 257, 258–259
- Ionic selectivity, of ion channels, 256
- Ionization sources, for mass spectrometers, 228, 229–230
- Ion trap analyzer, for mass spectrometers, 230–231
- Iris screw, 243
- Iron (Fe). *See also* [4Fe–4S] cluster entries; Heme
- ascorbate reactions with, 23
 - cellular storage of, 168
 - in cytochrome P450 reaction cycle, 100, 101
 - export from cells, 169
 - genetic disorders in metabolism of, 171–172
 - heme oxygenases and, 131
 - hydrogen peroxide and, 50
 - intracellular distribution of, 166
 - metabolism of, 163–164
 - mitochondria and, 168
 - in oxidative immune-system damage to bacteria, 221
 - perturbed metabolism of, 172–173
 - post-transcriptional regulation of, 169–171

- post-translational regulation of, 171
 in protein oxidation, 184–187
 pterins and, 44
 in superoxide dismutation, 56, 57
 transcriptional regulation of, 169
 uptake from the extracellular environment,
 164–165
- Iron regulatory proteins (IRPs), in post-
 transcriptional iron regulation, 169–171
- Iron response elements (IREs), in post-
 transcriptional iron regulation, 169–171
- Iron-responsive protein-1 (IRP-1), in
 immune- system oxidative stress
 response regulation, 223
- Iron–sulfur cluster loop (FCL) motif, of
 glycosylases, 89–91, 92
- Iron–sulfur (Fe–S) clusters
 heme and, 168
 in intracellular iron transport, 166
 in iron regulation, 169, 170
 in oxidative immune-system damage to
 bacteria, 221, 222
- Isocitrate, in aconitase activity measurement,
 274
- Isoflavones, 32
- Isomerases, PDI, 125–126
- Isomerization reactions, 111
 of protein disulfide bonds, 117–119, 122,
 124
- Isoniazide, inactivation of, 52
- Isoprenoid intermediates, nitric oxide
 synthase and, 138
- Isoprenoids, 30
- Isoprostanes (IsoP), in lipid peroxide
 detection, 276–277
- Isotopes, in peptide analysis mass
 spectrometry, 231, 232
- Isotropic EPR spectra, 240, 242
- JNK (c-Jun N-terminal kinase)
 apoptosis and, 160, 161
 in cardiac myocyte hypertrophy/death,
 209
- K⁺ (potassium ion)
 ATP-sensitive, 262
 Ca²⁺ influx into cardiac myocytes and,
 208
 ionic selectivity for, 256, 259, 261
- K⁺ channels, hypoxia inhibition of, 271–272
- Kadokura, Hiroshi, xiv, 113
- K_{ATP} channels, in H₂S biological signaling,
 147
- K-band EPR, 243
- Ketoaldehydes, 191
- Kidney, ascorbate biosynthesis in, 23
- King, Charles, 22
- Klystron tubes, 242–243
- K_m, of monofunctional catalases, 52
- Knockout mice, superoxide dismutase, 58
- Ko-jo-kon, 33
- Kunitz-trypsin inhibitor, in ascorbate
 recycling, 25
- Lactone oxidase, 23–24
- Lee, Cheng Chi, xiv, 177
- Lee, Jaekwon, xiv, 162
- Lens, 194
 anatomical structure of, 195
 antioxidant defenses of, 197–198, 199
 oxidation damages to, 198–199
 oxidative-stress pathology of, 195–199
- Lens membrane, oxidation damage to, 198
- Lens proteins, oxidation damage to, 198–199
- Leukemia, thioredoxins and, 70
- Leukotrienes, glutathione in synthesis of, 13,
 14
- Life
 evolution of, 1–4
 global redox cycling and, 4–5
 major bioenergetic cycles for, 6–8
- Ligand binding, potentiometry and,
 248–249
- Light
 folic acid and, 47
 retinal damage from, 201–202
- Lin, Ming-Fong, xiv, 212
- Lipid peroxidation, detection *in vivo*,
 276–277
- Lipids, ascorbate and, 22
- Lipid-soluble antioxidant molecules, 28–31
- Lipofuscin, 201
 macular degeneration and, 202
- Lipoic acid, molecular structure of, 29
- α-Lipoic acid
 as antioxidant, 30–31
 human health and, 34
- Liposomes, carotenoids in, 30

- Lipoxidation, in macular degeneration, 202
- Liquid chromatography and mass spectrometry (LC-MS), 228
- Lithosphere, global redox cycling and, 4, 5
- Liver
 - ascorbate biosynthesis in, 23–24
 - detoxification by GSH transferases in, 107–109
 - glutathione biosynthesis in, 16
- Longevity. *See also* Aging
 - catalases and, 53
 - free radicals and, 33
- Long term potentiation (LTP), in H₂S
 - biological signaling, 147
- Lorentzian EPR signals, 244, 245
- Lou, Marjorie F., xiv, 74, 194
- Low-molecular-weight thioredoxin reductase, 72
- Lucigenin, in superoxide generation measurement, 274
- Lysine, in cross-linked protein derivative formation, 192, 193
- Lysine tyrosylquinone (LTQ), 40
- Lysyl residue oxidation, 189, 190
- Mac1 transcription regulator, 169
- Macrophage NOS (iNOS), 149
- Macrophages
 - bacterial blocking of, 223–224
 - export of iron from, 169
 - in host–pathogen interaction, 219
 - ion channel regulation in, 260
 - thioredoxins in, 70
- Macula, 199, 202
- Macular degeneration, 194–195, 201, 202, 203
- Magnesium (Mg). *See* Mg²⁺ (magnesium ion)
- Magnetic fields, for EPR, 243, 244, 245
- Magnetic moments, nuclear, 238
- Magnets, for EPR, 241–242
- Malaria, glutathione reductase and, 77–78
- Malate dehydrogenase, 174
- Malondialdehyde-acetaldehyde
 - hybrid-protein adducts, ROS induction of, 215
- Mammals
 - 3-aminotriazole catalase inactivation in, 54
 - apoptosis in, 158–159
 - ascorbate biosynthesis in, 23–24
 - circadian clock in, 178, 181–182
 - detoxification by GSH transferases in, 107–109
 - γ -glutamyltranspeptidase in, 17–18
 - glutaredoxin in, 79
 - heme oxygenases in, 132
 - high-molecular-weight thioredoxin reductase from, 72–74
 - metal metabolism in, 163–164
 - metal uptake from the extracellular environment in, 164–165
 - methionine sulfoxide reductases of, 85
 - NAD⁺ biosynthesis in, 40
 - nitric oxide in, 153
 - peroxyredoxins in, 94, 95
 - reactive oxygen species in, 196–197
 - selenoproteins of unknown function in, 130
 - thioredoxin reductase in, 72
 - thioredoxins in, 69
- Manganese (Mn). *See also* MnSODs (manganese superoxide dismutases)
 - in catalases, 51–52
 - in dismutases, 50
 - in superoxide dismutation, 56, 57
- MAPEG (membrane-associated proteins in eicosanoid and GSH) GSTs, 107, 110
 - as enzymes, 112
 - in human health, 110–113
- MAPK (mitogen activated protein kinase), in redox regulation of genes, 154–155
- MAPK family, carbon dioxide and, 143
- MAPKKK (mitogen active protein kinase kinase kinase), apoptosis and, 160, 161
- Mass spectrometers, 228–231
 - types of, 228
- Mass spectrometry (MS), 228–237
 - applications of, 231–236
 - hydrogen exchange, 236
- Masters, Bettie Sue, xiv, 148
- Matrix-assisted laser desorption ionization (MALDI)
 - as mass spectrometer source, 230
 - in quantitative mass spectrometry, 234
- Matrix metalloproteinases (MMPs), in chronic heart failure, 210

- mCry* genes, in circadian clock, 178–179, 180
- Mechanically gated ionic channels, 257
- Mediterranean diet, 218
- Meister, Alton, 17, 18
- Membranes
 - cytochrome P450 enzymes in, 98
 - in electrophysiological techniques, 263–272
 - ion channels across, 257–260, 263
 - MAPEG GSTs in, 107
- Menaquinone, DsbA and DsbB proteins and, 116
- Mendel, R., 45
- Menkes disease, 167, 172
- Metabolism
 - GSTs in therapeutic drug, 113
 - of metals, 162–173
- Metabolomics, mass spectrometry for, 236
- Metal-binding proteins, conserved cysteines in, 253
- Metal catalysis, of protein carbonyl derivative formation, 189
- Metal-catalyzed disulfide bond formation, 121
- Metal complexes, glutathione in, 14
- Metal-containing enzymes, activation of, 175–176
- Metal-coordinating cysteines, 252
- Metal homeostasis, 162–173
 - genetic disorders in, 171–172
 - mechanisms for, 163
 - perturbation of, 172–173
 - regulation of, 169–171
- Metallic ions, in electron transfer, 162
- Metallocofactors, for redox enzymes, 173
- Metalloproteins, formation of, 162–163
- Metallothionein, in cellular metal storage, 168
- Metal oxidation, as redox pathway, 175
- Metal reduction, as redox pathway, 175
- Metals
 - cellular storage of, 168
 - export from cells, 168–169
 - intracellular distribution of, 165–166
 - metabolism of, 162–173
 - as paramagnetic species, 237
 - in protein oxidation, 184–187
 - uptake from the extracellular environment, 164–165
- Metal transporters, subcellular, 167–168
- Metazoans, evolution of, 4
- Methane monooxygenase, 174
- Methanogenesis, as redox pathway, 175
- Methanol dehydrogenase, 174
- Methionine reduction pathway, 84
- Methionine residues, oxidation to methionine sulfoxide, 84
- Methionine-*R*-sulfoxide (Met-*R*-SO), 84
 - methionine sulfoxide reductases for, 85–87
- Methionine-*R*-sulfoxide reductases (MsrBs), as selenoproteins, 129. *See also* MsrB (methionine sulfoxide reductase B)
- Methionine-*S*-sulfoxide (Met-*S*-SO), 84
 - methionine sulfoxide reductases for, 85–87
- Methionine-*S*-sulfoxide reductases (MsrAs), as selenoproteins, 129. *See also* MsrA (methionine sulfoxide reductase A)
- Methionine sulfoxide, from methionine residues, 84
- Methionine sulfoxide reductases (Msrs), 85–87. *See also* Msr entries
 - crystal structures of, 86
 - as lens antioxidants, 197
 - physiological functions of, 86
 - properties of, 86
 - selenoprotein forms of, 86
- Methyl-Com reductase, 174
- Methyl donors, in enzyme redox activation, 176
- Methylenetetrahydrofolate, 43, 46, 47
- Methyltransferases, ROS effects on, 216
- Mg²⁺ (magnesium ion), in NMDA-type glutamate channels, 261
- MgrA global regulator, in redox control of gene expression, 156
- MGST enzymes, 107
- MHC Class I molecules, in peptide editing, 156
- Mice
 - catalases and longevity of, 53
 - γ -glutamyltranspeptidase-deficient, 20–21
- Microelectrodes, for intracellular recording, 264–265, 265–266

- Microsomal glutathione transferases, 14
 Microwaves, for EPR, 241, 242–243
 Midpoint potential (E_m), 247–248
 measuring, 249–250
 Misfolded proteins, correction of, 117–119
 Missense mutations, hemochromatosis
 resulting from, 172
 Mitochondria
 in aerobic respiration, 8
 apoptosis and, 160
 catalases and, 53
 in chronic heart failure, 206, 207
 circadian enzyme regulation and, 177–178
 flavoenzymes in, 38
 glutathione in, 13
 high-molecular-weight thioredoxin
 reductase in, 73
 in intracellular metal distribution,
 165–168
 lipoic acid in, 30
 methionine sulfoxide reductases in, 85
 nitric oxide and, 140
 ROS-induced mutations in, 216
 superoxide dismutases in, 57
 thioredoxins in, 68–70
 ubiquinone and ubiquinol in, 31
 uncontrolled ROS production and, 214
 Mitochondrial biogenesis, 140
 Mitochondrial glutathione transferases, 14,
 107
 Mitochondrial NOS (mtNOS), 140
 MNK copper carrier, 165, 167
 in post-translational copper regulation,
 171
 MnSODs (manganese superoxide
 dismutases), 57, 58. *See also*
 Manganese (Mn)
 MODELER software, 255
 Modeling, protein structure, 254–255
 Molecular oxygen. *See also* Oxygen (O)
 flavin coenzymes and, 37–38
 superoxide from, 55
 Molecular redox regulation studies,
 electrophysiological techniques in, 271
 Molecular weight, in peptide analysis mass
 spectrometry, 231–233
 Molecules
 mass spectrometry of, 228
 potentiometry of, 248–249, 249–251
 MolScript software, xvii
 Molybdenum (Mo), molybdopterins and,
 44–45
 Molybdopterin cofactors, molecular
 structures of, 45
 Molybdopterins, 42–46
 Monocytes, thioredoxins in, 70
 Monodehydroascorbate, 22
 in ascorbate recycling, 25–26
 molecular structure of, 23
 Monofunctional catalases, 51–52
 Monooxygenases, 37–38, 43–44, 97
 Monothiol mechanism, of glutaredoxin, 83
mPer genes, in circadian clock, 178–179,
 180, 181
 mRNA UTRs (untranslated regions), in post-
 transcriptional iron regulation, 169–171
 MsrA (methionine sulfoxide reductase A),
 85–87. *See also* Methionine-*S*-sulfoxide
 reductases (MsrAs)
 catalytic mechanisms of, 87
 crystal structure of, 86
 MsrB (methionine sulfoxide reductase B),
 85–87. *See also* Methionine-*R*-sulfoxide
 reductases (MsrBs)
 catalytic mechanisms of, 87
 crystal structure of, 86
 mtDNA (mitochondrial DNA), ROS-induced
 mutations in, 216
 Müller cells, in retina, 199, 200
 Multiple reaction monitoring (MRM), by
 mass spectrometers, 230, 231
 Multiple superoxide dismutases, 56
 Multiunit recordings, electrophysiological,
 264
 Murad, Ferid, 137, 152–153
 Mutations, hemochromatosis resulting from,
 172
 Mut Y glycosylase, 89–91
 redox properties of, 91–92, 93
Mycobacterium tuberculosis, 52
 immune system blocking by, 224
 Mycothiol, 21
 molecular structure of, 20
 Myeloperoxidase, innate immune response
 and, 219–220
 Myocytes, expansion–contraction coupling
 in cardiac, 204–206
 Myoglobin, mass spectrogram of, 233–234

- Na⁺ (sodium ion)
 in cardiac myocyte expansion-contraction coupling, 205
 ionic selectivity for, 256, 261
- Na⁺/Ca²⁺ exchanger (NCX), in cardiac myocyte expansion-contraction coupling, 205
- Na⁺/Ca²⁺ exchange transporter, SERCA2a and, 208–209
- N*-acetyl cysteine (NAC)
 growth signaling and, 212
 in redox regulation of genes, 154
- NAD⁺ (nicotinamide adenine dinucleotide), 39–40
 biosynthesis of, 40
- NADH (reduced NAD⁺)
 in aerobic respiration, 7–8
 apoptosis and, 160
 cytochrome P450 and, 99–100, 101
 molybdopterins and, 44–45
 in nitrite and nitrate quantification, 278
- NAD⁺/NADH redox potential, 39
- NADP⁺ domain, of glutathione reductase, 76–77. *See also* Phosphorylated NAD⁺ (NADP⁺)
- NADPH (reduced phosphorylated NAD⁺)
 apoptosis and, 160
 in ascorbate recycling, 25–26
 carbon dioxide and, 141
 catalase binding of, 53
 cytochrome P450 and, 99–100
 glutaredoxin and, 78, 82
 glutathione and, 12, 13
 glutathione reductase and, 75–76, 76–77
 in glutathione system, 74
 growth signaling and, 212, 213
 in lens oxidation defenses, 197–198
 in nitrite and nitrate quantification, 278
 synthesis of, 6, 7
 thioredoxin reductase and, 71, 72, 73
 thioredoxins and, 68
- NADPH-cytochrome P450 reductase, nitric oxide synthases and, 149–150
- NADPH oxidases (NOXs), 39–40, 271
 in chronic heart failure, 206, 207
 innate immune response and, 219, 220
 in ion channel regulation, 260–261
 superoxide/hydrogen peroxide pathways and, 145, 146–147
 uncontrolled ROS production and, 214
- NADP⁺/NADPH redox potential, 39
- 2,3-Naphthotriazole (NAT), in NO determination, 278, 279
- National Cancer Institute, 218
- NCBI Conserved Domains database, 255
- NCBI sequence databases, 252
- Necrotic cell death, 158
- Neisseria gonorrhoeae*, methionine sulfoxide reductase of, 86
- Nernst equation, 247–248, 258, 259
- N*-ethylmaleamide (NEM), 140
- N*-ethylmaleamide sensitive factor (NSF), 140
- Neuronal NOS (nNOS; NOS1), 140, 149, 151–152
 discovery of, 137
- Neurons, ion channels in, 262
- Neutral blue semiquinone, 150
- Neutrophil oxidases (NOXs), superoxide/hydrogen peroxide pathways and, 145, 146
- Neutrophils
 bacterial blocking of, 223–224
 in host-pathogen interaction, 218–219
 innate immune response and, 219–220
- NF- κ B transcription factor
 in cardiac myocyte extracellular matrix remodeling, 210
 uncontrolled ROS production and, 214
- Niacin, 40
- Nickel (Ni), superoxide dismutase with, 57–58
- NifL flavoprotein, 38
- Nitrate, quantification of, 278, 279
- Nitrate reductase, 44, 45
- Nitration, retinal damage and, 201–202
- Nitric oxide (NO)
 apoptosis and, 161–162
 biological response to, 138–140
in vivo and *in vitro* detection of, 277–280
 protein and enzymatic interactions of, 152–153
 as signal transduction molecule, 136–140
 superoxide and, 55
- Nitric oxide synthases (NOSs)
 characterization of, 149–150

- Nitric oxide synthases (NOSs) (*Cont.*)
 in chronic heart failure, 206, 207
 discovery of, 137
 extrinsic regulation of, 152
 intrinsic regulation of, 150–152
 isoforms of, 149–150, 151–152
 molecular structures of, 151
 occurrence and function of, 137–138, 139, 140
 protein and enzymatic NO interactions, 152–153
 in redox signaling, 148–154
 tetrahydrobiopterin and, 45–46
- Nitrification, 5
- Nitrite
 in detecting peroxynitrite, 284
 quantification of, 277, 278, 279
- Nitrogen (N)
 evolution of life and, 2
 global equilibrium redox cycling of, 4–5
- Nitrogen dioxide, 277, 278, 279
- Nitrogen fixation, flavoenzymes in, 38
- Nitrogen-fixing bacteria, 4–5
- S*-Nitrosoglutathione (GSNO), in chronic heart failure, 206, 207
- Nitrosonium ion (NO⁺), in RSNO detection, 281, 282
- S*-Nitrosothiols (RSNOs), detection of, 281–282
- Nitrotyrosine (NT), retinal damage and, 201–202
- 3-Nitrotyrosine, in detecting peroxynitrite, 283–284
- Nitroxyl (HNO/NO), 280
 in detecting peroxynitrite, 284
- Nitryl chloride, in detecting peroxynitrite, 284
- NMDA (N-methyl-D-aspartate), 261
- NMDA receptor, in H₂S biological signaling, 147
- NMDA-type glutamate channels, 261–262
- Nonflavonoids, 31–32, 33
- Npas2* gene, in circadian clock, 180–182
- NPAS2 transcription factor, carbon dioxide and, 143
- N-terminal nucleophile hydrolase superfamily, 18–19
- Nuclear hyperfine interactions, in EPR, 246
- Nuclear magnetic resonance (NMR)
 spectroscopy, EPR versus, 237–238
- Nuclear spins, NMR and, 237
- OG (7,8-dihydro-8-oxo-2'-deoxyguanosine)
 DNA repair and, 88–89
 formation of, 93
- OG glycosylases, 89
- Ohm's Law, for ion channels, 257–260
- Oligomerization, of peroxyredoxins, 60–63
- 1-cys peroxyredoxins, 60, 61
- Opacity, age-related lens, 195–196
- Opsins, in retina, 199
- Ore, Joyce, xviii
- Organic free radicals, as paramagnetic species, 237, 239
- Organic peroxides, peroxyredoxins versus, 59
- Organ transplantation, carbon dioxide and, 143
- Osborne, Robert L., xiv, 97
- Outside-out patch configuration, for patch-clamp technique, 266–267
- Oxidants, sources of, 196–197
- Oxidant signaling, 136–148
- Oxidases, 38. *See also* Aldehyde oxidase; Copper amine oxidase; Cytochrome *c* oxidases; ER oxidases; Lactone oxidase; NADPH oxidases (NOXs); Neutrophil oxidases (NOXs); Peroxidases; Sulfite oxidase; Xanthine oxidase (XO)
- Oxidate activation, of enzymes, 175–176
- Oxidation. *See also* Oxidation/reduction; Redox entries
 aging-related protein, 184, 185, 186, 193
 cataract and, 196, 197
 in cross-linked protein derivative formation, 192, 193
 of dihydrodichlorofluorescein, 274–275
 protein carbonyl derivative formation via, 189–191
 protein modification via, 184–187, 193
 as redox pathway, 175
- Oxidation defense systems
 in the lens, 197–198, 199
 in the retina, 202–203
- Oxidation/reduction, of ascorbate, 23
- Oxidation states, of cysteines in protein, 235

- Oxidative damage, to bacteria via immune system, 220–221
- Oxidative folding
 by antioxidant enzymes, 113–127
 misfolding correction during, 117–119
 pathways for, 114–117, 117–120
- Oxidative potentiometric measurements, 250
- Oxidative stress, 11–12
 apoptosis and, 160, 161
 bacterial response to, 223
 in chronic heart failure, 206, 207
 DNA damage and, 87–88
 in the eye, 194–204
 glutaredoxin versus, 83
 GSH transferases versus, 109–110
 host–pathogen interaction and, 218–225
 by immune system, 221–224
- Oxidized nitric oxide metabolites, *in vivo* and *in vitro* detection of, 277–280
- Oxidoreductases, thiol-based, 251–255
- 5-Oxoprolinase, in GSH homeostasis, 17
- Oxyferrous P450 complex, molecular structure of, 99
- Oxygen (O). *See also* Molecular oxygen
 in aerobic respiration, 8
 in cytochrome P450 reaction cycle, 100–101
 as electron acceptor, 3
 global equilibrium redox cycling of, 4, 5
 glutathione and, 13
 increase in atmospheric, 4
 in inhibition of K⁺ channels, 271–272
 as metabolic waste, 3
 molybdopterins and, 44–45
 in potentiometry, 250–251
 in superoxide generation measurement, 274
- Oxygen activation
 in cytochrome P450 distal charge relay, 103–104
 in cytochrome P450 “thiolate push,” 102–103
- Oxygenase domain, of nitric oxide synthase molecules, 149, 151
- Oxygenases. *See* Heme oxygenases (HOs)
- Oxygen evolving center, 174
- Oxygenic photosynthesis, 3–4, 6–7
- Oxygen sensing
 in bacteria, 156
 carbon dioxide and, 141–142
- OxyR transcriptional regulator, 65
- OxyR transcription factor, 144
 in immune-system oxidative stress response regulation, 222
- p53 tumor suppressor gene, 155
- P450-CAM protein
 in cytochrome P450 distal charge relay, 103–104
 molecular structure of, 98–99
- P450 enzymes. *See* Cytochrome P450 enzymes
- Paracrine signaling, 137
- Paramagnetic species, 237
- Parkinson’s disease, perturbed metal homeostasis and, 173
- PAS domain structure, in heme-binding proteins, 179–180, 181
- Patch-clamp techniques
 advantages and disadvantages of, 269–270
 for intracellular recording, 265–270
 in redox regulation studies, 270–272
- Pathological processes, redox-related, 183–225
- Pauling, Linus, 22
- PDGF peptide growth factor, 144–145, 146
- PDI1* gene, 125, 126
- Pellagra, 40
- Peptide analysis, mass spectrometry for, 231–233
- Peptide bond cleavage, 189, 190
 protein modification via, 187–188
- Peptide editing, thiol-mediated redox regulation and, 156–157
- Perforated whole-cell patch-clamp configuration, for intracellular recording, 267, 269
- Period regulator, in circadian clock, 178
- Periplasm, DsbA, DsbB, DsbC, and SsbD proteins in, 120
- Peroxidases
 catalases and, 50
 in detecting peroxyxynitrite, 283–284
 glutathione, 13
K_m of, 52
 mechanism of action of, 52

- Peroxidation, in macular degeneration, 202
- Peroxides, glutathione versus, 13–14. *See also* Hydrogen peroxide (H₂O₂)
- Peroxide-sensitive switch, 63–64
- 4a-Peroxyflavin, 44
- Peroxyl radical, in protein oxidation, 184–187
- Peroxynitrite (ONOO⁻), 140
 - in chronic heart failure, 206, 207
 - 3-nitrotyrosine in detection of, 283–284
 - peroxyredoxins versus, 59
 - superoxide and, 55
- Peroxyredoxins (Prxs), 59–64
 - AhpF and, 65–67
 - classification of, 59–60
 - decamers of, 60–63
 - dimers of, 60–63
 - glutathione and, 13
 - during growth stimulation, 213–214
 - hyperoxidation of, 94, 95
 - mechanistic and structural features of, 59–60, 61
 - occurrence of, 59
 - oligomerization of, 60–63
 - in prokaryotes and eukaryotes, 63
 - protein–protein interactions and, 64
 - in redox-dependent cell signaling, 63–64
 - regulatory mechanisms for, 63–64
 - as selenoproteins, 130
- Phagocytes
 - alkyl hydroperoxide reductases of, 65
 - bacterial blocking of, 223–224
 - in host–pathogen interaction, 218–219
 - innate immune response and, 219–220
 - ion channel regulation in, 260
- Phagocytosis
 - bacterial inhibition of, 224
 - retinal, 201
- Phagosomes, bacterial inhibition of, 224
- Pharmacological redox regulation studies, electrophysiological techniques in, 270–271. *See also* Drugs
- Phenol red oxidation, in hydrogen peroxide detection, 276
- Phenylalanine hydroxylase, mutations in, 44
- Phenylketonuria, 44
- Phosphatases
 - during growth stimulation, 212–214
 - superoxide/hydrogen peroxide pathways and, 145–146
- Phosphofructokinase, glutaredoxin reactivation of, 83
- Phospholamban (PLN), 205
 - SERCA2a and, 208–209
- Phosphorus (P), global equilibrium redox cycling of, 4
- Phosphorylated NAD⁺ (NADP⁺), 39. *See also* NADP⁺ domain; NADPH entries
- Phosphorylation, in peroxyredoxin regulation, 64
- Photolyases, 38
 - folic acid and, 47
- Photoreactivation, folic acid and, 47
- Photoreceptor cells
 - light damage to, 201
 - in retina, 199–200, 200–201
- Photosynthesis
 - anoxygenic bacterial, 2–3
 - heme oxygenases and, 131
 - oxygenic, 3–4, 6–7
 - as redox pathway, 175
- Photosystem I, 6, 7
- Photosystem II, 6–7
- Physiological function, of glutathione reductase, 77–78
- Physiological processes, redox regulation of, 135–182
- Physiology, of metal metabolism, 163–164
- Phytoestrogens, 32
- Plants
 - ascorbate biosynthesis in, 24–25
 - ascorbate recycling in, 25–26
 - carotenoids and vitamin A from, 30
 - cytosolic GSTs in, 106
 - flavonoids in, 31–32
 - peroxidases in, 53
 - photosynthesis by, 6
 - quinones in, 40
 - thioredoxins in, 69
 - a-tocopherol from, 28–30
- Plasma membrane,
 - γ -glutamyltranspeptidase in, 17–18
- Plasmodium falciparum*, glutathione reductase and, 77–78
- Plastocyanin, in photosynthesis, 6, 7
- Platelet-derived growth factor (PDGF), growth signaling and, 212, 213

- Platelet-derived growth factor receptor (PDGFR), growth signaling and, 212, 213
- Polymorphonuclear white blood cells, in host–pathogen interaction, 218–219
- Polyphenols
as antioxidants, 31–33
“French Paradox” and, 33
in green tea, 32–33
- Poole, Leslie B., xiv, 59, 65, 94
- Post-transcriptional regulation, of metal metabolism, 169–171
- Post-translational modifications (PTMs), mass spectrometry of, 235
- Post-translational regulation, of metal metabolism, 171
- Potassium (K). *See* K⁺ entries
- Potentiometry, 247–251
midpoint potential in, 247–248
of redox-linked processes, 248–249
techniques of, 249–251
- PQQ. *See* Pyrroloquinoline quinone (PQQ)
- Precursor availability, in GSH homeostasis, 16–17
- Primates, uric acid in, 34
- Proapoptotic proteins, 158–159
- Probability density function, for ion channels, 268–269
- Programmed cell death, 158. *See also* Apoptosis of cardiac myocytes, 209
- Prokaryotes
glutaredoxin in, 79
methionine sulfoxide reductases of, 85, 86
peroxyredoxins in, 63
thioredoxins in, 68, 69
- Prolyl residue oxidation, 189, 190
- Pro-MMPs (MMP proenzymes), in chronic heart failure, 210
- Pro-oxidant, ascorbate as, 23
- PROSITE database, 253
- Prostaglandins
glutathione in synthesis of, 13, 14
synthesis of, 111
- “Protector protein,” 59
- Protein adducts, carcinogenic, 215–216
- Protein analysis
mass spectrometry for, 233–234
quantitative, 234
- Protein Data Bank, 254
- Protein disulfide isomerases (PDIs), 70
in endoplasmic reticulum, 124, 125–126
as selenoproteins, 129
- Protein disulfides, glutaredoxin mechanism and, 81–82, 83
- Protein kinase A (PKA)
in cardiac myocyte expansion–contraction coupling, 205, 206
SERCA2a and, 209
- Protein kinase G (PKG), nitric oxide and, 153
- Protein modification, 184–194
amino acid residue side-chain oxidation, 188–189
amino acid side-chain beta-scission, 189
associated with aging, 184, 185, 186, 193
carbonyl derivative generation, 189–191
cross-linked derivative formation, 192, 193
oxidation mechanisms, 184–187, 193
peptide bond cleavage, 187–188
- Protein oxidation, aging-related, 184, 185, 186, 193
- Protein phosphatases, in redox regulation of genes, 154–155
- Protein–protein interactions, in peroxyredoxin regulation, 64
- Proteins. *See also* Ca²⁺-handling proteins; Heme-binding proteins; Metal-binding proteins; Metalloproteins
as carbon monoxide targets, 141–143
disulfide bond formation in, 113–114, 120–127
glutaredoxin repair of, 83
ion-channel, 256–262
in lens, 195–196
methionine reduction pathway and, 84
nitric oxide interactions with, 152–153
oxidation damage to lens, 198–199
peroxyredoxins as, 60–63
potentiometry of, 247, 248–249, 249–251
proapoptotic, 158–159
quantitative mass spectrometry of, 234
redox state changes in, 263
sequence analysis of, 255
sulfinic acid-containing, 96–97
thioredoxins as, 70–71, 72

- Protein secondary structure modeling, 254–255
 redox-active cysteines and, 253–254
- Proteins with cysteine (PSSC), in lens oxidation damage, 199
- Proteins with glutathione (PSSG), in lens oxidation damage, 199
- Protein tyrosine phosphatases (PTPs) during growth stimulation, 212–214s
 superoxide/hydrogen peroxide pathways and, 145–146
- Proteolysis, in peroxyredoxin regulation, 64
- Proteomics, mass spectrometry for, 235
- Protonation/deprotonation reactions, of ascorbate, 23. *See also* Hydrogen (H); Hydrogen donors
- Protoporphyrin IX, 148. *See also* Heme
- Pseudocatalases, 51–52
- Pseudomonas aeruginosa*, phagocytosis inhibition by, 224
- PSI-BLAST software, 253. *See also* BLAST (Basic Local Alignment Search Tools) software
- PSIPRED software, 253
- PSSC (proteins with cysteine), in lens oxidation damage, 199
- PSSG (proteins with glutathione), in lens oxidation damage, 199
- Pterin-dependent aromatic amino acid hydroxylases, 43–44
- Pterins, 42–46
- PTPIB protein, superoxide/hydrogen peroxide pathways and, 147
- Purple bacteria, 2
- PutA flavoprotein, potentiometry of, 251
- Pyranopterin, 44
- Pyroloquinoline quinone (PQQ), 40, 41–42
 molecular structure of, 41
 redox states of, 41
 as vitamin, 41–42
- Pyruvate dehydrogenase, 174
- Pyruvate-ferredoxin oxidoreductase, 174, 175
- QACXG motif, apoptosis and, 160
- Q-band EPR, 243
- Quadrupole analyzer, for mass spectrometers, 230
- Quadrupole ion trap analyzer, for mass spectrometers, 231
- Quadrupole time-of-flight (Quad TOF) analyzer, for mass spectrometers, 231
- Qualitative markers, in hydrogen peroxide detection, 275
- Quantitation, 234
- Quantitative analysis, mass spectrometry for, 234
- Quantum mechanical resonance, EPR and, 240, 241
- Quercetin, 32
- Quinone/quinonoid cofactors, 40
- Quinones, 40–42
- Quinonoid dihydrobiopterin, 42
- Quinoproteins, 40–41
- Rac family proteins, superoxide/hydrogen peroxide pathways and, 145, 146
- Ragsdale, Stephen W., xiv, xvii, 131, 173, 237
- Rat thioredoxin reductase 1, molecular structure of, 73
- Raza, Ashraf, xiv, 228
- Reaction cycle, cytochrome P450, 100–102
- Reactive nitrogen species (RNS)
 in aging-related protein oxidation, 184, 185, 186, 193
 in cardiac myocyte extracellular matrix remodeling, 210–211
 in cardiac myocyte hypertrophy/death, 209
 in chronic heart failure, 206, 207
 detection of, 272–284
 in redox regulation of genes, 155
- Reactive oxygen species (ROS), 3, 11–12
 in aerobic respiration, 8
 in aging-related protein oxidation, 184, 185, 186, 193
 alkyl hydroperoxide reductases versus, 65
 apoptosis and, 159–162
 in carcinogenesis, 212–218
 carcinogenic DNA/protein adducts induced by, 215–216
 carcinogenic uncontrolled production of, 214
 in cardiac myocyte extracellular matrix remodeling, 210–211

- in cardiac myocyte hypertrophy/death, 209
- cataract and, 196–197
- in chronic heart failure, 206, 207
- detection of, 272–284
- DNA damage via oxidative stress from, 87–88
- DNA methylation and, 216
- gene expression and, 216
- glutathione versus, 13–14
- as growth signaling messengers, 212, 213
- innate immune response and, 219
- in ion channel regulation, 260–26
- lipoic acid and, 30–31
- mitochondrial mutations induced by, 216
- nitric oxide and, 140
- in oxidative immune-system damage to bacteria, 220–221
- and phosphatases during growth stimulation, 212–214
- in photosynthesis, 6
- in protein carbonyl derivative formation, 191
- in redox regulation of genes, 154–155
- in signal transduction, 156–157
- superoxide/hydrogen peroxide pathways and, 144–145, 146
- uric acid versus, 34
- vitamin E versus, 28–30
- Receptor protein tyrosine kinases (RPTKs), uncontrolled ROS production and, 214
- Receptor tyrosine kinases, superoxide/hydrogen peroxide pathways and, 145, 146
- Recording, electrophysiological, 263–266
- Recycling, of ascorbate, 25–26
- Redox activation, of enzymes, 175–176
- Redox-active cysteine residues, 252, 253–254
- Redox-active cysteines, in bioinformatics, 251–255
- Redox-active prosthetic groups, in redox enzymes, 173
- Redox-active signal molecules, heme oxygenases and, 132
- Redox biochemistry, xvii–xviii
 - bioinformatics methods in, 251–255
 - electron paramagnetic resonance techniques in, 237–247
 - electrophysiology in, 256–272
 - evolution of life and, 1–4
 - mass spectrometry in, 228–237
 - pathological processes related to, 183–225
 - potentiometry in, 247–251
 - reactive oxygen and nitrogen metabolite detection in, 272–284
 - specialized methods in, 227–284
- Redox buffers, thiol-based, 21. *See also* Glutathione (GSH)
- Redox center, in potentiometry, 247, 248, 249
- Redox coenzymes, 11, 35–47
 - flavin, 35–39
 - folic acid, 46–47
 - molybdopterins, 42–46
 - NAD⁺, 39–40
 - pterins, 42–46
 - quinones, 40–42
- Redox cofactors, pterins as, 42. *See also* Redox coenzymes
- Redox cycles, global, 4–5
- Redox-dependent cell signaling, peroxyredoxins in, 63–64
- Redox enzymes, 173–177
 - inhibition of, 271–272
 - pathways of, 175
 - table of selected, 174
- Redox factor-1, in cardiac myocyte extracellular matrix remodeling, 210
- Redox-linked processes, potentiometry of, 248–249
- Redox modulation, of Ca²⁺-handling proteins, 206–209
- Redox regulation
 - of apoptosis, 158–162
 - of genes, 154–158
 - ion channels in, 260–261, 270–272
 - of physiological processes, 135–182
 - thiol-mediated, 156–157
- Redox signaling, nitric oxide synthases in, 148–154
- Reduced cysteines, in redox regulation of genes, 155

- Reduced thioredoxin, 70–71, 72
- Reductase domain, of nitric oxide synthase molecules, 149, 151
- Reductases, alkyl hydroperoxide, 65–67. *See also* AhpC peroxyreductase; AhpF flavoprotein disulfide reductase; Alkyl hydroperoxide reductases; Biliverdin reductase; Cytochrome P450 reductase; Dcvtb reductase; Disulfide reductase system; Ferredoxin–thioredoxin reductase; Flavoprotein disulfide oxidoreductases; Flavoprotein disulfide reductase; Fumarate reductase; Glutathione reductase (GR); High-molecular-weight thioredoxin reductase; Human glutathione reductase; Hydroperoxide reductases; Low-molecular-weight thioredoxin reductase; Methionine-*R*-sulfoxide reductases (MsrBs); Methionine-*S*-sulfoxide reductases (MsrAs); Methionine sulfoxide reductases; Methyl-Com reductase; MsrA (methionine sulfoxide reductase A); MsrB (methionine sulfoxide reductase B); NADPH–cytochrome P450 reductase; Nitrate reductase; Oxidoreductases; Rat thioredoxin reductase 1; Ribonucleotide reductase; Superoxide reductases; Thiol-based oxidoreductases; Thiol–disulfide oxidoreductases; Thioredoxin reductases
- Reduction. *See also* Redox entries
of DsbC protein, 119–120
by DsbD protein, 119–120
by GSH transferases, 109–110
in protein disulfide bond isomerization, 118
- Reductive activation, of enzymes, 175–176
- Regulation. *See also* Redox regulation
circadian, 177–182
of immune-system oxidative stress response, 221–223
of metal metabolism, 169–171
of nitric oxide synthases, 150–152
- Regulatory cysteines, 252
- Regulatory pathways, flavoenzymes in, 38
- Respiration
aerobic, 3, 7–8
as redox pathway, 175
- Resveratrol
longevity and, 33
molecular structure of, 29
- Retina, 194
age-related macular degeneration in, 201, 202, 203
antioxidant defense systems of, 202–203
light damage to, 201–202
oxidative-stress pathology of, 199–203
structure and function of, 199–200
- Retinal pigment epithelium
light damage to, 201
oxidative damage to, 201
- Rev-Erb α receptor, circadian clock and, 181–182
- Reversal potential (V_{rev}), 259
- Rhodopsin
light damage to, 201
oxidative damage to, 200–201
in retina, 199
- Rho GTPase subfamily, nitric oxide synthase and, 138, 139
- Rhombic EPR spectra, 240, 242
- Riboflavin, 36
in humans, 38–39
synthesis of, 38
- Ribonucleotide reductase, 174
- RNA (ribonucleic acid). *See* mRNA UTRs (untranslated regions)
- ROS-dependent antioxidant enzymes, 50–67. *See also* Reactive oxygen species (ROS)
- ROS scavenging enzymes, 223
- Rovira, Ilsa I., xiv, 136
- Rozanski, George J., xiv, 204
- [Ru(phen)₂dppz]²⁺, photolysis of, 93
- Ryanodine receptors (RyR2)
Ca²⁺ release from cardiac myocytes and, 208
in cardiac myocyte expansion–contraction coupling, 204
- Saccharomyces cerevisiae*
ER oxidases in, 125
thioredoxins in, 70

- Salmonella typhimurium*
 alkyl hydroperoxide reductases of, 65, 66
 peroxiredoxin in, 60
- Sample composition/dose, for EPR, 243
- Sarcoplasmic reticulum (SR), in cardiac
 myocyte expansion–contraction
 coupling, 204. *See also* SERCA2a
 (sarco[endo]plasmic reticulum calcium
 ATPase)
- Saturation, in EPR experiments, 244, 245
- Saville reaction, in RSNO detection, 281,
 282
- Schiff bases, 191, 193
- Schultz, Harold D., xv, 263
- Schwartz, G., 45
- Sco1 membrane protein, 167
- Scopoletin, in hydrogen peroxide detection,
 275
- Scurvy, ascorbate and, 27
- SECIS (selenocysteine insertion sequence)
 element, 128
- Secondary protein structure
 modeling, 254–255
 redox-active cysteines and, 253–254
- SELECT (selenium and vitamin E cancer
 prevention trial), 217
- Selectivity, of ion channels, 256
- Selenium (Se)
 biological occurrence of, 127–128
 clinical cancer trials of, 217–218
 high-molecular-weight thioredoxin
 reductase and, 73–74
 methionine sulfoxide reductases and, 86
- Selenocysteine (Sec)
 biological occurrence of, 127–128
 molecular structure of, 127
 thioredoxin reductase and, 72, 73, 74
- Selenocysteine residues, in bioinformatics,
 251, 255
- Selenophosphate synthetase, as
 selenoprotein, 129
- Selenoprotein forms, of methionine
 sulfoxide reductases, 86, 87
- Selenoprotein P (SelP), 130
- Selenoproteins, 127–131
 functions of, 130–131
 with known functions, 128–130
 occurrence of, 127–128
 with unknown functions, 130
- Semiquinone, 150
 flavin and, 35–36
 molecular structure of, 29
- Senile cataract, 196
 oxidation and, 196, 197
- Sensitivity, of EPR experiments, 244, 245
- Sequence analysis, of thiol-based
 oxidoreductases, 255
- Seravalli, Javier, xv, 237
- SERCA2a (sarco[endo]plasmic reticulum
 calcium ATPase), 204–205, 206
 Na⁺/Ca²⁺ exchange transporter and,
 208–209
- Serine, molecular structure of, 127
- Sestrins, peroxiredoxins and, 94
- Shen Nung, Emperor, 32
- Signal detection, in EPR, 241–244, 245
- Signaling. *See also* Growth signaling
 messengers; Redox signaling
 oxidant, 136–148
 paracrine, 137
 redox-dependent, 63–64
- Signaling cascades, RNS/ROS and, 272
- Signaling pathways, flavoenzymes in, 38
- Signal transduction molecules
 carbon monoxide, 141–143
 hydrogen peroxide, 143–147
 nitric oxide, 136–140
 novel, 147–148
 reactive oxygen species as, 156–157
 superoxide, 143–147
- Single-channel conductance, by ionic
 channels, 256, 257, 258–259
- Single-channel patch-clamp technique, for
 intracellular recording, 266–267,
 268–269
- Single-unit recordings, electrophysiological,
 264, 267–268
- Sirtuins, 33
- Smirnoff–Wheeler–Running pathway, in
 ascorbate biosynthesis, 24–25
- S-nitrosylation (S-NO), by nitric oxide, 139,
 140
- sodA* (superoxide dismutase) gene, in
 immune-system oxidative stress
 response regulation, 222
- Sodium (Na). *See* Na⁺ entries
- Sodium-dependent vitamin C transporters
 (SVCTs), 26

- Soluble guanylyl cyclase (sGC)
 carbon dioxide and, 141
 nitric oxide and, 138–140, 153
- Somerville, Greg A., xv, 218
- Sources, for mass spectrometers, 228, 229–230
- SoxRS pathway, 144
- SoxR transcriptional regulator, 65
 in immune-system oxidative stress response regulation, 222
- Spin concentration, in EPR experiments, 244–246
- Spin inversion, 55
- Spin–lattice relaxation, in EPR experiments, 244
- Spin–orbit coupling, in EPR experiments, 244
- Spin relaxation, in EPR experiments, 244
- Spin restriction, 55
- Spiroiminodihydantoin (Sp), DNA damage and, 87–88
- Stable radicals, EPR studies on, 239
- Stadtman, Earl R., xv
- Staphylococcal complement inhibitor, immune system blocking by, 223–224
- Staphylococcus aureus*
 immune system blocking by, 223–224
 redox buffers in, 21
 redox control of gene expression in, 156
- Statins (HMG-CoA inductase inhibitors), nitric oxide synthase and, 138, 139
- Stone, Julie M., xv, 27
- Streptococcus*, acatalasemia and, 54
- Streptomyces*, superoxide dismutase in, 57–58
- Stress, ascorbate and, 26–27. *See also* Oxidative stress
- Stress-activated protein MAP kinases (SAPKs)
 apoptosis and, 161
 in redox regulation of genes, 154
- STRING database, 255
- Structural cysteines, 252
- Structure Prediction Meta Server, 254–255
- Stuehr, Dennis, 43
- Subcellular metal transporters, 167–168
- Succinate dehydrogenase, 174
- Sulfanilamide, in RSNO detection, 281, 282
- Sulfate reduction, as redox pathway, 175
- Sulfenic acid
 in oxidative immune-system damage to bacteria, 221
 as peroxide-sensitive switch, 63–64
- Sulfhydryl groups, in oxidative immune-system damage to bacteria, 221
- Sulfinic acid, reduction by sulfiredoxins, 94–96
- Sulfinic acid-containing proteins, sulfiredoxins and, 96–97
- Sulfiredoxins (Srxs), 61, 94–97
 crystal structure of, 96
 peroxyredoxins and, 94, 95
 reduction of sulfinic acid by, 94–96
 sulfinic acid-containing proteins and, 96–97
- Sulfite oxidase, 44, 45
- Sulfur (S). *See also* [4Fe–4S] cluster entries; Iron–sulfur entries
 global equilibrium redox cycling of, 4
 glutaredoxin mechanism and, 81–82, 83
 methionine sulfoxide reductase and, 85
- Sulfur bacteria, 2
- Sulfur oxidation, as redox pathway, 175
- Sun, photosynthesis and, 5, 6
- Superoxide (SO)
 as catalase inhibitor, 52–53
 cataract and, 196
 elimination of, 56
 formation of, 55
 harmful effects of, 55
 hydrogen peroxide and, 50
 perceived toxicity of, 136
 in photosynthesis, 6
 in protein oxidation, 184–187
 as signal transduction molecule, 143–147
- Superoxide anion radical, detection of, 273–274
- Superoxide dismutases (SODs), 13, 50, 52, 55–59, 174
 copper–zinc, 56–57, 163, 165
 effectiveness of, 58–59
 innate immune response and, 219
 in lens oxidation damage, 199
 manganese, iron, and cambialistic, 57
 molecular structures of, 53
 multiple, 56

- murine knockouts of, 58
 - nickel, 57–58
 - in retinal antioxidant defense systems, 203
- Superoxide reductases, 50
- “Switch-clamp” method, for intracellular recording, 266
- Systemic-disease-associated cataract, 196
- Szent-Györgyi, Albert, 22

- Takahara’s disease, 54
- Tandem mass spectrometry (MS/MS), 230, 231
- Target-specific chaperones, intracellular metal distribution by, 165–166
- Tetrachloroquinone, dehalogenation of, 111
- Tetrahydrobiopterin, 42–43, 151
 - in chronic heart failure, 206
 - nitric oxide synthase and, 45–46
 - redox reactions catalyzed by, 43
- Tetrahydrofolic acid, 46
- Tetramethylbenzidine oxidation, in hydrogen peroxide detection, 276
- TfR (transferrin receptor) complex, 166
- TGA codon, selenocysteine and, 127–128
- Therapeutic potential
 - of carbon monoxide, 143
 - of glutathione reductase, 77–78
- Thermodynamics
 - of ion channels, 258
 - of protein-ligand binding, 248–249
- Thermus thermophilus*, glycosylases in, 91, 92
- “Thiolate push,” cytochrome P450 and, 102–103
- Thiolate anions
 - in oxidative immune-system damage to bacteria, 221
 - in peptide editing, 157
- Thiol-based oxidoreductases. *See also* Thioredoxins (Trxs)
 - bioinformatics in studies of, 251–255
 - sequence analysis of, 255
- Thiol-based redox buffers, 21
- Thiol–disulfide exchange, 122–123
 - in disulfide bond stability, 121–122
- Thiol–disulfide oxidoreductases, 78
- Thiol groups, in peroxyredoxins, 62

- Thiol-mediated redox regulation, peptide editing and, 156–157
- Thiols (RSH)
 - redox control of, 71, 72
 - in RSNO detection, 281, 282
- Thiol-specific antioxidant (TSA), 59
- Thioltransferase, 78. *See also* Glutaredoxins (Grxs)
- Thioredoxin domain, in DsbA and DsbC proteins, 115
- Thioredoxin reductases, 61, 68, 71–74
 - high-molecular-weight, 72–74
 - low-molecular-weight, 72
 - molecular structure of, 73
 - occurrence of, 71–72
 - as selenoproteins, 129
- Thioredoxins (Trxs), 61, 68, 79, 81
 - DsbC and DsbD proteins and, 119
 - during growth stimulation, 213–214
 - isoforms of, 68–70
 - reduced, 70–71, 72
 - secondary structure of, 253–254
 - as selenoproteins, 130
 - structure and mechanism of, 70–71, 72
- Thioredoxin system
 - antioxidants in, 68–74
 - functions of, 68
 - glutathione system and, 75
- Thomas, Mark P., xv, 256
- Thylakoids, 6
- Thymine, DNA damage and, 88
- Thymine glycol (Tg), DNA damage and, 88
- Thyroid hormone deiodinases, as selenoproteins, 130
- Timeless* gene, in circadian clock, 178
- Time-of-flight (TOF) analyzer, for mass spectrometers, 231
- Tissue, measurement of GSH:GSSG redox couple in, 377
- Titrations, potentiometric, 249, 250, 251
- Tocols, 28
- α -Tocopherol
 - as antioxidant, 28–30
 - molecular structure of, 29
- Tocopherols, as antioxidants, 27–28
- Tocopheroxyl radical, 29–30
- Tocotrienols, as antioxidants, 27–28
- Topaquinone (TPQ), 40
- “Torin,” 60

- Toxicity. *See also* Detoxification
of carbon monoxide, 141
of copper and iron, 173
of metals, 163, 164
of reactive oxygen species, 136
RNS/ROS mediation of, 272–273
- Tpx catalase, versus hydrogen peroxide, 67
- Transcriptional regulators, alkyl
hydroperoxide reductases and, 65
- Transcriptional regulation
of glutathione biosynthesis, 15, 16
of metal metabolism, 169
- Transcription factor activity, in redox control
of gene expression, 155–156
- Transferases, glutathione, 13–14
- Transferrin (Tf)
atransferrinemia from lack of, 172
in iron uptake from extracellular
environment, 164–165, 166
- Transferrin receptor 1, in post-transcriptional
iron regulation, 170
- Transferrin receptor 2 mutations,
hemochromatosis resulting from, 172
- Transgenic mice, catalases and longevity of,
53
- Trans-Golgi network, in copper metabolism,
167, 171
- Transient reactive organic radicals, EPR
studies on, 239
- Transition metal ions, in electron transfer,
162
- Transition metals
as catalysts, 164
as paramagnetic species, 237, 239
- Transmembrane electron transfer, DsbD
protein catalysis of, 119–120
- Transmembrane recording, 264. *See also*
Intracellular recording
- Transparency, loss of lens, 195–196
- Transport, of ascorbate, 26. *See also*
Electron transport entries
- Transsulfuration pathway, in GSH
homeostasis, 16–17
- Tricarboxylic acid (TCA) cycle, in oxidative
immune-system damage to bacteria,
221, 222–223
- Triple quadrupole analyzer, for mass
spectrometers, 230
- Triplet organic radicals, EPR studies on, 239
- Trypanosoma brucei*, trypanothione from,
21
- Trypanothione, 21
molecular structure of, 20
- Tryptic peptides, in mass-spectrometry
proteomics, 235
- Tryptophan hydroxylase, 44
- Tryptophan tryptophylquinone (TTQ), 40
- Tumor necrosis factor- α (TNF- α), 63
- Tungsten (W), molybdopterins and, 44
- 2-cys peroxyredoxins, 60–63
robust, 62
sensitive, 62
“typical,” 60, 61, 62, 63
- Tyrosine
in cross-linked protein derivative
formation, 192, 193
in detecting peroxynitrite, 283–284
- Tyrosine hydroxylase, 44, 174
- Tyrosine nitration, retinal damage and,
201–202
- Tyrosine phosphatases, during growth
stimulation, 212–214
- Ubiquinol, 31
human health and, 34–35
molecular structure of, 29
- Ubiquinone, 31
DsbA and DsbB proteins and, 116
human health and, 34–35
molecular structure of, 29
- Ultraviolet (UV) radiation
cataract and, 196–197
shielding against, 2
- Unit conductance, of ion channels, 268
- Uric acid
human health and, 35
molecular structure of, 29
as water-soluble antioxidant, 34
- Veeramani, Suresh, xv, 212
- Vitamin A
as antioxidant, 30
antioxidants and, 27–28
clinical cancer trials of, 218
human health and, 34
- Vitamin B₂, synthesis of, 38
- Vitamin B₂. *See also* Riboflavin
- Vitamin B₃, 40

- Vitamin C, 22. *See also* Ascorbate
clinical cancer trials of, 218
- Vitamin E
antioxidants and, 27–28
clinical cancer trials of, 217–218
forms of, 28
human health and, 34
as lens antioxidant, 197
versus ROS, 28–30
- Voltage-clamp method, for intracellular recording, 265–266
- Voltage–current relationships, for ion channels, 257–260, 263–264, 265–266, 268, 269
- Voltage-gated ionic channels, 257
- Water
in ascorbate recycling, 25–26
glutathione and, 13
in photosynthesis, 6–7
- Water-soluble antioxidant molecules, 31–34
- Water-splitting reaction, 2–3
- Waveguides, for EPR, 243
- W-band EPR, 243
- Whole-cell patch-clamp configurations, for intracellular recording, 267, 269
- Wilson, Mark A., xv, 27
- Wilson disease, 167, 172
- WND copper carrier, 165, 167
in export of copper from cells, 168–169
in post-translational copper regulation, 171
- Women's Health Study of 1999, 217
- Xanthine dehydrogenase, 44, 45, 174
- Xanthine oxidase (XO)
in chronic heart failure, 206, 207
uncontrolled ROS production and, 214
- Xanthophylls, 30
- X-band EPR, 241, 242–243
- Xenopus*, 266
- Yamanishi, Mamoru, xviii
- Yeast glutathione synthetase, 16
- Yeasts
ER oxidases in, 125, 126
glutathione reductase in, 77–78
metallothionein in, 168
peroxyredoxins in, 59
post-transcriptional regulation in, 171
quinones in, 40
sulfiredoxins in, 94–96
thioredoxins in, 69
- Zeaxanthin, 30
- Zeeman effect, 237, 239–240, 246
- Zif268 protein–DNA complex
crystal structure of, 155
in redox control of gene expression, 155, 156
- Zinc (Zn), glutathione reductase inhibition by, 77. *See also* Copper- and zinc-containing superoxide dismutases (Cu,ZnSODs)
- Zinc finger motifs, in redox control of gene expression, 155, 156
- Zinc superoxide dismutase, 52
molecular structure of, 53
- Z-scheme, 6, 7